

Development of *Pseudomonas aeruginosa* Biofilm-targeted Antibiotic-Carbohydrate Conjugates

Dissertation

Zur Erlangung des Grades des Doktors der Naturwissenschaften
der Naturwissenschaftlich-Technischen Fakultät der Universität des
Saarlandes

von

Dipl.-Apotheker Joscha Meiers

Saarbrücken
2022

Tag des Kolloquiums: 10. Juni 2022
Dekan: Prof. Dr. Jörn Eric Walter
Berichterstatter: Prof. Dr. Alexander Titz
Prof. Dr. Anna K. H. Hirsch
Prof. Dr. Boris Schmidt

Vorsitz: Prof. Dr. Marc Schneider
Akad. Mitarbeiterin: Dr. Angelika Ulrich

Preface

Die vorliegende Arbeit wurde von Dezember 2017 bis Januar 2022 unter Anleitung von Herrn Prof. Dr. Alexander Titz in der Fachrichtung Pharmazie der Naturwissenschaftlich-Technischen Fakultät der Universität des Saarlandes sowie am Helmholtz-Institut für Pharmazeutische Forschung Saarland (HIPS) in der Arbeitsgruppe Chemische Biologie der Kohlenhydrate angefertigt.

Acknowledgements

Ich möchte mich ganz herzlich bei allen bedanken, die zum Gelingen dieser Arbeit beigetragen haben.

Zu Beginn möchte ich mich bei Prof. Dr. Alexander Titz bedanken, der mir dieses spannende Projekt zum Anfertigen meiner Doktorarbeit anvertraut hat. Alex, es ist und war mir eine riesige Freude mit Dir zusammen arbeiten zu dürfen und ich bedanke mich für dein Vertrauen, deine Geduld, deine Zeit, deine Energie und vor allen Dingen für Deinen wissenschaftlichen Geist.

Weiterhin möchte ich mich bei Prof. Dr. Rolf Müller und Dr. Jennifer Herrmann für die exzellente wissenschaftliche Betreuung bedanken. Ich danke Prof. Anna K. H. Hirsch für die Übernahme des Zweitgutachtens. Weiterer Dank gilt allen, die diese Arbeit begutachtet haben, sowie meinem Prüfungsausschuss.

Ganz besonderer Dank gilt natürlich dem Team CBCH: Meine direkten Bürokolleg:innen Dr. Stefanie Wagner, Olga Metelkina und Mario Fares sorgten immer für eine gute Atmosphäre.

Besonderer Dank geht an Eva Zahorska und Eike Siebs, mit denen ich immer eine tolle Zeit beim Brettspielen hatte. Bei Eva bedanke ich mich ausserdem für eine tolle Freundschaft, wissenschaftliche Diskussionen und die schöne Zeit die man hat, sobald sie in der Nähe ist.

Dirk Hauck möchte ich ein riesengroßes Dankeschön ausrichten: Dirk hat mich geduldig in das Labor eingewiesen und ist mir vor allem aber ein ausserordentlicher Arbeitskollege, Skitrainer, Tennistrainer, Squashtrainer, Nachbar und Freund. Es wird mir immer völlig schleierhaft sein, wie ein Labor ohne Dirk nicht sofort in Flammen aufgehen kann.

Ein großer Dank gilt ausserdem Lisa-Marie Denig: Ohne deine Hilfe wäre ich bestimmt mehr als nur einmal im Biolabor verzweifelt. Lisa, danke dass Du mir so oft geholfen hast und danke für die vielen schönen Kaffeepausen zusammen. Jemanden wie dich sollte man immer in seinem Freundeskreis haben.

Ich möchte mich ausserdem bei meinen Studierenden Johanna Knigge, Steffen Leusmann, Alina Aubel, Laura Kosmalla, Oceane Monfret und Lovette Azap für ihre Unterstützung in der Synthese bedanken. Besonderer Dank gilt dabei Johanna, Laura und Steffen, die das neue Labor in Gebäude C4 2 mit eingerichtet haben.

Bei Marta Czekanska, Aketza Romaniega Bilbao, Zeyue Zhang, Dr. Ghamdan Beshr bedanke ich mich für eine tolle Arbeitsatmosphäre.

Ein weiteres Dankeschön gilt dem Kollegium der Gruppe DDOP unter der Leitung von Prof. Dr. Anna K. H. Hirsch. Bei Simone Amann, Jeannine Jung, Selina Wolter, Tabea Wittmann, Dennis Jener, möchte ich mich für die technische Unterstützung und viele lustige Momente ganz herzlich bedanken. Bei Teresa Röhrig und Katharina Rox bedanke ich mich für die Planung und Auswertung der *in vitro* PK Experimente. Bei Andreas Kany, a.k.a. 2m-Kany, a.k.a. Kanyboy möchte ich mich für seine Expertise an der HPLC-MS/MS bedanken. Mögen die Maschinen gnädig mit uns sein und unsere Proben vollständig messen. Bei Sandra Johannsen a.k.a. Sandy und Christina Kosch möchte ich mich für die spannenden Gossip-Kaffeepausen bedanken.

Für eine solche Arbeit ist gutes wissenschaftliches Umfeld zwar unverzichtbar, jedoch ist ohne die Unterstützung von Familie und Freunde am wertvollsten: Zuerst möchte ich mich bei den vier wichtigsten Menschen meines Lebens bedanken: Bei meiner Mutter Maria, die mich gross gezogen hat, mich immer unterstützt hat und die ich sehr liebe; Bei meiner Tante Sandra, die mich auch immer bei allem unterstützt hat, an die ich mich immer wenden kann und ohne die ich nicht so wäre wie ich bin; Bei meiner Oma Christa, die mir durch ihre ausserordentliche Resilienz und Gutmütigkeit ein grosses Vorbild ist; Bei meiner Freundin Michèle, die ich sehr liebe und auf deren Geduld, Freundschaft und Liebe ich immer zählen kann. Ich danke euch von ganzem Herzen. Ich bedanke mich auch bei meinem Vater und allen anderen Familienmitgliedern, sowie Freunden und Bekannten für Ihre grossartige Unterstützung. Dabei gilt auch ein großer Dank meinen Kolleg:innen des MV Harmonie Wahlen und der Stadtkapelle Saarbrücken für die musikalische Abwechslung während den letzten Jahren.

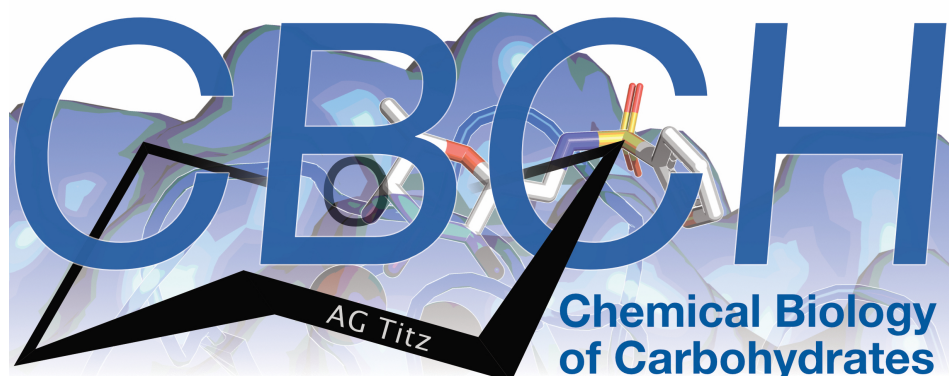


Table of Contents

| | |
|--|-------|
| Preface | III |
| Acknowledgements | IV |
| Table of Contents | VII |
| Summary | IX |
| Zusammenfassung..... | XI |
| Curriculum vitae | XII |
| Presentations at Scientific Conferences | XIII |
| Publications and Patents Resulting from this Thesis | XV |
| Contributions report..... | XVI |
| Abbreviations | XVIII |
| 1. Introduction | 1 |
| 1.1. <i>Pseudomonas aeruginosa</i> | 1 |
| 1.2. Lectin Antagonists in Infection, Immunity and Inflammation | 6 |
| 1.3. Antibiotics | 24 |
| 2. Aim of the Thesis..... | 33 |
| 3. Results..... | 34 |
| 3.1. Directing Drugs to Bugs: Antibiotic-Carbohydrate Conjugates Targeting Biofilm-Associated Lectins of <i>Pseudomonas aeruginosa</i> .. | 34 |
| 3.2. <i>P. aeruginosa</i> Lectin-targeted Conjugates of Tobramycin | 53 |
| 3.3. Smart Lectin-targeted Antibiotic-Carbohydrate Prodrugs activated by <i>Pseudomonas aeruginosa</i> | 63 |

| | |
|--|-----|
| 3.4. Synthesis of a <i>P. aeruginosa</i> Biofilm-targeted antibiotic Prodrug, based on a bivalent high-affinity LecA-Probe | 90 |
| 3.5. On the Carbohydrate binding-Specificity of the Pineapple-derived Lectin Acn-JRL and its Potential Use against SARS-CoV-2..... | 97 |
| 4. Global Summary and Future Perspectives..... | 114 |
| 5. Appendix | 120 |
| 5.1. Supporting Information for Chapter 3.1 | 120 |
| 5.2. Supporting Information for Chapter 3.2 | 152 |
| 5.3. Supporting Information for Chapter 3.3 | 162 |
| 5.4. Supporting Information for Chapter 3.4 | 252 |
| 5.5. Supporting Information for Chapter 3.5 | 267 |
| 5.6. Isosteric Substitution of Acylhydrazones yields highly potent divalent LecA Inhibitors with excellent Solubility and metabolic Stability | 286 |
| References | 301 |

Summary

Pseudomonas aeruginosa is an opportunistic Gram-negative bacterium and a serious threat to our health system. Further, resistances against a plethora of antibiotic drugs are constantly on the rise. Thus, new therapeutic strategies are urgently needed.

This work focuses on lectin-targeted antibiotic drug conjugates that specifically act on the *P. aeruginosa* biofilm, a hallmark of chronic infections. Antibiotics, in particular fluoroquinolones and tobramycin, were chemically linked to monovalent and bivalent carbohydrate-based lectin probes to target the *P. aeruginosa* biofilm.

In a first attempt, conjugation to ciprofloxacin and tobramycin was based on a non-cleavable triazole linker. Lectin-inhibition was confirmed for all conjugates. While the tobramycin-based compounds remained antibiotically inactive, conjugates of ciprofloxacin showed antibiotic activity and reduced cytotoxicity compared to their parent drug. Eventually, biofilm-accumulation experiments proved their enrichment within *P. aeruginosa* biofilm *in vitro*.

Based on these results, a peptide-based linker was introduced that is cleavable in presence of *P. aeruginosa*. The resulting prodrugs efficiently released their parent fluoroquinolone drugs and reached high antimicrobial activity *in vitro*. Further, their promising *in vitro* ADMET parameters and low cell permeability pave the way for a new class of antibiotic drug conjugates with strongly reduced side effects.

Zusammenfassung

Pseudomonas aeruginosa ist ein Gram-negatives, opportunistisches Bakterium und eine ernste Gefahr für unser Gesundheitssystem. Aufgrund der schnellen Entstehung multiresistenter Keime ist die Entwicklung neuartiger Antibiotika extrem wichtig.

Die vorliegende Arbeit beschreibt Antibiotika-Konjugate, die Lektine von *P. aeruginosa* adressieren und somit den Wirkstoff gezielt an den Ort der Infektion bringen sollen. Antibiotika aus der Klasse der Fluorchinolone sowie Tobramycin wurden chemisch an mono- sowie bivalente Lektinsonden geknüpft.

Der erste Teil behandelt Konjugate von Ciprofloxacin und Tobramycin, basierend auf einem nicht spaltbaren Linker. Alle Konjugate banden ihre entsprechenden Lektine mit hoher Affinität. Während die Tobramycin-Konjugate jedoch antibiotisch inaktiv waren, zeigten die Konjugate von Ciprofloxacin antibiotische Aktivität und verminderte Zytotoxizität im Vergleich zu ihrer Stammverbindung *in vitro*. Tatsächlich konnte eine Anreicherung im Biofilm von *P. aeruginosa in vitro* nachgewiesen werden.

Basierend auf diesen Ergebnissen wurde ein Peptidlinker eingeführt, der in Gegenwart von *P. aeruginosa* gespalten werden kann. Die entsprechenden Prodrugs zeigten eine schnelle Wirkstofffreisetzung und somit hohe antibiotische Aktivität *in vitro*. Aufgrund der exzellenten pharmakokinetischen Charakteristiken *in vitro*, sowie wie ihrer niedrigen Zellaufnahme begründen diese Prodrugs eine neue Wirkstoffklasse in der Therapie von Infektionen mit *P. aeruginosa*.

Curriculum vitae

Name: **Joscha Meiers**
Anschrift: Heidenkopferdell 25,
66123 Saarbrücken
Telefon: 0160-8384367
E-Mail: joscha.meiers@gmx.de
Geburtsdatum/-ort: 03.02.1994 in Wadern



BILDUNGSWEG

Universität des Saarlandes

Studium der Pharmazie

Erstes Staatsexamen (Note: 1.5)

Zweites Staatsexamen (Note: 1.2)

Drittes Staatsexamen (Note: 1.5)

Universität des Saarlandes, Pharmazeutische und Medizinische Chemie Prof. Dr. Christian Ducho

Anfertigen einer Diplomarbeit

Thema: Entwicklung eines LC-MS basierten Assays zur Evaluierung der bakteriellen Zellaufnahme

(schriftlich: 1.0, Kolloquium: 1.0)

Landmann Apotheke, Filiale Saarbrücken

Pharmazeut im Praktikum

Helmholtz Institut für Pharmazeutische Forschung Saarland Chemische Biologie der Kohlenhydrate, Prof. Dr. Alexander Titz

Anfertigen einer Doktorarbeit

Thema: Design and Synthesis of Antibiotic-Carbohydrate Conjugates Targeting Biofilm-Associated Lectins of *Pseudomonas aeruginosa*

LEHRE (Auszug seit 2017)

Betreuer im Seminar Medizinische Chemie für Pharmazeuten

Betreuung von Studierenden im Wahlpflichtpraktikum für Pharmazeuten

Betreuung von DAAD-Student:innen

Betreuung Vertiefungspraktikum/Masterarbeit von Frau J. Knigge

FÖRDERUNGEN

Studienstiftung Saarland

Saarlandstipendium (150€/Monat)

Studienstiftung des deutschen Volkes

Volles Stipendium (300€/Monat)

Französische Botschaft in Deutschland

Stipendium Procope - Mobilität (2800€), Grenoble (Frankreich)

HOBBIES

Stadtkapelle Saarbrücken und MV „Harmonie“ Wahlen 1924 e.V.

Musiker (Trompete)

2012 - 2017

2014

2016

2017

Nov. 2016 - Juli 2017

Mai - Okt. 2017

Dez. 2017 -
vs. Ende 2021

2017 - Heute

2020 - Heute

2019

2021

2014 - 2015

2015 - 2017

Sep. - Dez. 2021

Presentations at Scientific Conferences

ORAL PRESENTATIONS AT SCIENTIFIC CONFERENCES:

- VII. Symposium of the Interdisciplinary Graduate School of Natural Product Research, **2018**, Saarbrücken, oral presentation: „Sweet targeting with hybrid antimicrobials“.
- Gordon Research Seminar on Glycobiology, **2019**, Lucca (Italy), oral presentation: „Synthesis and Evaluation of *P. aeruginosa* Biofilm targeting Antibiotics“.
- HIPS-Symposium, **2019**, Saarbrücken, oral presentation: „Synthesis and Evaluation of *P. aeruginosa* Biofilm targeting Antibiotics“.

POSTER PRESENTATIONS AT SCIENTIFIC CONFERENCES:

- Advances in Chemical Biology, **2019**, Frankfurt am Main, poster presentation: „Targeting Antibiotics via Carbohydrate Probes against *Pseudomonas aeruginosa* Biofilm“.
- Gordon Research Conference on Glycobiology, **2019**, Lucca (Italy), poster presentation: „Sweet Targeting in Bitter Infections: Targeting Antibiotics via Carbohydrate Probes against *P. aeruginosa* Biofilm“.
- Frontiers in Medicinal Chemistry, **2021**, virtual conference, poster presentation: „Directing Drugs to Bugs: Antibiotic-Carbohydrate Conjugates targeting Biofilm-Associated Lectins of *Pseudomonas aeruginosa*“ (awarded with „Best Poster Award“, Arch. Pharm., Wiley)

Publications and Patents Resulting from this Thesis

Lectin antagonists in infection, immunity and inflammation

Joscha Meiers, Eike Siebs, Eva Zahorska and Alexander Titz

Curr. Opin. Chem. Biol. **2019**, 53, 51-67.

DOI: 10.1016/j.cbpa.2019.07.005.

Directing Drugs to Bugs: Antibiotic-Carbohydrate Conjugates Targeting Biofilm-associated Lectins of *Pseudomonas aeruginosa*

Joscha Meiers, Eva Zahorska, Teresa Röhrig, Dirk Hauck, Stefanie Wagner and Alexander Titz

J. Med. Chem. **2020**, 63, 11707-11724.

DOI: 10.1021/acs.jmedchem.0c00856.

Smart Antibiotic-Carbohydrate Prodrugs activated by *Pseudomonas aeruginosa*

Joscha Meiers, Katharina Rox and Alexander Titz

Manuscript in preparation.

Lectin-targeting Conjugates

Joscha Meiers, Eva Zahorska, Lisa Denig, Stefanie Wagner and Alexander Titz

Patent filed (07.12.2021, EP21212989).

Glycan Array Analysis of the Mannose-specific Pineapple- (*Ananas comosus*) derived Jacalin-related Lectin AcmJRL and its Potential against SARS-CoV-2

contributing authors (order not yet defined): Joscha Meiers, Jan Dastbaz, Sebastian Adam, Sari Rasheed, Peter Gross, Rolf Müller and Alexander Titz

Manuscript in preparation.

other publications:

Isosteric substitution of acylhydrazones yields highly potent divalent LecA inhibitors with excellent solubility and metabolic stability

Eva Zahorska, Sakonwan Kuhaudomlarp, Joscha Meiers, Dirk Hauck, Emilie Gillon, Katharina Rox, Anne Imberty and Alexander Titz

Manuscript in preparation

Contributions report

Chapter 1.2: Lectin antagonists in infection, immunity and inflammation

Joscha Meiers, Eike Siebs, Eva Zahorska and Alexander Titz

Curr. Opin. Chem. Biol. **2019**, 53, 51-67.

DOI: 10.1016/j.cbpa.2019.07.005.

All authors contributed equally and wrote parts of the review

Chapter 3.1: Directing Drugs to Bugs: Antibiotic-Carbohydrate Conjugates Targeting Biofilm-associated Lectins of *Pseudomonas aeruginosa*

Joscha Meiers, Eva Zahorska, Teresa Röhrig, Dirk Hauck Stefanie Wagner and Alexander Titz

J. Med. Chem. **2020**, 63, 11707-11724.

DOI: 10.1021/acs.jmedchem.0c00856.

J.M. designed and synthesised conjugates and individual building blocks. D.H. synthesised compound **17**. J.M. and E.Z. performed lectin inhibition assays. J.M. performed gyrase supercoiling inhibition, antibiotic susceptibility, and biofilm accumulation assays. T.R. analysed data for metabolic stability in human plasma, plasma protein binding, and acute cytotoxicity. S.W. provided conceptual advice and analysed the data. J.M. and A.T. conceived the study. J.M. and A.T. wrote the paper with input from all coauthors.

Chapter 3.2: *P. aeruginosa* Lectin-targeted Conjugates of Tobramycin

Joscha Meiers and Alexander Titz

J.M. designed and synthesised conjugates and individual building blocks and performed lectin inhibition assays and antibiotic susceptibility assays. J.M. and A.T. conceived the study. J.M wrote the chapter with input from A.T..

Chapter 3.3: Smart Lectin-targeted Antibiotic-Carbohydrate Prodrugs activated by *Pseudomonas aeruginosa*

Joscha Meiers, Katharina Rox and Alexander Titz

Manuscript in preparation.

J.M. designed and synthesised conjugates and individual building blocks and performed lectin inhibition assays, antibiotic susceptibility assays and characterised prodrug activation. K.R. analysed data for metabolic stability, plasma protein binding, acute cytotoxicity and cell accumulation. J.M. and A.T. conceived the study and wrote the paper with input from all coauthors.

Chapter 3.4: Synthesis of a *P. aeruginosa* Biofilm-targeted Antibiotic Prodrug, based on a bivalent high-affinity LecA-Probe

Joscha Meiers, Eva Zahorska and Alexander Titz

J.M. designed and synthesised peptidyl-fluoroquinolone **12**. E.Z. designed and synthesised divalent LecA-ligand **1**. J.M. synthesised the final compound **13**. J.M. and A.T. conceived the study.

Chapter 3.5: On the carbohydrate binding-specificity of the Pineapple-derived Lectin Acm-JRL and its Potential Use against SARS-CoV-2

Joscha Meiers and Alexander Titz

J.M. isolated and characterised the protein. J.M. performed fluorescent labelling. CFG performed glycan binding analysis on CFG glycan array. Semiotik developed the Semiotik glycan array. J.M. performed glycan binding analysis on Semiotik glycan array. J.M. assessed the data for both glycan arrays. J.M. and A.T. conceived the study. J.M. wrote this chapter with input from A.T..

Abbreviations

| | |
|-------------------|---|
| 3WJ | three-way junction |
| aa | amino acids |
| AAC | aminoglycoside acetyl transferase |
| ADC | Antibody-drug conjugate |
| AMP | antimicrobial peptide |
| ANT | aminoglycoside nucleotidyl transferase |
| APH | aminoglycoside phosphotransferase |
| Ara | L-Arabinose |
| Boc | <i>tert</i> -butyloxycarbonyl |
| calcd | calculated |
| CBCH | Chemical Biology of Carbohydrates |
| CD | Crohn's disease |
| CF | cystic fibrosis |
| CFG | Center for Functional Glycomics |
| CHES | <i>N</i> -Cyclohexyl-2-aminoethanesulfonic acid |
| cipro | ciprofloxacin |
| CL _{int} | intrinsic microsomal clearance |
| CL _{MIC} | microsomal clearance |
| COSY | homonuclear correlation spectroscopy |
| COVID-19 | coronavirus disease 2019 |
| cPr | cyclopropyl |
| Cy3 | cyanine 3 |
| DAD | diode array detector |
| DC-SIGN | Dendritic Cell-Specific Intercellular adhesion molecule-3-Grabbing Non-integrin |
| DEPT | distortionless enhanced by polarisation transfer |
| DIAD | Diisopropyl azodicarboxylate |
| DIPEA | Diisopropylethylamine |
| DLS | dynamic light scattering |
| DMF | Dimethylformamide |

| | |
|----------------|---|
| DMSO | Dimethylsulfoxide |
| DOL | degree of labelling |
| DPPA | Diphenylphosphoryl azide |
| DSMZ | Deutsche Sammlung für Mikroorganismen und Zellkulturen |
| ECDC | European Centre for Disease Prevention and Control |
| EDC | 1-ethyl-3(3-dimethylaminopropyl)carbodiimide hydrochloride |
| eDNA | extracellular DNA |
| Eis | enhanced intercellular survival |
| ESBL | extended spectrum β -lactamases |
| FDA | Food and Drug Administration |
| FITC | fluoresceinisothiocyanate |
| FL | fucosyl-lactose |
| FP | fluorescence polarisation |
| FQ | fluoroquinolone |
| Fuc | L-Fucose |
| Gal | D-Galactose |
| Gb3 | globotriaosylceramide |
| GID | glycan identification number |
| Glc | D-Glucose |
| GlcNAc | D-(<i>N</i> -Acetyl) glucosamine |
| H _a | hydrogen in axial position |
| HBGA | human blood group antigen |
| HBTU | O-(Benzotriazol-1-yl)- <i>N,N,N,N</i> -tetramethyluronium-hexafluorophosphate |
| H _e | hydrogen in equatorial position |
| HEK cells | human embryonic kidney cells |
| HIV | human immunodeficiency virus |
| HLM | human liver microsomes |
| HRMS | high resolution mass spectroscopy |
| HSQC | Heteronuclear multiple bond correlation spectroscopy |
| Ibcf | isobutyl chloroformate |

| | |
|------------------|--|
| IC ₅₀ | half maximal inhibitory concentration |
| ICU | intensive-care unit |
| JRL | jacalin related lectin |
| LB | lysogeny broth |
| LC | liquid chromatography |
| LRMS | low resolution mass spectroscopy |
| Lyx | D-Lyxose |
| MAG | myelin-associated glycoprotein |
| MDCK | Madin-Darby canine kidney cells |
| MDR | multidrug resistance |
| MHB II | Müller-Hinton broth II |
| MIC | minimal inhibitory concentration |
| MLM | mouse liver microsomes |
| MPLC | medium pressure liquid chromatography |
| MS | mass spectroscopy |
| msec | milliseconds |
| MWCO | molecular weight cutoff |
| n.s. | not significant |
| NCFG | National Centre for Functional Glycomics |
| NHS | <i>N</i> -Hydroxysuccinimide |
| NMI | <i>N</i> -Methylimidazole |
| NMR | nuclear magnetic resonance |
| NP | normal phase |
| OD | optical density at 600 nm |
| ONP | <i>ortho</i> -nitrophenol |
| PBS | phosphate buffered saline |
| PDB | protein database |
| PE | petroleum ether |
| PhMe | toluene |
| PMBN | polymyxin B nonapeptide |
| PPB | plasma protein binding |

| | |
|---------------------|--|
| PRR | pattern recognition receptor |
| QS | quorum-sensing |
| RBD | receptor binding domain |
| rcf | relative centrifugal force |
| Rha | L-Rhamnose |
| RP | reversed phase |
| s.d. | standard deviation |
| SAR | structure activity relationship |
| SARS-CoV-2 | severe acute respiratory syndrome coronavirus type 2 |
| satd | saturated |
| SGID | semiotic glycan identification number |
| SL | sialyl-lactose |
| sLe ^x | sialyl Lewis X |
| SPR | surface plasmon resonance |
| TAMRA | carboxymethylrhodamine |
| TBAHSO ₄ | Tetrabutylammonium hydrogensulfate |
| TBS | tris-buffered saline |
| TBSCl | <i>tert</i> -Butyldimethylsilylchlorid |
| TBTU | 2-(1H-Benzotriazole-1-yl)-1,1,3,3-tetramethylaminium tetrafluoroborate |
| TLC | thin layer chromatography |
| TNF | tumor necrosis factor |
| ToF | time-of-flight |
| UTI | urinary tract infection |
| UV | ultraviolet |
| WHO | World Health Organisation |
| Xyl | D-Xylose |

1. Introduction

1.1. *Pseudomonas aeruginosa*

Every day, our body carries an unimaginably high number of bacteria. In fact, the average 'reference man' is colonised by approximately 4×10^{13} bacterial cells.^[1] Interestingly, the number of human cells was estimated to 3×10^{13} cells, resulting in an approximately 1 : 1 ratio. To put these numbers in perspective, the number of stars in our galaxy, the milky way, is estimated around 3×10^{11} , thus 2 orders of magnitude less. Most of these bacteria contribute to a normal state of health, most prominently the intestinal microbiome, e.g. by constantly challenging the host's immune system, healthy digestion and nutrient uptake. In consequence, the human microbiome can be referred to as the 'second genome' or 'invisible organ'. However, it is quite obvious that beyond these 'healthy' bacteria, dangerous pathogenic bacteria can make us seriously ill.

One particularly perilous group of bugs are the ESKAPE pathogens, consisting of *Enterococcus faecium*, *Staphylococcus aureus*, *Klebsiella pneumoniae*, *Acinetobacter baumannii*, *Pseudomonas aeruginosa* and *Enterobacter* species.

This work focusses on the Gram-negative, opportunistic bacterium *P. aeruginosa*, which is a serious threat to immunocompromised patients (e.g. geriatrics, transplant patients, HIV patients and patients in ICU) and people suffering from cystic fibrosis.^[2-4] According to the Annual Epidemiological Report for 2017 from the European Centre for Disease Prevention and Control (ECDC), *P. aeruginosa* is the most frequently isolated pathogen in ICU-acquired pneumonia (19.9%).^[5] Further, over 50% of all adult cystic fibrosis patients are chronically infected with *P. aeruginosa*.^[6]

Almost any part of the body provided with sufficient humidity can be infected by *P. aeruginosa*. Prominent examples are wound infections (especially from burn victims), urinary-tract infections (UTI), infections of eye and brain as well as pneumonia and infections on indwelling medical devices.^[7] These diverse infection sites demand a careful choice of appropriate antibiotics with their specific pharmacokinetic properties. For instance, fluoroquinolones penetrate better over the blood-brain barrier than aminoglycosides, thus enabling therapy of *P. aeruginosa* brain infections.^[8]

The genome of *P. aeruginosa* ranges from 5.5 to 7 Mbp and is thereby larger than the genome of many other bacteria. Although the core genome is highly conserved, the accessory genome varies extensively within clinical isolates.^[9] Two *P. aeruginosa* clinical isolates PA14 and PAO1 are recognised most in research and most clinical isolates can

be clustered in PA14-like and PAO1 like strains, with PA14 being generally more virulent than PAO1.^[10] High genetic adaptability can lead to increased pathogenicity, antibiotic resistance and resilience against rough growth conditions, either by horizontal gene transfer or spontaneous mutations.^[11]

The pathogenicity of a bacterium is, among others, characterised by its virulence factors. Virulence factors are defined as biomolecular structures and machineries that allow the pathogen to effectively establish and sustain infections.^[12] *P. aeruginosa* has a particularly diverse arsenal of highly efficacious virulence factors: small cytotoxic molecules like cyanic acid or pyocyanin directly harm the host, whilst siderophores supply the bacterial cells with iron in nutrition-low environments. Further, biopolymers like polysaccharides (e.g. Psl and Pel), rhamnolipids and proteins (e.g. LecA, LecB and LasB) are also potent virulence factors.^[13] Most virulence factors are regulated by one or more of the the four *P. aeruginosa* quorum sensing systems *las*, *rhs*, *iqs*, and *pqs*.^[14]

1.1.1. *P. aeruginosa* biofilm and the lectins LecA and LecB

The formation of a biofilm is a hallmark in chronic infections of *P. aeruginosa* and is critical for its pathogenicity and thus a potent virulence factor.^[15] In contrast to single planktonic cells, a biofilm consists of accumulated bacterial cells, surrounded by a biofilm matrix. Within the biofilm, the cells are protected from antibiotic drugs (antibiotic resistance increased by up to factor 10,000^[16]) and components of the host's immune system. The biofilm matrix is a complex hydrogel, held together by exopolysaccharides (alginate, Pel, Psl), extracellular DNA (eDNA) and various proteins. The polysaccharide Psl consists of repeating units of mannose, rhamnose, and glucose (3:1:1).^[17] The exact chemical structure of Pel is yet not fully determined. There is evidence for the presence of (partially *N*-acetylated) galactosamine and glucosamine together with glucose.^[18] The three-dimensional structure of a biofilm is comparable to a sponge: micropores traverse the biofilm and guarantee access to nutrients and oxygen.^[19] In fact, only 10% of the dry biofilm mass are microorganisms themselves, while the other 90% are matrix components.^[20]

The two extracellular carbohydrate-binding proteins LecA and LecB (also known as PA-IL and PA-IIL, respectively)^[21-23] are vital for *P. aeruginosa* biofilm formation.^[24, 25] Both genes *lecA* and *lecB* are encoded in its core genome and are regulated by the quorum sensing systems *rhl* and *pqs*.^[26, 27] While *lecA* is highly conserved, *lecB* and its corresponding protein vary among clinical isolates and can be clustered in PA14- and PAO1-like families.

Both homologs LecB_{PAO1} and LecB_{PA14} bind similar glycans, however, with significantly different affinities.^[28]

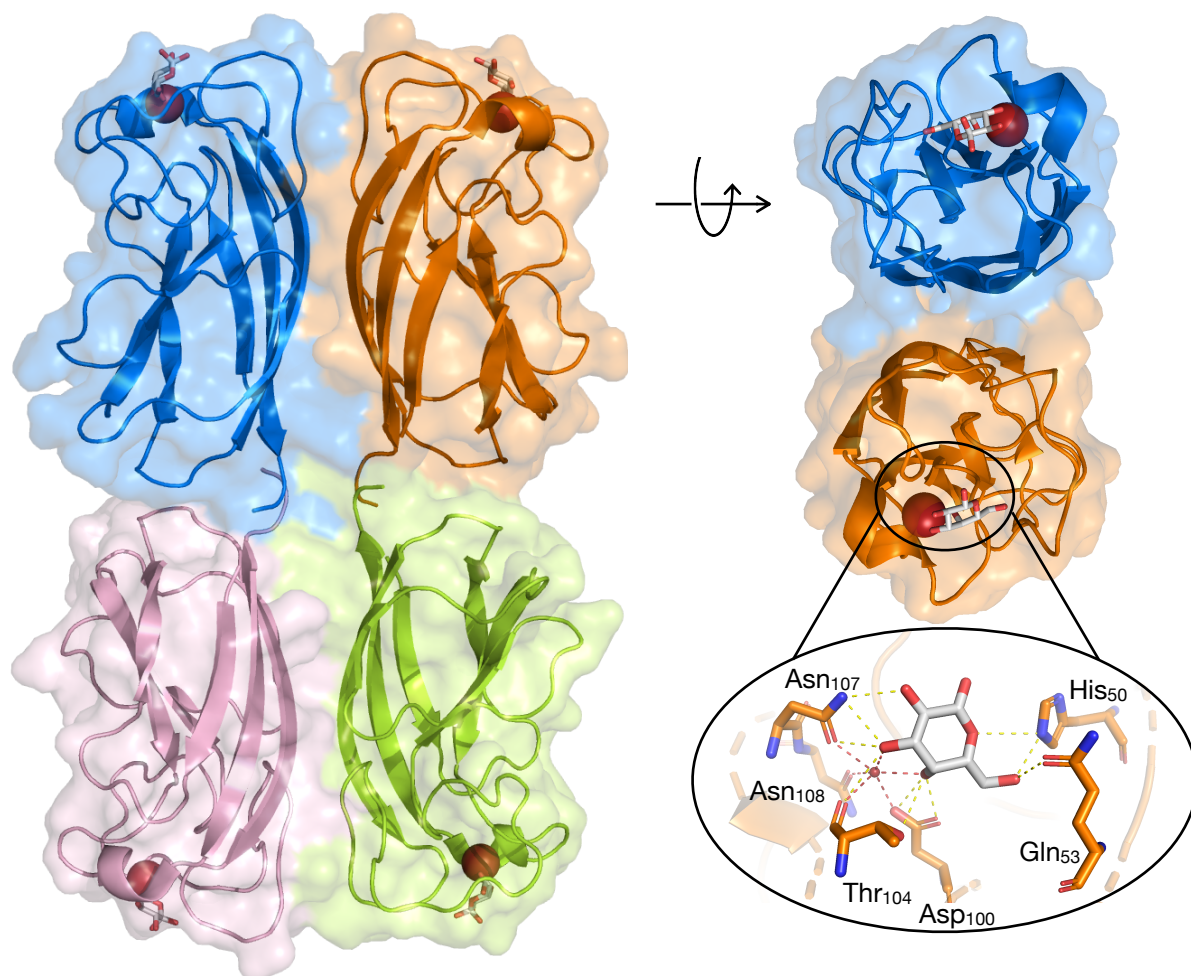


Figure 1. Co-crystal structure of homotetrameric *P. aeruginosa* lectin LecA (PDB code 1OKO) in complex with D-galactose (grey). Ca²⁺-ion (red) binds C3- and C4-hydroxy groups of D-galactose. Representation as cartoon, coloured by chain.

Carbohydrate-binding proteins beyond antibodies and without enzymatic activity are called lectins. LecA is a homotetramer (121 aa, 12.8 kDa, per monomer) and binds to D-galactose and D-galactosamine, however with decreased affinity. The galactose-binding sites each depend on a single calcium(II)-ion, chelated by the galactose C3- and C4-hydroxy groups upon binding (figure 1). The affinity of LecA towards galactosides is in the micromolar range and can be improved by the introduction of aromatic aglycons in the β -position.^[29] Due to the shallow binding side of LecA, the SAR towards monovalent ligands is rather flat. However, the relative presentation of the four LecA-monomers in the quaternary structure allows the design of highly potent divalent inhibitors, in particular for simultaneous binding to two adjacent monomers.^[30]

LecB (114 aa, 11.7 kDa) also forms tetramers in solution and binds to L-fucosides and D-mannosides. In contrast to LecA, each carbohydrate-binding site contains two calcium(II)-ions that coordinate their ligands by their C2-, C3- and C4- hydroxy groups (figure 2). The affinity of LecB to monovalent fucosides can reach up to sub-micromolar ranges (e.g. K_d of Me- α -L-fucoside is 430 nM and 202 nM for LecB_{PAO1} and LecB_{PA14}, respectively^[28]). In contrast to LecA, a detailed SAR has been described for LecB-inhibitors.^[31] As described above, the sequence of LecB varies within clinical isolates.^[28] In general, PA14-like homologs show two- to three-fold lower binding constants compared to LecB from PAO1-like strains (vide supra). For LecB, the carbohydrate-binding sites of the individual monomers are slightly tilted. As a result, the design of divalent inhibitors is not straight forward.

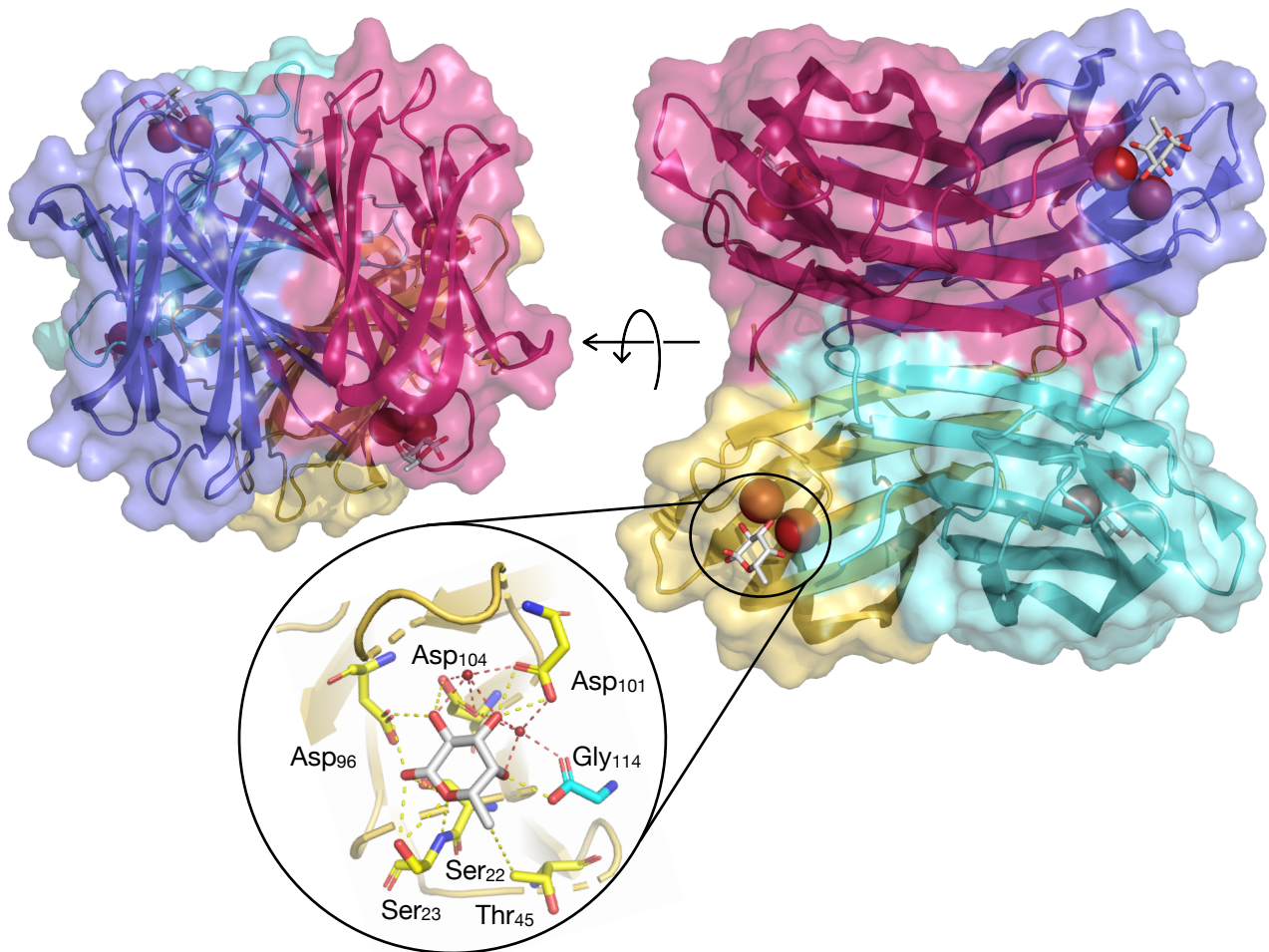


Figure 2: Co-crystal structure (PDB code 1OCX) of homotetrameric *P. aeruginosa* lectin LecB in complex with ligand L-fucose (grey). Ca^{2+} -ions (red) bind C2-, C3- and C4-hydroxy groups of L-fucose. Representation as cartoon, coloured by chain.

The intrinsically low monovalent binding affinity of LecA and LecB is compensated by multivalency. Both proteins can bind up to four ligands at once, which leads to high avidity, a common trick in nature to achieve receptor-ligand systems with 'variable' binding affinity (more details in chapter 1.2). Psl is a ligand of LecB and it is believed that LecB retains Psl within the biofilm matrix.^[32] Although LecA binds to galactosides (and also weakly to glucosides), it is not fully understood if it binds to Pel, Psl or both.^[33] However, our working hypothesis is that LecA and LecB act as biofilm-stabilisers by crosslinking glycans within the biofilm matrix. Further, they can also bind to glycosides presented on host and bacterial cell membranes.^[34]

Both lectins are also involved in the infection process. The glycosphingolipid Gb3 is decorated with the trisaccharide Gal α (1 \rightarrow 4)Gal β (1 \rightarrow 4)Glc β and is presented on various mammalian cells.^[35, 36] It is involved in LecA-mediated cell adhesion of *P. aeruginosa* on human lung epithelial cells. Further, it has been shown that binding of Gb3 by LecA triggers host cell invasion and host cell signalling.^[37, 38]

LecB binds glycosylated integrins on the basolateral side of human cells and causes integrin internalisation, leading to cell depolarisation. Internalisation of β 1-integrin could be associated with LecB-mediated inhibition of wound healing (figure 3).^[39] In cystic fibrosis patients, LecB impairs mucus transport by inhibition of lung ciliary beating.^[40] Interestingly, the effects described above can be inhibited by addition of the LecB-inhibitor L-Fuc, pronouncing the role of LecB-inhibitors as pathoblockers.

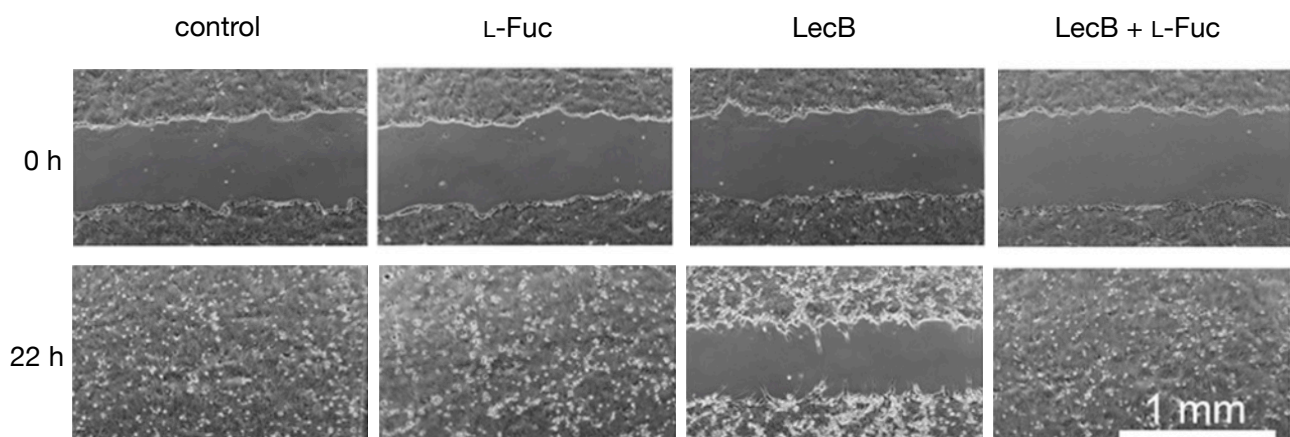


Figure 3. LecB inhibits epithelial wound healing. Polarised monolayers of MDCK cells were wounded with a pipette tip. Wound closure was observed with a wide-field microscope. Wound healing reduced by LecB can be restored by addition of L-fuc. Adapted from Thuenauer *et al.*^[39]

1.2. Lectin Antagonists in Infection, Immunity and Inflammation

Authors: Joscha Meiers, Eike Siebs, Eva Zahorska and Alexander Titz
(all authors contributed equally)

Published in: *Current Opinion in Chemical Biology* **2019**, 53, 51-67.

DOI: 10.1016/j.cbpa.2019.07.005

The references of this chapter are listed at the end of this chapter.



Lectin antagonists in infection, immunity, and inflammation

Joscha Meiers^{1,2,3,4}, Eike Siebs^{1,2,3,4}, Eva Zahorska^{1,2,3,4} and Alexander Titz^{1,2,3}



Lectins are proteins found in all domains of life with a plethora of biological functions, especially in the infection process, immune response, and inflammation. Targeting these carbohydrate-binding proteins is challenged by the fact that usually low affinity interactions between lectin and glycoconjugate are observed. Nature often circumvents this process through multivalent display of ligand and lectin. Consequently, the vast majority of synthetic antagonists are multivalently displayed native carbohydrates. At the cost of disadvantageous pharmacokinetic properties and possibly a reduced selectivity for the target lectin, the molecules usually possess very high affinities to the respective lectin through ligand epitope avidity. Recent developments include the advent of glycomimetic or allosteric small molecule inhibitors for this important protein class and their use in chemical biology and drug research. This evolution has culminated in the transition of the small molecule GMI-1070 into clinical phase III. In this opinion article, an overview of the most important developments of lectin antagonists in the last two decades with a focus on the last five years is given.

Addresses

¹Chemical Biology of Carbohydrates, Helmholtz Institute for Pharmaceutical Research Saarland (HIPS), Helmholtz Centre for Infection Research, D-66123 Saarbrücken, Germany

²Deutsches Zentrum für Infektionsforschung (DZIF), Standort Hannover-Braunschweig, Germany

³Department of Pharmacy, Saarland University, D-66123 Saarbrücken, Germany

Corresponding author: Titz, Alexander (alexander.titz@helmholtz-hzi.de)

⁴These authors contributed equally.

Current Opinion in Chemical Biology 2019, **53**:51–67

This review comes from a themed issue on **Mechanistic biology**

Edited by **Hermen S Overkleef** and **David J Vocadlo**

<https://doi.org/10.1016/j.cbpa.2019.07.005>

1367-5931/© 2019 Elsevier Ltd. All rights reserved.

Introduction

Lectins are a highly diverse family of proteins found in all domains of life [1,2]. Various folds and classes have been identified and the common functional feature is their specificity for carbohydrate ligands. These glycan-binding

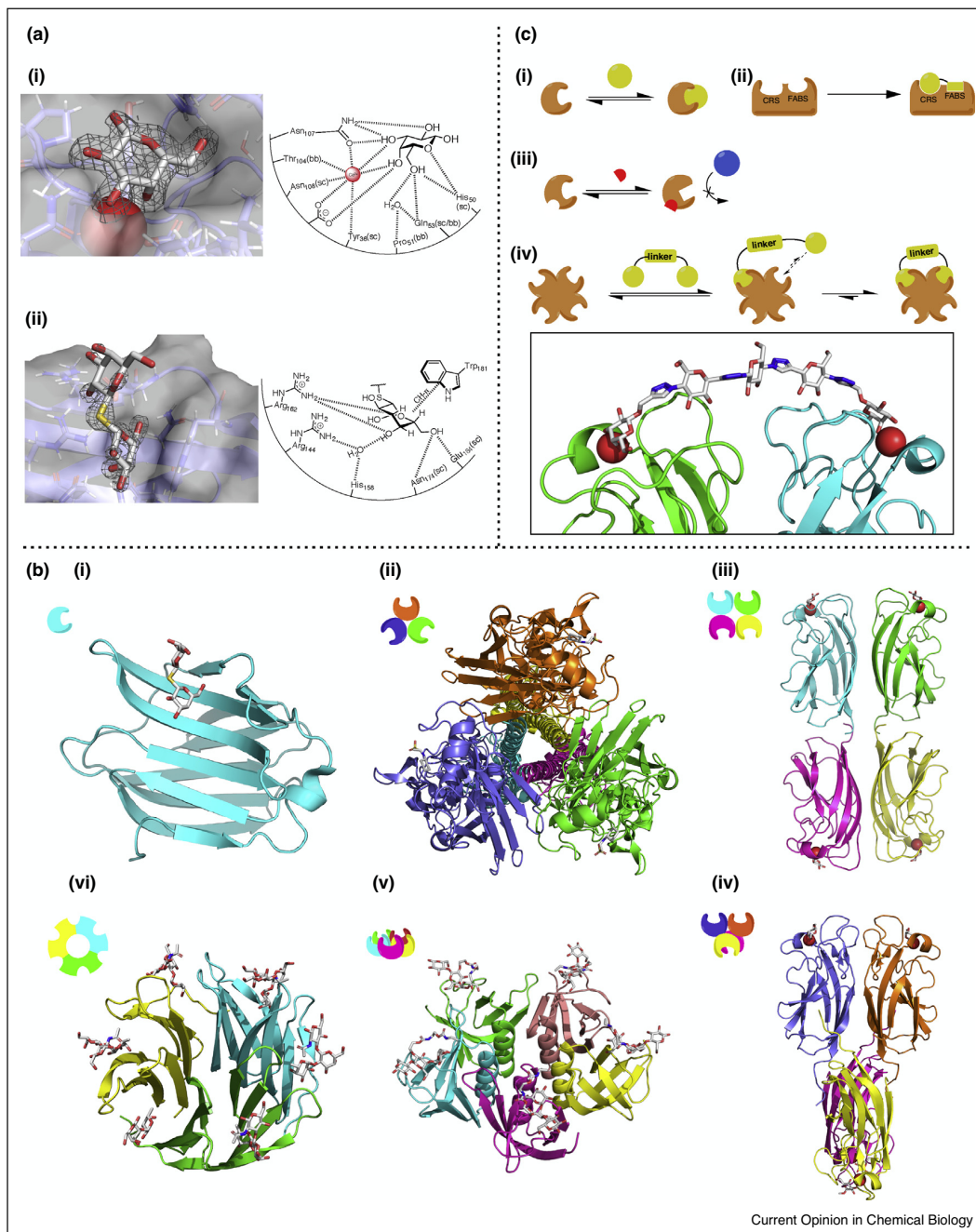
proteins have many important roles in infection, cell recognition, communication and various intracellular processes, such as protein folding and protein targeting.

Numerous viral, bacterial, fungal, and parasitic pathogens employ lectins for initiation and maintenance of an infection by adhering to surface-exposed glycoconjugates of their host organisms [3–5]. In contrast, the mammalian host has developed a plethora of lectin-containing pattern recognition receptors of the innate immune system recognizing glycan structures on intruders [6–8]. In addition to recognizing these non-self structures, other mammalian lectins bind to self-epitopes and thus mediate cell-recognition processes like inflammation and cancer metastasis [9–11].

The natural ligands of lectins are mostly bacterial or fungal polysaccharides, bacterial lipopolysaccharide and peptidoglycan, or eukaryotic glycoconjugates of lipids or proteins [1,12]. Except for bacteria which can have a high diversity among their monosaccharides, generally a relatively small set of different monosaccharide subunits are shared between animals, plants, fungi, parasites, bacteria, and other organisms. These building blocks are assembled into more diverse oligosaccharides where a very high complexity can be achieved due to many possible stereoisomers and regioisomers. In many cases, this leads to organism-specific oligosaccharides, which can then be recognized by innate immunity as non-self antigens and induce neutralization of the intruder [13], or elicit allergic reactions as observed for insect glycans, for example, in bee venom [14]. The opposite phenomenon that pathogen and host have identical glycoconjugates is also observed. The latter has been termed molecular mimicry or glycomimicry, a stealth process of the pathogen believed to be an evolutionary adaptation for evasion of immune surveillance of the host [15,16].

Despite the complexity of those oligosaccharide structures, lectins often recognize terminal monosaccharides or smaller oligosaccharides on a given glycoconjugate. Two common binding modes of carbohydrate ligands are shown in **Figure 1a**: (i) vicinal hydroxyl groups chelate a Ca^{2+} -ion present in the binding site, or (ii) carbon-bound hydrogen atoms of the carbohydrate ring interact via $\text{CH}-\pi$ stacking with aromatic amino acids in the binding site. Because of the recognition of rather small epitopes, common ligand specificity of different lectins with diverse functional roles often occurs. An example are

Figure 1



(a) Schematic representation of two important recognition modes of carbohydrates by lectins: (i) calcium-ion mediated binding of the ligands, example β -galactoside and LecA (PDB: 1OKO) (ii) tryptophan-mediated stacking on hydrophobic faces of carbohydrates, example galactoside with galectin-3 (PDB: 4JC1). **(b)** Various strategies for domain/binding site orientation: (i) monomeric in galectin-3 (4JC1), (ii) trimeric virus hemagglutinin (6CF5), (iii) tetrameric LecA (1OKO), (iv) tetrameric LecA ortholog PIIA with altered domain orientation (5ODU), (v) pentameric Shiga-like toxin B subunit (1QNU), (vi) trimeric BamBL containing 6 carbohydrate binding sites in and between subunits (3ZW2). **(c)** Schematic representation of different lectin inhibition approaches: (i) direct inhibition of carbohydrate binding sites, (ii) growing toward non-carbohydrate binding sites, (iii) allosteric inhibition (iv) multivalent inhibition which refers to clustered binding sites, either multivalent proteins or monovalent lectins clustering on cell membranes.

the functionally different human DC-SIGN and the bacterial lectin LecB with shared specificity for Lewis blood group antigens [17–19]. A large data set for the glycan specificity of many lectins using microarrays is provided by the Consortium for Functional Glycomics (see <http://www.functionalglycomics.org>).

Specificity of the lectins can be further tuned by recognizing functional groups attached to the essential carbohydrate, and, for example, lipids are recognized by a secondary site of the lectin Mincle [20,21], *O*-methylation is required for recognition by the tectonins [22,23], sulfates on nearby amino acids enhance binding of P-selectin to the Lewis-blood groups on glycoproteins [24] and phosphates are required for intracellular trafficking of proteins by the mannose-6-phosphate receptor [25].

Lastly, the spatial presentation of ligands and/or lectin's carbohydrate binding sites (Figure 1b), as well as clustering of several lectin protomers into oligomeric bundles or membrane embedded protein complexes can contribute significantly to specificity by augmentation of apparent binding affinity through avidity [7,26].

Carbohydrate specificity, requirements of additional functional groups and spatial presentation of binding sites are important aspects for the design and success of lectin-targeting probes in chemical biology and drug research. Therefore, the design of lectin antagonists usually follows various approaches from (i) competitive inhibition of a carbohydrate recognition site, (ii) targeting adjacent binding sites, (iii) allosteric inhibition, to (iv) multivalent competitive inhibition of two or more binding sites (Figure 1c).

Consequently, lectins have developed into attractive targets for chemical biology and medicinal chemistry over the past two decades [27,28]. Very active areas of research are the targeting of (i) lectins of pathogenic origin to interfere with mechanisms of infection by viruses and bacteria, and to a smaller extent also fungi and parasites, (ii) the selectins as a family of three closely related proteins crucial for cell migration in inflammation and cancer, as well as (iii) immunotherapeutic or immunomodulatory approaches for the mammalian lectins langerin in vaccine delivery, DC-SIGN in HIV infection or the galectins in cancer and immune modulation. Lectins discussed in this opinion article are summarized in Table 1.

Bacterial lectin antagonists

Bacterial antibiotic resistance is increasing worldwide at an alarming rate. As one consequence, antivirulence drugs have gained considerable research interest as alternative treatment approach with the aim to avoid the rapid onset of resistance [50]. In this context, the inhibition of bacterial lectins to prevent infection and persistence is a newly exploited strategy [3,27]. Targeting lectins involved in

the formation of bacterial biofilms are of particular interest since bacteria embedded in their self-produced biofilm matrix exhibit increased antimicrobial resistance compared to free floating planktonic bacteria. Biofilm-associated bacterial infections are responsible for a broad range of chronic/recurring diseases [51].

The Gram-negative bacterium *Escherichia coli* is the prime pathogen in urinary tract infections (UTIs) and important for intestinal infections as a consequence of Crohn's disease (CD). *E. coli* can build various organelles called pili and fimbriae which are oligomeric cell appendices built up of several proteins. These organelles are often employed for bacterial adhesion. The pilus or fimbria lectins FimH and FmlH, localized on the top of the different organelles, play decisive roles in host colonization, invasion, and biofilm formation [52]. Thus, inhibition of these lectins to antagonize infections presents a viable therapeutic strategy [53,54].

FimH is located on the tip of fimbriae and usually binds to mannosylated glycoconjugates in the bladder endothelium. Pathogenicity of *E. coli* clinical isolates expressing different *fimH* alleles varies, but the mannose binding pocket is invariant [52,55,56]. Hultgren's group demonstrated the activity of a high affinity mannoside FimH inhibitor against different uropathogenic *E. coli* strains [57]. In recent years, several research groups have been developing FimH antagonists for treatment of urinary tract infections and gut inflammations associated with CD. X-ray crystallography guided drug design focused on optimization of interactions with the so-called tyrosine gate adjacent to the mannose binding site. Introduction of aryl and alkyl aglycons increased the binding affinity significantly compared to simple mannose [58–60]. Nanomolar binding affinities were achieved by introducing biaryl aglycons that are tightly coordinated by the tyrosine gate [61–63]. High affinity biaryl mannosides were further optimized to increase metabolic stability by replacing the labile *O*-glycosidic bond with carbon-based linkers to the aglycon [29**,64]. Ester and phosphorylated prodrugs were successfully explored to improve oral bioavailability of both *O*-mannosides and *C*-mannosides [29**,65,66*]. Rational design and optimization of FimH antagonists are summarized in a recent review by Mydock-McGrane et al. [67]. The promising preclinical candidate **1** (EC₉₀ = 31 nM, Figure 2) is one example of a highly optimized FimH inhibitor with good metabolic stability and high efficacy in mouse models of acute and chronic UTI [29**]. Recent optimization attempts yielded thio-mannosides (e.g. **2**, EC₉₀ = 0.31 μM, Figure 2) with improved metabolic stability compared to respective *O*-mannosides, ability to inhibit biofilm formation *in vitro* and with a prophylactic effect in a mouse UTI model [30]. The first FimH antagonist entering clinical trials was EB8018 from Enterome (Paris, France) designed for the treatment of CD, but its structure has not been

| | Origin | Binding specificity | Key roles | Status of development/indicator |
|-----------------------------|--|---|---|---|
| Bacterial lectins | | | | |
| FimH | <i>E. coli</i> | Man | Adhesion, biofilm formation | Lead optimization (1, 2) [29*,30], EB8018 in Phase I clinical trials (www.clinicaltrials.gov , NCT03709628) |
| FmlH | <i>E. coli</i> | Gal, GalNAc | Adhesion, biofilm formation | Hit optimization (3) [31] |
| LecA | <i>P. aeruginosa</i> | Gal | Adhesion, biofilm formation | Exploratory studies |
| LecB | <i>P. aeruginosa</i> | Man, Fuc | Adhesion, biofilm formation | First covalent lectin inhibitor (5) [32**] Lead optimization (6, 7) [33,34**] |
| Shiga toxins | <i>S. dysenteriae</i> , <i>E. coli</i> | Gal, Glc | Toxin | Lead optimization on hold, First peptide-based inhibitor [35] |
| Cholera toxin | <i>V. cholerae</i> | Gal, Fuc | Toxin | Hit optimization (8) [36] |
| Viral Lectins | | | | |
| Hemagglutinin | Human influenza virus | Neu5Ac | Adhesion, cell entry | Hit optimization (12) [37–39] and exploratory studies (10, 11) [40*,41*,42**] |
| Hemagglutinin–neuraminidase | Human parainfluenza virus | Neu5Ac | Adhesion and detachment, cell entry | Hit optimization [43,44] |
| Capsid protein P domain | Norovirus | HBGAs | Adhesion, cell entry | Exploratory studies (14, citric acid) [45–47] |
| Mammalian Lectins | | | | |
| Langerin | Langerhans cells | Man, Fuc, GlcNAc, sulfated Gal, Glc | Immune response | Exploratory studies First allosteric mammalian lectin inhibitor (15) [48**] |
| DC-SIGN Selectins | Dendritic cells L-selectin: leukocytes P-selectin: platelets and endothelial cells E-Selectin: endothelial cells | Man, Fuc, GlcNAc sLe ^x P/L-selectins: Man, Gal and Sulfation [49] | Immune response Cell adhesion | Exploratory studies GMI-1070 (20) in Phase III clinical trials against vaso-occlusive anemia (www.clinicaltrials.gov , NCT02187003) |
| Mincle | Immune system | Glycolipids with terminal Glc or Man | Immune response | Exploratory studies |
| Galectin | Circulating proteins | Gal, for example, <i>N</i> -acetylglucosamine | Regulate cell death | TD139 (24) in Phase II clinical trials against idiopathic pulmonary fibrosis (www.clinicaltrials.gov , NCT03832946) |
| Siglecs | Immune-cells | Neu5Ac | Cell-cell signaling, immune response and adhesion | Exploratory studies |

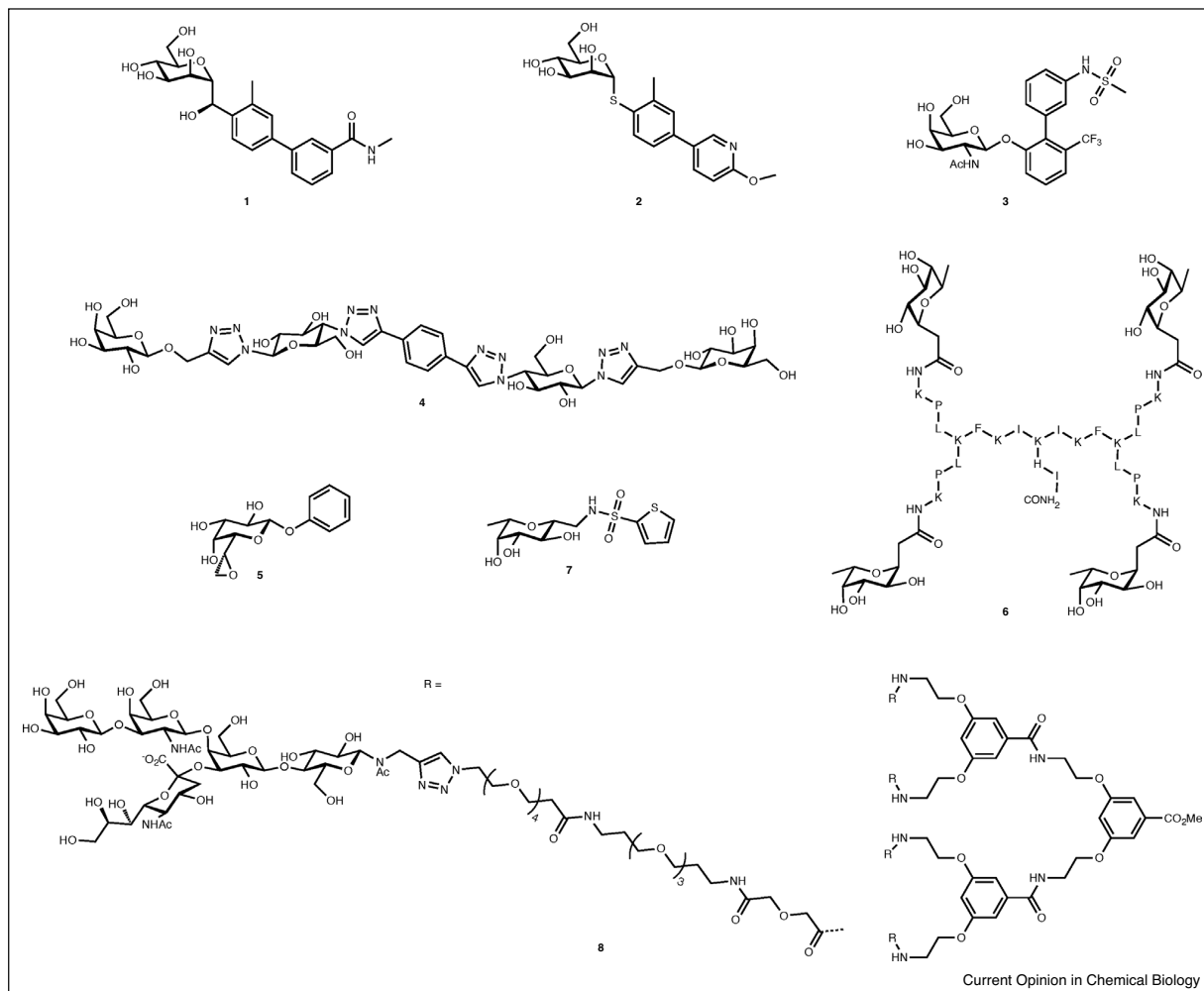
disclosed. In collaboration with Takeda, EB8018 has completed Phase Ia and the Phase Ib trial is ongoing in early 2019 (www.clinicaltrials.gov, NCT03709628). Furthermore, Fimbrion Therapeutics (St. Louis, MO) has announced the selection of a not further specified clinical candidate as antibiotic sparring molecule against UTIs in collaboration with GSK (www.fimbrion.com, press release Dec 06, 2018).

As a secondary target of uropathogenic *E. coli*, the FimH-like adhesin FmlH recognizes Gal(β1-3)GalNAc epitopes on bladder epithelium and enhances *E. coli* urinary tract colonization [54]. Recently, first structure-based inhibitor design approaches for FmlH have been reported [31,68**]. To date, the best FmlH inhibitor **3** (Figure 2) is based on *N*-acetyl galactosamine carrying a further substituted biphenyl aglycon and displays very high binding affinity (IC₅₀ = 34 nM), good aqueous solubility and high metabolic stability. Unfortunately, **3** showed

only low oral bioavailability in rats of less than 1% and further optimization is therefore mandatory [31,68**].

The opportunistic pathogen *Pseudomonas aeruginosa* has two soluble lectins, the extracellularly secreted proteins LecA (Figure 1) and LecB, both mediating bacterial virulence and being crucial components for biofilm formation [69–71]. Consequently, both proteins have been subject to intense research toward biofilm modulators and in drug discovery for antivirulence drugs [27,28,72–74]. LecA binds to various α-galactoside-terminating glycoconjugates with the glycosphingolipid Gb3 as proposed natural ligand [75]. This homotetrameric lectin was later shown to mediate bacterial uptake via Gb3 where it acts as a lipid zipper [76,77]. The affinity of LecA to galactose and simple glycosides thereof is rather weak in the 50–100 μM range. Consequently, development of LecA antagonists mainly focused on multivalent display of galactosides using many different linkers and maximizing

Figure 2



Inhibitors targeting lectins of pathogenic bacteria in *E. coli* (1-3), *P. aeruginosa* (4-7), and toxins of *V. cholerae* (8).

the number of presented epitopes [28,78]. Very potent tetravalent galactoclusters with low nanomolar binding affinities toward LecA have been developed [79^{**},80,81^{*},82,83]. In contrast to the high target-binding affinity, they showed only moderate inhibition of biofilm growth in the micromolar range *in vitro*.

The Pieters group has undertaken a different approach and focused on divalent galactosides oriented in a perfect manner to bridge two adjacent binding sites in the LecA tetramer. Several highly potent divalent inhibitors with the rigid spacers consisting of glucose and triazole groups were obtained, including the most potent LecA inhibitor reported so far with a K_d of 12 nM (4, Figure 2) [84^{**},85]. Again, recent optimization of these highly potent molecules on the target revealed a need for additional

multimerization and rather high micromolar concentrations for biofilm blocking [82,86].

Monovalent galactose-derived ligands with binding affinities in low micromolar range could be obtained after introduction of a β -aryl aglycon which establishes a π -stacking interaction with an imidazole-CH of His50 adjacent to the carbohydrate binding site (Figure 1a) [87^{**},88,89]. However, the specificity for further variations appears relaxed and changing substituents at the phenyl aglycon did not lead to significant potency improvements. As an alternative approach to the generally employed glycosides of unmodified galactose residues in LecA ligands, we have embarked on the modification of the galactose residue itself. A cysteine residue in the carbohydrate binding site of LecA was targeted with

the aim to develop a covalent lectin inhibitor using a small electrophilic headgroup in a modified galactose [32^{••}]. Despite the fact that covalent inhibitors are widespread for many other protein classes, epoxide **5** (Figure 2) was established as the first-in-class covalent lectin inhibitor. Because of its moderate affinity toward LecA ($IC_{50} = 64 \mu\text{M}$), the molecule was converted into a tool compound after synthetic derivatization and conjugation to fluorescein enabling the visualization of *P. aeruginosa* biofilm aggregates by confocal fluorescence microscopy [32^{••}].

The second *P. aeruginosa* lectin LecB also forms a homotetrameric quaternary structure, binds broadly to fucosides and mannosides and the highest affinity was determined for Lewis blood group antigens [17,90]. In contrast to LecA, the protein sequence of LecB varies among clinical isolates and two important types occurring in the clinical isolates PAO1 and PA14 have been identified as representative for all studied isolates [18,91]. Despite the observed amino acid sequence differences in LecB between strains, its carbohydrate binding specificity is conserved, underpinning the suitability of LecB as a drug target with conserved specificity among all isolates. Also for LecB, multivalent inhibitors have been the first choice for inhibition [28,78]. However, because of a sterically more distant and less favorable orientation of binding sites in LecB compared to LecA, the obtained multivalent ligands could not achieve a comparable boost in affinity. Nevertheless, two types of multivalent ligands carrying fucosides stand out of the very broad field: tetravalent glycopeptide dendrimer **6** ($IC_{50} = 140 \text{ nM}$, Figure 2) was able to efficiently prevent biofilm formation of *P. aeruginosa* at a concentration of $20 \mu\text{M}$ *in vitro*; [33] furthermore, a calixarene carrying four fucose residues was tested in an infection model in mice [79^{••}]. This compound significantly reduced the number of bacteria colonizing lung and spleen, but was unable to inhibit bacterial biofilms *in vitro* at a concentration of $100 \mu\text{M}$ despite its high affinity at the target ($K_d = 48 \text{ nM}$).

To overcome the intrinsic disadvantages associated with large molecules and multidirectional valency in biofilm formation, we have used the small molecule LecB ligand mannose as a starting point for the rational design of monovalent biofilm targeting glycomimetics [92]. These compounds exhibited rather good target-binding potency ($K_d = 3\text{--}20 \mu\text{M}$) and prevented bacterial adhesion to a glycosylated surface at $100 \mu\text{M}$. Further optimization [93] and removal of the anomeric center [94] finally yielded C-glycosidic inhibitors of LecB (e.g. **7**, Figure 2) with good target-binding potency ($K_d = 290 \text{ nM}$) and very long receptor residence times ($t_{1/2} = 28 \text{ min}$) [34^{••}]. Glycomimetic **7** showed approx. 85% inhibition of biofilm growth *in vitro* at $100 \mu\text{M}$, which contrasts the lack of antibiofilm activity of the natural LecB binder methyl α -L-fucoside, despite its very high target binding affinity ($K_d = 430 \text{ nM}$). Furthermore, glycomimetic **7** is orally

bioavailable which is not possible for large multivalent molecules.

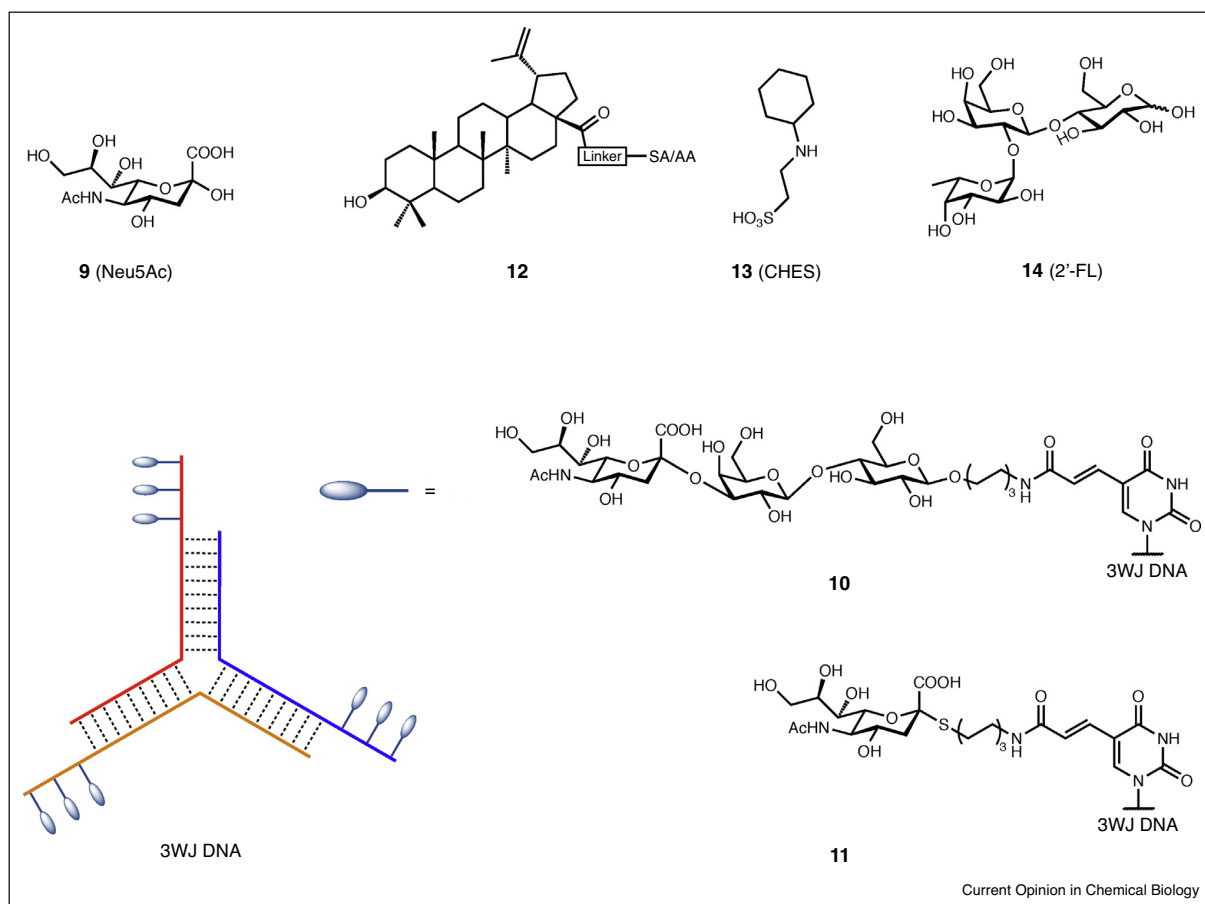
Shiga and cholera toxins are bacterial proteins responsible for severe symptoms in gastrointestinal infections. These so-called AB₅ toxins consist of one catalytic A-subunit and five lectin-like B-subunits (Figure 1b) which are responsible for the binding of the complex to the host cell surface in the gut. Inhibition of the B-subunits and thereby preventing adhesion is a potential treatment strategy [95].

Shiga toxins (Stxs) are produced by *Shigella dysenteriae* and some enteropathogenic *E. coli* strains, for example, enterohemorrhagic *E. coli* (EHEC). Kitov *et al.* designed the pentavalent ligand STARFISH to match the carbohydrate binding sites of the five B-subunits with subnanomolar inhibitory activity against Shiga-like toxins I and II (Stx1 and Stx2) [96]. A modified version of STARFISH, called DAISY, improved the *in vivo* activity and provided full protection against the toxins when administered simultaneously in a mouse model despite its lower target-binding potency [97]. However, further development of DAISY-based inhibitors appears halted (no further publications) since the compound proved ineffective in a treatment scenario, that is, drug administration after infecting mice with the Shiga toxin producing strain *E. coli* O91:H21. Nishikawa *et al.* designed a series of carbosilane dendrimers called SUPERTWIG. The most potent compound of the series was able to completely neutralize Stxs in the blood stream and protect mice against a fatal dose of the Shiga toxin producing strain *E. coli* O157:H7 even when administered after establishment of infection [98]. The rather complex synthesis of multivalent-trisaccharide inhibitors is hindering further clinical development.

From a peptide library, the branched proline and arginine rich high molecular weight peptide Ac-PPP-tet was identified to bind to Stx2 B-subunit and inhibit Stx2 cytotoxicity [35]. This peptide affects the intracellular transport of Stx2 and protected mice from a fatal dose of *E. coli* O157:H7 even when administered after an established infection; this molecule further protected rabbit intestines *ex vivo* against the toxic effect of Stx2 [35,99]. Recent efforts include the synthesis of sugar-amino acid hybrid polymers with highly clustered globotriaosyl residues that showed low micromolar affinities to both Stxs with the ability to neutralize the toxic effects on Vero cells [100].

Vibrio cholerae produces cholera toxin where each B-subunit (CTB) has two binding sites – one primary binding site recognized by the ganglioside GM₁ and a secondary low affinity site recognized by fucosylated glycans [101]. A number of derivatives mimicking the terminal galactose from GM₁ has been screened and m-nitrophenyl α -D-galactoside and 3,5-disubstituted phenylgalactosides were identified as monovalent CTB inhibitors [102,103]. Numerous multivalent inhibitors targeting the primary

Figure 3



Inhibitors of influenza hemagglutinin: Neu5Ac (**9**), macromolecular sialylated three way junctioned DNA **10** and **11** and small molecules **12-13**; or, Norovirus spike protein can be blocked using the trisaccharide 2'-fucosyl lactose **14**. SA: sialic acid, AA: ascorbic acid.

site with down to picomolar binding affinities (e.g. **8**, $IC_{50} = 34 \text{ pM}$, Figure 2) [36] have been developed and were summarized in a recent review by Kumar and Turnbull [104]. Targeting the fucose binding site as new strategy was published by Wands *et al.* who reported inhibition of CTB binding to cell surfaces with 2'-fucosyllactose and a fucosylated polymer [105**].

Viral lectin inhibitors

Viral infections are difficult to treat, control and prevent. Frequent antigen variation, for which the influenza virus is a perfect example, prevents efficient protection and virus clearance by the human immune system. In many viruses, lectin-carbohydrate interactions are crucial for an efficient infection of the host. Hemagglutinin is the sialic acid binding lectin on the surface of the influenza viral envelope and plays a key role in the host cell-virus interaction. Sialic acids are defined as a family of acidic sugars with a nine

carbon atom backbone and the most abundant member found in vertebrates is *N*-acetyl neuraminic acid (**9**, Neu5Ac, Figure 3) [106]. Because the binding interaction of one monomeric hemagglutinin to sialylated glycans is weak ($K_d > 1 \text{ mM}$) [107], trimerization of hemagglutinin on the viral envelope and a high sialic acid density on the host cell lead to an increased avidity. This binding event then triggers the internalization of the virus by endocytosis [108]. Therefore, inhibition of the hemagglutinin-sialic acid interaction could yield prophylactic as well as therapeutic treatments of an influenza virus infection.

For this purpose, Strauch *et al.* [42**] developed a trimeric influenza neutralizing protein, targeting the hemagglutinin receptor binding site. This protein was designed to mimic the key interactions of broadly neutralizing antibodies and its optimization led to a highly avid protein with a trimeric binding mode and nanomolar apparent K_d

values. *In vivo*, using an H3 HK68 influenza infection mouse model, prophylactic and therapeutic treatment significantly protected mice from establishing disease and weight loss. Unfortunately, this designed protein does not show broad spectrum activity since it does not bind to the pathogenic ‘bird flu’ subtype H5N1. Limitations in high scale production and price, together with challenging pharmacokinetic properties will impact on its commercial use as an anti-influenza drug.

A recent review by Li *et al.* describes a wide range of chemical scaffolds and strategies to inhibit the hemagglutinin – host cell interaction. Mostly, trimeric sialosides are presented as binders to the receptor binding site [109].

2,3-Sialyllactose (2,3-SL) conjugated to three way junction (3WJ) DNA, with each DNA strand presenting one, three or five 2,3-SL molecules complementary to the hemagglutinin trimer geometry was reported by Yamabe *et al.* [40,41]. Hemagglutinin inhibition revealed 3WJ DNA with three sialic acid residues per arm in compound **10** as best inhibitor with a $K_i = 0.25 \mu\text{M}$, which corresponds to an 80 000-fold increase compared to monomeric 2,3-SL and an eightfold increase compared to 3WJ DNA with only one sialic acid per strand. Surprisingly, 3WJ DNA presenting five sialic acid per strand led to a reduction in activity ($K_i^{\text{HAI}} > 4.0 \mu\text{M}$) which probably originates from an altered orientation of the carbohydrate epitopes induced by steric hindrance. In contrast to the neuraminidase labile *O*-linked **10**, the more stable thio-linked sialic acid derivative **11** was synthesized as a follow up. For **11**, an increased stability toward influenza neuraminidase present on the viral envelope was observed, while its activity was retained. However, in presence of the full virus both derivatives, that is, *O*-glycoside and *S*-glycoside, were stable under the conditions tested. Another approach using a macromolecular scaffold by Nagao *et al.* yielded a trimeric star-shaped glycopolymer presenting 6'-sialyllactose on each of the three arms, synthesized by reversible addition-fragmentation chain transfer polymerization [110]. The degree of polymerization dictated the length of each arm. Hemagglutinin inhibition clearly depended on the arm-length, resulting in a $K_i = 21 \mu\text{M}$ for their best glycopolymer.

Conjugation of sialic acid or ascorbic acid derivatives onto pentacyclic triterpenes by Zhou and co-workers [37,38] was inspired by the broad antiviral activity of *Dipsacus asperoides* triterpenes and the corresponding synthetic leads [39]. In both cases, conjugation to betulinic acid as in **12** led to a strong reduction of infection by influenza A/WSN/33 in MDCK cells. Cytotoxicity of the triterpenes was also reduced by conjugation to sialic acid or ascorbic acid and a hemagglutination assay and SPR experiments with immobilized hemagglutinin suggested hemagglutinin as the putative target ($K_d = 17 \mu\text{M}$ for the sialic acid conjugate, $K_d = 8.0 \mu\text{M}$ for the ascorbic acid conjugate). Interestingly, the synthetic 2,3-di-*O*-benzyl

ascorbic acid intermediate showed a higher affinity for hemagglutinin ($K_d = 3.78 \mu\text{M}$) and improved inhibition of viral plaque formation (IC_{50} 's of $8.7 \mu\text{M}$ versus $41.3 \mu\text{M}$).

Small molecules possess superior pharmacokinetic properties for drug development than the rather large structures described above. Kadam and Wilson [111] identified the common buffer molecule CHES (**13**) by X-ray crystallography in complex with hemagglutinin. The molecule's binding mode with hemagglutinin mimics the one of sialic acid and its sulfonic acid superimposes with the carboxylate of sialic acid in the complex. Furthermore, the cyclohexyl moiety of CHES forms a CH- π interaction with W153 of hemagglutinin which is normally established by the *N*-acetyl group of sialic acid. As binding of CHES, although in slightly different binding modes, was confirmed for H3-hemagglutinin and H5-hemagglutinin, Kadam and Wilson proposed this non-carbohydrate molecule as a starting point for fragment growing to overcome its very low affinity ($K_d > 20 \text{mM}$) in the discovery of new types of hemagglutinin inhibitors.

The human parainfluenza virus causes respiratory tract diseases in children and elderly patients. In contrast to other influenza viruses, its multifunctional hemagglutinin–neuraminidase protein possesses both receptor-binding (hemagglutinin-function) and receptor-processing (neuraminidase-function) functionalities in one binding site [112]. Usually, lectins are defined as carbohydrate binding proteins without catalytic activity. However, this multifunctionality makes this parainfluenza virus protein an interesting topic for this review. Von Itzstein and co-workers synthesized a set of enzymatic intermediate-like *N*-acylated Neu-2-en and substrate-like *N*-acylated 2,3-difluoro-Neu derivatives to block both functionalities with a single molecule [43,44]. Especially the *N*-isobutyramido Neu-2-en derivatives showed potent hemagglutinin inhibition ($\text{IC}_{50} = 1.15 \mu\text{M}$) as well as inhibition of neuraminidase activity and virus growth.

Norovirus, a worldwide cause of mild to severe acute gastroenteritis, can lead to life-threatening infections for pediatric and geriatric patients and outbreaks, especially in day care centers or nursing homes, which are particularly problematic. To date, therapy of norovirus infections is only supportive and limited to reversal of dehydration and loss of electrolytes [113]. Thus, to control and prevent outbreaks, new drugs are needed. The human norovirus capsid protein P domain interacts with human blood group antigens (HBGA) and plays an important role in infection [114]. This virus–host interaction can be blocked by human milk oligosaccharides such as 2'-fucosyl lactose (**14**, 2'-FL) as shown by Hansman and co-workers [45,46]. The very high concentrations of 2'-FL needed to inhibit the interaction of virus like particles with HBGA *in vitro* ($\text{IC}_{50} = 13\text{--}50 \text{mM}$), could be achieved because of the low toxicity of 2'-FL, its

metabolic stability and low gastrointestinal absorption [115]. Indeed, 2'-FL is a major constituent of human milk with a concentration in the mM range and has been postulated to prevent infections in breast-fed newborns [116]. Another commonly used and safe food supplement, citrate, was shown to bind norovirus in a HBGA-like manner [47].

Mammalian lectin antagonists

There are numerous mammalian lectins and the three important classes, siglecs, galectins and the C-type lectins, are currently addressed in chemical biology and medicinal chemistry. Sialic acid-binding immonoglobulin-like lectins, siglecs, are cell-surface receptors, mainly expressed by cells of the immune system. They are involved in various processes ranging from self-/non-self discrimination to regulating inflammation caused by damage-associated or pathogen-associated molecular patterns (DAMP/PAMP) [117,118]. Galectins, a family of soluble secreted lectins with 14 members, generally bind to β -galactosides [119]. Their functions are diverse and comprise mediation of cell-cell interactions, cell-matrix adhesion and transmembrane signaling [120–122]. C-type lectins are the largest and most diverse lectin family which share a conserved protein fold. The name giving Ca^{2+} -ion present in all carbohydrate recognizing family members directly mediates the binding to the glycan ligand [7]. Only a few examples exist for which Ca^{2+} is dispensable for carbohydrate recognition with dectin-1 being the most prominent example. The C-type lectin receptor family in mammals contains 17 members and many are part of innate immunity [123,124].

Langerin, DC-SIGN

All cells of the innate immune system express a variety of pattern recognition receptors (PRR) such as toll-like receptors, NOD-like receptors and C-type lectin receptors, which allow the orchestration of an appropriate biological response to an incoming microbial threat. These PRRs are specialized to recognize PAMPs such as bacterial cell wall structures, fungal polysaccharides, the viral envelope and foreign RNA/DNA [127,128]. The signaling cascades initiated by these recognition events as well as the antigen uptake and processing pathways eventually lead to activation of cells of the adaptive immune system and hence are central elements bridging these two arms of immunity. For example, PAMPs recognized and processed by dendritic cells can lead to differentiation of CD4^+ -cells into T-helper cells [123,126]. Important C-type lectin receptors are langerin, DC-SIGN and dectin-1 [123].

The homotrimeric protein langerin is expressed on Langerhans cells in epithelial and mucosal tissues and binds to D-mannose, L-fucose, and D-GlcNAc as well as sulfated D-galactose. Langerin mediates the uptake of *Yersinia pestis* and influenza A virus amongst others in host infection [7,8]. Capitalizing on these carbohydrate-mediated

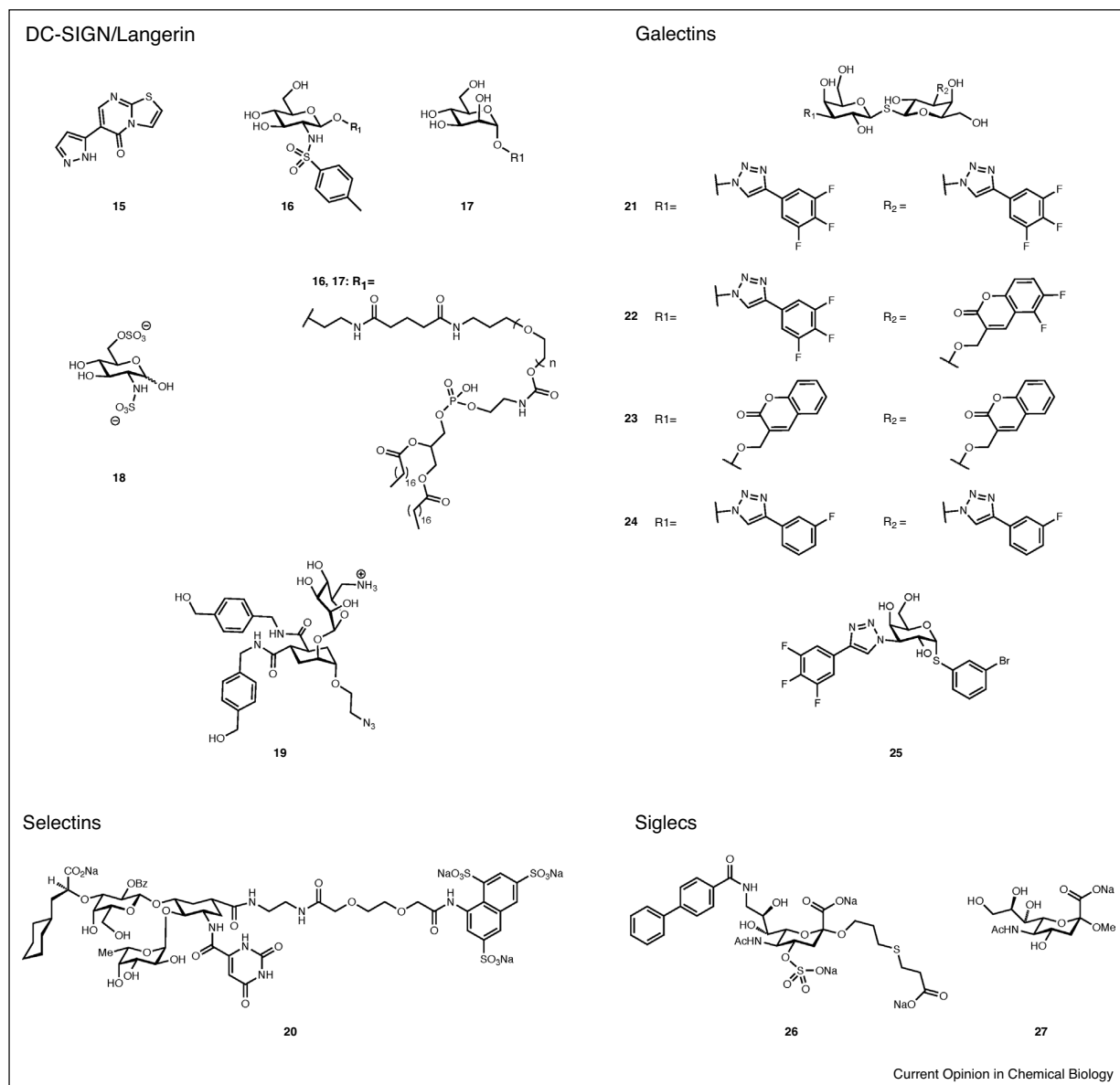
antigen uptake and processing pathways, langerin has also been described as an attractive target for targeted drug-delivery approaches to Langerhans cells [129,130]. This raised the interest in specific langerin ligands and, for example, Aretz *et al.* reported the discovery of thiazolopyrimidines as murine langerin antagonists, revealing the first allosteric inhibition of a mammalian lectin [48**]. Optimization of the initial hit **15** (Figure 4) was found beneficial at position 6 and led to up to 10-fold lower K_d and IC_{50} -values (K_d (**15**) = 0.7 mM; IC_{50} = 0.6 mM). Overall, a large series of langerin inhibitors was presented with IC_{50} values ranging in the two digit micromolar range.

Furthermore, it is well known that langerin has high affinity for sulfated polysaccharides or large oligosaccharides, for example, heparin ($K_d = \sim 2.4$ nM). As the binding affinity is electrostatically driven, no binding was detected with pH values below 4 or at high salt concentrations above 0.5 M [131]. A screening for langerin binding molecules revealed a sulfonamide of glucosamine as weakly binding langerin ligand [132**,133**]. Considering this screening hit, the modified phospholipids **16** and **17** were synthesized with the aim to produce glycomimetic modified liposomes for langerin targeting. These were tested against Langerin⁺, DC-SIGN⁺ or Dectin-1⁺ Raji cells. Liposomes consisting of mannosylated phospholipid **17** bound specifically to DC-SIGN⁺ cells and those consisting of sulfonamide **16** specifically to Langerin⁺ cells. Intracellular trafficking of the langerin targeting liposomes consisting of **16** was then observed in Langerin⁺ COS-7 cells by confocal microscopy.

Tetrameric DC-SIGN is expressed by myeloid dendritic cells and macrophages. Since DC-SIGN shares the same EPN amino acid motif with langerin, both proteins recognize similar monosaccharide ligands. While langerin was reported to be protective against HIV infections [134], DC-SIGN promotes viral dissemination via a process called *trans*-infection. Targeting DC-SIGN is therefore of interest to stop the transmission of HIV [135].

One common approach to increase affinity for DC-SIGN is the multivalent presentation of monosaccharide ligands. Following such an avidity-driven strategy, a dodecavalent fuco-dendrimer with a 420-fold potency increase compared to fucose was reported [136]. However, unspecific binding to langerin due to its similar binding specificity imposes a selectivity issue. GlcNAc is recognized by both C-type lectins but sulfation of position six and replacement of the *N*-acetyl group by a *N*-sulfate led to a favored recognition of the negatively charged compound **18** by langerin [125*]. The development of positively charged amino species in the pseudo-1,2-mannobioside **19** favored the selectivity toward DC-SIGN ($\text{IC}_{50} = 254 \mu\text{M}$; (langerin $\text{IC}_{50} > 4400 \mu\text{M}$) [125*]. Pseudo-1,2-mannobiosides were shown to bind to the carbohydrate recognition domain in DC-SIGN using X-ray crystallography [137]. As an alternative approach to

Figure 4



Allosteric (**15**) and carbohydrate-binding site directed (**16-27**) mammalian lectin antagonists.

generate specificity, a recent report highlighted the presence of five secondary binding sites on DC-SIGN. These sites recognize drug-like compounds unrelated to carbohydrates, and hence constitute a potential starting point for future development [138*].

Dectin-1, a mammalian lectin of the innate immune system, recognizes β -glucans found on fungal cell walls and is able to function as a PRR in fungal-infection [124]. Liposomes carrying the currently used antifungal drug

amphotericin B intercalated into the lipid membrane reduce the antifungal's toxicity compared to detergent-solubilized drugs. Coating of these liposomes with dectin-1 for the specific targeting toward fungal cells showed a 200-fold higher affinity to those cells than untargeted liposomes [139]. These dectin-modified delivery vehicles also reduced growth and viability of the mold *Aspergillus fumigatus* with higher efficiency and thus provide a new opportunity to fight those resistant and difficult to treat infections.

Selectins

Selectins are a subfamily of the C-type lectins consisting of three single-chain transmembrane glycoproteins, which are found on endothelial cells (E-selectin or CD62E), leukocytes (L-selectin or CD62L) and platelets (P-selectin or CD62P). They are involved in constitutive lymphocyte homing, chronic and acute inflammation processes and their minimal common binding epitope is the blood group antigen sialyl Lewis X (sLe^x). [140]

In accordance with the bioactive conformation of the tetrasaccharide sLe^x for E-selectin, this carbohydrate lead was successively optimized in a series of papers from Ernst and co-workers [141–145]. NMR screening of fragments allowed the identification of a second site binder and upon merging with the first site sLe^x mimic, 30 nM lectin antagonists were obtained from a 1 mM lead [146]. Subsequent addressing of the additional sulfate-binding domain in P-selectins/L-selectins led to the successful pan-selectin antagonist Rivipansel (GMI-1070, **20**) out of the development program by Ernst and Magnani that started in the mid-1990s, despite the common fashion to drop selectin research in pharmaceutical industry in the early 2000s [147]. Since June 2015, Rivipansel is in clinical phase III studies against vaso-occlusive anemia in hospitalized subjects with sickle cell disease (trial end date: June 2019, clinicaltrials.gov Identifier: NCT02187003).

Mincle

Mincle has been identified as a C-type lectin receptor of the innate immune system with glycolipid binding specificity that plays an important role in infection by mycobacteria. Mincle binds the mycobacterial glycolipid trehalose dimycolate [20,21] and has recently been addressed by a number of groups describing synthetic molecules based on the bacterial glycolipid [148^{••},149,150,151].

Galectins

Galectin-3, the best described member of the galectin family, is involved in many biological processes, *inter alia*, cell growth, cell adhesion and apoptosis. Consequently, it plays an important role in many diseases, among them are cancer, inflammation, fibrosis, heart disease and stroke [152–154]. For that reason, galectin-3 became an important drug target, recently reviewed by Cagnoni *et al.* [11].

Symmetric C3-aryltriazolyl-substituted thiodigalactosides have shown high affinities for galectin-3 down to $K_d = 1\text{--}2$ nM. However, most of the compounds also bound to galectin-1 raising concerns about the specificity (e.g.: **21**, K_d (galectin-1) = 69 nM; K_d (galectin-3) = 2.3 nM). After combining C3 aryltriazolyl groups with O3-coumaryl groups into asymmetrical thiodigalactosides the selectivity toward galectin-3 increased: specificity of compound **22** toward galectin-3 was achieved with a high affinity (K_d (galectin-1) = 340 nM; K_d (galectin-3) = 7.5 nM) [155^{••}]. Dicumaryl digalactoside **23** (K_d (galectin-1) = 16 μ M; K_d (galectin-

3) = 91 nM) was then analyzed *in vivo* in mice against bleomycin-induced lung fibrosis. At a dose of 3.5 mg/kg of digalactoside **23** the fibrosis score could be reduced but no effect on the inflammatory score was observed [156]. TD139 (**24**) is a derivative of **21** with a single fluorine atom in *meta*-position of the phenyl rings which is in clinical trials phase II as a galectin-3 inhibitor in idiopathic pulmonary fibrosis since February 2019 using the pulmonary route of administration (www.clinicaltrials.gov, NCT03832946) [157,158]. Oral administration of these disaccharides is impeded by their poor membrane permeability. Currently, various research groups are optimizing this property and a new galectin-inhibitor class with only one sugar residue and low nanomolar affinity was discovered, for example, **25**, $K_d = 37$ nM [159].

Siglecs

A number of siglecs have attracted the attention in the past decades and several antibodies targeting siglecs are approved drugs or in clinical trials [160,161]. Many publications report the development of antagonists for siglec-4, also called myelin-associated glycoprotein (MAG) [162–164]. This protein is important for glial scar formation after central nervous system lesions and inhibition of MAG is considered one therapeutic approach to prevent scar formation and enable axonal regeneration [165,166].

Siglec-2 (CD22) is a target receptor in anti-cancer therapy of lymphoma, leukemia as well as in the treatment of autoimmune diseases such as lupus and rheumatoid arthritis [167]. Biphenylcarboxamidated sialic acid derivative **26** ($IC_{50} = 2$ nM) was developed with an over 500 000-fold stronger binding affinity compared to the minimal siglec ligand α Me-Neu5Ac (**27**, $IC_{50} = 1.5$ mM) against siglec-2 [168^{••}]. Despite the fact that this protein is a monomeric protein, divalent or trivalent *N*-glycans show a very high affinity in the low nM/high pM range. The group by Paulson suggest that this high affinity in their assays originates from simultaneous binding to several CD22 lectins clustering on the cell surface within 30–50 Å to each other [169^{••}].

Conclusions

Lectins are a large family of proteins that are present in each domain of life. These carbohydrate-binding proteins possess numerous functions, both intracellularly and outside the cell. Research toward lectin antagonists has developed rapidly over the past two decades focusing on lectins from selected fields, mainly related to immunity and infection involving mammalian lectins and those from pathogenic bacteria and viruses. The largest block of literature focusses on the assembly of native carbohydrates onto a plethora of different multivalent scaffolds. With some important exceptions discussed here, these publications usually center around the chemical synthesis and compounds are only evaluated in a target-binding assay and not employed further for questions of chemical biology and drug research.

However, in the last decade, a number of strategies toward glycomimetic lectin antagonists has been published that led to drug-like structures which proved equally useful in chemical biology research and early preclinical drug discovery. Antibacterial glycomimetic drugs applied alone or in combination with conventional antibiotics will provide new effective therapies for multi-resistant bacterial infections. And because of an increasing resistance toward established drugs and the absence of effective drugs against several, so far untreated viruses, viral lectins have become attractive targets in recent years and further research will likely yield new tools for chemical biology and drug therapy. Despite the intrinsic difficulty of developing probes/therapeutics for these low affinity carbohydrate–protein interactions, the field is developing rapidly and the first lectin antagonist currently in phase III clinical trials is GMI-1070 (20, Figure 4).

Many new lectins are being uncovered every year providing a large playground for new lectin antagonists for chemical biology and potentially as therapeutic targets. Lectins from other organisms, such as fungi or bacteria that are not pathogenic to humans are active areas of research. It will be interesting to probe, for example, fungal lectins [22,23,170,171] with a distinct specificity for methylated glycans or those of bacteria [172–174] that live in symbiosis with nematodes and kill invaded insects. Furthermore, a large number of bacterial adhesins in pathogenic bacteria are being uncovered, for example, the *Burkholderia* lectins [175–178] or carbohydrate binding adhesins from *Salmonella enterica* [179], and thus, there is a bright future for the chemical biology of lectin antagonists ahead.

Conflict of interest statement

Nothing declared.

Acknowledgements

The authors thank Dr. Christoph Rademacher for constructive comments on the manuscript. We further acknowledge funding by the Helmholtz Association (VH-NG-934).

References and recommended reading

Papers of particular interest, published within the period of review, have been highlighted as:

- of special interest
 - of outstanding interest
1. Cummings RD, Schnaar RL, Esko JD, Drickamer K, Taylor ME: **Principles of glycan recognition**. In *Essentials of Glycobiology*. Edited by Varki A, Cummings RD, Esko JD, Stanley P, Hart GW, Aebi M, Darvill AG, Kinoshita T, Packer NH, Prestegard JH, Schnaar RL, Seeberger PH. Cold Spring Harbor Laboratory Press; 2015.
 2. Lis H, Sharon N: **Lectins: carbohydrate-specific proteins that mediate cellular recognition**. *Chem Rev* 1998, **98**:637-674.
 3. Sharon N: **Carbohydrates as future anti-adhesion drugs for infectious diseases**. *Biochim Biophys Acta* 2006, **1760**:527-537.
 4. Rodrigues JA, Acosta-Serrano A, Aebi M, Ferguson MAJ, Routier FH, Schiller I, Soares S, Spencer D, Titz A, Wilson IBH, Izquierdo L: **Parasite glycobiology: a bittersweet symphony**. *PLoS Pathog* 2015, **11**:e1005169.
 5. Thompson AJ, de Vries RP, Paulson JC: **Virus recognition of glycan receptors**. *Curr Opin Virol* 2019, **34**:117-129.
 6. van Kooyk Y, Rabinovich GA: **Protein-glycan interactions in the control of innate and adaptive immune responses**. *Nat Immunol* 2008, **9**:593-601.
 7. Drickamer K, Taylor ME: **Recent insights into structures and functions of C-type lectins in the immune system**. *Curr Opin Struct Biol* 2015, **34**:26-34.
 8. Dam TK, Brewer CF: **Lectins as pattern recognition molecules: the effects of epitope density in innate immunity**. *Glycobiology* 2010, **20**:270-279.
 9. McEver RP: **Selectins: initiators of leucocyte adhesion and signalling at the vascular wall**. *Cardiovasc Res* 2015, **107**:331-339.
 10. Borsig L: **Selectins in cancer immunity**. *Glycobiology* 2018, **28**:648-655.
 11. Cagnoni AJ, Pérez Sáez JM, Rabinovich GA, Mariño KV: **Turning-off signaling by siglecs, selectins, and galectins: chemical inhibition of glycan-dependent interactions in cancer**. *Front Oncol* 2016, **6**:109.
 12. Varki A, Gagneux P: **Biological functions of glycans**. In *Essentials of Glycobiology*. Edited by Varki A, Cummings RD, Esko JD, Stanley P, Hart GW, Aebi M, Darvill AG, Kinoshita T, Packer NH, Prestegard JH, Schnaar RL, Seeberger PH. Cold Spring Harbor Laboratory Press; 2015.
 13. Fujita T: **Evolution of the lectin-complement pathway and its role in innate immunity**. *Nat Rev Immunol* 2002, **2**:346-353.
 14. Hoffmann-Sommergruber K, Paschinger K, Wilson IBH: **Glycomarkers in parasitic infections and allergy**. *Biochem Soc Trans* 2011, **39**:360-364.
 15. Moran AP: **Molecular mimicry of host glycosylated structures by bacteria**. In *Microbial Glycobiology*. Edited by Holst O, Brennan PJ, von Itzstein M. Academic Press; 2010:847-870.
 16. Comstock LE, Kasper DL: **Bacterial glycans: key mediators of diverse host immune responses**. *Cell* 2006, **126**:847-850.
 17. Perret S, Sabin C, Dumon C, Pokorná M, Gautier C, Galanina O, Iliá S, Bovin N, Nicaise M, Desmadril M *et al.*: **Structural basis for the interaction between human milk oligosaccharides and the bacterial lectin PA-III of *Pseudomonas aeruginosa***. *Biochem J* 2005, **389**:325-332.
 18. Sommer R, Paulson JC, Titz A, Varrot A, Wagner S, Khaledi A, Häussler S, Nycholat CM, Imberty A: **The virulence factor LecB varies in clinical isolates: consequences for ligand binding and drug discovery**. *Chem Sci* 2016, **7**:4990-5001.
 19. Guo Y, Feinberg H, Conroy E, Mitchell DA, Alvarez R, Blixt O, Taylor ME, Weis WI, Drickamer K: **Structural basis for distinct ligand-binding and targeting properties of the receptors DC-SIGN and DC-SIGNR**. *Nat Struct Mol Biol* 2004, **11**:591-598.
 20. Williams SJ: **Sensing lipids with mincle: structure and function**. *Front Immunol* 2017, **8**:1662.
 21. Furukawa A, Kamishikiryō J, Mori D, Toyonaga K, Okabe Y, Toji A, Kanda R, Miyake Y, Ose T, Yamasaki S, Maenaka K: **Structural analysis for glycolipid recognition by the C-type lectins Mincle and MCL**. *Proc Natl Acad Sci U S A* 2013, **110**:17438-17443.
 22. Wohlschläger T, Butschli A, Grassi P, Sutov G, Gauss R, Hauck D, Schmieder SS, Knobel M, Titz A, Dell A, Haslam SM, Hengartner MO, Aebi M, Künzler M: **Methylated glycans as conserved targets of animal and fungal innate defense**. *Proc Natl Acad Sci U S A* 2014, **111**:E2787-E2796.
 23. Sommer R, Makshakova ON, Wohlschläger T, Hutin S, Marsh M, Titz A, Künzler M, Varrot A: **Crystal structures of fungal tectonin in complex with O-methylated glycans suggest key role in innate immune defense**. *Structure* 2018, **26**:391-402.e4.
 24. Wilkins PP, Moore KL, McEver RP, Cummings RD: **Tyrosine sulfation of P-selectin glycoprotein ligand-1 is required for**

- high affinity binding to P-selectin. *J Biol Chem* 1995, **270**:22677-22680.**
25. Dahms NM, Olson LJ, Kim J-JP: **Strategies for carbohydrate recognition by the mannose 6-phosphate receptors.** *Glycobiology* 2008, **18**:664-678.
 26. Weis WI, Drickamer K: **Structural basis of lectin-carbohydrate recognition.** *Annu Rev Biochem* 1996, **65**:441-473.
 27. Ernst B, Magnani JL: **From carbohydrate leads to glycomimetic drugs.** *Nat Rev Drug Discov* 2009, **8**:661-677.
 28. Cecioni S, Imberty A, Vidal S: **Glycomimetics versus multivalent glycoconjugates for the design of high affinity lectin ligands.** *Chem Rev* 2015, **115**:525-561.
 29. Mydock-McGrane L, Cusumano Z, Han Z, Binkley J, Kostakioti M, Hannan T, Pinkner JS, Klein R, Kalas V, Crowley J et al.: **Antivirulence C-mannosides as antibiotic-sparing, oral therapeutics for urinary tract infections.** *J Med Chem* 2016, **59**:9390-9408.
- Design, synthesis, *in vitro* and *in vivo* evaluation of the new class of C-mannosides as FimH inhibitors. The lead compounds showed improved PK and metabolic stability compared to O-mannosides and high efficacy in mouse UTI model.
30. Sattigeri JA, Garg M, Bhateja P, Soni A, Rauf ARA, Gupta M, Deshmukh MS, Jain T, Alekar N, Barman TK et al.: **Synthesis and evaluation of thiomannosides, potent and orally active FimH inhibitors.** *Bioorg Med Chem Lett* 2018, **28**:2993-2997.
 31. Kalas V, Hibbing ME, Maddirala AR, Chugani R, Pinkner JS, Mydock-McGrane LK, Conover MS, Janetka JW, Hultgren SJ: **Structure-based discovery of glycomimetic FimH ligands as inhibitors of bacterial adhesion during urinary tract infection.** *Proc Natl Acad Sci U S A* 2018, **115**:E2819-E2828.
 32. Wagner S, Hauck D, Hoffmann M, Sommer R, Joachim I, Müller R, Imberty A, Varrot A, Titz A: **Covalent lectin inhibition and application in bacterial biofilm imaging.** *Angew Chem—Int Ed* 2017, **56**:16559-16564.
- Design and synthesis of the first covalent lectin inhibitor. The covalent inhibitor targeting a cysteine residue of LecA was conjugated to fluorescein and used for LecA-specific staining of *P. aeruginosa* biofilm aggregates.
33. Johansson EMV, Cruz SA, Kolomiets E, Buts L, Kadam RU, Cacciarini M, Bartels KM, Diggle SP, Cámara M, Williams P et al.: **Inhibition and dispersion of *Pseudomonas aeruginosa* biofilms by glycopeptide dendrimers targeting the fucose-specific lectin LecB.** *Chem Biol* 2008, **15**:1249-1257.
 34. Sommer R, Wagner S, Rox K, Varrot A, Hauck D, Wamhoff EC, Schreiber J, Ryckmans T, Brunner T, Rademacher C et al.: **Glycomimetic, orally bioavailable lecb inhibitors block biofilm formation of *Pseudomonas aeruginosa*.** *J Am Chem Soc* 2018, **140**:2537-2545.
- Development of small molecule LecB inhibitors with high potency, excellent receptor binding kinetics, thermodynamics, selectivity, and pharmacokinetic properties. These glycomimetic inhibitors showed inhibition of *P. aeruginosa* biofilm formation *in vitro* and are promising leads for drug development.
35. Nishikawa K, Watanabe M, Kita E, Igai K, Omata K, Yaffe MB, Natori Y: **A multivalent peptide library approach identifies a novel Shiga toxin inhibitor that induces aberrant cellular transport of the toxin.** *FASEB J* 2006, **20**:2597-2599.
 36. Fu Q, Pukin AV, Vanufford HCQ, Branson TR, Thies-Weesie DME, Turnbull WB, Visser GM, Pieters RJ: **Tetra-versus pentavalent inhibitors of cholera toxin.** *Chem Open* 2015, **4**:471-477.
 37. Han X, Shi Y, Si L, Fan Z, Wang H, Xu R, Jiao P, Meng K, Tian Z, Zhou X et al.: **Design, synthesis and biological activity evaluation of novel conjugated sialic acid and pentacyclic triterpene derivatives as anti-influenza entry inhibitors.** *MedChemComm* 2016, **7**:1932-1945.
 38. Wang H, Xu R, Shi Y, Si L, Jiao P, Fan Z, Han X, Wu X, Zhou X, Yu F et al.: **Design, synthesis and biological evaluation of novel I-ascorbic acid-conjugated pentacyclic triterpene derivatives as potential influenza virus entry inhibitors.** *Eur J Med Chem* 2016, **110**:376-388.
 39. Yu M, Si L, Wang Y, Wu Y, Yu F, Jiao P, Shi Y, Wang H, Xiao S, Fu G et al.: **Discovery of pentacyclic triterpenoids as potential entry inhibitors of influenza viruses.** *J Med Chem* 2014, **57**:10058-10071.
 40. Yamabe M, Kaihatsu K, Ebara Y: **Sialyllactose-modified three-way junction DNA as binding inhibitor of influenza virus hemagglutinin.** *Bioconjug Chem* 2018, **29**:1490-1494.
- Sialic acid presented on a three-way junction DNA matches the hemagglutinin receptor binding site. The authors studied the structure activity relationship and showed highly active hemagglutinin inhibitors.
41. Yamabe M, Fujita A, Kaihatsu K, Ebara Y: **Synthesis of neuraminidase-resistant sialoside-modified three-way junction DNA and its binding ability to various influenza viruses.** *Carbohydr Res* 2019, **474**:43-50.
- As a follow-up study of Ref. 40, the introduction of a S-glycosidic bond instead of an O-glycosidic bond increased the stability against neuraminidase.
42. Strauch E-M, Bernard SM, La D, Bohn AJ, Lee PS, Anderson CE, Nieuwma T, Holstein CA, Garcia NK, Hooper KA et al.: **Computational design of trimeric influenza-neutralizing proteins targeting the hemagglutinin receptor binding site.** *Nat Biotechnol* 2017, **35**:667-671.
- A highly avid trimeric protein, specifically *in silico* designed to match the binding site architecture of hemagglutinin. The resulting hemagglutinin inhibitor shows prophylactic and therapeutic activity against H3N2 in a mouse model.
43. Guillon P, Dirr L, El-Deeb IM, Winger M, Bailly B, Haselhorst T, Dyason JC, Von Itzstein M: **Structure-guided discovery of potent and dual-acting human parainfluenza virus haemagglutinin-neuraminidase inhibitors.** *Nat Commun* 2014, **5**:5268.
 44. Dirr L, El-Deeb IM, Chavas LMG, Guillon P, Von Itzstein M: **The impact of the butterfly effect on human parainfluenza virus haemagglutinin-neuraminidase inhibitor design.** *Sci Rep* 2017, **7**.
 45. Koromyslova A, Tripathi S, Morozov V, Schrotten H, Hansman GS: **Human norovirus inhibition by a human milk oligosaccharide.** *Virology* 2017, **508**:81-89.
 46. Weichert S, Koromyslova A, Singh BK, Hansman S, Jennewein S, Schrotten H, Hansman GS: **Structural basis for norovirus inhibition by human milk oligosaccharides.** *J Virol* 2016, **90**:4843-4848.
 47. Koromyslova AD, White PA, Hansman GS: **Treatment of norovirus particles with citrate.** *Virology* 2015, **485**:199-204.
 48. Aretz J, Anumala UR, Fuchsberger FF, Molavi N, Ziebart N, Zhang H, Nazaré M, Rademacher C: **Allosteric inhibition of a mammalian lectin.** *J Am Chem Soc* 2018, **140**:14915-14925.
- The first allosteric inhibition of a mammalian lectin (langerin) using thiazolopyrimidines led to binding affinities in a double-digit micromolar range.
49. Mcever RP: **Selectins: initiators of leucocyte adhesion and signalling at the vascular wall.** *Cardiovasc Res* 2015, **107**:331-339.
 50. Clatworthy AE, Pierson E, Hung DT: **Targeting virulence: a new paradigm for antimicrobial therapy.** *Nat Chem Biol* 2007, **3**:541-548.
 51. Davies D: **Understanding biofilm resistance to antibacterial agents.** *Nat Rev Drug Discov* 2003, **2**:114-122.
 52. Hung C, Bouckaert J, Hung D, Pinkner J, Widberg C, Defusco A, Auguste CG, Strouse R, Langermann S, Waksman G, Hultgren SJ: **Structural basis of tropism of *Escherichia coli* to the bladder during urinary tract infection.** *Mol Microbiol* 2002, **44**:903-915.
 53. Hartmann M, Lindhorst TK: **The bacterial lectin FimH, a target for drug discovery – carbohydrate inhibitors of Type 1 fimbriae-mediated bacterial adhesion.** *Eur J Org Chem* 2011, **2011**:3609.
 54. Conover MS, Ruer S, Taganna J, Kalas V, De Greve H, Pinkner JS, Dodson KW, Remaut H, Hultgren SJ: **Inflammation-induced adhesin-receptor interaction provides a fitness advantage to uropathogenic *E. coli* during chronic infection.** *Cell Host Microbe* 2016, **20**:482-492.

64 Mechanistic biology

55. Chen SL, Hung CS, Pinkner JS, Walker JN, Cusumano CK, Li Z, Bouckaert J, Gordon JI, Hultgren SJ: **Positive selection identifies an *in vivo* role for FimH during urinary tract infection in addition to mannose binding.** *Proc Natl Acad Sci U S A* 2009, **106**:22439-22444.
56. Schwartz DJ, Kalas V, Pinkner JS, Chen SL, Spaulding CN, Dodson KW, Hultgren SJ: **Positively selected FimH residues enhance virulence during urinary tract infection by altering FimH conformation.** *Proc Natl Acad Sci U S A* 2013, **110**:15530-15537.
57. Spaulding CN, Klein RD, Ruer S, Kau AL, Schreiber IVHL, Cusumano ZT, Dodson KW, Pinkner JS, Fremont DH, Janetka JW *et al.*: **Selective depletion of uropathogenic *E. coli* from the gut by a FimH antagonist.** *Nature* 2017, **546**:528-532.
58. Firon N, Ashkenazi S, Mirelman D, Ofek I, Sharon N: **Aromatic alpha-glycosides of mannose are powerful inhibitors of the adherence of type 1 fimbriated *Escherichia coli* to yeast and intestinal epithelial cells.** *Infect Immun* 1987, **55**:472-476.
59. Bouckaert J, Berglund J, Schembri M, De Genst E, Cools L, Wuhler M, Hung CS, Pinkner J, Slättegård R, Zavalov A *et al.*: **Receptor binding studies disclose a novel class of high-affinity inhibitors of the *Escherichia coli* FimH adhesin.** *Mol Microbiol* 2005, **55**:441-455.
60. Sivignon A, Yan X, Dorta DA, Bonnet R, Bouckaert J, Fleury E, Bernard J, Gouin SG, Darfeuille-Michaud A, Barnich N: **Development of heptylmannoside-based glycoconjugate antiadhesive compounds against adherent-invasive *Escherichia coli* bacteria associated with crohn's disease.** *mBio* 2015, **6**:1-9.
61. Chalopin T, Alvarez Dorta D, Sivignon A, Caudan M, Dumych TI, Bilyy RO, Deniaud D, Barnich N, Bouckaert J, Gouin SG: **Second generation of thiazolymannosides, FimH antagonists for *E. coli*-induced Crohn's disease.** *Org Biomol Chem* 2016, **14**:3913-3925.
62. Jarvis C, Han DZ, Kalas V, Klein R, Pinkner JS, Ford B, Binkley J, Cusumano CK, Cusumano Z, Mydock-McGrane L *et al.*: **Antivirulence isoquinolone mannosides: optimization of the biaryl aglycone for FimH lectin binding affinity and efficacy in the treatment of chronic UTI.** *ChemMedChem* 2016, **11**:367-373.
63. Schönemann W, Cramer J, Mühlethaler T, Fiege B, Silbermann M, Rabbani S, Dätwyler P, Zihlmann P, Jakob RP, Sager CP *et al.*: **Improvement of aglycone π -stacking yields nanomolar to sub-nanomolar FimH antagonists.** *ChemMedChem* 2019, **14**:749-757.
64. Alvarez Dorta D, Sivignon A, Chalopin T, Dumych TI, Roos G, Bilyy RO, Deniaud D, Krammer EM, De Ruyck J, Lensink MF *et al.*: **The antiadhesive strategy in crohn's disease: orally active mannosides to decolonize pathogenic *Escherichia coli* from the gut.** *ChemBioChem* 2016, **17**:936-952.
65. Schönemann W, Kleeb S, Dätwyler P, Schwardt O, Ernst B: **Prodrugability of carbohydrates — oral FimH antagonists.** *Can J Chem* 2016, **94**:909-919.
66. Kleeb S, Jiang X, Frei P, Sigl A, Bezençon J, Bamberger K, Schwardt O, Ernst B: **FimH antagonists: phosphate prodrugs improve oral bioavailability.** *J Med Chem* 2016, **59**:3163-3182.
- Phosphate-prodrugs have been synthesized and increased drug availability at the site of infection.
67. Mydock-McGrane LK, Hannan TJ, Janetka JW: **Rational design strategies for FimH antagonists: new drugs on the horizon for urinary tract infection and Crohn's disease.** *Expert Opin Drug Discov* 2017, **12**:711-731.
68. Maddirala AR, Klein R, Pinkner JS, Kalas V, Hultgren SJ, Janetka JW: **Biphenyl Gal and GalNAc FmIH lectin antagonists of uropathogenic *E. coli* (UPEC): optimization through iterative rational drug design.** *J Med Chem* 2019, **62**:467-479.
- Structure-guided optimization was used to develop very potent FmIH inhibitors with excellent metabolic stability and good PK, but low oral bioavailability. This represents a good starting point for drug development for the recently identified target FmIH.
69. Tielker D, Hacker S, Loris R, Strathmann M, Wingender J, Wilhelm S, Rosenau F, Jaeger KE: ***Pseudomonas aeruginosa* lectin LecB is located in the outer membrane and is involved in biofilm formation.** *Microbiology* 2005, **151**:1313-1323.
70. Diggle SP, Stacey RE, Dodd C, Cámara M, Williams P, Winzer K: **The galactophilic lectin, LecA, contributes to biofilm development in *Pseudomonas aeruginosa*.** *Environ Microbiol* 2006, **8**:1095-1104.
71. Gilboa-Garber N: ***Pseudomonas aeruginosa* lectins.** *Methods Enzymol* 1982, **83**:378-385.
72. Wagner S, Sommer R, Hinsberger S, Lu C, Hartmann RW, Empting M, Titz A: **Novel strategies for the treatment of *Pseudomonas aeruginosa* infections.** *J Med Chem* 2016, **59**:5929-5969.
73. Calvert MB, Jumde VR, Titz A: **Pathoblockers or antivirulence drugs as a new option for the treatment of bacterial infections.** *Beilstein J Org Chem* 2018, **14**:2607-2617.
74. Titz A: **Carbohydrate-based anti-virulence compounds against chronic *Pseudomonas aeruginosa* infections with a focus on small molecules.** *Top Med Chem* 2014, **12**:169-186.
75. Blanchard B, Nurisso A, Hollville E, Tétaud C, Wiels J, Pokorná M, Wimmerová M, Varrot A, Imberty A: **Structural basis of the preferential binding for globo-series glycosphingolipids displayed by *Pseudomonas aeruginosa* Lectin I.** *J Mol Biol* 2008, **383**:837-853.
76. Eierhoff T, Bastian B, Thuenauer R, Madl J, Audfray A, Aigal S, Juillot S, Rydell GE, Muller S, de Bentzmann S *et al.*: **A lipid zipper triggers bacterial invasion.** *Proc Natl Acad Sci U S A* 2014, **111**:12895-12900.
77. Imberty A, Wimmerová M, Mitchell EP, Gilboa-Garber N: **Structures of the lectins from *Pseudomonas aeruginosa*: insights into the molecular basis for host glycan recognition.** *Microbes Infect* 2004, **6**:221-228.
78. Bernardi A, Jiménez-Barbero J, Casnati A, De Castro C, Darbre T, Fieschi F, Finne J, Funken H, Jaeger K-E, Lahmann M *et al.*: **Multivalent glycoconjugates as anti-pathogenic agents.** *Chem Soc Rev* 2013, **42**:4709-4727.
79. Boukerb AM, Rousset A, Galanos N, Méar JB, Thépaut M, Grandjean T, Gillon E, Cecioni S, Abderrahmen C, Faure K *et al.*: **Antiadhesive properties of glycoclusters against *Pseudomonas aeruginosa* lung infection.** *J Med Chem* 2014, **57**:10275-10289.
- Lectin-targeting clusters show beneficial effects in a *Pseudomonas aeruginosa* co-institution mouse model of acute lung infection.
80. Kadam RU, Bergmann M, Hurley M, Garg D, Cacciarini M, Swiderska MA, Nativi C, Sattler M, Smyth AR, Williams P *et al.*: **A Glycopeptide dendrimer inhibitor of the galactose-specific lectin LecA and of *Pseudomonas aeruginosa* biofilms.** *Angew Chem Int Ed* 2011, **50**:10631-10635.
81. Michaud G, Visini R, Bergmann M, Salerno G, Bosco R, Gillon E, Richichi B, Nativi C, Imberty A, Stocker A *et al.*: **Overcoming antibiotic resistance in *Pseudomonas aeruginosa* biofilms using glycopeptide dendrimers.** *Chem Sci* 2016, **7**:166-182.
- Lectin-antagonistic peptide dendrimers targeting LecB restored efficacy of the antibiotic tobramycin in biofilms of *Pseudomonas aeruginosa*.
82. Visini R, Jin X, Bergmann M, Michaud G, Pertici F, Fu O, Pukin A, Branson TR, Thies-Weesie DME, Kemmink J *et al.*: **Structural insight into multivalent galactoside binding to *Pseudomonas aeruginosa* Lectin LecA.** *ACS Chem Biol* 2015, **10**:2455-2462.
83. Ligeour C, Vidal O, Dupin L, Casoni F, Gillon E, Meyer A, Vidal S, Vergoten G, Lacroix J, Souteyrand E *et al.*: **Mannose-centered aromatic galactocusters inhibit the biofilm formation of *Pseudomonas aeruginosa*.** *Org Biomol Chem* 2015, **13**:8433-8444.
84. Pertici F, Pieters RJ: **Potent divalent inhibitors with rigid glucose click spacers for *Pseudomonas aeruginosa* lectin LecA.** *Chem Commun* 2012, **48**:4008-4010.
- Synthesis of divalent LecA inhibitors using azide-alkyne click chemistry. The most potent divalent inhibitor showed 545-fold increased potency compared to the monovalent alkyne ligand.
85. Yu G, Vicini AC, Pieters RJ: **Assembling of divalent ligands and their effect on divalent binding to *Pseudomonas aeruginosa* lectin LecA.** *J Org Chem* 2019, **84**:2470-2488.

86. Yu G, Thies-Weesie DME, Pieters RJ: **Tetravalent *Pseudomonas aeruginosa* adhesion lectin leca inhibitor for enhanced biofilm inhibition.** *Helv Chim Acta* 2019, **102**:e1900014.
87. Kadam RU, Garg D, Schwartz J, Visini R, Sattler M, Stocker A, Darbre T, Reymond JL: **CH- π "t-shape" interaction with histidine explains binding of aromatic galactosides to *Pseudomonas aeruginosa* lectin LecA.** *ACS Chem Biol* 2013, **8**:1925-1930.
- CH- π interaction between galactoside aryl aglycon and His50 increases ligand binding potency. Identification and exploiting such interactions may help with design of small molecule inhibitors.
88. Rodrigue J, Ganne G, Blanchard B, Saucier C, Giguère D, Shiao TC, Varrot A, Imberty A, Roy R: **Aromatic thioglycoside inhibitors against the virulence factor LecA from *Pseudomonas aeruginosa*.** *Org Biomol Chem* 2013, **11**:6906-6918.
89. Joachim I, Rikker S, Hauck D, Ponader D, Boden S, Sommer R, Hartmann L, Titz A: **Development and optimization of a competitive binding assay for the galactophilic low affinity lectin LecA from: *Pseudomonas aeruginosa*.** *Org Biomol Chem* 2016, **14**:7933-7948.
90. Mitchell E, Houles C, Sudakevitz D, Wimmerova M, Gautier C, Pérez S, Wu AM, Gilboa-Garber N, Imberty A: **Structural basis for oligosaccharide-mediated adhesion of *Pseudomonas aeruginosa* in the lungs of cystic fibrosis patients.** *Nat Struct Biol* 2002, **9**:918-921.
91. Boukerb AM, Decor A, Ribun S, Tabaroni R, Rousset A, Commin L, Buff S, Doléans-Jordheim A, Vidal S, Varrot A et al.: **Genomic rearrangements and functional diversification of lecA and lecB lectin-coding regions impacting the efficacy of glycomimetics directed against *Pseudomonas aeruginosa*.** *Front Microbiol* 2016, **7**:1-16.
92. Hauck D, Joachim I, Frommeyer B, Varrot A, Philipp B, Möller HM, Imberty A, Exner TE, Titz A: **Discovery of two classes of potent glycomimetic inhibitors of *Pseudomonas aeruginosa* LecB with distinct binding modes.** *ACS Chem Biol* 2013, **8**:1775-1784.
93. Sommer R, Hauck D, Varrot A, Wagner S, Audfray A, Prestel A, Möller HM, Imberty A, Titz A: **Cinnamide derivatives of d-mannose as inhibitors of the bacterial virulence factor LecB from *Pseudomonas aeruginosa*.** *ChemistryOpen* 2015, **4**:756-767.
94. Sommer R, Exner TE, Titz A: **A biophysical study with carbohydrate derivatives explains the molecular basis of monosaccharide selectivity of the *Pseudomonas aeruginosa* lectin lecB.** *PLoS One* 2014, **9**:1-22.
95. Fan E, Merritt EA, Verlinde CLMJ, Hol WGJ: **AB5 toxins: structures and inhibitor design.** *Curr Opin Struct Biol* 2000, **10**:680-686.
96. Kitov PI, Sadowska JM, Mulvey G, Armstrong GD, Ling H, Pannu NS, Read RJ, Bundle DR: **Shiga-like toxins are neutralized by tailored multivalent carbohydrate ligands.** *Nature* 2000, **403**:669-672.
97. Mulvey GL, Marcato P, Kitov PI, Sadowska J, Bundle DR, Armstrong GD: **Assessment in mice of the therapeutic potential of tailored, multivalent shiga toxin carbohydrate ligands.** *J Infect Dis* 2003, **187**:640-649.
98. Nishikawa K, Matsuoka K, Kita E, Okabe N, Mizuguchi M, Hino K, Miyazawa S, Yamasaki C, Aoki J, Takashima S et al.: **A therapeutic agent with oriented carbohydrates for treatment of infections by Shiga toxin-producing *Escherichia coli* O157:H7.** *Proc Natl Acad Sci U S A* 2002, **99**:7669-7674.
99. Watanabe-Takahashi M, Sato T, Dohi T, Noguchi N, Kano F, Murata M, Hamabata T, Natori Y, Nishikawa K: **An orally applicable Shiga toxin neutralizer functions in the intestine to inhibit the intracellular transport of the toxin.** *Infect Immun* 2010, **78**:177-183.
100. Matsuoka K, Nishikawa K, Goshu Y, Koyama T, Hatano K, Matsushita T, Watanabe-Takahashi M, Natori Y, Terunuma D: **Synthetic construction of sugar-amino acid hybrid polymers involving globotriaose or lactose and evaluation of their biological activities against Shiga toxins produced by *Escherichia coli* O157:H7.** *Bioorg Med Chem* 2018, **26**:5792-5803.
101. Cervin J, Wands AM, Casselbrant A, Wu H, Krishnamurthy S, Cvjetkovic A, Estelius J, Dedic B, Sethi A, Wallom KL et al.: **GM1 ganglioside-independent intoxication by Cholera toxin.** *PLoS Pathog* 2018, **14**:e1006862.
102. Merritt EA, Sarfaty S, Feil IK, Hol WGJ: **Structural foundation for the design of receptor antagonists targeting *Escherichia coli* heat-labile enterotoxin.** *Structure* 1997, **5**:1485-1499.
103. Mitchell DD, Pickens JC, Korotkov K, Fan E, Hol WGJ: **3,5-Substituted phenyl galactosides as leads in designing effective cholera toxin antagonists: synthesis and crystallographic studies.** *Bioorg Med Chem* 2004, **12**:907-920.
104. Kumar V, Turnbull WB: **Carbohydrate inhibitors of cholera toxin.** *Beilstein J Org Chem* 2018, **14**:484-498.
105. Wands AM, Cervin J, Huang H, Zhang Y, Youn G, Brautigam CA, Matson Dzebo M, Björklund P, Wallenius V, Bright DK et al.: **Fucosylated molecules competitively interfere with cholera toxin binding to host cells.** *ACS Infect Dis* 2018, **4**:758-770.
- Inhibition of cholera toxin by targeting the neglected fucose binding site compared to the well studied GM1 primary binding site. For the first time, the fucosylated polymers were used to inhibit cholera toxin binding to human cells *in vitro*.
106. Varki A, Schnaar RL, Schauer R: *Sialic Acids and Other Nonulosonic Acids.* Cold Spring Harbor Laboratory Press; 2015.
107. Sauter NK, Bednarski MD, Wurzburg BA, Hanson JE, Whitesides GM, Skehel JJ, Wiley DC: **Hemagglutinins from two influenza virus variants bind to sialic acid derivatives with millimolar dissociation constants: a 500-MHz proton nuclear magnetic resonance study.** *Biochemistry* 1989, **28**:8388-8396.
108. Nizet V, Varki A, Aebi M: **Microbial lectins: hemagglutinins, adhesins, and toxins.** In *Essentials of Glycobiology*. Edited by Varki A, Cummings RD, Esko JD, Stanley P, Hart GW, Aebi M, Darvill AG, Kinoshita T, Packer NH, Prestegard JH, Schnaar RL, Seeberger PH. Cold Spring Harbor Laboratory Press; 2015.
109. Li F, Ma C, Wang J: **Inhibitors targeting the influenza virus hemagglutinin.** *Curr Med Chem* 2015, **22**.
110. Nagao M, Matsubara T, Hoshino Y, Sato T, Miura Y: **Topological design of star glycopolymers for controlling the interaction with the influenza virus.** *Bioconjug Chem* 2019, **30**:1192-1198 <http://dx.doi.org/10.1021/acs.bioconjchem.9b00134>.
111. Kadam RU, Wilson IA: **A small-molecule fragment that emulates binding of receptor and broadly neutralizing antibodies to influenza A hemagglutinin.** *Proc Natl Acad Sci U S A* 2018, **115**:4240-4245.
112. Moscona A: **Entry of parainfluenza virus into cells as a target for interrupting childhood respiratory disease.** *J Clin Invest* 2005, **115**:1688-1698.
113. Robilotti E, Deresinski S, Pinsky BA: **Norovirus.** *Clin Microbiol Rev* 2015, **28**:134-164.
114. Taube S, Mallagaray A, Peters T: **Norovirus, glycans and attachment.** *Curr Opin Virol* 2018, **31**:33-42.
115. Coulet M, Phothisrath P, Allais L, Schilter B: **Pre-clinical safety evaluation of the synthetic human milk, nature-identical, oligosaccharide 2'-O-Fucosyllactose (2'FL).** *Regul Toxicol Pharmacol* 2014, **68**:59-69.
116. Morrow AL, Ruiz-Palacios GM, Altaye M, Jiang X, Lourdes Guerrero M, Meinen-Derr JK, Farkas T, Chaturvedi P, Pickering LK, Newburg DS: **Human milk oligosaccharides are associated with protection against diarrhea in breast-fed infants.** *J Pediatr* 2004, **145**:297-303.
117. Pillai S, Netravali IA, Cariappa A, Mattoo H: **Siglecs and immune regulation.** *Annu Rev Immunol* 2012, **30**:357-392.
118. Macauley MS, Crocker PR, Paulson JC: **Siglec-mediated regulation of immune cell function in disease.** *Nat Rev Immunol* 2014, **14**:653-666.
119. Barondes SH, Cooper DN, Gitt MA, Leffler H: **Galectins. Structure and function of a large family of animal lectins.** *J Biol Chem* 1994, **269**:20807-20810.

120. Thiemann S, Baum LG: **Galectins and immune responses-just how do they do those things they do?** *Annu Rev Immunol* 2016, **34**:243-264.
121. Compagno D, Jaworski FM, Gentilini L, Contrufo G, González Pérez I, Elola MT, Prego N, Rabinovich GA, Laderach DJ: **Galectins: major signaling modulators inside and outside the cell.** *Curr Mol Med* 2014, **14**:630-651.
122. Rabinovich GA, Toscano MA: **Turning "sweet" on immunity: galectin-glycan interactions in immune tolerance and inflammation.** *Nat Rev Immunol* 2009, **9**:338-352.
123. van den Berg LM, Gringhuis SI, Geijtenbeek TBH: **An evolutionary perspective on C-type lectins in infection and immunity.** *Ann N Y Acad Sci* 2012, **1253**:149-158.
124. Brown GD, Willment JA, Whitehead L: **C-type lectins in immunity and homeostasis.** *Nat Rev Immunol* 2018, **18**:374-389.
125. Porkolab V, Chabrol E, Varga N, Ordanini S, Sutkevičiūtė I, Thépaut M, Garcia-Jiménez MJ, Girard E, Nieto PM, Bernardi A, Fieschi F: **Rational-differential design of highly specific glycomimetic ligands: targeting DC-SIGN and excluding langerin recognition.** *ACS Chem Biol* 2018, **13**:600-608.
- GlcNAc is recognized by both lectins- langerin and DC-SIGN. Selectivity toward langerin was achieved by sulfation on position six.
126. Wilson NJ, Boniface K, Chan JR, McKenzie BS, Blumenschein WM, Mattson JD, Basham B, Smith K, Chen T, Morel F *et al.*: **Development, cytokine profile and function of human interleukin 17-producing helper T cells.** *Nat Immunol* 2007, **8**:950-957.
127. Yang K, Park CG, Cheong C, Bulgheresi S, Zhang S, Zhang P, He Y, Jiang L, Huang H, Ding H *et al.*: **Host Langerin (CD207) is a receptor for *Yersinia pestis* phagocytosis and promotes dissemination.** *Immunol Cell Biol* 2015, **93**:815-824.
128. Ng WC, Londrigan SL, Nasr N, Cunningham AL, Turville S, Brooks AG, Reading PC: **The C-type lectin langerin functions as a receptor for attachment and infectious entry of Influenza A virus.** *J Virol* 2016, **90**:206-221.
129. Idoyaga J, Suda N, Suda K, Park CG, Steinman RM: **Antibody to Langerin/CD207 localizes large numbers of CD8alpha+ dendritic cells to the marginal zone of mouse spleen.** *Proc Natl Acad Sci U S A* 2009, **106**:1524-1529.
130. Flacher V, Tripp CH, Stoitzner P, Haid B, Ebner S, Del Frari B, Koch F, Park CG, Steinman RM, Idoyaga J, Romani N: **Epidermal Langerhans cells rapidly capture and present antigens from C-type lectin-targeting antibodies deposited in the dermis.** *J Invest Dermatol* 2010, **130**:755-762.
131. Zhao J, Liu X, Kao C, Zhang E, Li Q, Zhang F, Linhardt RJ: **Kinetic and structural studies of interactions between glycosaminoglycans and langerin.** *Biochemistry* 2016, **55**:4552-4559.
132. Wamhoff E-C, Schulze J, Bellmann L, Bachem G, Fuchsberger FF, Rademacher J, Hermann M: **A specific, glycomimetic Langerin ligand for human Langerhans cell targeting.** *bioRxiv* 2018 <http://dx.doi.org/10.1101/286021>.
- Intracellular trafficking of synthesized langerin targeting liposomes was observed in Langerin+ COS-7 cells by confocal microscopy. It paves the way for trans-cutaneous vaccinations using these liposomes in therapeutic applications.
133. Wamhoff E-C, Schulze J, Bellmann L, Rentsch M, Bachem G, Fuchsberger FF, Rademacher J, Hermann M, Del Frari B, van Dalen R *et al.*: **A specific, glycomimetic langerin ligand for human langerhans cell targeting.** *ACS Cent Sci* 2019, **5**:808-820 <http://dx.doi.org/10.1021/acscentsci.9b00093>.
- Intracellular trafficking of synthesized langerin targeting liposomes was observed in Langerin+ COS-7 cells by confocal microscopy. It paves the way for trans-cutaneous vaccinations using these liposomes in therapeutic applications.
134. de Witte L, Nabatov A, Pion M, Fluitsma D, de Jong MAWP, de Grijl T, Piguat V, van Kooyk Y, Geijtenbeek TBH: **Langerin is a natural barrier to HIV-1 transmission by Langerhans cells.** *Nat Med* 2007, **13**:367-371.
135. Geijtenbeek TB, Kwon DS, Torensma R, van Vliet SJ, van Duijnhoven GC, Middel J, Cornelissen IL, Nottet HS, KewalRamani VN, Littman DR *et al.*: **DC-SIGN, a dendritic cell-specific HIV-1-binding protein that enhances trans-infection of T cells.** *Cell* 2000, **100**:587-597.
136. Bertolotti B, Sutkevičiūtė I, Ambrosini M, Ribeiro-Viana R, Rojo J, Fieschi F, Dvořáková H, Kašáková M, Parkan K, Hlaváčková M *et al.*: **Polyvalent C-glycomimetics based on l-fucose or d-mannose as potent DC-SIGN antagonists.** *Org Biomol Chem* 2017, **15**:3995-4004.
137. Thépaut M, Guzzi C, Sutkevičiūtė I, Sattin S, Ribeiro-Viana R, Varga N, Chabrol E, Rojo J, Bernardi A, Angulo J *et al.*: **Structure of a glycomimetic ligand in the carbohydrate recognition domain of C-type Lectin DC-SIGN. Structural requirements for selectivity and ligand design.** *J Am Chem Soc* 2013, **135**:2518-2529.
138. Aretz J, Baukmann H, Shanina E, Hanske J, Wawrzinek R, Zapol'skii VA, Seeberger PH, Kaufmann DE, Rademacher C: **Identification of multiple druggable secondary sites by fragment screening against DC-SIGN.** *Angew Chem Int Ed* 2017, **56**:7292-7296.
- Increased number of druggable pockets on DC-SIGN allows the development of new multivalent compounds with higher binding affinities. The inhibition of the cell-surface receptor DC-SIGN is important due to pathogenic threats.
139. Ambati S, Ferraro AR, Kang SE, Lin J, Lin X, Momany M, Lewis ZA, Meagher RB: **Dectin-1-targeted antifungal liposomes exhibit enhanced efficacy.** *mSphere* 2019, **4**:e00025-19.
140. Ley K: **The role of selectins in inflammation and disease.** *Trends Mol Med* 2003, **9**:263-268.
141. Peters T, Scheffler K, Ernst B, Katopodis A, Magnani JL, Wang WT, Weisemann R: **Determination of the bioactive conformation of the carbohydrate ligand in the E-selectin/Sialyl LewisX complex.** *Angew Chem Int Ed Engl* 1995, **34**:1841-1844.
142. Thoma G, Magnani JL, Patton JT, Ernst B, Jahnke W: **Preorganization of the bioactive conformation of Sialyl LewisX analogues correlates with their affinity to E-selectin.** *Angew Chem Int Ed* 2001, **40**:1941-1945.
143. Norman KE, Anderson GP, Kolb HC, Ley K, Ernst B: **Sialyl Lewis X (sLe(x)) and an sLe(x) mimetic, CGP69669A, disrupt E-selectin-dependent leukocyte rolling in vivo.** *Blood* 1998, **91**:475-483.
144. Schwizer D, Patton JT, Cutting B, Smieško M, Wagner B, Kato A, Weckerle C, Binder FPC, Rabbani S, Schwardt O, Magnani JL, Ernst B: **Pre-organization of the core structure of E-selectin antagonists.** *Chem - A Eur J* 2012, **18**:1342-1351.
145. Kolb HC, Ernst B: **Development of tools for the design of selectin antagonists.** *Chem - A Eur J* 1997, **3**:1571-1578.
146. Egger J, Weckerle C, Cutting B, Schwardt O, Rabbani S, Lemme K, Ernst B: **Nanomolar E-selectin antagonists with prolonged half-lives by a fragment-based approach.** *J Am Chem Soc* 2013, **135**:9820-9828.
147. Chang J, Patton JT, Sarkar A, Ernst B, Magnani JL, Frenette PS: **GMI-1070, a novel pan-selectin antagonist, reverses acute vascular occlusions in sickle cell mice.** *Blood* 2010, **116**:1779-1786.
148. Decout A, Silva-Gomes S, Drocourt D, Barbe S, André I, Cueto FJ, Lioux T, Sancho D, Pérouzel E, Vercellone A *et al.*: **Rational design of adjuvants targeting the C-type lectin Mincle.** *Proc Natl Acad Sci U S A* 2017, **114**:2675-2680.
- Structure-based design of mincle inhibitors as promising vaccine adjuvants.
149. Feinberg H, Rambaruth NDS, Jégouzo SAF, Jacobsen KM, Djurhuus R, Poulsen TB, Weis WI, Taylor ME, Drickamer K: **Binding sites for acylated trehalose analogs of glycolipid ligands on an extended carbohydrate recognition domain of the macrophage receptor mincle.** *J Biol Chem* 2016, **291**:21222-21233.
150. Matsumaru T, Ikeno R, Shuchi Y, Iwamatsu T, Tadokoro T, Yamasaki S, Fujimoto Y, Furukawa A, Maenaka K: **Synthesis of glycerolipids containing simple linear acyl chains or aromatic rings and evaluation of their Mincle signaling activity.** *Chem Commun (Camb)* 2019, **55**:711-714.

151. Bird JH, Khan AA, Nishimura N, Yamasaki S, Timmer MSM, Stocker BL: **Synthesis of branched trehalose glycolipids and their muncle agonist activity.** *J Org Chem* 2018, **83**:7593-7605.
152. Dumić J, Dabelić S, Flügel M: **Galectin-3: an open-ended story.** *Biochim Biophys Acta – Gen Subj* 2006, **1760**:616-635.
153. Sharma UC, Pokharel S, van Brakel TJ, van Berlo JH, Cleutjens JPM, Schroen B, Andre' S, Crijns HJGM, Gábius H-J, Maessen J, Pinto YM: **Galectin-3 marks activated macrophages in failure-prone hypertrophied hearts and contributes to cardiac dysfunction.** *Circulation* 2004, **110**:3121-3123128.
154. Raimond J, Zimonjic DB, Mignon C, Mattei M-G, Popescu NC, Monsigny M, Legrand A: **Mapping of the galectin-3 gene (LGALS3) to human chromosome 14 at region 14q21-22.** *Mamm Genome* 1997, **8**:706-707.
155. Peterson K, Kumar R, Stenström O, Verma P, Verma PR, Håkansson M, Kahl-Knutsson B, Zetterberg F, Leffler H, Akke M et al.: **Systematic tuning of fluoro-galectin-3 interactions provides thiodigalactoside derivatives with single-digit nM affinity and high selectivity.** *J Med Chem* 2018, **61**:1164-1175.
- Selectivity for galectin-3 inhibitors over galectin-1 is important for the targeting of galectin-3, for example, in cancer, inflammation and fibrosis. Asymmetric thiodigalactosides were designed and synthesized for the selective inhibition of galectin-3.
156. Rajput VK, MacKinnon A, Mandal S, Collins P, Blanchard H, Leffler H, Sethi T, Schambye H, Mukhopadhyay B, Nilsson UJ: **A selective galactose-coumarin-derived Galectin-3 inhibitor demonstrates involvement of Galectin-3-glycan interactions in a pulmonary fibrosis model.** *J Med Chem* 2016, **59**:8141-8147.
157. Delaine T, Collins P, MacKinnon A, Sharma G, Stegmayr J, Rajput VK, Mandal S, Cumpstey I, Larumbe A, Salameh BA et al.: **Galectin-3-binding glycomimetics that strongly reduce bleomycin-induced lung fibrosis and modulate intracellular glycan recognition.** *ChemBioChem* 2016, **17**:1759-1770.
158. Chen W-S, Cao Z, Leffler H, Nilsson UJ, Panjwani N: **Galectin-3 inhibition by a small-molecule inhibitor reduces both pathological corneal neovascularization and fibrosis.** *Invest Ophthalmol Vis Sci* 2017, **58**:9.
159. Zetterberg FR, Peterson K, Johnsson RE, Brimert T, Håkansson M, Logan DT, Leffler H, Nilsson UJ: **Monosaccharide derivatives with low-nanomolar lectin affinity and high selectivity based on combined fluorine-amide, phenyl-arginine, sulfur- π , and halogen bond interactions.** *ChemMedChem* 2018, **13**:133-137.
160. Angata T, Nycholat CM, Macauley MS: **Therapeutic targeting of siglecs using antibody- and glycan-based approaches.** *Trends Pharmacol Sci* 2015, **36**:645-660.
161. O'Reilly MK, Paulson JC: **Siglecs as targets for therapy in immune cell mediated disease.** *Trends Pharmacol Sci* 2009, **30**:240.
162. Schwardt O, Kelm S, Ernst B: **SIGLEC-4 (MAG) antagonists: from the natural carbohydrate epitope to glycomimetics.** *Top Curr Chem* 2013:151-200.
163. Zaccai NR, Maenaka K, Maenaka T, Crocker PR, Brossmer R, Kelm S, Jones EY: **Structure-guided design of sialic acid-based Siglec inhibitors and crystallographic analysis in complex with sialoadhesin.** *Structure* 2003, **11**:557-567.
164. Zeng Y, Rademacher C, Nycholat CM, Futakawa S, Lemme K, Ernst B, Paulson JC: **High affinity sialoside ligands of myelin associated glycoprotein.** *Bioorg Med Chem Lett* 2011, **21**:5045-5049.
165. Lopez PHH: **Role of myelin-associated glycoprotein (Siglec-4a) in the nervous system.** *Adv Neurobiol* 2014:245-262.
166. Schnaar RL, Collins BE, Wright LP, Kiso M, Tropak MB, Roder JC, Crocker PR: **Myelin-associated glycoprotein binding to gangliosides. Structural specificity and functional implications.** *Ann N Y Acad Sci* 1998, **845**:92-105.
167. Macauley MS, Crocker PR, Paulson JC: **Siglec-mediated regulation of immune cell function in disease.** *Nat Rev Immunol* 2014, **14**:653-666.
168. Prescher H, Schweizer A, Kuhfeldt E, Nitschke L, Brossmer R: **Discovery of multifold modified sialosides as Human CD22/Siglec-2 ligands with nanomolar activity on B-cells.** *ACS Chem Biol* 2014, **9**:1444-1450.
- Modified sialoside inhibitors against CD22 were synthesized and showed increased binding affinities. These compounds are useful for further investigation of the function of CD22.
169. Peng W, Paulson JC: **CD22 ligands on a natural N-glycan scaffold efficiently deliver toxins to B-lymphoma cells.** *J Am Chem Soc* 2017, **139**:12450-12458.
- A chemically defined natural N-linked glycan scaffold showed 1500-fold increase in potency compared to the monovalent ligand. Conjugates of auristatin and saporin toxins with this scaffold resulted in efficient killing of the B-cell lymphoma cells. This represents an alternative strategy to the antibody and nanoparticle mediated approaches for drug delivery.
170. Cabanettes A, Perkams L, Spies C, Unverzagt C, Varrot A: **Recognition of complex core-fucosylated N-glycans by a mini lectin.** *Angew Chem Int Ed Engl* 2018, **57**:10178-10181.
171. Varrot A, Basheer SM, Imberty A: **Fungal lectins: structure, function and potential applications.** *Curr Opin Struct Biol* 2013, **23**:678-685.
172. Kumar A, Sýkorová P, Demo G, Dobeš P, Hyršl P, Wimmerová M: **A novel fucose-binding lectin from *Photobacterium luminescens* (PLL) with an unusual heptabladed β -propeller tetrameric structure.** *J Biol Chem* 2016, **291**:25032-25049.
173. Jančaříková G, Houser J, Dobeš P, Demo G, Hyršl P, Wimmerová M: **Characterization of novel bangle lectin from *Photobacterium asymbotica* with dual sugar-binding specificity and its effect on host immunity.** *PLoS Pathog* 2017, **13**: e1006564.
174. Beshr G, Sikandar A, Jemiller E-M, Klymiuk N, Hauck D, Wagner S, Wolf E, Koehnke J, Titz A: ***Photobacterium luminescens* lectin A (PLIA): a new probe for detecting α -galactoside-terminating glycoconjugates.** *J Biol Chem* 2017, **292**:19935-19951.
175. Lameignere E, Malinová L, Sláviková M, Duchaud E, Mitchell EP, Varrot A, Sedo O, Imberty A, Wimmerová M: **Structural basis for mannose recognition by a lectin from opportunistic bacteria *Burkholderia cenocepacia*.** *Biochem J* 2008, **411**:307-318.
176. Beshr G, Sommer R, Hauck D, Siebert DCB, Hofmann A, Imberty A, Titz A: **Development of a competitive binding assay for the *Burkholderia cenocepacia* lectin BC2L-A and structure activity relationship of natural and synthetic inhibitors.** *MedChemComm* 2016, **7**:519-530.
177. Šulák O, Cioci G, Delia M, Lahmann M, Varrot A, Imberty A, Wimmerová M: **A TNF-like trimeric lectin domain from *Burkholderia cenocepacia* with specificity for fucosylated human histo-blood group antigens.** *Structure* 2010, **18**:59-72.
178. Šulák O, Cioci G, Lameignère E, Balloy V, Round A, Gutsche I, Malinová L, Chignard M, Kosma P, Aubert DF et al.: ***Burkholderia cenocepacia* BC2L-C is a super lectin with dual specificity and proinflammatory activity.** *PLoS Pathog* 2011, **7**: e1002238.
179. Wagner C, Barlag B, Gerlach RG, Deiwick J, Hensel M: **The *Salmonella enterica* giant adhesin SiiE binds to polarized epithelial cells in a lectin-like manner.** *Cell Microbiol* 2014, **16**:962-975.

1.3. Antibiotics

1.3.1. Antibiotic Crisis

Homo sapiens and its predecessors suffer from infectious diseases for already more than 100,000 years.^[41] A prominent example is the 'iceman' Ötzi, who was infected by *Helicobacter pylori* 5300 years ago.^[42] Until the discovery of antibiotic substances, mostly crude phytopharmaceuticals were empirically used to treat infection-associated diseases. For example, Ötzi carried the fungus *Fomitopsis betulina*, which is believed to have served as antibacterial medicine.^[43] The first antibiotic substances were isolated and characterised in the early 20th century (figure 4, top).^[44] Since then, many of our most common antibiotic classes like β -lactams, tetracyclins and aminoglycosides accessed the market. Antibacterial research reached a peak between 1940 and 1960. On the other hand, antibiotic resistances appeared very quickly (figure 4, bottom).

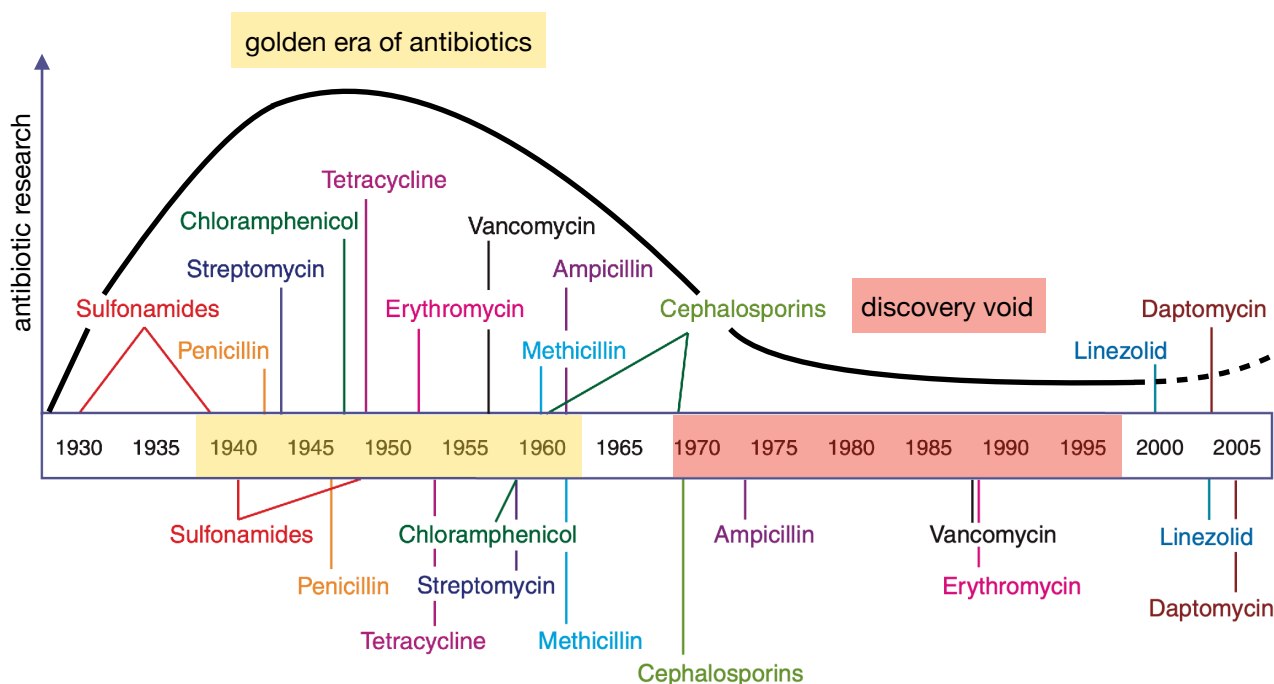


Figure 4. Timeline of antibiotic deployment and the appearance of first antibiotic resistances with a schematic plot of antibiotic research focus along the 20th century. The 'golden era' of antibiotics ended in the 1960's. A long discovery void started since the 1970's despite the emergence of further antibiotic resistances. The figure is adapted from Clathworthy *et al.*, 2007.^[45]

According to C. Walsh^[44], antibiotic drugs can be characterised by their biomolecular mode of actions. Four classical target mechanisms can be described. The

inhibition of bacterial cell wall biosynthesis or impairment of the outer cell membrane leads to reduced cell growth or lysis (figure 5a). Common examples are β -lactam antibiotics or antimicrobial peptides (AMP). Ribosomal protein biosynthesis is inhibited by various antibiotic classes, e.g. aminoglycosides, macrolides, tetracyclines and oxazolidinones. DNA and RNA replication (figure 5c) is the target of fluoroquinolone antibiotics (gyrase) and rifampin (RNA polymerase) and can further be impaired by inhibition of the folate metabolism (figure 5d). Although this list is certainly not claiming completeness, it becomes quite evident, that the number of antibacterial targets is indeed limited.

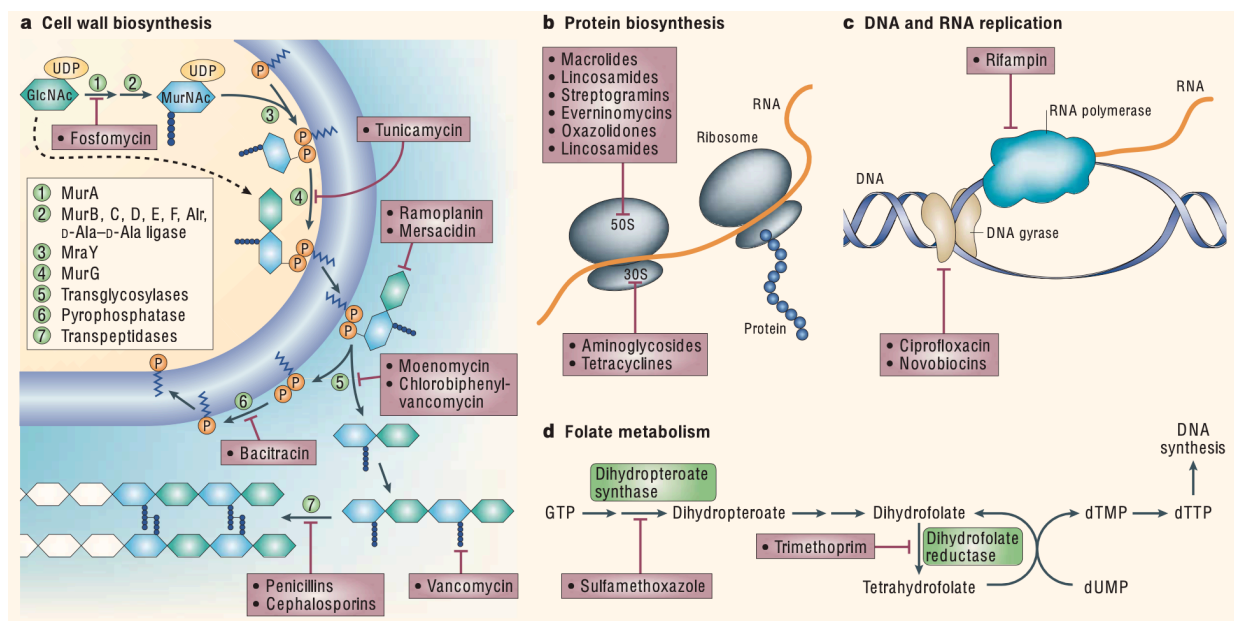


Figure 5. Common antimicrobial targets and their inhibitors. Adapted from C. Walsh.^[44]

Antibiotic resistance mechanisms can be clustered in four categories: (1) modification and inactivation of antibiotics (e.g. β -lactamases^[46]); (2) modification of target structures (e.g. point mutations in *gyrB*^[47]); (3) use of alternative pathways to circumvent inhibited metabolism (e.g. overproduction of dihydrofolate reductase to circumvent inhibition by trimethoprim^[48]) and (4) reduced intracellular concentrations by reduced permeability (e.g. additional outer membrane of Gram-negative bacteria, biofilm formation) or increased drug efflux.

The large discovery void of antibiotics and antimicrobial targets, together with the rise of antibiotic resistances leads into an antibiotic crisis. In fact, it is estimated that up to 10 million deaths per year will be related to drug-resistant infectious diseases by 2050.^[49] Thus it is obvious, that new antibiotics, preferably with new mode of actions need to be discovered.

1.3.2. Treatment of *P. aeruginosa* Infections

The treatment of *P. aeruginosa* with antibiotic drugs is characterised by several resistance mechanisms.^[11] Gram-negative bacteria are intrinsically resistant due their additional outer phospholipid membrane. This barrier limits permeation of many antibiotics, e.g. glycopeptide antibiotics.^[50] Further, *P. aeruginosa* developed a very efficacious efflux pump system, reducing the intracellular drug concentration.^[51, 52] In addition to its intrinsic drug resistance, *P. aeruginosa* is also genetically highly adaptable. In consequence, it can easily acquire further resistances by spontaneous mutations or horizontal gene transfer, leading to extremely drug-resistant bacteria with very limited therapeutic options.

The number of antimicrobial treatment options against *P. aeruginosa* is limited. Only very specific representatives of the antibiotic classes aminoglycosides, fluoroquinolones and β -lactams and the antimicrobial peptide colistin are active against *P. aeruginosa* infections (table 1).^[53] Although these drugs are considered safe, they can result in side effects (table 1). Especially colistin, a polymyxin-derivative, is associated to severe nephrotoxicity and is thus used as a last resort antibiotic.

Table 1. Antibiotics in clinical use against *P. aeruginosa* infections together with exemplary side-effects, grouped by (sub-)classes.^[53]

| antibiotic class | sub-class | drugs | exemplary side-effects |
|-----------------------------|--------------------------------|--------------------------------|-------------------------------------|
| aminoglycosides | <i>micromonospora</i> -derived | gentamicin, amikacin | nephrotoxicity, ototoxicity |
| | <i>streptomyces</i> -derived | tobramycin | |
| fluoroquinolones | 2 nd generation | ciprofloxacin | tendon rupture, neuropathy |
| | 3 rd generation | levofloxacin | |
| β -lactam antibiotics | penicillins | ticarcillin, penicillin | rash, urticaria, allergic reactions |
| | cephalosporins | ceftazidime, cefepime | |
| | monobactams | aztreonam | |
| | carbapenems | imipenem-cilastatin, meropenem | |
| antimicrobial peptides | polymyxins | colistin (only last resort) | strong nephrotoxicity |

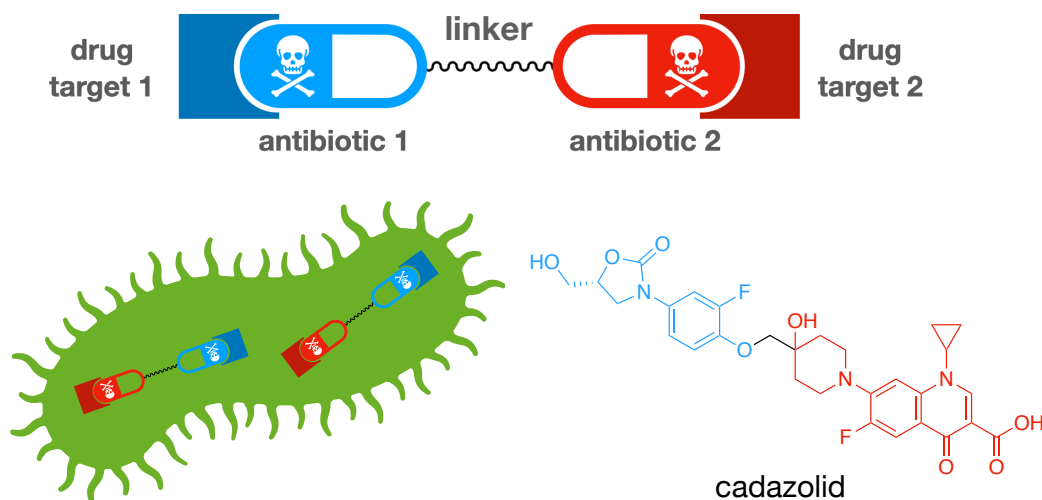
Due to the rapid emergence of drug-resistant *P. aeruginosa*, new antibiotics with novel mode-of-actions or innovative strategies are necessary (reviewed by Wagner *et al*^[54]). Beyond the established groups of therapeutics, new compound classes like argyriins^[55]

and cystobactamids^[56] are currently of high interest. The *P. aeruginosa*-specific antimicrobial peptide Murepavadin (also known as POL7080)^[57] was a very promising new antibiotic in the pipeline^[58] and even reached phase III clinical studies. Unfortunately, systemic therapy suffered from kidney toxicity and the studies had to be terminated.^[59] At the moment, the compound is under investigation for inhalation therapy.

Pathoblockers are an alternative strategy to antibiotic drugs. In contrast to bactericidal or bacteriostatic antibiotics, pathoblockers disarm bacterial cells by inhibiting their virulence factors.^[60, 61] Recent *P. aeruginosa*-specific anti-virulence strategies focussed on the inhibition of the quorum sensing system PQS^[62], the cytotoxic peptidase LasB^[63] and biofilm formation^[31, 64, 65] (for LecA and LecB inhibitors, see chapter 1.2). In fact, combining pathoblockers with antibiotics can lead to synergistic effects.^[66] For example, it was shown that inverse agonists of the Pqs-receptor increase the susceptibility of *P. aeruginosa* biofilms against tobramycin.^[67] Currently, most pathoblocker strategies are still in the preclinical phase. However, some of them are likely to reach clinical trials in the next decade.

1.3.3. Antibiotic Drug Conjugates

New antibiotic strategies are desperately needed in order to deal with the antibiotic resistance crisis. As described before, there is a huge innovation gap since the 1970's and the antibacterial pipeline is rather half empty than half full.^[68] Antibiotic-drug conjugates are multifunctional molecules and consist of at least one antibiotic substance that is chemically linked to another antimicrobial compound or functional moiety.

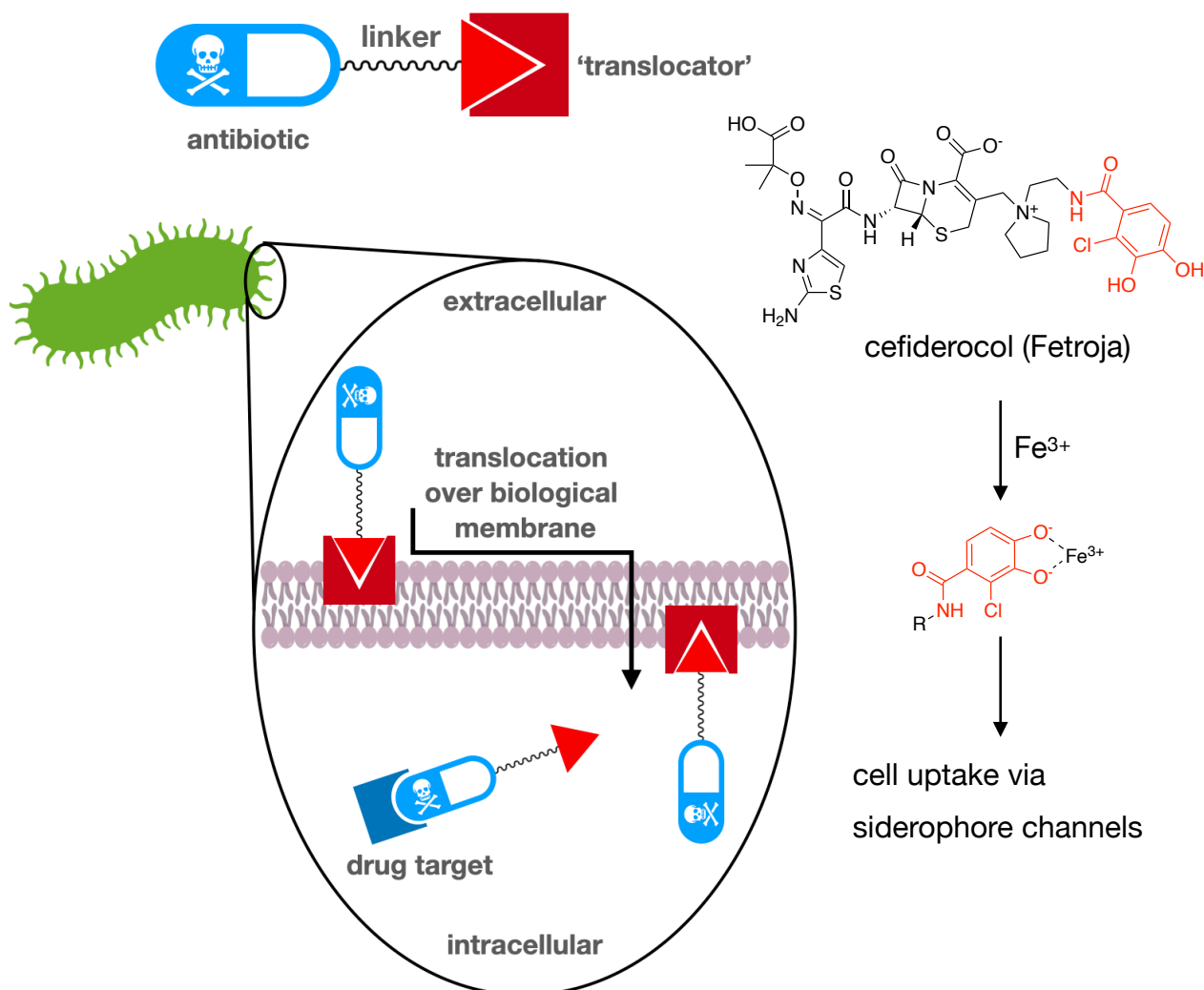


- + simplifies PK of included drugs
- + less likely to form resistances
- + works for almost all targets
- SAR of two highly optimised antibiotic have to be considered
- big molecular size

Figure 6. Schematic representation of hybrid antimicrobials.

Linking two antibiotics leads to so-called hybrid antimicrobials (figure 6). Two antibiotics can often result in a synergistic effect and potentiate each other in their antimicrobial activity. A comprehensible example for a potentiating effect is the combination of a membrane-destabilising polymyxin with a low-permeating drug against gram-negative bacteria (e.g. colistin + Rifampin^[69]). Different pharmacokinetic properties of the individual antibiotic molecules can nullify the *in vitro* synergism when used *in vivo*. Thus, chemical conjugation results in a new molecule with a unique pharmacokinetic parameters. However, these can be significantly altered to the initial molecules, potentially resulting in unfavourable characteristics. Theoretically, the hybrid antimicrobial approach works for all potential target combinations. However, the structure-activity activity relationships of two

(usually highly optimised) antibiotics have to be taken into account for the design of hybrid conjugates. So far, many hybrid conjugates have been studied^[70], however with limited success.^[71] For example, development of the fluoroquinolone-oxazolidinone hybrid-antibiotic cadazolid (Johnson & Johnson) was discontinued in 2018 due to inconsistent results from clinical phase III studies.

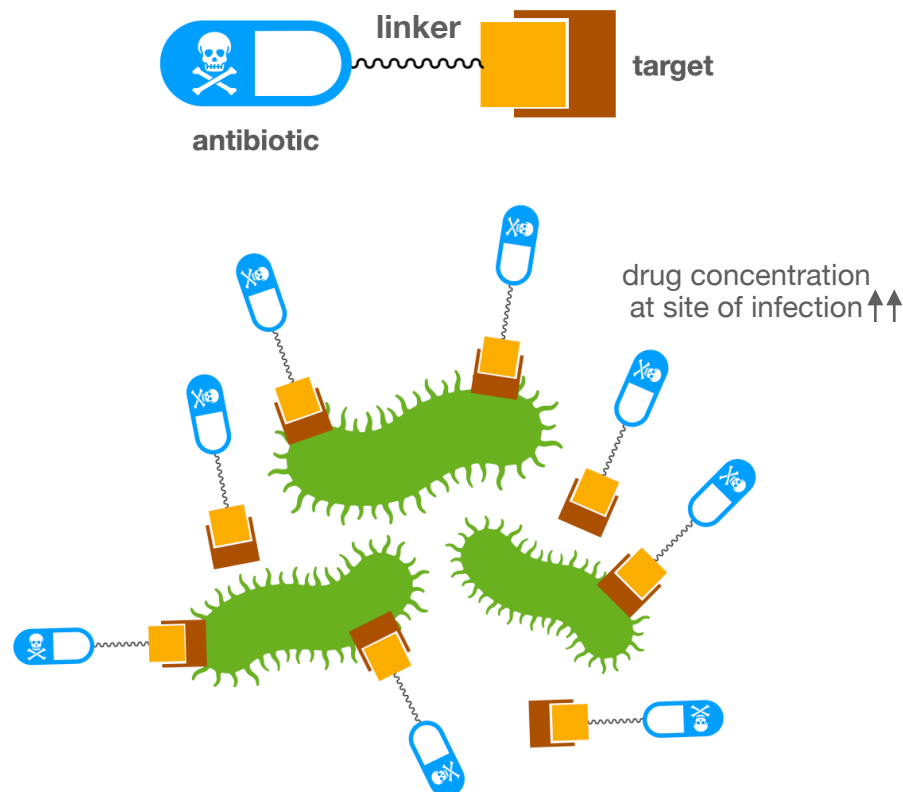


- + increased intracellular drug concentration
- + organism-specific (e.g. by targeting specific siderophore-transporters)
- big molecular size
- best for intracellular drug-targets

Figure 7. Schematic representation of cell permeating antimicrobial conjugates.

Instead of linking two antibiotic substances, antimicrobial conjugates containing an antibiotic linked to a functional molecule is very promising (figure 7). Very popular are components that mediate intracellular drug accumulation by exploiting specific cell

uptake mechanisms. Gram-negative bacteria reduce the permeability of antimicrobial compounds like β -lactams by their additional outer membrane. By conjugation to iron-chelators (i.e. siderophores) drug conjugates can traverse the Gram-negative outer membrane by exploitation of iron transporter systems and eventually reach its antibiotic target. This so-called Trojan horse approach was successfully introduced on the market with the catechol-conjugated cephalosporin cefiderocol (commercial name: Fetroja, sold by Shionogi Inc., figure 7).



- + increased drug concentration at site of infection → reduced side effects
- + organism-specific (e.g. by targeting *P. aeruginosa*-specific proteins)
- big molecular size
- best for extracellular targets

Figure 8. Schematic representation of targeted antimicrobial conjugates.

Targeted drug-delivery is a huge field in drug discovery. Conjugation of a highly cytotoxic drug to a targeted moiety, often specific antibodies, is currently a trending strategy in cancer therapy. Increased local drug concentration at pathogenic tissues and cell-specificity result in higher pharmacological effects and can reduce side effects. Antibody-drug conjugates (ADC) like trastuzumab-emtisine or brentuximab-vedotin are available

on the market and reach high efficacy in the clinics.^[72] For antimicrobials, targeted drug delivery, especially in the field of small molecules, is yet under-represented.^[73] However, conjugation of antibiotics to strain-specific (e.g. *P. aeruginosa*) probes could relieve the healthy microbiome and reduce side effects. Higher concentrations at the site of infection could eventually break antimicrobial resistance (figure 8). A very promising example of targeted antimicrobial conjugates is the antibody-antibiotic conjugate (AAC) DSTA4637S (figure 9).^[74] In clinical phase 1A studies, it was shown that this AAC is safe in healthy patients.^[75] Phase 1B studies in patients with *S. aureus* bacteremia were completed early 2020.^[76] The outcome has however not been published yet.

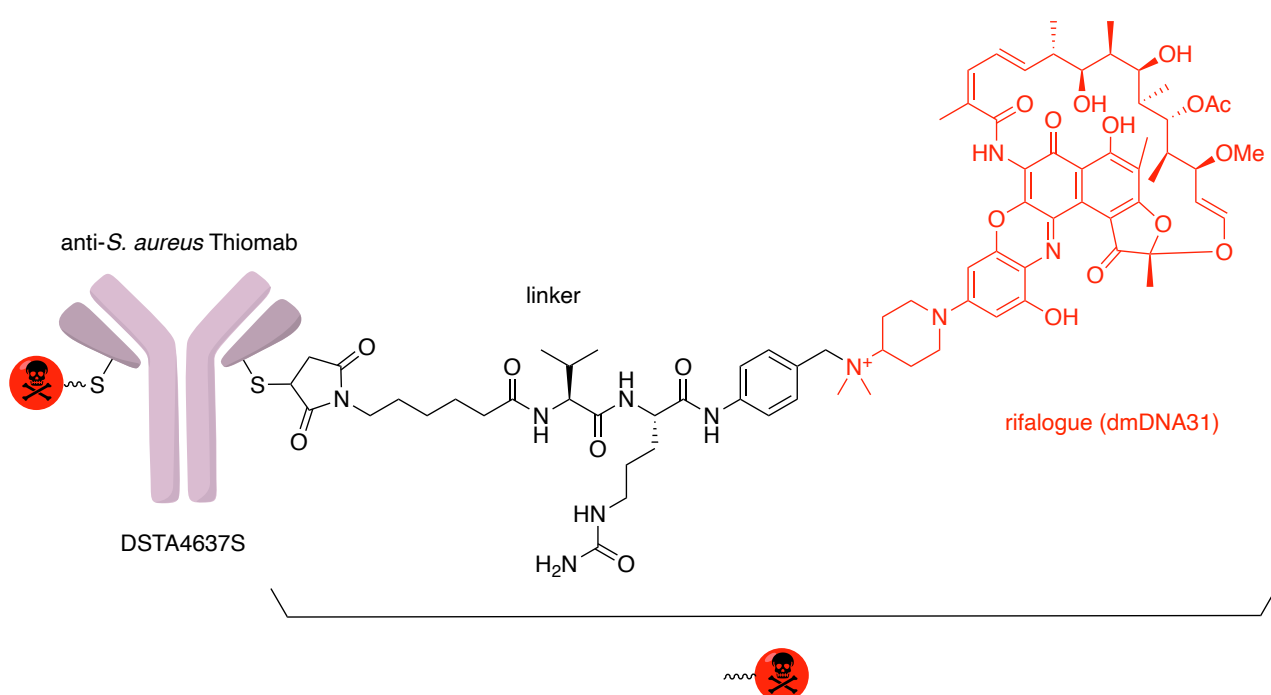


Figure 9. Structure of the *S. aureus*-targeted ADC 1 that is currently in clinical phase I^[75]. The antibiotic payload is drawn in red, the linker is drawn in black.

Huge molecular size and the complex molecular structure of ADCs are problematic. Oral bioavailability is virtually impossible and their large-scale production is complicated and expensive. Further, IgG antibodies extravasate slowly, thus reaching the site of infection correspondingly at reduced speed.^[77] These disadvantages can be avoided by small molecule targeted antibiotic conjugates.^[78] Recently, Tegge *et al.*^[79] presented targeted antimicrobial conjugates based on colistin. They used an Ubiquicidin-based antimicrobial peptide for the specific targeting of bacterial cell membranes. The authors showed that

their molecules indeed preferentially target the Gram-negative cell membrane, even in the presence of human erythrocytes, thrombocytes and white blood cells.

Please note that the classifications described above do not have strict borders, and can contain more than two features at once. Thus, antimicrobial conjugates can also belong to several classes at once, e.g. strain-specific antibiotic-siderophore conjugates. Bifunctional antimicrobial conjugates and hybrid antimicrobials were carefully and comprehensively reviewed by Klahn and Brönstrup.^[80]

Antibiotics that are active against Gram-negative bacteria tend to have a molecular weight below 600 Da and are usually rather hydrophilic.^[81] However, this is in contrast to the structures of most antimicrobial conjugates. To circumvent this problem, conjugates can be designed as prodrugs. Prodrugs have no or only little bioactivity, but can be transformed into the active principle by chemical or biological triggers, e.g. pH, Red/Ox-potential or enzymes. The introduction of a cleavable linker that releases the antibiotic cargo, e.g. triggered by neutrophil elastase, is a promising development in the design of antimicrobial conjugates. In fact, the two examples described above (DSTA4637S and Colistin-AMP conjugate) both contain cleavable linkers, that are processed by human enzymes and eventually release the antibiotic cargo.

2. Aim of the Thesis

The rise of new multi-resistant infections runs contrary to the development of new antibacterial agents. Less than a handful of antibacterial drugs with innovative chemical structures or new mode of actions found their way on the market in the last four decades (figure 4).^[44] The Gram-negative opportunistic *P. aeruginosa* is a particularly perilous pathogen leading to chronic and potentially deadly infections. Its ability to form biofilms during chronic infections results in increased antibiotic drug resistance. The extracellular *P. aeruginosa* lectins LecA and LecB are crucial for biofilm formation and could serve as anchors for targeted drug-delivery. Several LecA-/LecB-inhibitors have yet been synthesised in the department 'Chemical Biology of Carbohydrates', which will be used as lectin probes for this work.

The aim of this work was the design, synthesis and evaluation of carbohydrate-based antimicrobial conjugates, that target LecA and LecB within the *P. aeruginosa* biofilm. Increased drug concentrations at the site of infection can overcome antimicrobial resistance and reduce adverse side effects that are associated with unspecific drug distribution and inhibition of off-targets.

Three iterative generations of lectin-targeted antibiotic conjugates were envisaged for this work:

1. Design and synthesis of modular building blocks (lectin probes & antibiotic cargo) based on copper-click chemistry to rapidly access a small library of uncleavable antibiotic conjugates.
2. Introduction of a cleavable linker to obtain smart biofilm-targeted antibiotic prodrugs, that release their antibiotic cargo at the site of infection.
3. Introduction of divalent LecA-inhibitors to increase the target-affinity of the LecA-targeted smart conjugates.

3. Results

3.1. Directing Drugs to Bugs: Antibiotic-Carbohydrate Conjugates Targeting Biofilm-Associated Lectins of *Pseudomonas aeruginosa*

Authors: Joscha Meiers, Eva Zahorska, Teresa Röhrig, Dirk Hauck, Stefanie Wagner and Alexander Titz

Published in: *Journal of Medicinal Chemistry* **2020**, 63, 11707-11724.

DOI: 10.1021/acs.jmedchem.0c00856

The references of this chapter are listed at the end of the chapter.

Directing Drugs to Bugs: Antibiotic-Carbohydrate Conjugates Targeting Biofilm-Associated Lectins of *Pseudomonas aeruginosa*

Joscha Meiers, Eva Zahorska, Teresa Röhrig, Dirk Hauck, Stefanie Wagner, and Alexander Titz*

Cite This: *J. Med. Chem.* 2020, 63, 11707–11724

Read Online

ACCESS |



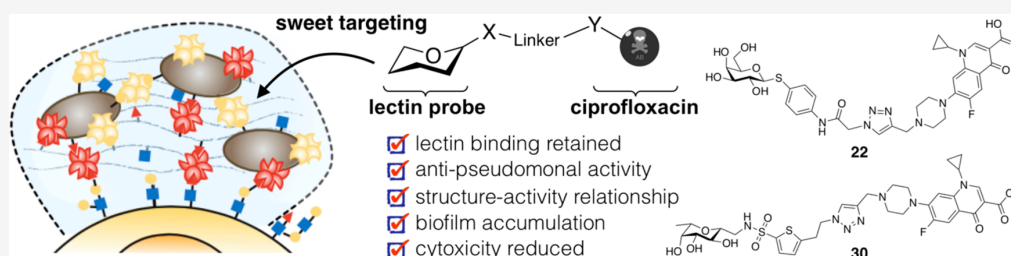
Metrics & More



Article Recommendations



Supporting Information



ABSTRACT: Chronic infections by *Pseudomonas aeruginosa* are characterized by biofilm formation, which effectively enhances resistance toward antibiotics. Biofilm-specific antibiotic delivery could locally increase drug concentration to break antimicrobial resistance and reduce the drug's peripheral side effects. Two extracellular *P. aeruginosa* lectins, LecA and LecB, are essential structural components for biofilm formation and thus render a possible anchor for biofilm-targeted drug delivery. The standard-of-care drug ciprofloxacin suffers from severe systemic side effects and was therefore chosen for this approach. We synthesized several ciprofloxacin-carbohydrate conjugates and established a structure–activity relationship. Conjugation of ciprofloxacin to lectin probes enabled biofilm accumulation *in vitro*, reduced the antibiotic's cytotoxicity, but also reduced its antibiotic activity against planktonic cells due to a reduced cell permeability and on target activity. This work defines the starting point for new biofilm/lectin-targeted drugs to modulate antibiotic properties and ultimately break antimicrobial resistance.

INTRODUCTION

The Gram-negative, opportunistic pathogen *Pseudomonas aeruginosa* has become a serious threat^{1–3} for immunocompromised patients (e.g., geriatrics, untreated HIV patients,^{4,5} and cancer patients⁶) and people suffering from cystic fibrosis (CF). Severe infections with *P. aeruginosa* can lead to recurrent pneumonia, lung damage, and sepsis.⁷ Its intrinsic antimicrobial resistance and its ability to acquire further resistances, which often lead to multidrug-/extensively drug-resistant (MDR/XDR) strains, are major obstacles for therapeutic treatment.⁸ As a consequence, the WHO stated *P. aeruginosa* in 2017 to be a critical priority 1 pathogen, which increases research and therapeutic focus on this particular Gram-negative pathogen.⁹ The ability to colonize almost any part of the human body can lead to various infected tissues, e.g., chronic wound infections, catheter-associated urinary tract infections or pneumonia, and further challenges clinicians to find an appropriate antibiotic therapy. Additionally, pharmacokinetic properties such as tissue distribution, oral bioavailability, and others vary from antibiotic to antibiotic. Thus, not every drug can reach the specific site of infection. Further, high drug levels at sensitive tissues can lead to hazardous side effects, e.g., ototoxicity of many aminoglycosides or tendon rupture and neuropathy after extensive use of fluoroquinolones.

The ability to form biofilms is a hallmark of chronic *P. aeruginosa* infections. During this stage of living, the cells cluster together in a biofilm matrix and produce a highly impenetrable barrier against host immune defense or antibiotics.^{10,11} These biofilm cells can show an up to 1000-fold increase in resistance against antibiotic drugs.¹² Despite the highly complex composition of the *P. aeruginosa* biofilm, the two quorum-sensing¹³ regulated extracellular virulence factors LecA¹⁴ and LecB¹⁵ (formerly called PA-IL and PA-IIL^{16–18}) stand out. It is assumed that these Ca²⁺-dependent tetravalent proteins crosslink bacteria with the biofilm matrix as well as host tissue via glycan binding (Figure 1). It was shown that these carbohydrate-binding proteins (i.e., lectins), amongst other biological roles, are crucial for biofilm formation and its structural integrity by *P. aeruginosa*.^{14,15} In the case of the D-mannose(D-Man)- and L-fucose(L-Fuc)-binding LecB, da Silva et al. recently showed that it organizes the localization of the

Received: May 20, 2020

Published: September 14, 2020



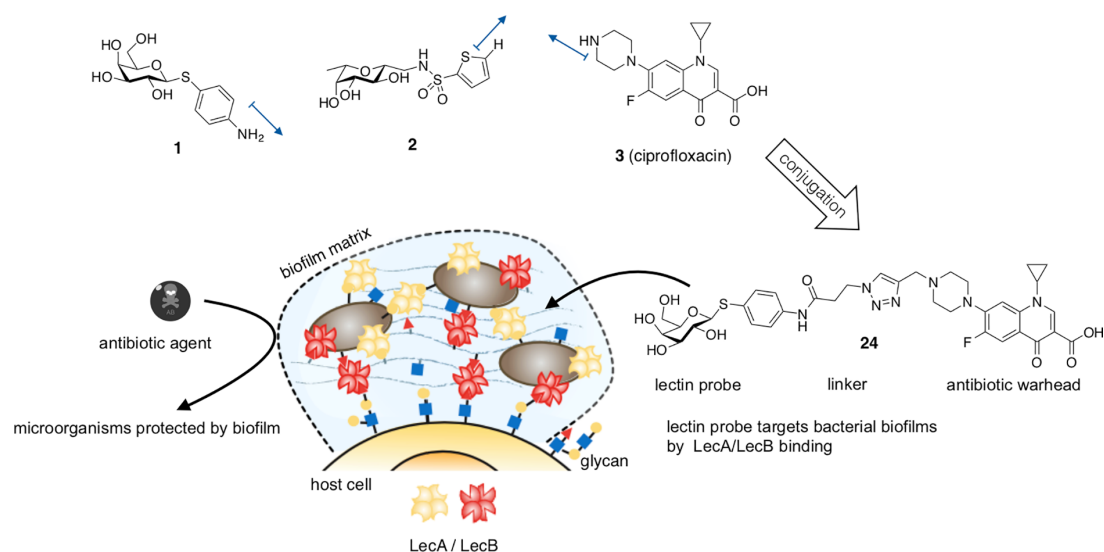


Figure 1. The lectin inhibitors **1** and **2** are conjugated to the antibiotic ciprofloxacin (**3**) resulting in pathogen-specific, lectin-targeted antibiotics. These compounds target the biofilm-associated lectins LecA and LecB and therefore increase local antibiotic concentration at the site of infection, resulting in fewer side effects caused by unspecific distribution and tissue accumulation. Blue arrows display growth vectors used in this work.

exopolysaccharide Psl in the biofilm matrix.¹⁹ Further, both lectins also play roles in the direct infection process: LecB conveys virulence through carbohydrate-dependent inhibition of human ciliary beating,²⁰ interference with repair of wounded tissues,^{21,22} and activation of B-cells.²³ Next to its biofilm-related roles, it was shown that the D-galactose-binding LecA triggers host cell signaling pathways²⁴ and mediates membrane invaginations after binding to its cellular receptor, the glycosphingolipid Gb3.²⁵ *In vivo*, both proteins are involved in the *P. aeruginosa* infection process and host colonization in a murine infection model.^{26,27} Interestingly, a study of *P. aeruginosa* infected CF patients and a case report on a pulmonary infected infant reported that the bacterial load in infected airways can be reduced by intrapulmonary application of fucose and galactose.^{28–30} Although *P. aeruginosa* is genetically highly diverse and adaptable,^{31,32} the protein sequence of LecA is highly conserved amongst clinical isolates. On the other hand, LecB does vary and can be clustered in either PAO1-like or PA14-like structures.³³ However, both LecB variants bind to same glycosides, making the design of LecB-inhibitors against a wide range of clinical *P. aeruginosa* strain isolates possible.^{33,34}

Lectin-carbohydrate interactions are usually characterized by weak binding affinity, which Nature circumvents by multivalent presentation of ligand or receptor.³⁵ Due to the high therapeutic interest, many compounds have been designed to inhibit LecA or LecB,^{36–38} most of them showing high affinity on the target in a multivalent fashion.^{39,40} Interestingly, LecB-directed multivalent molecules with nanomolar on-target activity required millimolar concentrations to inhibit biofilm formation of *P. aeruginosa*.²⁶ One possible explanation is the creation of additional crosslinks due to the protein's and ligand's multivalent structure, resulting in an undesired stabilization of the biofilm at therapeutic concentrations of the multivalent ligand.

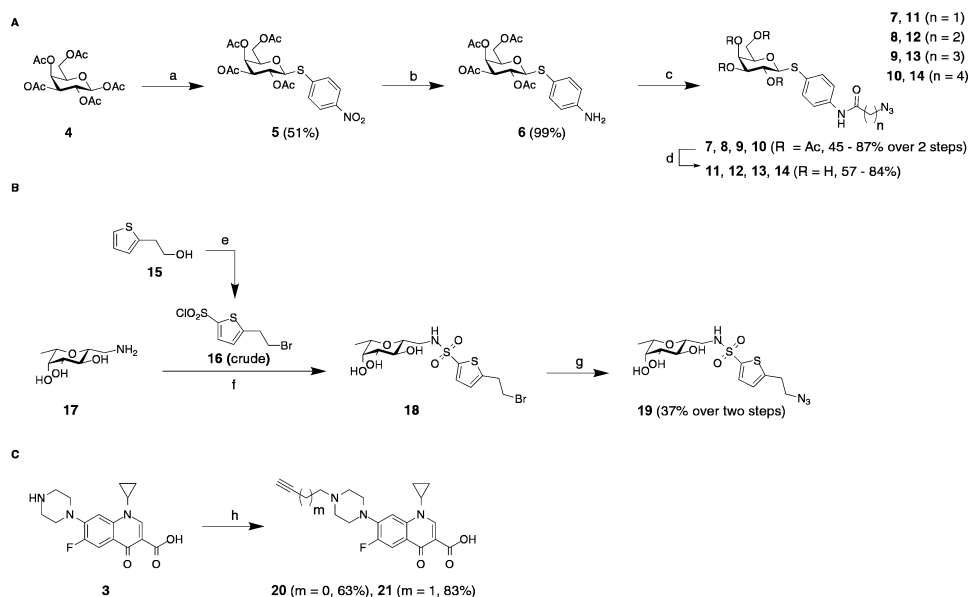
We have previously identified monovalent LecB inhibitors, sulfonamide-capped mannosides, and C-glycosides combining pharmacophores of its natural ligands, fucose and man-

nose.^{41–43} Recently, we reported the first drug-like, oral bioavailable LecB inhibitor **1** and established its SAR.^{44,45} Glycomimetic **1** showed excellent binding affinity against LecB and inhibited biofilm formation *in vitro* at micromolar concentrations. In mice, high plasma and urine concentrations were obtained after oral application.

Whilst LecB can be inhibited with high affinity ligands, LecA only shows moderate binding affinity against monovalent galactose-based compounds.^{36–38,46} Instead of a multivalent ligand presentation, we circumvented the rapid dissociation of the ligand–receptor complex by introduction of an electrophilic warhead in the first covalent lectin inhibitor. After conjugation of this galactose-based epoxide to a fluorescent dye, we used the resulting LecA-targeted dye to stain *P. aeruginosa* biofilms *in vitro*, proposing its potential use as biofilm-recognizing diagnostic tools.⁴⁷

Fluoroquinolone antibiotics are frequently used to treat a plethora of bacterial infections. The most common representative of this class is the drug ciprofloxacin, which is amongst other indications being used in cystic fibrosis-associated bronchopulmonary *P. aeruginosa* infections. Although fluoroquinolones were originally described to be pharmacologically safe, clinical phase IV studies revealed partially irreversible side effects like tendon ruptures or neuropathy, resulting from high tissue penetration and off-target effects. As a consequence, the fluoroquinolones have been categorized by drug agencies as high risk drugs and the U.S. Food and Drug Administration (FDA) issued a “black box” warning label,⁴⁸ and the German Federal Institute for Drugs and Medical devices (BfArM) informed medical professionals about prescription restrictions in 2019.

Paul Ehrlich coined the concept of a “magic bullet”, describing molecules that would specifically target only pathogenic bacteria or tumor cells.⁴⁹ One hundred fifty years later, this approach is on the way to become common therapeutic practice: Antibody-drug conjugates like trastuzumab-emtansine⁵⁰ led to a great success in cancer therapy and are also being studied in antimicrobial research.⁵¹ Further,

Scheme 1. Chemical Synthesis of the (A) LecA-Targeting (11–14) and (B) LecB-Targeting (19) Probes and (C) Alkyne Ciprofloxacin Derivatives 20 and 21^a

^aReagents and conditions: (a) *p*-nitrothiophenol, BF₃·Et₂O, CH₂Cl₂, 0 °C to r.t., 16 h; (b) H₂, Pd/C, CH₂Cl₂, r.t., 24 h; (c) (i) Br(CH₂)_nCOH, Et₃N, or K₂CO₃, DMF, 0 °C to r.t., 1–4 h, (ii) NaN₃, DMF, r.t., 4 h; (d) cat. NaOMe, MeOH, r.t., 1 h; (e) (i) PBr₃, CH₂Cl₂, 0 °C to r.t., 1 h, (ii) HSO₃Cl, CH₂Cl₂, 0 °C to r.t., 3 h; (f) crude **16**, K₂CO₃, DMF, r.t., 5 h; (g) NaN₃, DMF, r.t., 5 h; (h) propargyl bromide or 4-bromo-but-1-yne, Et₃N, DMF, 70 °C, 1–4 d.

many antibiotic conjugates have been described so far, mainly targeting bacterial uptake mechanisms or non-targeted dual acting antibiotics (reviewed in refs 52, 53). Interestingly, carbohydrate conjugates of ciprofloxacin were described to increase bacterial cell uptake via sugar transporters.^{54,55} Inspired by the successful detection of *P. aeruginosa* biofilms with LecA-directed dyes, we aimed to conjugate glycomimetics to ciprofloxacin in order to target the extracellular *P. aeruginosa*-specific, biofilm-related virulence factors LecA and LecB. By exploiting lectin accumulation in the *P. aeruginosa* biofilm, the targeted conjugates shall deliver their antibiotic cargo specifically to the site of infection. Thus, an enhanced local drug concentration could overcome antimicrobial resistance and lower nonspecific drug distribution, potentially reducing systemic side effects (Figure 1). Here, we report the synthesis of the first lectin-targeted antibiotic conjugates and their microbiological and biochemical evaluation. We describe an antimicrobial structure–activity relationship of these lectin binding conjugates and show their biofilm accumulation *in vitro*.

RESULTS AND DISCUSSION

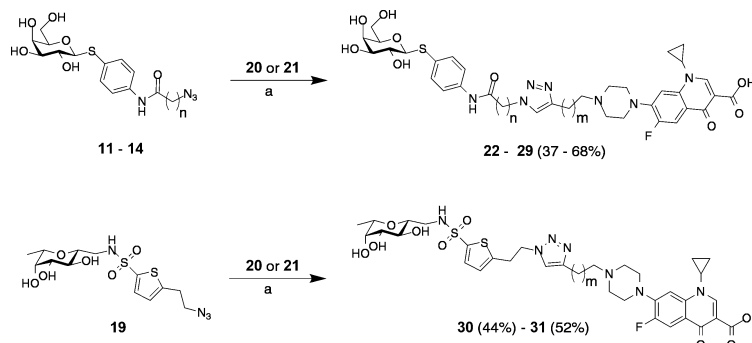
Design. The design of the lectin-targeted conjugates followed the established structure–activity relationships (SAR) of their individual components, i.e., targeting moiety and ciprofloxacin cargo.

The targeted lectins LecA and LecB both show shallow carbohydrate binding sites on their protein surfaces. As a consequence, linking a cargo to specific sites at the published probes without losing lectin inhibition activity was plausible. The SAR of D-galactose-based LecA inhibitors revealed β-linked aromatic aglycons to be vital for potent LecA inhibition. Further substitutions at the aromatic aglycon only result in

minor changes in binding affinity.^{56–58} In the complex with LecA, the ligand's surface-exposed phenyl aglycon reveals a potential growth vector for the conjugation of cargo to the para-position.⁵⁹ As this linking strategy was used to stain *P. aeruginosa* biofilms *in vitro*,⁴⁷ we decided to similarly link an antibiotic cargo, using **1** as a LecA targeting probe. To increase the metabolic stability, the O-glycosidic structure was replaced with a thioglycoside. The potent LecB inhibitor **2** displays a C-glycosidic hybrid structure, merging target interactions of D-mannose and L-fucose. The attachment of an aromatic sulfonamide addressed an additional subpocket on LecB.^{41–44} Analysis of the co-crystal structure of LecB in complex with **2** and extensive SAR studies⁴⁵ revealed a potential growth vector on position 5 of the thiophene ring for subsequent conjugation to the antibiotic cargo.

Fluoroquinolones represent a highly active class of antibiotics, deriving from their predecessor nalidixic acid. The SAR of the fluoroquinolones^{60–63} is well described and exploited in several antimicrobial conjugates. Its main pharmacophore, 6-fluoro-quinolone-3-carboxylic acid, is essential for inhibition of its intracellular target, bacterial gyrase. Substitutions at position 7 mainly modify and fine-tune pharmacokinetic properties and strain specificity. In the case of ciprofloxacin, the presence of a piperazine increases anti-pseudomonal activity.⁶⁴ We chose to derivatize the synthetically accessible secondary amine of the piperazine ring to a tertiary amine as this would result only in a smaller change of its physicochemical properties that influence porin-mediated bacterial cell uptake, as compared to, e.g., amide formation. Furthermore, analysis of the co-crystal structure⁶⁵ of ciprofloxacin with the GyrA/GyrB heterodimer showed a possible growth vector at this position (Figure 1).

Copper-catalyzed Huisgen-type [3+2] cycloaddition of terminal alkynes and terminal azides was chosen as a

Scheme 2. Assembly of the Lectin-Targeted Ciprofloxacin Conjugates⁴

^aReagents and conditions: (a) cat. CuSO_4 , cat. sodium ascorbate, DMF/ H_2O , r.t. 16 h, r.t. (for 11–14) or 40 °C (for 19).

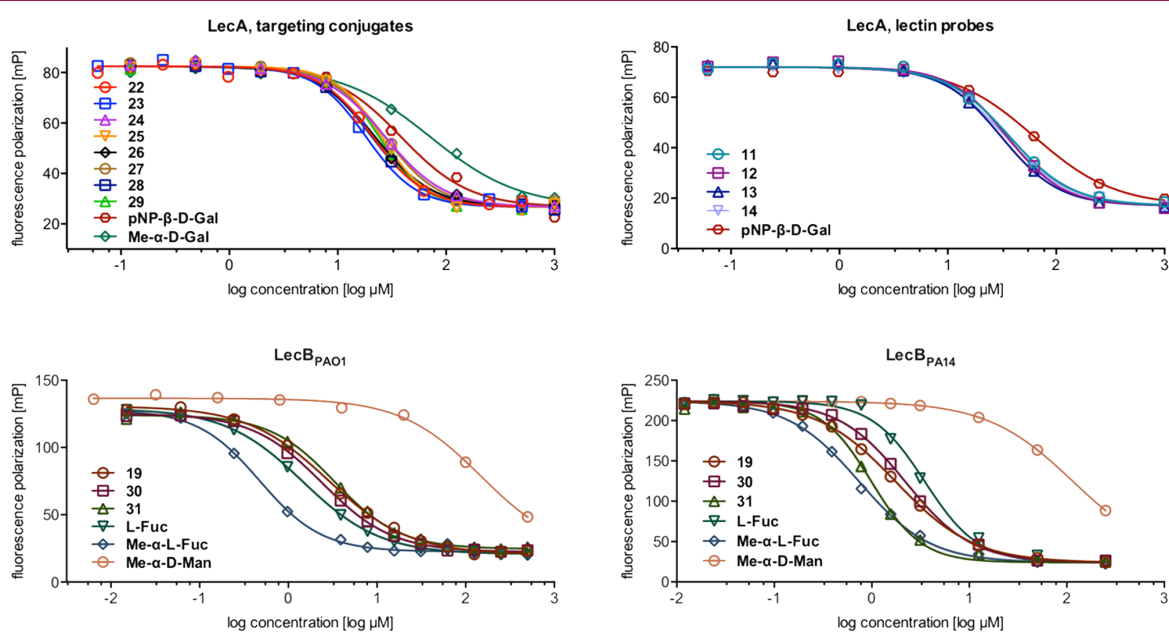


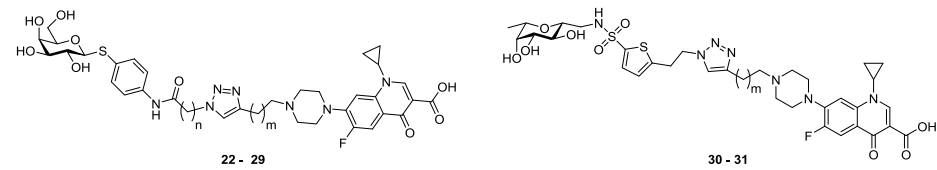
Figure 2. Competitive binding assay of lectin-targeted ciprofloxacin conjugates 22–31, lectin probes 11–14 and 19, and control compounds with LecA, LecB_{PA01}, and LecB_{PA14}. One representative titration of triplicates on one plate is shown for each compound (IC_{50} in Table 1 and K_i in Table S1).

convenient and modular way of linking both moieties. Further, we decided to analyze the impact of the linker length and flexibility on antibiotic activity by stepwise introduction of methylene spacers.

Synthesis. The LecA-targeting precursor 6 (Scheme 1) was synthesized in analogy to Casoni et al.⁶⁶ Glycosylation of the acceptor *para*-nitrothiophenol with galactose pentaacetate (4) using $\text{BF}_3 \cdot \text{Et}_2\text{O}$ as a Lewis acid resulted in thioglycoside 5 in 51% yield. Palladium-catalyzed hydrogenation gave the corresponding aniline 6 quantitatively. Compound 6 was then treated with various ω -bromo acylhalides followed by a nucleophilic substitution with sodium azide to the corresponding azides 7–10 in one pot. The usage of triethylamine during the amide coupling led to β -elimination in the case of the propionic acid derivative 7 or γ -lactam formation in the case of bromide 13, which could be circumvented by using potassium carbonate as a base. Deprotection of acetates 7–10 under Zemplén conditions resulted in the LecA-probes 11–14.

Based on the results from the antimicrobial susceptibility testing (*vide infra*), we synthesized only one LecB probe (Scheme 1). β -C-glycoside 17 was synthesized as reported.⁴² Thiophene building block 16 was synthesized from 15 in two steps: The primary alcohol 15 was transformed to the corresponding bromide with phosphorous tribromide followed by chlorosulfonation of the thiophene in position 5 with chlorosulfonic acid. Crude sulfonylchloride 16 was reacted with amine 17 to yield sulfonamide 18. This intermediate was stirred with sodium azide to give compound 19 in an overall yield of 37% over two steps based on the amine starting material 17.

Alkylation of ciprofloxacin with propargyl bromide or 4-bromobut-1-yne in DMF at elevated temperatures yielded the corresponding terminal alkynes 20 and 21. Finally, copper-catalyzed 1,3-dipolar cycloaddition of alkynes 20 and 21 with azides 11–14 and 19 resulted in the lectin-targeted ciprofloxacin conjugates 22–31 (Scheme 2).

Table 1. Competitive Binding Assay of Lectin-Targeted Ciprofloxacin Conjugates and Control Compounds with LecA, LecB_{PAO1}, and LecB_{PA14}^a


| LecA | | | |
|----------------------|------------|------------------------------|------------------------------|
| compound | n | m | IC ₅₀ ± s.d. [μM] |
| 11 | 1 | | 31.7 ± 11 |
| 12 | 2 | | 30.9 ± 8.7 |
| 13 | 3 | | 31.1 ± 8.3 |
| 14 | 4 | | 29.9 ± 9.5 |
| 22 | 1 | 0 | 30.4 ± 8.0 |
| 23 | 1 | 1 | 21.6 ± 5.5 |
| 24 | 2 | 0 | 32.2 ± 3.3 |
| 25 | 2 | 1 | 28.0 ± 1.8 |
| 26 | 3 | 0 | 27.3 ± 4.0 |
| 27 | 3 | 1 | 29.3 ± 3.7 |
| 28 | 4 | 0 | 28.3 ± 8.1 |
| 29 | 4 | 1 | 26.2 ± 2.4 |
| Me-α-D-Gal | | controls | 71.7 ± 16 |
| pNP-β-D-Gal | | | 52.7 ± 13 |
| LecB _{PAO1} | | | |
| compound | m | IC ₅₀ ± s.d. [μM] | LecB _{PA14} |
| 19 | LecB-probe | 3.91 ± 1.6 | IC ₅₀ ± s.d. [μM] |
| 30 | 0 | 2.37 ± 1.2 | 1.87 ± 0.21 |
| 31 | 1 | 2.53 ± 0.87 | 2.24 ± 0.23 |
| Me-α-D-Man | | 166 ± 22 | 1.00 ± 0.06 |
| L-Fuc | controls | 2.63 ± 1.7 | 101 ± 10 |
| Me-α-L-Fuc | | 0.534 ± 0.07 | 2.46 ± 0.33 |
| | | | 0.79 ± 0.11 |

^aMeans and standard deviations were determined from a minimum of three independent experiments. K_i calculated from IC₅₀ is shown in Table S1.

Biophysical and Microbiological Evaluation. *Competitive Lectin Binding Assay Based on Fluorescence Polarization.* To analyze lectin binding of the targeted antibiotics, we quantified their binding affinity to LecA or LecB in the previously reported competitive binding assays.^{33,41,58}

The binding affinity of the LecA-targeting conjugates 22–29 did not significantly differ from their corresponding lectin probes 11–14 (Figure 2 and Table 1), reaching IC₅₀ values from 26 to 30 μM. Thus, they show an up to 2-fold increased inhibitory activity against LecA compared to *p*-nitrophenyl β-D-galactoside (pNP-β-D-Gal, IC₅₀ = 52.7 ± 13 μM) and an up to 3-fold increase compared to methyl α-D-galactoside (Me-α-D-Gal, IC₅₀ = 71.7 ± 16 μM), which served as reference compounds in this study.

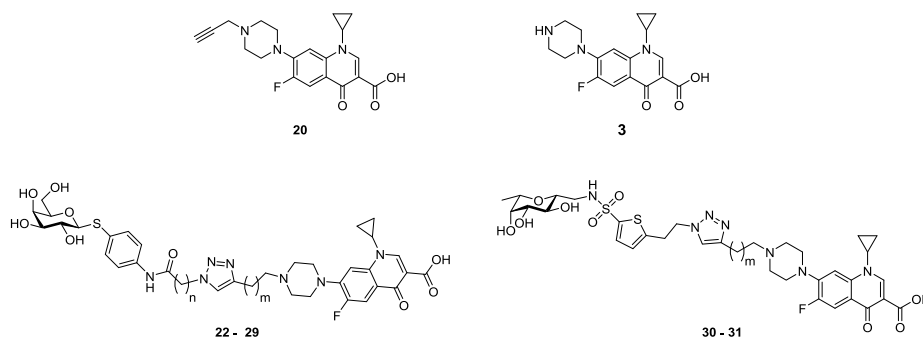
Competitive binding assays against LecB_{PAO1} (Figure 2 and Table 1) revealed IC₅₀ values in the one digit micromolar range for LecB probe 19 (IC₅₀ = 3.91 ± 1.6 μM) and its corresponding conjugates 30 and 31 (IC₅₀ = 2.37 ± 1.2 and 2.53 ± 0.87 μM, respectively), which is in the range of L-fucose (IC₅₀ = 2.63 ± 1.7 μM). The two glycosides, methyl α-D-mannoside (Me-α-D-Man) and methyl α-L-fucoside (Me-α-L-Fuc), which resemble terminal glycan structures recognized by LecB showed IC₅₀ values of 166 ± 22 and 0.534 ± 0.07 μM, respectively. The inhibition assay on LecB_{PA14} showed similar trends (Table 1). As observed previously,³³ LecB_{PA14} binds its ligands with higher affinity (e.g., IC₅₀ of 1.00 μM vs 2.53 μM for compound 31). Since *P. aeruginosa* PA14 and PAO1 are

representative for many clinical isolates, a broad range of *P. aeruginosa* strains can be targeted by these conjugates.

Comparing the conjugates with the unlinked lectin probes showed in all cases a comparable binding affinity. Further, all compounds showed better binding than Me-α-D-Gal (LecA) or Me-α-D-Man (LecB). Due to the highly optimized structure of the fucose-mannose pharmacophore, the LecB targeting compounds were comparably active on LecB as L-fucose. In conclusion, the topology of the carbohydrate binding sites in both proteins allowed the conjugation with an antibiotic cargo without influencing lectin binding.

Antibiotic Susceptibility Assay. The antibiotic activity of lectin-targeted ciprofloxacin conjugates 22–31 was tested against a panel of Gram-positive and Gram-negative bacteria (Table 2). The model organisms *E. coli* MG1655 (a common lab strain), *E. coli* DSM 1116 (an antibiotic susceptibility reference strain recommended by the DSMZ), and the Gram-positive *Staphylococcus carnosus* DSM 20501 were tested first to assess Gram-negative specific antibiotic activity and strain specificity. Afterward, the antibiotic activity against the two *P. aeruginosa* strains PA14 and PAO1 was studied. These two important reference strains represent a broad range of clinical isolates and are well studied in the literature.³³ To determine the effect of the lectins' presence on antibiotic activity, we used the lectin-deficient knockout mutants of *P. aeruginosa* PA14, i.e., PA14 Δ*lecA* and PA14 Δ*lecB*. Ciprofloxacin (3) and the synthetic intermediate 20 were used as reference compounds

Table 2. Antibacterial Activity of Lectin Targeted Conjugates 22–31, 20, and Ciprofloxacin (3) against a Panel of Bacterial Organisms. LecA-targeting galactosides were generally more active than the LecB-targeting conjugates. A shorter linker length on the side of the antibiotic led to increased antimicrobial activity^a



| compound | target: LecA | | | | | | target: LecB | | | | references | |
|---|--------------------------|-----------|-------|-------|-------|-------|--------------|-----------|-----------|-----------|------------|------------|
| | 22 | 23 | 24 | 25 | 26 | 27 | 28 | 29 | 30 | 31 | 20 | 3 |
| molecular mass [g/mol] | 739.8 | 753.8 | 753.8 | 767.8 | 767.8 | 781.9 | 781.9 | 795.9 | 761.8 | 775.9 | 369.4 | 331.3 |
| linker length n/m | 1/0 | 1/1 | 2/0 | 2/1 | 3/0 | 3/1 | 4/0 | 4/1 | -/0 | -/1 | 0 | |
| test organism | MIC [$\mu\text{g/mL}$] | | | | | | | | | | | |
| <i>E. coli</i> K12 MG1655 | 2 | 8–16 | 2 | 16 | 1–2 | 16 | 2–4 | 16 | 8–16 | 16 | n.d. | <0.125 |
| <i>E. coli</i> DSM 1116 | 2–4 | 16 | 2–4 | 32 | 2–32 | 4–32 | 4–32 | 4–32 | 16–32 | 32 | n.d. | <0.125 |
| <i>S. carnosus</i> DSM 20501 | 32 | 64 | 32 | >64 | 16 | 64 | 8 | ≥ 64 | >64 | >64 | n.d. | <0.125 |
| <i>P. aeruginosa</i> PA14 wt | 16 | ≥ 64 | 8–16 | >64 | 8–16 | >64 | 32 | >64 | >64 | >64 | 2–4 | 0.025–0.1 |
| <i>P. aeruginosa</i> PA14 wt + 1 $\mu\text{g/mL}$ PMBN | 4–16 | 16–64 | 8–16 | 32–64 | 4 | 32–64 | 2–8 | 32–64 | 64 | 64 | 0.025–0.5 | 0.025 |
| <i>P. aeruginosa</i> PA14 ΔlecA | 16–32 | ≥ 64 | 8–16 | >64 | 8–16 | >64 | 32 | >64 | ≥ 64 | >64 | 4–8 | 0.05–0.08 |
| <i>P. aeruginosa</i> PA14 ΔlecB | 16–32 | ≥ 64 | 8–32 | >64 | 8–16 | >64 | 32–64 | >64 | 64 | >64 | 4 | 0.05–0.08 |
| <i>P. aeruginosa</i> PAO1 wt | 16–32 | >64 | 16 | >64 | 16–32 | >64 | 32–64 | >64 | ≥ 64 | >64 | 4–8 | 0.025–0.08 |
| <i>P. aeruginosa</i> PAO1 wt + 1 $\mu\text{g/mL}$ PMBN | 4–8 | 32–64 | 4–8 | 32–64 | 4–8 | 32–64 | 8–16 | 32–64 | 32–64 | ≥ 64 | 1–2 | 0.025–0.05 |

^aData is presented as minimal inhibitory concentration (MIC) range from at least three independent experiments. Molar MIC is given in Table S2. n.d. = not determined.

to study the effect of piperazine N-alkylation on antibiotic activity.

Ciprofloxacin is known to be particularly active against Gram-negative compared to Gram-positive organisms. Both *E. coli* strains showed higher susceptibility against the ciprofloxacin conjugates than the Gram-positive organism *S. carnosus*. Comparing both *E. coli* strains, the antibiotic susceptibility reference strain (DSM 1116) showed similar or slightly higher MIC values (Table 2).

Compared to *E. coli*, *P. aeruginosa* PA14 and PAO1 both showed lower susceptibility against all compounds tested, which was expected due to the well-known increased intrinsic antimicrobial resistance of *P. aeruginosa*. It was also observed that the clinical isolate PAO1 was similarly or slightly less susceptible than the clinical isolate PA14. Importantly, some of the lectin-targeted conjugates reached antibiotic activity down to 8 $\mu\text{g/mL}$ against planktonic *P. aeruginosa* (Table 2).

Comparing the MIC values amongst the different conjugates and the reference compounds 20 and ciprofloxacin (3), we observed a structure–activity relationship: Conjugates containing galactosides as lectin-targeting probes showed higher antimicrobial activity than LecB-targeting compounds, which are based on a C-glycosidic hybrid structure. It has been previously postulated that galactosides are recognized by the bacterial sugar uptake machinery,^{54,55} which would result in an active transportation over the Gram-negative cell wall. A comparative study by O’Shea and Moser⁶⁵ on commonly used

antibiotics showed that especially *P. aeruginosa* active compounds have clogD values of <0 . LogD calculation (data not shown) of all conjugates 22–31 and 20 revealed positive values, which could explain the reduction in antimicrobial activity with respect to ciprofloxacin (3) showing a clogD of <0 .

Further, a decreased linker length between triazole and ciprofloxacin (entitled m in the structure drawings) amplified the antibiotic activity in all cases, independent of the carbohydrate probe or microorganism tested. This effect becomes most evident in case of *E. coli* K12 MG1655, where an up to 8-fold increase in MIC could be observed (e.g., 24 vs 25, Table 2). We assume that changing the distance between the tertiary amine and the electron-withdrawing triazole affects the amine’s basicity, which is believed to play a role in porin diffusion.⁶⁷ The parent drug ciprofloxacin reached MIC values of 0.025–0.1 $\mu\text{g/mL}$ against *P. aeruginosa*, while the propargylated derivative 20 showed MIC values of 2–4 $\mu\text{g/mL}$ against *P. aeruginosa* PA14 and 4–8 $\mu\text{g/mL}$ against *P. aeruginosa* PAO1, thereby reaching the concentration range of the most potent conjugates. As alkylation of ciprofloxacin alone already led to a significant decrease in activity, conjugation at the secondary amine in the piperazine ring is most likely responsible for the decreased antibiotic activity.^{60–62}

Regarding total linker size, increasing length resulted in higher MIC values (e.g., 22 vs 29), which can be explained by a size exclusion effect of outer membrane porins. It is believed

that these barrel-formed, hydrophilic channels play crucial roles for membrane permeation of hydrophilic compounds and are limited to a certain molecular weight or three-dimensional molecular structure.^{67,68} Further, the introduction of additional methylene groups results in an increased number of rotatable bonds and increased lipophilicity, which is also described to reduce bacterial cell uptake.^{67,68} We compared retention times from reversed-phase HPLC analyses as a surrogate parameter for lipophilicity (Table S4 and Figure S4). Two trends were observed that correlated with the antimicrobial activity assays: (i) In general, all galactose-based conjugates showed lower retention times than the C-glycosides indicative for higher polarity, and (ii) the stepwise introduction of methylene groups in both linkers led to a stepwise increase in retention times indicating higher lipophilicity, which correlated with the reduced antimicrobial activity. Only the shortest galactose-based conjugates **22** and **23** ($n = 1$, $m = 0$ or 1 , respectively) showed retention times slightly higher than expected in their series, which may be a result of an intramolecular hydrogen bonding between the amide NH and the central nitrogen atom of the triazole for $n = 1$ altering their conformation and thus their physicochemical properties. We observed that the most anti-*Pseudomonas* active compound **24** showed the lowest retention time amongst the conjugates. Thus, we conclude that the conjugates' lipophilicity is an important parameter for antimicrobial activity. Ciprofloxacin (**3**) was eluted much earlier than all conjugates, reflecting its higher hydrophilicity.

Polymyxin B nonapeptide (PMBN) is a membrane-active antimicrobial compound that is used at sub-MIC concentrations to increase outer membrane permeability. Without being lethal to the microbe, this can provide information on bacterial cellular uptake of antimicrobial drugs. In our studies, all conjugates, except **24** and **30**, benefit from the presence of the permeabilizer at least twofold (e.g., **26**, Table 2). Interestingly, the MIC of reference compound **20** was increased most and reached high antimicrobial activity approximating ciprofloxacin. Thus, the drop in antibiotic activity for the conjugates can partially be explained by decreased cell wall permeability, as a consequence of derivatization of the secondary amine. As expected, unmodified ciprofloxacin benefitted only marginally by the addition of PMBN.

Gyrase-Dependent DNA Supercoiling Inhibition Assay. The antimicrobial susceptibility assays revealed a decrease in antibiotic activity after conjugation (Table 2). We showed that this decrease is most likely caused by a reduced bacterial cellular uptake as shown by the co-incubation experiments with membrane permeabilizer. However, the addition of PMBN did not result in MIC values comparable to ciprofloxacin, suggesting that further features are affected by conjugation of ciprofloxacin to the lectin probes. Thus, we investigated the compounds' ability to inhibit bacterial gyrase, the target of ciprofloxacin.

We compared the gyrase inhibition activity of three conjugates (**22**, **23**, and **30**), while the propargylated ciprofloxacin derivative **20** and unmodified ciprofloxacin (**3**) were used as controls (Figure 3). Gyrase-inhibition leads to a reduction of supercoiled DNA, which can be visualized by gel electrophoresis. Ciprofloxacin was the most active compound, reaching full inhibition of plasmid supercoiling in the nanomolar range. Compound **20** ($IC_{50} = 0.7 \pm 0.1 \mu M$) was less active than ciprofloxacin; however, it still showed an IC_{50} in the nanomolar range, suggesting that modification in this

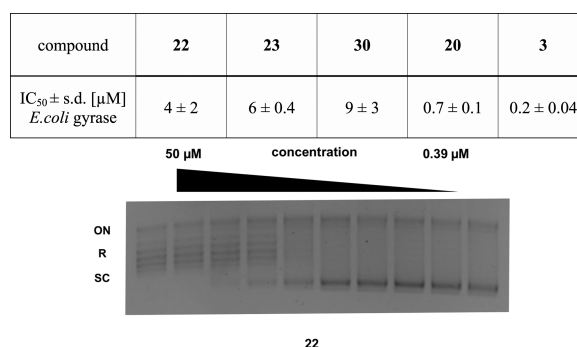


Figure 3. Effect of **20**, **22**, **23**, **30**, and ciprofloxacin (**3**) on gyrase-catalyzed DNA supercoiling. Propargylation (**20**) decreased the inhibitory concentration only by a factor of 3.5 compared to **3**. Gyrase inhibition as a putative mode of action was confirmed as all conjugates inhibit gyrase-catalyzed DNA supercoiling. Mean and standard deviations were determined from three independent experiments. A representative titration of *E. coli* gyrase with **22** in a supercoiling inhibition assay is shown. Controls: plasmid without gyrase and inhibitor (leftmost band) and plasmid with gyrase and without inhibitor (rightmost band). ON, open circular/nicked plasmid; R, relaxed topoisomers; SC, supercoiled topoisomers of *E. coli* DNA.

region of the molecule as concluded from the crystal structure analysis is indeed possible. The lectin-targeting conjugates were also potent inhibitors of gyrase supercoiling activity in the single digit micromolar range, although they were not as potent as reference compounds **20** and **3**. This decrease in activity explains why the compounds did not reach the antibiotic activity of *N*-propargyl ciprofloxacin (**20**) after membrane permeabilization with PMBN.

***P. aeruginosa* Biofilm Accumulation Assay.** Since the carbohydrate-ciprofloxacin conjugates **22–31** bind their respective lectins in a competitive binding assay, we investigated the ability of two representative lectin-targeting conjugates to accumulate in *P. aeruginosa* biofilms *in vitro* (Figure 4).

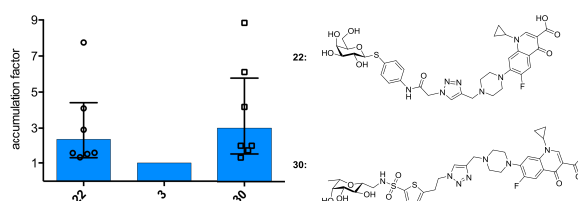


Figure 4. Accumulation of **22** (targeting LecA) and **30** (targeting LecB) in *P. aeruginosa* PAO1 biofilm relative to ciprofloxacin (**3**). Each data point reflects the relative accumulation compared to ciprofloxacin of a single independent assay with at least three technical replicates. Bars show geometric mean and 95% confidence interval (see the Supporting Information for more detailed information, Figure S2).

For this purpose, biofilms were grown on peg lids in a 96-well format that allows incubation and washing steps in a batch format. After 24 h of bacterial growth, *P. aeruginosa* PAO1 formed a visible biofilm on the pegs, which was used for compound accumulation assays. After one washing step to remove planktonic bacteria, the biofilm was immersed for 10 min into solutions containing two lectin-targeting conjugates (**22** and **30**) or ciprofloxacin (**3**) at $100 \mu M$. After a

Table 3. Early ADMET Data on Two Representative Lectin-Targeted Conjugates (22 and 30) and Ciprofloxacin (3): All Compounds Were Metabolically Stable in Human Plasma and Microsomal Fractions. Cytotoxicity was reduced compared to ciprofloxacin^a

| compound | metabolic stability | | | plasma protein binding [%] | cytotoxicity @ 100 μ M [% inhibition] | | |
|----------|---------------------|--------------------------------------|------|----------------------------|---|-------------|------|
| | $t_{1/2}$ [min] | CL_{MIC} [μ L/min/mg protein] | | | human plasma | HEK293 | AS49 |
| | human plasma | MLM | HLM | | | | |
| 22 | >150 | 10 | 10 | 69 \pm 7 | 8 \pm 4 | 5 \pm 22 | |
| 30 | >150 | 10 | 15 | 75 \pm 10 | 11 \pm 12 | -9 \pm 15 | |
| 3 | >150 | n.d. | n.d. | 33 \pm 2 | 48 \pm 5 | 18 \pm 11 | |

^aData is presented as mean and standard deviation from at least two independent experiments (exception: one experiment for CL_{MIC} data). MLM, mouse liver microsomes; HLM, human liver microsomes; n.d., not determined.

subsequent washing step to remove an unspecifically bound compound, the biofilm was disrupted and the amount of bound compound was quantified by LC-MS/MS.

Although the assay showed variation in absolute compound binding between biological replicates (Figure S2), we observed an obvious trend: the lectin targeted conjugates reached higher concentrations in the bacterial biofilm than the unmodified ciprofloxacin, independent of their lectin targeting moiety (Figure 4). These results are fundamental for the future development of further biofilm targeting antibiotic conjugates.

In Vitro Early ADMET. Metabolic stability of two representative conjugates (22 and 30) and ciprofloxacin (3) as the parent molecule was studied *in vitro* against human plasma, human liver microsomes, and mouse liver microsomes (Table 3). The data reveals high metabolic stability in all matrices tested: half-life in human plasma was above 150 min for all compounds and microsomal clearance by mouse and human liver microsomes was very low on the lectin-targeting compounds. Both conjugates showed clearance of 10 μ L/min/mg protein by human liver microsomes, reaching the assay's lower limit. Against mouse liver microsomes, compound 22 also reached the assay limit of 10 μ L/min/mg protein, whereas 30 was slightly less stable (CL_{MIC} = 15 μ L/min/mg protein) but still classified in the most stable category of this assay (≤ 15 μ L/min/mg protein). Thus, the compounds are considered metabolically stable, fitting the molecular design approach as S-/C-glycosides. Both conjugates showed higher plasma protein binding than ciprofloxacin (69 \pm 7% for 22, 75 \pm 10% for 30 vs 33 \pm 2% for 3).

Acute cytotoxicity was tested against a human embryonic kidney cell line (HEK 293) and adenocarcinoma human alveolar basal epithelial cells (AS49). Compounds 22 and 30 showed no cytotoxicity at 100 μ M after 48 h incubation, whereas ciprofloxacin showed detectable cytotoxicity (48 \pm 5% inhibition) against HEK 293 cells (Table 3). Furthermore, penetration over cultured human airway epithelial cells (Calu-3 HTB-55) was assessed *in vitro* via a Transwell system to analyze the compounds ability to permeate over mammalian cell membranes. No detectable permeation (apical to basal) was observed for compounds 22 and 30 after 4 h, while 10% ciprofloxacin was permeated after 4 h (data not shown). The low acute toxicity against human alveolar basal epithelial cells and the low lung cell permeation suggest the possibility of pulmonary application routes for patients suffering from cystic fibrosis.

CONCLUSIONS AND OUTLOOK

Biofilms present a hallmark in chronic *P. aeruginosa* infections. The ability to protect against the host immune system and

antibiotic treatment renders this chemo-mechanic barrier as a strong virulence factor. Notably, it is not advisable to solely focus MIC optimization on planktonic cells during the development of new antibiotics but rather to find new therapeutic strategies. As an example, Müsken et al. showed that biofilm susceptibility of clinical *P. aeruginosa* isolates cannot be deduced from commonly studied phenotypes like MIC or minimal bactericidal concentration values.⁶⁹ Delivering antibiotics specifically to the site of infection could decrease potential side effects and enhance efficacy. In this work, we developed and characterized the first *P. aeruginosa* lectin-targeted antibiotic conjugates. Based on our previous work, we conjugated ciprofloxacin to LecA and LecB probes and varied the linker length.

The antibiotic conjugates showed effective lectin binding against LecA and both LecB variants from *P. aeruginosa* PAO1 and PA14, which represent a broad range of clinical isolates of *P. aeruginosa*. A structure–activity relationship regarding the antimicrobial activity of the synthesized conjugates could be established. In general, a shorter spacer between triazole and antibiotic as well as a D-galactose-based lectin probe was preferred. The observed reduction in antibiotic activity could be rationalized due to a higher molecular weight, decreasing the ability to penetrate the Gram-negative cell wall. Comparison with N-propargylated ciprofloxacin showed, that alkylation of the secondary amine of the piperazine ring already resulted in a decreased antibiotic activity. Further, we proved the inhibition of gyrase-catalyzed DNA supercoiling as the conjugates' antimicrobial mode of action.

In the first *P. aeruginosa* biofilm accumulation assay, we observed an enrichment of lectin-targeting conjugates compared to ciprofloxacin, which could compensate for the decrease in antimicrobial activity. Since cytotoxicity of both conjugates was decreased compared to ciprofloxacin especially against kidney cells, and the biofilm accumulation was achieved, a reduction of the severe systemic side effects of ciprofloxacin is possible. Further, *in vitro* metabolism assays showed good metabolic stability supporting the conjugates' design as S- or C-glycosides.

This work reports the first *P. aeruginosa* biofilm-targeted antibiotics and analyzes their properties on lectin binding, antimicrobial activity, target inhibition, and biofilm enrichment. *In vitro* studies revealed a reduced cytotoxicity of the conjugates compared to the parent drug ciprofloxacin. Future work will address the improvement of antimicrobial activity of the antibiotic conjugates. Our modular synthesis allows the conjugation of lectin probes to other antibiotics, leading to future generations of biofilm targeting antibiotics.

EXPERIMENTAL SECTION

Chemical Synthesis. Thin layer chromatography (TLC) was performed on Silica Gel 60 coated aluminum sheets containing a fluorescence indicator (Merck KGaA, Darmstadt, Germany) and developed under UV light (254 nm) and aqueous KMnO_4 solution or a molybdate solution (a 0.02 M solution of ammonium cerium sulfate dihydrate and ammonium molybdate tetrahydrate in aqueous 10% H_2SO_4). Self-packed Silica Gel 60 columns (60 Å, 400 mesh particle size, Fluka, for normal-phase liquid chromatography) or Chromabond Flash RS15 C₁₈ ec columns (Macherey-Nagel, Düren, Germany, for reversed-phase liquid chromatography), and a Teledyne Isco Combiflash Rf200 system were used for preparative medium pressure liquid chromatography (MPLC). Nuclear magnetic resonance (NMR) spectroscopy was performed on a Bruker Avance III 500 UltraShield spectrometer at 500 MHz (^1H) or 126 MHz (^{13}C). Chemical shifts are given in parts per million (ppm) and were calibrated on residual solvent peaks as an internal standard. Multiplicities were specified as s (singlet), d (doublet), t (triplet), q (quartet), or m (multiplet). The signals were assigned with the help of ^1H , ^1H COSY, and DEPT-135-edited ^1H , ^{13}C HSQC experiments. Assignment numbering of the C-glycoside atoms and groups corresponds to the numbering in fucose. Assignment numbering of the galactoside atoms and groups corresponds to the numbering in galactose. Assignment numbering of the ciprofloxacin atoms and groups corresponds to the numbering in ciprofloxacin (cipro).⁷⁰ Commercial chemicals and solvents were used without further purification. Deuterated solvents were purchased from Eurisotop (Saarbrücken, Germany). Ciprofloxacin and polymyxin B nonapeptide-HCl (PMBN) was purchased from Sigma-Aldrich (purity $\geq 98\%$, HPLC, Merck KGaA, Darmstadt, Germany), and ciprofloxacin-HCl was purchased from Cayman Chemical (Ann Arbor, Michigan, USA). If not stated otherwise, the purity of the final compounds was further analyzed by HPLC-UV, and all UV active compounds had a purity of at least 95%. Chromatographic separation was performed on a Dionex Ultimate 3000 HPLC (Thermo Scientific, Germany) with UV detection at 254 nm using a RP-18 column (100/2 Nucleoshell RP18plus, 2.7 μm , from Macherey-Nagel, Germany) as a stationary phase. LCMS-grade distilled MeCN and double distilled H_2O were used as mobile phases containing formic acid (0.1% v/v). In a gradient run, an initial concentration of 5% MeCN in H_2O was increased to 95% during 7 min at a flow rate 600 $\mu\text{L}/\text{min}$. The injection volume was 4 μL of 1 mM compound in $\text{H}_2\text{O}/\text{DMSO} = 100:1$. UPLC-HRMS for key compounds were obtained using a RP-18 column (EC 150/2 Nucleodur C18 Pyramid, 3 μm , from Macherey-Nagel, Germany) and a Q Exactive Focus Orbitrap spectrometer (Thermo Scientific, Germany). The data was analyzed using Xcalibur data acquisition and interpretation software (Thermo Scientific, Germany).

General procedure (i) for amide couplings of **6**: Aniline **6** and K_2CO_3 (2 eq.) were dispersed in dry DCM (0.1 M) and cooled (0 °C). The corresponding (*o*-bromo)acylhalide was added dropwise under vigorous stirring. After stirring for 15 min, the reaction was allowed to warm to r.t. and stirred for 1–4 h until full conversion as monitored by TLC (PE:EtOAc) or HPLC-MS. The reaction was quenched with ice-cold water. The organic phase was washed with brine, and combined organic layers were dried over anhydrous Na_2SO_4 . After filtration, the solvent was evaporated *in vacuo*.

General procedure (ii) for $\text{S}_{\text{N}}2$ reactions with NaN_3 toward **7–10**: The crude starting material was dissolved in dry DMF (0.1 M). A 5 eq. solution of NaN_3 was added, and the reaction was stirred at r.t. until completion (monitored by HPLC-MS). Then, the reaction was diluted with an excess of water and extracted with EtOAc (3x). The combined organic layers were washed with half satd. brine and dried over anhydrous Na_2SO_4 . After filtration, the solvent was evaporated *in vacuo* and the products were purified by MPLC (PE:EtOAc, 30–80%).

General procedure (iii) for the Zemplén deprotection of **7–10**: The starting material was suspended in dry MeOH (0.1 M) and a freshly prepared solution of NaOMe in MeOH (1 M) was added

dropwise to 10 mol %. The reaction was stirred for 1–2 h until the disappearance of the starting material, monitored by TLC (PE:EtOAc, 4:6). Then, the reaction was diluted with MeOH and neutralized with Amberlite IR-120 H^+ exchange resin. The resin was filtered off, and the solvent was evaporated *in vacuo*. Purification was performed by reversed-phase MPLC (MeCN: H_2O , 10–20%, 0.1% formic acid). The solvent was removed by lyophilization.

General procedure (iv) for the copper-catalyzed click reaction toward conjugates **22–31**: Alkyne (1.1 eq.) and azide (1 eq.) were dissolved in 1 mL of dry DMF (purged with argon). $\text{CuSO}_4 \cdot 7\text{H}_2\text{O}$ (10 mol %) and sodium ascorbate (20 mol %) were added as aqueous solutions from freshly prepared stock solutions (100 mM). The mixture was stirred at r.t. or 40 °C for 16–24 h. Reaction progress was monitored by HPLC-MS. After full conversion, the solvents were evaporated *in vacuo* followed by purification via RP-MPLC (MeCN: H_2O , 10–20%, 0.1% formic acid). The solvent was removed by lyophilization.

p-Nitrophenyl 2,3,4,6-Tetra-O-acetyl- β -D-thiogalactopyranoside (5). Galactose pentaacetate (**4**, 2.0 g, 5.1 mmol, 1 eq.) and *p*-nitrothiophenol (2.4 g, 15.3 mmol, 3 eq.) were dissolved in 20 mL dry CH_2Cl_2 in a heat-dried flask under a N_2 atmosphere. The mixture was cooled (0 °C), and $\text{BF}_3 \cdot \text{Et}_2\text{O}$ (3.2 mL, 25.5 mmol, 5 eq.) was added dropwise under vigorous stirring. Afterward, the reaction was allowed to warm to r.t. and stirred overnight (17 h). Reaction progress was monitored by TLC (Tol:EtOAc, 9:1). After consumption of the starting material, the reaction was poured on ice water. The organic phase was isolated and washed with aq. satd. NaHCO_3 . The combined organic layers were washed with half satd. brine and dried over anhydrous Na_2SO_4 . After filtration, the solvent was removed *in vacuo*. Purification by MPLC (SiO_2 , EtOAc in toluene, 5–20%) gave the product as a pale yellow amorphous solid (1.3 g, 51%). ^1H NMR (500 MHz, CHCl_3 -*d*) δ 8.16 (d, *J* = 8.8 Hz, 2H, Ar-H), 7.61 (d, *J* = 8.8 Hz, 2H, Ar-H), 5.47 (d, *J* = 3.2 Hz, 1H, glyco-H-4), 5.29 (t, *J* = 10.0 Hz, 1H, glyco-H-2), 5.10 (dd, *J* = 9.9, 3.3 Hz, 1H, glyco-H-3), 4.86 (d, *J* = 10.0 Hz, 1H, glyco-H-1), 4.21 (dd, *J* = 11.5, 7.2 Hz, 1H, glyco-H-6), 4.14 (dd, *J* = 11.5, 5.8 Hz, 1H, glyco-H-6'), 4.04 (t, *J* = 6.5 Hz, 1H, glyco-H-5), 2.35 (s, 3H, Ac- CH_3), 2.16 (s, 3H, Ac- CH_3), 2.09 (s, 3H, Ac- CH_3), 2.08 (s, 3H, Ac- CH_3), 1.99 (s, 3H, Ac- CH_3); ^{13}C NMR (126 MHz, CHCl_3 -*d*) δ 170.44 (C=O), 170.15 (C=O), 170.08 (C=O), 169.50 (C=O), 146.96 (Ar-C), 142.52 (Ar-C), 130.52 (Ar-C), 123.97 (Ar-C), 84.97 (glyco-C-1), 74.97 (glyco-C-5), 71.85 (glyco-C-3), 67.20 (glyco-C-4), 66.84 (glyco-C-2), 61.81 (glyco-C-6), 20.88 (Ac- CH_3), 20.84 (Ac- CH_3), 20.79 (Ac- CH_3), 20.68 (Ac- CH_3). LR-MS: *m/z* = 503.16, $[\text{M} + \text{Na}]^+$. Spectroscopic data is in accordance with the literature.⁷¹

p-Aminophenyl 2,3,4,6-Tetra-O-acetyl- β -D-thiogalactopyranoside (6). Compound **6** was synthesized according to Casoni et al.:⁶⁶ *p*-nitrophenyl 2,3,4,6-tetra-O-acetyl- β -D-galactothiopyranoside (**5**, 1.0 g, 2.06 mmol, 1 eq.) was dissolved in 70 mL of dry DCM and Pd/C (50 mg, 5 wt %) was added. The reaction vessel was flushed several times with hydrogen and subsequently stirred under a hydrogen atmosphere (1 bar) for 48 h. The reaction was followed by TLC (PE:EtOAc, 1:1). After completion, the reaction was filtered over celite. The solvent was removed *in vacuo*, and the pure product was obtained as a pink amorphous solid (903 mg, 96%), which was used without further purification in the next step. ^1H NMR (500 MHz, $\text{DMSO}-d_6$) δ 7.18–7.08 (m, 2H, ArH), 6.57–6.48 (m, 2H, ArH), 5.39 (s, 2H, NH_2), 5.25 (dd, *J* = 3.5, 1.0 Hz, 1H, glyco-H-4), 5.18 (dd, *J* = 9.7, 3.5 Hz, 1H, glyco-H-3), 4.93 (t, *J* = 9.9 Hz, 1H, glyco-H-2), 4.78 (d, *J* = 10.0 Hz, 1H, glyco-H-1), 4.21–4.13 (m, 1H, glyco-H-5), 4.11–3.93 (m, 2H, glyco-H-6), 2.09 (s, 3H, Ac- CH_3), 2.06 (s, 3H, Ac- CH_3), 2.00 (s, 3H, Ac- CH_3), 1.90 (s, 3H, Ac- CH_3). ^{13}C NMR (126 MHz, $\text{DMSO}-d_6$) δ 169.93 (C=O), 169.84 (C=O), 169.46 (C=O), 169.17 (C=O), 149.42 (ArC), 135.15 (ArC), 115.20 (ArC), 114.07 (ArC), 86.07 (glyco-C-1), 73.25 (glyco-C-5), 71.20 (glyco-C-3), 67.62 (glyco-C-4), 67.24 (glyco-C-2), 61.66 (glyco-C-6), 20.63 (Ac- CH_3), 20.51 (Ac- CH_3), 20.40 (Ac- CH_3), 20.36 (Ac- CH_3). LR-MS: *m/z* = 456.2, $[\text{M} + \text{H}]^+$.

p-(α -Azidoacetamido)phenyl 2,3,4,6-Tetra-O-acetyl- β -D-thiogalactopyranoside (7). **7** was synthesized starting from **6** in two

chemical steps in analogy to Casoni et al.:⁶⁶ Aniline **6** (300 mg, 0.66 mmol, 1 eq.) and triethylamine (140 μ L, 1.01 mmol, 1.6 eq.) were dissolved in 6 mL of dry DCM. The solution was cooled (0 °C), and bromoacetyl bromide (86 μ L, 0.99 mmol, 1.5 eq.) was added dropwise under vigorous stirring. The reaction was stirred for 1 h followed by TLC (PE:EtOAc, 7:3). After completion, the mixture was quenched with ice water. The organic phase was washed with aq. satd. NH_4Cl (3x), water (2x), and brine (1x) and dried over anhydrous Na_2SO_4 . After filtration, the solvent was removed *in vacuo* to yield the crude intermediate as an oil (370 mg), which was transformed according to general procedure ii. Product **7** was obtained as a white amorphous solid (283.2 mg, 80% over two steps). ¹H NMR in accordance with the literature⁶⁶ (500 MHz, CHCl_3 -d) δ 8.04 (s, 1H, Amide-NH), 7.52 (s, 4H, ArH), 5.41 (d, J = 3.0 Hz, 1H, glyco-H-4), 5.20 (t, J = 9.9 Hz, 1H, glyco-H-2), 5.04 (dd, J = 9.9, 3.3 Hz, 1H, glyco-H-3), 4.65 (d, J = 10.0 Hz, 1H, glyco-H-1), 4.18 (dd, J = 11.3 Hz, overlaps with 4.16, 1H, glyco-H-6), 4.16 (s, 2H, CH_2N_3), 4.11 (dd, J = 11.3, 6.3 Hz, 1H, glyco-H-6'), 3.92 (t, J = 6.6 Hz, 1H, glyco-H-5), 2.12 (s, 3H, Ac- CH_3), 2.10 (s, 3H, Ac- CH_3), 2.05 (s, 3H, Ac- CH_3), 1.97 (s, 3H, Ac- CH_3). ¹³C NMR (126 MHz, CHCl_3 -d) δ 170.54 (C=O), 170.33 (C=O), 170.20 (C=O), 169.55 (C=O), 164.64 (C=O), 137.21 (ArC), 134.29 (ArC), 128.05 (ArC), 120.34 (ArC), 86.79 (glyco-C-1), 74.60 (glyco-C-5), 72.12 (glyco-C-3), 67.32 (glyco-C-4), 61.72 (glyco-C-2), 53.11 (glyco-C-6), 53.07 ($\text{C}_2\text{H}_2\text{N}_3$), extracted from HSQC), 21.01 (Ac- CH_3), 20.85 (Ac- CH_3), 20.81 (Ac- CH_3), 20.73 (Ac- CH_3). LR-MS: m/z = 539.1, $[\text{M} + \text{H}]^+$.

p-(β -Azidopropamido)phenyl 2,3,4,6-Tetra-O-acetyl- β -D-thiogalactopyranoside (**8**). The title compound was synthesized starting from **6** (300 mg, 0.66 mmol, 1 eq.) according to general procedures i and ii and was obtained as a white amorphous solid over two chemical steps (316 mg, 87%). However, the elimination product could not be separated, resulting in a <10% contamination of the corresponding Michael-acceptor side product (quantified by ¹H NMR). ¹H NMR (500 MHz, CHCl_3 -d) δ 7.49 (s, 4H, ArH), 7.44 (s, 1H, NH), 6.44 (d, J = 16.9 Hz, 1H, $-\text{COCHCH}_2$, from impurity), 6.24 (dd, J = 16.8, 10.3 Hz, 1H, $-\text{COCHCH}-\text{H}$, from impurity), 5.80 (d, J = 10.2 Hz, 1H, $-\text{COCHCH}-\text{H}'$, from impurity), 5.40 (d, J = 3.1 Hz, 1H, glyco-H-4), 5.19 (t, J = 9.9 Hz, 1H, glyco-H-2), 5.03 (dd, J = 9.9, 3.1 Hz, 1H, glyco-H-3), 4.63 (d, J = 9.9 Hz, 1H, glyco-H-1), 4.17 (dd, J = 11.3, 6.9 Hz, 1H, glyco-H-6), 4.10 (dd, J = 11.5, 6.3 Hz, 1H, glyco-H-6'), 3.90 (t, J = 6.5 Hz, 1H, glyco-H-5), 3.72 (t, J = 6.2 Hz, 2H, COCH_2), 2.60 (t, J = 6.2 Hz, 2H, CH_2N_3), 2.11 (s, 3H, Ac- CH_3), 2.10 (s, 3H, Ac- CH_3), 2.05 (s, 3H, Ac- CH_3), 1.97 (s, 3H, Ac- CH_3). ¹³C NMR (126 MHz, CHCl_3 -d) δ 170.45 (C=O), 170.25 (C=O), 170.10 (C=O), 169.48 (C=O), 168.22 (C=O), 137.92 (ArC), 134.23 (ArC), 127.27 (ArC), 120.14 (ArC), 86.78 (glyco-C-1), 74.43 (glyco-C-5), 72.00 (glyco-C-3), 67.24 (glyco-C-4), 67.20 (glyco-C-2), 61.58 (glyco-C-6), 47.24 ($\text{COCH}_2\text{CH}_2\text{N}_3$), 36.96 ($\text{COCH}_2\text{CH}_2\text{N}_3$), 20.88 (Ac- CH_3), 20.72 (Ac- CH_3), 20.67 (Ac- CH_3), 20.60 (Ac- CH_3). LR-MS: m/z = 553.1, $[\text{M} + \text{H}]^+$.

p-(γ -Azidobutyramido)phenyl 2,3,4,6-Tetra-O-acetyl- β -D-thiogalactopyranoside (**9**). The title compound was synthesized starting from **6** (300 mg, 0.66 mmol, 1 eq.) according to general procedures i and ii and was obtained as a white amorphous solid over two chemical steps (296 mg, 79%). ¹H NMR (500 MHz, CHCl_3 -d) δ 7.48 (s, 4H, Ar-H), 7.44 (s, 1H, NH), 5.40 (d, J = 3.4 Hz, 1H, glyco-H-4), 5.20 (t, J = 9.9 Hz, 1H, glyco-H-2), 5.02 (dd, J = 10.0, 3.3 Hz, 1H, glyco-H-3), 4.62 (d, J = 9.9 Hz, 1H, glyco-H-1), 4.17 (dd, J = 11.3, 6.9 Hz, 1H, glyco-H-6), 4.09 (dd, J = 11.3, 6.3 Hz, 1H, glyco-H-6'), 3.90 (t, J = 6.6 Hz, 1H, glyco-H-5), 3.41 (t, J = 6.4 Hz, 2H, COCH_2), 2.47 (t, J = 7.1 Hz, 2H, CH_2N_3), 2.12 (s, 3H, Ac- CH_3), 2.10 (s, 3H, Ac- CH_3), 2.04 (s, 3H, Ac- CH_3), 2.00 (t, J = 6.8 Hz, 2H, $-\text{CH}_2-$), 1.97 (s, 3H, Ac- CH_3). ¹³C NMR (126 MHz, CHCl_3 -d) δ 170.57 (C=O), 170.35 (C=O), 170.26 (C=O), 170.21 (C=O), 169.61 (C=O), 138.25 (ArC), 134.31 (ArC), 127.14 (ArC), 120.11 (ArC), 86.95 (glyco-C-1), 74.52 (glyco-C-5), 72.10 (glyco-C-3), 67.36 (glyco-C-4), 67.32 (glyco-C-2), 61.68 (glyco-C-6), 50.78 (COCH_2), 34.26 (CH_2N_3), 24.66 (CH_2), 20.99 (Ac- CH_3), 20.82 (Ac- CH_3), 20.77 (Ac- CH_3), 20.71 (Ac- CH_3). LR-MS: m/z = 567.1, $[\text{M} + \text{H}]^+$.

p-(δ -Azidovalerylamido)phenyl 2,3,4,6-Tetra-O-acetyl- β -D-thiogalactopyranoside (**10**). The title compound was synthesized starting from **6** (300 mg, 0.66 mmol, 1 eq.) according to general procedures i and ii and was obtained as a white amorphous solid over two chemical steps (327 mg, 85%). ¹H NMR (500 MHz, CHCl_3 -d) δ 7.48 (s, 4H, Ar-H), 7.24 (s, 1H, NH), 5.40 (d, J = 3.2 Hz, 1H, glyco-H-4), 5.19 (t, J = 9.9 Hz, 1H, glyco-H-2), 5.03 (dd, J = 9.9, 3.3 Hz, 1H, glyco-H-3), 4.63 (d, J = 10.0 Hz, 1H, glyco-H-1), 4.17 (dd, J = 11.3, 6.9 Hz, 1H, glyco-H-6), 4.10 (dd, J = 11.3, 6.3 Hz, 1H, glyco-H-6'), 3.90 (t, J = 6.6 Hz, 1H, glyco-H-5), 3.34 (t, J = 6.7 Hz, 2H, $-\text{COCH}_2-$), 2.41 (t, J = 7.3 Hz, 2H, $-\text{CH}_2\text{N}_3$), 2.11 (s, 3H, Ac- CH_3), 2.10 (s, 3H, Ac- CH_3), 2.05 (s, 3H, Ac- CH_3), 1.97 (s, 3H, Ac- CH_3), 1.82 (p, J = 7.4 Hz, 2H, $-\text{CH}_2\text{CH}_2\text{N}_3$), 1.74–1.64 (p, 2H, $-\text{COCH}_2\text{CH}_2-$). ¹³C NMR (126 MHz, CHCl_3 -d) δ 170.69 (C=O), 170.56 (C=O), 170.36 (C=O), 170.21 (C=O), 169.59 (C=O), 138.34 (ArC), 134.39 (ArC), 127.03 (ArC), 120.05 (ArC), 86.99 (glyco-C-1), 74.55 (glyco-C-5), 72.13 (glyco-C-3), 67.37 (glyco-C-4), 67.33 (glyco-C-2), 61.70 (glyco-C-6), 51.31 ($\text{CO}-\text{CH}_2-$), 37.07 ($-\text{CH}_2\text{N}_3$), 28.43 ($-\text{COCH}_2\text{CH}_2-$), 22.75 ($-\text{CH}_2\text{CH}_2\text{N}_3$), 21.01 (Ac- CH_3), 20.85 (Ac- CH_3), 20.80 (Ac- CH_3), 20.72 (Ac- CH_3). LR-MS: m/z = 581.2, $[\text{M} + \text{H}]^+$.

p-(α -Azidoacetamido)phenyl- β -D-thiogalactopyranoside (**11**). The title compound was synthesized from **7** (275 mg, 0.51 mmol, 1 eq.) according to general procedure iii and was obtained as a white solid (142 mg, 75%). ¹H NMR (500 MHz, $\text{MeOH}-d_4$) δ 7.54 (s, 4H, ArH), 4.51 (d, J = 9.7 Hz, 1H, glyco-H-1), 4.01 (s, 2H, $-\text{CH}_2\text{N}_3$), 3.89 (d, J = 3.2 Hz, 1H, glyco-H-4), 3.76 (dd, J = 11.5, 6.8 Hz, 1H, glyco-H-6), 3.70 (dd, J = 11.5, 5.2 Hz, 1H, glyco-H-6'), 3.62–3.52 (m, 2H, glyco-H-2 + glyco-H-5), 3.49 (dd, J = 9.2, 3.3 Hz, 1H, glyco-H-3). ¹³C NMR (126 MHz, $\text{MeOH}-d_4$) δ 168.47 (C=O), 138.61 (ArC), 133.58 (ArC), 130.91 (ArC), 121.59 (ArC), 90.50 (glyco-C-1), 80.61 (glyco-C-5), 76.30 (glyco-C-3), 70.93 (glyco-C-2), 70.40 (glyco-C-4), 62.60 (glyco-C-6), 53.26 ($-\text{CH}_2\text{N}_3$). HR-MS calcd $[\text{C}_{14}\text{H}_{17}\text{N}_4\text{O}_6\text{S}]^-$: 369.0874, found 369.0877.

p-(β -Azidopropamido)phenyl- β -D-thiogalactopyranoside (**12**). The title compound was synthesized from **8** (309 mg, 0.56 mmol, 1 eq.) according to general procedure iii and was obtained as a white solid (216 mg, 54%). ¹H NMR (500 MHz, $\text{MeOH}-d_4$) δ 7.53 (d, J = 1.1 Hz, 4H, ArH), 4.50 (d, J = 9.6 Hz, 1H, glyco-H-1), 3.88 (d, J = 2.5 Hz, 1H, glyco-H-4), 3.76 (dd, J = 11.5, 6.8 Hz, 1H, glyco-H-6), 3.70 (dd, J = 11.5, 5.3 Hz, 1H, glyco-H-6'), 3.64 (t, J = 6.4 Hz, 2H, $-\text{COCH}_2-$), 3.60–3.52 (m, 2H, glyco-H-2 + glyco-H-5), 3.48 (dd, J = 9.2, 3.3 Hz, 1H, glyco-H-3), 2.63 (t, J = 6.4 Hz, 2H, $-\text{CH}_2\text{N}_3$). ¹³C NMR (126 MHz, $\text{MeOH}-d_4$) δ 171.27 (C=O), 139.20 (ArC), 133.68 (ArC), 130.38 (ArC), 121.39 (ArC), 90.59 (glyco-C-1), 80.61 (glyco-C-5), 76.33 (glyco-C-3), 70.93 (glyco-C-2), 70.43 (glyco-C-4), 62.63 (glyco-C-6), 48.43 ($-\text{COCH}_2-$), 37.08 ($-\text{CH}_2\text{N}_3$). HR-MS calcd $[\text{C}_{15}\text{H}_{19}\text{N}_4\text{O}_6\text{S}]^-$: 383.1031, found 383.1036.

p-(γ -Azidobutyramido)phenyl- β -D-thiogalactopyranoside (**13**). The title compound was synthesized from **9** (296 mg, 0.52 mmol, 1 eq.) according to general procedure iii and was obtained as a white solid in 81% yield. ¹H NMR (500 MHz, $\text{MeOH}-d_4$) δ 7.52 (s, 4H, ArH), 4.50 (d, J = 9.6 Hz, 1H, glyco-H-1), 3.88 (d, J = 3.2 Hz, 1H, glyco-H-4), 3.76 (dd, J = 11.5, 6.8 Hz, 1H, glyco-H-6), 3.70 (dd, J = 11.5, 5.3 Hz, 1H, glyco-H-6'), 3.61–3.52 (m, 2H, glyco-H-2 + glyco-H-5), 3.48 (dd, J = 9.2, 3.3 Hz, 1H, glyco-H-3), 3.39 (t, J = 6.7 Hz, 2H, $-\text{COCH}_2-$), 2.47 (t, J = 7.3 Hz, 2H, $-\text{CH}_2\text{N}_3$), 1.94 (p, J = 7.0 Hz, 2H, $-\text{CH}_2-$). ¹³C NMR (126 MHz, $\text{MeOH}-d_4$) δ 173.37 (C=O), 139.37 (ArC), 133.70 (ArC), 130.21 (ArC), 121.38 (ArC), 90.62 (glyco-C-1), 80.62 (glyco-C-5), 76.34 (glyco-C-3), 70.94 (glyco-C-2), 70.43 (glyco-C-4), 62.63 (glyco-C-6), 51.92 ($-\text{COCH}_2-$), 34.73 ($-\text{CH}_2\text{N}_3$), 25.94 ($-\text{CH}_2-$). HR-MS calcd $[\text{C}_{16}\text{H}_{21}\text{N}_4\text{O}_6\text{S}]^-$: 397.1187, found 397.1189.

p-(δ -Azidovalerylamido)phenyl- β -D-thiogalactopyranoside (**14**). The title compound was synthesized from **10** (327 mg, 0.56 mmol) according to general procedure iii and was obtained as a white solid (235 mg, 84%). ¹H NMR (500 MHz, $\text{MeOH}-d_4$) δ 7.52 (s, 4H, ArH), 4.49 (d, J = 9.6 Hz, 1H, glyco-H-1), 3.88 (dd, J = 3.3, 0.8 Hz, 1H, glyco-H-4), 3.76 (dd, J = 11.5, 6.8 Hz, 1H, glyco-H-6), 3.70 (dd, J = 11.5, 5.3 Hz, 1H, glyco-H-6'), 3.62–3.50 (m, 2H, glyco-H-2 + glyco-

H-5), 3.48 (dd, $J = 9.2, 3.3$ Hz, 1H, glyco-H-3), 3.34 (t, $J = 6.7$ Hz, 2H, $-\text{COCH}_2-$), 2.40 (t, $J = 7.4$ Hz, 2H, $-\text{CH}_2\text{N}_3$), 1.82–1.72 (m, 2H, $-\text{CH}_2\text{CH}_2\text{N}_3$), 1.70–1.60 (m, 2H, $-\text{COCH}_2\text{CH}_2-$). ^{13}C NMR (126 MHz, MeOH- d_4) δ 174.06 (C=O), 139.39 (ArC), 133.72 (ArC), 130.18 (ArC), 121.37 (ArC), 90.62 (glyco-C-1), 80.62 (glyco-C-5), 76.34 (glyco-C-3), 70.94 (glyco-C-2), 70.43 (glyco-C-4), 62.63 (glyco-C-6), 52.16 ($-\text{COCH}_2-$), 37.27 ($-\text{CH}_2\text{N}_3$), 29.45 ($-\text{COCH}_2\text{CH}_2-$), 23.99 ($-\text{CH}_2\text{CH}_2\text{N}_3$). HR-MS calcd [$\text{C}_{17}\text{H}_{23}\text{N}_4\text{O}_6\text{S}$] $^-$: 411.1344, found 411.1350.

N-Propargyl-ciprofloxacin (20). The title compound was synthesized in analogy to McPherson et al.⁷² Ciprofloxacin (500 mg, 1.5 mmol, 1 eq.) was dispersed in 10 mL of dry DMF together with Et_3N (310 μL , 2.25 mmol, 1.5 eq.) and propargyl bromide (250 μL , 2.25 mmol, 1.5 eq.). The mixture was stirred at 90 °C for 24 h, and further equivalents of Et_3N (309 μL , 2 mmol, 2 eq.) and propargyl bromide (250 μL , 2 mmol, 2 eq.) were added stepwise until the disappearance of the starting material, monitored by TLC (DCM:MeOH, 9:1). The reaction was poured on ice water. After filtration, the precipitate was redissolved and purified by MPLC (DCM:MeOH, 1–10%) to yield the title compound as a beige amorphous solid (353 mg, 64%). ^1H NMR (500 MHz, CHCl_3 - d) δ 14.99 (br s, 1H, COOH), 8.77 (s, 1H, ArH-2), 8.02 (d, $J = 13.0$ Hz, 1H, ArH-5), 7.37 (d, $J = 6.7$ Hz, 1H, ArH-8), 3.55 (br s, 1H, cPr-H), 3.43 (s, 2H, HCCCH $_2$ -), 3.41 (br s, 4H, 2x piperazine-CH $_2$ -), 2.84 (br s, 4H, 2x piperazine-CH $_2$ '-), 2.33 (s, 1H, alkyne-H), 1.39 (d, $J = 6.3$ Hz, 2H, cPr-CH $_2$), 1.20 (br s, 2H, cPr-CH $_2$ '). ^{13}C NMR (126 MHz, CHCl_3 - d) δ 177.28 (C4=O), 167.17 (COOH), 153.82 (d, $J = 251.4$ Hz, cipro-C-6), 147.61 (cipro-C-2), 145.86 (d, $J = 10.1$ Hz, cipro-C-7), 139.21 (cipro-C-8a), 120.14 (d, $J = 7.6$ Hz, cipro-C-4a), 112.67 (d, $J = 23.4$ Hz cipro-C-5), 108.35 (cipro-C-3), 105.04 (d, $J = 2.4$ Hz, cipro-C-8), 74.23 (HCCCH $_2$ -), 51.52 (HCCCH $_2$ -), 49.67 (piperazine), 46.95 (piperazine), 35.42 (cPr-CH), 8.39 (cPr-CH $_2$), $-\text{HCCCH}_2-$ (not observed). HR-MS calcd [$\text{C}_{20}\text{H}_{21}\text{FN}_3\text{O}_3$] $^+$: 370.1561, found 370.1552.

N-Butynyl-ciprofloxacin (21). Ciprofloxacin (500 mg, 1.5 mmol, 1 eq.) was dissolved in dry DMF and heated to 70 °C. Over 72 h, Et_3N (1512 μL , 10.5 mmol, 7 eq.) and 4-bromo-1-butyne (982 μL , 10.5 mmol, 7 eq.) were added portionwise in 1 eq. steps until the disappearance of the starting material, monitored by TLC (DCM:MeOH, 9:1). The reaction was poured on ice-cold water. After precipitation, the precipitate was purified by MPLC (DCM:MeOH, 1–10%) to yield the product as a beige amorphous solid (245 mg, 43%). ^1H NMR (500 MHz, DMSO- d_6) δ 15.22 (br s, 1H, COOH), 8.66 (s, 1H, ArH-2), 7.89 (d, $J = 13.3$ Hz, 1H, ArH-5), 7.56 (d, $J = 7.3$ Hz, 1H, ArH-8), 3.85–3.77 (br s, 1H, cPr-H), 3.32 (br s, 4H, 2x piperazine-CH $_2$ -), 2.81 (s, 1H, HCCCH $_2$ CH $_2$ -), 2.64 (br s, 4H, piperazine-CH $_2$ -), 2.56 (t, $J = 7.2$ Hz, 2H, RR'NCH $_2$ CH $_2$ CCH-), 2.38 (t, $J = 6.2$ Hz, 2H, RR'NCH $_2$ CH $_2$ CCH-), 1.31 (q, $J = 6.0$ Hz, 2H, cPr-CH $_2$ -), 1.17 (br s, 2H, cPr-CH $_2$ '-). ^{13}C NMR (126 MHz, DMSO- d_6) δ 176.40 (C4=O), 166.01 (COOH), 153.04 (d, $J = 249.4$ Hz, cipro-C-6), 148.05 (cipro-C-2), 145.22 (cipro-C-7), 139.20 (cipro-C-8a), 118.63 (cipro-C4a), 110.94 (d, $J = 23.0$ Hz, cipro-C-5), 106.74 (cipro-C-3), 106.44 (cipro-C-8), 83.16 (HCCCH $_2$ CH $_2$ -), 71.87 (HCCCH $_2$ CH $_2$ -), 56.26 (HCCCH $_2$ CH $_2$ -), 51.98 (piperazine), 49.41 (piperazine), 49.38 (piperazine), 35.88 (cPr-CH), 16.19 (HCCCH $_2$ CH $_2$ -), 7.59 (cPr-CH $_2$). HR-MS calcd [$\text{C}_{21}\text{H}_{23}\text{FN}_3\text{O}_3$] $^+$: 384.1718, found 384.1711.

Gal-ciprofloxacin Conjugate 22 ($n = 1, m = 0$). The title compound was synthesized from **11** (20 mg, 0.054 mmol, 1 eq.) and **20** (40 mg, 0.108 mmol, 2 eq.) according to general procedure iv and was obtained as a beige amorphous solid (22 mg, 55%). ^1H NMR (500 MHz, DMSO- d_6) δ 15.22 (br s, 1H, COOH), 10.51 (s, 1H, $-\text{CONH}-$), 8.65 (s, 1H, cipro-ArH-2), 8.06 (s, 1H, triazole-H), 7.88 (d, $J = 13.3$ Hz, 1H, cipro-ArH-5), 7.55 (d, $J = 7.4$ Hz, 1H, cipro-ArH-8), 7.52 (d, $J = 8.6$ Hz, 2H, Phenyl-H), 7.43 (d, $J = 8.7$ Hz, 2H, Phenyl-H), 5.32 (s, 2H, $-\text{HNCO}-\text{CH}_2$ -triazole), 5.11 (br s, 1H, OH), 4.85 (br s, 1H, OH), 4.62 (br s, 1H, OH), 4.48 (d, $J = 9.4$ Hz, 1H, glyco-H-1), 4.44 (br s, 1H, OH), 3.81 (s, 1H, cPr-H), 3.70 (s, 2H, $-\text{NHCOCH}_2\text{CH}_2$ -N-cipro), 3.69 (br s, 1H, glyco-H-4), 3.53–3.45 (m, 2H, glyco-H-6 + H-6'), 3.43 (glyco-H-2, extracted from HSQC), 3.38

(glyco-H-5, extracted from HSQC), 3.33 (glyco-H-3, extracted from HSQC), 3.33 (2x piperazine-CH $_2$, extracted from HSQC), 2.65 (s, 4H, 2x piperazine-CH $_2$), 1.31 (d, $J = 6.5$ Hz, 2H, cPr-CH $_2$), 1.17 (br s, 2H, cPr-CH $_2$ '). ^{13}C NMR (126 MHz, DMSO- d_6) δ 176.41 (cipro-C4=O), 166.05 (COOH), 164.34 (C=O), 153.06 (d, $J = 249.3$ Hz, cipro-C-6), 148.03 (cipro-C-2), 145.23 (d, $J = 10.1$ Hz, cipro-C-7), 142.84 (triazole-C), 139.24 (cipro-C-8a), 137.09 (phenyl-C), 131.00 (phenyl-C), 129.46 (phenyl-C), 125.67 (triazole-CH), 119.60 (phenyl-C), 118.59 (d, $J = 7.5$ Hz, cipro-C-4a), 110.98 (d, $J = 23.4$ Hz, cipro-C-5), 106.75 (cipro-C-3), 106.43 (d, $J = 3.9$ Hz, cipro-C-8), 88.17 (glyco-C-1), 79.22 (glyco-C-5), 74.72 (glyco-C-3), 69.26 (glyco-C-2), 68.40 (glyco-C-4), 60.63 (glyco-C-6), 52.29 ($-\text{triazole}-\text{CH}_2$ -N-cipro), 52.17 ($-\text{HNCO}-\text{CH}_2$ -triazole), 51.83 (piperazine), 49.40 (piperazine), 35.92 (cPr-CH), 7.61 (cPr-CH $_2$). HR-MS calcd [$\text{C}_{34}\text{H}_{39}\text{FN}_7\text{O}_9\text{S}$] $^+$: 740.2509, found 740.2500.

Gal-ciprofloxacin Conjugate 23 ($n = 1, m = 1$). The title compound was synthesized from **11** (20 mg, 0.054 mmol, 1 eq.) and **21** (41 mg, 0.108 mmol, 2 eq.) according to general procedure iv and was obtained as a beige amorphous solid (15 mg, 37%). ^1H NMR (500 MHz, DMSO- d_6) δ 15.23 (br s, 1H, COOH), 10.50 (s, 1, CONH), 8.66 (s, 1H, cipro-ArH-2), 7.94 (s, 1H, triazole-H), 7.90 (d, $J = 13.3$ Hz, 1H, cipro-ArH-5), 7.57 (d, $J = 6.6$ Hz, 1H, cipro-ArH-8), 7.52 (d, $J = 8.4$ Hz, 2H, Phenyl-H), 7.42 (d, $J = 8.7$ Hz, 2H, Phenyl-H'), 5.28 (s, 2H, $-\text{HNCOCH}_2-$), 4.48 (d, $J = 9.4$ Hz, 1H, glyco-H-1), 3.82 (s, 1H, cPr-H), 3.69 (d, $J = 2.8$ Hz, 1H, glyco-H-4), 3.49 (glyco-H-6 + H-6', extracted from HSQC), 3.43 (glyco-H-2, extracted from HSQC), 3.38 (glyco-H-5, extracted from HSQC), 3.35 (2x piperazine-CH $_2$, extracted from HSQC), 3.33 (glyco-H-3, extracted from HSQC), 2.88 (t, $J = 7.5$ Hz, 2H, $-\text{triazole}-\text{CH}_2\text{CH}_2\text{NRR}'$), 2.68 (br s, 6H, 2x piperazine-CH $_2$ + $-\text{triazole}-\text{CH}_2\text{CH}_2\text{NRR}'$), 1.31 (d, $J = 6.0$ Hz, 2H, cPr-CH $_2$), 1.18 (br s, 2H, cPr-CH $_2$ '). ^{13}C NMR (126 MHz, DMSO- d_6) δ 176.42 (cipro-C4=O), 166.06 (COOH), 164.39 (C=O), 153.09 (d, $J = 249.8$ Hz, cipro-C-6), 148.05 (cipro-C-2), 145.27 (d, $J = 9.9$ Hz, cipro-C-7), 144.96 (triazole-C), 139.26 (cipro-C-8a), 137.11 (phenyl-C), 131.00 (phenyl-C), 129.44 (phenyl-C), 124.00 (triazole-CH), 119.59 (phenyl-C), 118.58 (d, $J = 8.0$ Hz, cipro-C-4a), 110.99 (d, $J = 23.1$ Hz, cipro-C-5), 106.76 (cipro-C-3), 106.38 (d, $J = 3.1$ Hz, cipro-C-8), 88.17 (glyco-C-1), 79.21 (glyco-C-5), 74.72 (glyco-C-3), 69.25 (glyco-C-2), 68.39 (glyco-C-4), 60.63 (glyco-C-6), 57.29 (linker-CH $_2$), 52.27 (piperazine), 52.18 (linker-CH $_2$), 49.43 (piperazine), 35.92 (cPr-CH), 22.97 (linker-CH $_2$), 7.62 (cPr-CH $_2$). HR-MS calcd [$\text{C}_{35}\text{H}_{41}\text{FN}_7\text{O}_9\text{S}$] $^+$: 754.2665, found 754.2658.

Gal-ciprofloxacin Conjugate 24 ($n = 2, m = 0$). The title compound was synthesized from **12** (20 mg, 0.052 mmol, 1 eq.) and **20** (20 mg, 0.054 mmol, 1 eq.) according to general procedure iv and was obtained as a beige amorphous solid (26 mg, 66%). ^1H NMR (500 MHz, DMSO- d_6) δ 15.23 (br s, 1H, COOH), 10.09 (s, 1H, CONH), 8.66 (s, 1H, cipro-ArH-2), 7.97 (s, 1H, triazole-H), 7.90 (d, $J = 13.3$ Hz, 1H, cipro-ArH-5), 7.53 (d, $J = 7.4$ Hz, 1H, cipro-ArH-8), 7.48 (d, $J = 8.6$ Hz, 2H, phenyl-H), 7.37 (d, $J = 8.5$ Hz, 2H, phenyl-H'), 5.07 (br s, 1H, OH), 4.84 (br s, 1H, OH), 4.65 (t, $J = 6.6$ Hz, 2H, $-\text{NHCOCH}_2\text{CH}_2-$), 4.60 (br s, 1H, OH), 4.43 (d, $J = 9.2$ Hz, 1H, glyco-H-1), 4.43 (br s, 1H, OH), 3.90–3.79 (br s, 1H, cPr-H), 3.67 (s, 1H, glyco-H-4), 3.64 (s, 2H, $-\text{triazole}-\text{CH}_2$ -NRR'), 3.47 (glyco-H-6 + H-6', extracted from HSQC), 3.39 (glyco-H-2, extracted from HSQC), 3.35 (glyco-H-5, extracted from HSQC), 3.30 (glyco-H-3, extracted from HSQC), 3.29–3.25 (m, 4H, 2x piperazine-CH $_2$), 2.96 (t, $J = 6.6$ Hz, 2H, $-\text{NHCOCH}_2\text{CH}_2-$), 2.61–2.57 (m, 4H, 2x piperazine-CH $_2$ '-), 1.34–1.25 (m, 2H, cPr-CH $_2$), 1.18–1.15 (m, 2H, cPr-CH $_2$ '). ^{13}C NMR (126 MHz, DMSO- d_6) δ 176.43 (cipro-C4=O), 168.22 (COOH), 166.07 (C=O), 153.07 (d, $J = 250.0$ Hz, cipro-C-6), 148.07 (cipro-C-2), 145.23 (d, $J = 10.1$ Hz, cipro-C-7), 142.88 (triazole-C), 139.25 (cipro-C-8a), 137.65 (phenyl-C), 131.13 (phenyl-C), 128.70 (phenyl-C), 124.23 (triazole-CH), 119.48 (phenyl-C), 118.61 (d, $J = 7.5$ Hz, cipro-C-4a), 110.99 (d, $J = 22.9$ Hz, cipro-C-5), 106.77 (cipro-C-3), 106.40 (d, $J = 2.5$ Hz, cipro-C-8), 88.28 (glyco-H-1), 79.19 (glyco-H-5), 74.73 (glyco-H-3), 69.24 (glyco-H-2), 68.36 (glyco-H-4), 60.60 (glyco-H-6), 52.30 (linker-CH $_2$), 51.80 (piperazine), 49.39 (piperazine), 45.58 (linker-CH $_2$),

36.56 (linker-CH₂), 35.91 (cPr-CH), 7.61 (cPr-CH₂). HR-MS calcd [C₃₅H₄₁FN₇O₉S]⁺: 754.2665, found 754.2657.

Gal-ciprofloxacin Conjugate 25 (*n* = 2, *m* = 1). The title compound was synthesized from **12** (30 mg, 0.078 mmol, 1 eq.) and **21** (33 mg, 0.086 mmol, 1.1 eq.) according to general procedure iv and was obtained as a beige amorphous solid (35 mg, 58%). ¹H NMR (500 MHz, DMSO-*d*₆) δ 15.23 (br s, 1H, COOH), 10.07 (s, 1H, CONH), 8.66 (s, 1H, cipro-ArH-2), 7.91 (d, *J* = 13.3 Hz, 1H, cipro-ArH-5), 7.87 (s, 1H, triazole-H), 7.55 (d, *J* = 7.3 Hz, 1H, cipro-ArH-8), 7.49 (d, *J* = 8.7 Hz, 2H, phenyl-H), 7.38 (d, *J* = 8.8 Hz, 2H, phenyl-H), 5.06 (br s, 1H, OH), 4.83 (br s, 1H, OH), 4.61 (t, *J* = 6.7 Hz, 2H, -NHCOCH₂CH₂- + OH), 4.43 (d, *J* = 9.3 Hz, 1H, glyco-H-1), 4.42 (s, 1H, OH), 3.83 (s, 1H, OH), 3.68 (s, 1H, glyco-H-4), 3.48 (ddd, *J* = 10.8, 6.5, 5.5 Hz, 2H), 3.40 (t, *J* = 6.3 Hz, 2H, glyco-H-2), 2.95 (t, *J* = 6.6 Hz, 2H, -NHCOCH₂CH₂-), 2.82 (t, *J* = 7.5 Hz, 2H, -triazole-CH₂CH₂NRR'), 2.65 (br s, 6H, 2x piperazine-CH₂ + -triazole-CH₂CH₂NRR'), 1.31 (q, *J* = 7.1 Hz, 2H, cPr-CH₂), 1.20–1.16 (m, 2H, cPr-CH₂). ¹³C NMR (126 MHz, DMSO-*d*₆) δ 176.37 (cipro-C4=O), 168.15 (C=O), 165.98 (COOH), 153.02 (d, *J* = 248.9 Hz, cipro-C-6), 148.02 (cipro-C-2), 145.16 (d, *J* = 10.5 Hz, cipro-C-7), 144.88 (cipro-C-7), 139.21 (cipro-C-8a), 137.65 (phenyl-C), 131.05 (phenyl-C), 128.66 (phenyl-C), 122.58 (triazole-CH), 119.38 (phenyl-C), 118.55 (d, *J* = 7.4 Hz, cipro-C-4a), 110.96 (d, *J* = 23.1 Hz, cipro-C-5), 106.73 (cipro-C-3), 106.32 (d, *J* = 3.8 Hz, cipro-C-8), 88.26 (glyco-C-1), 79.17 (glyco-C-5), 74.69 (glyco-C-3), 69.19 (glyco-C-2), 68.33 (glyco-C-4), 60.57 (glyco-C-6), 57.18 (linker-CH₂), 52.16 (piperazine), 49.35 (piperazine), 45.35 (linker-CH₂), 36.48 (linker-CH₂), 35.88 (cPr-CH), 22.87 (linker-CH₂), 7.58 (cPr-CH₂). HR-MS calcd [C₃₆H₄₃FN₇O₉S]⁺: 768.2822, found 768.2822.

Gal-ciprofloxacin Conjugate 26 (*n* = 3, *m* = 0). The title compound was synthesized from **13** (30 mg, 0.075 mmol, 1 eq.) and **20** (31 mg, 0.083 mmol, 1.1 eq.) according to general procedure iv and was obtained as a beige amorphous solid (30 mg, 52%). ¹H NMR (500 MHz, DMSO-*d*₆) δ 15.21 (br s, 1H, COOH), 9.96 (s, 1H, CONH), 8.65 (s, 1H, cipro-ArH-2), 8.06 (s, 1H, triazole-H), 7.89 (d, *J* = 13.3 Hz, 1H, cipro-ArH-5), 7.54 (d, *J* = 7.3 Hz, 1H, cipro-ArH-8), 7.51 (d, *J* = 8.6 Hz, 2H, phenyl-H), 7.39 (d, *J* = 8.8 Hz, 2H, phenyl-H), 5.06 (br s, 1H, OH), 4.84 (br s, 1H, OH), 4.60 (br s, 1H, OH), 4.44 (d, *J* = 9.4 Hz, 1H, glyco-H-1), 4.42 (OH, extracted from COSY), 4.41 (t, *J* = 6.9 Hz, 1H, -NHCOCH₂CH₂CH₂-), 3.81 (s, 1H, cPr-H), 3.68 (s, 1H, glyco-H-4), 3.66 (s, 2H, -triazole-CH₂-NRR'), 3.56–3.44 (m, 2H, glyco-H-6 + H-6'), 3.41 (t, *J* = 6.3 Hz, 1H, glyco-H-5), 3.37 (glyco-H-2, extracted from HSQC), 3.32 (glyco-H-3, extracted from HSQC), 3.32 (2x piperazine-CH₂, extracted from HSQC) 2.64 (br s, 4H, 2x piperazine-CH₂), 2.33 (t, *J* = 7.2 Hz, 2H, -NHCOCH₂CH₂CH₂-), 2.13 (tt, *J* = 7.1 Hz, 2H, -NHCOCH₂CH₂CH₂-), 1.33–1.27 (m, 2H, cPr-CH₂), 1.23–1.14 (br s, 2H, cPr-CH₂). ¹³C NMR (126 MHz, DMSO-*d*₆) δ 176.36 (cipro-C4=O), 170.11 (C=O), 165.96 (COOH), 153.01 (d, *J* = 249.7 Hz, cipro-C-6), 148.00 (cipro-C-2), 145.17 (d, *J* = 10.1 Hz, cipro-C-7), 143.11 (triazole-C), 139.19 (cipro-C-8a), 137.97 (phenyl-C), 131.15 (phenyl-C), 128.26 (phenyl-C), 123.81 (triazole-CH), 119.34 (phenyl-C), 118.56 (d, *J* = 7.5 Hz, cipro-C-4a), 110.94 (d, *J* = 23.1 Hz, cipro-C-5), 106.72 (cipro-C-3), 106.36 (d, *J* = 3.7 Hz, cipro-C-8), 88.34 (glyco-C-1), 79.17 (glyco-C-5), 74.70 (glyco-C-3), 69.20 (glyco-C-2), 68.34 (glyco-C-4), 60.58 (glyco-C-6), 52.41 (linker-CH₂), 51.87 (piperazine), 49.39 (piperazine), 48.84 (linker-CH₂), 35.85 (cPr-CH), 32.91 (linker-CH₂), 25.51 (linker-CH₂), 7.57 (cPr-CH₂). HR-MS calcd [C₃₆H₄₃FN₇O₉S]⁺: 768.2822, found 768.2815.

Gal-ciprofloxacin Conjugate 27 (*n* = 3, *m* = 1). The title compound was synthesized from **13** (30 mg, 0.075 mmol, 1 eq.) and **21** (32 mg, 0.083 mmol, 1.1 eq.) according to general procedure iv and was obtained as a beige amorphous solid (31 mg, 53%). ¹H NMR (500 MHz, DMSO-*d*₆) δ 15.22 (br s, 1H, COOH), 9.94 (s, 1H, CONH), 8.66 (s, 1H, cipro-ArH-2), 7.93 (s, 1H, triazole-H), 7.90 (d, *J* = 13.3 Hz, 1H, cipro-ArH-5), 7.56 (d, *J* = 7.2 Hz, 1H, cipro-ArH-8), 7.51 (d, *J* = 8.6 Hz, 2H, phenyl-H), 7.38 (d, *J* = 8.8 Hz, 2H, phenyl-H), 5.06 (br s, 1H, OH), 4.83 (br s, 1H, OH), 4.59 (br s, 1H, OH), 4.44 (d, *J* = 9.4 Hz, 1H, glyco-H-1), 4.42 (br s, 1H, OH), 4.38 (t, *J* =

6.8 Hz, 2H, -NHCOCH₂CH₂CH₂-), 3.82 (br s, 1H, cPr-H), 3.68 (s, 1H, glyco-H-4), 3.53–3.44 (m, 2H, glyco-H-6 + H-6'), 3.41 (t, *J* = 6.3 Hz, 1H, glyco-H-5), 3.37 (glyco-H-2, extracted from HSQC), 3.34 (2x piperazine-CH₂, extracted from HSQC), 3.32 (glyco-H-3) 2.84 (t, *J* = 7.6 Hz, 2H, -triazole-CH₂CH₂NRR'), 2.67 (br s, 6H, 2x piperazine-CH₂ + -triazole-CH₂CH₂NRR'), 2.31 (t, *J* = 7.3 Hz, 2H, -NHCOCH₂CH₂CH₂-), 2.11 (tt, *J* = 8.1, 7.5 Hz, 2H, -NHCOCH₂CH₂CH₂-), 1.36–1.28 (m, 2H, cPr-CH₂), 1.21–1.13 (m, 2H, cPr-CH₂). ¹³C NMR (126 MHz, DMSO-*d*₆) δ 176.37 (cipro-C4=O), 170.11 (CO), 165.97 (COOH), 153.03 (d, *J* = 249.5 Hz, cipro-C-6), 148.01 (cipro-C-2), 145.19 (d, *J* = 9.9 Hz, cipro-C-7), 145.05 (triazole-C), 139.20 (cipro-C-8a), 137.95 (phenyl-C), 131.12 (phenyl-C), 128.27 (phenyl-C), 122.21 (triazole-CH), 119.33 (phenyl-C), 118.56 (d, *J* = 8.0 Hz, cipro-C-4a), 110.94 (d, *J* = 23.1 Hz, cipro-C-5), 106.73 (cipro-C-3), 106.35 (d, *J* = 3.2 Hz, cipro-C-8), 88.33 (glyco-C-1), 79.17 (glyco-C-5), 74.70 (glyco-C-3), 69.20 (glyco-C-2), 68.34 (glyco-C-4), 60.58 (glyco-C-6), 57.21 (linker-CH₂), 52.19 (piperazine), 49.40 (piperazine), 48.74 (linker-CH₂), 35.87 (cPr-CH), 32.90 (linker-CH₂), 25.53 (linker-CH₂), 22.98 (linker-CH₂), 7.58 (cPr-CH₂). HR-MS calcd [C₃₇H₄₅FN₇O₉S]⁺: 782.2987, found 782.2965.

Gal-ciprofloxacin Conjugate 28 (*n* = 4, *m* = 0). The title compound was synthesized from **14** (30 mg, 0.073 mmol, 1 eq.) and **20** (30 mg, 0.08 mmol, 1.1 eq.) according to general procedure iv and was obtained as a beige amorphous solid (25 mg, 43%). ¹H NMR (500 MHz, DMSO-*d*₆) δ 15.21 (br s, 1H, COOH), 9.93 (s, 1H, CONH), 8.65 (s, 1H, cipro-ArH-2), 8.05 (s, 1H, triazole-H), 7.89 (d, *J* = 13.3 Hz, 1H, cipro-ArH-5), 7.54 (d, *J* = 8.1 Hz, 1H, cipro-ArH-8), 7.51 (d, *J* = 8.5 Hz, 2H, phenyl-H), 7.38 (d, *J* = 8.4 Hz, 2H, phenyl-H), 5.06 (br s, 1H, OH), 4.84 (br s, 1H, OH), 4.59 (br s, 1H, OH), 4.43 (d, *J* = 9.4 Hz, 2, glyco-H-1 + OH), 4.37 (t, *J* = 6.9 Hz, 2H, -NHCOCH₂CH₂CH₂CH₂-), 3.81 (s, 1H, cPr-H), 3.68 (br s, 1H, glyco-H-4), 3.65 (s, 2H, -triazole-CH₂CH₂NRR'), 3.56–3.44 (m, 2H, glyco-H-6 + H-6'), 3.41 (d, *J* = 6.0 Hz, 19H), 3.40 (glyco-H-5, extracted from HSQC), 3.37 (glyco-H-2, extracted from HSQC), 3.32 (2x piperazine-CH₂, extracted from HSQC), 2.63 (br s, 4H, 2x piperazine-CH₂'), 2.34 (t, *J* = 7.4 Hz, 2H, -NHCOCH₂CH₂CH₂CH₂-), 1.86 (tt, *J* = 7.1 Hz, 2H, -NHCOCH₂CH₂CH₂CH₂-), 1.55 (tt, *J* = 7.5 Hz, 2H, -NHCOCH₂CH₂CH₂CH₂-), 1.39–1.26 (m, 2H, cPr-CH₂), 1.22–1.12 (m, 2H, cPr-CH₂). ¹³C NMR (126 MHz, DMSO-*d*₆) δ 176.36 (cipro-C4=O), 170.82 (C=O), 165.96 (COOH), 153.01 (d, *J* = 249.9 Hz, cipro-C-6), 148.01 (cipro-C-2), 145.17 (d, *J* = 9.9 Hz, cipro-C-7), 143.02 (triazole-C), 139.19 (cipro-C-8a), 138.03 (phenyl-C), 131.15 (phenyl-C), 128.20 (phenyl-C), 123.77 (triazole-CH), 119.31 (phenyl-C), 118.56 (d, *J* = 7.8 Hz, cipro-C-4a), 110.94 (d, *J* = 23.2 Hz, cipro-C-5), 106.72 (cipro-C-3), 106.37 (d, *J* = 3.0 Hz, cipro-C-8), 88.35 (glyco-C-1), 79.17 (glyco-C-5), 74.69 (glyco-C-3), 69.20 (glyco-C-2), 68.33 (glyco-C-4), 60.57 (glyco-C-6), 52.40 (linker-CH₂), 51.86 (piperazine), 49.39 (piperazine), 49.03 (linker-CH₂), 35.85 (cPr-CH), 35.59 (linker-CH₂), 29.34 (linker-CH₂), 22.01 (linker-CH₂), 7.57 (cPr-CH₂). HR-MS calcd [C₃₇H₄₅FN₇O₉S]⁺: 782.2987, found 782.2972.

Gal-ciprofloxacin Conjugate 29 (*n* = 4, *m* = 1). The title compound was synthesized from **14** (30 mg, 0.073 mmol, 1 eq.) and **21** (56 mg, 0.146 mmol, 2 eq.) according to general procedure iv and was obtained as a beige amorphous solid (28 mg, 48%). ¹H NMR (500 MHz, DMSO-*d*₆) δ 15.23 (br s, 1H, COOH), 9.93 (s, 1H, CONH), 8.66 (s, 1H, cipro-ArH-2), 7.93–7.86 (m, 2H, triazole-H + cipro-ArH-5), 7.55 (d, *J* = 7.2 Hz, 1H, cipro-ArH-8), 7.50 (d, *J* = 8.6 Hz, 2H, phenyl-H), 7.37 (d, *J* = 8.6 Hz, 2H, phenyl-H), 5.07 (br s, 1H, OH), 4.84 (br s, 1H, OH), 4.62 (br s, 1H, OH), 4.43 (d, *J* = 9.2 Hz, 2H, glyco-H-1 + OH), 4.34 (t, *J* = 6.9 Hz, 2H, -NHCOCH₂CH₂CH₂CH₂-), 3.81 (br s, 1H), 3.68 (s, 1H, glyco-H-4), 3.49 (glyco-H-6 + H-6', extracted from HSQC), 3.41 (glyco-H-5, extracted from HSQC), 3.37 (glyco-H-2, extracted from HSQC), 3.34 (2x piperazine-CH₂, extracted from HSQC), 3.32 (glyco-H-3, extracted from HSQC), 2.84 (t, *J* = 7.5 Hz, 2H, -triazole-CH₂CH₂NRR'), 2.67 (br s, 6H, 2x piperazine-CH₂ + -triazole-

$\text{C}_2\text{H}_2\text{C}_2\text{NRR}'$), 2.33 (t, $J = 7.3$ Hz, 2H, $-\text{NHCOCH}_2\text{CH}_2\text{CH}_2\text{CH}_2-$), 1.83 (tt, $J = 6.9$ Hz, 2H, $-\text{NHCOCH}_2\text{CH}_2\text{CH}_2\text{CH}_2-$), 1.54 (tt, $J = 7.4$ Hz, 2H, $-\text{NHCOCH}_2\text{CH}_2\text{CH}_2\text{CH}_2-$), 1.36–1.24 (m, 2H, cPr-CH_2), 1.25–1.06 (br s, 2H, cPr-CH_2). ^{13}C NMR (126 MHz, $\text{DMSO-}d_6$) δ 176.41 (cipro-C4=O), 170.89 (C=O), 166.04 (COOH), 153.07 (d, $J = 249.6$ Hz, cipro-C-6), 148.04 (cipro-C-2), 145.23 (d, $J = 9.9$ Hz, cipro-C-7), 144.99 (triazole-C), 139.24 (cipro-C-8a), 138.05 (phenyl-C), 131.19 (phenyl-C), 128.23 (phenyl-C), 122.23 (triazole-CH), 119.35 (phenyl-C), 118.58 (d, $J = 7.5$ Hz, cipro-C-4a), 110.98 (d, $J = 23.2$ Hz, cipro-C-5), 106.75 (cipro-C-3), 106.36 (d, $J = 3.0$ Hz, cipro-C-8), 88.37 (glyco-C-1), 79.19 (glyco-C-5), 74.72 (glyco-C-3), 69.24 (glyco-C-2), 68.38 (glyco-C-4), 60.62 (glyco-C-6), 57.25 (linker- CH_2), 52.21 (piperazine), 49.41 (piperazine), 49.00 (linker- CH_2), 35.90 (cPr-CH), 35.66 (linker- CH_2), 29.40 (linker- CH_2), 22.99 (linker- CH_2), 22.07 (linker- CH_2), 7.61 (cPr- CH_2). HR-MS calcd [$\text{C}_{37}\text{H}_{45}\text{FN}_7\text{O}_9\text{S}_2$] $^+$: 796.3135, found 796.3128.

5-(2'-Bromoethyl)thiophene-2-sulfonyl Chloride (16). **16** was synthesized in two chemical steps: thiopheneethanol **15** (1.0 mL, 9.0 mmol, 1 eq.) was dissolved in 40 mL of dry CH_2Cl_2 . The solution was cooled (0 °C), and a solution of PBr_3 (846 μL , 9.0 mmol, 1 eq.) in dry CH_2Cl_2 was added dropwise under vigorous stirring; the reaction was stirred for 1 h until full transformation, monitored by TLC (PE:EtOAc, 95:5). The reaction was quenched with ice water. The organic phase was washed with water (2x), aq. half satd. Na_2CO_3 (2x), and brine and dried over anhydrous Na_2SO_4 . The organic phase was reduced *in vacuo* and filtered over silica. After evaporation of the solvent *in vacuo* crude 2-(2'-bromoethyl)thiophene was obtained as a yellow oil (490 mg, 28%). ^1H NMR (500 MHz, CHCl_3 - d) δ 7.20 (dd, $J = 5.1, 1.2$ Hz, 1H, ArH-5), 6.97 (dd, $J = 5.1, 3.5$ Hz, 1H, ArH-4), 6.90 (dd, $J = 3.4, 1.0$ Hz, 1H, ArH-3), 3.58 (t, $J = 7.4$ Hz, 2H, $-\text{CH}_2\text{CH}_2\text{Br}$), 3.38 (t, $J = 7.5$ Hz, 2H, $-\text{CH}_2\text{CH}_2\text{Br}$). 2-(2'-Bromoethyl)thiophene (255 mg, 1.33 mmol, 1 eq.) was dissolved in 10 mL of dry CH_2Cl_2 , and the mixture was cooled (0 °C). HSO_3Cl (266 μL , 4 mmol, 3 eq.) was dissolved in 5 mL of dry CH_2Cl_2 and added dropwise to the starting material under vigorous stirring. The reaction was stirred 1 h until full transformation, monitored by TLC (PE:EtOAc, 95:5). The reaction was quenched with ice water. The aqueous phase was extracted with CH_2Cl_2 (3x). The combined organic phases were washed with half satd. brine (x) and brine (1x) and dried over anhydrous Na_2SO_4 . The solvent was evaporated *in vacuo* to obtain the crude product as a dark yellow oil (261 mg).

β -L-Fucopyranosyl-1-methylamine (17). β -L-Fucopyranosyl-1-nitromethane was synthesized according to Phiasivongsa et al.⁷³ with subsequent reduction to the amine as previously described in Sommer et al.⁴² NMR in agreement with literature data.⁴²

***N*- β -L-Fucopyranosylmethyl-2-(5-(2'-azidoethyl)thiophene)sulfonamide (19).** β -L-Fucopyranosyl-1-methylamine (**17**, 128 mg, 0.60 mmol, 1 eq.) and K_2CO_3 (166 mg, 1.2 mmol, 2 eq.) were dispersed in 6 mL of dry DMF and cooled to 0 °C. Crude 2-chlorosulfonyl-5-(2'-bromoethyl)thiophene (261 mg, 0.90 mmol) was dissolved in 6 mL of dry DMF and added dropwise to the starting material under vigorous stirring. The reaction was stirred for 3 h until full conversion, as monitored by TLC (MeOH:EtOAc:aq. NH_4OH 25%, 4:4:2). After quenching with water, the aqueous phase was extracted with EtOAc (4x). The combined organic layers were washed with half satd. brine (3x) and brine (1x) and dried over anhydrous Na_2SO_4 . After filtration, the solvent was evaporated *in vacuo* and the crude material (191 mg) was dissolved in 10 mL of dry DMF. NaN_3 (143 mg, 2.2 mmol) was added, and the mixture was stirred for 3 h. After full transformation (monitored by HPLC-MS), the reaction was diluted with water and extracted with EtOAc (3x). The combined organic layers were washed with half satd. brine (3x) and satd. brine (1x) and dried over anhydrous Na_2SO_4 . After filtration, the solvent was evaporated *in vacuo*, and the product was purified by MPLC (DCM:MeOH, 1–11%) to yield the target compound as a white amorphous solid (141 mg, 60% after three chemical steps, 8% impurity of the corresponding alkyl chloride, determined by ^1H NMR). ^1H NMR (500 MHz, $\text{MeOH-}d_4$) δ 7.46 (d, $J = 3.8$ Hz, 1H, Ar-H), 6.97 (d, $J = 3.7$ Hz, 1H, Ar-H), 3.65–3.57 (m, 3H,

$-\text{CH}_2\text{CH}_2\text{N}_3 + \text{H-4}$), 3.50 (q, $J = 7.0$ Hz, 1H, H-5), 3.45–3.34 (m, 3H, $-\text{CH}_2\text{N-} + \text{H-2}$), 3.17 (td, $J = 9.1, 8.6, 2.4$ Hz, 1H, H-1), 3.12 (t, $J = 6.6$ Hz, 2H, $-\text{CH}_2\text{CH}_2\text{N}_3$), 3.06 (dd, $J = 12.9, 7.2$ Hz, 1H, $-\text{CH}_2'\text{N-}$), 1.20 (d, $J = 6.5$ Hz, 3H, H-6). ^{13}C NMR (126 MHz, $\text{MeOH-}d_4$) δ 149.48 (Ar-C), 141.03 (Ar-C), 132.98 (Ar-C), 127.32 (Ar-C), 79.55 (glyco-C-2), 76.37 (glyco-C-3), 75.57 (glyco-C-5), 73.61 (glyco-C-4), 69.74 (glyco-C-1), 53.08 (glyco-C-2), 45.75 (linker- CH_2), 30.71 (linker- CH_2), 17.07 (glyco-C-6). HR-MS calcd [$\text{C}_{13}\text{H}_{19}\text{N}_4\text{O}_6\text{S}_2$] $^-$: 391.0751, found 391.0759.

Hybrid-Ciprofloxacin Conjugate 30 ($m = 0$). The title compound was synthesized from **19** (35 mg, 0.09 mmol, 1 eq.) and **20** (35 mg, 0.095 mmol, 1.1 eq.) according to general procedure iv and was obtained as a beige amorphous solid (30 mg, 44%). ^1H NMR (500 MHz, $\text{DMSO-}d_6$) δ 15.23 (br s, 1H, -COOH), 8.66 (s, 1H, cipro-H-2), 7.98 (s, 1H, triazole-H), 7.90 (d, $J = 13.3$ Hz, 1H, cipro-H-5), 7.66 (t, $J = 5.9$ Hz, 1H, $-\text{NHSO}_2-$), 7.55 (d, $J = 7.4$ Hz, 1H, cipro-H-8), 7.37 (d, $J = 3.7$ Hz, 1H, thienyl-H), 6.89 (d, $J = 3.8$ Hz, 1H, thienyl-H), 4.80 (br s, 1H, OH), 4.65 (t, $J = 6.7$ Hz, 1H, thiophene- CH_2CH_2 -triazole), 4.59 (br s, 1H, OH), 4.28 (d, $J = 5.5$ Hz, 1H, OH), 3.86–3.77 (m, 1H, cPr-H), 3.63 (s, 2H, triazole- CH_2 -NRR'), 3.47 (t, $J = 6.7$ Hz, 2H, thiophene- CH_2CH_2 -triazole), 3.39 (s, 1H, glyco-H-4), 3.37, 3.25–3.18 (m, 2H, $-\text{CH}_2\text{NHSO}_2-$ + glyco-H-3), 3.14 (t, $J = 9.3$ Hz, 1H, glyco-H-2), 3.01 (td, $J = 8.8, 2.3$ Hz, 1H, glyco-H-1), 2.73 (ddd, $J = 13.4, 8.4, 5.6$ Hz, 1H, $-\text{CH}_2\text{NHSO}_2-$), 2.59 (2.63–2.56 m, 4H, 2x piperazine- CH_2), 1.39–1.30 (m, 2H, cPr- CH_2), 1.20–1.14 (m, 4H, cPr- CH_2), 1.07 (d, $J = 6.4$ Hz, 3H, glyco-H-3). ^{13}C NMR (126 MHz, $\text{DMSO-}d_6$) δ 176.38 (cipro-C4=O), 165.98 (COOH), 153.02 (d, $J = 249.2$ Hz, cipro-C-6), 147.98 (cipro-C-2), 146.07 (Ar-C), 145.23 (d, $J = 10.1$ Hz, cipro-C-7), 143.18 (triazole-C), 139.65 (Ar-C), 139.23 (cipro-C-8a), 131.14 (Ar-C), 126.59 (Ar-C), 124.22 (triazole-CH), 118.56 (d, $J = 7.4$ Hz, cipro-C-4a), 110.95 (d, $J = 22.9$ Hz, cipro-C-5), 106.72 (cipro-C-3), 106.34 (d, $J = 2.6$ Hz, cipro-C-8), 78.24 (glyco-C-2), 74.64 (glyco-C-3), 73.64 (glyco-C-5), 71.56 (glyco-C-4), 68.30 (glyco-C-1), 52.41 (linker- CH_2), 51.88 (piperazine), 50.01 (linker- CH_2), 49.40 (piperazine), 44.74 (glyco- CH_2), 35.90 (cPr-CH), 29.97 (linker- CH_2), 16.93 (glyco-C-6), 7.57 (cPr- CH_2). HR-MS calcd [$\text{C}_{33}\text{H}_{41}\text{FN}_7\text{O}_9\text{S}_2$] $^+$: 762.2386, found 762.2382.

Hybrid-Ciprofloxacin Conjugate 31 ($m = 1$). The title compound was synthesized from **19** (56 mg, 0.14 mmol, 1 eq.) and **21** (59 mg, 0.15 mmol, 1.1 eq.) according to general procedure iv and was obtained as a beige amorphous solid (57 mg, 52%). ^1H NMR (500 MHz, $\text{DMSO-}d_6$) δ 15.23 (s, 1H, COOH), 8.67 (s, 1H, cipro-ArH-2), 7.93–7.89 (m, 2H, triazole-H + cipro-ArH-5), 7.68 (t, $J = 5.9$ Hz, 1H, $-\text{NHSO}_2-$), 7.58 (d, $J = 7.4$ Hz, 1H, cipro-ArH-8), 7.38 (d, $J = 3.7$ Hz, 1H, thienyl-H), 6.89 (d, $J = 3.8$ Hz, 1H, thienyl-H), 4.82 (br s, 1H, OH), 4.62 (t, $J = 6.9$ Hz, 2H, thiophene- CH_2CH_2 -triazole + OH), 4.29 (s, 1H, OH), 3.84 (s, 1H, cPr-H), 3.44 (t, $J = 6.9$ Hz, 2H, thiophene- CH_2CH_2 -triazole), 3.40 (s, 1H, glyco-H-4), 3.37 (1H, glyco-H-5, extracted from HSQC), 3.35 (4H, 2x piperazine- CH_2), 3.28–3.20 (m, 2H, $-\text{CH}_2\text{NSO}_2-$ + glyco-H-3), 3.15 (t, $J = 9.3$ Hz, 1H, glyco-H-2), 3.02 (td, $J = 8.8, 2.3$ Hz, 1H, glyco-H-1), 2.85 (t, $J = 7.5$ Hz, 2H, $-\text{triazole-CH}_2\text{CH}_2\text{NRR}'$), 2.74 (ddd, $J = 13.6, 8.4, 5.7$ Hz, 1H, $-\text{CH}_2'\text{NSO}_2-$), 2.68 (br s, 6H, 2x piperazine- CH_2 + $-\text{triazole-CH}_2\text{CH}_2\text{NRR}'$), 1.91 (s, OH), 1.35–1.29 (m, 2H, cPr- CH_2), 1.22–1.16 (m, 2H, cPr- CH_2), 1.08 (d, $J = 6.4$ Hz, 3H, glyco-H-6). ^{13}C NMR (126 MHz, $\text{DMSO-}d_6$) δ 176.37 (cipro-C4=O), 165.97 (COOH), 153.03 (d, $J = 250.0$ Hz, cipro-C-6), 148.02 (cipro-C-2), 146.17 (Ar-C), 145.17 (d, $J = 10.4$ Hz, cipro-C-7), triazole-C not found, 139.66 (Ar-C), 139.21 (cipro-C-8a), 131.18 (Ar-C), 126.45 (Ar-C), 122.47 (triazole-CH), 118.57 (d, $J = 7.4$ Hz, cipro-C-4a), 110.95 (d, $J = 23.1$ Hz, cipro-C-5), 106.73 (cipro-C-3), 106.37 (d, $J = 2.5$ Hz, cipro-C-8), 78.24 (glyco-C-2), 74.65 (glyco-C-3), 73.63 (glyco-C-5), 71.57 (glyco-C-4), 68.31 (glyco-C-1), 57.16 (linker- CH_2), 52.15 (piperazine), 49.88 (linker- CH_2), 49.32 (piperazine), 44.74 (glyco- CH_2), 35.89 (cPr-CH), 29.99 (linker- CH_2), 22.87 (linker- CH_2), 16.93 (glyco-C-6), 7.59 (cPr- CH_2). HR-MS calcd [$\text{C}_{34}\text{H}_{43}\text{FN}_7\text{O}_9\text{S}_2$] $^+$: 776.2542, found 776.2538.

Competitive Binding Assays. LecA (According to Joachim et al.⁵⁸). A serial dilution of the test compounds was prepared in TBS/

Ca (8.0 g/L NaCl, 2.4 g/L Tris, 0.19 g/L KCl, 0.15 g/L $\text{CaCl}_2 \cdot 2\text{H}_2\text{O}$), with 30% DMSO as a co-solvent. A concentrated solution of LecA was diluted in TBS/Ca together with the fluorescent reporter ligand (*N*-(fluorescein-5-yl)-*N'*-(β -D-(*m*-aminophenyl)-galactopyranosyl)thiocarbamide) to yield concentrations of 40 μM and 20 nM, respectively. A 10 μL solution of this mix was added to 10 μL serial dilutions of the test compounds in a black 384-well microtiter plates (Greiner Bio-One, Germany, cat. no. 781900) in triplicate. After centrifugation (2680 rcf, 1 min, r.t.), the reactions were incubated for 30–60 min at r.t. in a humidity chamber. Fluorescence (excitation 485 nm, emission 535 nm) was measured in parallel and perpendicular to the excitation plane on a PheraStar FS plate reader (BMG Labtech GmbH, Germany). The measured intensities were reduced by the values of only LecA in TBS/Ca, and fluorescence polarization was calculated. The data were analyzed with the MARS Data Analysis Software (BMG Labtech GmbH, Germany) and fitted according to the four-parameter variable slope model. Bottom and top plateaus were fixed according to the control compounds in each assay (*p*-nitrophenyl)- β -D-galactoside, and the data was reanalyzed with these values fixed. A minimum of three independent measurements on three plates was performed for each inhibitor.

LecB (LecB_{PAO1} According to Hauck et al.⁴¹ and LecB_{PA14} According to Sommer et al.³³). A serial dilution of the test compounds was prepared in TBS/Ca, with 10% DMSO as a co-solvent. A concentrated solution of LecB PAO1 or PA14 was diluted in TBS/Ca together with the fluorescent reporter ligand (*N*-(fluorescein-5-yl)-*N'*-(α -L-fucopyranosyl ethylene)thiocarbamide) to yield concentrations of 300 nM and 20 nM, respectively. A 10 μL solution of this mix was added to 10 μL serial dilutions of the test compounds in a black 384-well microtiter plates (Greiner Bio-One, Germany, cat. no. 781900) in triplicate. After centrifugation (2680 rcf, 1 min, r.t.), the reactions were incubated for 4–8 h at r.t. in a humidity chamber. Fluorescence was measured and analyzed as for LecA. Bottom and top plateaus were fixed according to the control compound in each assay (*L*-fucose), and the data were reanalyzed with these values fixed. A minimum of three independent measurements on three plates was performed for each inhibitor.

Gyrase Supercoiling Inhibition. The assay was performed with the *E. coli* gyrase supercoiling kit (Inspiralis, Norwich, UK) according to the manufacturer's instructions. All pipetting steps before the reaction was started were performed on ice. A serial dilution of the test compounds was prepared in 5% DMSO in water. A mix of relaxed pBR322 DNA (5.5 μg), 66 μL assay buffer (5x), and 192.5 μL water was prepared. 3 μL of the dilution series (or 3 μL 5% DMSO in water for control reactions) was added. 10 U gyrase (2 μL , 5 U/ μL) was diluted in 28 μL dilution buffer. 3 μL of the gyrase (1 U) solution was added to the reaction mixtures. For the negative control, 3 μL of dilution buffer was added instead of the enzyme. The reaction was incubated for 30 min at 37 °C. The reactions were stopped by the addition of 30 μL of STE-buffer (40% (m/v) sucrose, 100 mM Tris-HCl, pH 8, 10 mM EDTA, pH 8, 0.5 mg/mL bromophenol blue) and 30 μL of CHCl_3 /isoamyl alcohol (24:1) and vortexing. After centrifugation (17,600 rcf, 1 min, 4 °C), 50 μL of the aqueous layer was loaded on an agarose gel (1%, Tris-EDTA-acetate buffer). The gel was run for 3 h at 85 V, and DNA was visualized afterward by staining with ethidium bromide. Agarose gels were digitalized using the E-box VX2 gel documentation instrument (Vilber, Eberhardzell, Germany). The fluorescence intensity of each supercoiled band was quantified using ImageJ (Version 1.52a, National Institute of Health, USA). The data were analyzed using GraphPad Prism (Version 6.0 h, GraphPad Software, USA) and fitted against inhibitor concentration according to the four-parameter variable slope model to determine IC_{50} values. Bottom plateaus were fixed to 0. A minimum of three different experiments was performed for each inhibitor.

Bacterial Strain List. All microorganisms were obtained from the German Collection of Microorganisms and Cell Cultures (DSMZ) and the American Type Culture Collection (ATCC) or were part of our internal strain collection. The following strains were used: *Escherichia coli* DSM 1116 (source: Rolf Müller, HIPS), *Escherichia*

coli K12 MG1655 (source: Winfried Boos, Universität Konstanz), *Staphylococcus carnosus* DSM 20501 (source: Rolf Müller, HIPS), *Pseudomonas aeruginosa* PA14 wt (DSM 19882), *Pseudomonas aeruginosa* PAO1 wt (DSM 19880), *Pseudomonas aeruginosa* PA14 ΔlecA (Wagner et al., in preparation), and *Pseudomonas aeruginosa* PA14 ΔlecB (Wagner et al., in preparation).

Antibiotic Susceptibility (MIC Assay). The antibiotic activity of the synthesized conjugates was determined by broth microdilution assay based on the EUCAST guidelines, according to Wiegand, Hilpert, and Hancock.⁷⁴ Serial dilutions in sterile Müller-Hinton broth II (Fluka analytical, cat. no. 90922: 17.5 g/L casein acid hydrolysate, 3 g/L beef extract, 1.5 g/L starch, supplemented with 20–25 mg/L Ca^{2+} and 10–15 mg/L Mg^{2+} , pH 7.3) of the conjugates 21–31 and 20 were prepared from 100 mM DMSO stocks (for ciprofloxacin (3), a 10 mM aq. stock of ciprofloxacin-HCl was used), in sterile 96-well plates, yielding a concentration range from 128 to 0.125 $\mu\text{g}/\text{mL}$ (12.8–0.0125 for ciprofloxacin). Bacterial strains were streaked on LB-agar plates (1% agar) from glycerol stocks and incubated at 37 °C overnight. Colonies were picked from plate and dispersed in fresh Müller-Hinton broth II (MHB II) to yield an OD_{600} of 0.08–0.13. This dispersion was diluted 1:100 in fresh MHB II, which was then used for the assay to achieve a final inoculum of 5×10^5 CFU/mL. If indicated, PMBN was added to this inoculum at 2 $\mu\text{g}/\text{mL}$. A 50 μL inoculum was mixed with 50 μL of the serial dilution in the corresponding well of the 96-well plate. The plates were incubated at 37 °C for 18–20 h in a humid incubator. Growth inhibition was assessed by visual inspection, and the given MIC values are the lowest concentration of the antibiotic at which there was no visible growth.

Biofilm Accumulation Assay. Bacterial precultures of *P. aeruginosa* PAO1 were prepared in 10 mL of LB and grown at 37 °C and 180 rpm overnight. The bacterial precultures were diluted in fresh LB to 50 mL and centrifuged (5925 rcf, 10 min, r.t.). The supernatant was discarded, and the pellet was resuspended and washed in 50 mL of fresh LB and centrifuged again (5925 rcf, 10 min, r.t.). The supernatant was discarded and the pellet was again resuspended in fresh LB to yield an OD_{600} of 0.1. Then, 150 μL of this inoculum were transferred to each well of a 96-well MBEC assay plate (SKU: 19113, Category: Well Base, Innovotech Inc., Canada). The outer wells were filled with 150 μL of sterile LB as a control. Plates were incubated at 37 °C, 125 rpm, and 75% humidity for 24 h. Compound solutions (170 μL , 200 μM , 1% DMSO) in phosphate-buffered saline pH 7.4, supplemented with 100 μM CaCl_2 (PBS/Ca) were dispensed in a 96-well plate (cat. no. 167008, Nunc MicroWell 96-Well Microplates, Thermo Scientific) in quintuplicate on plates. Each peg of the biofilm covered peg lid was washed in 200 μL of PBS/Ca in a 96-well plate (Nunc) for 1 min at r.t. and then incubated with the compound solution for 5 or 10 min at 37 °C, and 80 rpm under humid conditions. After the incubation step, the pegs were again washed with 200 μL of PBS/Ca in a 96-well format for 30 s at r.t. and transferred to a last 96-well plate (Nunc) filled with 170 μL PBS/Ca per well. The plate was sealed with parafilm and sonicated for 15 min using an ultrasound bath. A 100 μL sample of each well was transferred to a vial and treated with 100 μL of MeCN (spiked with 1.5 μM diphenhydramine-HCl as an internal standard). After centrifugation (17,600 rcf, 10 min, 4 °C), the compound concentration in the supernatant was determined by LC-MS/MS. Fresh calibration curves for each compound were prepared in the same matrix for each experiment. In each assay, the accumulation factor relative to ciprofloxacin was determined. Statistical analysis (unpaired *t*-test) was performed using the GraphPad-Prism QuickCalcs online tool (<https://www.graphpad.com/quickcalcs/contMenu/>).

LC-MS/MS. LC-MS/MS analysis was performed on an Ultimate 3000 system (degasser, pump, autosampler, column compartment) equipped with a Nucleodur C18 Pyramid column (150 \times 2 mm, 3 μm , Macherey-Nagel, Düren, Germany) coupled to a TSQ Quantum Access MAX (Thermo Fisher Scientific, Waltham MA) with the following gradient conditions: A, water (0.1% formic acid); B, acetonitrile (0.1% formic acid); flow 0.600 mL/min; 90% A for 1.0 min; 90–5% A in 0.7 min; 5% A for 1.8 min; equilibration at 90% A

for 1.0 min. MS was operated in positive SRM mode with the following mass transitions:

Diphenhydramin (IS): 256.04–164.90; 256.04–166.90.

Ciprofloxacin (3): 332.063–230.908; 332.063–244.968; spray voltage: 4001 V, vaporizer temperature: 420 °C, sheath gas pressure: 50 psi, ion sweep pressure: 2.5 psi, aux gas pressure: 30 psi, capillary temperature: 260 °C, tube lens offset: 97 V, skimmer offset: 0 V, collision pressure: 1.5 mTorr, collision energy: 36 eV (230.908), 23 eV (244.968).

(21): 740.140–559.933; 740.140–577.966; spray voltage: 3000 V, vaporizer temperature: 470 °C, sheath gas pressure: 60 psi, ion sweep pressure: 0 psi, aux gas pressure: 55 psi, capillary temperature: 296 °C, tube lens offset: 99 V, skimmer offset: 0 V, collision pressure: 1.5 mTorr, collision energy: 36 eV (559.933), 27 eV (577.966).

(29): 762.124–726.026; 762.124–744.061; spray voltage: 4500 V, vaporizer temperature: 223 °C, sheath gas pressure: 60 psi, ion sweep pressure: 0 psi, aux gas pressure: 55 psi, capillary temperature: 284 °C, tube lens offset: 99 V, skimmer offset: 0 V, collision pressure: 1.5 mTorr, collision energy: 33 eV (726.026), 29 eV (744.061).

Cytotoxicity (MTT Assay, According to Haupenthal et al.⁷⁵). HEK293 or A549 cells (2×10^5 cells per well) were seeded in 24-well, flat-bottom plates. Culturing of cells, incubations, and OD measurements were performed as described with small modifications. Twenty-four hours after seeding the cells, the incubation was started by the addition of compounds in a final DMSO concentration of 1%. The living cell mass was determined after 48 h in a PHERAstar microplate reader (BMG Labtech, Ortenberg, Germany). Two independent measurements were performed for each compound.

Microsomal Stability. Microsomal stability was performed as previously described in Sommer et al.⁴⁴

Plasma Protein Binding. Plasma protein binding was measured with a rapid equilibrium dialysis assay plate (Thermo Fisher Scientific, Waltham MA). On one side of the membrane, 150 μ L of human plasma (seralab-BioIVT, West Sussex United Kingdom) and 150 μ L of PBS pH 7.4 (Gibco Thermo Fisher Scientific, Waltham MA) were added to the well; on the other side, 550 μ L of PBS was added to the well. The compound was added to a final concentration of 1 μ M to the plasma-containing well. The plate was closed and incubated in an orbital shaker at 37 °C for 6 h at 750 rpm. Samples of 10 μ L from each well were taken at 0, 5, and 6 h and mixed with 90 μ L of ice-cold acetonitrile with internal standard diphenhydramine (1 μ M). The concentration of compound in the supernatant was analyzed with LC-MS/MS. Plasma protein binding was calculated from the concentration difference between the wells. Five and 6 h samples were compared to ensure equilibrium. Warfarin was used as an assay control.

Human Plasma Stability. Compound stability in plasma was measured by incubation with plasma and LC-MS/MS quantification of the remaining compound. A 195 μ L solution of human plasma (seralab-BioIVT, West Sussex, United Kingdom) was incubated with 5 μ L of compound (40 μ M stock) at 37 °C for 0, 5, 60, and 150 min. Then, 800 μ L of ice-cold acetonitrile containing internal standard diphenhydramine (1 μ M) was added. The concentration of remaining compound in the supernatant was determined via LC-MS/MS measurement. Procaine was used as an activity control of plasma metabolism.

Cell Permeability. Permeability of the compound was assessed *in vitro* with Calu-3 HTB-55 cell line (ATCC). Cells were cultivated in minimum essential medium supplemented with Earle's salts, L-glutamine, 10% FCS, 1% non-essential amino acids (NEAA), and 1 mM sodium pyruvate. Passages between 35 and 55 were used, and the medium was changed every 2–3 days. For experiments, cells were harvested using Trypsin/EDTA and 1×10^5 cells seeded on Transwell inserts 3460. Cells were grown in an air–liquid interface beginning at day 3 and used for transport studies on days 11–13. TEER values exceeded 300 Ω ·cm² before beginning transport studies. For experiments, Krebs-Ringer solution with 1% BSA was used and cells were accommodated to the buffer for at least 1 h with no decrease in TEER. Samples (200 μ L) were taken in regular intervals from the apical side (time intervals of 0, 20, 40, 60, 90, 120, 180, and 240 min)

and replenished with fresh buffer. TEER was monitored during the experiment, and epithelial barriers were considered compromised if the TEER fell below 300 Ω ·cm² during 4 h of experiment duration. Fluorescein sodium salt and ciprofloxacin-HCl were used as a control. A 50 μ L sample was mixed with 150 μ L of ice-cold acetonitrile containing internal standard diphenhydramine (1 μ M), and the concentration of compound was analyzed with LC-MS/MS.

■ ASSOCIATED CONTENT

Supporting Information

The Supporting Information is available free of charge at <https://pubs.acs.org/doi/10.1021/acs.jmedchem.0c00856>.

¹H and ¹³C NMR spectra of new compounds; gyrase supercoiling inhibition assay gels; *P. aeruginosa* PAO1 biofilm accumulation raw data; lectin inhibition K_i values calculated from IC₅₀; antibiotic susceptibility in molar concentration; key compounds and intermediates as SMILES; purity of key compounds 11–14, 19–31 by HPLC-UV; and retention times and a representative chromatogram of conjugates 22–31 and ciprofloxacin (3) from slow gradient HPLC runs for lipophilicity comparison (PDF)

Molecular formula strings for all new compounds and key compounds (5–14, 16, and 19–31) (CSV)

■ AUTHOR INFORMATION

Corresponding Author

Alexander Titz – Chemical Biology of Carbohydrates (CBCH), Helmholtz Institute for Pharmaceutical Research Saarland (HIPS), Helmholtz Centre for Infection Research, D-66123 Saarbrücken, Germany; Deutsches Zentrum für Infektionsforschung (DZIF), Standort Hannover-Braunschweig, D-38124 Braunschweig, Germany; Department of Pharmacy and Department of Chemistry, Saarland University, D-66123 Saarbrücken, Germany; orcid.org/0000-0001-7408-5084; Phone: +49 681 99806 2500; Email: alexander.titz@helmholtz-hzi.de

Authors

Joscha Meiers – Chemical Biology of Carbohydrates (CBCH), Helmholtz Institute for Pharmaceutical Research Saarland (HIPS), Helmholtz Centre for Infection Research, D-66123 Saarbrücken, Germany; Deutsches Zentrum für Infektionsforschung (DZIF), Standort Hannover-Braunschweig, D-38124 Braunschweig, Germany; Department of Pharmacy and Department of Chemistry, Saarland University, D-66123 Saarbrücken, Germany

Eva Zahorska – Chemical Biology of Carbohydrates (CBCH), Helmholtz Institute for Pharmaceutical Research Saarland (HIPS), Helmholtz Centre for Infection Research, D-66123 Saarbrücken, Germany; Deutsches Zentrum für Infektionsforschung (DZIF), Standort Hannover-Braunschweig, D-38124 Braunschweig, Germany; Department of Pharmacy and Department of Chemistry, Saarland University, D-66123 Saarbrücken, Germany

Teresa Röhrig – Deutsches Zentrum für Infektionsforschung (DZIF), Standort Hannover-Braunschweig, D-38124 Braunschweig, Germany; Drug Design and Optimization (DDOP), Helmholtz Institute for Pharmaceutical Research Saarland (HIPS), Helmholtz Centre for Infection Research, D-66123 Saarbrücken, Germany

Dirk Hauck – Chemical Biology of Carbohydrates (CBCH), Helmholtz Institute for Pharmaceutical Research Saarland

(HIPS), Helmholtz Centre for Infection Research, D-66123 Saarbrücken, Germany; Deutsches Zentrum für Infektionsforschung (DZIF), Standort Hannover-Braunschweig, D-38124 Braunschweig, Germany

Stefanie Wagner – Chemical Biology of Carbohydrates (CBCH), Helmholtz Institute for Pharmaceutical Research Saarland (HIPS), Helmholtz Centre for Infection Research, D-66123 Saarbrücken, Germany; Deutsches Zentrum für Infektionsforschung (DZIF), Standort Hannover-Braunschweig, D-38124 Braunschweig, Germany

Complete contact information is available at:
<https://pubs.acs.org/10.1021/acs.jmedchem.0c00856>

Author Contributions

J.M. synthesized conjugates and individual building blocks. D.H. synthesized compound 17. J.M. and E.Z. performed lectin inhibition assays. J.M. performed gyrase supercoiling inhibition, antibiotic susceptibility, and biofilm accumulation assays. T.R. analyzed data for metabolic stability in human plasma, plasma protein binding, and acute cytotoxicity. S.W. provided conceptual advice and analyzed the data. J.M. and A.T. conceived the study. J.M. and A.T. wrote the paper with input from all coauthors.

Notes

The authors declare no competing financial interest.

ACKNOWLEDGMENTS

The authors are thankful to Prof. Dr. Rolf Müller and Dr. Jennifer Hermann (HIPS) for scientific discussions and for providing the bacterial strains *S. carnosus* DSM 20501 and *E. coli* DSM 1116. We are grateful to Dr. Thomas Ryckmans (F. Hoffmann la Roche, Basel) for metabolic stability assays against human liver microsomes and mouse liver microsomes, Tabea Wittmann and Dennis Jener (HIPS) for plasma stability, plasma protein binding, and cytotoxicity assays, and Justus Horstmann (HIPS) for cell permeation measurements. A.T. acknowledges financial support from the Helmholtz Association (VH-NG-934), the European Research Council (ERC Starting Grant, Sweetbullets), and DZIF.

LIST OF ABBREVIATIONS

XDR, extensively drug-resistant; WHO, World Health Organization; *P. aeruginosa*, *Pseudomonas aeruginosa*; MLM, mouse liver microsomes; HLM, human liver microsomes; PE, petroleum ether; CL_{MIC}, microsomal clearance; cPr, cyclopropyl; rcf, relative centrifugal force; LR-MS, low-resolution mass spectrometry

REFERENCES

- (1) Rice, L. B. Federal funding for the study of antimicrobial resistance in nosocomial pathogens: no ESKAPE. *J. Infect. Dis.* **2008**, *197*, 1079–1081.
- (2) Boucher, H. W.; Talbot, G. H.; Bradley, J. S.; Edwards, J. E.; Gilbert, D.; Rice, L. B.; Scheld, M.; Spellberg, B.; Bartlett, J. Bad bugs, no drugs: no ESKAPE! An update from the Infectious Diseases Society of America. *Clin. Infect. Dis.* **2009**, *48*, 1–12.
- (3) Rice, L. B. Progress and challenges in implementing the research on ESKAPE pathogens. *Infect. Control Hosp. Epidemiol.* **2010**, *31*, S7–S10.
- (4) Meynard, J.-L.; Barbut, F.; Guiguet, M.; Batisel, D.; Lalande, V.; Lesage, D.; Guiard-Schmid, J.-B.; Petit, J.-C.; Frottier, J.; Meyohas, M.-C. *Pseudomonas aeruginosa* infection in human immunodeficiency virus infected patients. *J. Infect.* **1999**, *38*, 176–181.

- (5) Rizzi, E. B.; Schininà, V.; Bordi, E.; Buontempo, G.; Narciso, P.; Bibbolino, C. HIV-related bronchopulmonary infection by *Pseudomonas aeruginosa* in the HAART era: radiological findings. *Acta Radiol.* **2006**, *47*, 793–797.

- (6) Bodey, G. P. *Pseudomonas aeruginosa* infections in cancer patients: have they gone away? *Curr. Opin. Infect. Dis.* **2001**, *14*, 403–407.

- (7) Hauser, A. R.; Rello, J. *Severe infections caused by Pseudomonas aeruginosa*; Springer Science & Business Media: Boston, MA, 2012.

- (8) Poole, K. *Pseudomonas aeruginosa*: resistance to the max. *Front. Microbiol.* **2011**, *2*, 65.

- (9) WHO publishes list of bacteria for which new antibiotics are urgently needed; World Health Organization: Geneva, 2017 Available at: <https://www.who.int/news-room/detail/27-02-2017-who-publishes-list-of-bacteria-for-which-new-antibiotics-are-urgently-needed>. (accessed January 2020)

- (10) Suci, P. A.; Mittelman, M. W.; Yu, F. P.; Geesey, G. G. Investigation of ciprofloxacin penetration into *Pseudomonas aeruginosa* biofilms. *Antimicrob. Agents Chemother.* **1994**, *38*, 2125–2133.

- (11) Flemming, H.-C.; Wingender, J. The biofilm matrix. *Nat. Rev. Microbiol.* **2010**, *8*, 623–633.

- (12) Davies, D. Understanding biofilm resistance to antibacterial agents. *Nat. Rev. Drug Discovery* **2003**, *2*, 114–122.

- (13) Winzer, K.; Falconer, C.; Garber, N. C.; Diggle, S. P.; Camara, M.; Williams, P. The *Pseudomonas aeruginosa* lectins PA-IL and PA-III are controlled by quorum sensing and by RpoS. *J. Bacteriol.* **2000**, *182*, 6401–6411.

- (14) Diggle, S. P.; Stacey, R. E.; Dodd, C.; Cámara, M.; Williams, P.; Winzer, K. The galactophilic lectin, LecA, contributes to biofilm development in *Pseudomonas aeruginosa*. *Environ. Microbiol.* **2006**, *8*, 1095–1104.

- (15) Tielker, D.; Hacker, S.; Loris, R.; Strathmann, M.; Wingender, J.; Wilhelm, S.; Rosenau, F.; Jaeger, K.-E. *Pseudomonas aeruginosa* lectin LecB is located in the outer membrane and is involved in biofilm formation. *Microbiology* **2005**, *151*, 1313–1323.

- (16) Gilboa-Garber, N. *Pseudomonas aeruginosa* lectins. *Methods Enzymol.* **1982**, *83*, 378–385.

- (17) Gilboa-Garber, N.; Mizrahi, L.; Garber, N. Mannose-binding hemagglutinins in extracts of *Pseudomonas aeruginosa*. *Can. J. Biochem.* **1977**, *55*, 975–981.

- (18) Gilboa-Garber, N. Purification and properties of hemagglutinin from *Pseudomonas aeruginosa* and its reaction with human blood cells. *Biochim. Biophys. Acta, Gen. Subj.* **1972**, *273*, 165–173.

- (19) da Silva, D. P.; Matwchuk, M. L.; Townsend, D. O.; Reichhardt, C.; Lamba, D.; Wozniak, D. J.; Parsek, M. R. The *Pseudomonas aeruginosa* lectin LecB binds to the exopolysaccharide Psl and stabilizes the biofilm matrix. *Nat. Commun.* **2019**, *10*, 2183.

- (20) Adam, E. C.; Mitchell, B. S.; Schumacher, D. U.; Grant, G.; Schumacher, U. *Pseudomonas aeruginosa* II lectin stops human ciliary beating: therapeutic implications of fucose. *Am. J. Respir. Crit. Care Med.* **1997**, *155*, 2102–2104.

- (21) Landi, A.; Mari, M.; Kleiser, S.; Wolf, T.; Gretzmeier, C.; Wilhelm, I.; Kiritsi, D.; Thünaier, R.; Geiger, R.; Nyström, A.; Reggiori, F.; Claudinon, J.; Römer, W. *Pseudomonas aeruginosa* lectin LecB impairs keratinocyte fitness by abrogating growth factor signalling. *Life Sci. Alliance* **2019**, *2*, No. e201900422.

- (22) Cott, C.; Thuenauer, R.; Landi, A.; Kühn, K.; Juillot, S.; Imberty, A.; Madl, J.; Eierhoff, T.; Römer, W. *Pseudomonas aeruginosa* lectin LecB inhibits tissue repair processes by triggering β -catenin degradation. *Biochim. Biophys. Acta, Mol. Cell Res.* **2016**, *1863*, 1106–1118.

- (23) Wilhelm, I.; Levit-Zerdoun, E.; Jakob, J.; Villringer, S.; Frensch, M.; Übelhart, R.; Landi, A.; Müller, P.; Imberty, A.; Thuenauer, R.; Claudinon, J.; Jumaa, H.; Reth, M.; Eibel, H.; Hobeika, E.; Römer, W. Carbohydrate-dependent B cell activation by fucose-binding bacterial lectins. *Sci. Signaling* **2019**, *12*, No. eaao7194.

- (24) Zheng, S.; Eierhoff, T.; Aigal, S.; Brandel, A.; Thuenauer, R.; de Bentzmann, S.; Imberty, A.; Römer, W. The *Pseudomonas aeruginosa*

- lectin LecA triggers host cell signalling by glycosphingolipid-dependent phosphorylation of the adaptor protein CrkII. *Biochim. Biophys. Acta, Mol. Cell Res.* **2017**, *1864*, 1236–1245.
- (25) Eierhoff, T.; Bastian, B.; Thuenauer, R.; Madl, J.; Audfray, A.; Aigal, S.; Juillot, S.; Rydell, G. E.; Muller, S.; de Bentzmann, S.; Imberty, A.; Fleck, C.; Romer, W. A lipid zipper triggers bacterial invasion. *Proc. Natl. Acad. Sci. U. S. A.* **2014**, *111*, 12895–12900.
- (26) Boukerb, A. M.; Rousset, A.; Galanos, N.; Méar, J.-B.; Thépaut, M.; Grandjean, T.; Gillon, E.; Cecioni, S.; Abderrahmen, C.; Faure, K.; Redelberger, D.; Kipnis, E.; Dessen, R.; Havet, S.; Darblade, B.; Matthews, S. E.; de Bentzmann, S.; Guéry, B.; Cournoyer, B.; Imberty, A.; Vidal, S. Antiadhesive properties of glycoclusters against *Pseudomonas aeruginosa* lung infection. *J. Med. Chem.* **2014**, *57*, 10275–10289.
- (27) Chemani, C.; Imberty, A.; de Bentzmann, S.; Pierre, M.; Wimmerová, M.; Guery, B. P.; Faure, K. Role of LecA and LecB lectins in *Pseudomonas aeruginosa*-induced lung injury and effect of carbohydrate ligands. *Infect. Immun.* **2009**, *77*, 2065–2075.
- (28) von Bismarck, P.; Schneppenheim, R.; Schumacher, U. Successful treatment of *Pseudomonas aeruginosa* respiratory tract infection with a sugar solution - a case report on a lectin based therapeutic principle. *Klin. Paediatr.* **2001**, *213*, 285–287.
- (29) Hauber, H.-P.; Schulz, M.; Pforte, A.; Mack, D.; Zabel, P.; Schumacher, U. Inhalation with fucose and galactose for treatment of *Pseudomonas aeruginosa* in cystic fibrosis patients. *Int. J. Med. Sci.* **2008**, *5*, 371–376.
- (30) Bucior, I.; Abbott, J.; Song, Y.; Matthay, M. A.; Engel, J. N. Sugar administration is an effective adjunctive therapy in the treatment of *Pseudomonas aeruginosa* pneumonia. *Am. J. Physiol.: Lung Cell. Mol. Physiol.* **2013**, *305*, L352–L363.
- (31) Klockgether, J.; Cramer, N.; Wiehlmann, L.; Davenport, C. F.; Tümmler, B. *Pseudomonas aeruginosa* genomic structure and diversity. *Front. Microbiol.* **2011**, *2*, 150.
- (32) Dötsch, A.; Schniederjans, M.; Khaledi, A.; Hornischer, K.; Schulz, S.; Bielecka, A.; Eckweiler, D.; Pohl, S.; Häussler, S. The *Pseudomonas aeruginosa* transcriptional landscape is shaped by environmental heterogeneity and genetic variation. *MBio* **2015**, *6*, No. e00749.
- (33) Sommer, R.; Wagner, S.; Varrot, A.; Nycholat, C. M.; Khaledi, A.; Häussler, S.; Paulson, J. C.; Imberty, A.; Titz, A. The virulence factor LecB varies in clinical isolates: consequences for ligand binding and drug discovery. *Chem. Sci.* **2016**, *7*, 4990–5001.
- (34) Boukerb, A. M.; Decor, A.; Ribun, S.; Tabaroni, R.; Rousset, A.; Commin, L.; Buff, S.; Doléans-Jordheim, A.; Vidal, S.; Varrot, A.; Imberty, A.; Cournoyer, B. Genomic rearrangements and functional diversification of lecA and lecB lectin-coding regions impacting the efficacy of glycomimetics directed against *Pseudomonas aeruginosa*. *Front. Microbiol.* **2016**, *7*, 811.
- (35) Varki, A.; Etzler, M. E.; Cummings, R. D.; Esko, J. D. Discovery and classification of glycan-binding proteins. In *Essentials of Glycobiology*; 2nd edition, Eds: Varki, A.; Cummings, R. D.; Esko, J. D.; Freeze, H. H.; Stanley, P.; Bertozzi, C. R.; Hart, G. W.; Etzler, M. E. Cold Spring Harbor Laboratory Press: 2009, Chapter 26. Available at: <http://www.ncbi.nlm.nih.gov/books/NBK1923/>.
- (36) Calvert, A. B.; Jumde, V. R.; Titz, A. Pathoblockers or antivirulence drugs as a new option for the treatment of bacterial infections. *Beilstein J. Org. Chem.* **2018**, *14*, 2607–2617.
- (37) Meiers, J.; Siebs, E.; Zahorska, E.; Titz, A. Lectin antagonists in infection, immunity, and inflammation. *Curr. Opin. Chem. Biol.* **2019**, *53*, 51–67.
- (38) Wagner, S.; Sommer, R.; Hinsberger, S.; Lu, C.; Hartmann, R. W.; Empting, M.; Titz, A. Novel strategies for the treatment of *Pseudomonas aeruginosa* infections. *J. Med. Chem.* **2016**, *59*, 5929–5969.
- (39) Cecioni, S.; Imberty, A.; Vidal, S. Glycomimetics versus multivalent glycoconjugates for the design of high affinity lectin ligands. *Chem. Rev.* **2015**, *115*, 525–561.
- (40) Bernardi, A.; Jiménez-Barbero, J.; Casnati, A.; De Castro, C.; Darbre, T.; Fieschi, F.; Finne, J.; Funken, H.; Jaeger, K.-E.; Lahmann, M.; Lindhorst, T. K.; Marradi, M.; Messner, P.; Molinaro, A.; Murphy, P. V.; Nativi, C.; Oscarson, S.; Penadés, S.; Peri, F.; Pieters, R. J.; Renaudet, O.; Reymond, J.-L.; Richichi, B.; Rojo, J.; Sansone, F.; Schäffer, C.; Turnbull, W. B.; Velasco-Torrijos, T.; Vidal, S.; Vincent, S.; Wennekes, T.; Zuilhof, H.; Imberty, A. Multivalent glycoconjugates as anti-pathogenic agents. *Chem. Soc. Rev.* **2013**, *42*, 4709–4727.
- (41) Hauck, D.; Joachim, I.; Frommeyer, B.; Varrot, A.; Philipp, B.; Möller, H. M.; Imberty, A.; Exner, T. E.; Titz, A. Discovery of two classes of potent glycomimetic inhibitors of *Pseudomonas aeruginosa* LecB with distinct binding modes. *ACS Chem. Biol.* **2013**, *8*, 1775–1784.
- (42) Sommer, R.; Exner, T. E.; Titz, A. A biophysical study with carbohydrate derivatives explains the molecular basis of monosaccharide selectivity of the *Pseudomonas aeruginosa* lectin LecB. *PLoS One* **2014**, *9*, No. e112822.
- (43) Sommer, R.; Hauck, D.; Varrot, A.; Wagner, S.; Audfray, A.; Prestel, A.; Möller, H. M.; Imberty, A.; Titz, A. Cinnamide derivatives of D-mannose as inhibitors of the bacterial virulence factor LecB from *Pseudomonas aeruginosa*. *ChemistryOpen* **2015**, *4*, 756–767.
- (44) Sommer, R.; Wagner, S.; Rox, K.; Varrot, A.; Hauck, D.; Wamhoff, E.-C.; Schreiber, J.; Ryckmans, T.; Brunner, T.; Rademacher, C.; Hartmann, R. W.; Brönstrup, M.; Imberty, A.; Titz, A. Glycomimetic, orally bioavailable LecB inhibitors block biofilm formation of *Pseudomonas aeruginosa*. *J. Am. Chem. Soc.* **2018**, *140*, 2537–2545.
- (45) Sommer, R.; Rox, K.; Wagner, S.; Hauck, D.; Henrikus, S. S.; Newsad, S.; Arnold, T.; Ryckmans, T.; Brönstrup, M.; Imberty, A.; Varrot, A.; Hartmann, R. W.; Titz, A. Anti-biofilm agents against *Pseudomonas aeruginosa*: a structure-activity relationship study of C-glycosidic LecB inhibitors. *J. Med. Chem.* **2019**, *62*, 9201–9216.
- (46) Cioci, G.; Mitchell, E. P.; Gautier, C.; Wimmerová, M.; Sudakevitz, D.; Pérez, S.; Gilboa-Garber, N.; Imberty, A. Structural basis of calcium and galactose recognition by the lectin PA-IL of *Pseudomonas aeruginosa*. *FEBS Lett.* **2003**, *555*, 297–301.
- (47) Wagner, S.; Hauck, D.; Hoffmann, M.; Sommer, R.; Joachim, I.; Müller, R.; Imberty, A.; Varrot, A.; Titz, A. Covalent lectin inhibition and application in bacterial biofilm imaging. *Angew. Chem., Int. Ed.* **2017**, *56*, 16559–16564.
- (48) Tanne, J. H. FDA adds 'black box' warning label to fluoroquinolone antibiotics. *BMJ* **2008**, *337*, a816.
- (49) Schwartz, R. S. Paul Ehrlich's magic bullets. *N. Engl. J. Med.* **2004**, *350*, 1079–1080.
- (50) Barok, M.; Joensuu, H.; Isola, J. Trastuzumab emtansine: mechanisms of action and drug resistance. *Breast Cancer Res.* **2014**, *16*, 209.
- (51) Lehar, S. M.; Pillow, T.; Xu, M.; Staben, L.; Kajihara, K. K.; Vandlen, R.; DePalatis, L.; Raab, H.; Hazenbos, W. L.; Morisaki, J. H.; Kim, J.; Park, S.; Darwish, M.; Lee, B.-C.; Hernandez, H.; Loyet, K. M.; Lupardus, P.; Fong, R.; Yan, D.; Chalouni, C.; Luis, E.; Khalif, Y.; Plise, E.; Cheong, J.; Lyssikatos, J. P.; Strandh, M.; Koefoed, K.; Andersen, P. S.; Flygare, J. A.; Tan, M. W.; Brown, E. J.; Mariathasan, S. Novel antibody-antibiotic conjugate eliminates intracellular *S. aureus*. *Nature* **2015**, *527*, 323–328.
- (52) Zhang, G.-F.; Liu, X.; Zhang, S.; Pan, B.; Liu, M.-L. Ciprofloxacin derivatives and their antibacterial activities. *Eur. J. Med. Chem.* **2018**, *146*, 599–612.
- (53) Klahn, P.; Brönstrup, M. Bifunctional antimicrobial conjugates and hybrid antimicrobials. *Nat. Prod. Rep.* **2017**, *34*, 832–885.
- (54) Milner, S. J.; Carrick, C. T.; Kerr, K. G.; Snelling, A. M.; Thomas, G. H.; Duhme-Klair, A.-K.; Routledge, A. Probing bacterial uptake of glycosylated ciprofloxacin conjugates. *ChemBioChem* **2014**, *15*, 466–471.
- (55) Howse, G. L.; Bovill, R. A.; Stephens, P. J.; Osborn, H. M. I. Synthesis and antibacterial profiles of targeted triclosan derivatives. *Eur. J. Med. Chem.* **2019**, *162*, 51–58.
- (56) Rodrigue, J.; Ganne, G.; Blanchard, B.; Saucier, C.; Giguère, D.; Shiao, T. C.; Varrot, A.; Imberty, A.; Roy, R. Aromatic thioglycoside inhibitors against the virulence factor LecA from *Pseudomonas aeruginosa*. *Org. Biomol. Chem.* **2013**, *11*, 6906–6918.

- (57) Kadam, R. U.; Garg, D.; Schwartz, J.; Visini, R.; Sattler, M.; Stocker, A.; Darbre, T.; Reymond, J.-L. CH- π 'T-shape' interaction with histidine explains binding of aromatic galactosides to *Pseudomonas aeruginosa* lectin LecA. *ACS Chem. Biol.* **2013**, *8*, 1925–1930.
- (58) Joachim, I.; Rikker, S.; Hauck, D.; Ponader, D.; Boden, S.; Sommer, R.; Hartmann, L.; Titz, A. Development and optimization of a competitive binding assay for the galactophilic low affinity lectin LecA from *Pseudomonas aeruginosa*. *Org. Biomol. Chem.* **2016**, *14*, 7933–7948.
- (59) Kadam, R. U.; Bergmann, M.; Hurley, M.; Garg, D.; Cacciarini, M.; Swiderska, M. A.; Nativi, C.; Sattler, M.; Smyth, A. R.; Williams, P.; Cámara, M.; Stocker, A.; Darbre, T.; Reymond, J.-L. A Glycopeptide dendrimer inhibitor of the galactose-specific lectin LecA and of *Pseudomonas aeruginosa* biofilms. *Angew. Chem., Int. Ed.* **2011**, *50*, 10631–10635.
- (60) Chu, D. T.; Fernandes, P. B. Structure-activity relationships of the fluoroquinolones. *Antimicrob. Agents Chemother.* **1989**, *33*, 131–135.
- (61) Gootz, T. D.; Brighty, K. E. Fluoroquinolone antibacterials: SAR, mechanism of action, resistance, and clinical aspects. *Med. Res. Rev.* **1996**, *16*, 433–486.
- (62) Idowu, T.; Schweizer, F. Ubiquitous nature of fluoroquinolones: the oscillation between antibacterial and anticancer activities. *Antibiotics* **2017**, *6*, 26.
- (63) Pham, T. D. M.; Ziora, Z. M.; Blaskovich, M. A. T. Quinolone antibiotics. *Med. Chem. Commun.* **2019**, *10*, 1719–1739.
- (64) Koga, H.; Itoh, A.; Murayama, S.; Suzue, S.; Irikura, T. Structure-activity relationships of antibacterial 6,7- and 7,8-disubstituted 1-alkyl-1,4-dihydro-4-oxoquinoline-3-carboxylic acids. *J. Med. Chem.* **1980**, *23*, 1358–1363.
- (65) Mustaev, A.; Malik, M.; Zhao, X.; Kurepina, N.; Luan, G.; Oppgaard, L. M.; Hiasa, H.; Marks, K. R.; Kerns, R. J.; Berger, J. M.; Drlica, K. Fluoroquinolone-gyrase-DNA complexes: two modes of drug binding. *J. Biol. Chem.* **2014**, *289*, 12300–12312.
- (66) Casoni, F.; Dupin, L.; Vergoten, G.; Meyer, A.; Ligeour, C.; Géhin, T.; Vidal, O.; Souteyrand, E.; Vasseur, J.-J.; Chevotot, Y.; Morvan, F. The influence of the aromatic aglycon of galactocusters on the binding of LecA: a case study with O-phenyl, S-phenyl, O-benzyl, S-benzyl, O-biphenyl and O-naphthyl aglycons. *Org. Biomol. Chem.* **2014**, *12*, 9166–9179.
- (67) Richter, M. F.; Drown, B. S.; Riley, A. P.; Garcia, A.; Shirai, T.; Svec, R. L.; Hergenrother, P. J. Predictive compound accumulation rules yield a broad-spectrum antibiotic. *Nature* **2017**, *545*, 299–304.
- (68) O'Shea, R.; Moser, H. E. Physicochemical properties of antibacterial compounds: implications for drug discovery. *J. Med. Chem.* **2008**, *51*, 2871–2878.
- (69) Müsken, M.; Klimmek, K.; Sauer-Heilborn, A.; Donnert, M.; Sedlacek, L.; Suerbaum, S.; Häussler, S. Towards individualized diagnostics of biofilm-associated infections: a case study. *NPJ Biofilms Microbiomes* **2017**, *3*, 22.
- (70) Zięba, A.; Maślankiewicz, A.; Sitkowski, J. ^1H , ^{13}C and ^{15}N NMR spectra of ciprofloxacin. *Magn. Reson. Chem.* **2004**, *42*, 903–904.
- (71) Driguez, H.; Szeja, W. Facile synthesis of 1,2-trans-nitrophenyl-1-thioglycopyranosides. *Synthesis* **1994**, *1994*, 1413–1414.
- (72) McPherson, J. C., III; Runner, R.; Buxton, T. B.; Hartmann, J. F.; Farcasiu, D.; Bereczki, I.; Róth, E.; Tollas, S.; Ostorházi, E.; Rozgonyi, F.; Herczegh, P. Synthesis of osteotropic hydroxybisphosphonate derivatives of fluoroquinolone antibacterials. *Eur. J. Med. Chem.* **2012**, *47*, 615–618.
- (73) Phiasivongsa, P.; Samoshin, V. V.; Gross, P. H. Henry condensations with 4,6-O-benzylidened and non-protected D-glucose and L-fucose via DBU-catalysis. *Tetrahedron Lett.* **2003**, *44*, 5495–5498.
- (74) Wiegand, I.; Hilpert, K.; Hancock, R. E. W. Agar and broth dilution methods to determine the minimal inhibitory concentration (MIC) of antimicrobial substances. *Nat. Protoc.* **2008**, *3*, 163–175.
- (75) Haupenthal, J.; Baehr, C.; Zeuzem, S.; Piiper, A. RNAse A-like enzymes in serum inhibit the anti-neoplastic activity of siRNA targeting polo-like kinase 1. *Int. J. Cancer* **2007**, *121*, 206–210.

3.2. *P. aeruginosa* Lectin-targeted Conjugates of Tobramycin

3.2.1. Introduction

Next to fluoroquinolones, aminoglycosides are first-line antibiotics in the therapy against *P. aeruginosa* infections.^[53] Aminoglycosides are broad-spectrum antibiotics with very characteristic structures. Typically, they contain one aminocyclitol ring (most commonly 2-desoxystreptamine), glycosidically linked to two amino sugars. Aminoglycosides disturb bacterial protein biosynthesis by binding to the 16S rRNA of the bacterial 30S ribosomal subunit. In consequence, these drugs have to permeate the bacterial cell wall. In Gram-negative bacteria, their cell uptake mechanism is supposed to be self-promoted. The multiple positive charges of aminoglycosides destabilise the outer membrane by electrostatic interaction with phospholipids. Additionally, accumulation of mistranslated proteins in the cytoplasmic cell membrane leads to further cell wall damage.^[82] In fact, it is supposed that membrane destabilisation might be a second, although less pronounced mode of action.^[83] Membrane disruption can increase permeability for other antibiotics, increasing their antimicrobial activity when used in combination.^[84]

Although aminoglycoside antibiotics are in regular clinical use, they suffer from several disadvantages. The highly polar structure of aminoglycosides prevents oral bioavailability, that is why they are only in parenteral use. Especially for intravenous drug delivery, small therapeutic windows due to nephro- and ototoxicity make close therapeutic drug monitoring vital. Targeted drug delivery could reduce unspecific drug accumulation in sensitive tissues and thus reduce side effects.

Tobramycin (**1**) is particularly effective against *P. aeruginosa* and is (amongst other indications) used via inhalation therapy against chronic *P. aeruginosa* infections. However, the *P. aeruginosa* biofilm protects individual cells from tobramycin.^[67, 85] It is very likely that negatively charged EPS of the biofilm matrix (e.g. alginate and eDNA) trap positively charged molecules and hinder their diffusion towards the biofilm core.^[86-89]

In parallel to chapter 3.1, the design, synthesis and evaluation of *P. aeruginosa* lectin-targeted conjugates of tobramycin is presented here.

3.2.2. Results and Discussion

3.2.2.1. Design and Synthesis

Tobramycin (**1**) is a highly functionalised molecule with five hydroxy groups and five amino groups, most of them involved in target binding (figure 1A, B). Thus, the anchor point for site-specific conjugation to lectin probes must be carefully chosen. On the other hand, synthetic accessibility has to be considered.

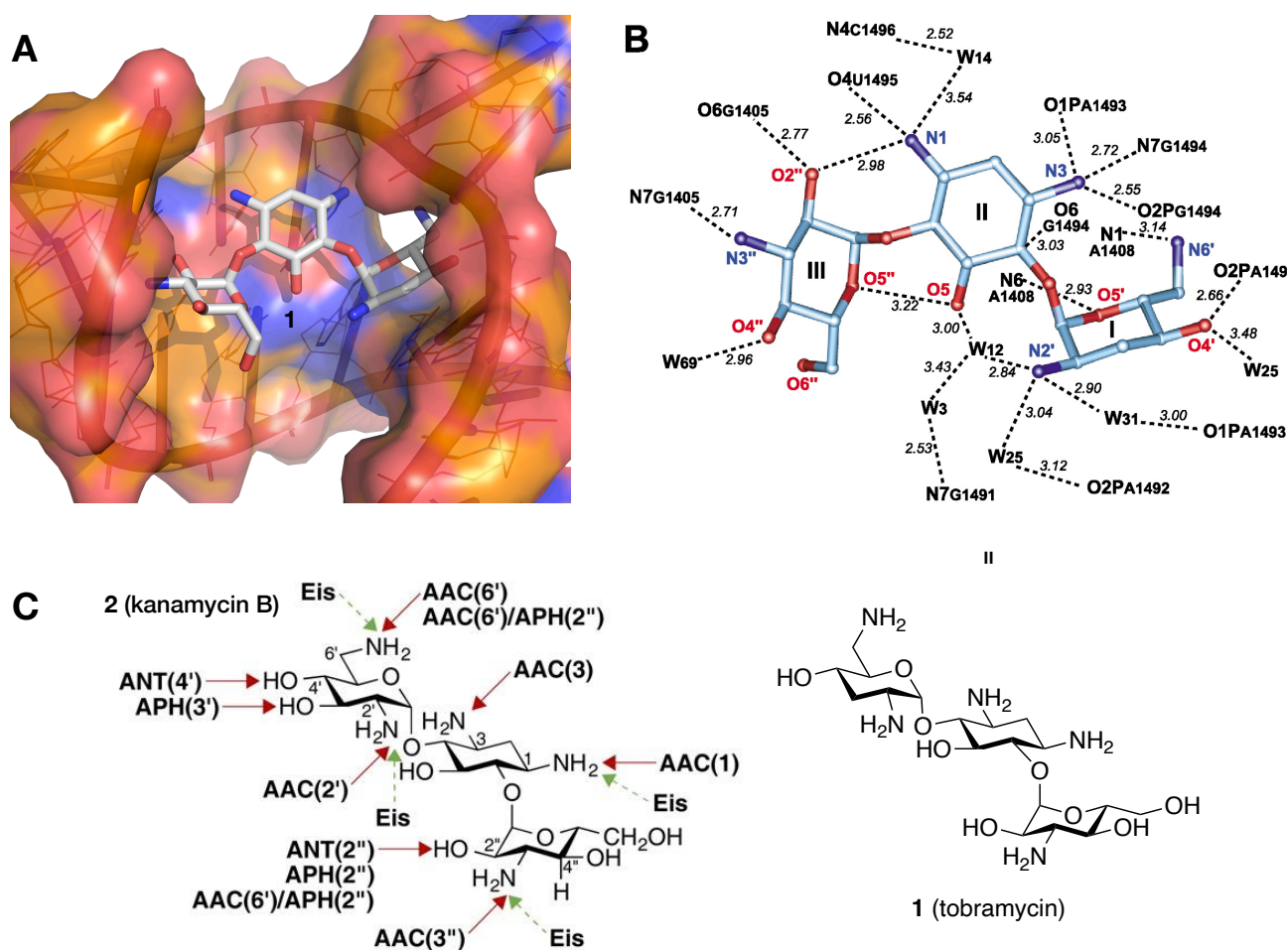
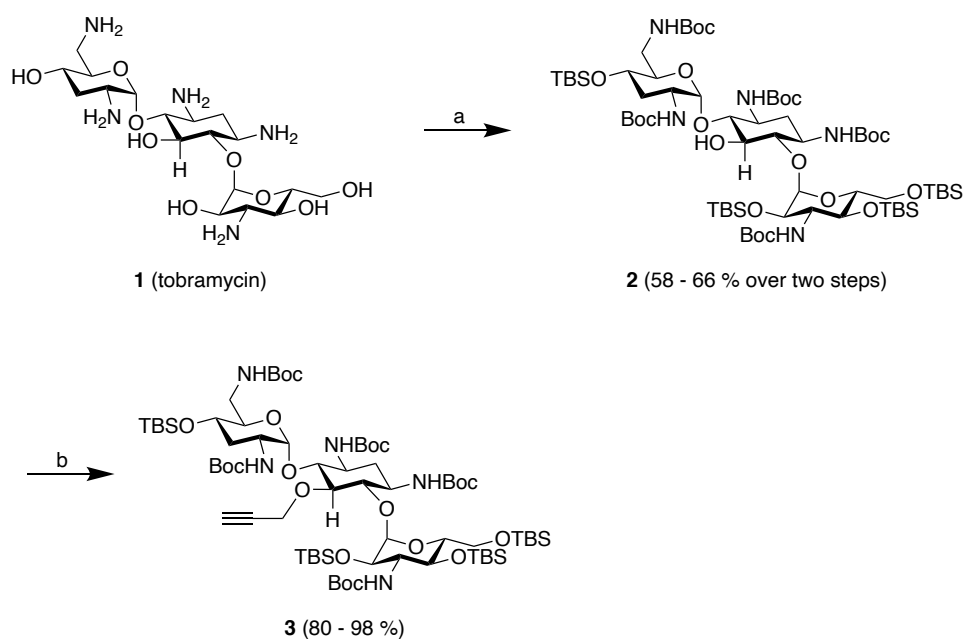


Figure 1. **A** Crystal structure of tobramycin (**1**) in complex with an oligonucleotide containing the ribosomal decoding A site (PDB code: 1LC4^[90]). Tobramycin and RNA are shown in grey and orange, respectively (functional groups coloured according to atom type). **B** Interaction network of tobramycin and bacterial RNA. Ring numbers and atom numbers are specified. Adapted from Vicens and Westhof.^[90] **C** Functional groups of kanamycin B (**2**) affected by aminoglycoside-modifying enzymes (AAC, ANT, APH, Eis) resulting in antimicrobial resistance. Adapted from Garneau-Tsodikova and Labby.^[91] Chemical structure of tobramycin (**1**) is shown for comparison (tobramycin = 3'-desoxykanamycin B).

Resistance against aminoglycoside antibiotics is most commonly mediated by aminoglycoside-modifying enzymes (figure 1C), e.g. *N*-acetylation (AAC), *O*-phosphorylation (APH) and *O*-adenylation (ANT).^[91] The modification of any amino group by aminoglycoside *N*-acetyltransferases disturbs target interaction and results in antimicrobial resistance. For example, the enhanced intracellular survival (Eis) protein is a acetyltransferase and a major cause of resistance against kanamycin in *mycobacterium tuberculosis* clinical isolates.^[92]

Interestingly, *O*5 of tobramycin (ring II) does not seem to serve as a substrate for aminoglycoside modifying enzymes. Further, it is only weakly involved in target binding (figure 1B). Together with its straight forward synthetic accessibility, *O*3 was chosen as a suitable starting point for conjugation.

Previous experiments (chapter 3.1) showed that short linker structures result in better antimicrobial activity due to improved bacterial cell uptake. However, self-promoted cell uptake should tolerate bigger molecular sizes. The modular approach of our triazole-based linkers allowed the use the same lectin probes as described before.



Scheme 1. Chemical synthesis of Boc-/TBS-protected 5-propargyl tobramycin (**3**). Reagents and conditions: (a) 1. Boc_2O , Et_3N , $\text{MeOH} : \text{H}_2\text{O}$ (2:1), 55 °C, 18 h; 2. TBSCl , NMI , DMF , r.t., 36 h; (b) propargylbromide, TBAHSO_4 , PhMe , r.t. 24 h.

Regiospecific propargylation of tobramycin was performed in analogy to Guchhait *et al.*^[93] (scheme 1): After tert-butyloxycarbonyl-protection (Boc) of the five primary amines, the sterically accessible hydroxy groups (i.e. *O*4', *O*2'', *O*4'' and *O*6'') were protected as tert-

interaction liquid chromatography (HILIC) and obtained as the corresponding formate salts (figure 2).

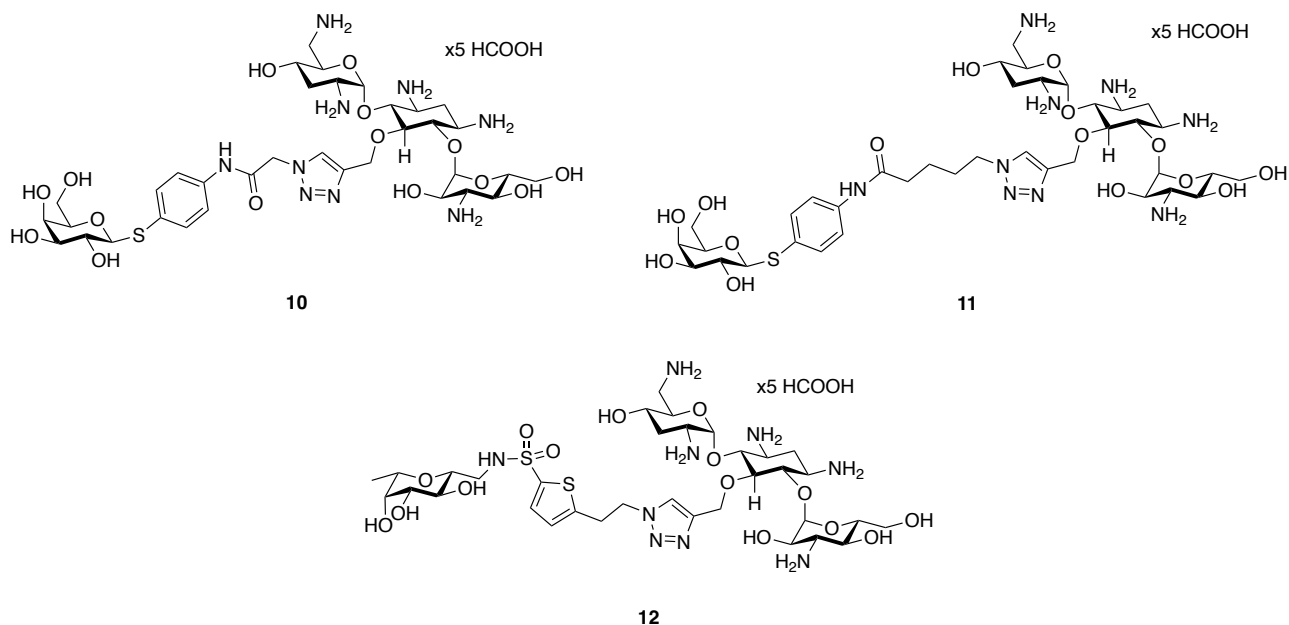


Figure 2. Chemical structures of the lectin-targeted tobramycin conjugates after purification by HILIC. All compounds were isolated as their penta-formate salt, determined by $^1\text{H-NMR}$.

3.2.2.2. Biophysical and microbiological evaluation

The binding affinity of the lectin-targeted tobramycin-conjugates was determined by reporter ligand displacement assay based on fluorescence polarisation.

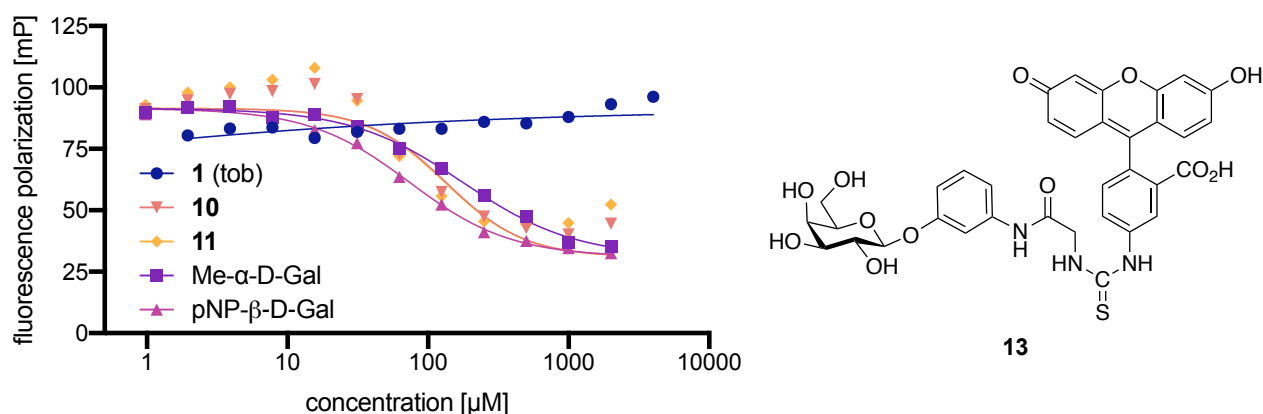


Figure 3. Competitive binding assay of tobramycin (**1**), its LecA-targeted conjugates **10** and **11** and reference carbohydrates against LecA, using fluorescein-based reporter ligand **13**. Fluorescence polarisation increased with increasing concentration for tobramycin-based compounds **1**, **10** and **11**. One representative titration of triplicates on plate is shown for each compound.

In the first experiments, fluorescein-galactose probe **13** was used to determine the conjugates' affinity towards LecA. Binding to LecA could be confirmed for both conjugates, while tobramycin (**1**) remained inactive (figure 3). However, all tobramycin-based compounds (**1**, **10**, **11**) showed an overall increase of fluorescence polarisation with increasing concentration, which was partially compensated by lectin binding around IC_{50} (for **10** and **11**). One reason could be an unspecific interaction with the protein. LecAs' calculated isoelectric point is around pH 5. Thus, LecA is negatively charged under the conditions of the binding assay (calcium adjusted tris-buffer, 20 mM tris, pH 7.4). Consequently, an ionic interaction with the positively charged tobramycin derivatives is likely.

On the other hand, it has to be noted, that the buffer concentration in this assay was 20 mM, whilst compound concentrations reached up to 4 mM. Hence, the pH of the test solution might be influenced by the aminoglycosides. Although fluorescein is commonly used as fluorescence dye, its fluorescence properties are known to be pH-dependent.

Thus, it is possible that addition of basic tobramycin (**1**) or acidic formate salts **10** - **12** influence the fluorescence polarisation readout during the competitive binding assay. Consequently, the reporter ligand was changed to the less pH-sensitive Galactose sulfo-Cy5 (sCy5) conjugate (**14**, figure S1).

| compound | IC ₅₀ [μM] | s.d. [μM] | target |
|-------------|-----------------------|-----------|----------------------|
| 1 | n.b. | - | LecA |
| 10 | 46.3 | 4.1 | |
| 11 | 38.5 | 3.0 | |
| Me-α-D-gal | 204 | 27 | |
| pNP-β-D-Gal | 90.6 | 13 | |
| ----- | | | |
| 1 | n.d. | - | LecB _{PA14} |
| 12 | 2.33 | 0.19 | |
| Me-α-L-Fuc | 0.83 | 0.07 | |
| L-Fuc | 2.46 | 0.33 | |
| Me-α-D-Man | 115 | 2.1 | |
| ----- | | | |
| 1 | n.b. | - | LecB _{PAO1} |
| 12 | 3.62 | 0.28 | |
| Me-α-L-Fuc | 0.55 | 0.05 | |
| L-Fuc | 2.63 | 1.7 | |
| Me-α-D-Man | 166 | 22 | |

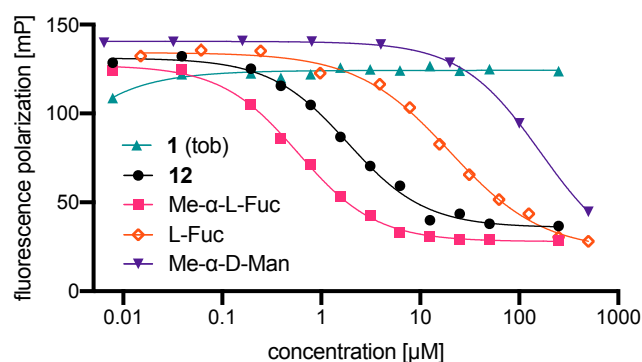
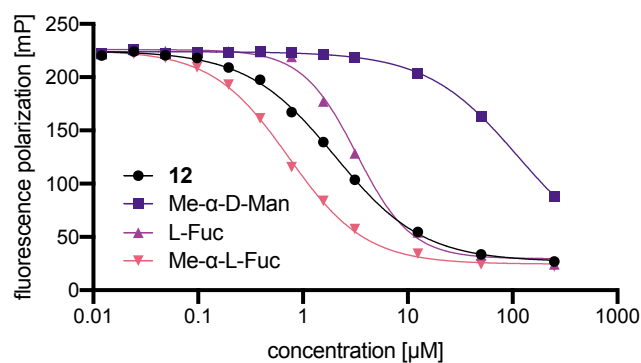
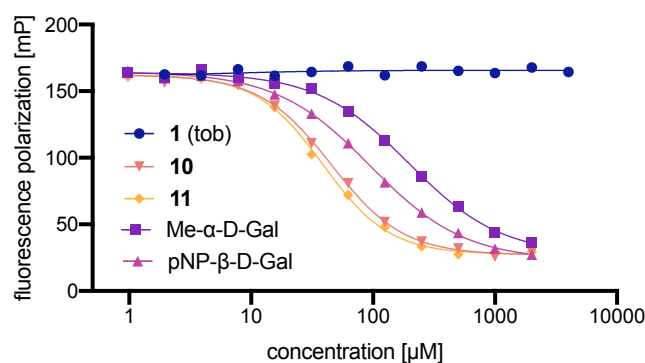


Figure 4. Competitive binding assay of tobramycin (**1**), its lectin-targeted conjugates **10** - **12** and reference carbohydrates with LecA, LecB_{PA14} and LecB_{PAO1}, using Cy5-based reporter ligand **14** (figure S1). One representative titration of triplicates on plate is shown for each compound. The corresponding IC₅₀-values were determined from at least three independent experiments and are given as mean and standard deviation. n.b., no binding; n.d., not determined.

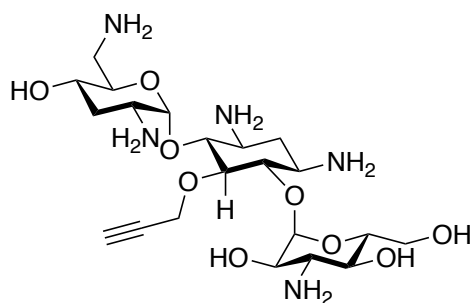
No ramp effect was observed under these conditions (figure 4), underpinning the latter theory described above. LecA-targeted tobramycin conjugates **10** and **11** bound their target protein with good affinity ($IC_{50} = 46.6 \mu\text{M} \pm 4.1 \mu\text{M}$ and $38.5 \pm 3.0 \mu\text{M}$, for **10** and **11**, respectively). In fact, the binding affinity was over factor two higher than the IC_{50} of reference compound pNP- β -D-Gal and around factor five for Me- α -D-gal. This can be explained by the fact that electron-rich aglycons stabilise the CH- π interaction with His50 of LecA.^[94] Further, an ion-ion interaction between positively charged conjugates **10** and **11** and negatively charged LecA could explain increased target affinity compared to pNP- β -D-Gal. However, unmodified tobramycin was found to have no affinity towards LecA below 4 mM. In conclusion, *P. aeruginosa* biofilm-targeting of lectin-targeted conjugates **10** - **12** is likely.

Next, minimal inhibitory concentration (MIC) of tobramycin-conjugates **10** - **12** against *E. coli* and *S. carnosus* was determined by broth dilution assay.^[95] In contrast to our expectations, all targeted conjugates showed no antibiotic activity at 64 $\mu\text{g}/\text{mL}$. Thus, planktonic *P. aeruginosa* was not considered for further experiments.

3.2.3. Conclusion and Outlook

In this study, the previously reported lectin-targeted building blocks (chapter 3.1) were conjugated to tobramycin by copper-click chemistry. Conjugates **10** - **12** were able to bind LecA or LecB with good affinity. However, they showed no antimicrobial activity below 64 $\mu\text{g}/\text{mL}$. Conjugation to lectin probes by the stable triazole linker results in sterically demanding molecules. The co-crystal structure of tobramycin with an RNA fragment suggests a possible growth vector at O5 (figure 1). However, it has to be noted that this binding site is surrounded by ribosomal proteins. It is very likely, that the conjugates do not fit in the target site, or do not reach the target site due to their molecular size. Although O5 is not an obvious target of deactivating enzymes, modifications at this position might not be tolerated due to target interactions. On the other hand, hindered membrane permeability might also limit the antimicrobial activity of the tobramycin conjugates, however less likely. It is very likely, that the conjugates are not in accordance with the target binding site of tobramycin. A possible control experiment would be the MIC-determination of propargyl-tobramycin (**15** which could unfortunately not be obtained in sufficient purity.

Despite the lost antimicrobial activity, conjugates **10** - **12** might still be used as *P. aeruginosa* biofilm-targeted sensitisers due to their potential to interfere with the Gram-negative outer membrane.



15

Figure 6. Control compound **15** needed for future experiments to evaluate the effect of O5 alkylation.

Further, the introduction of a cleavable linker in a prodrug-like fashion is of high interest and is currently under investigation (see chapter 3.3).

3.3. Smart Lectin-targeted Antibiotic-Carbohydrate Prodrugs activated by *Pseudomonas aeruginosa*

Authors: Joscha Meiers¹⁻³, Katharina Rox^{2,4} and Alexander Titz¹⁻³

Manuscript in preparation.

The references of this chapter are listed at the end of the chapter.

¹ Chemical Biology of Carbohydrates (CBCH), Helmholtz Institute for Pharmaceutical Research Saarland (HIPS), Helmholtz Centre for Infection Research, D-66123 Saarbrücken, Germany

² Deutsches Zentrum für Infektionsforschung (DZIF), Standort Hannover-Braunschweig, D-38124 Braunschweig, Germany

³ Department of Chemistry, Saarland University, D-66123 Saarbrücken, Germany

⁴ Chemical Biology (CBIO), Helmholtz Centre for Infection Research (HZI), Helmholtz Centre for Infection Research, D-38124 Braunschweig, Germany

This chapter is included in patent EP21212989 (priority date 07.12.21).

3.3.1. Abstract

The Gram-negative bacterium *Pseudomonas aeruginosa* is a critical threat for our health care system. Chronic infections are characterised by biofilm formation, which is a major virulence factor of *P. aeruginosa*, resulting in extensive drug resistance. Fluoroquinolones are very effective antibiotics, but are also linked to severe side effects resulting in medical contraindications. The two extracellular *P. aeruginosa*-specific lectins LecA and LecB are key structural biofilm components and can be exploited for targeted drug delivery. In this work, several fluoroquinolones were conjugated to lectin probes via a cleavable peptide linker to yield lectin-targeted prodrugs. The prodrugs rapidly released the antibiotic cargo in presence of *P. aeruginosa*. On the other hand, the prodrugs are stable against host metabolism and show good ADME properties *in vitro*. This work establishes the first biofilm-targeted antibiotic prodrugs against *P. aeruginosa* and serves as a starting point for a new class of antibiotics.

3.3.2. Introduction

Pseudomonas aeruginosa is a Gram-negative, opportunistic pathogen and has become a serious threat for our health care system.^[96-98] Chronic infections - especially in immunocompromised patients (e.g. hospitalised patients, geriatrics) and people suffering from cystic fibrosis - can lead to recurrent pneumonia, lung injuries, sepsis and other life-threatening conditions.^[7] In fact, 19.9% of ICU-acquired pneumonia is associated with *P. aeruginosa* in Europe.^[5] Its high pathogenicity is driven by various virulence factors together with intrinsic or acquired resistance against multiple antibiotic classes.

Almost any part of the human body can be infected by *P. aeruginosa*, leading to wound infections, urinary-tract infections, sepsis or pneumonia.^[99-101] Thus, it is vital to tailor the antibiotic treatment according to suitable pharmacokinetic properties. Targeted drug delivery is a yet underrepresented field in antibiotic therapy.^[73] In order to focus research activities on this perilous pathogen, carbapenem-resistant *P. aeruginosa* was declared critical priority I pathogen by the WHO.^[102]

The antibiotic resistance of *P. aeruginosa* is intrinsically caused by the additional outer membrane of Gram-negative bacteria and highly efficient efflux pumps, e.g. the MexAB-OprM system.^[51] Further resistances like antibiotic-modifying enzymes or reduced membrane permeability can be acquired by horizontal gene transfer or spontaneous mutations. In Europe 2019, 17.6% of all invasive *P. aeruginosa* isolates were resistant to at least two antibacterial groups.^[103] During chronic infections, *P. aeruginosa* can form biofilms, that are described as complex hydrogels stabilised by extracellular polymeric substances (EPS) like DNA (eDNA), polysaccharides (alginate, Psl and Pel) and a plethora of proteins.^[20] These biofilms can lead to an additional barrier towards antibiotics (up to 1,000-fold increase in antibacterial resistance) and the host immune system.^[104]

Ciprofloxacin and other fluoroquinolone antibiotics are standard-of-care drugs in the treatment of *P. aeruginosa* infections. Despite their overall drug safety, they are linked to rare severe side effects like tendon rupture, neuropathy or heart valve regurgitation. As a result, medical federal agencies like FDA and BfArM alert about the inappropriate use of fluoroquinolone antibiotics.^[105-107] Although the molecular principles are not yet fully understood, there is evidence for inhibition of the human mitochondrial topoisomerase II^[108, 109], production of ROS^[110], combined with an unspecific accumulation in sensitive tissues like muscle tissues^[111].

Targeted drug-delivery can reduce side-effects and improve therapeutic efficacy by increasing the drug concentration at specific tissues (e.g. site of infection) relative to

others. In addition, unfavourable pharmacokinetic parameters can be revised by a prodrug-approach. In general, prodrugs are described as chemically masked analogues of their parent drug molecules, showing no or only minor pharmacological effect. However, they can be activated towards their active principle by metabolising enzymes or specific chemical conditions.^[112] In the context of antibacterial research, the rational design of selectively cleavable prodrugs is a powerful but yet underrepresented approach. Currently, a very promising Antibody-Antibiotic Conjugate targeting *S. aureus* is under investigation. ^[74, 75] Antimicrobial conjugates were reviewed by Klahn and Brönstrup^[113]; targeted drug delivery in infectious diseases was reviewed by Devarajan *et al.*^[73]

Two highly relevant proteins in the *P. aeruginosa* biofilm are the quorum-sensing regulated carbohydrate-binding proteins, i.e. lectins, LecA (PA-IL) and LecB (PA-IIL).^[21-23] These homotetrameric, Ca²⁺-dependent lectins are essential for biofilm formation and are virulence factors. Due to their multivalency, they are believed to crosslink bacterial cells with the biofilm matrix, and the host cells via their glycan-epitopes. A genetic or functional knockout of either of the two proteins leads to a significantly reduced biofilm formation.^[25, 114] It has recently been shown, that the D-mannose- and L-fucose-binding LecB acts as a spatial organiser of Psl within the biofilm matrix.^[32]

LecA and LecB are not exclusively involved in biofilm formation, but also in the direct infection process: The D-galactose-binding LecA mediates cell invasion as a lipid zipper and triggers host cell signalling upon binding to glycosphingolipid Gb3 on the eukaryotic cell surface.^[38] On the other hand, LecB facilitates and sustains an infection by inhibition of lung ciliary beating^[40] and wound tissue healing^[115, 116]. Interestingly, LecB can also carbohydrate-dependently activate murine B-cells in murine infection models.^[117]

The high genetic diversity and adaptability of *P. aeruginosa* results in a wide range of clinical isolates with varying characteristics.^[28] Whilst the protein sequence of LecA is highly conserved within clinical isolates, LecB can be clustered into PAO1-like and PA14-like homologues. Both variants however bind the same glycosides, although with slightly different affinities, rendering the development of universal LecB-inhibitors possible.

The intrinsically low affinity of lectins towards their natural carbohydrate ligands is often compensated by multivalent presentation of receptors or receptor-binding domains (RBD). So far, mainly multivalent inhibitors of LecA and LecB have been studied by various groups (reviewed by Cecioni *et al.*^[118] and Bernardi *et al.*^[119]). However, also highly potent bivalent and non-carbohydrate based inhibitors of LecA were recently disclosed.^[120-122] The *P. aeruginosa* biofilm-related lectins LecA and LecB both show a flat SAR beyond the

carbohydrate core, due to their shallow receptor binding sites on the proteins surface. Thus, conjugation of lectin-probes to larger molecules like fluorescent dyes^[123] or antibiotics^[124] without reduction of the binding affinity is straight forward.

The Zn-dependent metalloprotease LasB is an important virulence factor of *P. aeruginosa* and well recognised as a target in antimicrobial research.^[63, 125-127] LasB is involved in tissue damaging and host immune system evasion by degradation of immunoglobulins, complement factors^[128] and the host-derived antimicrobial peptide LL-37^[129]. Further, it is involved in biofilm formation, e.g. by activation of the rhamnolipid and alginate biosynthesis machineries.^[130, 131]

In our previous work^[124], we presented lectin-targeted conjugates of ciprofloxacin that are connected to lectin-probes via a non-cleavable linker. These conjugates showed antibiotic activity and accumulation in *P. aeruginosa* biofilm *in vitro*. Their antibiotic activity was reduced compared to ciprofloxacin, most likely due to the big molecular size of the antibiotic conjugates and the resulting poor bacterial bioavailability.^[81, 132]

Here, the stable linker of the above mentioned conjugates was exchanged with a cleavable peptide linker in a prodrug-like fashion. After activation by the *P. aeruginosa* specific endoprotease LasB, these prodrugs shall release their antibiotic cargo and therefore circumvent cellular uptake issues of big molecules. Here, we report the design and synthesis of the first *P. aeruginosa* lectin-targeted antibiotic prodrugs. Further, their stability in biological matrices and context-specific activation was characterised as well as their antibiotic activity profile.

3.3.3. Results and Discussion

3.3.3.1. Design

Following the strategy of our previous work^[124], a beta-aromatic substituted thiogalactoside and a C-glycosidic hybrid structure based on L-fucose and D-mannose were used as LecA and LecB probes, respectively. In contrast to natural O-glycosidic bonds, these lectin probes should be chemically and metabolically highly stable. Our previously published conjugates were linked by a non-cleavable triazole linker, allowing fast and flexible chemistry. However, these molecules showed reduced antibacterial activity due to their big molecular size. In this work, a peptidic linker was introduced instead, which can be cleaved in presence of *P. aeruginosa* to release the antibiotic cargo and reach potent antibacterial activity.

The peptide sequence „Ala-Gly-Leu-Ala“ is an established substrate for the endopeptidase LasB, which specifically cuts between Gly and Leu.^[126, 133] This peptide-motif can thus be exploited as a cleavable linker between the carbohydrate lectin-probe and the antibiotic drug, conjugated to the *N*- and *C*-termini, respectively. This will protect the peptide from unspecific cleavage by other host-derived exopeptidases, resulting in high metabolic stability. Cleavage by LasB will release a lectin-probe-dipeptide and a dipeptide-antibiotic fragment. Due to its low molecular weight, this antibiotic dipeptide fragment could already show weak antibiotic activity. Eventually, these unprotected dipeptides get cleaved in biological matrices by proteolysis, either by *P. aeruginosa*-associated proteases or by host-derived enzymes, thus resulting in the release of the free cargo and full antimicrobial activity.

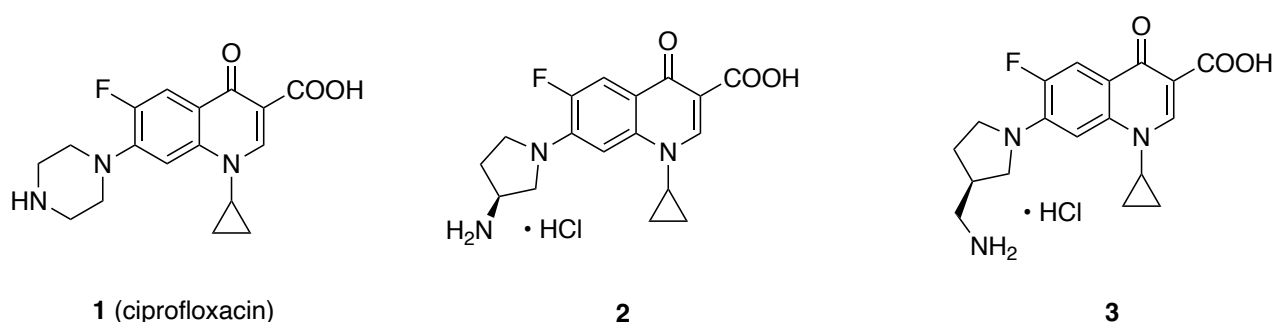


Figure 1. Anticipated antibiotic cargo for the lectin-targeted prodrug conjugates. Ciprofloxacin (**1**) is a very potent approved drug. Aminopyrrolidine fluoroquinolone **2** and aminomethylpyrrolidine fluoroquinolone **3** also show high antibiotic activity and carry a primary amine which serves as a handle for conjugation to the peptide linker.

Fluoroquinolones represent a highly efficient class of antibiotics and are active against a wide range of bacteria. Their most common representative, ciprofloxacin (**1**), is a vital antibiotic in the treatment of *P. aeruginosa* infections.^[53, 134, 135] However, fluoroquinolones can lead to severe side effects such as tendon ruptures, neuropathy or heart failures. These side effects are linked to undesired tissue accumulation and therefore they could be reduced by targeted drug delivery to the infected tissue only. In fact, we could show in our previous work, that conjugation of ciprofloxacin to lectin probes resulted in drug-accumulation in *P. aeruginosa* biofilms *in vitro*.^[124]

The structure-activity relationship of fluoroquinolone antibiotics allows the conjugation to larger moieties only at two positions: (i) the carboxylic acid at the 3-position of the quinolone-core or (ii) the heterocycle present at C-7 in almost all fluoroquinolone drugs

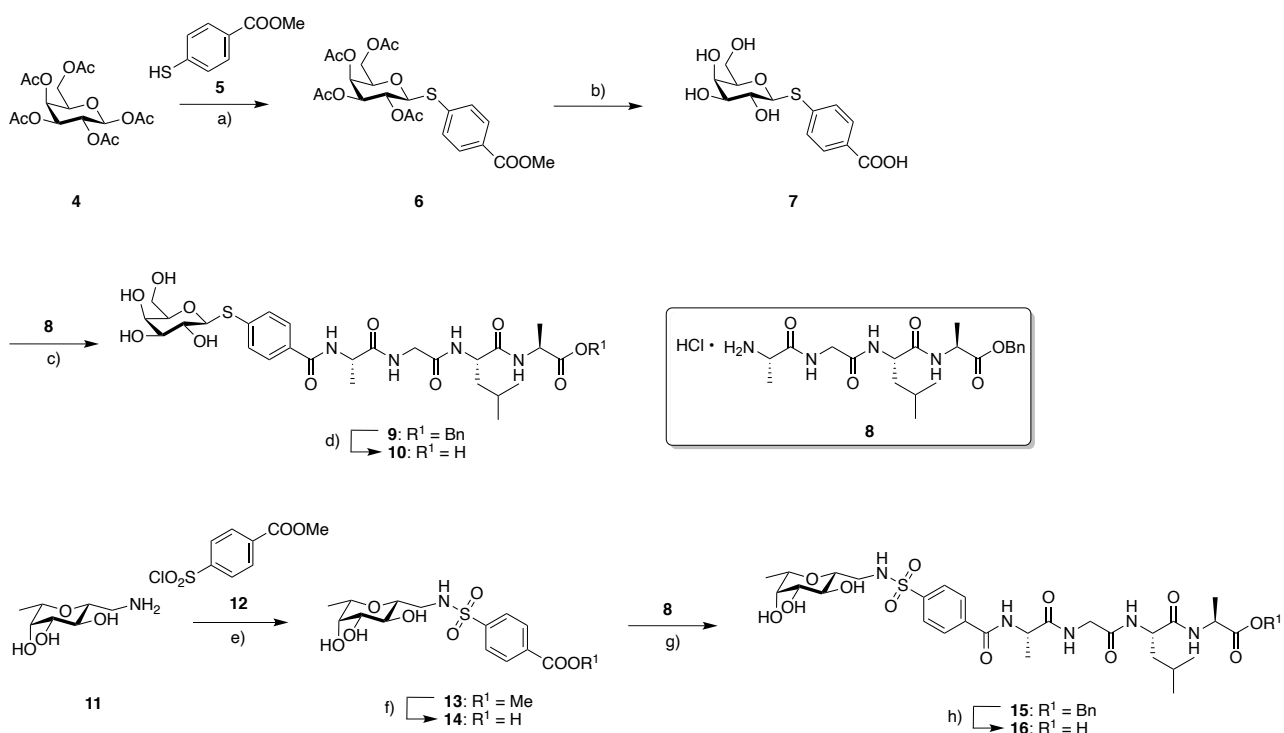
(reviewed by Gootz and Brighty, Chu and Fernandes^[136, 137]) For ciprofloxacin, conjugation of a peptide linker to its piperazine-*N* results in a secondary peptide. In general, secondary peptides are considered to have higher stability against proteases.^[138] This could result in a slow and inefficient drug release in case of ciprofloxacin-based prodrugs. Thus, conjugation of fluoroquinolones with a primary amine was envisaged as a strategy to circumvent these drawbacks. Compounds **2** and **3** share a very similar structure and antibiotic profile compared to ciprofloxacin and contain a primary amine.^[139-141] The 3-aminomethylpyrrolidine residue of fluoroquinolone **3** was chosen to improve the accessibility of the corresponding amide and thus potentially improve proteolysis (figure 1).

3.3.3.2. Synthesis

LECTIN-TARGETED CARBOHYDRATE-PEPTIDE CONJUGATES

The LecA-targeted galactoside precursor **7** was synthesised in analogy to Novoa *et al.* (scheme 1).^[142] In brief, Lewis acid-mediated glycosylation of methyl-4-mercaptobenzoate (**5**) with galactose pentaacetate (**4**) gave galactoside **6** in good yield. After subsequent global deprotection in two steps, LecA probe **7** was obtained quantitatively.

Scheme 1. Chemical synthesis of the lectin-targeted carbohydrate-peptide conjugates **10** (LecA-targeted) and **16** (LecB-targeted)^a.



^aReagents and conditions: (a) $\text{BF}_3 \cdot \text{Et}_2\text{O}$, 0 °C to r.t., 16 h, 58%; (b) first NaOMe, MeOH, r.t., 30 min; then LiOH, MeOH/H₂O (20:3), 1 h, quant.; (c) TBTU, DIPEA, DMF, r.t., 1 h, 58%; (d) LiOH, DMF/H₂O, 50 °C, 49%; (e) Et₃N, DMF, 0 °C to r.t., 16 h, 67%; (f) LiOH, THF/MeOH/H₂O (3/1/1), r.t., 16 h, 95%; (g) TBTU, DIPEA, DMF, r.t., 1 h, 80%; (h) H₂, cat. Pd/C, MeOH, r.t., 16 h, 95%.

Tetrapeptide **8** was synthesised in 5 chemical steps by solution-phase peptide synthesis (SI for details). Peptide coupling of linker **8** to LecA-probe **7** was performed with TBTU, yielding protected conjugate **9**. The following debenzoylation proved to be problematic: Only small amounts of product **10** could be isolated by hydrogenolysis, even under elevated H₂-

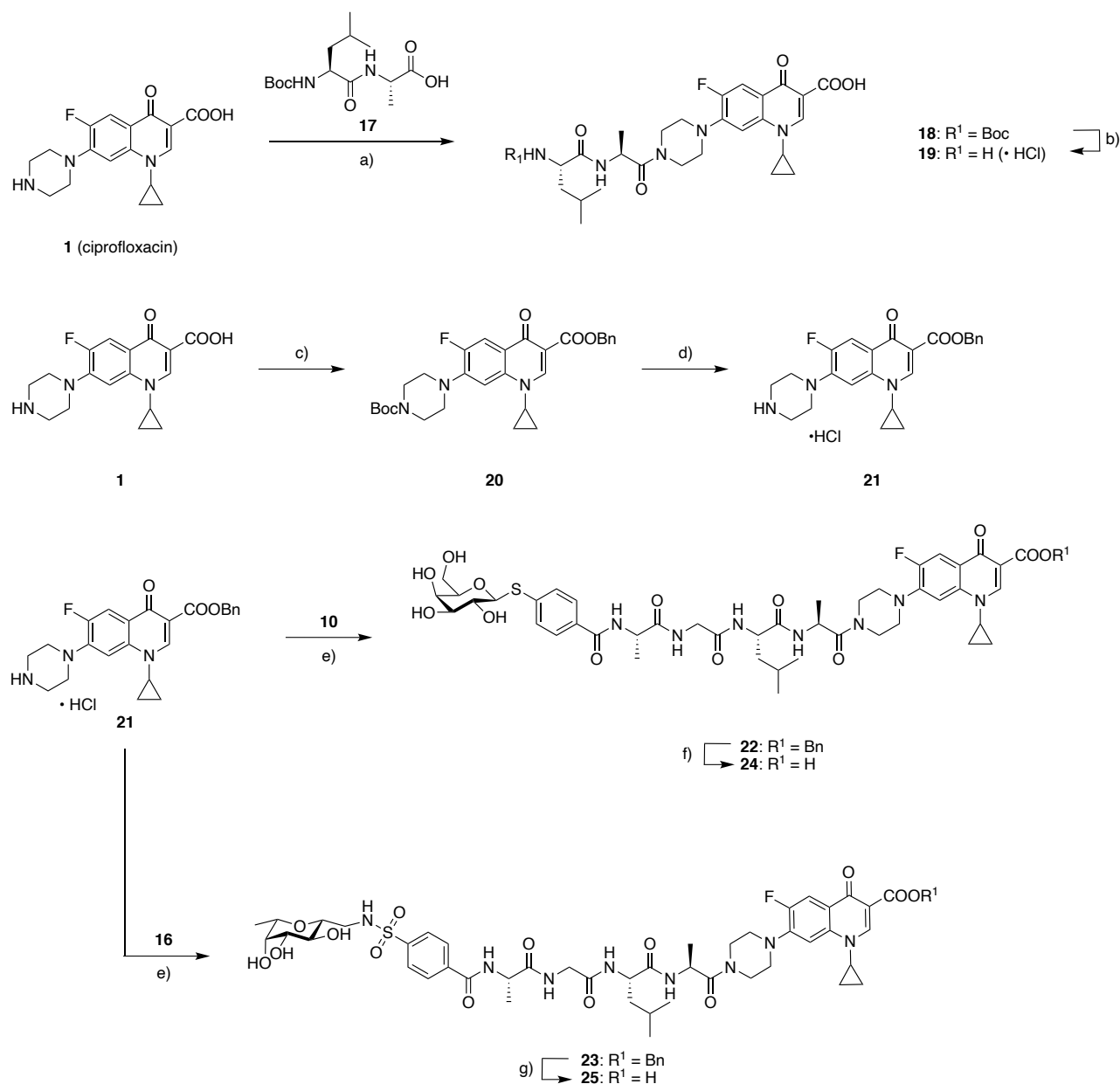
pressure (3.5 bar) and catalysis with elemental Pd. Eventually, saponification with LiOH gave the desired compound **10** in 49% yield (scheme 1).

LecB-targeted β -C-glycoside **11** was synthesised as reported.^[143] Reaction with sulfonylchloride **12** resulted in sulfonamide **13**, which was subsequently saponified with LiOH to yield the corresponding carboxylic acid **14**. Conjugation to tetrapeptide **8** was again performed with TBTU to give benzyl-protected intermediate **15**. In contrast to the troublesome deprotection of benzylester **9**, debenzylation towards compounds **16** was achieved by hydrogenolysis with catalytic amounts of palladium on charcoal in excellent yields (scheme 1). Lectin-targeted building blocks **10** and **16** were now available for the conjugation to the antibiotic cargo compounds **1 - 3**.

CIPROFLOXACIN SERIES

Ciprofloxacin-based prodrugs were synthesised starting from ciprofloxacin (scheme 2).

Scheme 2. Chemical synthesis of the ciprofloxacin-based lectin-targeted prodrugs **24** (LecA-targeted) and **25** (LecB-targeted) and control compound **19**.^a



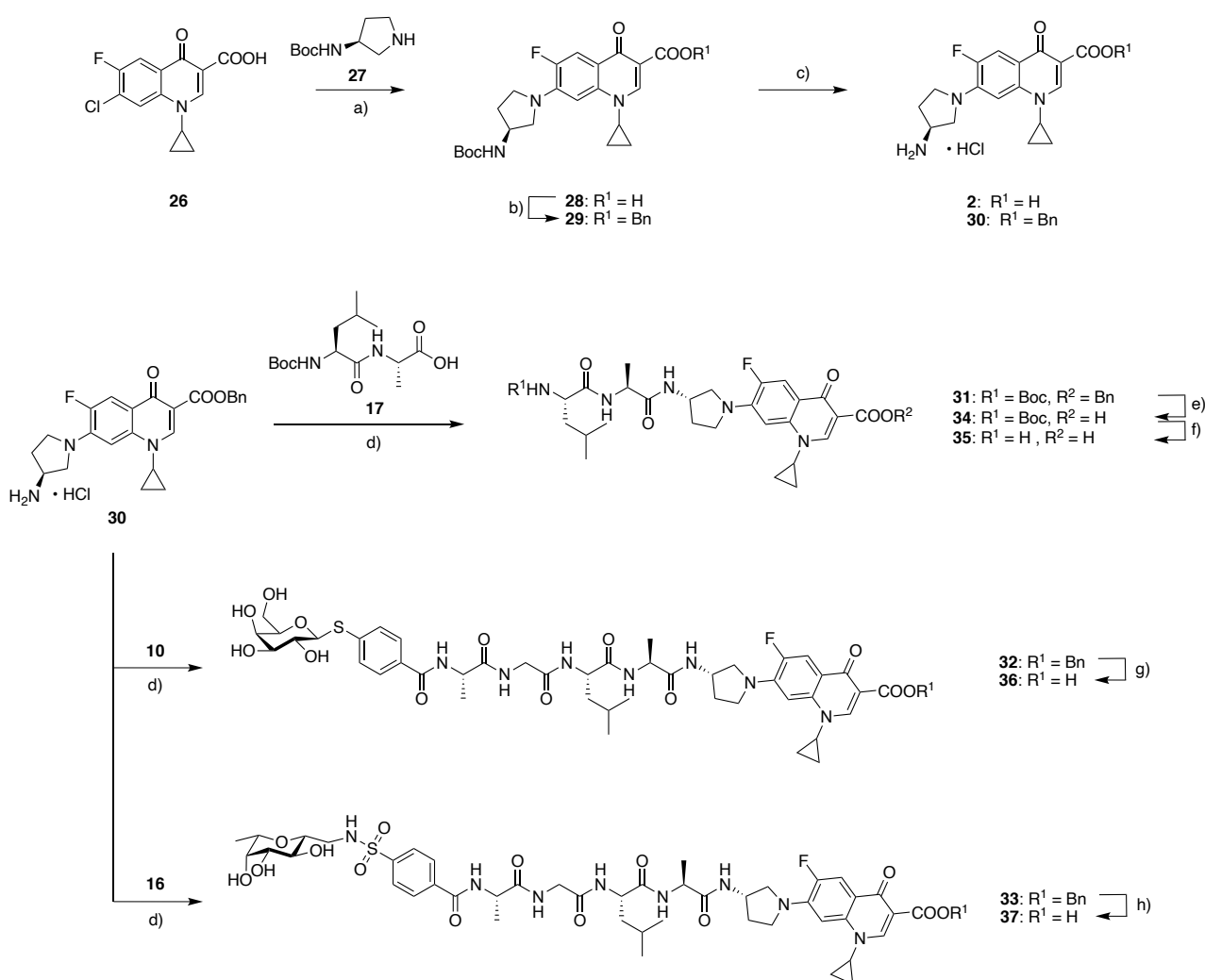
^aReagents and conditions: (a) first **17**, lbcf, NMM, THF, -15 °C, 20 min, then **1**, THF, r.t., 3 h, 25%; (b) HCl, dioxane, r.t. 1 h, 54%; (c) first Boc₂O, KHCO₃, DMF, 40 °C, 90 min, then BnBr, 115 °C, 86% over 2 chemical steps; (d) HCl, dioxane, r.t., 1 h, quant.; (e) TBTU, DIPEA, r.t., 1 h, 84% for **23**; (f) H₂, cat. Pd MeOH, r.t., 6 d 22% over two chemical steps; (g) H₂, cat. Pd, MeOH, r.t. 24 h, 74%.

Boc-Leu-Ala (**17**, SI for details) was coupled to ciprofloxacin (**1**) after activation with isobutyl chloroformate to give Boc-protected intermediate **18** which subsequently was deprotected by HCl to give dipeptidyl-ciprofloxacin **19** as reference compound. The conjugation of the lectin-targeted peptide precursors **10** (LecA-targeted) and **16** (LecB-targeted) with benzyl-protected ciprofloxacin (**21**) towards the protected prodrugs **22** and **23** was performed by activation with TBTU. Hydrogenolytic deprotection resulted in the ciprofloxacin-based lectin-targeted prodrugs **24** and **25** (scheme 2).

AMINOPYRROLIDINE SERIES

For the aminopyrrolidine series (scheme 3), fluoroquinolone (FQ) core structure **26** was refluxed with aminopyrrolidine **27** in dry pyridine, according to Sanchez *et al.*^[139] After chromatographic separation of the regioisomers, Boc-protected fluoroquinolone **28** was reacted with benzylbromide to give fully protected aminopyrrolidine-FQ **29** in good yield. On the other hand, a small amount of **28** was directly boc-deprotected under acidic conditions to obtain aminopyrrolidine-FQ **2** in excellent yield.

Scheme 3. Chemical synthesis of the aminopyrrolidine-based lectin lectin-targeted prodrugs **36** (LecA-targeted) and **37** (LecB-targeted) and control compounds **2** and **35**^a



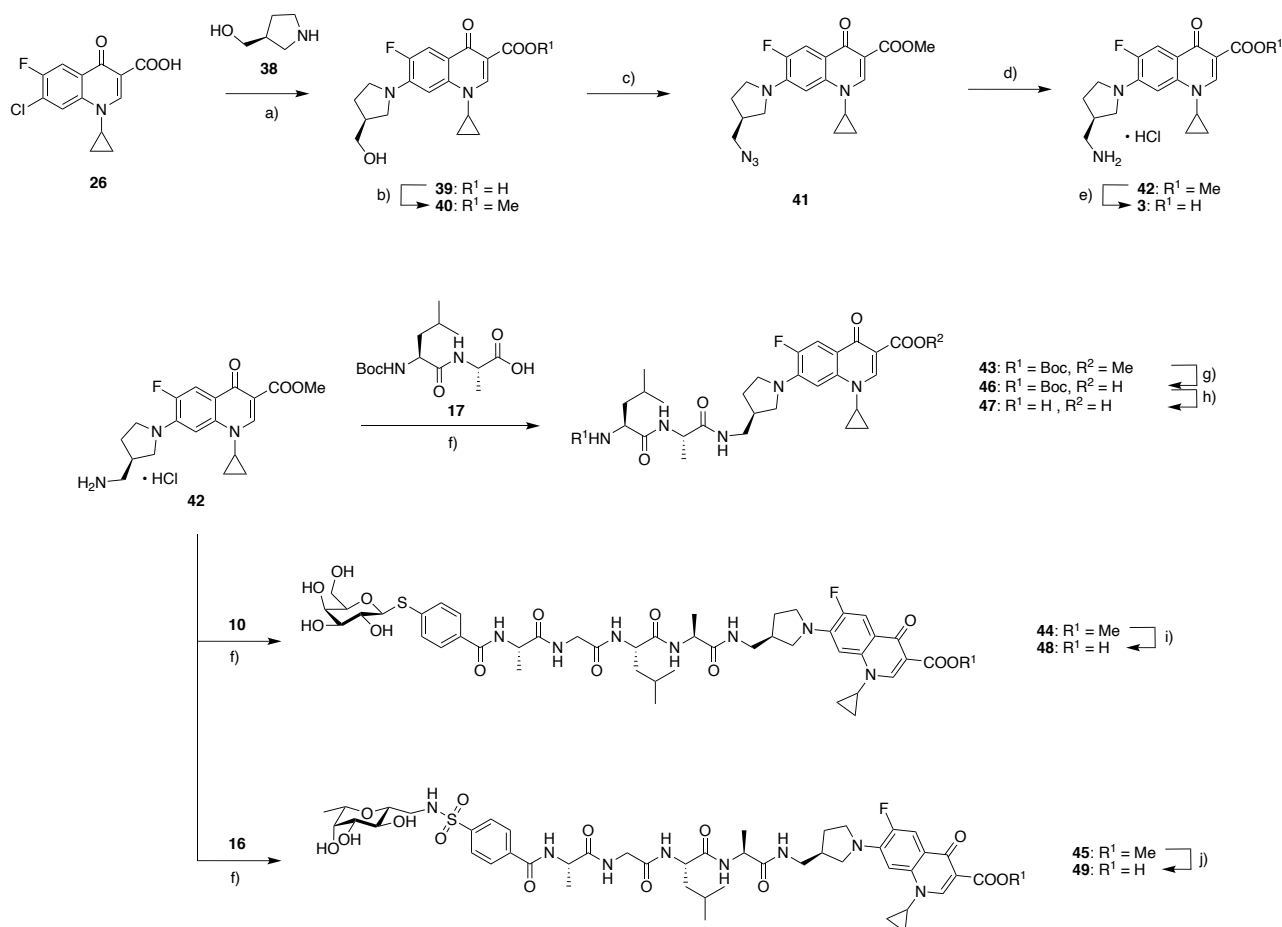
^aReagents and conditions: (a) pyridine, reflux, 16 h, 32-50%; (b) BnBr, K₂CO₃, DMF, 110° C, 60 min, 86%; (c) HCl, dioxane, r.t., 1 h, 97% for **2**, quant. for **30**; (d) TBTU, DIPEA, r.t., 1 h, 74% for **31**, 49% for **35**; (e) H₂, cat. Pd, MeOH, r.t., 16 h; (f) HCl, dioxane, r.t., 1 h, 61% over two chemical steps; (g) H₂, cat. Pd, MeOH, r.t., 24 h, 48% over two chemical steps; (h) H₂, cat. Pd/C, MeOH, r.t., 41%.

In parallel, **29** was deprotected towards the free amine **30** and subsequently conjugated to Boc-Leu-Ala (**17**), LecA-targeted tetrapeptide precursor **10** and LecB-targeted tetrapeptide precursor **16** by activation with TBTU to result in the protected conjugates **31**, **32** and **33**, respectively. Dipeptidyl-FQ **31** was first deprotected by hydrogenolysis towards intermediate compound **34**, which was then Boc-deprotected under acidic conditions to yield the aminopyrrolidine-FQ **35**. The protected lectin-targeted conjugates **32** and **33** were hydrogenolytically deprotected to yield the two aminopyrrolidine-based prodrugs **36** (LecA-targeted) and **37** (LecB-targeted).

AMINOMETHYLPYRROLIDINE SERIES

For the aminomethylpyrrolidine series (scheme 4), fluoroquinolone core structure **26** was refluxed with (*S*)- β -prolinol (**38**) in dry pyridine. The desired regioisomer **39** precipitated from the reaction at room temperature. After CSA-catalysed esterification, methylester **40** was obtained in excellent yield.

Scheme 4. Chemical synthesis of the aminomethylpyrrolidine-based lectin-targeted prodrugs **48** (LecA-targeted) and **49** (LecB-targeted) and control compounds **3** and **47**^a



^aReagents and conditions: (a) pyridine, reflux, 16 h, 62%; (b) (*R/S*)-CSA, MeOH, reflux, 72 h, 96%; (c) DIAD, P(Ph)₃, DPPA, THF, 1 h, 65%; (d) H₂, cat. Pd/C, MeOH, 16 h, then HCl, dioxane/Et₂O, 0 °C 78%; (e) LiOH, THF/MeOH/H₂O (3:1:1), 2 d, 43%; (f) TBTU, DIPEA, DMF, r.t., 1 h, 50% for **43**, 72% for **45**; (g) LiOH, THF/H₂O/MeOH (5:5:1), r.t., 3 h, 86%; (h) HCl, dioxane, r.t., 1 h, 54%; (i) LiOH, H₂O/THF (5:1), r.t., 3 h, 70% over two chemical steps; (j) LiOH, THF/H₂O/MeOH (3:1:1), r.t., 12 h, 96%.

The following step towards the corresponding azide **41** contained several pitfalls: Transformation of the primary alcohol to a leaving group, e.g. with PBr₃ or TsCl led to

decomposition of the starting material. Eventually, Bose-Mitsunobu conditions (diphenylphosphoryl azide, DPPA; diisopropyl azodicarboxylate, DIAD; PPh₃) gave azide **41** in one step.^[144] After hydrogenation, amine **42** was trapped as its HCl salt to prevent potential side-reaction with the methylester during workup. Saponification with LiOH yielded the corresponding reference antibiotic **3** in 43% yield. As in the aminopyrrolidine series, methyl-protected fluoroquinolone **42** was coupled to the peptides Boc-Leu-Ala (**17**), LecA-targeted tetrapeptide precursor **10** and LecB-targeted tetrapeptide precursor **16** after activation with TBTU to yield the protected intermediates **43**, **44** and **45**, respectively. Dipeptide **43** was then saponified with LiOH towards carboxylic acid **46**. After deprotection under acidic conditions, reference aminomethylpyrrolidine-FQ **47** was obtained. The methyl-protected lectin-targeted conjugates **44** and **45** were deprotected by saponification to yield the two aminomethylpyrrolidine-based prodrugs **48** (LecA-targeted) and **49** (LecB-targeted) in good yields.

3.3.3.3. Biophysical and microbiological evaluation

The compounds were analysed for their target affinity in our previously reported competitive binding assays, based on fluorescence polarisation (figure 2).[28, 94]

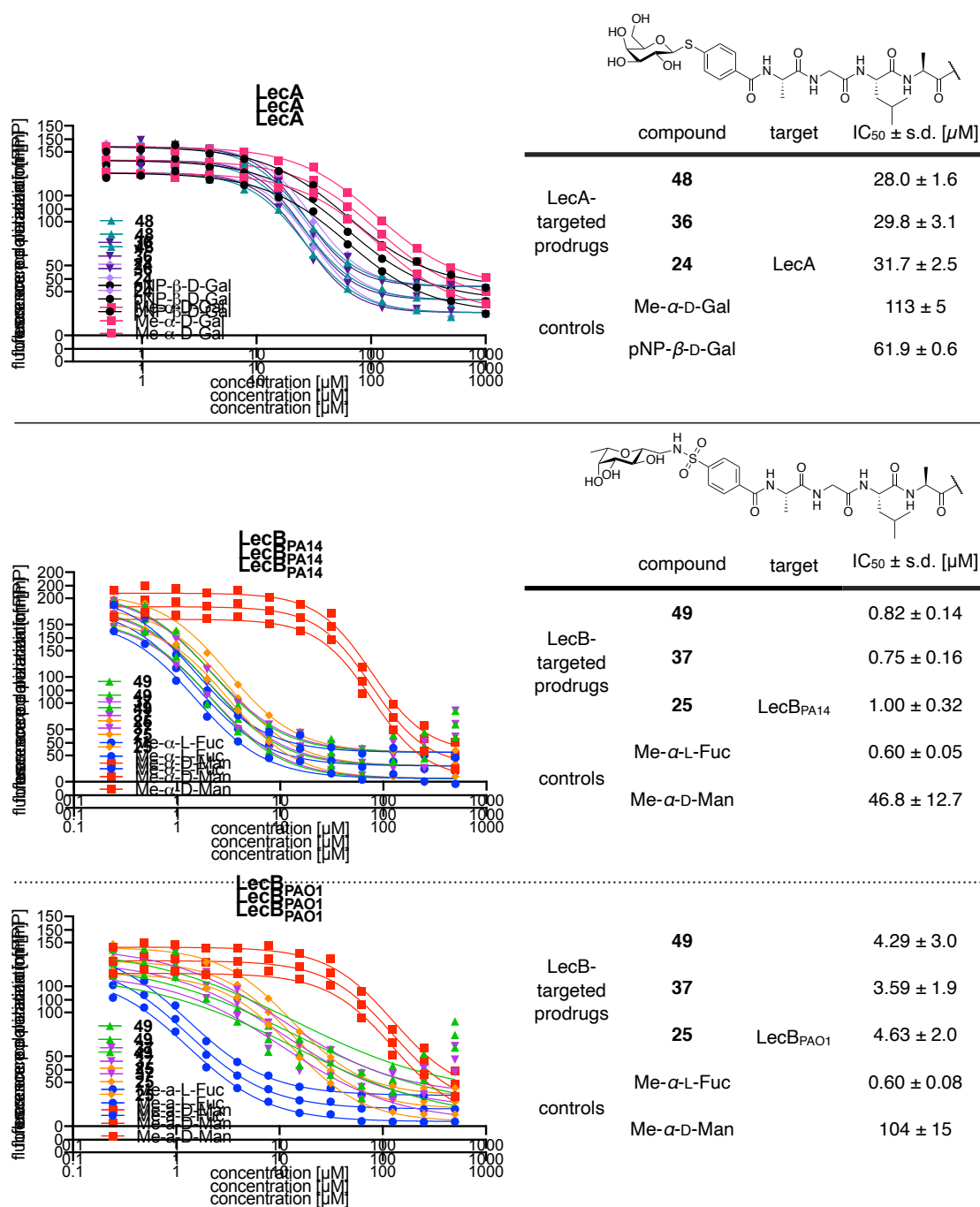


Figure 2. Competitive binding assay of the lectin-targeted prodrugs and reference carbohydrates with LecA, LecB_{PA14} and LecB_{PA01}. One representative titration of triplicates on plate is shown for each compound. The corresponding IC₅₀-values were determined from at least three independent experiments and are given as mean and standard deviation (K_i in Table S1).

In case of LecA (Figure 2, top), the lectin-targeted prodrugs **24** (ciprofloxacin-based), **36** (aminopyrrolidine-based) and **48** (aminomethylpyrrolidine-based) showed very similar binding affinities around 30 μM . Methyl α -D-galactoside (Me- α -D-Gal, $\text{IC}_{50} = 113 \pm 5 \mu\text{M}$) and *p*-nitrophenyl β -thiogalactoside (pNP- β -D-Gal, $\text{IC}_{50} = 61.9 \pm 0.6 \mu\text{M}$) were used as positive controls.

The two *P. aeruginosa* strains PAO1 and PA14 and their respective lectin homologues represent a broad range of clinical isolates. LecB_{PAO1} bound the LecB-targeted prodrugs **25** (ciprofloxacin-based), **37** (aminopyrrolidine-based) and **49** (aminomethylpyrrolidine-based) with high affinity in the one digit micromolar range (figure 2, middle), comparable to L-fucose ($\text{IC}_{50} = 2.63 \pm 1.7 \mu\text{M}$ ^[124]). As observed for LecA, the different prodrugs possessed comparable affinity independent of their cargo. Terminal mannosides and fucosides are the natural ligands of LecB. Thus, methyl α -D-mannoside (Me- α -D-Man, $\text{IC}_{50} = 104 \pm 15 \mu\text{M}$) and methyl α -L-fucoside (Me- α -L-Fuc, $\text{IC}_{50} = 0.60 \pm 0.08 \mu\text{M}$) were used as control compounds.

We further tested the LecB-homologue from *P. aeruginosa* PA14. As observed before^[28] for mannose- and fucose-based carbohydrates, LecB_{PA14} bound all conjugates and the control compounds with higher affinity compared to LecB_{PAO1}, reaching IC_{50} values in the low micromolar to high nanomolar range (e.g. $3.59 \pm 1.92 \mu\text{M}$ vs $0.75 \pm 0.16 \mu\text{M}$ for **37**, Figure 2, bottom).

In conclusion, the lectin-targeted prodrugs have the potential to target a broad field of *P. aeruginosa* strains.

PRODRUGS RELEASE ANTIBIOTIC CARGO IN DEPENDENCE OF BACTERIAL PROTEINS AND HUMAN BLOOD PLASMA

The peptide linker of the reported prodrugs was designed to be cleaved in presence of LasB, an endopeptidase expressed by *P. aeruginosa*. In order to resemble the complex variety of proteases, primary and secondary metabolites during an infection, a sterile filtrate of an overnight culture from *P. aeruginosa* PA14 was used instead of purified LasB. This matrix contains a plethora of enzymes, some of them being able to process the resulting dipeptides from the first LasB-mediated cleavage and finally release the parent antibiotic cargo. LasB-mediated cleavage of the tetrapeptide prodrugs was generally very fast (within minutes) and therefore not a rate limiting step. In contrast, preliminary scouting experiments showed that dipeptide **19** and **35** only slowly released their antibiotic cargo in PA14-filtrate (no full release after 24 h, Figure S1).

To increase complexity of the biological matrix and to mimic the infection scenario closer, human blood plasma was added to the cleavage experiments (figure 3). Indeed, in presence of PA14-filtrate and human blood plasma, the lectin-targeted prodrugs **36/37** and **48/49** released a significant amount of their antibiotic cargo within 3 h. The ciprofloxacin-based prodrugs **24** and **25** were also processed after initial cleavage by LasB and the resulting dipeptide **19** was further metabolised. However, degradation stopped at the stage of the secondary amide (Ala-ciprofloxacin), proving that the ciprofloxacin-based prodrugs are not fully metabolised to release their antibiotic cargo.

Comparing the aminopyrrolidine-FQ with the aminomethylpyrrolidine-FQ series, only minor differences could be observed. All primary amide-based prodrugs were quickly metabolised and efficiently released their parent fluoroquinolones. The aminopyrrolidine-based prodrugs **36** and **37** released their antibiotic cargo (**2**) faster than aminomethylpyrrolidine **3** was released from prodrugs **48** and **49**. This was unexpected, as the aminomethylpyrrolidine-series was designed to have an additional CH₂-spacer to increase accessibility for proteolytic enzymes.

The prodrugs' stability in presence of human blood plasma was assessed in a control experiment in absence of bacterial matrix (figure 4). Indeed, the compounds showed no release of fluoroquinolone or peptide-conjugated intermediates within three hours. In conclusion, activation of the prodrugs is efficiently triggered by the presence of proteases expressed by *P. aeruginosa*.

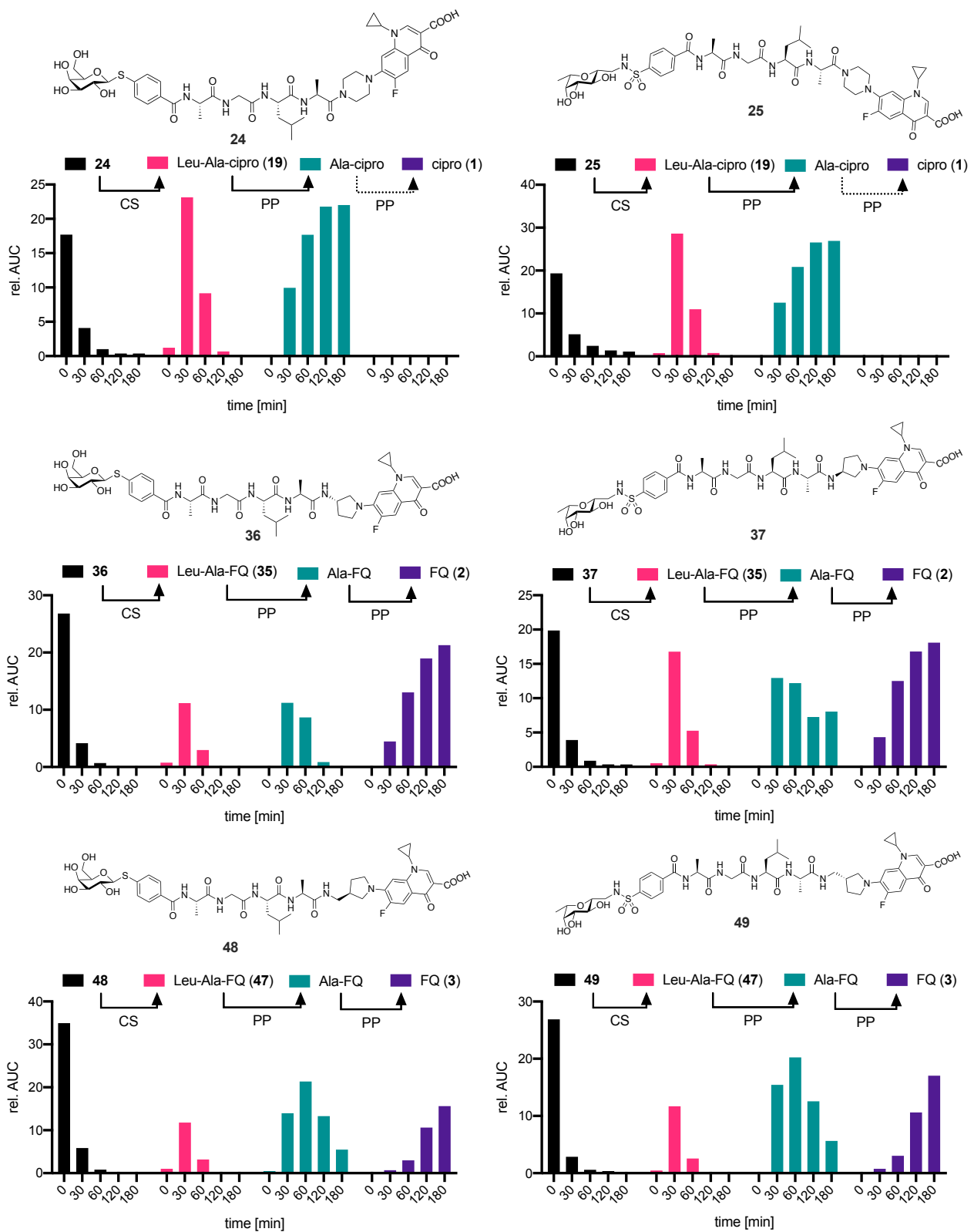


Figure 3. Activation of the lectin-targeted prodrugs in 50% human blood plasma spiked with 10% *P. aeruginosa* culture supernatant (CS): The ciprofloxacin-based prodrugs **24** and **25** do not release ciprofloxacin whilst the primary amide-based prodrugs **36**, **37**, **48** and **49** release their antibiotic cargo within the same time frame. PP = plasma proteins.

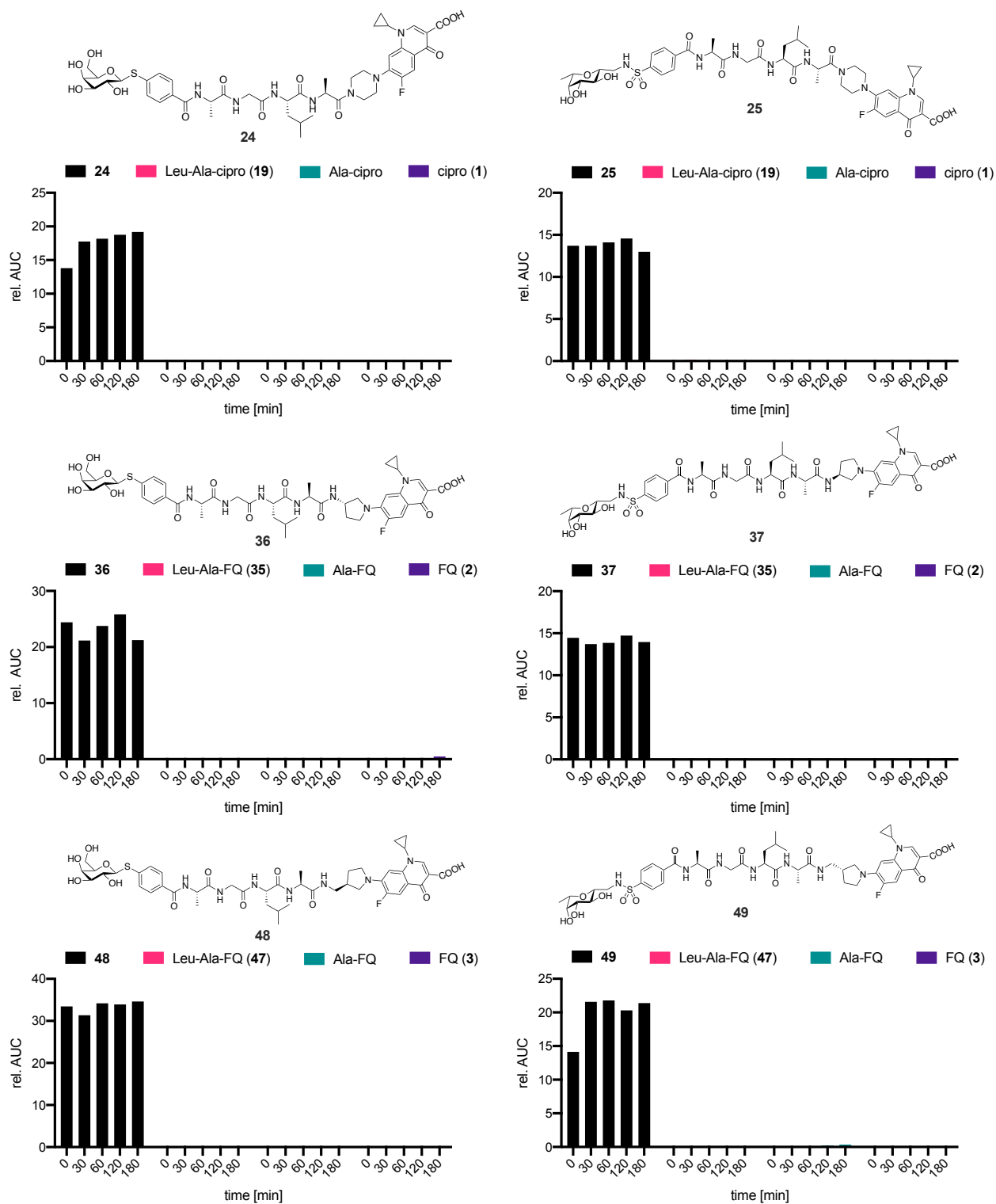


Figure 4. Stability of the lectin-targeted prodrugs in 50% human blood plasma spiked with 10% LB: All prodrugs (**24**, **25**, **36**, **37**, **48** and **49**) show no significant release of their antibiotic cargo within the observed time frame.

LECTIN-TARGETED PRODRUGS REACH HIGH ANTIBIOTIC ACTIVITY AFTER ACTIVATION BY *P. aeruginosa*

The antibiotic activity (MIC) of fluoroquinolones **2** and **3** against *P. aeruginosa* PA14 was analysed by microbroth dilution assay (table 1).^[95]

Table 1. Antibacterial activity of the control compounds **1**, **2**, **3**, **19**, **35** and **47** and of the lectin-targeted LasB-cleavable prodrugs **24**, **25**, **36**, **37**, **48** and **49** against *P. aeruginosa* PA14. Prodrugs were tested under different conditions, varying the pre-incubation time (< 10 min vs 3 h) in the different biological matrices 1 - 4 before addition of the inoculum.^a

| | 1 | 24 | 25 | 36 | 37 | 48 | 49 |
|---|---------------|---------------|---------------|---------------|---------------|---------------|---------------|
| | control | LecA-targeted | LecB-targeted | LecA-targeted | LecB-targeted | LecA-targeted | LecB-targeted |
| antibiotic cargo | | | | | | | |
| Matrix 1: PBS | | | | | | | |
| < 10 min | 0.125 - 0.156 | > 25 | > 25 | > 25 | > 25 | > 25 | > 25 |
| 3 h | 0.125 - 0.25 | > 25 | > 25 | > 25 | > 25 | > 25 | > 25 |
| Matrix 2: 50% human blood plasma + 10% <i>P. aeruginosa</i> culture supernatant in PBS | | | | | | | |
| < 10 min | 0.25 - 0.313 | ≥ 25 | ≥ 25 | 0.195 - 0.39 | 0.78 - 1.56 | 3.13 - 12.5 | 3.13 - 6.25 |
| 3 h | 0.156 - 0.25 | ≥ 25 | ≥ 25 | 0.1 | 0.1 - 0.195 | 1.56 | 1.56 - 3.13 |
| Matrix 3: 10% <i>P. aeruginosa</i> culture supernatant in PBS | | | | | | | |
| < 10 min | 0.125 - 0.313 | ≥ 25 | ≥ 25 | 0.78 - 3.13 | 1.56 - 12.5 | 1.56 - 3.13 | 3.13 - 6.25 |
| 3 h | 0.125 - 0.313 | ≥ 25 | ≥ 25 | 0.195 - 3.13 | 0.39 - 3.13 | 1.56 - 3.13 | 1.56 - 6.25 |
| Matrix 4: 50% human blood plasma + 10% LB in PBS | | | | | | | |
| < 10 min | 0.156 - 0.313 | > 25 | ≥ 25 | ≥ 25 | ≥ 25 | > 25 | ≥ 25 |
| 3 h | 0.156 - 0.313 | ≥ 25 | ≥ 25 | 0.78 - 6.25 | 0.78 - 6.25 | 12.5 - >25 | 12.5 - >25 |
| MIC (parent drug) | | 1 | 0.125 - 0.25 | 2 | 0.027 - 0.054 | 3 | 0.29 - 1.45 |
| MIC (dipeptide-FQ) | [μM] | 19 | 7.25 - 14.5 | 35 | 58 | 47 | 28 - 56 |

^aData is represented as minimal inhibitory concentration (MIC) range from at least three independent experiments (exception: N = 2 for matrix 1, < 10 min).

As reported by Sanchez *et al.* ^[141], fluoroquinolone **2** (MIC = 0.027 - 0.054 μM) was more active than ciprofloxacin (**1**, MIC = 0.125 - 0.25 μM). The antibacterial activity of aminomethylpyrrolidine **3** was (MIC = 0.29 - 1.45 μM) slightly weaker than the other two

antibiotics.^[139] The dipeptidyl-fluoroquinolone conjugates **19** (ciprofloxacin-based), **35** (aminopyrrolidine-based) and **47** (aminomethylpyrrolidine-based) - i.e. those that result after initial cleavage by LasB - only showed low antibiotic activity in the micromolar range. Previous experiments showed, that a majority of free antibiotic drug was released from the prodrugs within 3 h in presence of PA14-filtrate together with human blood plasma (figure 3). Therefore, the prodrugs were incubated for 3 h (and < 10 min as control) in different matrices before transferring them to the antibiotic susceptibility assay (**Table 1**): PBS (matrix 1), 50% human blood plasma spiked with 10% PA14-filtrate in PBS (matrix 2), 10% PA14-filtrate in PBS (matrix 3) and 50% human blood plasma spiked with 10% LB in PBS (matrix 4).

In adherence to the prodrug-definition (see above), the lectin-targeted prodrugs **24**, **25**, **35**, **36**, **48** and **49** (**Table 1**, matrix 1) did not show any antibiotic activity below 25 μM when they were added from PBS (MIC > 25 μM). In contrast, a brief pre-incubation of < 10 min in a mixture of human blood plasma and PA14-filtrate in PBS (matrix 2) activates the primary amide based prodrugs **36/37** (MIC = 0.195 - 0.39 μM and 0.78 - 0.156 μM , respectively) and **48/49** (MIC = 3.13 - 12.5 μM and 3.13 - 6.25 μM , respectively), while the ciprofloxacin based prodrugs **24** and **25** remained inactive (MIC \geq 25 μM). This trend became even stronger after 3 h of pre-incubation: while the ciprofloxacin series remained inactive, especially the aminopyrrolidine-based prodrugs (**36**, **37**) were highly potent (MIC = 0.098 - 0.195 μM) and almost reached the antibiotic activity of their parent fluoroquinolone **2** (MIC = 0.027 - 0.054 μM), indicating a very efficient drug release during the experiment. Under the same conditions (Matrix 2), the aminomethylpyrrolidine series (**48**, **49**) reached low micromolar antibacterial activities around 1.56 - 3.13 μM , which is close to the activity of parent fluoroquinolone **3** (MIC = 0.29 - 1.45 μM). It has to be noted, that MICs of the parent drugs (**1** - **3**) and the dipeptide-conjugates (**19**, **35**, **47**) were measured under conventional conditions, i.e. without the addition of a proteolytically active biological matrix like blood plasma or PA14 filtrate. Thus, effects like metabolism or plasma protein binding are drastically reduced, potentially resulting in lower MIC-values. The antibiotic activity difference within the different fluoroquinolone-series can be explained by the different drug-release kinetics of the prodrugs (figure 3) and by the intrinsically lower antibacterial activity of aminomethylpyrrolidine-FQ **3** compared to aminopyrrolidine-FQ **2** (MIC = 0.29 - 1.45 μM and MIC = 0.027 - 0.054 μM , respectively).

Interestingly, primary amide based prodrugs **36**, **37**, **48** and **49** still released a significant amount of active drug in presence of *P. aeruginosa* culture-filtrate only (**Table 1**, matrix 3),

resulting in antibiotic activities in the low micro molar range (e.g. MIC = 0.195 - 0.78 μ M for **36** after 3 h pre-incubation). We reason that the time frame of the experiment itself (18 h, 37 °C) is sufficient to release a significant amount of drug, despite the slower metabolism in culture-filtrate (figure S1). This assumption is in coherence to the fact that even with a pre-incubation time of 3 h, the antibiotic activity increased only mildly (e.g. for **36**: MIC (< 10 min pre-incubation) = 0.78 - 1.56 μ M vs MIC (3 h pre-incubation) = 0.195 - 0.78 μ M, for **49**: MIC (< 10 min pre-incubation) = 3.13 μ M vs MIC (3 h pre-incubation) = 1.56 - 3.13 μ M).

In all cases, the antibiotic activity reached after pre-incubation in human blood plasma alone (**Table 1**, matrix 4) was significantly lower than from the other biological matrices (matrices 2 & 3). Only the aminopyrrolidine-based prodrugs **36** (LecA-targeted) and **37** (LecB-targeted) reached significant potency, however, it varied extensively between the replicates (MIC = 0.78 - 6.25 μ M).

Overall, the antibiotic activity of the lectin-targeted prodrugs correlated well with their metabolic activation in the presence of human blood plasma proteins and PA14-filtrate. The ciprofloxacin-based prodrugs could not be fully activated due to the presence of a stable secondary amide and thus showed only weak antibiotic activity, despite their potent antibiotic cargo. In contrast, the primary amide-based prodrugs showed efficient release of their antibiotic cargo, resulting in highly potent antimicrobial activity.

PRODRUGS ARE METABOLICALLY STABLE AND SHOW NO ACUTE CYTOTOXICITY IN VITRO

Due to their excellent antibiotic activity profile against *P. aeruginosa* PA14 *in vitro*, aminopyrrolidine-FQ **2** and the corresponding lectin-targeted prodrugs **36** and **37** were chosen for further *early in vitro* ADMET studies (**Table 2**).

Metabolic stability was assessed against human and mouse liver microsomes and blood plasma. High metabolic stability in mouse and human S9 liver fractions was observed for the prodrugs **36** ($t_{1/2, MLM} = 100$ min, $t_{1/2, HLM} = 93$ min) and **37** ($t_{1/2, MLM} = 216$ min, $t_{1/2, HLM} = 178$ min). In contrast, metabolism of the parent fluoroquinolone **2** was twofold faster in human liver microsomes ($t_{1/2, HLM} = 41$ min), which is most likely due the presence of a free primary amine in fluoroquinolone **2**, that is masked in the prodrugs.

Plasma protein binding was assessed in mouse and human blood plasma since very high plasma protein binding (> 99%) can mask the prodrugs and prevent e.g. binding to their corresponding lectins and metabolic activation. LecA-targeted prodrug **36** showed comparable protein binding (74% for mouse blood plasma, 97% for human blood plasma)

to its parent fluoroquinolone **2** (78% for mouse blood plasma, 94% for human blood plasma). Interestingly, C-glycoside-based prodrug **37** showed significantly reduced plasma protein binding (30% for mouse blood plasma, 51% for human blood plasma).

Table 2. *In vitro* ADMET data of the two aminopyrrolidine-based lectin-targeted prodrugs **36** and **37** and their common fluoroquinolone cargo **2**. All compounds showed good metabolic stability in blood plasma and in presence of liver cell microsomal fractions. Acute cytotoxicity against A549-cells was not observed.^a

| compound | t _{1/2} [min] | | metabolic stability | | | | plasma protein binding [%] | | cytotoxicity A549 cells [μM] |
|-----------|------------------------|-----|---------------------------------------|---------------------|--|-------|----------------------------|-------------|---------------------------------|
| | MLM | HLM | CL _{mic} [μL/min/mg protein] | | plasma stability, t _{1/2} [min] | | mouse | human | |
| | | | S9 _{mouse} | S9 _{human} | mouse | human | | | |
| 36 | 100 | 93 | 14 | 15 | > 240 | > 240 | 74.0 ± 3.7 | 97.2 ± 4.8 | 21.7 |
| 37 | 216 | 178 | 6.4 | 7.8 | 74 | 135 | 30.1 ± 9.2 | 51.1 ± 13.3 | > 50 |
| 2 | > 60 | 41 | < 23 | 33.49 | > 240 | 135 | 77.7 ± 10.9 | 93.5 ± 1.3 | 20.8 |

^aData is presented as mean and standard deviation from at least three independent experiments. S9_{mouse}, mouse S9 liver fractions; S9_{human}, human S9 liver fractions; CL_{MIC}, microsomal clearance, calculated from t_{1/2}.

In mouse and human blood plasma, LecA-targeted prodrug **36** was fully stable (t_{1/2} > 240 min). LecB-targeted prodrug **37** was somewhat less stable under these conditions (t_{1/2, MBP} = 74 min, t_{1/2, HBP} = 135 min). Reference compound **2** showed high stability in blood plasma (t_{1/2, MBP} > 240 min, t_{1/2, HBP} = 135 min).

Cytotoxicity was assessed against A549 cells. Whereas **37** showed no cytotoxicity up to 50 μM, **36** and **2** gave IC₅₀ values of 21.7 μM and 20.8 μM, respectively. However, even for **36** and **2** this is acceptable as these values are more than 20-fold higher compared to their activity *in vitro* (table 1).

PRODRUGS CAN NOT REACH INTRACELLULAR OFF-TARGETS IN HUMAN CELLS

The specific mechanisms of fluoroquinolone-related side effects are not yet fully understood. There is evidence for oxidative stress^[110, 145] and the impairment of the mitochondrial DNA replication system^[108, 146, 147] induced by ciprofloxacin. In combination with an unspecific drug accumulation in sensitive tissues, the effects described above could lead to severe tissue damage.^[109, 111, 148] These intracellular side-effects benefit from excellent permeation of fluoroquinolone drugs across biological membranes. It was thus reasoned, that these side effects could be reduced by lower intracellular availability. To test this hypothesis, cell accumulation experiments were performed with prodrugs **36/37** and

with their parent fluoroquinolone **2** (figure 5). While compound **2** was highly intracellularly abundant, both prodrugs **36** and **37** showed very low intracellular concentrations (around 30-180 ng/ml after 15, 30 and 60 min for **36** and between 10-20 ng/mL for **37** after 15, 30 and 60 min, whereas **2** showed concentrations ranging from 2-8 $\mu\text{g}/\text{mL}$). It is interesting that **2** showed already high intracellular levels 15 min after incubation, suggesting that it is rapidly taken up whereas only low concentrations of **36** and **37** were found. Moreover, we assessed if **36** and **37** might have been cleaved intracellularly and, thus, looked for compound **2**. However, this was not the case.

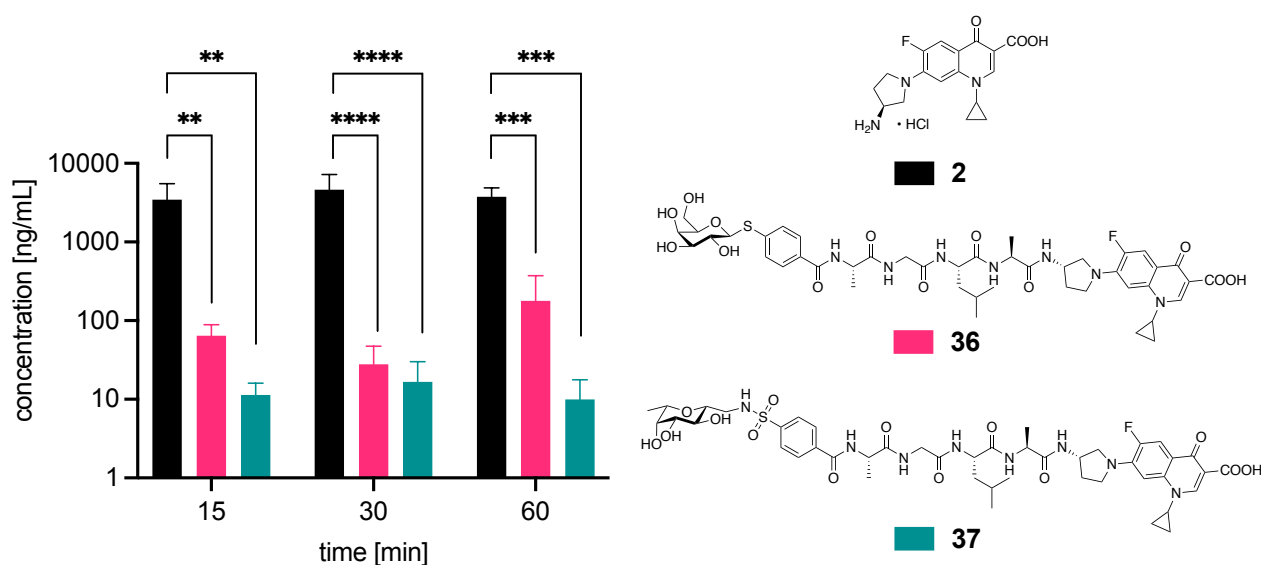


Figure 5. Intracellular drug accumulation assay of the lectin-targeted prodrugs **36/37** and their antibiotic cargo **2** on A549-cells at 10 $\mu\text{g}/\text{mL}$. While fluoroquinolone **2** easily permeates the cell membrane and can be found in high intracellular concentrations, the prodrugs are unable to reach intracellular off-targets. Data is shown as mean and standard deviation from two biological replicates with each two technical replicates. Statistical analysis was calculated with two-way ANOVA and Tukey post-hoc test. Incubation time has no statistical influence on concentration. ($p > 0.05$, ns; $p \leq 0.05$, *; $p \leq 0.01$, **; $p \leq 0.001$, ***; $p \leq 0.0001$, ****).

We conclude, the chemical nature of the prodrugs resulted in a decreased ability to permeate into human cells and reach intracellular off-targets. In combination with the targeted drug delivery approach, this could synergistically lead to drastic reduction of severe side-effects.

3.3.4. Conclusions and outlook

Chronic infections with *P. aeruginosa* can lead to life-threatening conditions, especially in vulnerable patients. Bacterial biofilms are a major contributor to pathogenicity and antibiotic resistance. The large discovery void of antibiotics with new mode of actions for the last 30 years culminated in the current antibiotic resistance crisis.

In this work, we present the first *P. aeruginosa* biofilm-targeted prodrugs. Carbohydrate-probes, targeting the two soluble lectins LecA and LecB of *P. aeruginosa*, were conjugated via a cleavable peptide linker to an antibiotic cargo. The linker was designed as substrate of LasB, the major secreted endopeptidase of *P. aeruginosa*. Three different fluoroquinolones were conjugated to the biofilm-targeted lectin probes and analysed in various assays.

All prodrugs showed effective target-binding to LecA and both homologs of LecB from *P. aeruginosa* PA14 and PAO1, thus covering a broad range of clinical isolates. Further, stability and activation of the prodrugs in different biological matrices were characterised. While unspecific activation by human blood plasma was not observed, the initial cleavage in a sterile filtrate of *P. aeruginosa* PA14 culture supernatant containing LasB was very fast for all prodrugs. When bacterial enzymes and human blood plasma were present, the primary amide based prodrugs **36**, **37**, **48** and **49** efficiently released their antibiotic cargo within 3 h. In contrast, proteolysis of ciprofloxacin-based prodrugs was halted at the stage of the secondary amide, resulting in poor release of ciprofloxacin.

In antimicrobial activity assays, it was shown that the unactivated prodrugs were inactive, while proteolytic activation leads to very potent antibiotic drugs. Especially in the case of aminopyrrolidine-based prodrugs, compounds **36** and **37** reached high antibiotic activities (0.098 - 0.195 μM), comparable to their parent fluoroquinolone **2** (0.027 - 0.054 μM). The ciprofloxacin-based prodrugs showed no significant antibiotic activity, independent of the activating biological matrix, which was consistent with our cleavage data (figure 3).

In vitro ADMET analysis of the most active aminopyrrolidine-based series **2**, **36**, and **37** proved their metabolic stability in microsomal liver fractions and blood plasma in both species, human and mouse. For both prodrugs, the stability in presence of human liver microsomes was enhanced compared to parent fluoroquinolone **2**. Acute cytotoxicity was not observed against A549 lung carcinoma cells using an MTT cytotoxicity assay for assessment. In cell accumulation experiments, the prodrugs showed strongly reduced cell permeability. This is a major improvement compared to the parent drugs, due to the

absence intracellular off-target inhibition and formation of ROS. In our previous work^[149], we reported an *in vitro* biofilm-accumulation assay. For the prodrugs reported above, the high analytic complexity of this assay is further increased by the described instability of the prodrugs towards the biofilm-component LasB. However, we believe that biofilm-accumulation is also plausible for these prodrugs due to the affinity towards their corresponding lectins. In conclusion, this work defines the starting point for the first *P. aeruginosa* biofilm-targeted antibiotic prodrugs.

3.4. Synthesis of a *P. aeruginosa* Biofilm-targeted antibiotic Prodrug, based on a bivalent high-affinity LecA-Probe

This chapter is included in patent EP21212989 (priority date 07.12.21).

Multivalent ligand presentation is a common tool to increase binding affinity of lectin inhibitors (chapter 1.2). In case of tetrameric LecA, carbohydrate binding sites of two neighbored monomers are spatially perfectly oriented for bivalent inhibitors. Importantly, geometry and molecular dimensions of multivalent inhibitors have to be carefully designed in order to avoid intermolecular lectin crosslinks. It is believed, that crosslinking of *P. aeruginosa* biofilm-related lectins rather results in a biofilm stabilisation than inhibition or eradication.^[151] A variety of multivalent^[152, 153] and bivalent^[142, 154-157] LecA-inhibitors have been synthesised so far, resulting in high on-target affinities *in vitro*. Notably, Zahorska *et al.* recently published a series of bivalent LecA inhibitors with exceptional inhibitory activity and selectivity over galectin-1.^[121] The authors systematically varied length and number of rotatable bonds of the spacer to fit the distance of two carbohydrate binding sites. Based on these inhibitors, a branched fluorescent LecA-ligand was designed and synthesised (EP19306432.6). However, these molecules suffered from low aqueous solubility and chemical stability at lower pH. Isosteric substitution of the labile acylhydrazones resulted in a new series of highly potent bivalent LecA-inhibitors with excellent solubility and metabolic stability (appendix 6.6, *manuscript in preparation*, PhD-Thesis of Eva Zahorska **2021**, *Saarland University*). Further, introduction of a central tertiary amine in the spacer unit allowed the instalment of cargo molecules, e.g. (fluorescent) dyes or antibiotics (*patent filed*, EP21212989). The rational design of bivalent LecA-probe **1** resulted in highly potent binding affinity ($K_d = 9.9 \pm 0.5$ nM, SPR). Conjugation to fluorescein via a PEG-alkyne linker only merely reduced binding affinity (19.3 ± 10.5 nM, SPR).

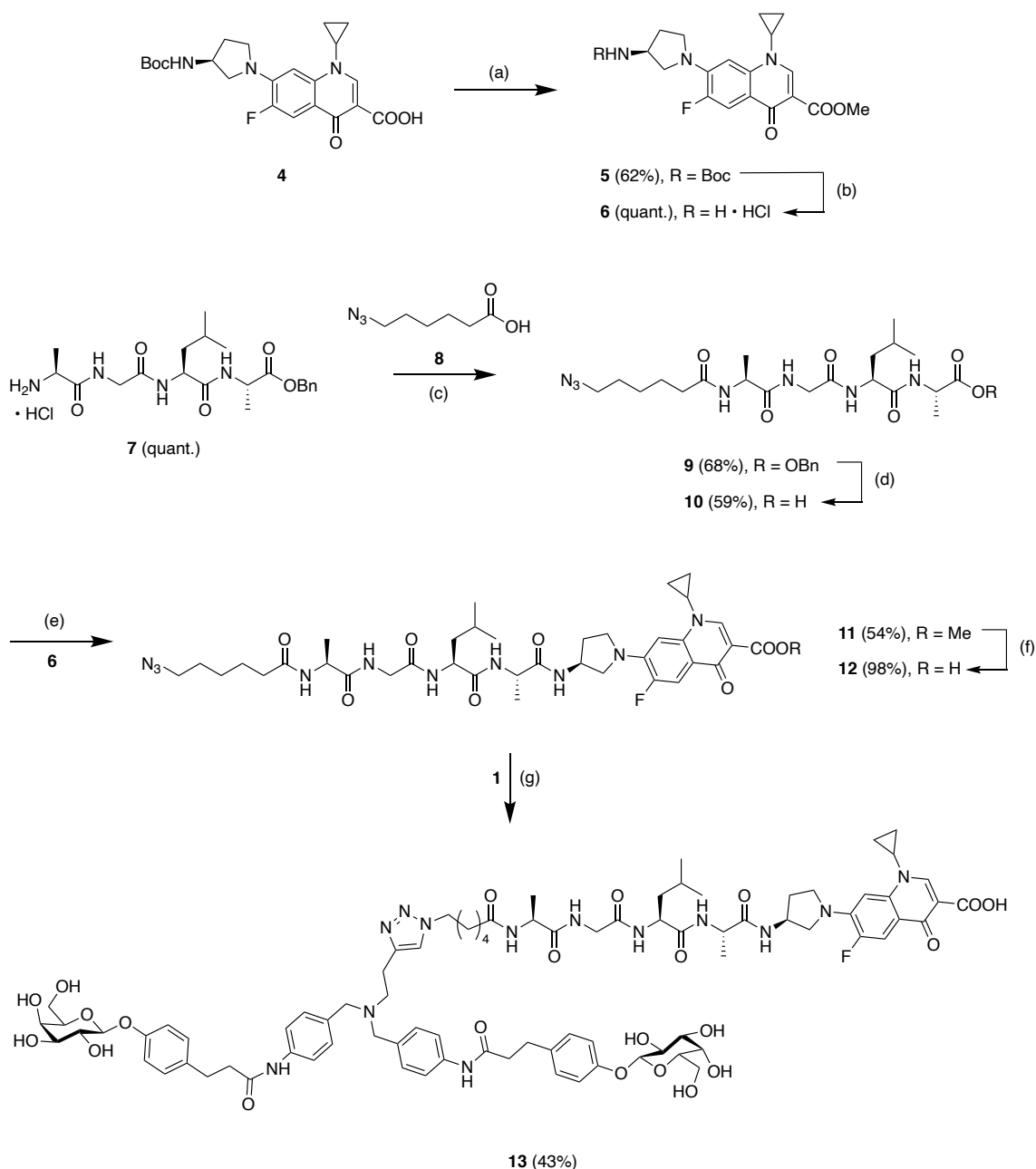
In the following chapter, the previously described bivalent LecA-inhibitor approach was combined with the LasB-cleavable antibiotic prodrugs described in chapter 3.3. Due to the nanomolar binding affinity of LecA-probe **1**, a prodrug strategy is indispensable. Uncleavable high-affinity conjugates are likely to stick with the target protein and are thus not able to enter the bacterial cell. According to chapter 3.3, a LasB-cleavable peptide motif (Ala-Gly-Leu-Ala) was elongated with an azide linker (**2**) for conjugation via copper catalysed alkyne azide [3+2]-cycloaddition (CuAAC) with alkyne **1**. Fluoroquinolone **3** was used as antibiotic cargo.

3.4.2. Results and discussion

3.4.2.1. Synthesis

Chemical synthesis is based on three building blocks: bivalent LecA-probe **1**, LasB-cleavable ω -azido-peptide-linker **2** and fluoroquinolone **3** (scheme 1).

Scheme 1: Synthesis of the bivalent LecA-targeted fluoroquinolone prodrug **13**.^a



^aReagents and conditions: (a) TBTU, DIPEA, MeOH, cat. DMAP, CH₂Cl₂, r.t., 16 h; (b) HCl, dioxane, r.t., 16 h; (c) TBTU, DIPEA, CH₂Cl₂, r.t. 16 h; (d) LiOH, THF/MeOH/H₂O (3:2:2), r.t. 30 min; (e) TBTU, DIPEA, DMF, r.t. 4 h, 90% pure; (f) LiOH, THF/MeOH/H₂O (3:1:1), r.t., 24 h, 90% pure; (g) cat. CuSO₄, cat. sodium ascorbate, DMF/H₂O (4:1), r.t., 2 h.

In the previous chapter 3.3, synthesis of a benzyl-protected aminopyrrolidine-substituted fluoroquinolone^[158] was presented. In order to increase orthogonality between the fluoroquinolone protecting groups and the azide in linker **2**, the benzyl-ester was substituted by a methyl ester. Methyl esters can be readily cleaved by saponification and allow a straight forward purification. Boc-protected fluoroquinolone **4** (synthesis described in chapter 3.3) was converted to the corresponding methyl ester **5** by activation with TBTU. After acidic deprotection, fluoroquinolone building block **6** was obtained in quantitative yield.

Tetrapeptide **7** (synthesis described in chapter 3.3) was reacted with ω -azido-hexanoic acid (**8**) under peptide coupling conditions by TBTU. Afterwards, benzyl-ester **9** was cleaved by saponification with LiOH towards carboxylic acid **10**. Building blocks **6** and **10** were then coupled via activation by TBTU to obtain compound **11**. Troublesome chromatographic purification of compound **11** resulted in a purity of approximately 90%. Subsequent LiOH-mediated saponification gave fluoroquinolone-peptide conjugate **12** in high yield with equal purity. Lastly, conjugate **11** was coupled to bivalent LecA-probe **1** by CuAAC and prodrug **13** was purified by preparative HPLC.

However, there is evidence that compound **13** is not diastereometrically pure (figure 2).

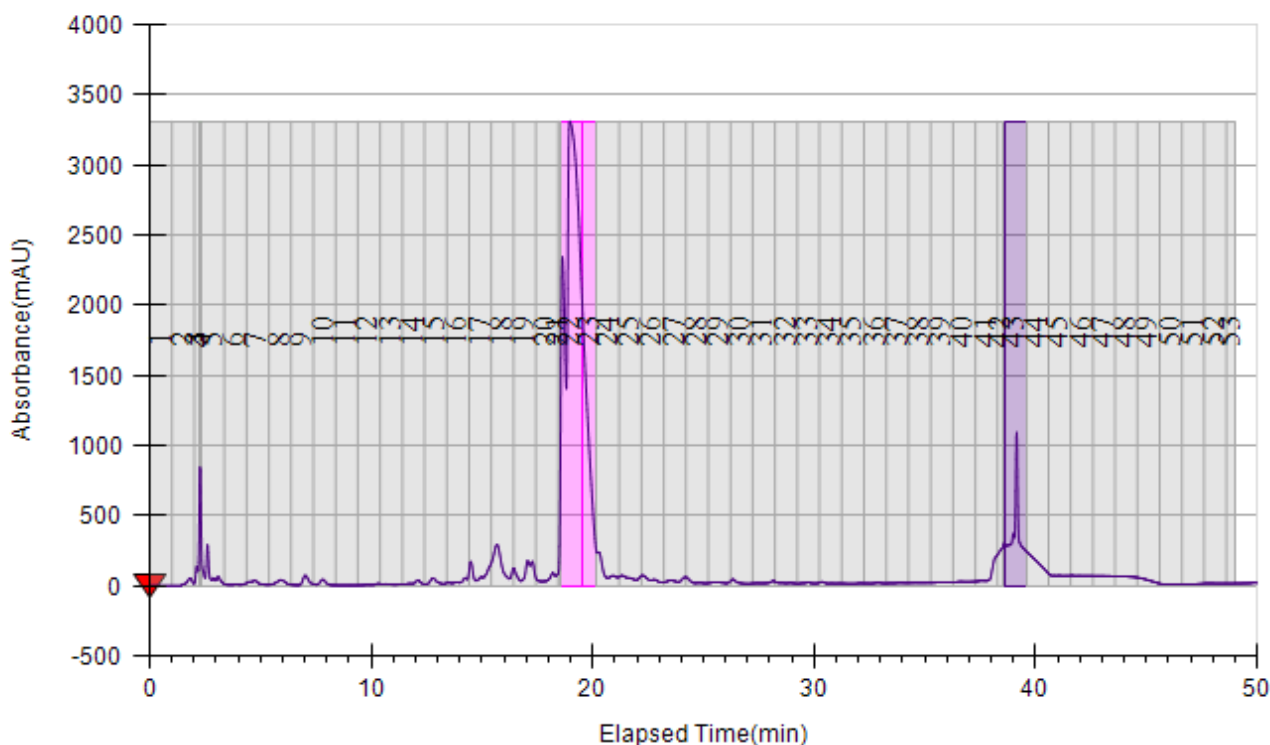


Figure 2. Preparative-HPLC chromatogram of prodrug **13**. Compound eluted at 18.5 - 20 min and was collected in tubes 22 and 23. An impurity was co-eluted at 18.5 - 19 min.

First, a small peak co-eluted with the main compound peak (figure 2). Second, there is an additional peak in the ^1H -NMR (8.03 ppm, $J = 0.25$) together with four unassigned peaks in the ^{13}C -NMR (51.60 ppm, 22.83 ppm, 21.72 ppm, 17.86 ppm, 17.73 ppm). According to $^1\text{H},^{13}\text{C}$ -HSQC and $^1\text{H},^1\text{H}$ -COSY analysis, the peak at 8.03 ppm in the ^1H -NMR corresponds to aminopyrrolidine NH at C3. Interestingly, its integral adds up together with the integral of NH at 7.97 ppm to $J = 1$. In the ^{13}C -NMR spectrum, there are additional peaks at 17.86 ppm, 17.73 ppm, 23.02 ppm, 21.43 ppm and 51.60 ppm. Similar signal patterns can be observed in the ^{13}C spectra of precursors **11** - **13**. Thus it is very likely that LecA-targeted prodrug **13** is not pure, but presumably contaminated with a diastereomer corresponding to the aminopyrrolidine stereocenter. So far, it is not clear whether the commercially available (*S*)-aminopyrrolidine was not enantiomerically pure or if epimerisation happened during the synthesis. Another, however less likely explanation would be the presence of rotamers or intramolecular bond formation that can result in artefacts.

3.4.3. Conclusion and Outlook

In this chapter, the synthesis of a *P. aeruginosa* biofilm-targeted, LasB-cleavable antibiotic prodrug based on a highly potent bivalent LecA-inhibitor was established. Although the purity of prodrug **13** has to be confirmed and (if necessary) improved, first experiments to evaluate their potential can be performed. First, prodrug activation by *P. aeruginosa* *in vitro* and release of antibiotic cargo have to be confirmed in analogy to experiments in chapter 3.3. Further, retention of high binding affinity towards LecA will be confirmed. In fact, based on our experience with the previously described lectin-targeted prodrugs and bivalent LecA-targeted fluorescein conjugate (compound not shown), we are very confident that prodrug **13** will behave as planned. Notably, preliminary experiments with the fluorescent dye mentioned above showed a lectin-dependent *P. aeruginosa* biofilm staining under flow conditions *in vitro* (Eva Zahorska and Lisa Denig, unpublished). Prodrug **13** will be further studied under similar conditions, followed by a dead-live staining in order to evaluate the compounds antibiotic effect.

As described in the previous chapters, the modular approach allows the exchange of its individual building blocks (i.e. targeting unit, cleavable linker, antibiotic) with other molecules. Carbohydrate-based molecules are likely to suffer from disadvantageous pharmacokinetic properties, i.e. low oral bioavailability and metabolic stability. Recently, our group published first non-carbohydrate glycomimetic LecA-inhibitors, based on a

catechol scaffold.^[122] Catechol-antibiotic conjugates are of particular interest due to their ability to exploit active iron-uptake mechanisms, so-called trojan horse approach.^[80, 159, 160] The cephalosporin-catechol conjugate Cefiderocol^[161] is a prominent example that entered the European market in 2020 for treatment of antibiotic-resistant, aerobic Gram-negative bacteria. Combination of trojan-horse approach with multivalent inhibition of catechol-based LecA-ligands could lead to synergistic targeting effects.

3.5. On the Carbohydrate binding-Specificity of the Pineapple-derived Lectin Acm-JRL and its Potential Use against SARS-CoV-2

3.5.1. Introduction

Since the beginning of 2020, society is facing the severe acute respiratory syndrome corona-virus 2 (SARS-CoV-2) pandemic. SARS-CoV-2 is a novel coronavirus, that spread within a short time all over the world. It can infect the respiratory tract and potentially results in a coronavirus associated disease (CoViD-19). Especially for older or immunocompromised patients, CoViD-19 is likely to be lethal. So far (October 2021), almost 240 million people were infected worldwide and more than 4.5 million deaths were reported in association with SARS-CoV-2.

A variety of novel and very potent vaccines entered the market at the end of 2020. Vaccination is an indispensable approach to protect society from a SARS-CoV-2 infection. However, a small fraction of vaccinated people still suffers from a severe infection. Further, there is a significant number of people who can not be vaccinated due to allergic preconditions. Thus, novel pharmaceutical therapies are urgently needed to treat infections.

Drug repurposing is especially interesting due to the acute nature of this pandemic. Bromelain is an approved drug that shows anti-edematous, anti-inflammatory and fibrinolytic properties and is thus used to cure trauma-induced swelling.^[162, 163]

Plants are a rich source of pharmaceuticals. As described in the introduction (chapter 1.3.1), plants, plant parts or their preparations (e.g. by extraction, fermentation, grinding) are of high pharmaceutical interest since thousands of years. Pineapple (*Ananas comosus*) is usually not considered as a classical pharmaceutical plant. However, bromelain is prepared by precipitation or ultracentrifugation of pineapple stem juice and is an approved drug in Germany.^[164]

Phytopharmaceuticals often not only consist of a single active ingredient responsible for their therapeutic action. Proteases, peptide based protease inhibitors and the lectin Acm-JRL (also called Anlec^[165]) are the three main protein components of bromelain. It is very likely that proteases are responsible for the anti-inflammatory properties of bromelain. Additionally, protease inhibitors prevent unspecific proteolysis like a safety mechanism that is slowly removed during the intake of bromelain. Acm-JRL was recently characterised by Azarkan *et al.*^[166] and its quantitative proportion in bromelain was determined by Gross *et al.* in collaboration with HIPS. Despite these recent studies, the molecular mode of action of Acm-JRL (if there is any) is not yet understood.

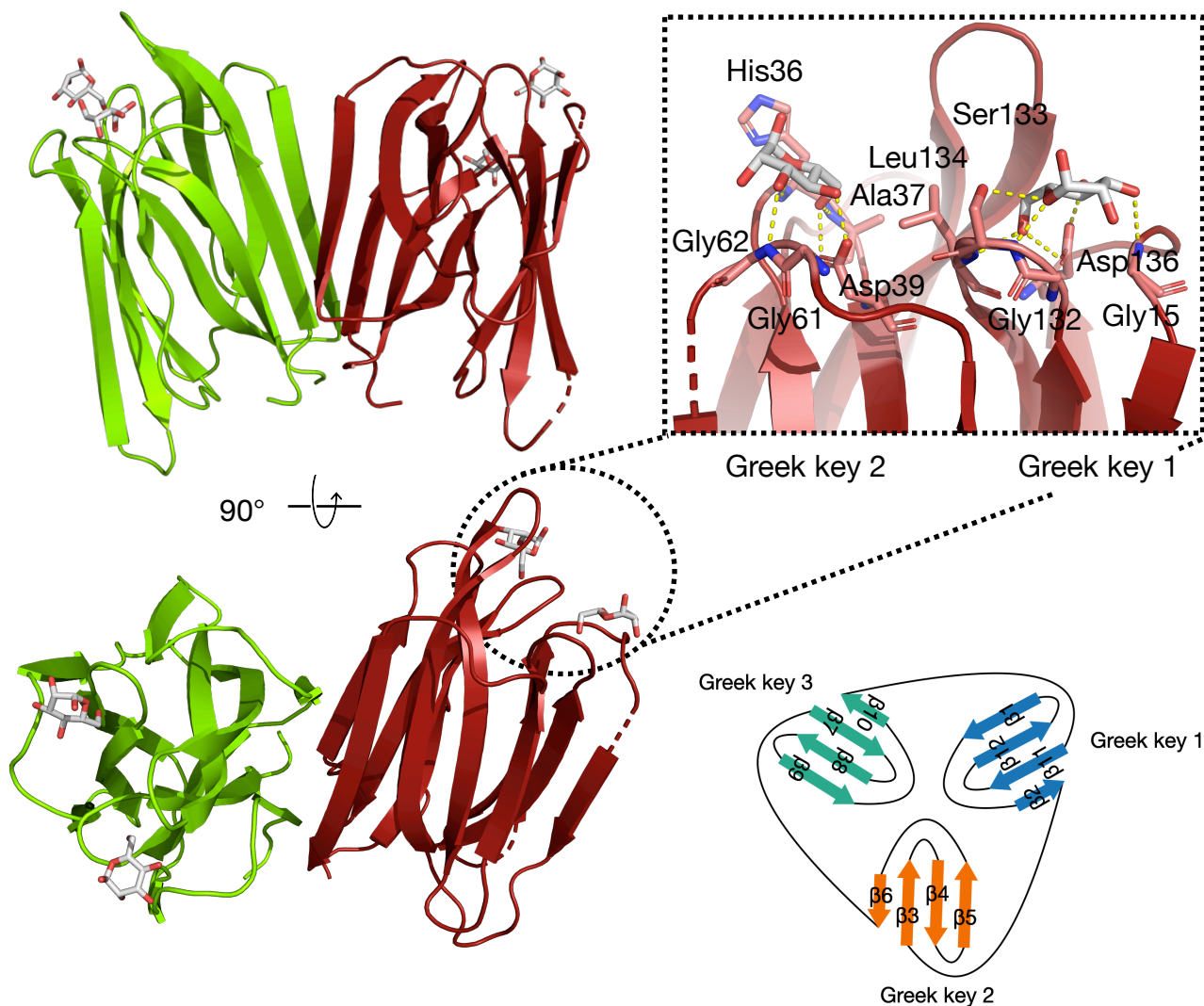


Figure 1. Overall structure of Acm-JRL in complex with D-mannose (PDB code: 6FLY^[166]). Protein is shown in cartoon representation with green and red colouring, according to the monomers. Ligands are shown as grey sticks and the involved amino acids in the carbohydrate binding site as red sticks. Key ligand-protein interactions are described in the text. Bottom right shows the general structure of one monomer in a β -prism fold together with the common nomenclature.

Acm-JRL belongs to the family of Jacalin-related lectins (JRL).^[167] One of the first representatives of this lectin family is jacalin, the lectin isolated from jack fruit (*Artocarpus integrifolia*). Lectins are carbohydrate binding proteins. The JRL family can be divided in two main classes, according to their ligand specificity.^[167] Galactose-specific JRL can almost exclusively be found in the *Moraceae* plant family, most typically in the seed. Structurally, those JRLs are tetramers of four identical protomers, each with one carbohydrate binding site. The biosynthesis of galactose-specific JRL is highly complex

and includes co- and post-translational modifications from one preproprotein together with *N*-glycosylation in the secretory pathway.

Mannose-specific jacalin-related lectins can be found in various plants. The structure of mannose-specific JRLs is less complex as they usually consist of two, four or eight unprocessed peptides. Due to the absence of a signal peptide, they are considered as cytoplasmic proteins.

The specific physiological roles of jacalin-related lectins is yet not fully clear. The main occurrence of galactose-specific JRL in seeds suggests a role as storage proteins. On the other hand, jacalin-related lectins were shown to have insecticidal or mitogenic properties. Thus, they could serve as defensive agents, e.g. against bacteria, fungi or predators.^[168]

Acm-JRL is a mannose-binding JRL and was first isolated and characterised by Azarkan and coworkers in 2018.^[166] Isothermal titration calorimetry experiments revealed a rather low binding affinity towards D-mannose ($K_a = 178 \pm 4 \text{ M}^{-1}$), D-glucose ($K_a = 83 \pm 3 \text{ M}^{-1}$) and GlcNAc ($K_a = 88 \pm 1 \text{ M}^{-1}$). On the other hand, high mannose structures like mannotriose (Man α 1-6[Man α 1-3]Man α , $K_a = 734 \pm 117 \text{ M}^{-1}$) and mannopentaose (Man α 1-6[Man α 1-3]Man α 1-6[Man α 1-3]Man β , $K_a = 1694 \pm 679 \text{ M}^{-1}$) showed significantly higher binding affinities.

Like other mannose-specific JRL, Acm-JRL adopts a characteristic β -prism fold with three Greek key four-stranded β -sheets. Two monomers align side-by-side, mostly involving β 1 and β 10 to form dimers with an angle of approximately 45° . Although also a tetrameric form of Acm-JRL could be assigned from the monomers in the asymmetric unit, this is rather an artefact due to the high protein concentrations during crystallisation. In Co-crystal structures with D-mannose and Me- α -D-mannopyranoside, two carbohydrates were bound by one monomer in a conserved binding pose. Site 1 is defined by interactions with Greek key 1, while site 2 is surrounded by Greek key 2. Key interactions within site 1 and D-mannose are hydrogen bonds of Man-O5 with S133-OH, Man-O4/O6 with D136-COOH and backbone-NH interactions of Man-O3 with G15, Man-O5 with S133 and Man-O6 with L134. Comparable to binding site 1, site 2 interacts with D-mannose via hydrogen bonding of Man-O4/O6 with D39-COOH and Man-O3, Man-O5 and Man-O6 with backbone nitrogens of G62, H36 and A37, respectively (figure 1). For Me- α -D-mannopyranoside, binding interactions were mostly conserved, except the interaction of S55-OH with with the ring oxygen in binding site 1 and a slight rotation of the carbohydrate in binding site 2. Overall, the interactions are comparable to the binding

of D-mannose by BanLec, a closely related mannose-specific JRL from banana (*Musa acuminata*). BanLec is reported to be a potent viral entry inhibitor of HIV-1, HCV and influenza virus.^[169, 170] However, the mitogenic activity of native BanLec limits its therapeutic use. Interestingly, the structure of Acm-JRL shares similarities of a genetically engineered BanLec^[170] with reduced mitogenic activity. Thus, Azarkan *et al.* postulated a potential use of Acm-JRL as an alternative to BanLec against mannosylated viruses. Consequently, it is very likely that mannose binding lectins like Acm-JRL can bind SARS-CoV2 Spike-protein and neutralise the virus.

3.5.2. Results and discussion

3.5.2.1. Isolation of Acm-JRL from bromelain and its biophysical characterisation

The mannophilic lectin Acm-JRL was isolated by affinity chromatography from pineapple stem extract (bromelain) following the procedure reported by Azarkan *et al.*^[166] Prior to purification, the soluble protein fraction of bromelain was obtained by aqueous extraction in presence of protease inhibitor (methyl methanesulfonate). Freshly prepared mannosylated sepharose beads were used as purification matrix.^[171] Elution with 1 M D-mannose yielded the desired lectin in a yield of 0.9 - 1.6 mg Acm-JRL per gram bromelain powder (figure 2A).

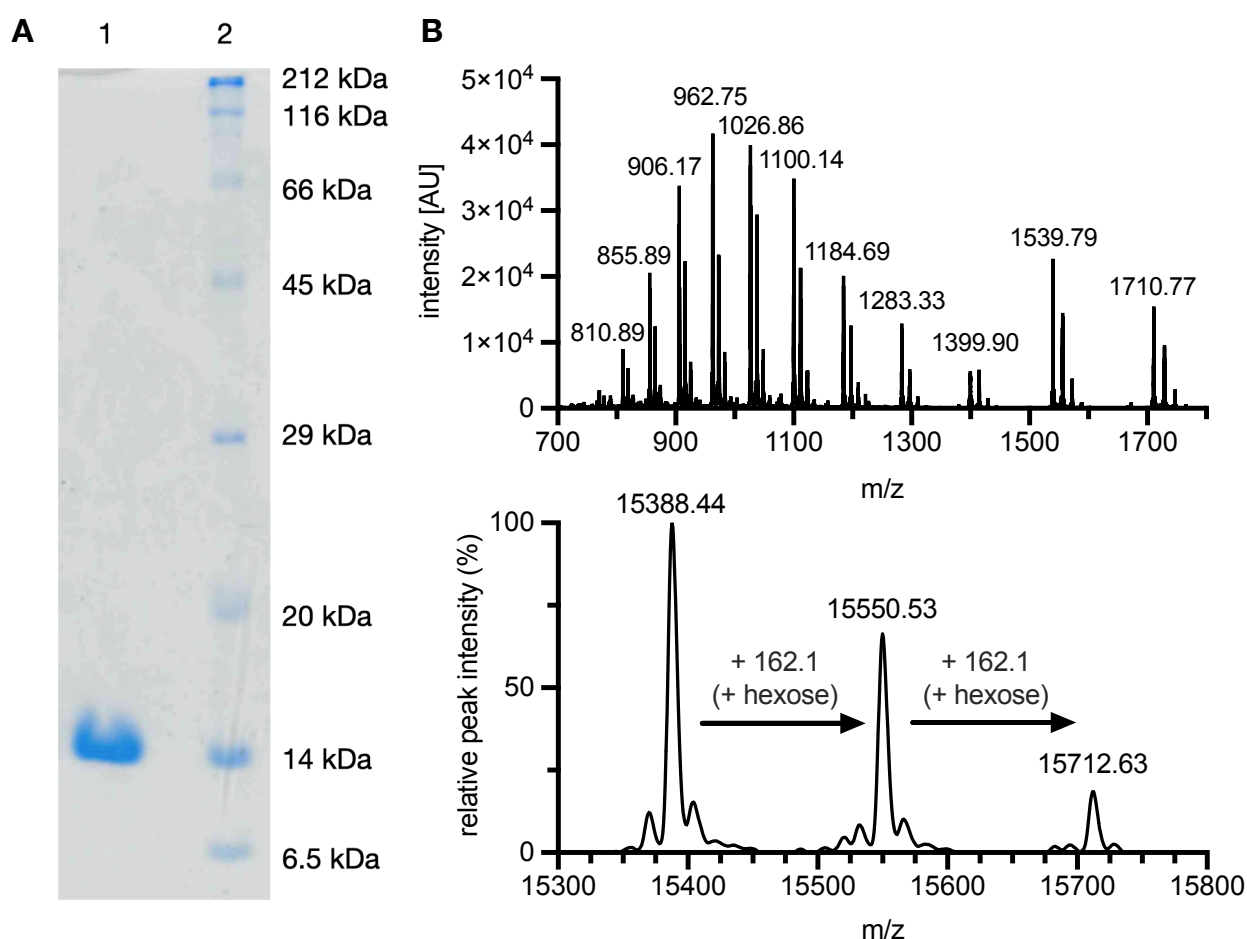
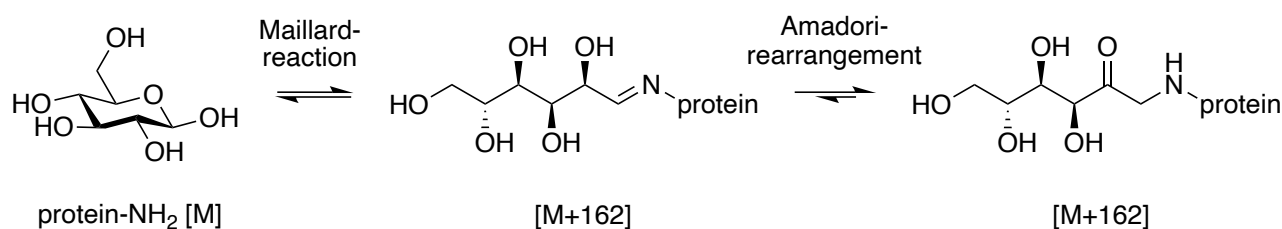


Figure 2. **A** Affinity purified Acm-JRL (lane 1) and molecular mass marker (lane 2) analysed by SDS-PAGE (18%). **B** ESI-MS-spectrum of Acm-JRL before (top) and after (bottom) maximum entropy deconvolution. Main peak ($m/z = 15388.44$) after deconvolution corresponds to acetonitrile adduct $[M+H+MeCN]^+$. Peaks at higher $m/z = 15550.53$ and $m/z = 15712.63$ most likely result from glycation.

The identity of the protein was confirmed by mass spectroscopy (average mass = 15346 Da, figure 2B). The main peak ($m/z = 15388.44$) can be assigned to the acetonitrile adduct $[M+H+MeCN]^+$. As reported by Gross *et al.*^[165] two additional mass peaks were observed in a ratio of 100 : 65 : 17, separated by a mass shift of 162 Da. During the industrial production of bromelain, the raw product is loaded on maltodextrin particles to simplify its handling. Maltodextrin is a mixture of soluble carbohydrates that result from hydrolysis of starch.



Scheme 1. Protein glycation by Schiff-base formation and Amadori-rearrangement. Primary amine, e.g. from Lysine or *N*-terminus forms an imine with an aldohexose, that can rearrange towards a α -amino-ketone. In case of multiple available nucleophiles, this reaction can occur repeatedly, always resulting in a mass shift of 162 Da. $[M]$, molecular mass of the protein.

Thus, it contains reactive reducing carbohydrates like glucose or glucose oligosaccharides. Reducing carbohydrates can react with primary amines of proteins (5 lysins present in Acm-JRL) to form a Schiff-base, presumably followed by Amadori rearrangement (figure 1) towards a stable α -amino ketone. The products of this reaction are called advanced glycation end products. Glycation results in a mass shift of 162 Da that was observed in the MS-spectrum (figure 2). The presence of two mass shifts suggest that this reaction occurs twice on the protein or one disaccharide of maltose reacts following the same reaction sequence. However, it is not clear if it is just a statistical mixture or if two specific lysins are affected by this reaction. A close look on the electron density map of crystallised Acm-JRL (PDB: 6FLY) did not show any evidence for unassigned electron density. Flexible residues, especially on the protein surface, are known to have no or only very faint electron density in crystal structures. Further, it was not reported whether the Acm-JRL isolated and crystallized by Azarkan *et al.* was actually glycated.

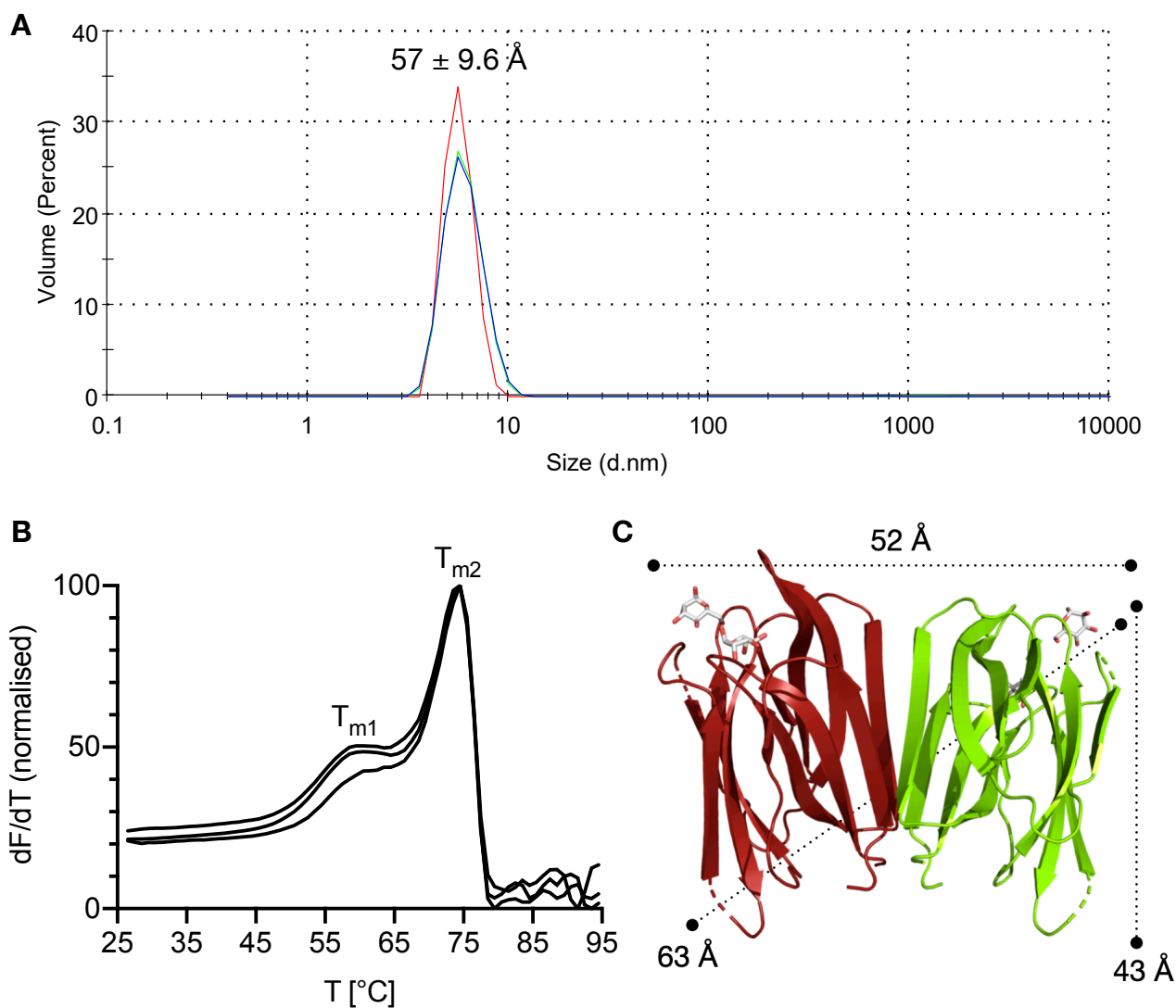


Figure 3. **A** Dynamic light scattering analysis of Acm-JRL (size distribution by volume). Peak at $57 \pm 9.6 \text{ \AA}$ indicates dimerisation in solution. **B** Differential scanning fluorimetry of Acm-JRL: biphasic denaturation together with two peaks T_{m1} and T_{m2} correspond to the reported dimeric structure in solution. **C** Global structure and dimensions of Acm-JRL in the crystal structure (PDB: 6FLY^[166]).

Next the protein's properties and purity were analysed (figure 2). Gel-electrophoresis under denaturing conditions (SDS-PAGE) showed a single protein band at $\approx 14 \text{ kDa}$ (figure 2A). Previous studies showed dimerisation of Acm-JRL in solution, determined by size exclusion chromatography and equilibrium unfolding experiments.^[166] However, the authors also showed that Acm-JRL crystallised as a tetramer. Dynamic light scattering (DLS) was used to determine the hydrodynamic radius of Acm-JRL in buffered solution (figure 3A). The measured hydrodynamic diameter of $57 \pm 9.6 \text{ \AA}$ corresponds to the radius of the dimer (figure 3C), rather than to monomeric or tetrameric quaternary structure.

Additionally, differential scanning fluorimetry studies suggested two unfolding events at $T_1 = 58 - 60^\circ\text{C}$ and $T_2 = 73 - 74^\circ\text{C}$ (figure 3B) which could correspond to dissociation of the dimer followed by denaturation of the monomers.

Protease impurities from the soluble protein fraction of bromelain can disturb future experiments and thus have to be quantitatively removed. Although the protease fraction should be removed by affinity chromatography, residual proteolytic activity of the eluted fraction was analyzed (figure 4). *N* $_{\alpha}$ -benzyloxycarbonyl-L-lysine *o*-nitrophenyl ester (Z-Lys-ONp) was used as a model substrate that releases chromogenic *o*-nitrophenol (HONp) upon proteolysis.

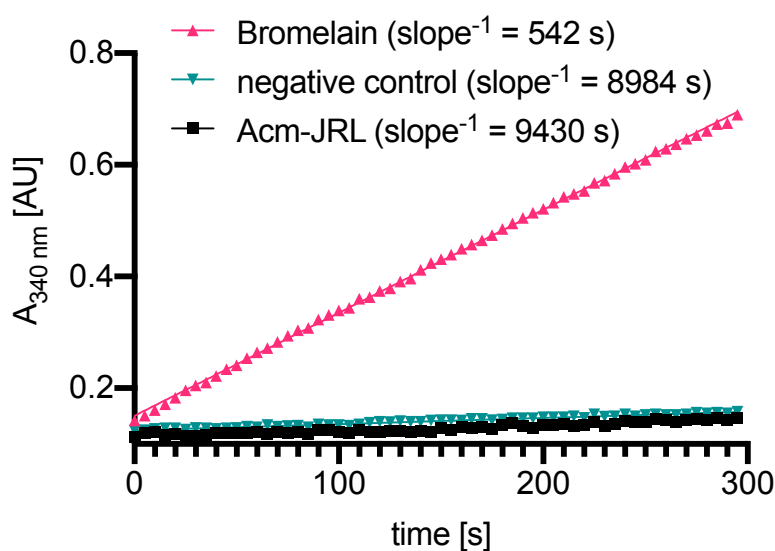


Figure 4. Protease activity of bromelain before and of Acm-JRL after purification by affinity chromatography. Negligible proteolytic activity was observed for the purified protein. Soluble protein fraction from bromelain and absence of protein were used as positive and negative control, respectively.

After linear regression fit of the raw data ($R^2 > 0.90$), the slope can be used to describe the proteolytic activity. Crude soluble protein fraction of bromelain led to a fast release of HONp (slope $^{-1} = 542$ s). In contrast, purified lectin showed only very little release of HONp (slope $^{-1} = 8984$ s), comparable to the absence of protein (negative control, slope $^{-1} = 9430$ s). In conclusion, Acm-JRL was obtained in good purity and can be used for further studies.

3.5.2.2. Fluorescence labelling of Acm-JRL and glycan array analysis

Fluorescence labelling of proteins is a handy tool in chemical biology. Many biophysical techniques like microscale thermophoresis, fluorescence microscopy or glycan array analysis are accessible after fluorescence labelling. Due to the presence of five lysins in Acm-JRL, urea- and amide-based conjugation chemistry was chosen for the attachment of a fluorophore. Fluorescein, and its activated derivative fluorescein isothiocyanate (FITC) are popular fluorescent dyes for molecular imaging. They share good water solubility and high fluorescent quantum yields. However, they are also pH-dependent and suffer from a high rate of photobleaching.^[172]

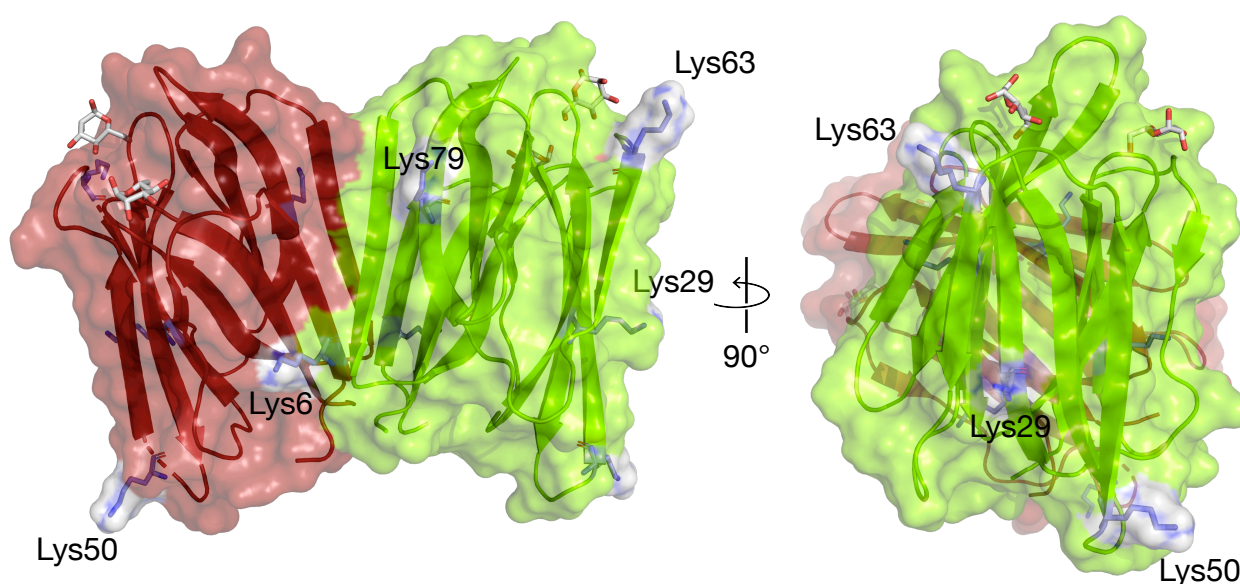


Figure 5. Accessible lysins on the protein surface of Acm-JRL (PDB: 6FLY, solvent radius 1.6 Å). Lys50 and Lys63 are most accessible and thus most likely already partially glycosylated. The reduced solvent accessibility of the residual lysins could explain low labelling efficiency (labelling efficiency = 0.44 and 0.55 for FITC and NHS-Cy3, respectively).

Interestingly, labelling with FITC yielded a rather low labelling efficiency of 0.44. Low labelling efficiency combined with high photobleaching could result in poor fluorescence sensitivity. Cyanine-3 (Cy3) is a bright, photostable and pH-insensitive orange fluorescent dye that was used as NHS-activated Cy3 to improve labelling efficiency and photochemical properties of the labelled protein. Unfortunately, Cy3-labelling also

resulted in a low labelling efficiency of 0.55. Notably, one to two of the five lysins of Acm-JRL are not available anymore for labelling as they are partially chemically modified by glycation (figure 1). According to the solvent accessible protein surface calculated from the crystal structure, Lys50 and Lys63 are most accessible (figure 5). The reduced availability of the other lysins (Lys6, Lys29 and Lys79) could explain the low labelling yields. On the other hand, only 10% of Acm-JRL is bis-glycosylated, 36% is mono-glycosylated and 54% is unmodified (figure 2).

In general, jacalin-related lectins can be clustered by their carbohydrate specificity into galactophilic and manno-/glucophilic subgroups. Acm-JRL is reported to have a millimolar affinity towards mannosides and glucosides. Glycan microarrays are two-dimensional arrangements of spatially-defined immobilised (oligo-)saccharides on solid support.^[173] This technique allows the analysis of binding specificities of glycan-binding proteins (GBP) in a high-throughput fashion.

To elucidate a more precise glycan specificity, Acm-JRL was submitted to the Consortium for Functional Glycomics for glycan array analysis with 585 distinct mammalian carbohydrate epitopes (figure 6). Confirming previous mannose specificity, the lectin showed a high specificity towards α -mannosides and a less pronounced affinity to α -glucosides/*N*-Acetyl glucosamines.

Although there was also a single glycan hit with a terminal β -galactoside, this is suspected to be a false positive due to dose-independent changes in signal intensity (5 vs 50 μ g/mL) and the close proximity to the solid support, induced by the absence of a linker moiety (Sp0). Bi- and trivalent mannosides, so-called, high-mannose structures, showed higher apparent binding affinities towards Acm-JRL than monovalent glycans (e.g. compare CFG glycan ID **312** vs. **207/209**). Increased binding affinity induced by multivalent ligand presentation is a common feature in glycan-lectin recognition. The mannotriose epitope (Man α 1-6[Man α 1-3]Man α , present in CFG glycan ID **211**, **213**, **51** and **50**) and the mannopentaose epitope (Man α 1-6[Man α 1-3]Man α 1-6[Man α 1-3]Man β , present in CFG glycan ID **310** and **214**) showed highest binding responses and their relative trends corresponded to previously published ITC data ($K_d(\text{mannotriose}) = 1.4 \pm 0.2$ mM, $K_d(\text{mannopentaose}) = 590 \pm 236$ μ M)^[166].

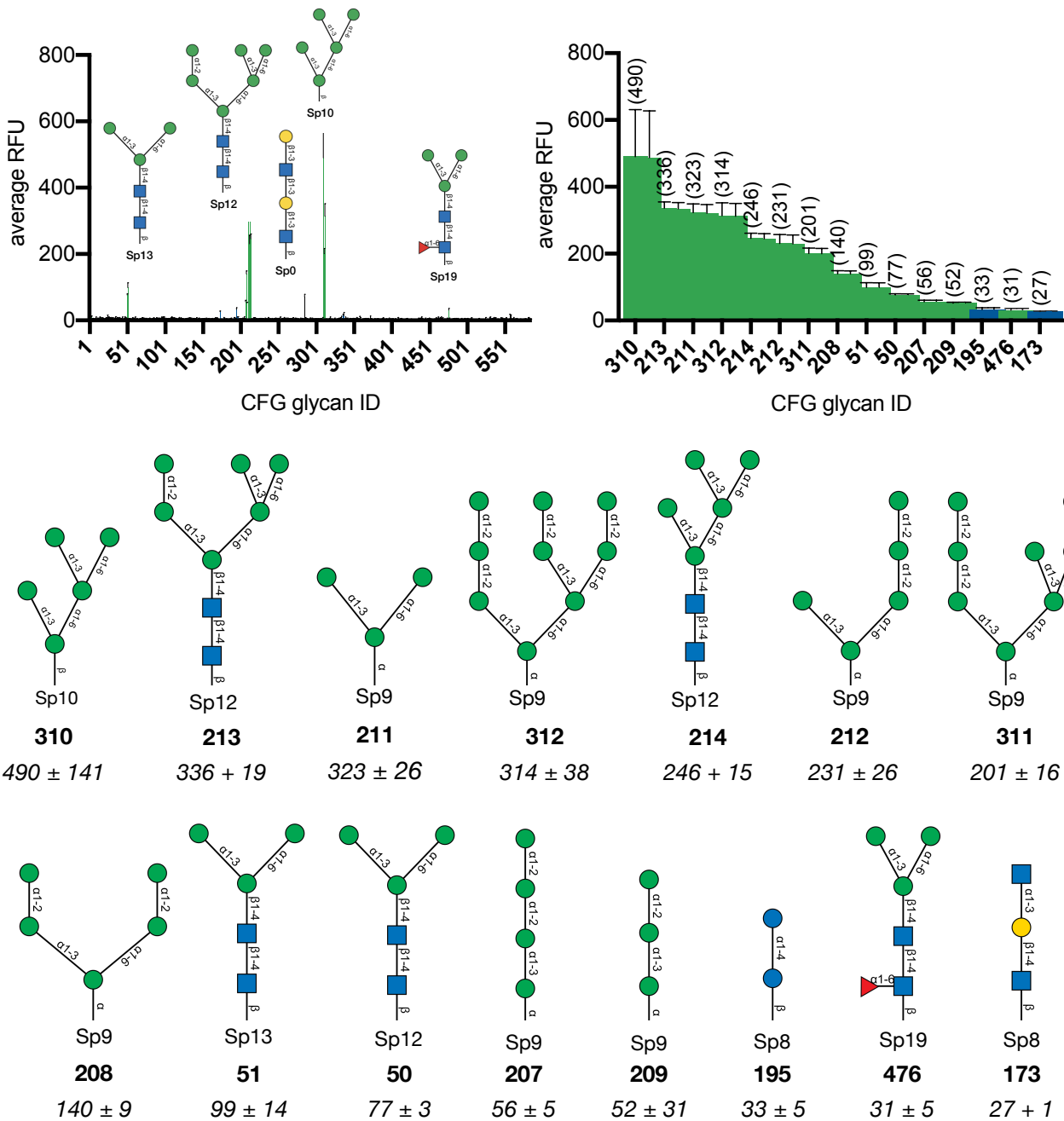


Figure 6. Mammalian glycan array (CFG) analysis of Acm-JRL (50 $\mu\text{g/mL}$): the protein recognises terminal α -mannosides and weakly binds terminal α -glucosides. Terminal galactoside hit (CFG glycan ID **285**) is most likely a false positive, possibly due to unspecific interactions with the matrix (Sp0 = no spacer). Glycans containing terminal mannosides are labelled green, terminal glucosides (Glc/GlcNAc) are labelled blue; others are labelled black. Data from CFG glycan microarray version 5.5 is shown as mean fluorescent intensity \pm s.d. from 6 replicates on the array. Glycan structures are illustrated according to CFG nomenclature. Legend: *av. RFU*, **glycan ID**.

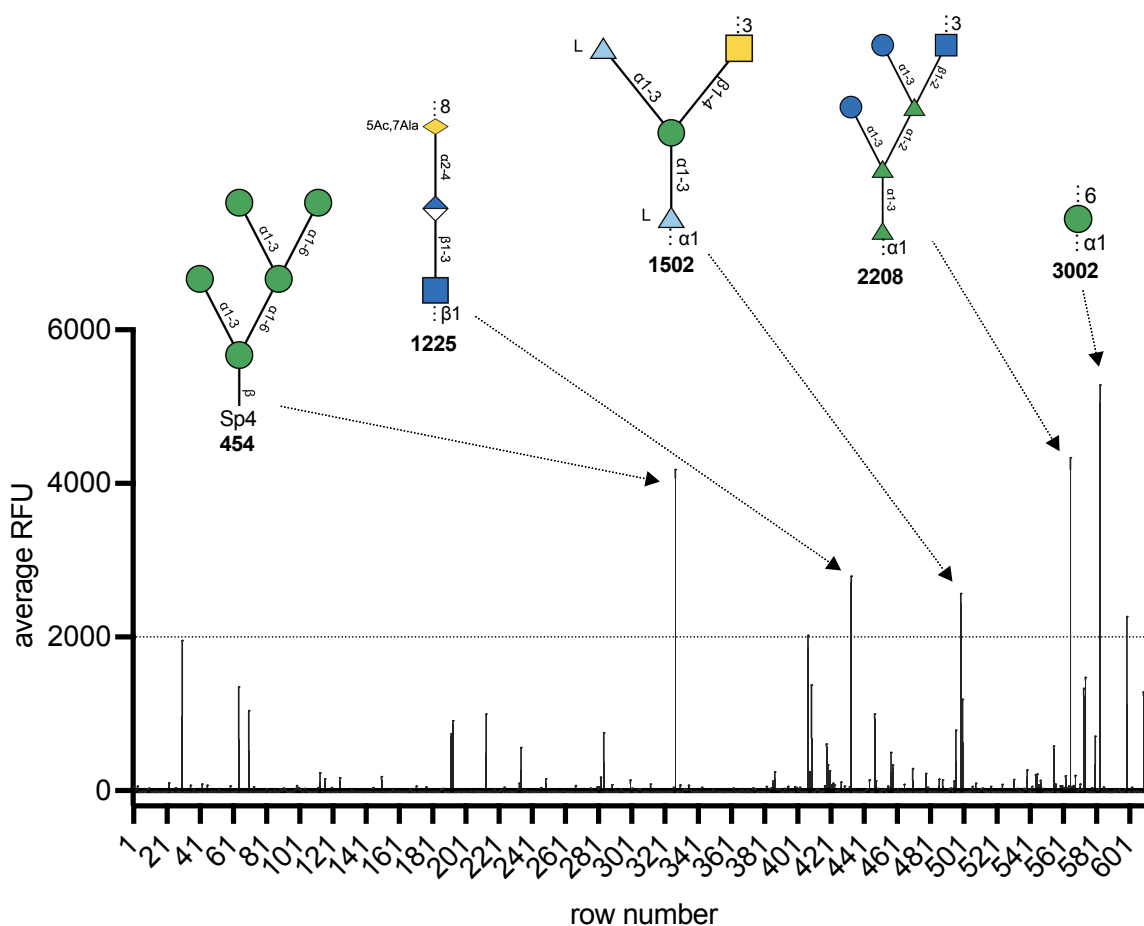


Figure 7. Analysis of Acm-JRL (20 $\mu\text{g}/\text{mL}$) on the Semiotik glycan array, with mammalian, bacterial and further glycans. 2000 RFU were defined as hit threshold. Mainly multivalent mannosides and glucosides were bound by the protein. L-6-deoxy-talose glycan (Semiotik glycan ID **1502**) is considered questionable due to irregular response with varying lectin-concentration (SI). Data from Semiotik glycan microarray is shown as median fluorescent intensity 6 replicates on the array. Glycan structures are illustrated according to CFG nomenclature. Three dots indicate the glycan is a repeating unit of undefined number of repetitions. Bold number underneath glycan structure corresponds to Semiotik glycan ID. Translation from row number to Semiotik glycan ID and short name can be found in table S1 and table S2.

Acm-JRL forms dimers in solution and can bind up to two mannosides per binding site. The distance from the binding site from one monomer to the other monomer is approximately 46 - 50 \AA . The distance from C1 to C1 of two mannosides within one binding site is approximately 14 \AA , which is in the range of distance of two mannoside C1s in mannopentaose. Consequently, it is possible that the increased binding affinity of the mannopentaose epitope results from a simultaneous bivalent binding event. On the

other hand, mannopentaose could also preorganise two α -mannosides in a way that allows the rapid alternating occupation of the two binding sites within one monomer.

Monovalent α -glucosides showed very low but significant binding. Unfortunately, no multivalent glucosides are available on this array to understand the influence of multivalency for these epitopes.

In addition to the CFG glycan array, we analyzed Acm-JRL on the Semiotik glycan array, which provides also mammalian glycans but furthermore presents a large variety of other glycans, mainly from bacterial species (figure 7). This array contains a plethora of glycans, e.g. ranging from very simple mannosides to complex bacterial O-antigens ($\Sigma = 610$). Although Mannopentaose (Semiotik glycan ID (SGID) **454**) and Man α 1-6 (mannan, SGID **3002**) could be confirmed as a ligand for Acm-JRL, the smaller mannotriose (SGID **258**) showed no binding, arguably due to a short linker length (Sp4) preventing accessibility by the protein. In contrast to the CFG glycan array, a multivalent α -glucoside is present on the Semiotik chip (SGID **2208**) and was well recognised by the lectin. This underlines again the affinity of Acm-JRL towards α -glucosides. Interestingly, two rather exotic structures were bound: -8(D-Ala1-7)Leg5Aca2-4GlcA β 1-3GlcNAc β 1- (SGID **1225**, *E. coli* O161) and -3GalNAc β 1-4(L-6dTal α 1-3)Man α 1-3L-6dTal α 1- (SGID **1502**, *A. hydrophila* O34deAc). However, it has to be noted, that SGID **1502** shows a nonlinear dose-response which asks for orthogonal analysis.

3.5.2.3. Development of a competitive binding assay for Acm-JRL

Glycan arrays provide valuable insight into carbohydrate specificity at high throughput. For commercially available glycan arrays, unnatural or uncommon carbohydrates are usually not available. Further, quantitative binding analysis is not possible. Therefore, a solution phase competitive binding assay based on fluorescence polarisation was developed in analogy to our previous work.^[28, 94, 174] Fluorescein labelled α -D-mannoside **1** was titrated with Acm-JRL. A binding affinity of $K_d = 58.9 \pm 5.9 \mu\text{M}$ was quantified (figure 8). The high binding affinity towards this α -mannoside was surprising, compared to the lectin's rather low affinity towards Man α 1-3Man ($K_d = 2.4 \text{ mM}$, determined by ITC^[166]). Interestingly, such a discrepancy between the carbohydrate alone and its fluorophore labeled derivative was already observed for α -galactosides and PIIA ($K_d = 62.7 \pm 3.8 \mu\text{M}$ and $K_d 520 \pm 70 \mu\text{M}$, for FITC- α -D-Gal and Me- α -D-Gal, respectively).^[175]

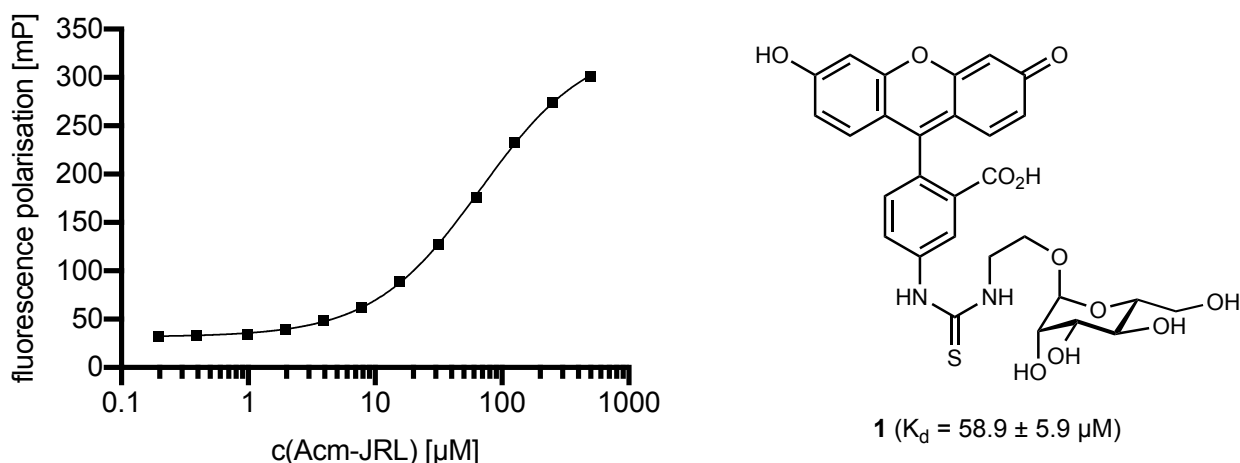


Figure 8. Development of a fluorescence polarisation-based binding assay against Acm-JRL. K_d of mannose-based fluorescent ligand **1** on Acm-JRL was determined from a four-parameter fit to the data points obtained from direct titration. Dissociation constant and standard deviations were obtained from three independent experiments with triplicates on plates.

This system was then used to screen several carbohydrates in competitive binding assays. Next to the glycan hits (D-mannose and D-glucose) and two non-recognised epitopes (D-galactose and L-fucose) from the previous glycan arrays, other plant carbohydrates like L-rhamnose (Rha), D-xylose (Xyl) and D-arabinose (Ara) were tested (figure 9). First, single concentration inhibition assays again confirmed the affinity of Acm-

JRL towards α -mannosides and α -glucosides (figure 9A). Additionally, glucosamines and *N*-Acetyl-glucosamines were confirmed as ligands. In accordance with literature and the glycan array results, none of the other tested carbohydrates were recognised.

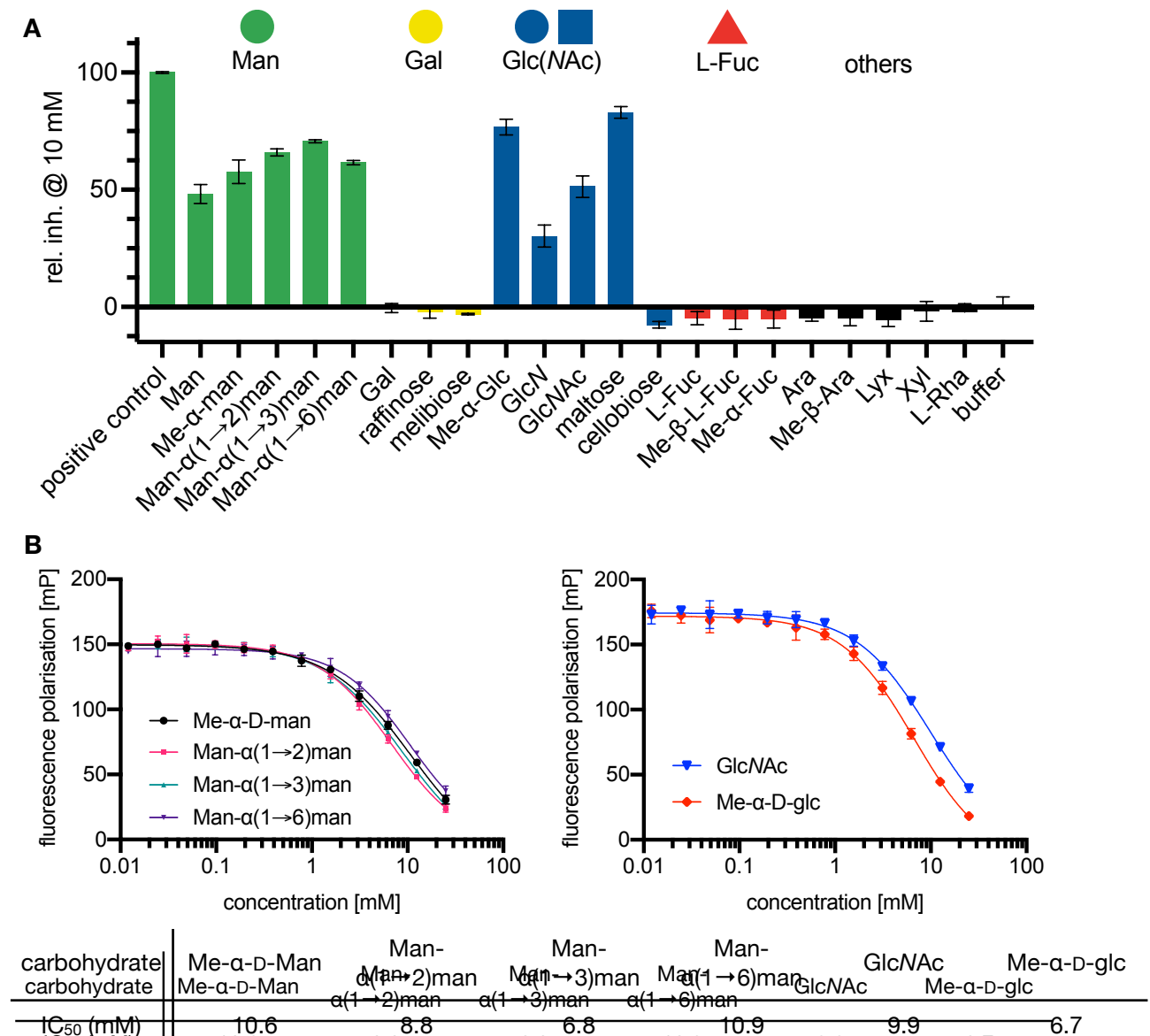


Figure 9. Carbohydrate ligand screening of Acm-JRL based on a reporter ligand displacement assay: **A** Single-point binding assay of Acm-JRL against a carbohydrate panel. Mannosides and glucosides could be confirmed as ligands. Fluorescence polarisation at 50 mM Man- α (1 \rightarrow 2)Man (positive control) was defined as 100% inhibition. One titration of triplicates on one plate is shown for each carbohydrate. **B** Dose-response curves of Acm-JRL with differently linked mannosides (left) or Glc(NAc) together with preliminary corresponding IC₅₀ values. Data is shown as mean \pm s.d. from three technical triplicates on plate. Both experiments were only performed once with technical triplicates.

In order to evaluate the influence of the glycosidic linkage ($\alpha 1 \rightarrow 2$ vs $\alpha 1 \rightarrow 3$ vs $\alpha 1 \rightarrow 6$) of the oligomannosides, a dose-response titration was performed. Only very subtle differences could be observed (figure 9), with Mana1 \rightarrow 3Man having the highest affinity. Comparing the glycan array results with this finding, could explain why the mannopentaose glycan was preferentially recognised over other bis-(Mana1 \rightarrow 2man)-presenting epitopes (e.g. CFG-GID **208**). Interestingly, Me- α -D-glucose showed higher affinity towards Acm-JRL than the mannosides. However, this experiment was only carried out once so far and has to be repeated in the future.

3.5.3. Conclusion and Outlook

Pineapple (*Ananas comosus*) lectin Acm-JRL was isolated from bromelain powder by affinity chromatography and characterised by mass spectrometry, differential scanning fluorimetry and dynamic light scattering. The lectin's ligand specificity was further explored by carbohydrate glycan array analysis using two complimentary arrays. The data supported the previously reported preference towards mannopentaose. A solution phase binding assay was then developed and various carbohydrates were screened and their inhibition of AcmJRL was quantified. The confirmed mannose-specificity of AcmJRL with preference for high mannose structures may serve as a scavenging agent for SARS-CoV2 viruses, whose major surface protein, the spike, was shown to be highly glycosylated carrying a high mannose fur^[176].

In fact, SPR experiments run by Sebastian Adam and Jan Dastbaz at MINS/HIPS showed mannose-dependent binding of SARS-CoV2 spike protein by Acm-JRL (*manuscript in preparation*, data not shown). In future experiments, the therapeutic potential of bromelain and Acm-JRL will be further explored.

4. Global Summary and Future Perspectives

The rising spread of drug-resistant *P. aeruginosa* infections calls for the development of new antibiotic drugs. More precisely, research towards novel antibacterial modes of actions and innovative strategies are of outmost importance. Biofilm formation is a serious resistance mechanism during chronic *P. aeruginosa* infections. However, only few biofilm-specific therapeutic approaches are currently available, e.g. LecA/LecB inhibitors or quorum sensing inhibitors. Targeted antibiotic drug delivery is an exciting approach with high therapeutic potential. Aim of this thesis was therefore the design and synthesis of *P. aeruginosa* biofilm-targeted antibiotic conjugates.

In the first project, uncleavable carbohydrate conjugates of ciprofloxacin and tobramycin were used as a proof of concept study. Previously published small molecule lectin inhibitors were used as biofilm-targeted probes. The modular design, based on copper-catalysed click chemistry, resulted in straight forward synthesis of a small conjugate library with varying linker lengths. Flat SAR of both LecA and LecB allowed retained binding affinity for all conjugates. While lectin-targeted conjugates of tobramycin showed no antibiotic activity against *E. coli* and *S. carnosus*, ciprofloxacin-based conjugates revealed a structure-activity relationship against *P. aeruginosa* (figure 1).

In general, conjugates with smaller linker lengths showed higher antibiotic activity compared to bigger conjugates, possibly linked to a lower bacterial bioavailability.

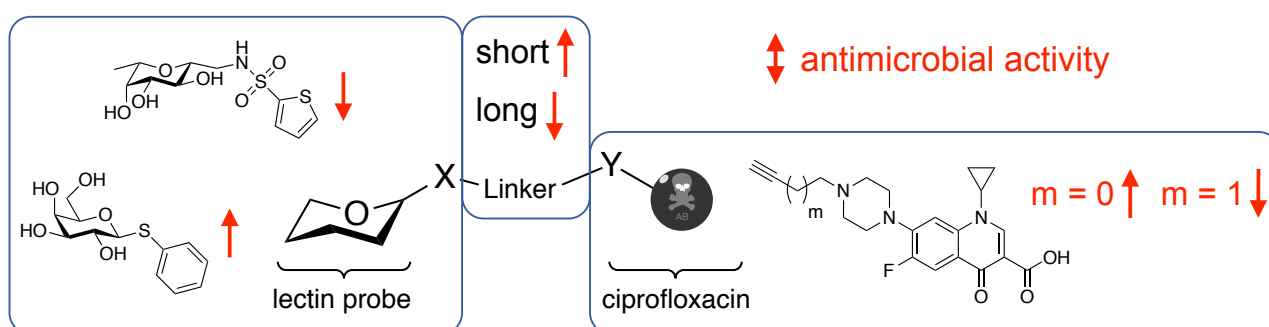


Figure 1. SAR of uncleavable *P. aeruginosa* biofilm-targeted ciprofloxacin conjugates. Red arrow depicts influence on antibiotic activity (up = higher antimicrobial activity, down = lower antimicrobial activity).

Next to the total linker length, an influence of the specific linker on the side attached to ciprofloxacin was observed. Methylene linkers always resulted in higher antibiotic activity compared to slightly longer ethylene linkers. As this linker defines the distance between the electron-withdrawing triazole and the basic nitrogen of piperazine, an influence on its

basicity is likely. The piperazine unit of ciprofloxacin is crucial for strain selectivity and could play a crucial role in diffusion through outer membrane porins. Future uncleavable conjugates of ciprofloxacin should use a different molecular handle than piperazine nitrogen in order to retain its physicochemical properties. For example, introduction of an additional alkyl amine on piperazine C3 could be a promising alternative.

A third observation was the fact that galactose-based conjugates showed higher antibiotic activity than their C-glycoside-based analogues. Active uptake mechanisms of galactose-based conjugates e.g. as a carbon source seem unlikely due to the presence of nutrient rich medium (LB) during the experiment. Low nutrient conditions, e.g. with minimal medium M63, or competition experiments under high galactose concentrations could provide clarity.

Decreased antibiotic activity can be counterbalanced by increased local drug concentration, i.e. targeted drug delivery. A novel assay based on HPLC-MS/MS analytics was developed to determine *P. aeruginosa* biofilm accumulation *in vitro*. Indeed, two representative lectin-targeted conjugates showed increased biofilm accumulation compared to unmodified ciprofloxacin. Although the assay has to be improved towards lower standard deviations, it could serve as an important tool to find biofilm-accumulating antibiotics. Eventually, this could yield a new set of rules for antibiotic drug design, comparable to the eNTRY-rules postulated by Hergenrother and co-workers.^[177]

Gyrase-inhibition was confirmed as antimicrobial mode of action for three representative conjugates, however with less inhibitory activity compared to ciprofloxacin and propargyl-ciprofloxacin. Notably, the conjugates showed reduced cytotoxicity against HEK293 cells *in vitro*. In summary, first generation *P. aeruginosa* biofilm-targeted were successfully developed based on ciprofloxacin as a cargo. With their increased biofilm accumulation and reduced cytotoxicity, these conjugates have the potential to reduce therapeutic side effects and break antimicrobial resistance.

Uncleavable drug-conjugates benefit from their simplicity in regards of chemical synthesis and metabolic stability. On the other side, permanent linkage asks for very careful drug design, according to structure-activity relationships of the single components. Further, they share high molecular weight, limiting their antimicrobial bioavailability (porin permeation^[81, 178]). Future compound generations could circumvent low cell permeability by conjugation to periplasmatic or extracellular antibiotics like β -lactams and colistin. Alternatively, exploitation of active uptake mechanisms, e.g. by additional conjugation to

siderophores could result in trifunctional antibiotic conjugates with high bacterial bioavailability.

In the second part of this work, the uncleavable linker of the first chapter was substituted with a cleavable peptide linker. This yielded the first *P. aeruginosa* biofilm-targeted antimicrobial prodrugs. Comparable to the approach of O’Leary *et al.*^[179], the linker was designed as a substrate of *P. aeruginosa* proteases, e.g. LasB. In contrast to the first project, a small variety of fluoroquinolones was used as antibiotic cargo in order to optimise drug release and antimicrobial activity.

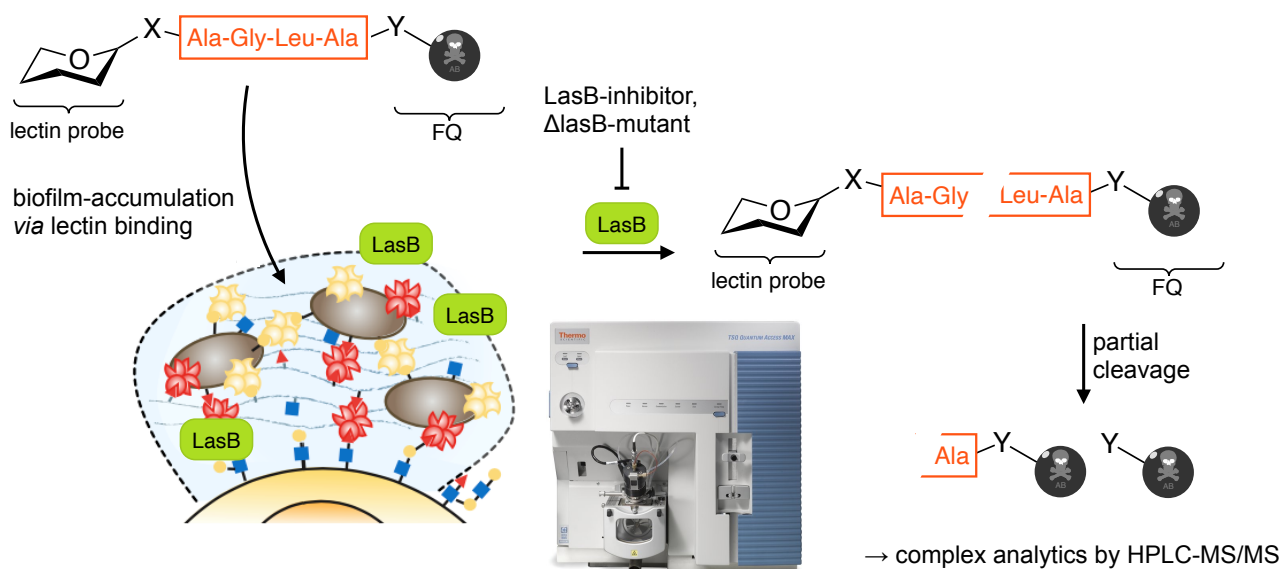


Figure 2. *In vitro P. aeruginosa* biofilm accumulation experiments with lectin-targeted prodrugs experience high analytical complexity: four different molecules, i.e. prodrug, LasB cleavage product (Leu-Ala-FQ) and further cleavage products (Ala-FQ and FQ) have to be detected simultaneously. Reduction of LasB-activity by addition of a LasB-inhibitor or usage of a LasB-knockout strain increases concentration of intact prodrug and simplifies analytics.

As described for uncleavable conjugates, all prodrugs were able to bind their lectin targets *in vitro*. Detailed prodrug activation experiments revealed fast drug release in presence of *P. aeruginosa* culture filtrate and human blood plasma for primary amide-based fluoroquinolone prodrugs. Ciprofloxacin-based prodrugs did not effectively release their antibiotic cargo due to the presence of a secondary amide. Fast releasing prodrugs had excellent antimicrobial activities against *P. aeruginosa in vitro*.

Due to the intrinsic complexity of the lectin-targeted prodrugs, no biofilm accumulation experiments were performed in this project. Further development of the biofilm-

accumulation assay, e.g. by co-incubation with a highly potent LasB-inhibitor could simplify the detection of accumulated prodrug molecules (figure 2). In fact, preliminary cleavage experiments in presence of a LasB-inhibitor show a significantly increased prodrug stability (data not shown). Alternatively, a LasB-knockout mutant strain of *P. aeruginosa* could be used (figure 2). The influence of genetically absent LasB on biofilm formation is not yet fully understood. However, it is very likely that biofilm accumulation observed for uncleavable conjugates (chapter 3.1) can be transferred to these prodrugs, as they share the same targeting units. Additionally, lectin-dependent *P. aeruginosa* biofilm staining experiments based on comparable lectin probes conjugated to fluorescent dyes gave similar results (Eva Zahorska and Lisa Denig, unpublished).

After extensive characterisation *in vitro*, early *in vivo* studies have to be performed in the near future. First, pharmacokinetic properties like drug distribution, metabolism and elimination are of particular interest. The high molecular weight of the prodrugs asks for systemic application via injection. Although the lectin-targeted prodrugs proved to be stable under *in vitro* conditions, strongly increased complexity of *in vivo* models can yield unexpected results. Especially the peptide linker could be a substrate of endopeptidases that were not present in the reported early ADMET-studies. In particular, matrix metalloproteinases (MMP) like MMP-2 and MMP-3 have a tendency to cleave in front of leucine. In case of fast degradation *in vivo*, the peptide linker has to be optimised towards higher host-derived metabolic stability while keeping its vulnerability against LasB or other *P. aeruginosa* endopeptidases. Possible options would be the introduction of unnatural amino acids (e.g. D- vs L-configured, unusual side chains) or peptide backbone *N*-methylation. Phage display^[180] or cellular libraries of peptide substrates (CLiPS^[181]) are very potent screening techniques with high throughput. With these tools, peptide fragments with high susceptibility against bacterial trigger enzymes (e.g. LasB) can be identified. In a second step, these hit peptides could be screened against human plasma or specific off-target peptidases. MMP-3 is commercially available and could serve as a, however very limited, model system to screen for peptide linkers with improved stability. Due to the traceless prodrug approach, conjugation of other antibiotic molecules is much easier compared to uncleavable conjugates. In fact, we are currently working on lectin-targeted prodrugs of tobramycin. An alternative application of the prodrug concept would be the development of *P. aeruginosa* sensitive fluorescent dyes (figure 3) as diagnostic tools.

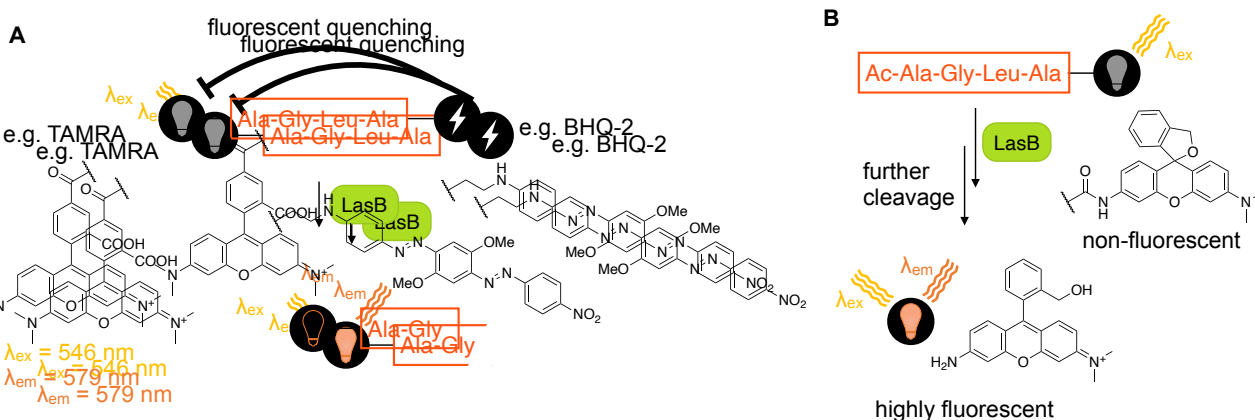


Figure 3. Turn-on fluorescent dyes for *P. aeruginosa* imaging based on enzymatic activation. **A** Fluorescence (e.g. TAMRA) is quenched by fluorescence quencher (e.g. black hole quencher 2, BHQ-2). Spatial segregation by enzymatic cleavage of linker peptide (e.g. LasB) reduces fluorescence quench. **B** Acylated rhodamine dye shows low fluorescence.^[182] Proteolytic digest of signal peptide by LasB and blood plasma proteins releases highly fluorescent dye.

In a follow-up project, monovalent LecA-probes were substituted by a bivalent LecA-inhibitor in order to increase target affinity. In this work, the synthesis of one bivalent antibiotic prodrug was described. This molecule will be further characterised in analogy to the monovalent prodrug series. Additionally, binding affinity will be confirmed by isothermal titration calorimetry.

In order to investigate the biofilm-targeting effect of the conjugates described in this work, visual *P. aeruginosa* biofilm experiments would be of high interest. Our group recently published a biofilm inhibition assay, that evaluated the effect of lectin inhibitors in a multi-well format, monitored by confocal laser scanning microscopy (CLSM). Addition of a dead-live staining protocol could enable us to understand antimicrobial activities of biofilm-targeted antibiotic conjugates. However, the published static biofilm assay has a major disadvantage: Buffer exchange and washing steps are almost impossible as formed biofilm aggregates are easily destroyed. Thus, comparison with highly active parent compound is difficult. For this reason, our group is currently implementing a *P. aeruginosa* biofilm assay under constant medium flow, comparable to the protocol of M \ddot{u} sken *et al.*^[85] Under these conditions, removal of residual, unbound antibiotics is easily possible.

To sum up, I synthesised the first antibiotic conjugates to specifically target *P. aeruginosa* biofilms. Starting with rather simple uncleavable conjugates, molecules were improved by

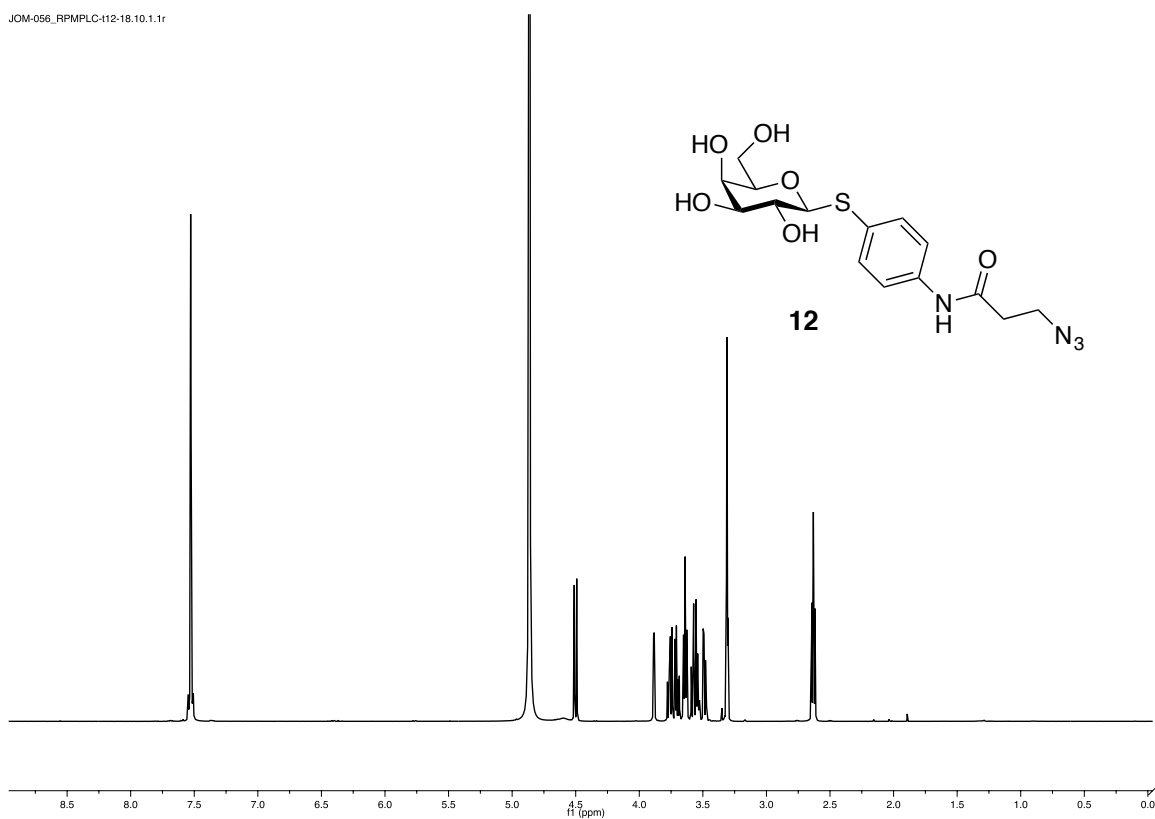
converting them into *P. aeruginosa* sensitive prodrugs. These approaches pave the way towards a new series of antibiotic drugs with novel mode-of-actions and promising properties.

In the last chapter of this thesis, Acm-JRL, a mannose-binding lectin from pineapple (*Ananas comosus*) was isolated from bromelain and further characterised by dynamic light scattering and differential scanning fluorimetry. The lectin was chemically labelled with two different fluorescent dyes. For the first time, ligand specificity towards multivalent mannosides, particularly mannotriose Man α 1-6[Man α 1-3]Man α , was analysed by glycan array analysis. Additionally, I developed a competitive binding assay based on fluorescence polarisation. With this assay in hand, glycan array hits can be validated in the future. The spike protein of SARS-CoV is highly mannosylated and vital for host cell entry. Preliminary SPR studies of Acm-JRL binding to heterologously expressed immobilised spike protein (Jan Dastbaz, Sebastian Adam and Sari Rasheed, manuscript in progress) indeed showed a mannose-dependent binding in the low micro molar range. Cellular infection experiments with SARS-CoV-2 and its simplified model organism hCoV-229E will be performed at Twincore in Hannover to analyse the potential of AcmJRL as an antiviral drug.

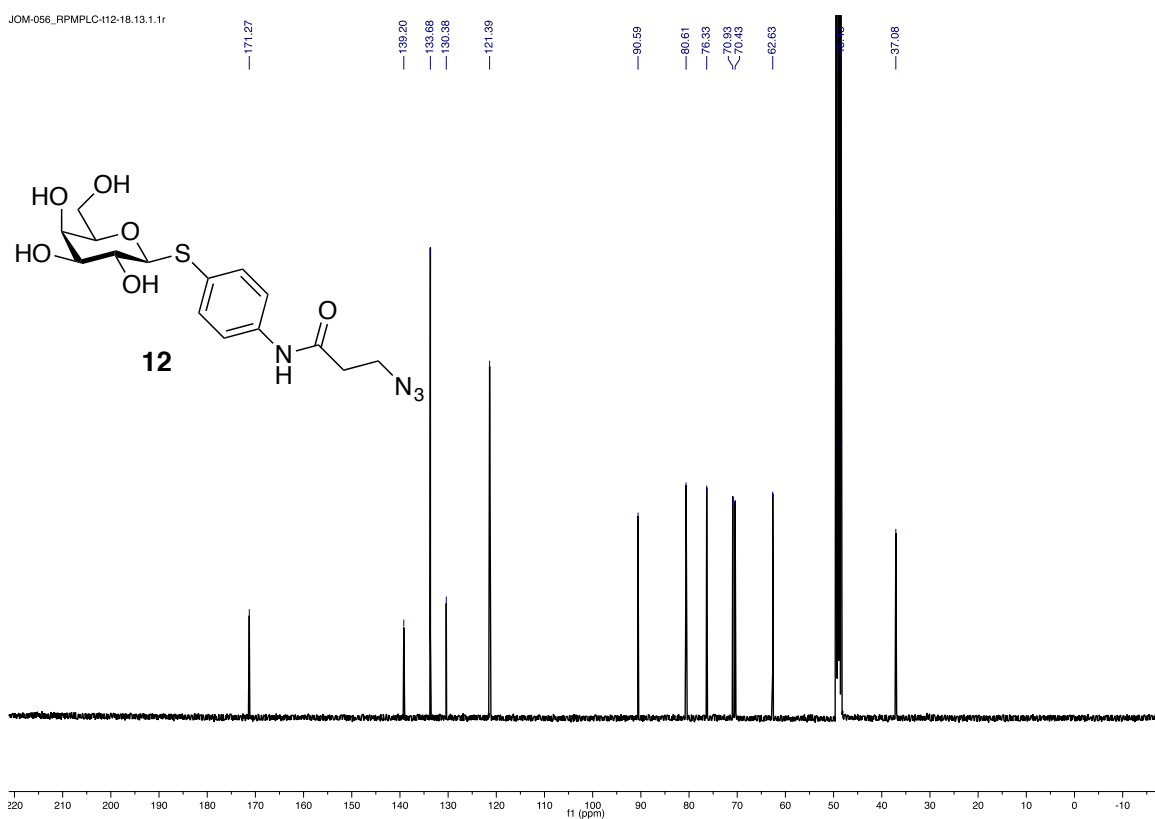
5. Appendix

5.1. Supporting Information for Chapter 3.1

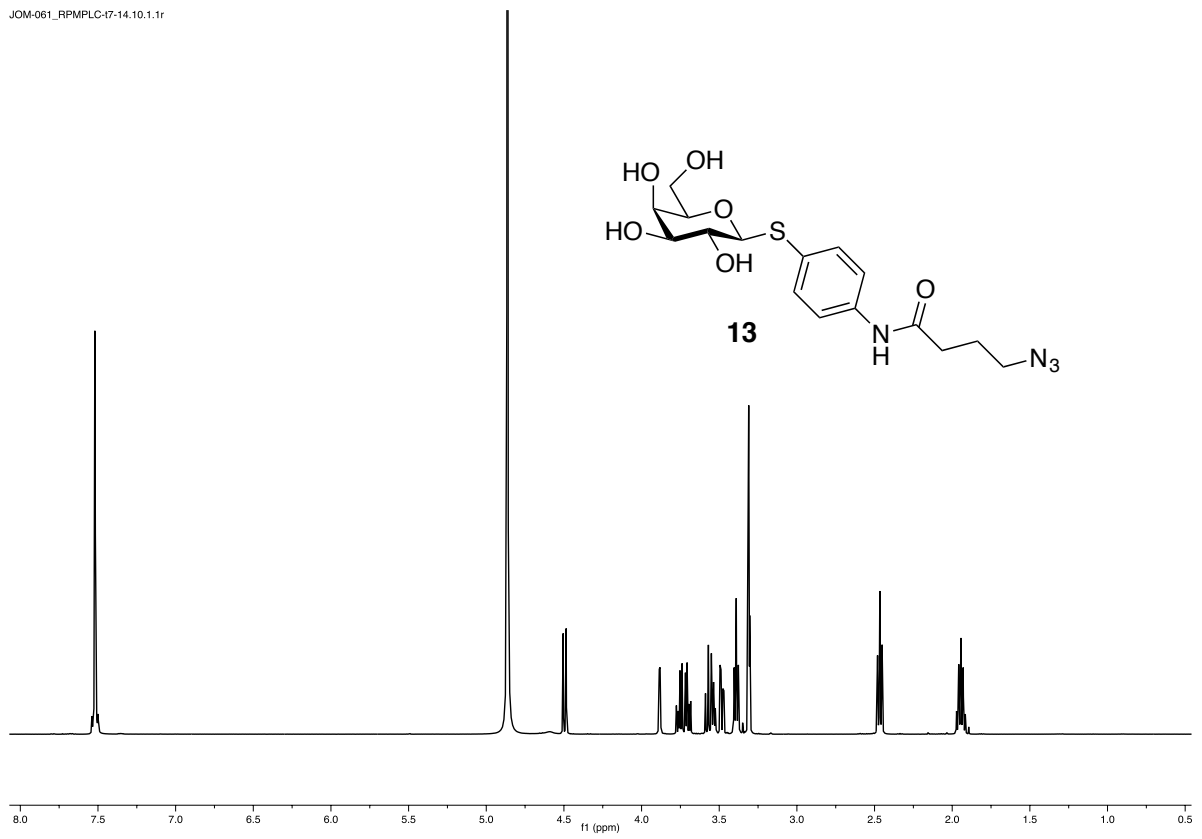
JOM-056_RPMLC-112-18.10.1.1f



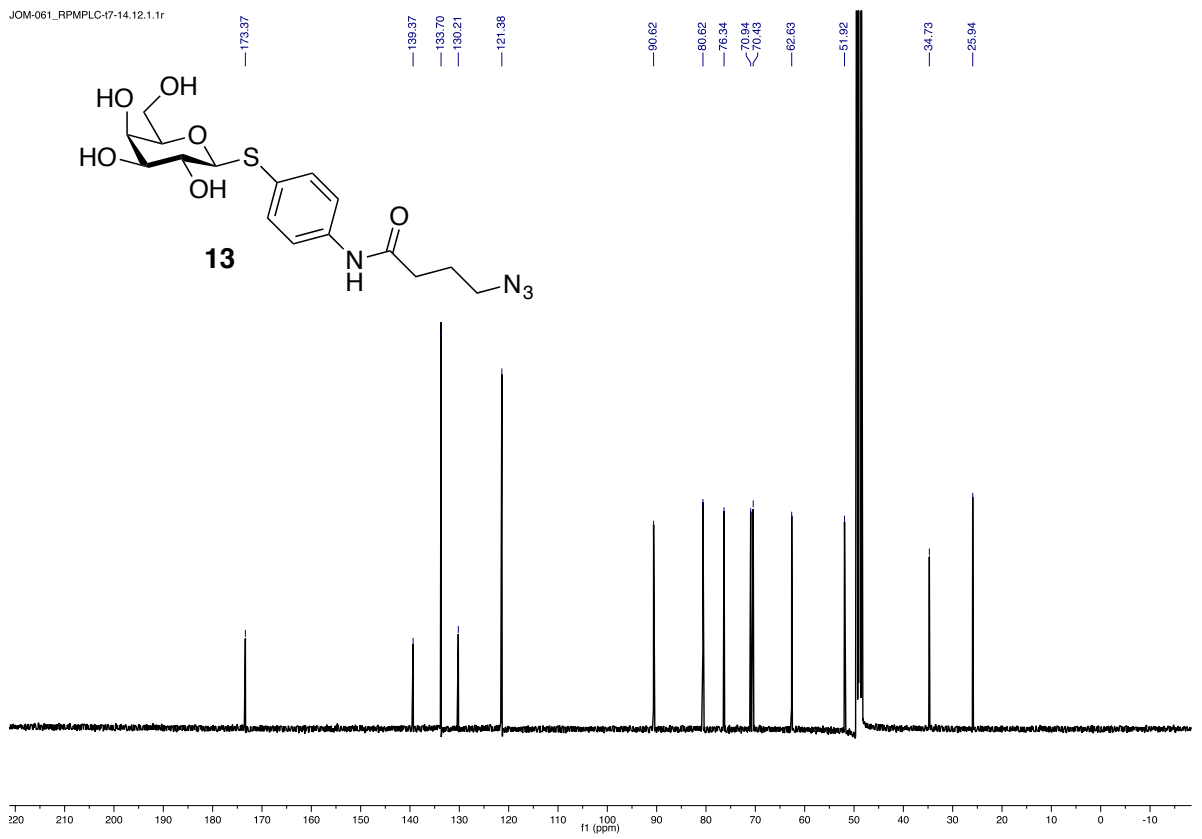
JOM-056_RPMLC-112-18.13.1.1f



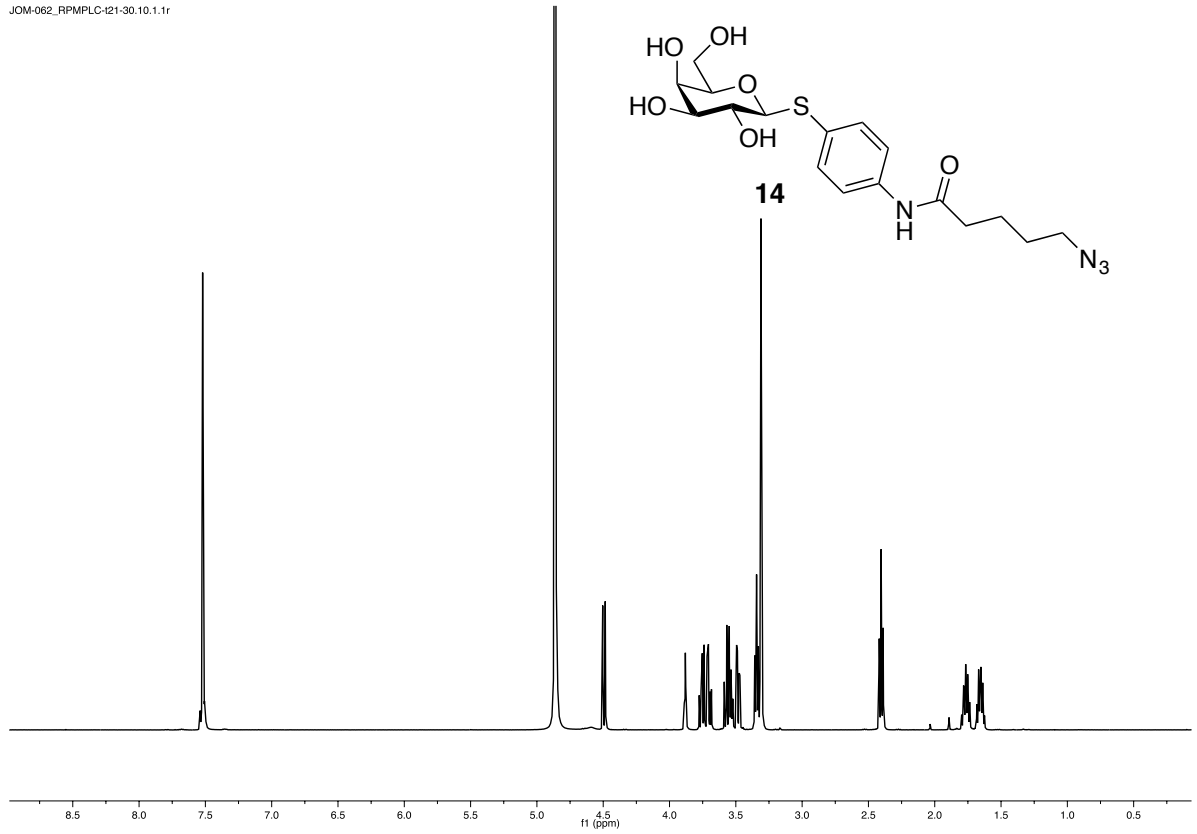
JOM-061_RPMPLC-17-14.10.1.1r



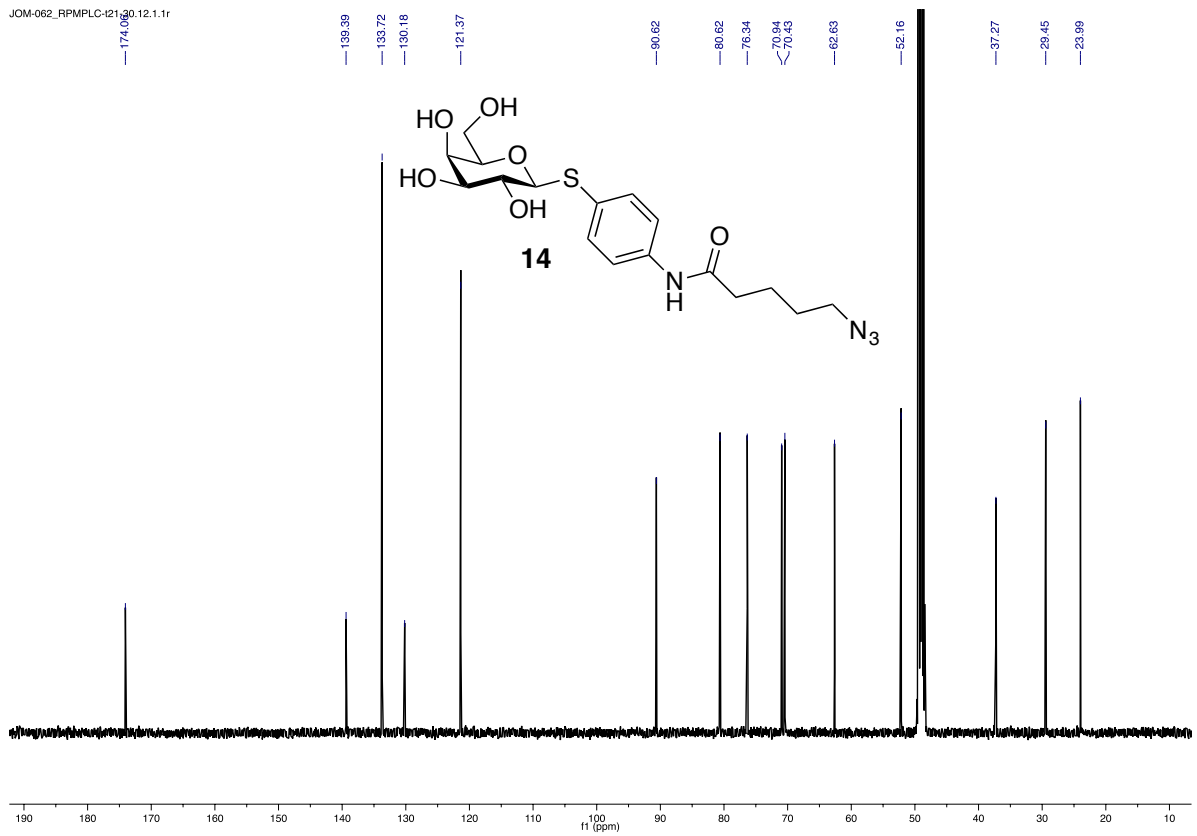
JOM-061_RPMPLC-17-14.12.1.1r

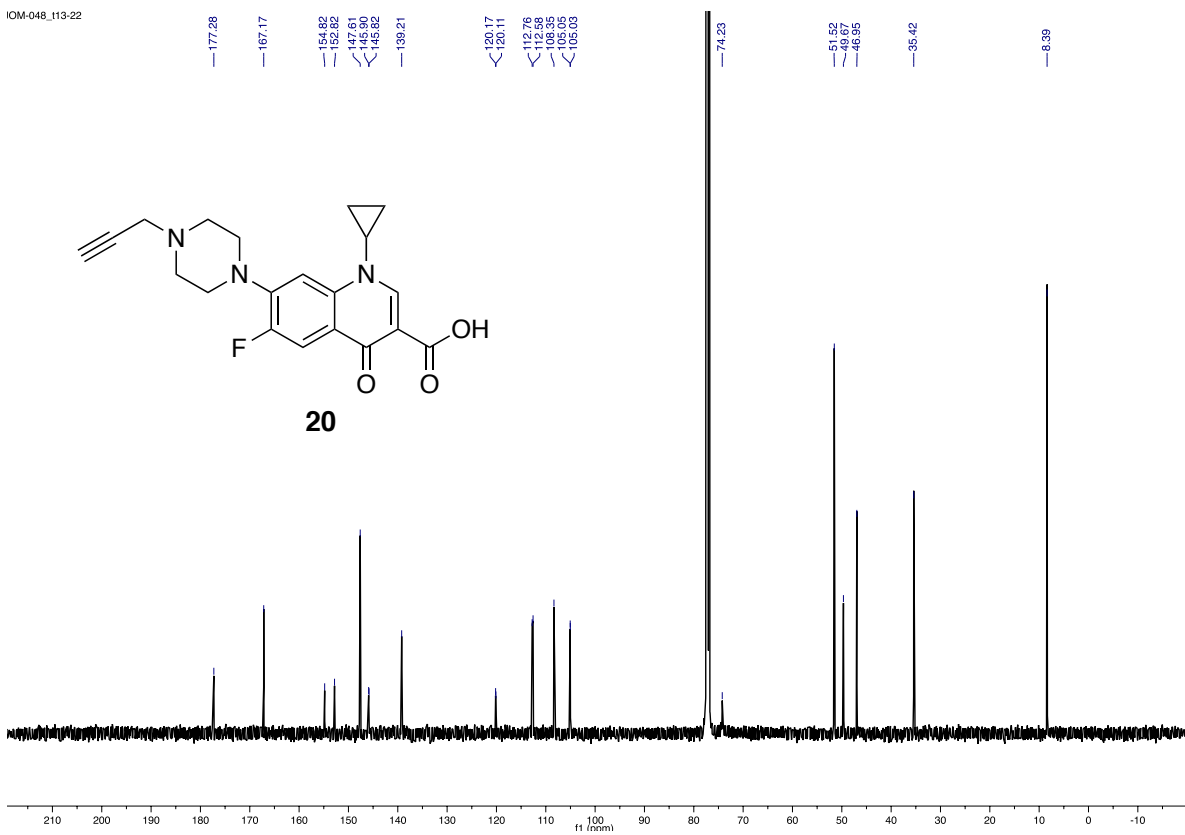
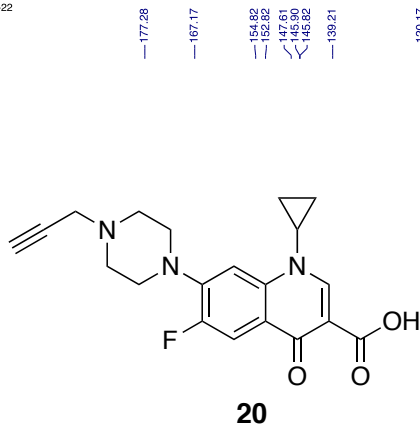
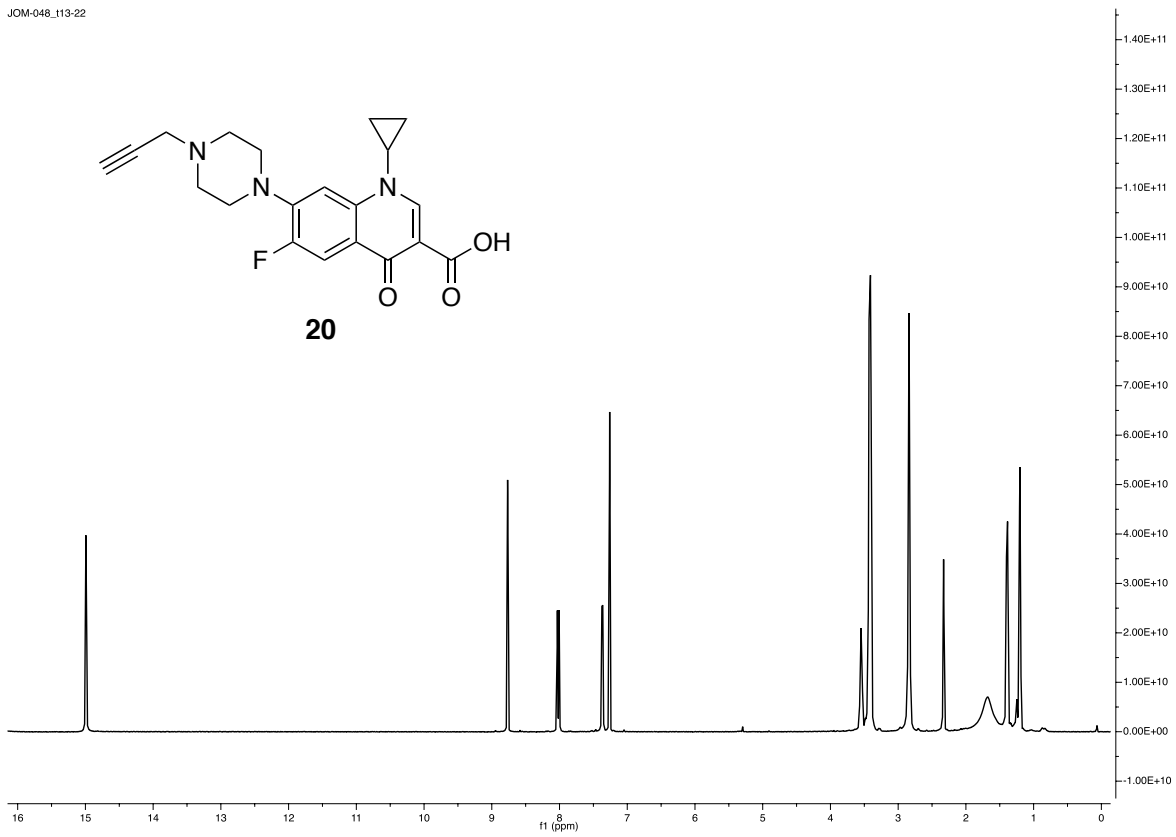
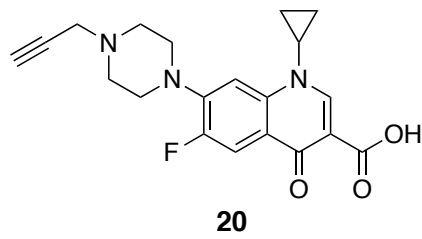


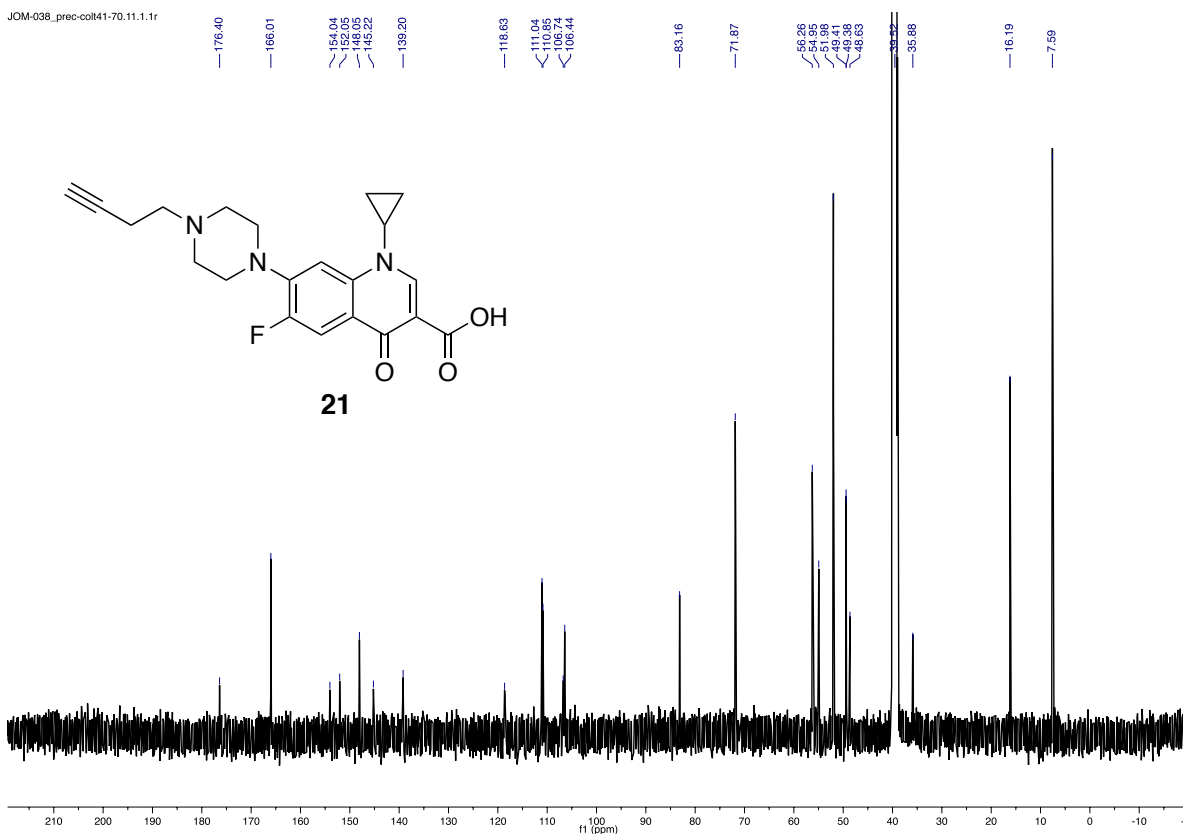
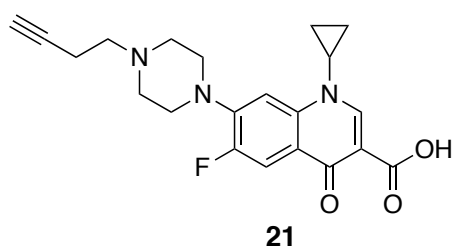
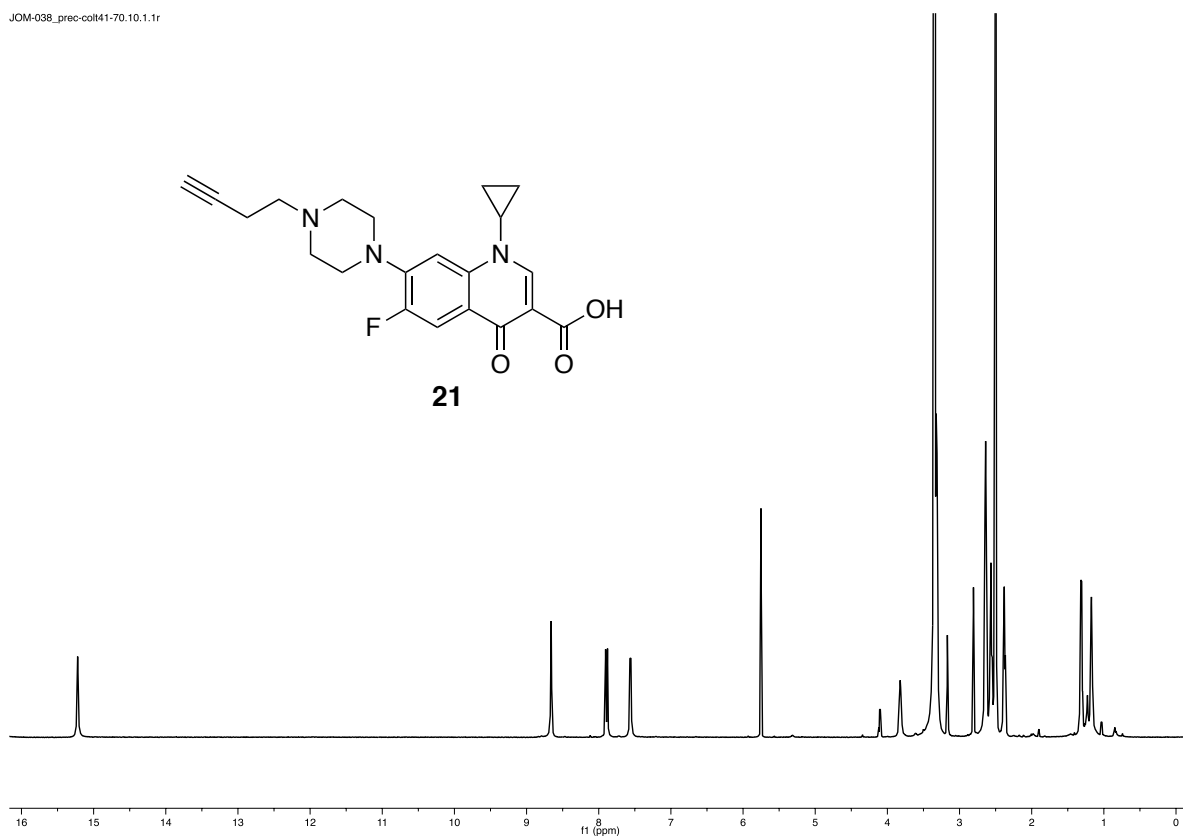
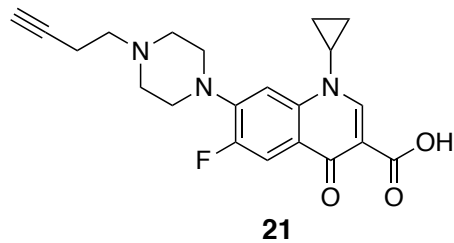
JOM-062_RPMPLC-121-30.10.1.1r



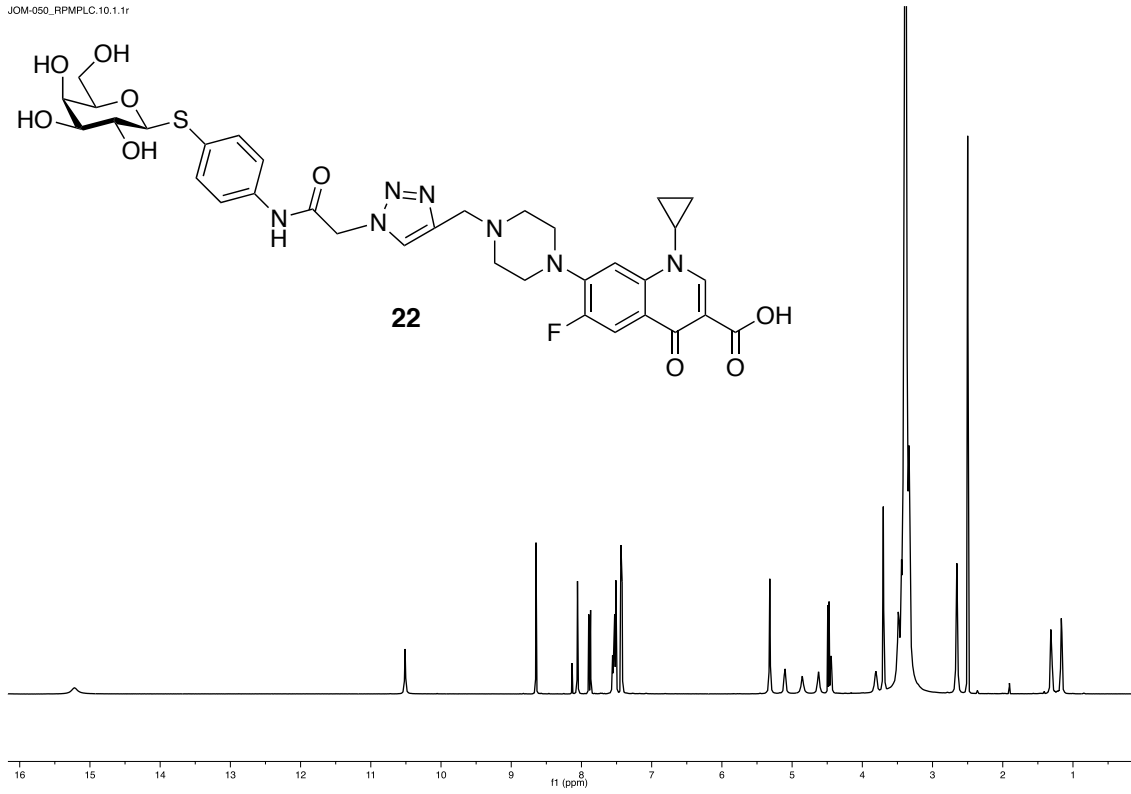
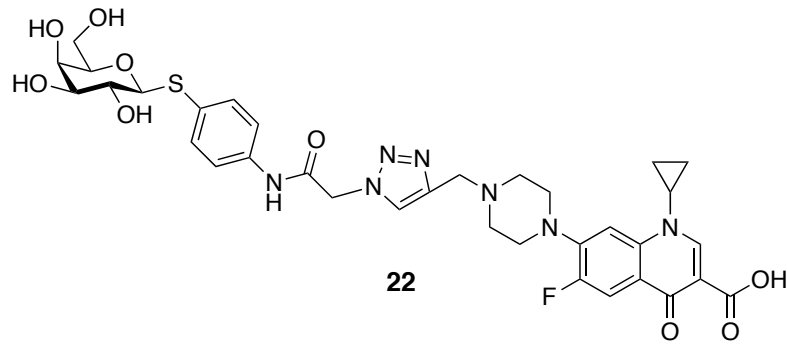
JOM-062_RPMPLC-121-30.12.1.1r



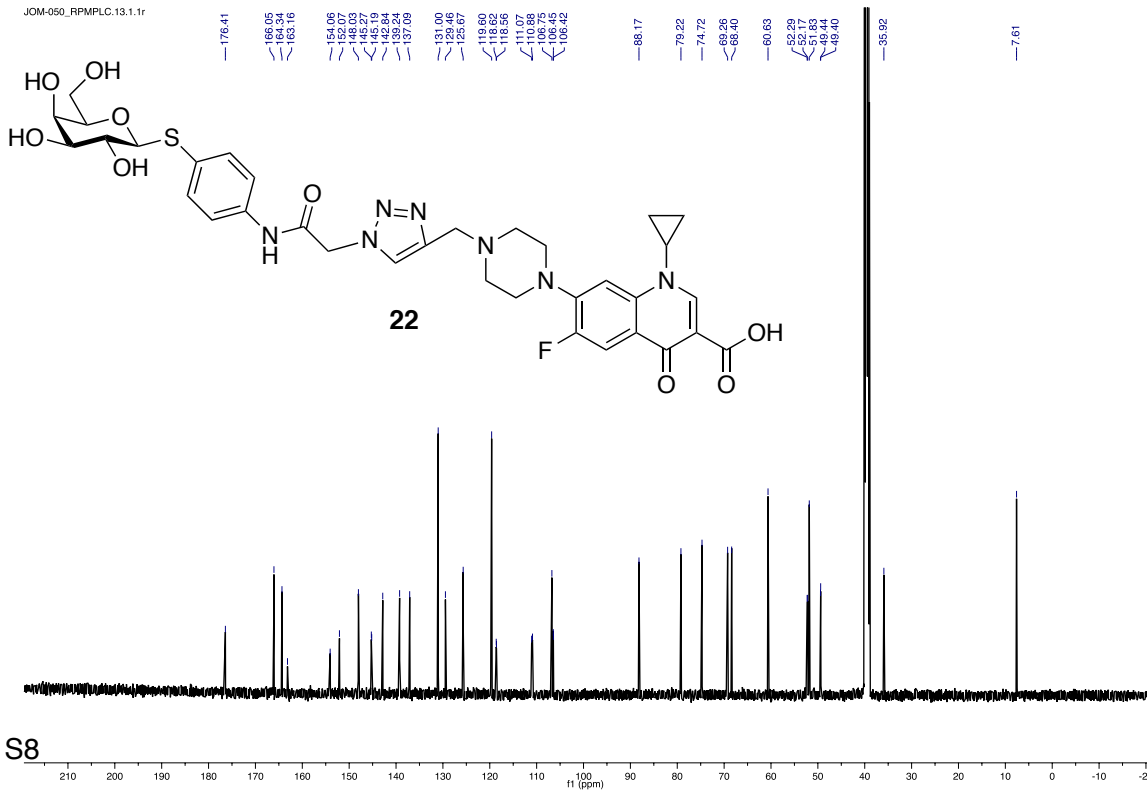
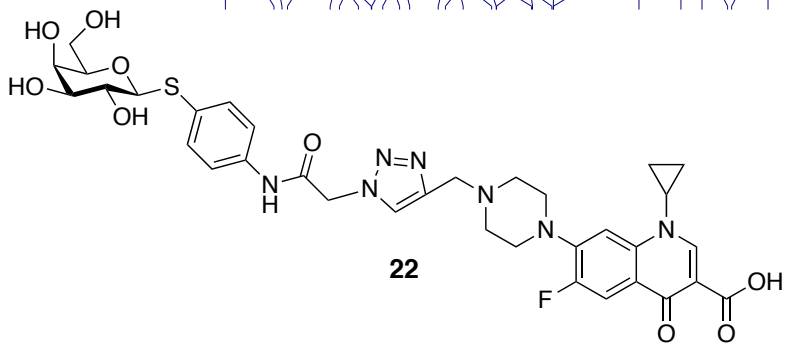




JOM-050_RPMP.LC.10.1.1r

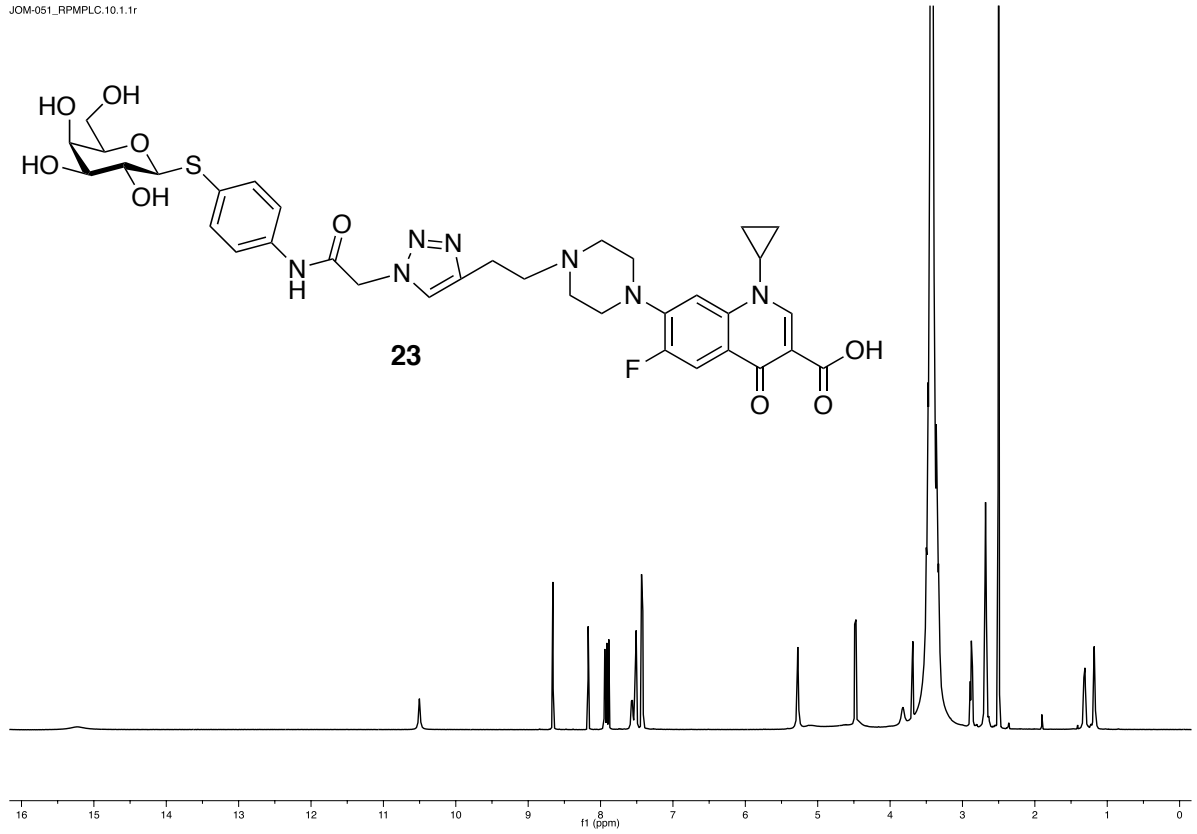


JOM-050_RPMP.LC.13.1.1r

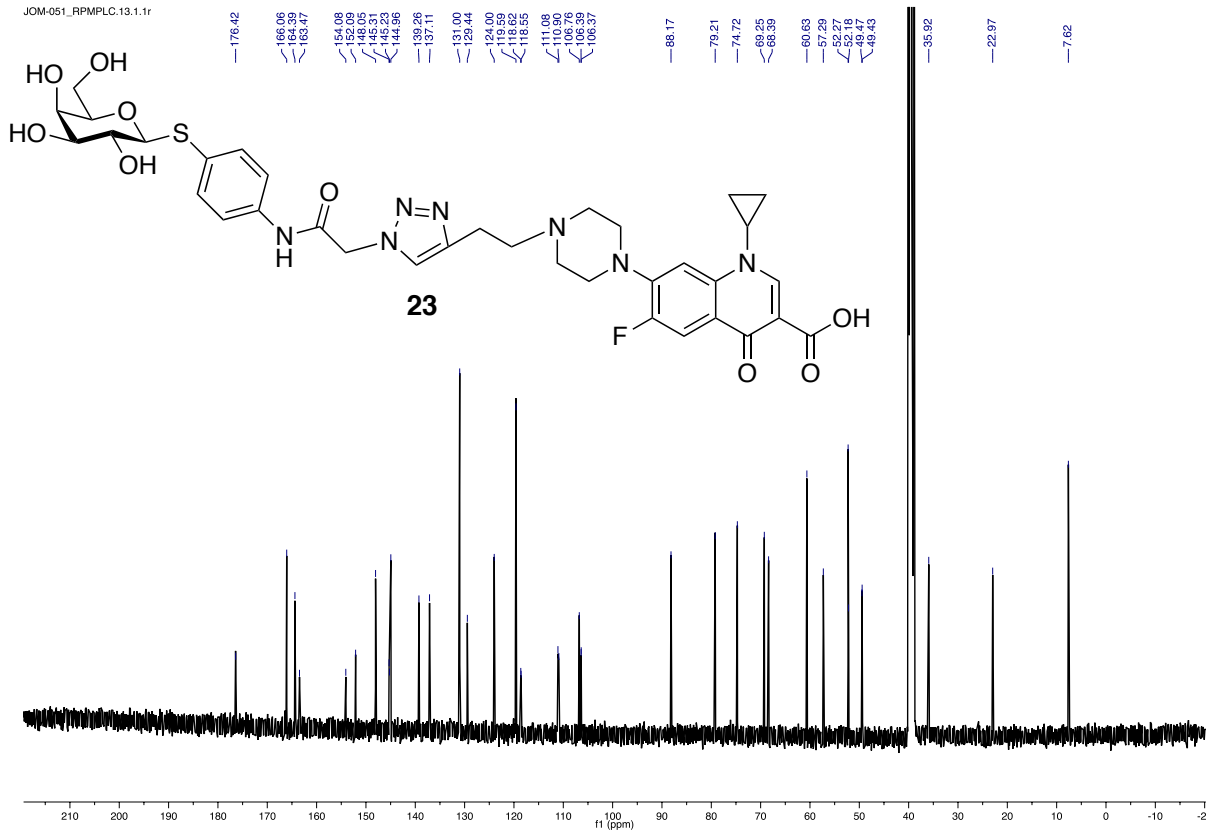


S8

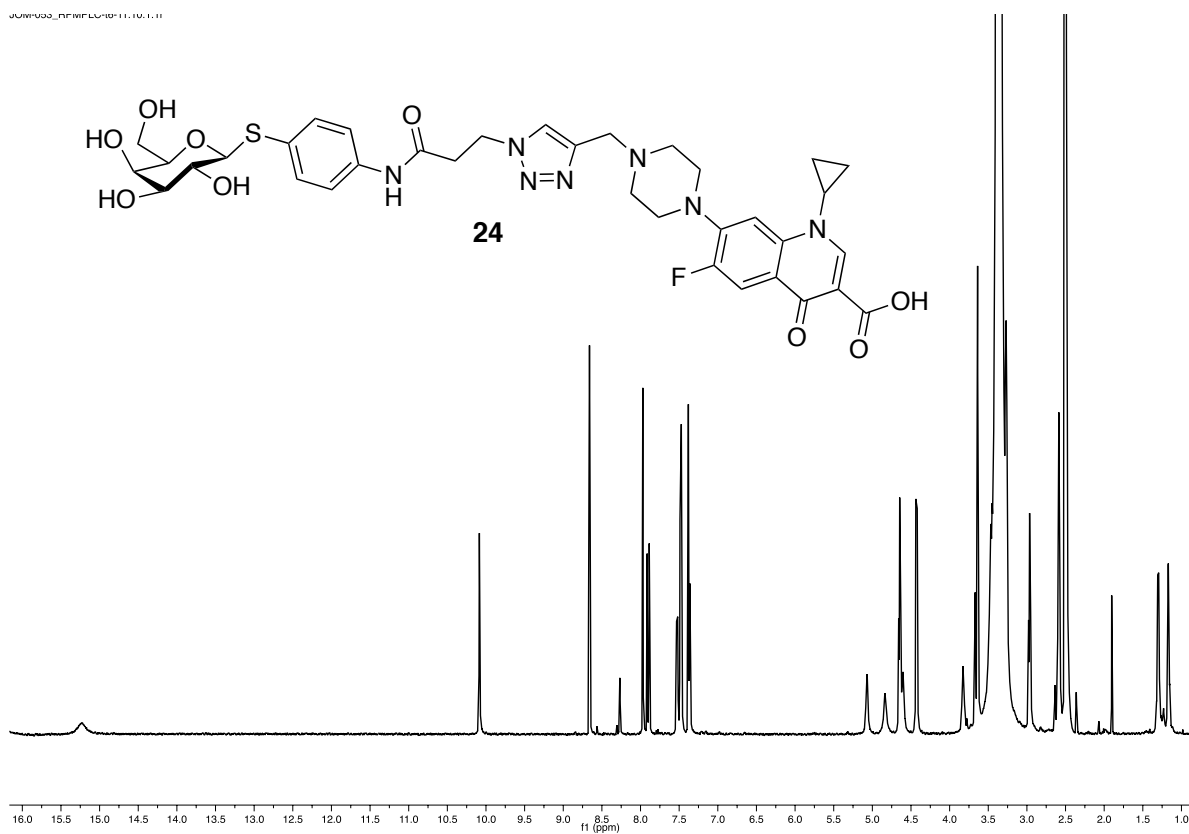
JOM-051_RPMPLC.10.1.1r



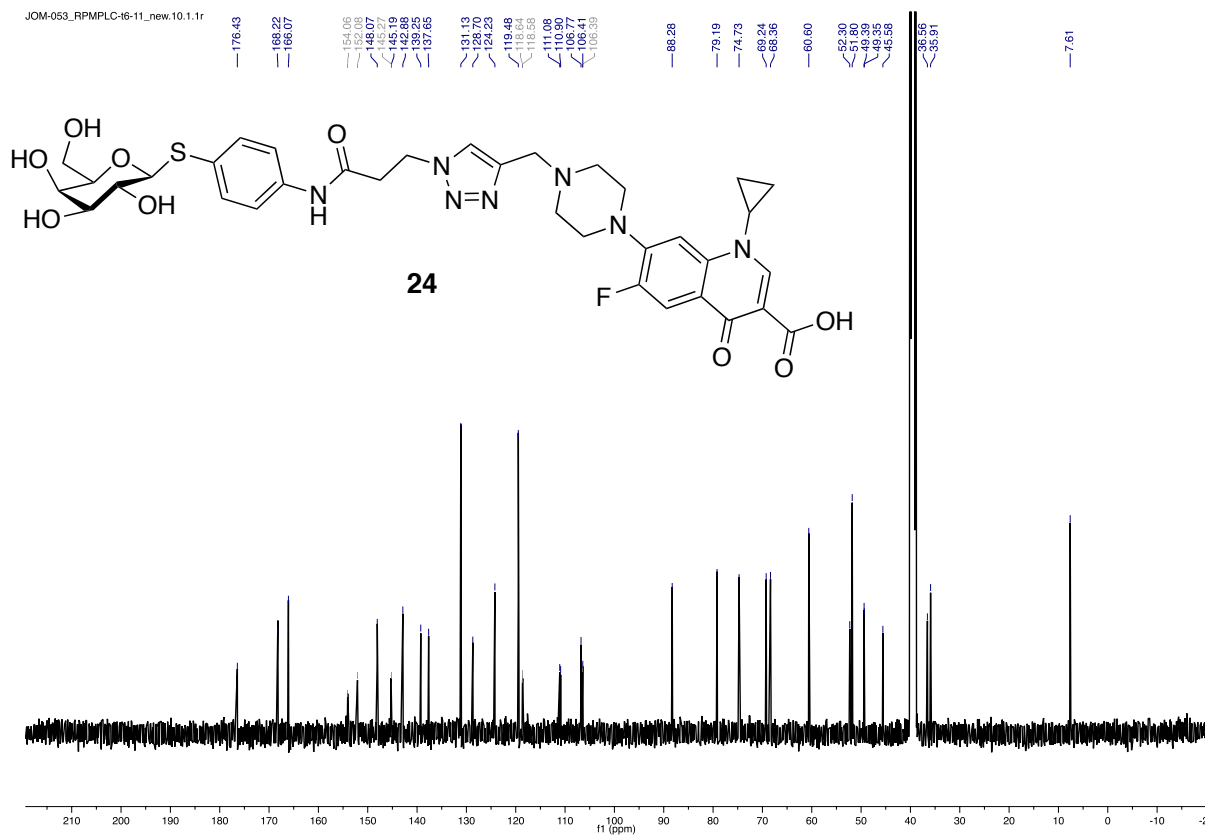
JOM-051_RPMPLC.13.1.1r



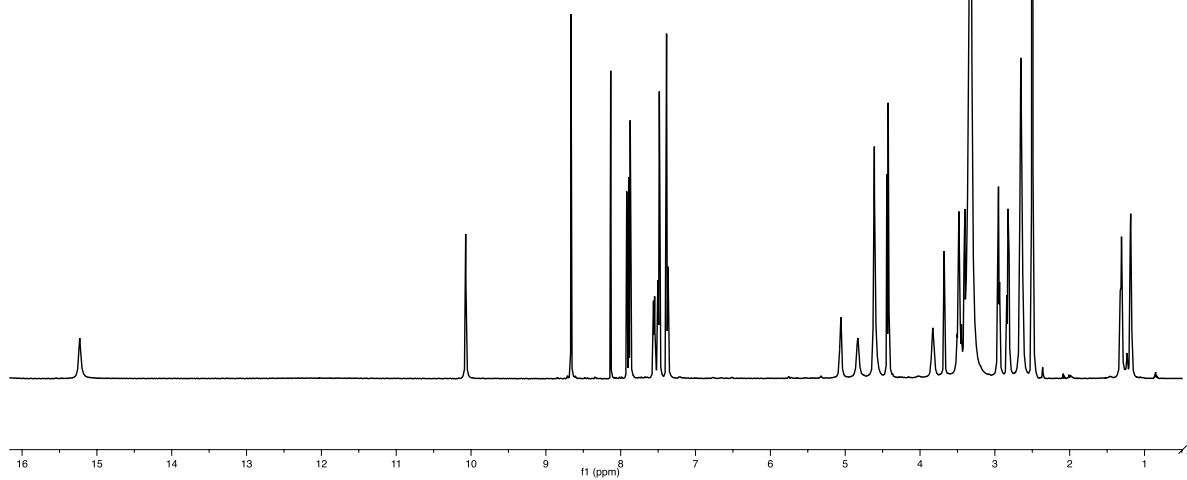
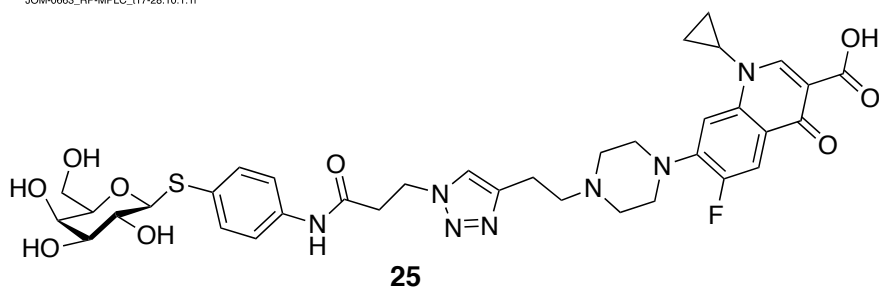
JOM-053_RPMPLC-16-11_10.1.11



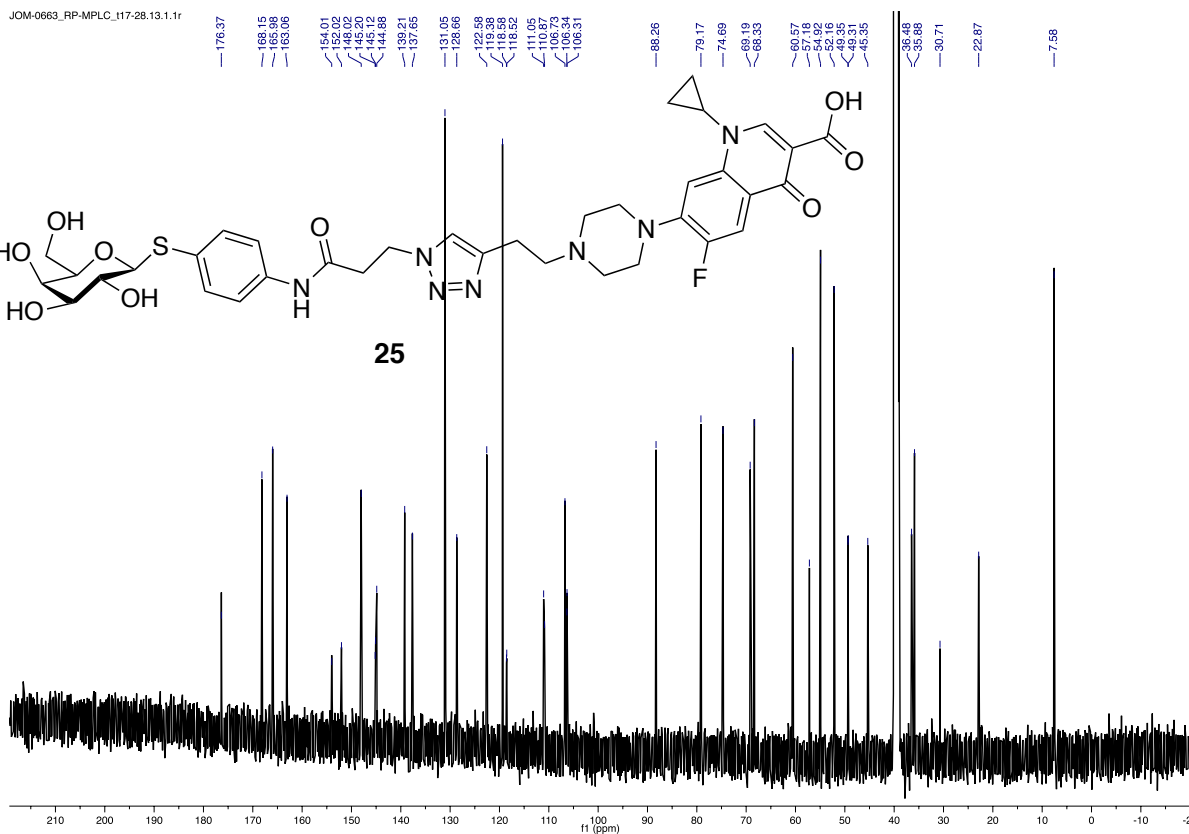
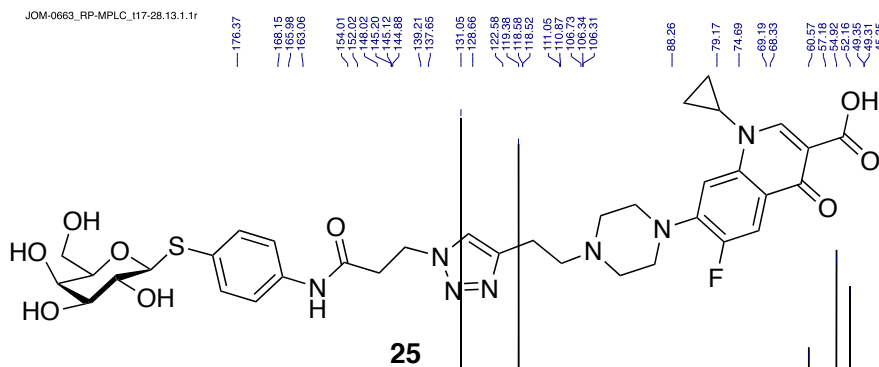
JOM-053_RPMPLC-16-11_new.10.1.1r



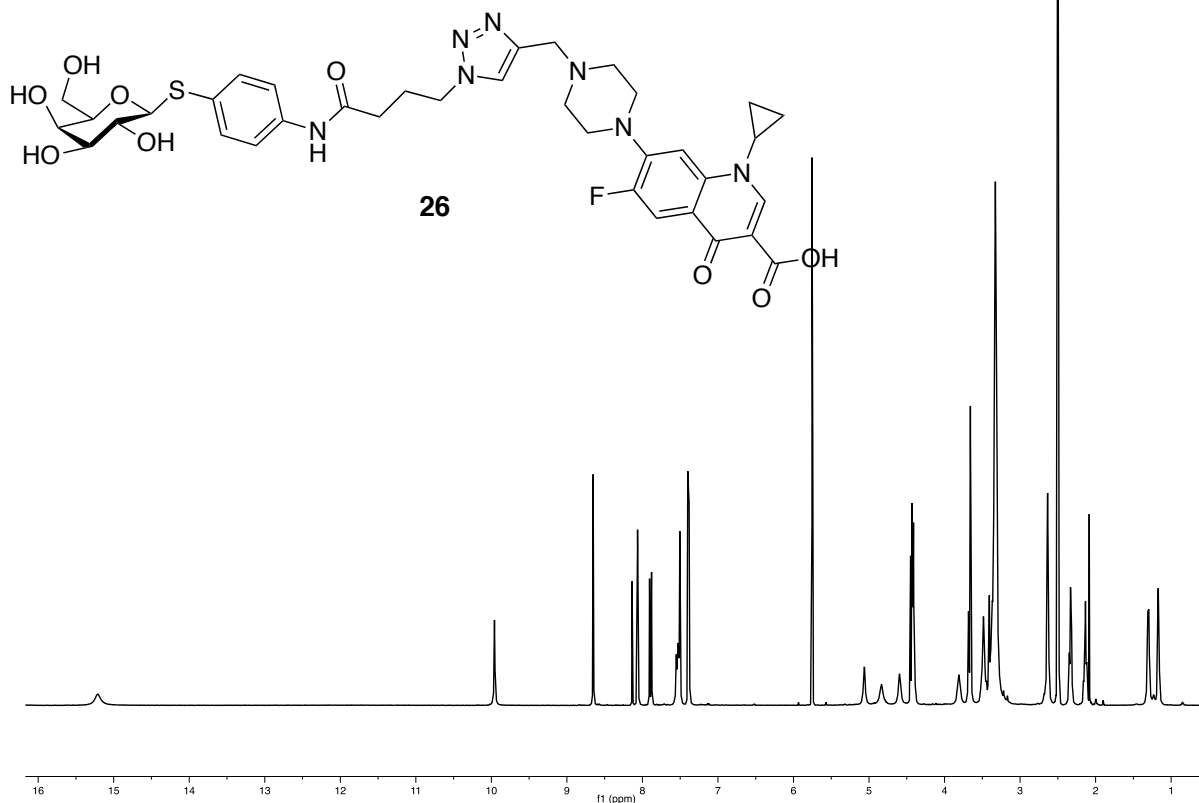
JOM-0663_RP-MPLC_117-28.10.1.1r



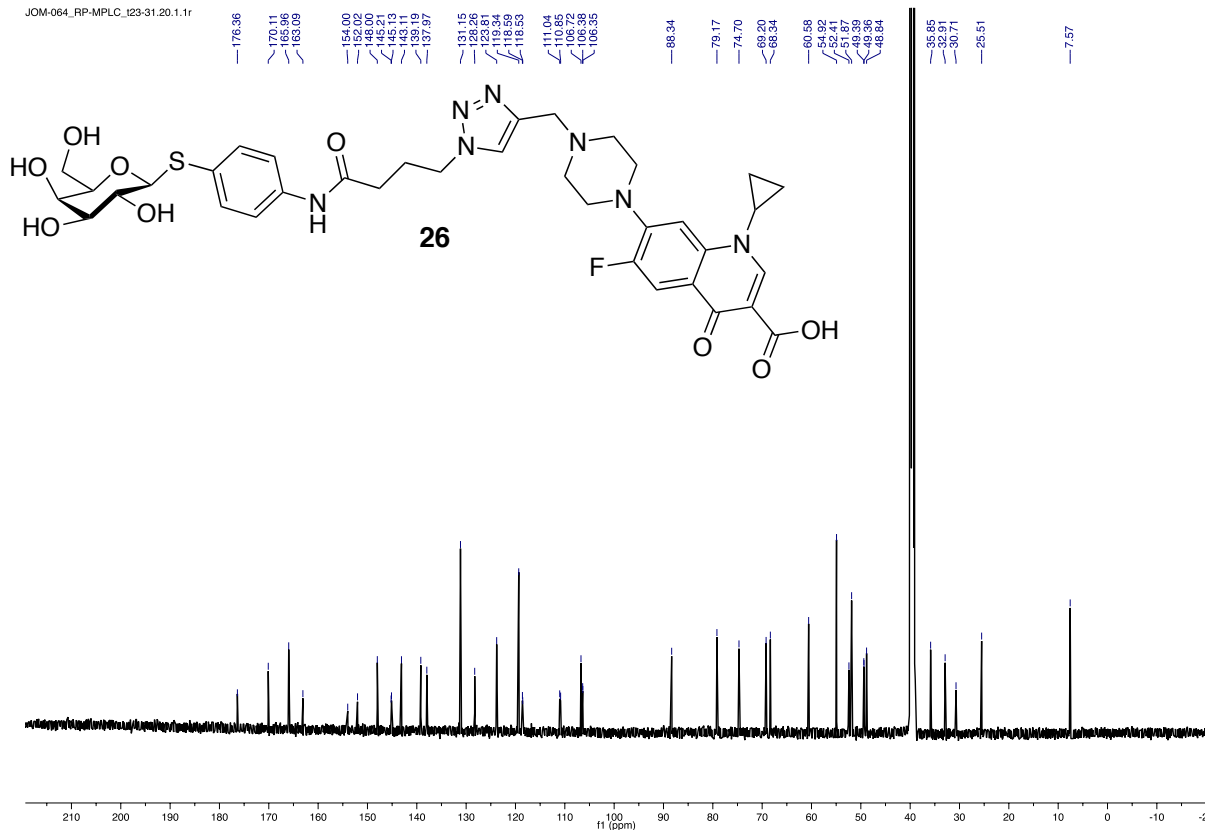
JOM-0663_RP-MPLC_117-28.13.1.1r



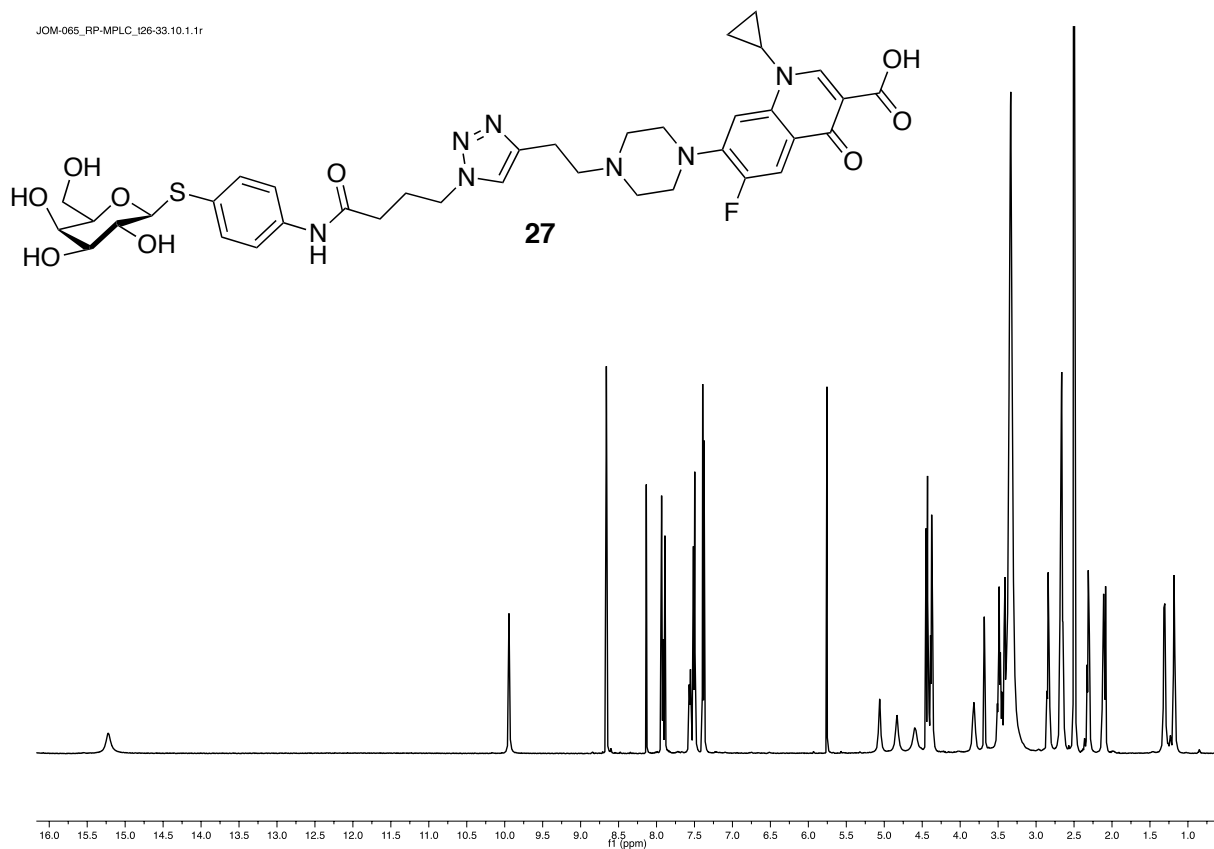
JOM-064_RP-MPLC_I23-31.10.1.1r



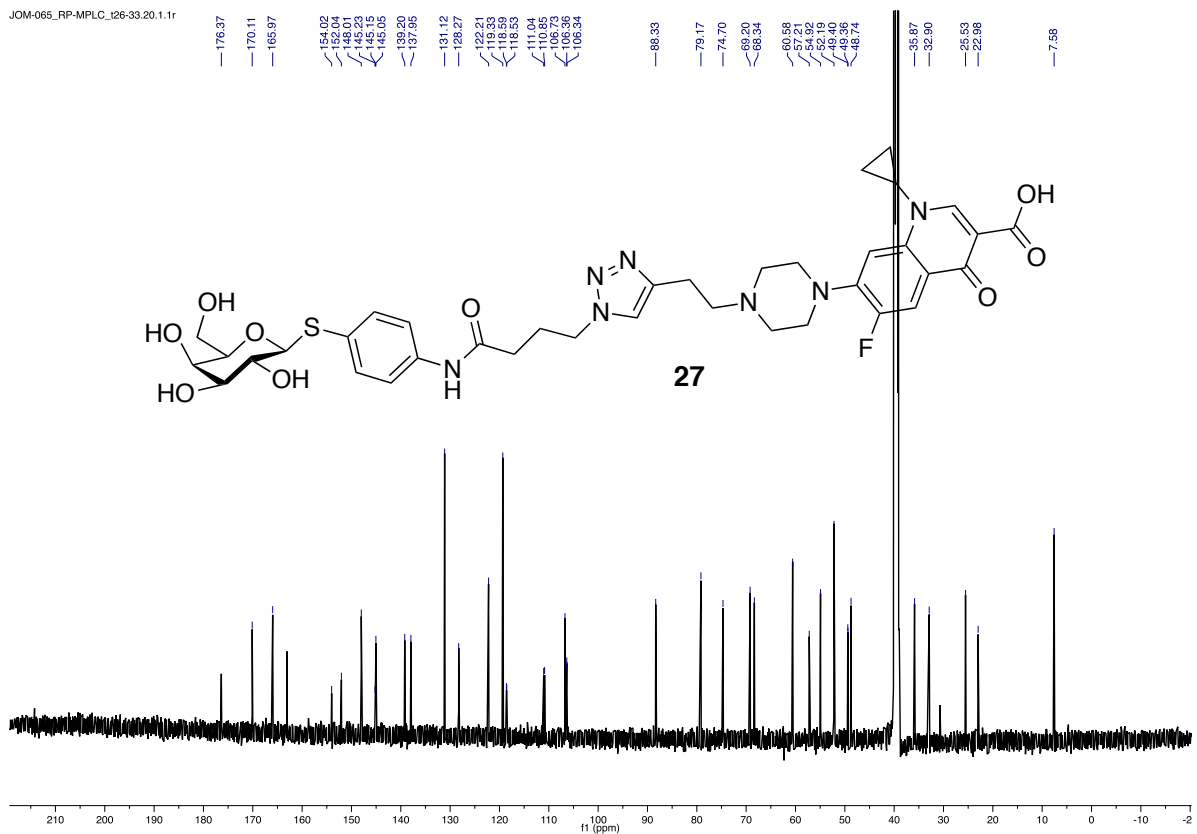
JOM-064_RP-MPLC_I23-31.20.1.1r



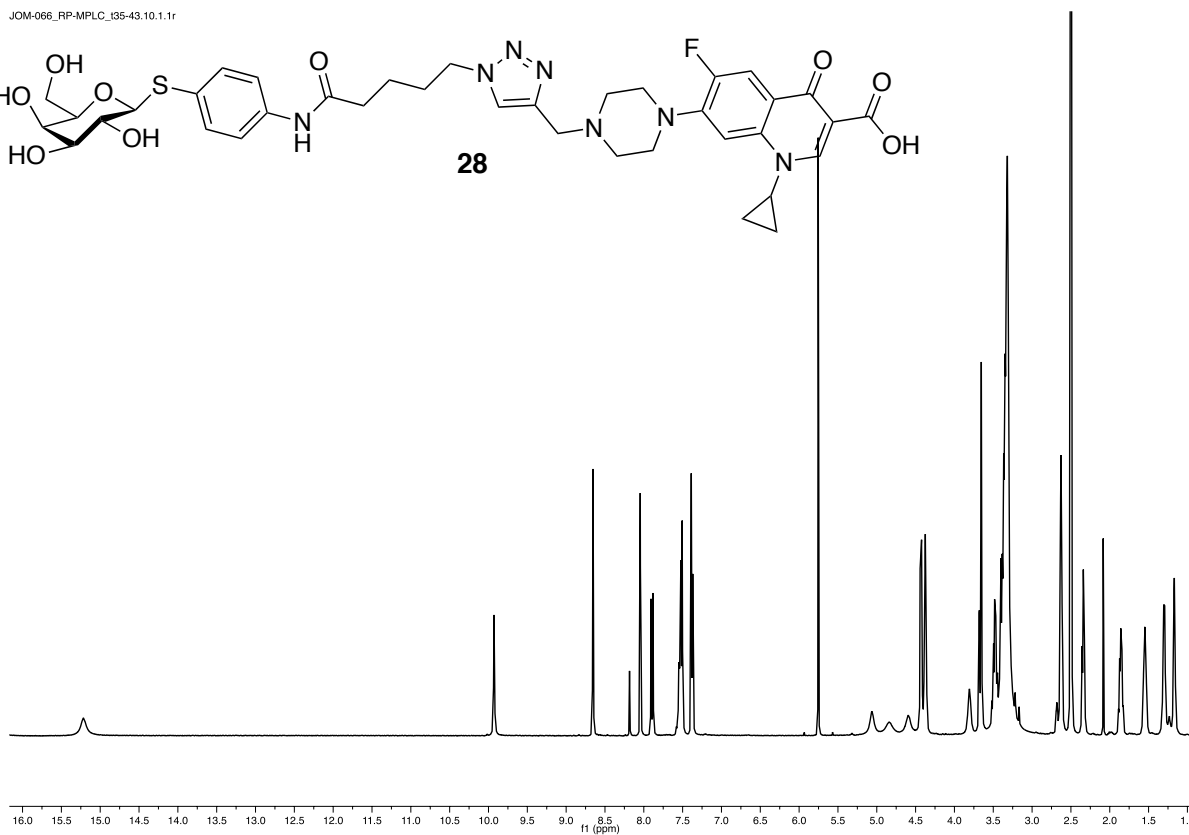
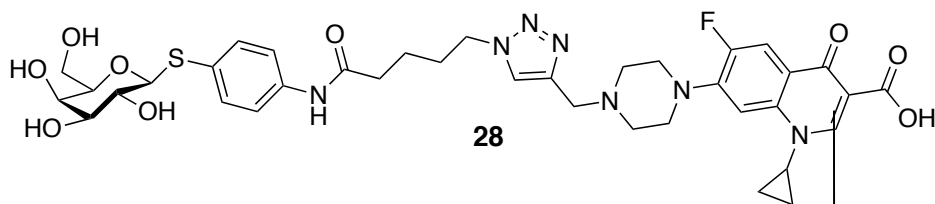
JOM-065_RP-MPLC_126-33.10.1.1r



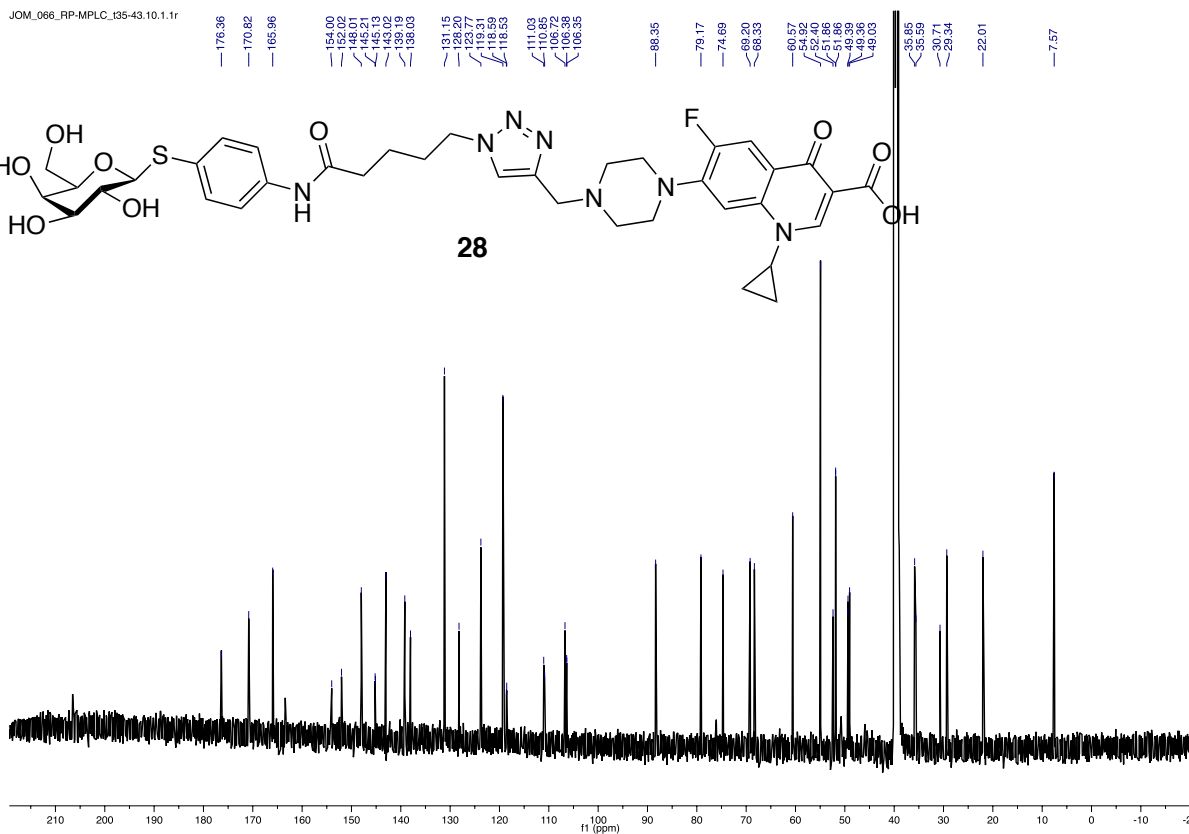
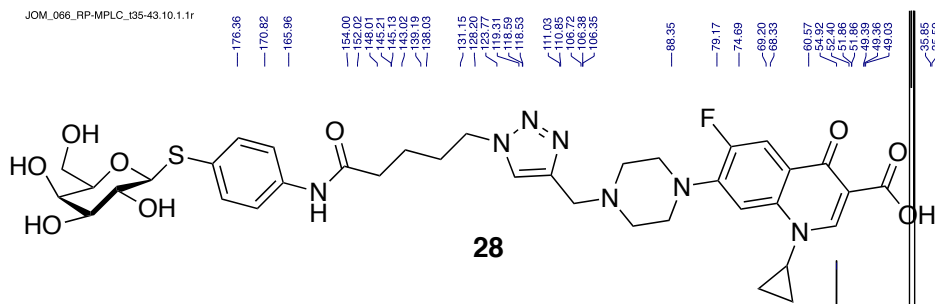
JOM-065_RP-MPLC_126-33.20.1.1r



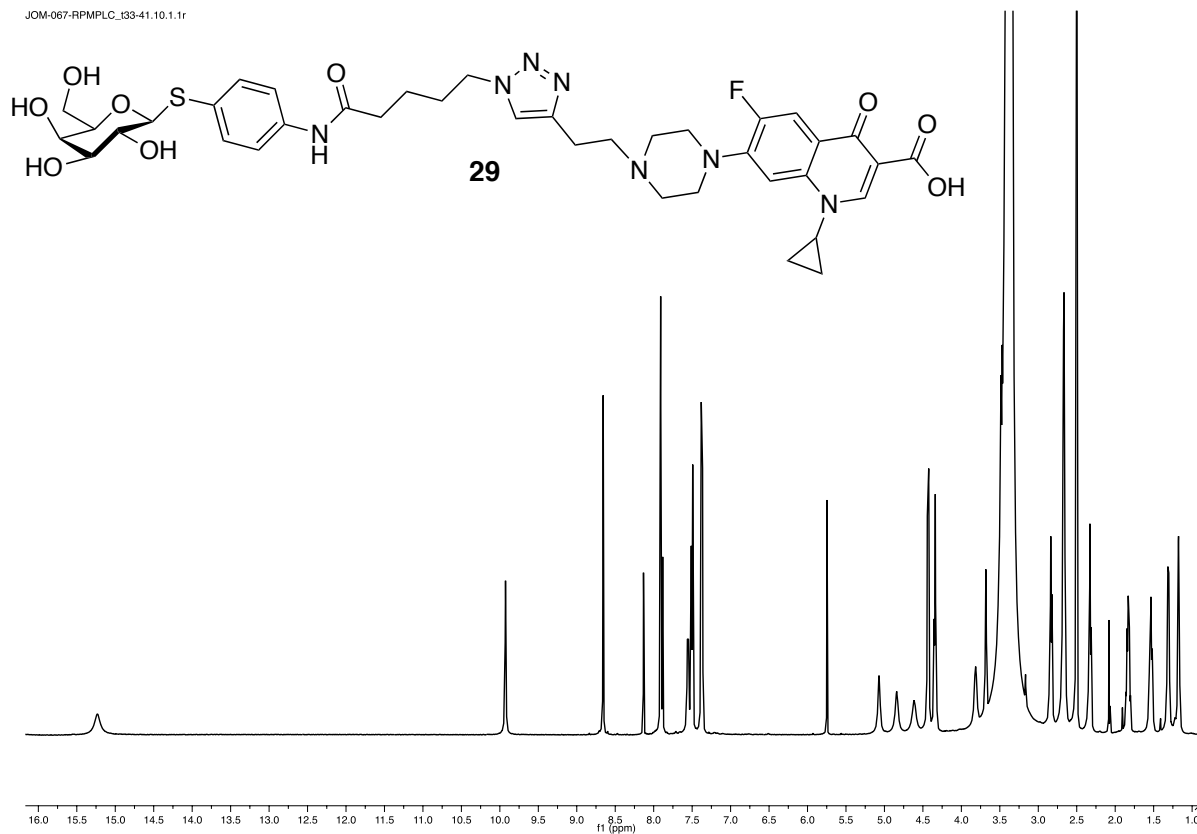
JOM-066_RP-MPLC_135-43.10.1.1r



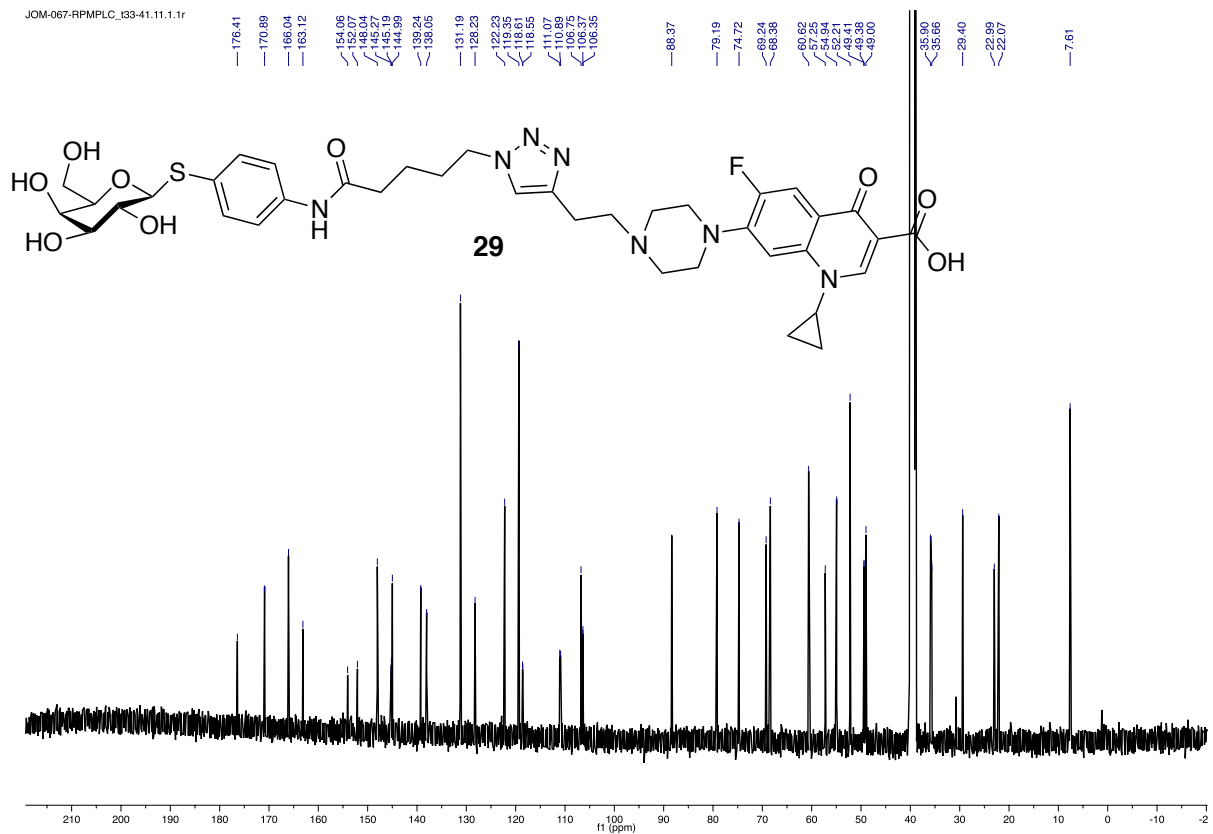
JOM_066_RP-MPLC_135-43.10.1.1r



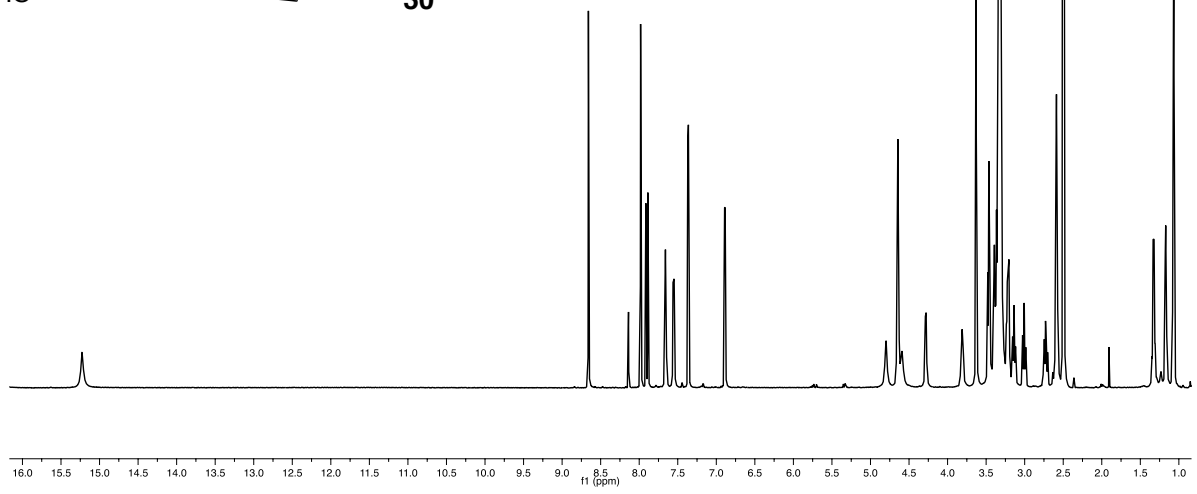
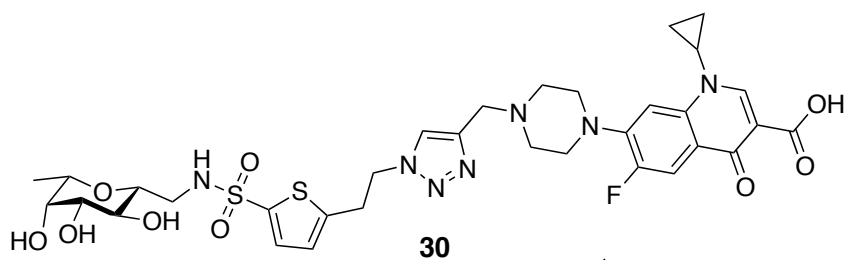
JOM-067-RPMPLC_133-41.10.1.1r



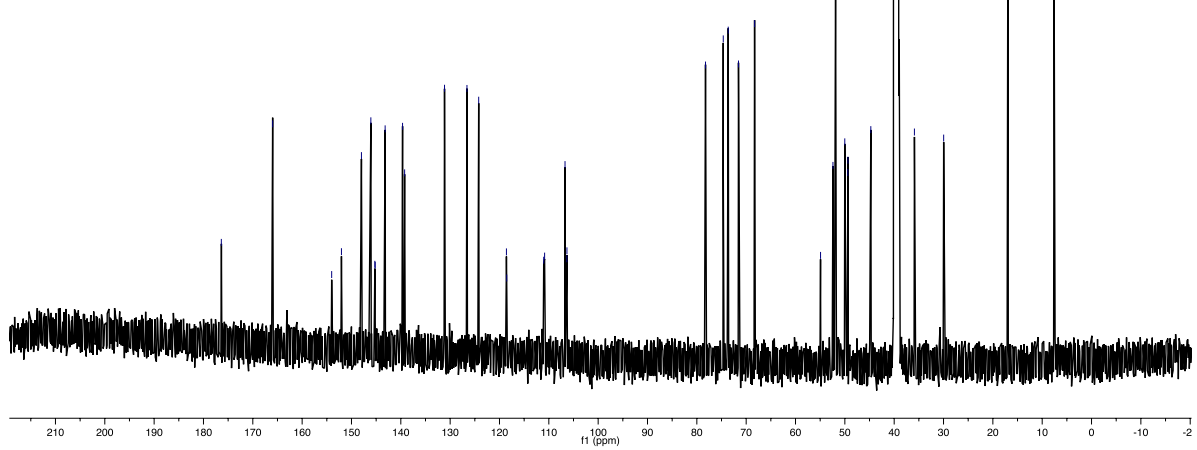
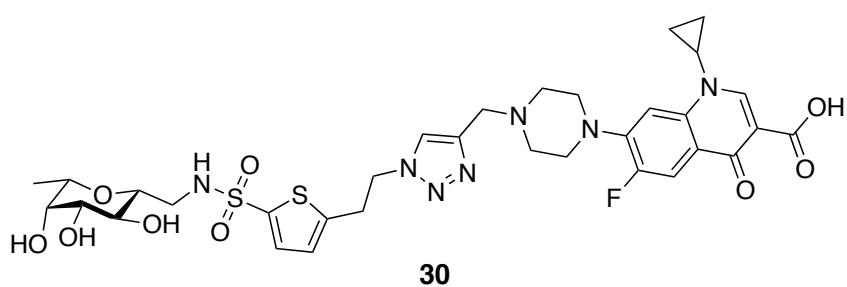
JOM-067-RPMPLC_133-41.11.1.1r



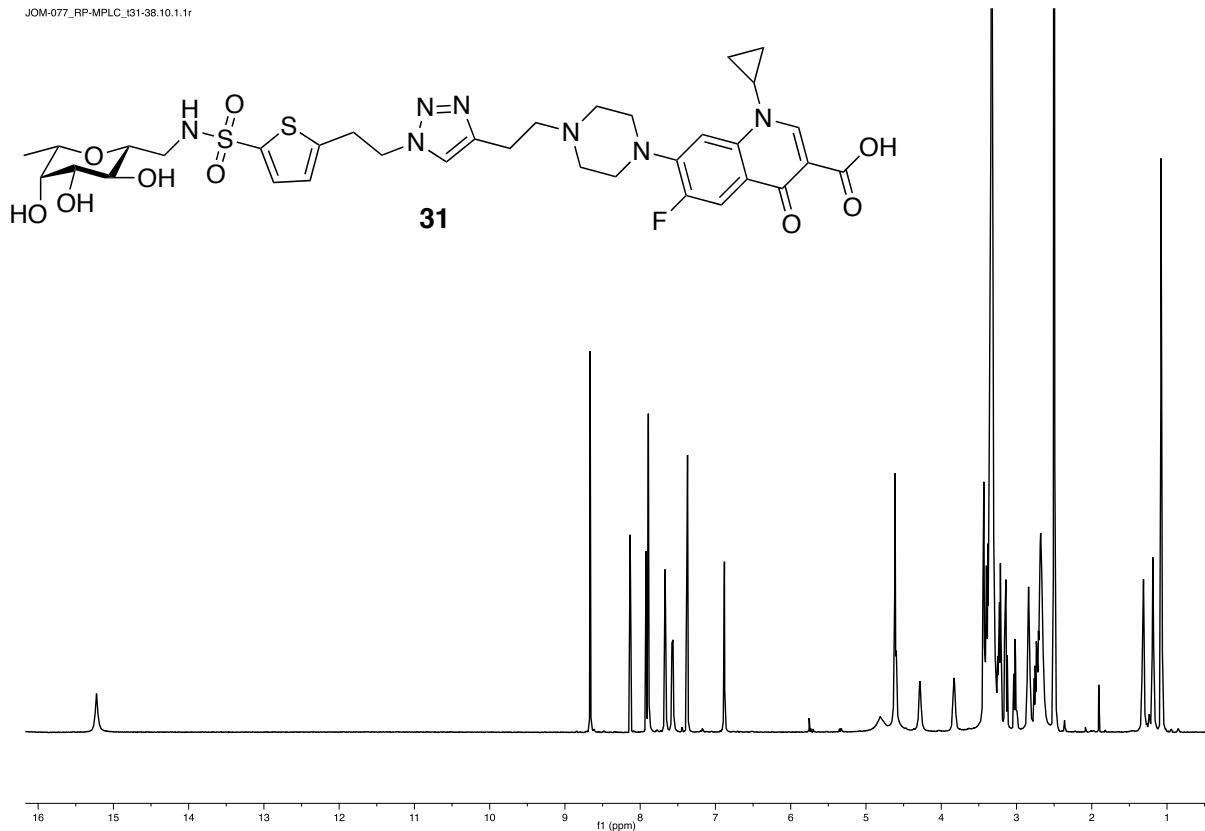
JOM-078_RP-MPLC_I34-39.10.1.1r



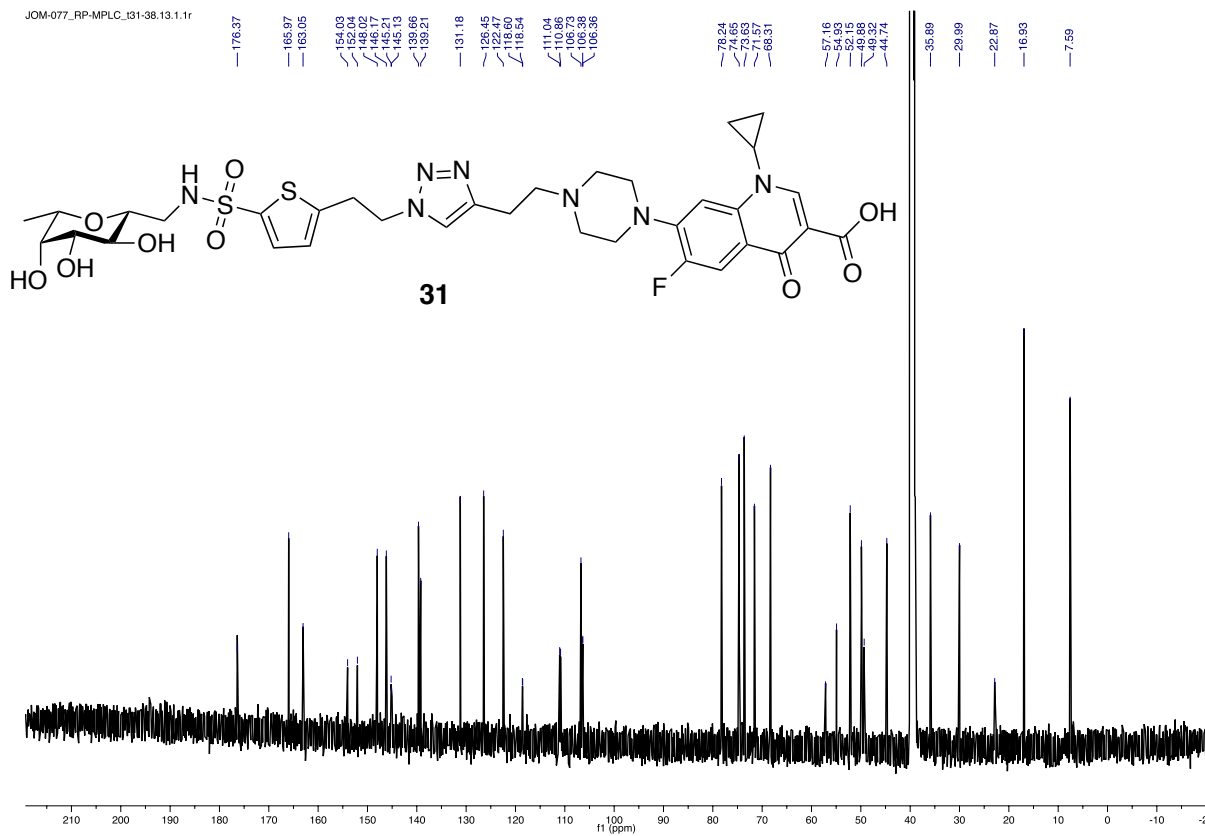
JOM-078_RP-MPLC_I34-39.13.1.1r



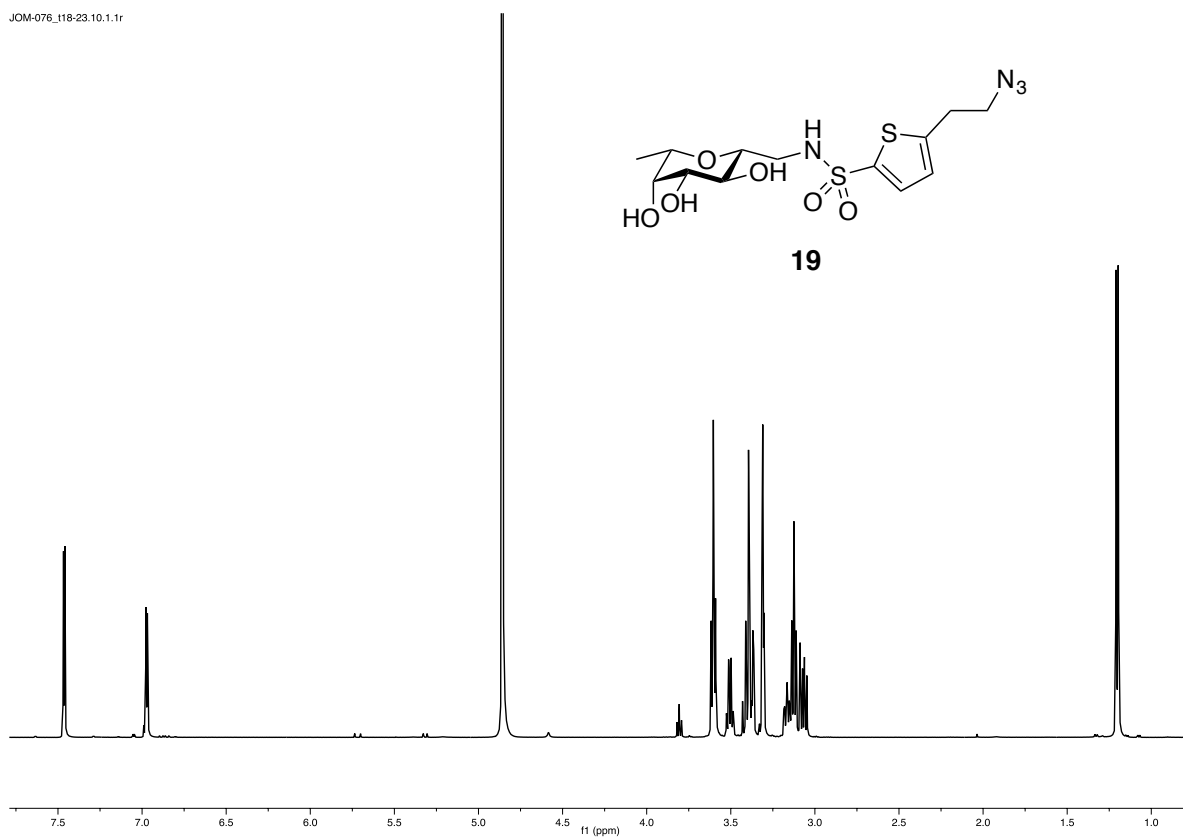
JOM-077_RP-MPLC_I31-38.10.1.1r



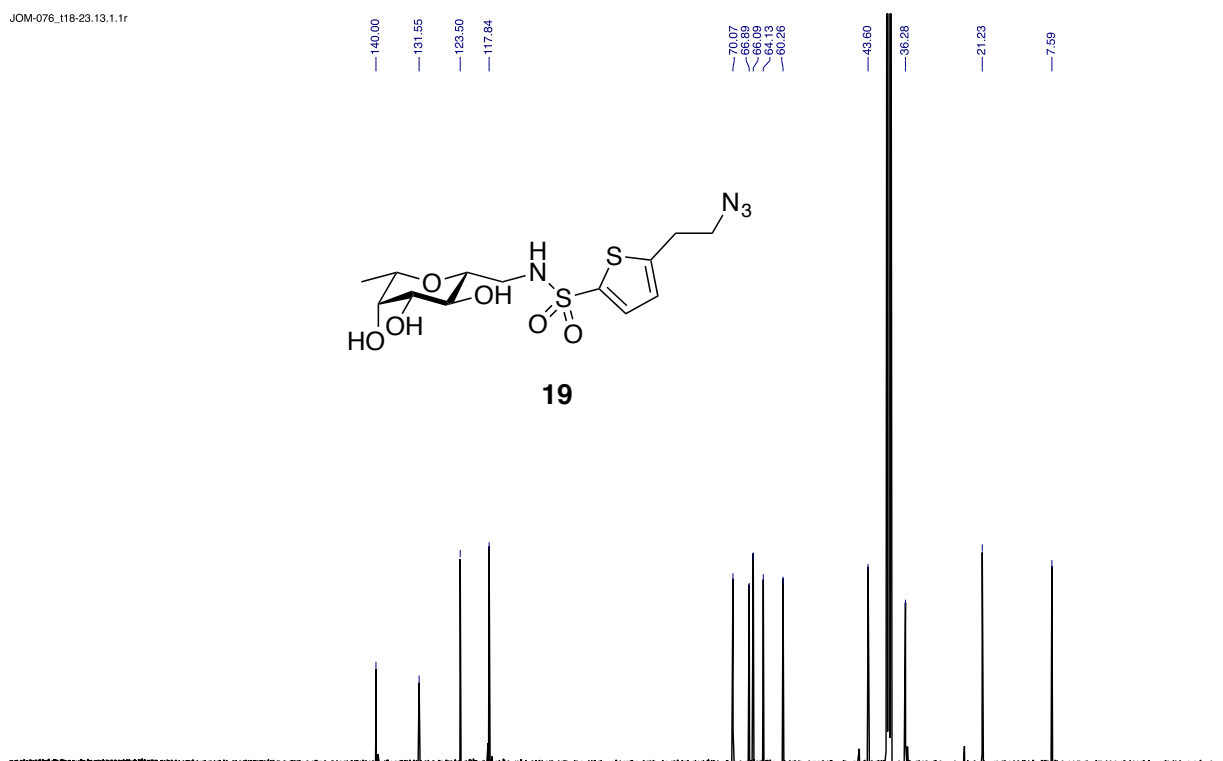
JOM-077_RP-MPLC_I31-38.13.1.1r



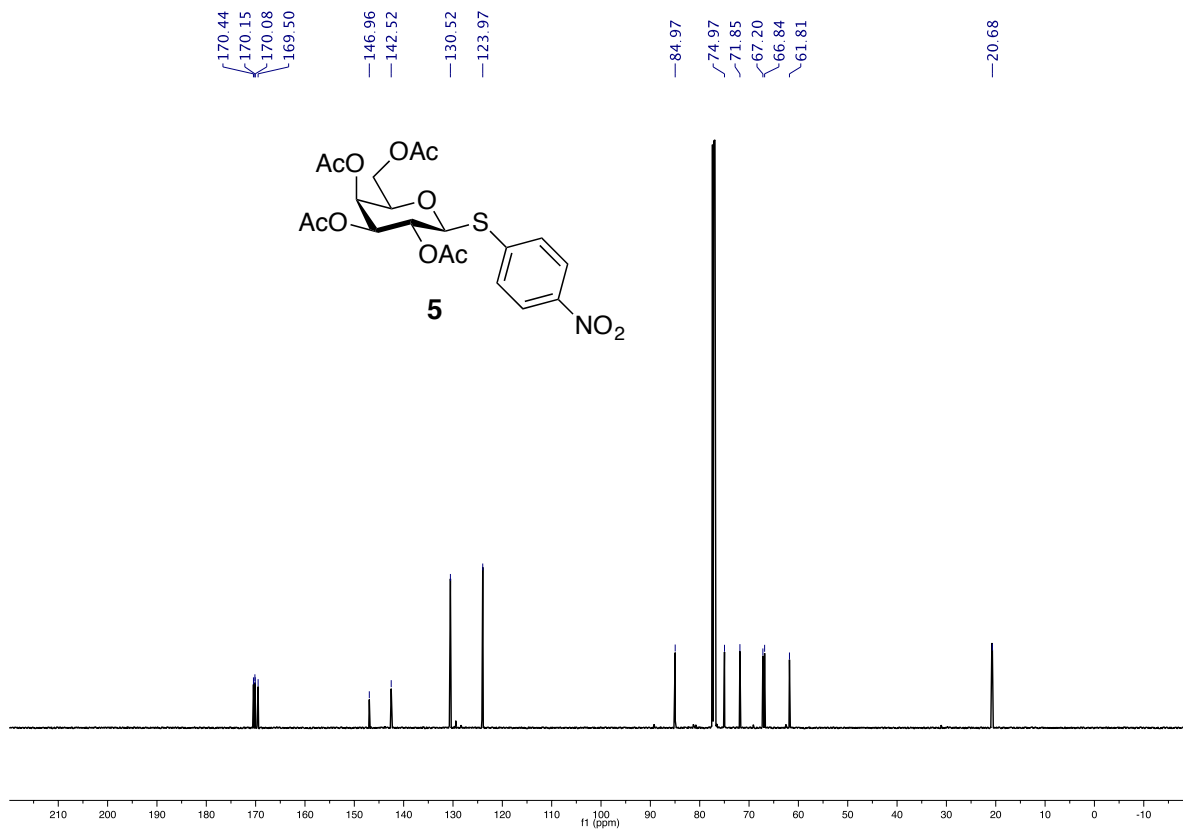
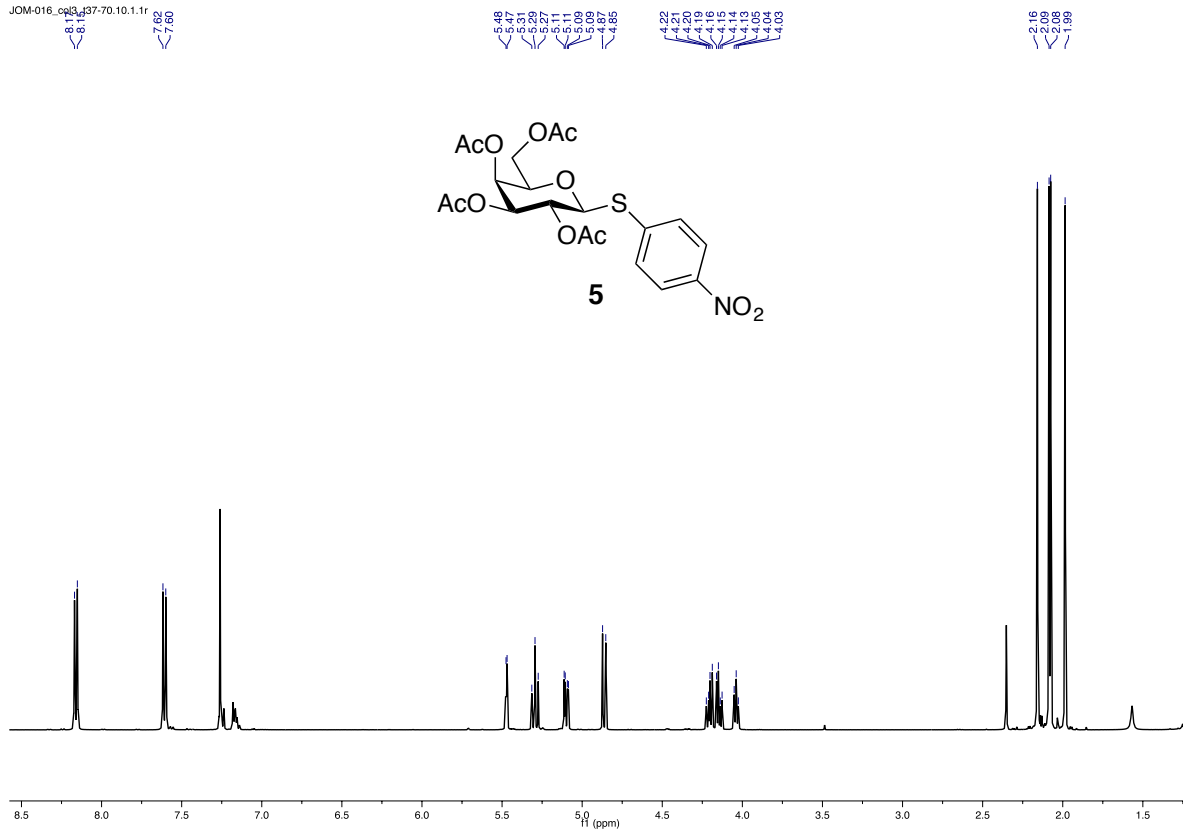
JOM-076_t18-23.10.1.1r

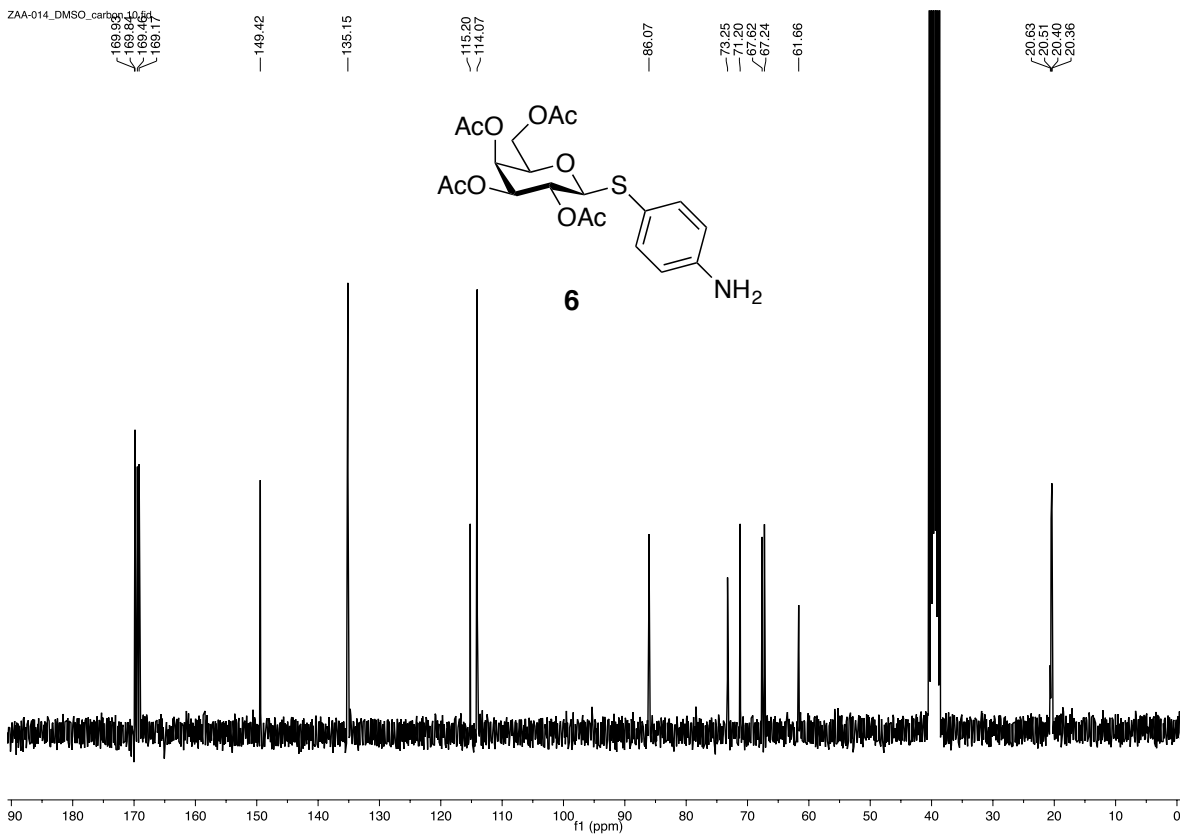
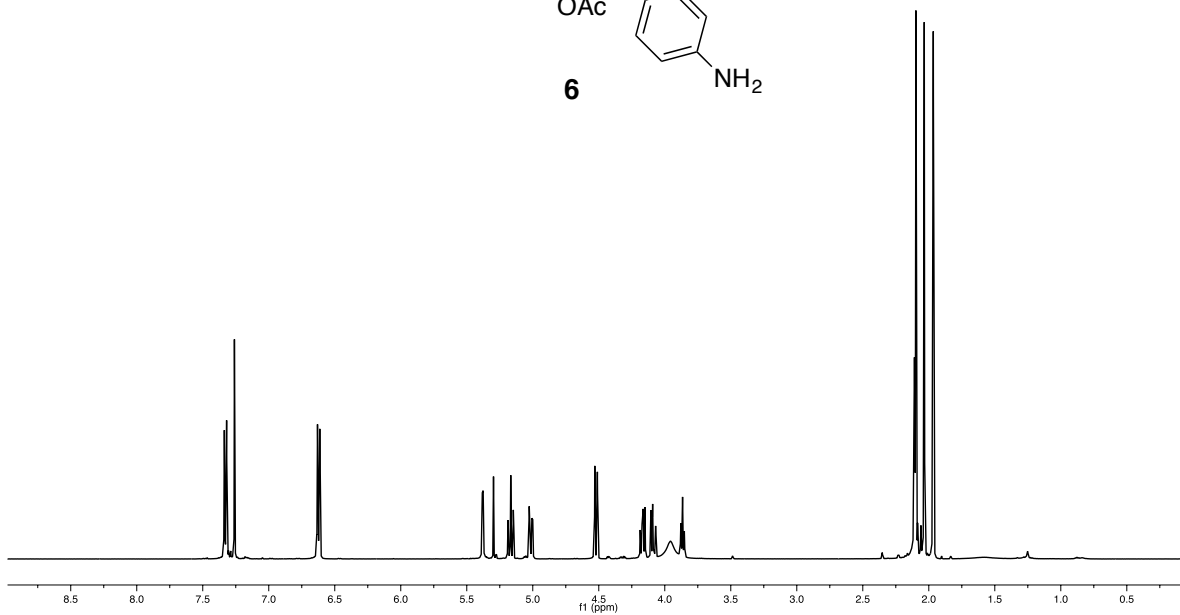
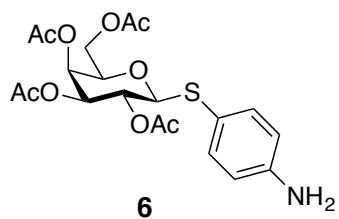


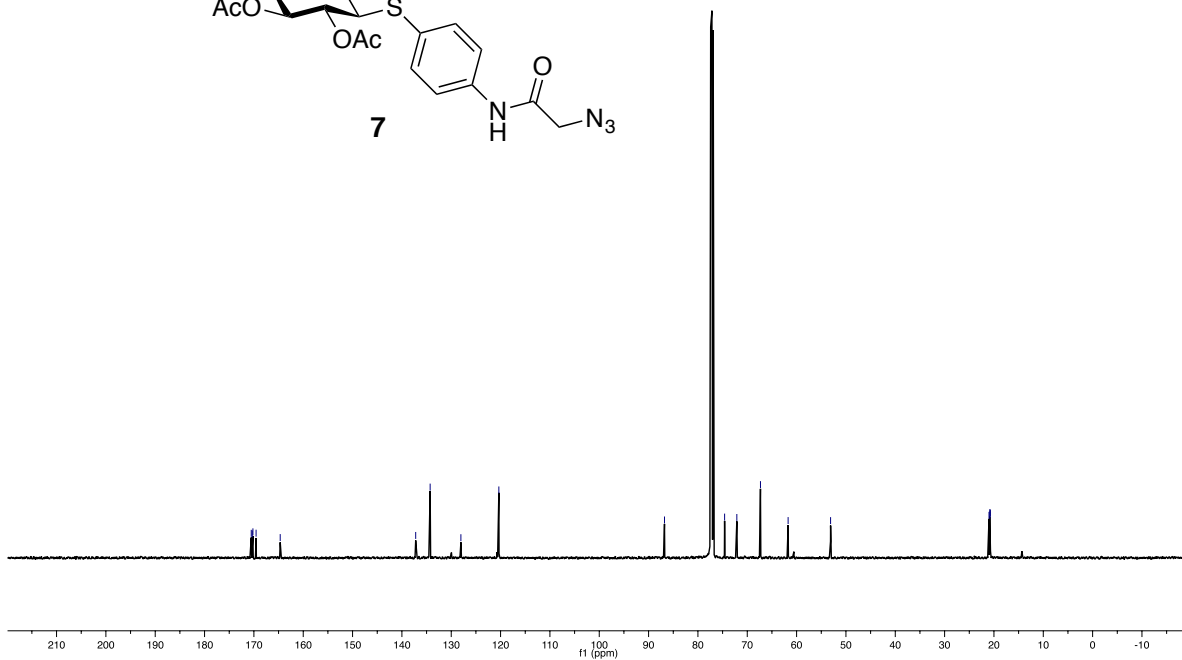
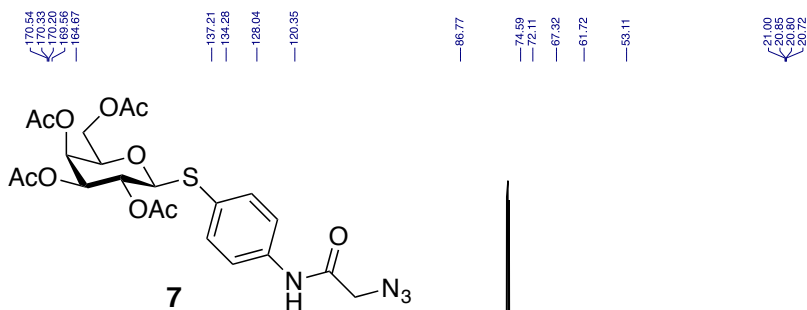
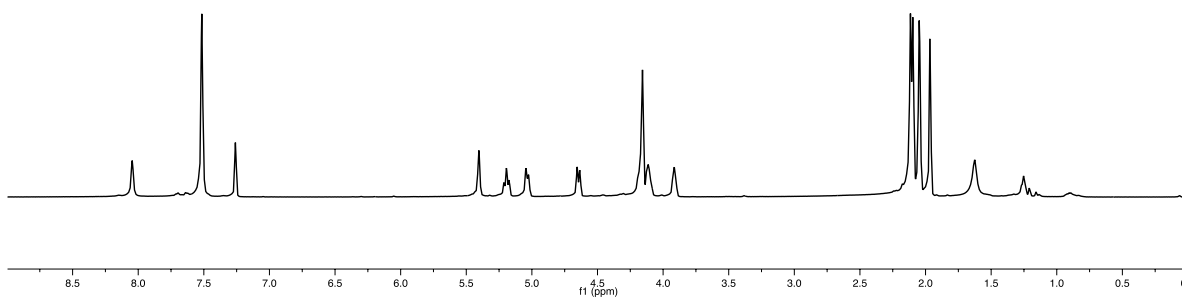
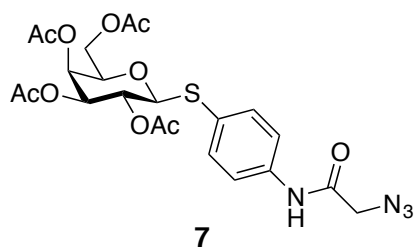
JOM-076_t18-23.13.1.1r

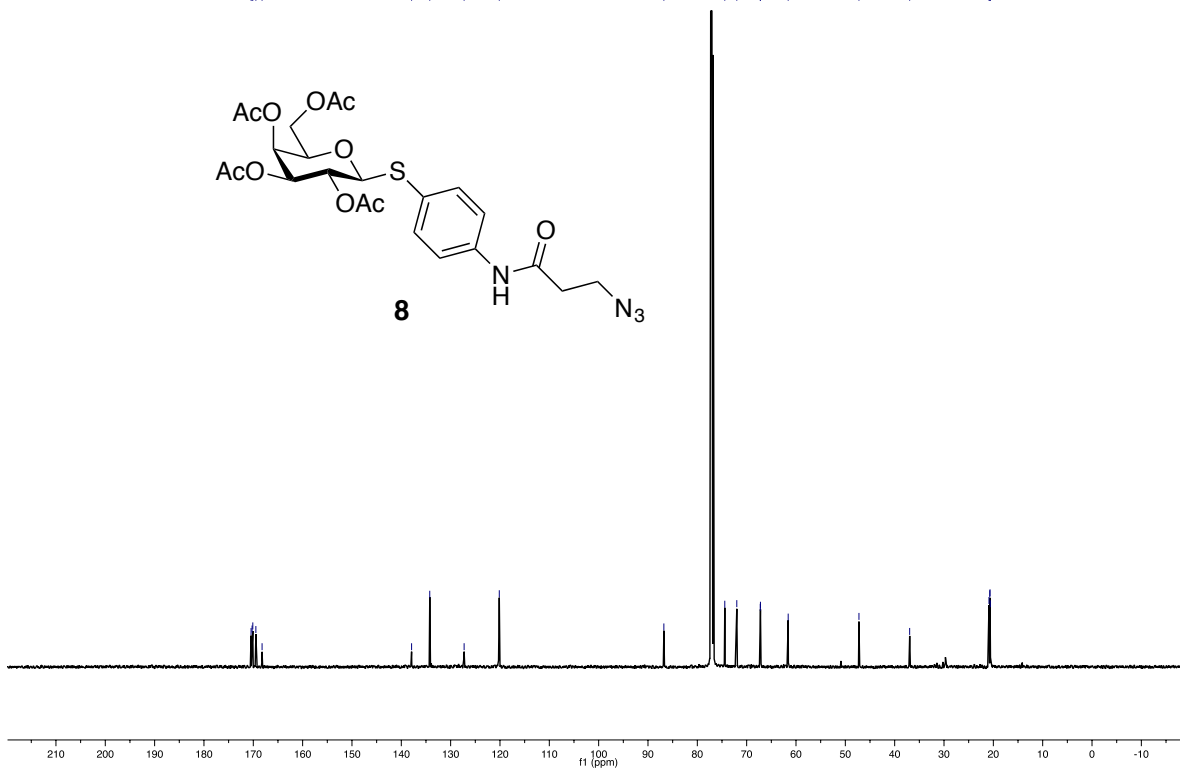
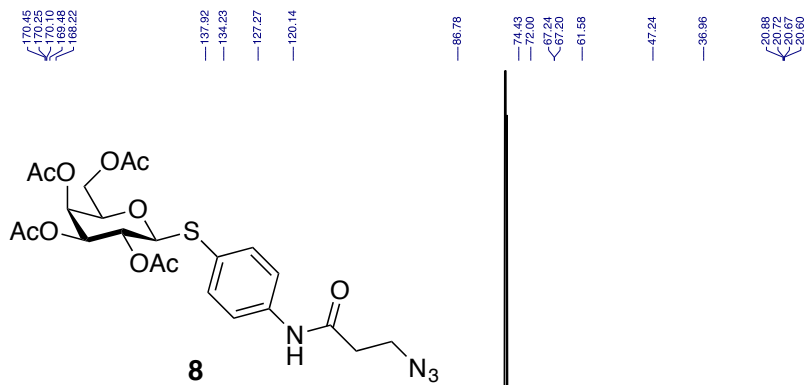
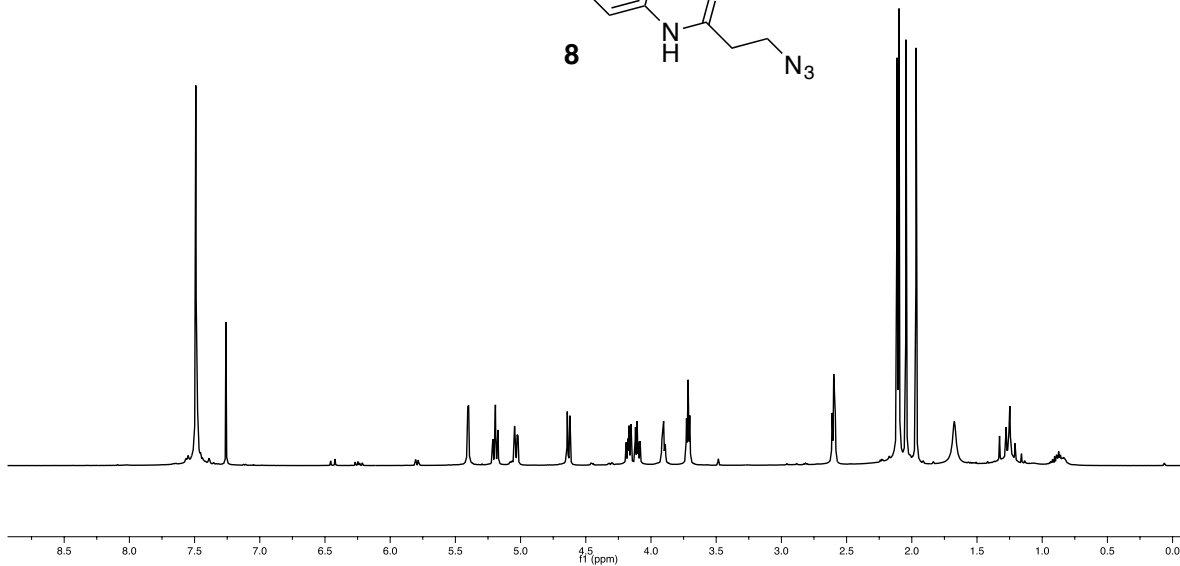
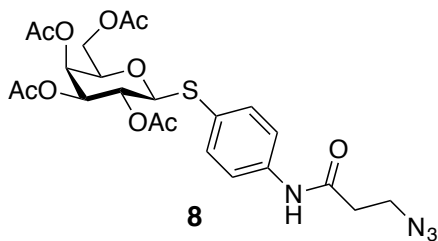


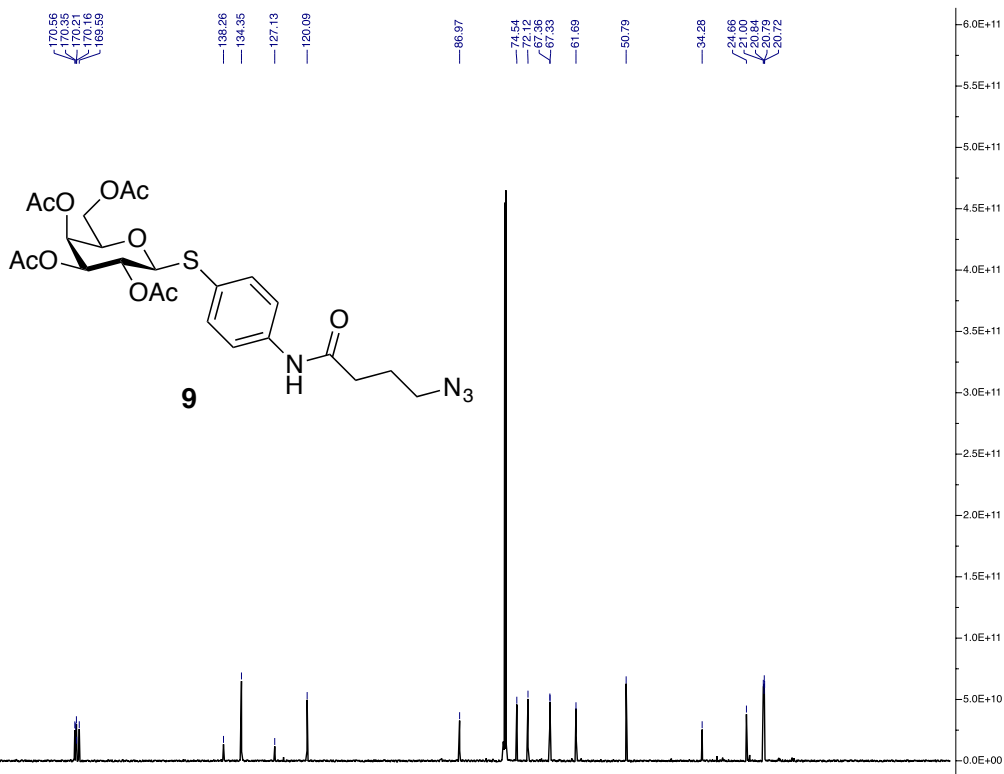
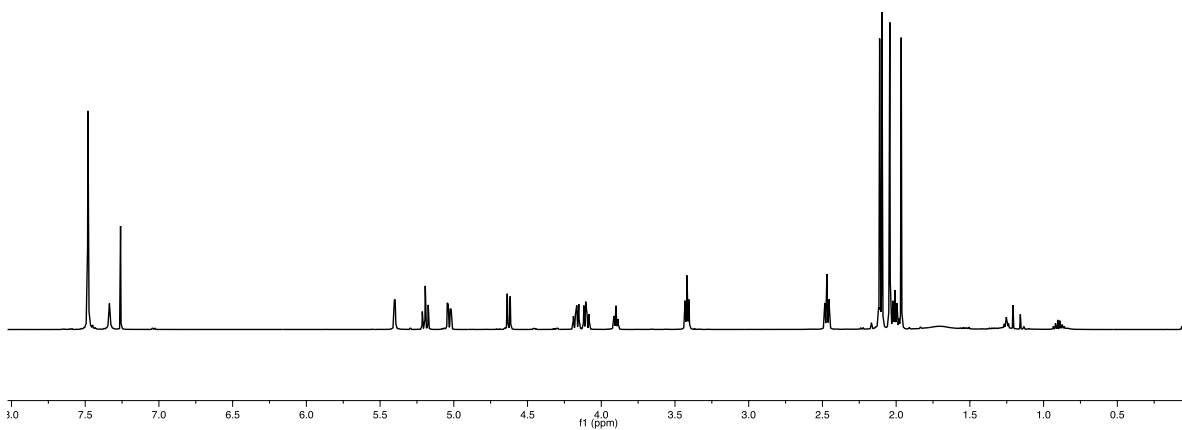
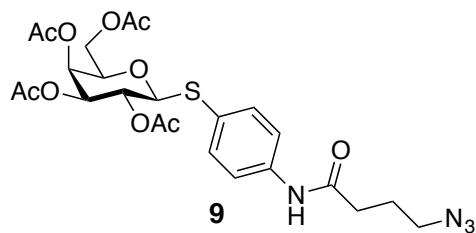
JOM-016_cq3_137-70.10.1.1r



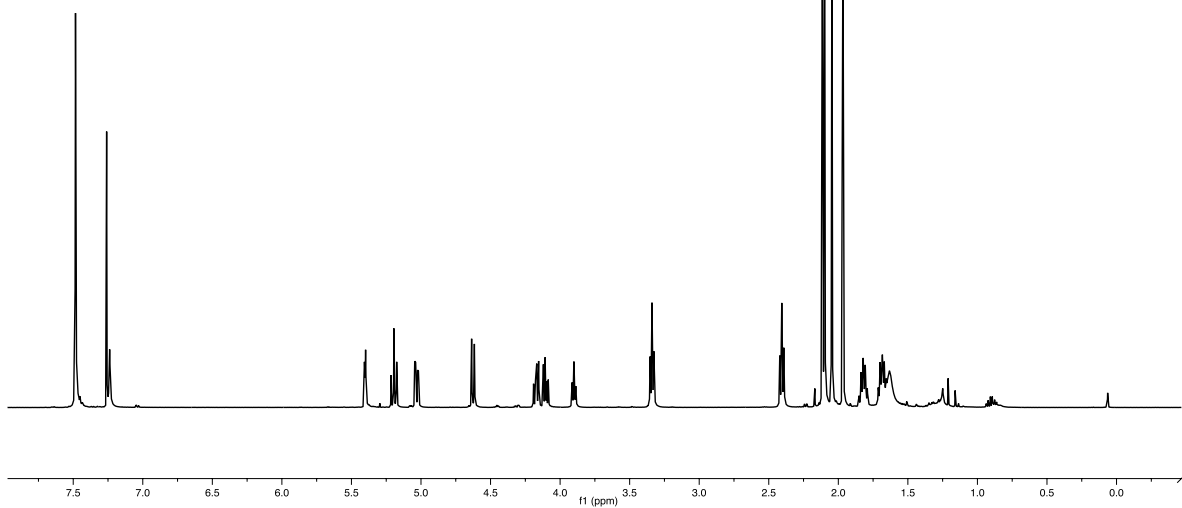
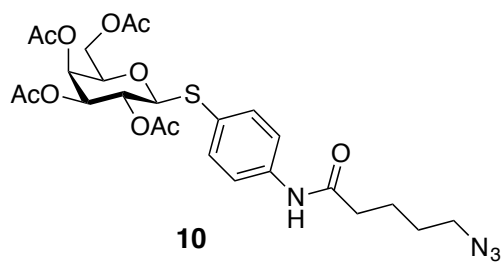








JOM-060_120-25.10.1.1r



JOM-060_120-25.20.1.1r

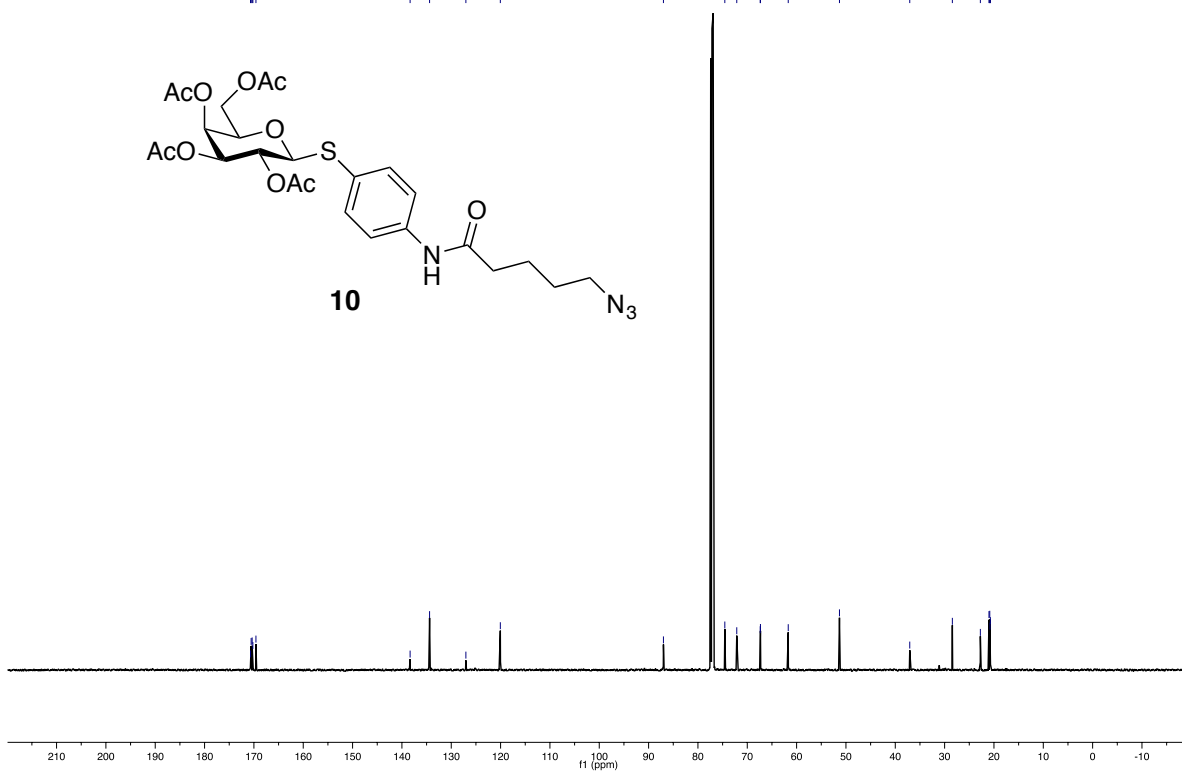
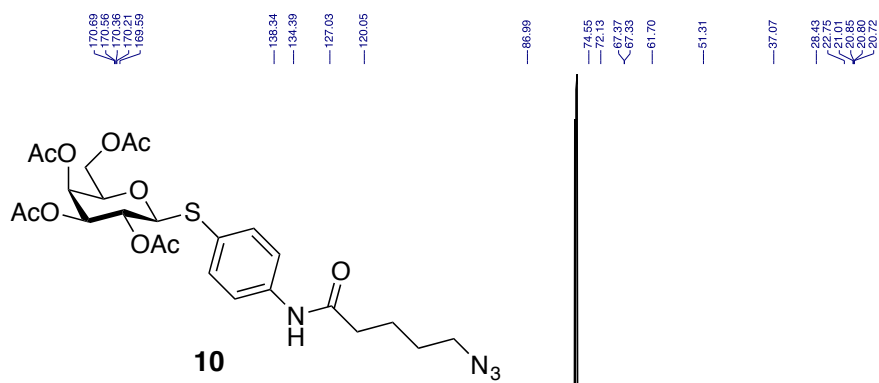


Figure S1: representative Gels for each compound in gyrase-catalyzed DNA supercoiling inhibition assays.

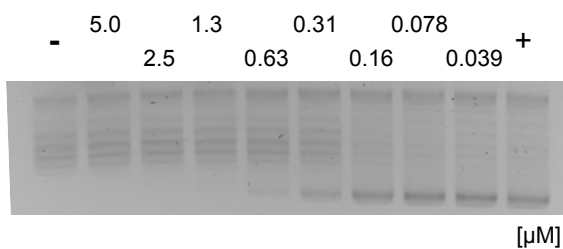
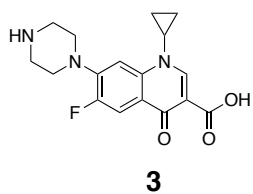
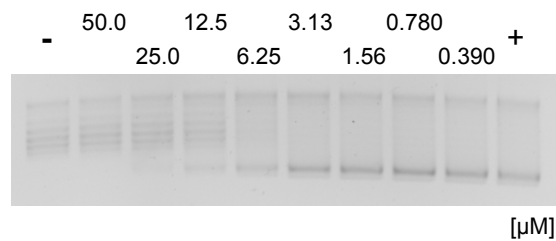
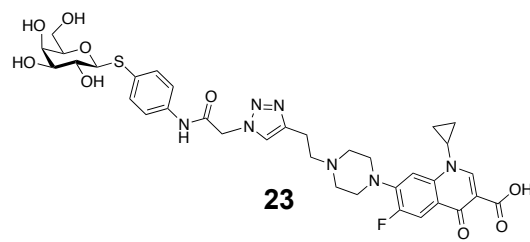
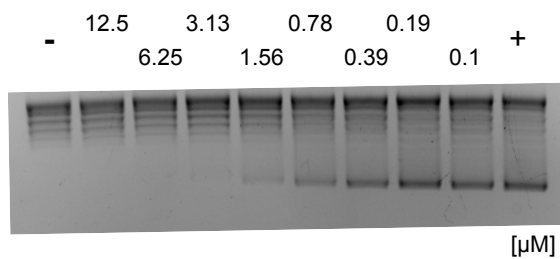
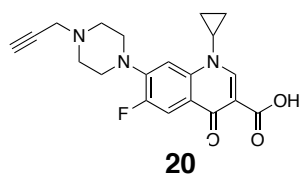
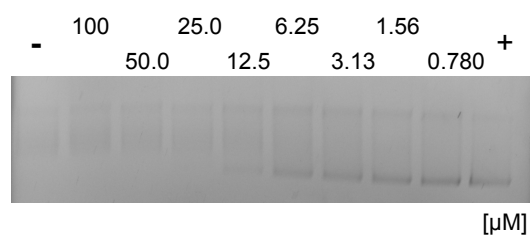
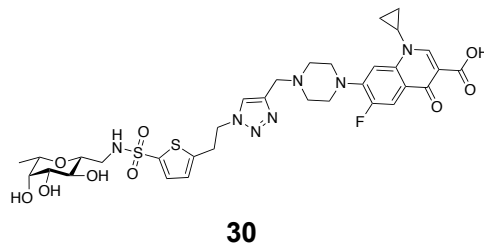
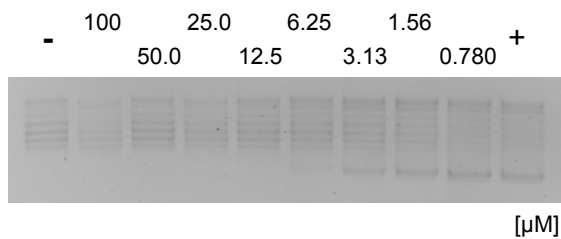
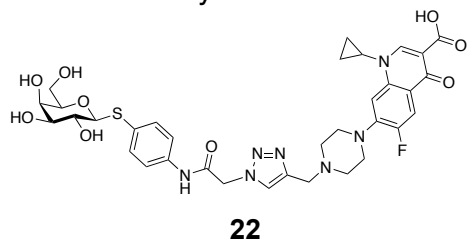
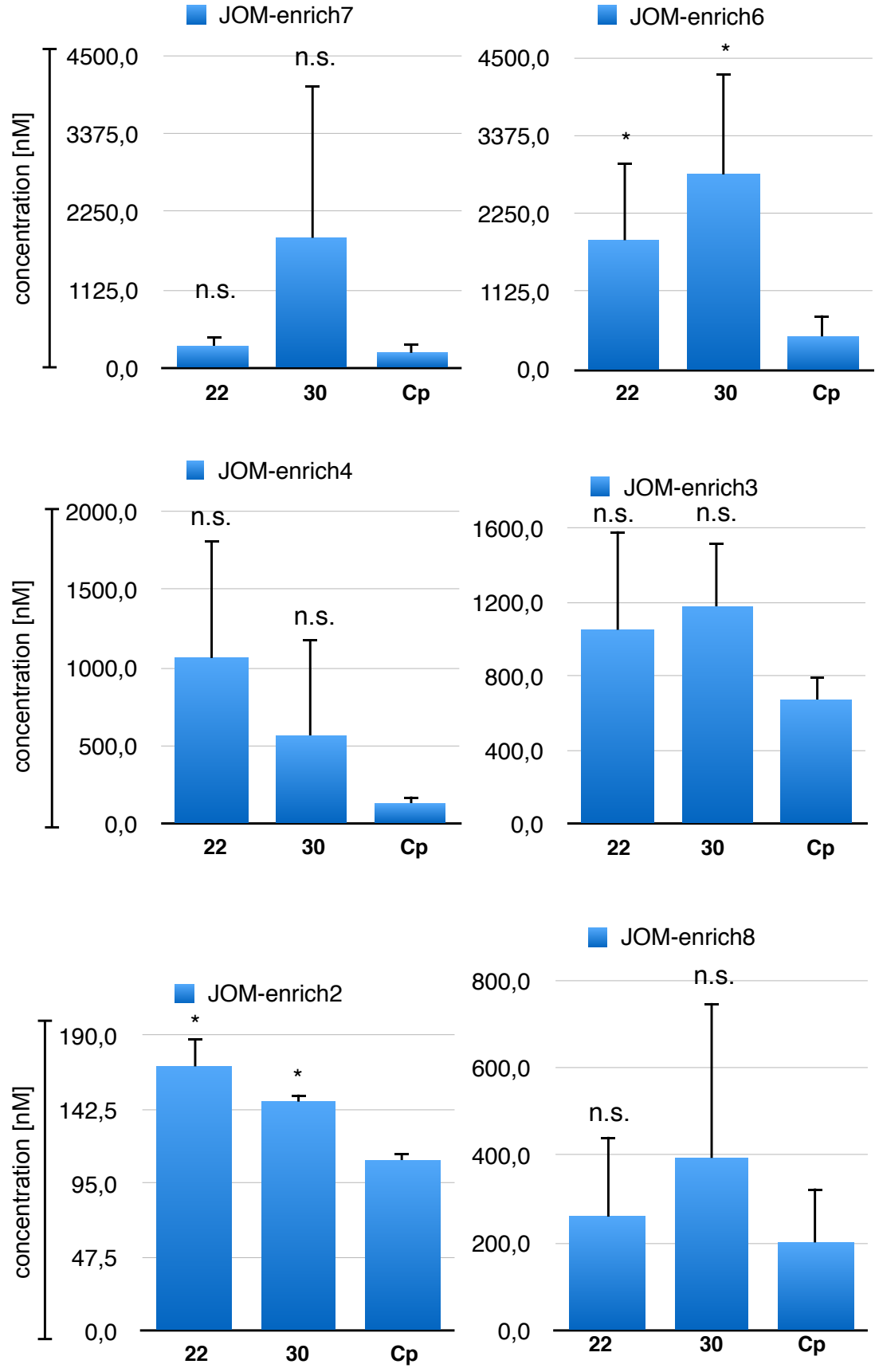


Figure S2: *P. aeruginosa* PAO1 biofilm accumulation raw data.



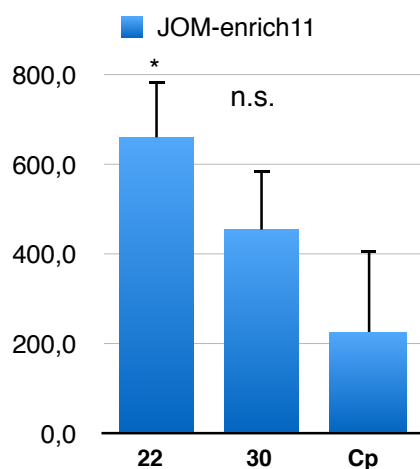


Table S1: Lectin inhibition, calculated as K_i [μM] from IC_{50} according to Huang et al. [1]. N.a. = not applicable. Data is comparable to experimental K_i -values, determined by ITC. [2]

| LecA | | | | | LecB _{PAO1} | | | | |
|-------------------------------------|---|-------------|-------------------------------------|--|-------------------------------------|-------------------------------------|-------------------------------------|--|------------------|
| compound | n | m | $K_i \pm \text{s.d.} [\mu\text{M}]$ | $\text{IC}_{50} \pm \text{s.d.} [\mu\text{M}]$ | compound | m | $K_i \pm \text{s.d.} [\mu\text{M}]$ | $\text{IC}_{50} \pm \text{s.d.} [\mu\text{M}]$ | |
| 11 | 1 | LecA-probes | 4.16 ± 2.99 | 31.7 ± 11 | 19 | LecB-probe | 1.52 ± 0.72 | 3.91 ± 1.6 | |
| 12 | 2 | | 3.96 ± 2.33 | 30.9 ± 8.7 | 30 | 0 | 0.82 ± 0.55 | 2.37 ± 1.2 | |
| 13 | 3 | | 4.01 ± 2.22 | 31.1 ± 8.3 | 31 | 1 | 0.89 ± 0.39 | 2.53 ± 0.87 | |
| 14 | 4 | | 3.67 ± 2.54 | 29.9 ± 9.5 | Me-α-D-Man | | 75.11 ± 9.79 | 166 ± 22 | |
| 22 | 1 | | 0 | 3.82 ± 2.13 | 30.4 ± 8.0 | L-Fuc | controls | 0.93 ± 0.78 | 2.63 ± 1.7 |
| 23 | 1 | | 1 | 1.48 ± 1.47 | 21.6 ± 5.5 | Me-α-L-Fuc | | n.a. | 0.534 ± 0.07 |
| 24 | 2 | | 0 | 4.29 ± 0.87 | 32.2 ± 3.3 | LecB _{PA14} | | | |
| 25 | 2 | | 1 | 3.19 ± 0.48 | 28.0 ± 1.8 | 19 | LecB-probe | 0.36 ± 0.04 | 1.87 ± 0.21 |
| 26 | 3 | | 0 | 3.00 ± 1.08 | 27.3 ± 4.0 | 30 | 0 | 0.18 ± 0.01 | 2.24 ± 0.23 |
| 27 | 3 | | 1 | 3.53 ± 0.99 | 29.3 ± 3.7 | 31 | 1 | 0.44 ± 0.05 | 1.00 ± 0.06 |
| 28 | 4 | 0 | 3.27 ± 2.17 | 28.3 ± 8.1 | Me-α-D-Man | | 21.21 ± 2.08 | 101 ± 10 | |
| 29 | 4 | 1 | 2.70 ± 0.64 | 26.2 ± 2.4 | L-Fuc | controls | 0.49 ± 0.07 | 2.46 ± 0.33 | |
| Me-α-D-Gal | | | 9.76 ± 3.53 | 71.7 ± 16 | Me-α-L-Fuc | | 0.14 ± 0.02 | 0.79 ± 0.11 | |
| pNP-β-D-Gal | | controls | 14.8 ± 4.25 | 52.7 ± 13 | | | | | |

Table S2: Antibiotic susceptibility assay data in molar concentration [μM].

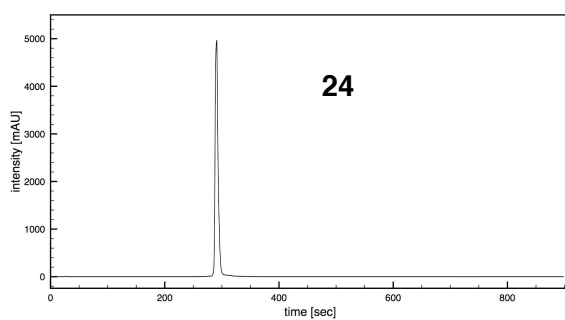
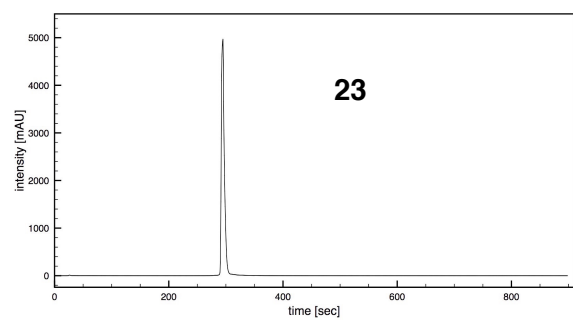
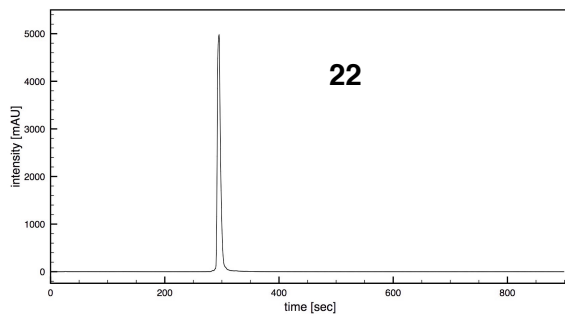
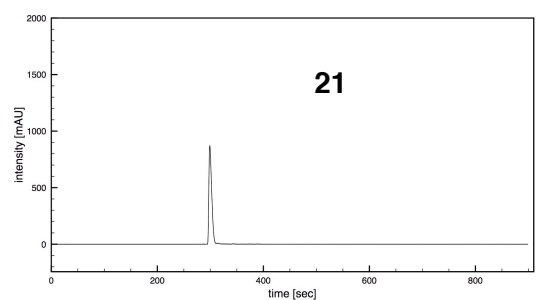
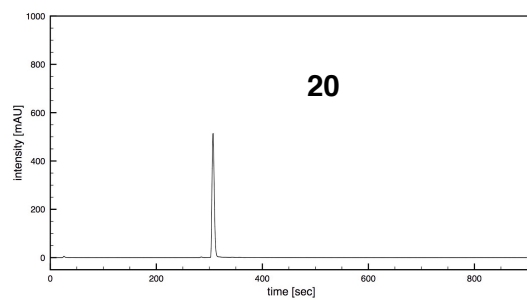
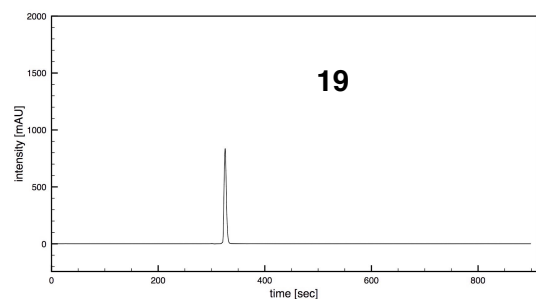
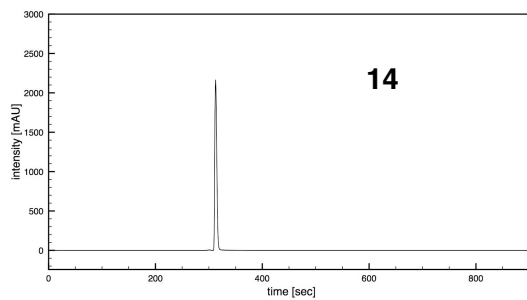
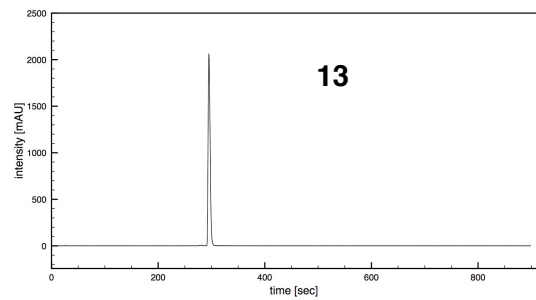
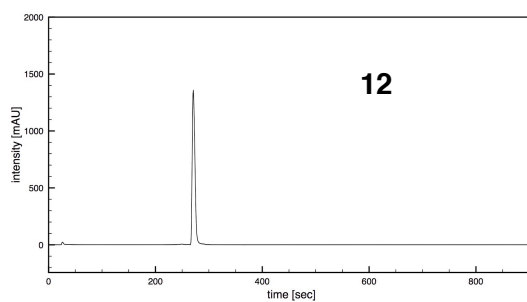
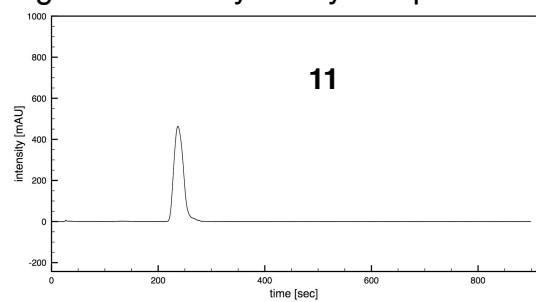
| compound | target: LecA | | | | | | | | | | | target: LecB | | | references | |
|--|---------------------------------------|-----------|-----------|---------|-----------|----------|------------|-----------|-----------|-----------|-------------|--------------|----|---|------------|--|
| | 22 | 23 | 24 | 25 | 26 | 27 | 28 | 29 | 30 | 31 | 20 | 3 | 20 | 3 | | |
| molecular mass [g/mol] | 739.8 | 753.8 | 753.8 | 767.8 | 767.8 | 781.9 | 781.9 | 795.9 | 761.8 | 775.9 | 369.4 | 331.3 | | | | |
| linker length n/m | 1/0 | 1/1 | 2/0 | 2/1 | 3/0 | 3/1 | 4/0 | 4/1 | -/0 | -/1 | 0 | - | | | | |
| test organism | MIC [μM] | | | | | | | | | | | | | | | |
| <i>E. coli</i> K12 MG1655 | 2.7 | 11 - 21 | 2.7 | 21 | 1.3 - 2.6 | 20 | 2.6 - 5.11 | 20 | 11 - 21 | 21 | n.d. | < 0.37 | | | | |
| <i>E. coli</i> DSM 1116 | 2.7 - 5.4 | 22 | 2.7 - 5.3 | 42 | 2.6 - 42 | 5.1 - 41 | 5.11 - 41 | 5 - 40 | 21 - 42 | 41 | n.d. | < 0.37 | | | | |
| <i>S. carnosus</i> ^[a] | 43 | 85 | 42 | > 83 | 21 | 82 | 10 | ≥ 80 | > 84 | > 82 | n.d. | < 0.37 | | | | |
| <i>P. aeruginosa</i> PA14 wt | 22 | ≥ 85 | 11 - 21 | > 83 | 10 - 21 | > 82 | 41 | > 80 | 84 | > 82 | 5.4 - 10.8 | 0.075 - 0.3 | | | | |
| <i>P. aeruginosa</i> PA14 wt + 1 $\mu\text{g/mL}$ PMBN | 5.4 - 22 | 21 - 85 | 11 - 21 | 42 - 83 | 5.2 | 41 - 82 | 2.6 - 10 | 40 - 80 | 84 | 82 | 0.068 - 1.4 | 0.075 | | | | |
| <i>P. aeruginosa</i> PA14 ΔlecA | 22 - 44 | ≥ 85 | 11 - 21 | > 83 | 10 - 21 | > 82 | 41 | > 80 | ≥ 84 | > 82 | 11 - 22 | 0.15 - 0.24 | | | | |
| <i>P. aeruginosa</i> PA14 ΔlecB | 22 - 44 | ≥ 85 | 11 - 42 | > 83 | 10 - 21 | > 82 | 41 - 82 | > 80 | 84 | > 82 | 11 | 0.15 - 0.24 | | | | |
| <i>P. aeruginosa</i> PAO1 wt | 22 - 44 | > 85 | 21 | > 83 | 21 - 42 | > 82 | 41 - 82 | > 80 | ≥ 84 | > 82 | 11 - 22 | 0.075 - 0.24 | | | | |
| <i>P. aeruginosa</i> PAO1 wt + 1 $\mu\text{g/mL}$ PMBN | 5.4 - 11 | 42 - 85 | 5.3 - 11 | 42 - 83 | 5.2 - 10 | 41 - 82 | 10 - 20 | 40 - 80 | 42 - 84 | ≥ 82 | 2.7 - 5.4 | 0.075 - 0.15 | | | | |

n.d. = not determined, ^[a] DSM 20501

| compound | SMILE | IC ₅₀ LecA ± s.d. [μM] | IC ₅₀ LecB _{PAO1} ± s.d. [μM] | IC ₅₀ LecB _{PA14} ± s.d. [μM] |
|----------|---|--------------------------------------|--|--|
| 11 | <chem>O[C@H]1[C@@H](O)[C@@H](CO)O[C@@H](SC2=CC=C(NC(CN=[N+]=[N-])=O)C=C2)[C@@H]1O</chem> | 31.7 ± 11 | n.a. | n.a. |
| 12 | <chem>O[C@H]1[C@@H](O)[C@@H](CO)O[C@@H](SC2=CC=C(NC(CCN=[N+]=[N-])=O)C=C2)[C@@H]1O</chem> | 30.9 ± 8.7 | n.a. | n.a. |
| 13 | <chem>O[C@H]1[C@@H](O)[C@@H](CO)O[C@@H](SC2=CC=C(NC(CCCN=[N+]=[N-])=O)C=C2)[C@@H]1O</chem> | 31.1 ± 8.3 | n.a. | n.a. |
| 14 | <chem>O[C@H]1[C@@H](O)[C@@H](CO)O[C@@H](SC2=CC=C(NC(CCCCN=[N+]=[N-])=O)C=C2)[C@@H]1O</chem> | 29.9 ± 9.5 | n.a. | n.a. |
| 19 | <chem>C[C@H]1[C@@H](O)[C@@H](O)[C@H](O)[C@@H](CNS(C2=CC=C(CCN=[N+]=[N-])S2)(=O)=O)O1</chem> | n.a. | 3.91 ± 1.6 | 1.87 ± 0.21 |
| 20 | <chem>O=C(O)C1=CN(C2=CC(N3CCN(CC#C)CC3)=C(F)C=C2C1=O)C4CC4</chem> | n.a. | n.a. | n.a. |
| 21 | <chem>O=C(O)C1=CN(C2=CC(N3CCN(CCC#C)CC3)=C(F)C=C2C1=O)C4CC4</chem> | n.a. | n.a. | n.a. |
| 22 | <chem>O=C(O)C1=CN(C2=CC(N3CCN(CC4=CN(CC(NC(C=C5)=CC=C5S[C@H]6[C@H](O)[C@@H](O)[C@@H](O)[C@@H](CO)O6)=O)N=N4)CC3)=C(F)C=C2C1=O)C7CC7</chem> | 30.4 ± 8.0 | n.a. | n.a. |
| 23 | <chem>O[C@H]1[C@@H](O)[C@@H](CO)O[C@@H](SC2=CC=C(NC(CN3N=NC(CCN(CC4)CCN4C5=C(F)C=C6C(N(C7CC7)C=C(C6=O)C(O)=O)=C5)=C3)=O)C=C2)[C@@H]1O</chem> | 21.6 ± 5.5 | n.a. | n.a. |
| 24 | <chem>O=C(O)C1=CN(C2=CC(N3CCN(CC4=CN(CCC(NC(C=C5)=CC=C5S[C@H]6[C@H](O)[C@@H](O)[C@@H](O)[C@@H](CO)O6)=O)N=N4)CC3)=C(F)C=C2C1=O)C7CC7</chem> | 32.2 ± 3.3 | n.a. | n.a. |
| 25 | <chem>O[C@H]1[C@@H](O)[C@@H](CO)O[C@@H](SC2=CC=C(NC(CCN3N=NC(CCN(CC4)CCN4C5=C(F)C=C6C(N(C7CC7)C=C(C6=O)C(O)=O)=C5)=C3)=O)C=C2)[C@@H]1O</chem> | 28.0 ± 1.8 | n.a. | n.a. |
| 26 | <chem>O=C(O)C1=CN(C2=CC(N3CCN(CC4=CN(CCCC(NC(C=C5)=CC=C5S[C@H]6[C@H](O)[C@@H](O)[C@@H](O)[C@@H](CO)O6)=O)N=N4)CC3)=C(F)C=C2C1=O)C7CC7</chem> | 27.3 ± 4.0 | n.a. | n.a. |
| 27 | <chem>O[C@H]1[C@@H](O)[C@@H](CO)O[C@@H](SC2=CC=C(NC(CCN3N=NC(CCN(CC4)CCN4C5=C(F)C=C6C(N(C7CC7)C=C(C6=O)C(O)=O)=C5)=C3)=O)C=C2)[C@@H]1O</chem> | 29.3 ± 3.7 | n.a. | n.a. |
| 28 | <chem>O[C@H]1[C@@H](O)[C@@H](CO)O[C@@H](SC2=CC=C(NC(CCCCN3N=NC(CN(CC4)CCN4C5=C(F)C=C6C(N(C7CC7)C=C(C6=O)C(O)=O)=C5)=C3)=O)C=C2)[C@@H]1O</chem> | 28.3 ± 8.1 | n.a. | n.a. |
| 29 | <chem>O[C@H]1[C@@H](O)[C@@H](CO)O[C@@H](SC2=CC=C(NC(CCCCN3N=NC(CCN(CC4)CCN4C5=C(F)C=C6C(N(C7CC7)C=C(C6=O)C(O)=O)=C5)=C3)=O)C=C2)[C@@H]1O</chem> | 26.2 ± 2.4 | n.a. | n.a. |
| 30 | <chem>C[C@H]1[C@@H](O)[C@@H](O)[C@H](O)[C@@H](CNS(C2=CC=C(CCN3N=NC(CN(CC4)CCN4C5=C(F)C=C6C(N(C7CC7)C=C(C6=O)C(O)=O)=C5)=C3)S2)(=O)=O)O1</chem> | n.a. | 2.37 ± 1.2 | 2.24 ± 0.23 |
| 31 | <chem>C[C@H]1[C@@H](O)[C@@H](O)[C@H](O)[C@@H](CNS(C2=CC=C(CCN3N=NC(CCN(CC4)CCN4C5=C(F)C=C6C(N(C7CC7)C=C(C6=O)C(O)=O)=C5)=C3)S2)(=O)=O)O1</chem> | n.a. | 2.53 ± 0.87 | 1.00 ± 0.06 |
| 5 | <chem>O=C(O)[C@H]1[C@@H](OC(C)=O)[C@@H](COC(C)=O)O[C@@H](SC2=CC=C([N+](O-)=O)C=C2)[C@@H]1OC(C)=O)C</chem> | n.a. | n.a. | n.a. |
| 6 | <chem>NC(C=C1)=CC=C1S[C@H]2[C@H](OC(C)=O)[C@@H](OC(C)=O)[C@@H](OC(C)=O)[C@@H](OC(C)=O)[C@@H](COC(C)=O)O2</chem> | n.a. | n.a. | n.a. |
| 7 | <chem>O=C(CN=[N+]=[N-])NC(C=C1)=CC=C1S[C@H]2[C@H](OC(C)=O)[C@@H](OC(C)=O)[C@@H](OC(C)=O)[C@@H](COC(C)=O)O2</chem> | n.a. | n.a. | n.a. |
| 8 | <chem>O=C(CCN=[N+]=[N-])NC(C=C1)=CC=C1S[C@H]2[C@H](OC(C)=O)[C@@H](OC(C)=O)[C@@H](OC(C)=O)[C@@H](COC(C)=O)O2</chem> | n.a. | n.a. | n.a. |
| 9 | <chem>O=C(CCCN=[N+]=[N-])NC(C=C1)=CC=C1S[C@H]2[C@H](OC(C)=O)[C@@H](OC(C)=O)[C@@H](OC(C)=O)[C@@H](COC(C)=O)O2</chem> | n.a. | n.a. | n.a. |
| 10 | <chem>O=C(CCCCN=[N+]=[N-])NC(C=C1)=CC=C1S[C@H]2[C@H](OC(C)=O)[C@@H](OC(C)=O)[C@@H](OC(C)=O)[C@@H](COC(C)=O)O2</chem> | n.a. | n.a. | n.a. |
| 16 | <chem>BrCC1=CC=C(S(=O)(Cl)=O)S1</chem> | n.a. | n.a. | n.a. |

Table S3: key compounds and intermediates as smiles (n.a. = not applicable).

Figure S3: Purity of key compounds by HPLC-UV.



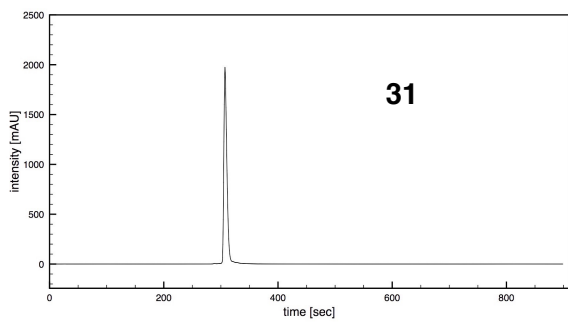
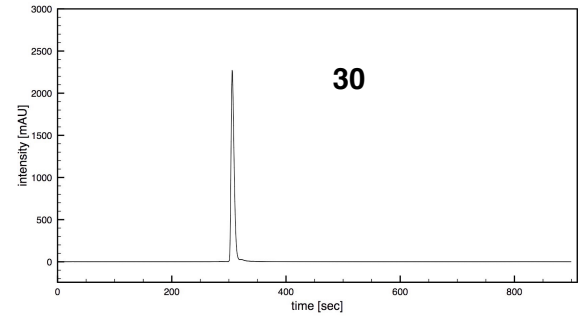
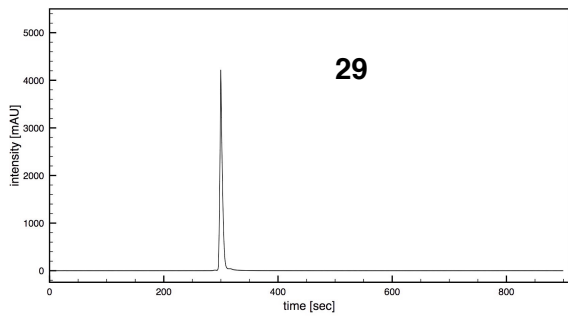
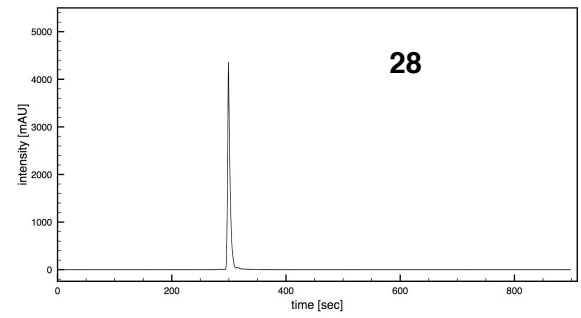
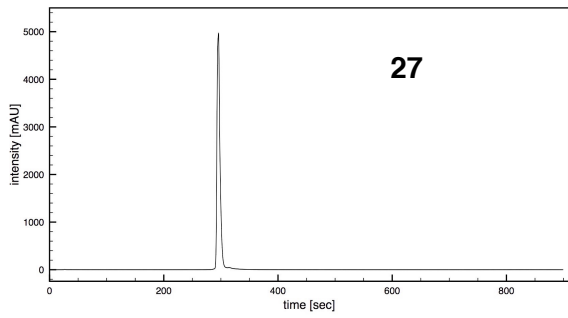
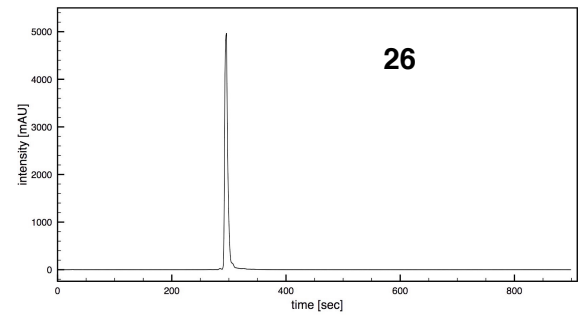
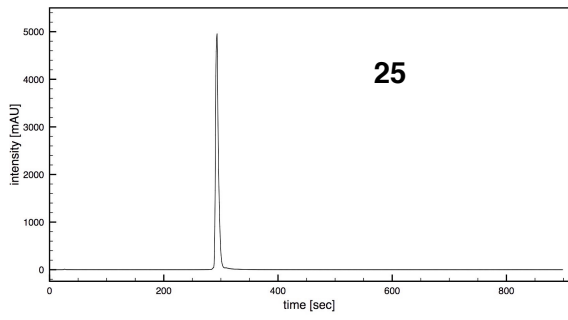
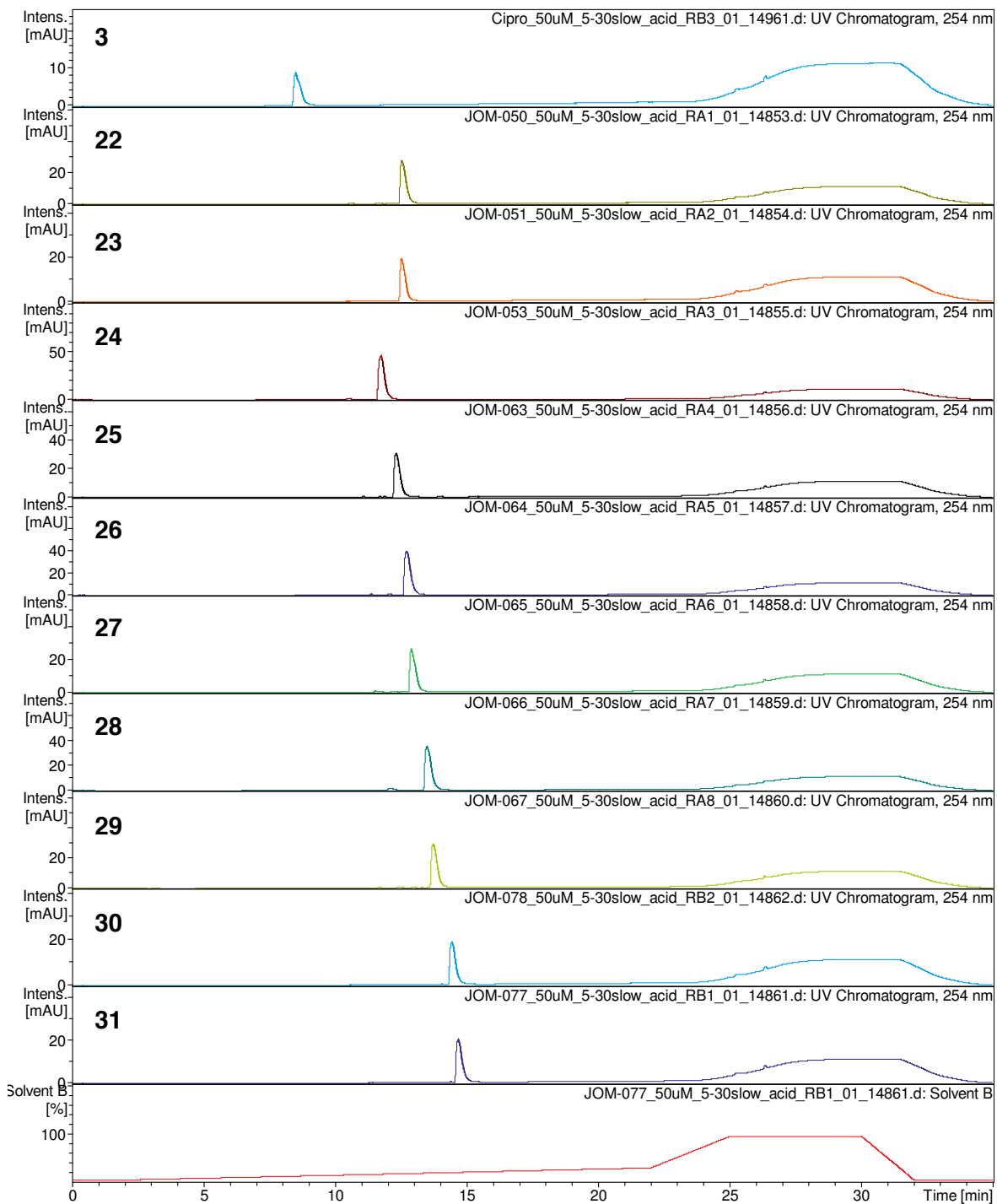
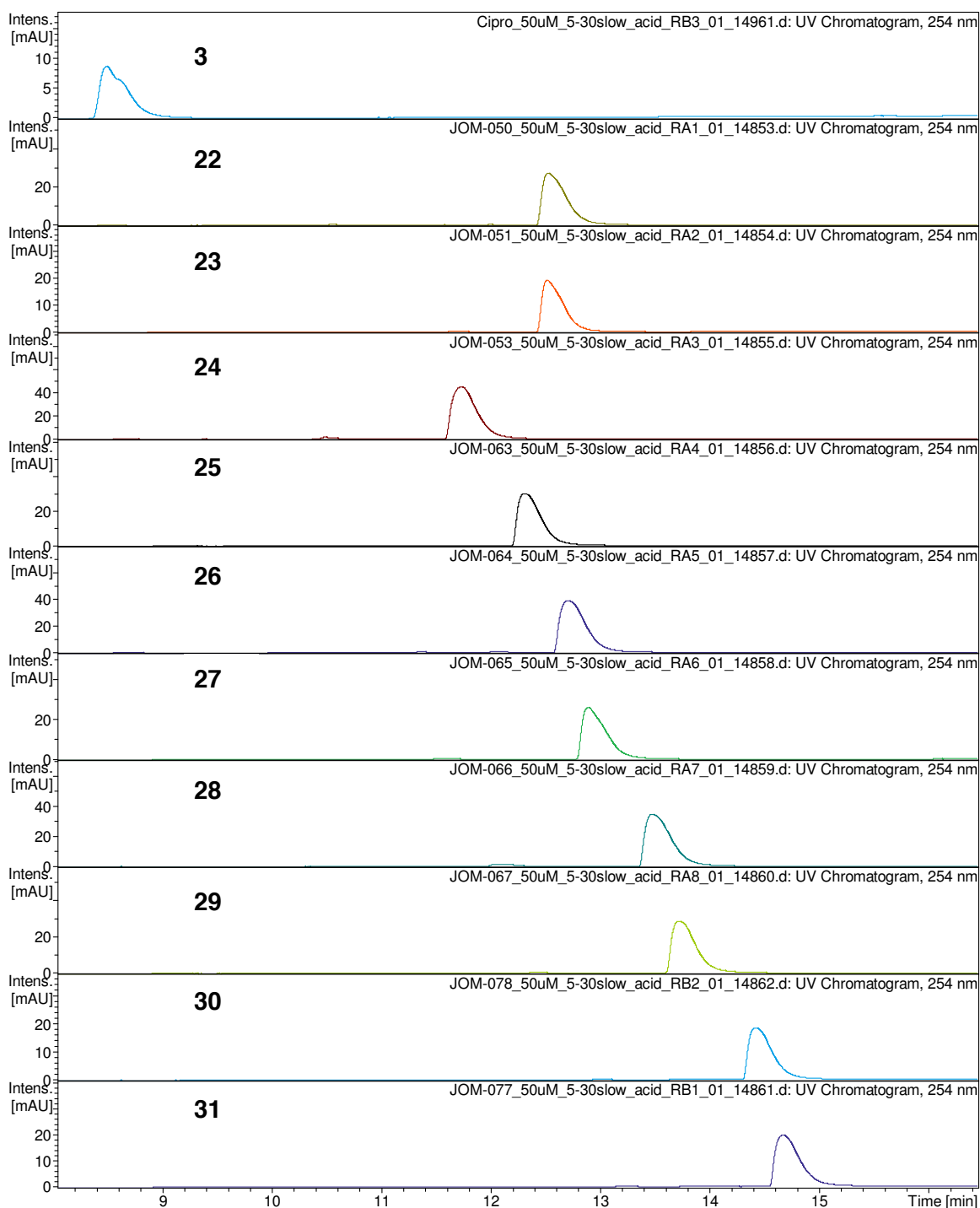


Table S4: Retention times measured by reversed-phase HPLC with a H₂O/MeCN system, using three gradients a-c: a. 5-55% B over 20 min; b. 5-30% B over 20 min; c. 2-25% B over 20 min. Eluent A: H₂O (0.1% formic acid), eluent B: MeCN (0.1% formic acid).

| compound | target | m | n | gradient | | |
|----------|--------|---|---|-------------------------------------|------|------|
| | | | | a | b | c |
| | | | | retention time t _R [min] | | |
| 22 | LecA | 0 | 1 | 9.0 | 12.5 | 15.7 |
| 23 | | 1 | 1 | 9.0 | 12.9 | 15.7 |
| 24 | | 0 | 2 | 8.6 | 11.7 | 14.9 |
| 25 | | 1 | 2 | 8.9 | 12.3 | 15.5 |
| 26 | | 0 | 3 | 9.1 | 12.7 | 15.9 |
| 27 | | 1 | 3 | 9.2 | 12.9 | 16.1 |
| 28 | | 0 | 4 | 9.5 | 13.5 | 16.7 |
| 29 | | 1 | 4 | 9.6 | 13.7 | 17.0 |
| 30 | LecB | 0 | - | 10.0 | 14.4 | 17.7 |
| 31 | | 1 | - | 10.2 | 14.7 | 18.0 |
| 3 | | - | - | 7.0 | 8.5 | 11.6 |

Figure S4: representative chromatogram of conjugates **22 - 31** and ciprofloxacin (**3**) from slow gradient b (see table S4) HPLC runs for lipophilicity comparison. Top: full UV-chromatogram and gradient for eluent B, bottom: UV-chromatogram from t = 8.2 - 16.4 min.

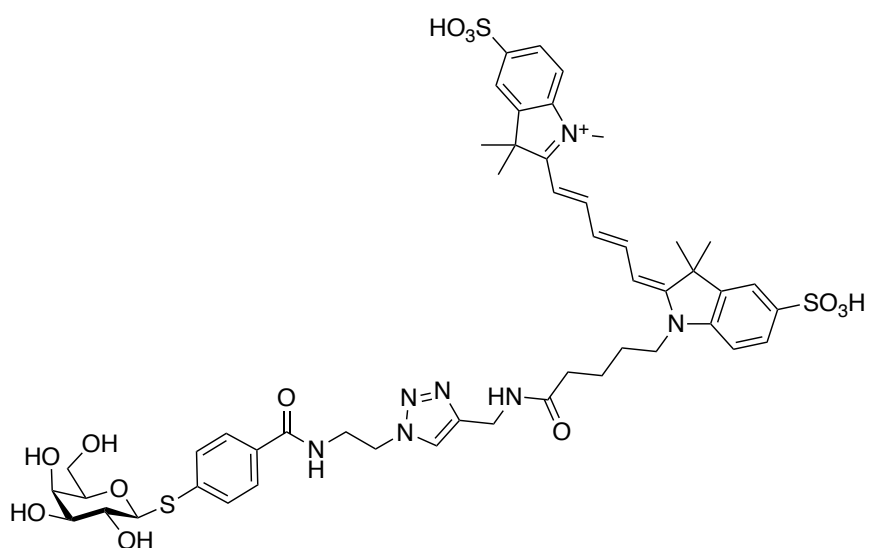




References

- Huang, X. Fluorescence polarization competition assay: the range of resolvable inhibitor potency is limited by the affinity of the fluorescent ligand. *J Biomol. Screen.* **2003**, *8*, 34-38.
- Sommer, R.; Wagner, S.; Varrot, A.; Nycholat, C. M.; Khaledi, A.; Häussler, S.; Paulson, J. C.; Imberty, A.; Titz, A. The virulence factor LecB varies in clinical isolates: consequences for ligand binding and drug discovery. *Chem. Sci.* **2016**, *7*, 4990–5001.

5.2. Supporting Information for Chapter 3.2



14

Figure S1. Chemical structure of the sCy5-based reporter ligand **14**.^[122] Fluorescence properties of cyanine-based fluorophores are less pH sensitive compared to fluorescein.

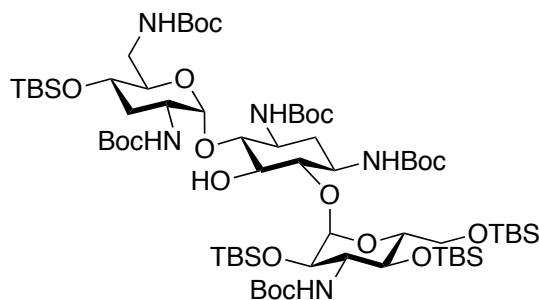
General information about chemistry, reporter ligand displacement assays and antibacterial susceptibility assays were described in chapters [3.1](#) and [5.3](#).

NMR analysis of protected tobramycin intermediates was not possible due to the high signal intensity of protecting groups and low resolution of residual signals. Further, protected intermediates were not analysable by HPLC-MS because they are not ionisable by electron spray ionisation. Additionally, they were not eluted from C18 column under standard conditions. The synthesis of Lectin probes **4**, **5** and **8** were described in chapter 3.1. Signals of LecB-targeted fucose/mannose-hybrid C-glycoside were assigned according to the nomenclature of fucose.

General procedure (i) for global deprotection of tobramycin conjugates **10** - **12**:

Protected lectin-targeted conjugate (**6**, **7**, **9**) was dissolved in HCl-saturated dioxane (3 - 4 mL, 4 M) while cooling on ice. H₂O (400 μ L) was added under vigorous stirring, and the reaction was allowed to warm to r.t.. Reaction progress was monitored by TLC (CH₂Cl₂ : MeOH, 9 : 1, for educt; CH₂Cl₂ : NH₄OH : MeOH, 3 : 2 : 1, for product) and stirred at r.t. until full consumption of the starting material. After completion, the solvent was evaporated *in vacuo* without heating. The residue was taken up in MeOH (1 mL) and the product was precipitated with chilled Et₂O. Afterwards, the precipitate was washed with chilled Et₂O and the solvent was evaporated *in vacuo*. The product was purified by HILIC (stationary phase: VP 250/10 Nucleodur HILIC, 5 μ m, Macharey-Nagel, mobile phase: 200 mM NH₄COOH : MeCN, 4 : 6, isocratic) on a semi-preparative scale.

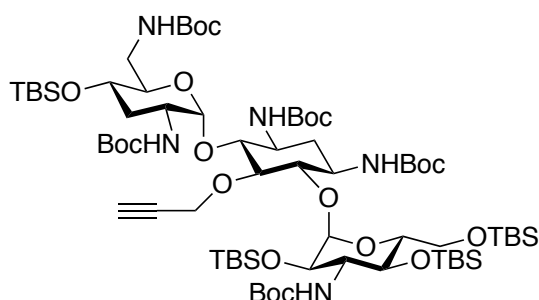
Boc-/TBS-protected tobramycin **2**:



The title compound was synthesised in two steps in analogy to Guchhait *et al.*^[93]: Tobramycin (**1**, 500 mg, 1.1 mmol, 1 eq.) was dissolved in MeOH/H₂O (2:1, 11 mL), together with Et₃N (3.35 mL, 24.2 mmol, 22 eq.) and Boc₂O (2.4 mL, 11 mmol, 10 eq.). The mixture was stirred at 55 °C for 20 h. The reaction was dried *in vacuo* by co-evaporation with CH₂Cl₂ and toluene. TBSCl (1.658 g, 11 mmol, 10 eq.) and *N*-Methyl imidazole (965 μ L, 12.1 mmol, 11 eq.) were dissolved in dry DMF (11 mL). This solution was then added to the dried residue and stirred at r.t. until disappearance of the starting material. After 36 h, reaction was poured on chilled water (100 mL), the precipitate was

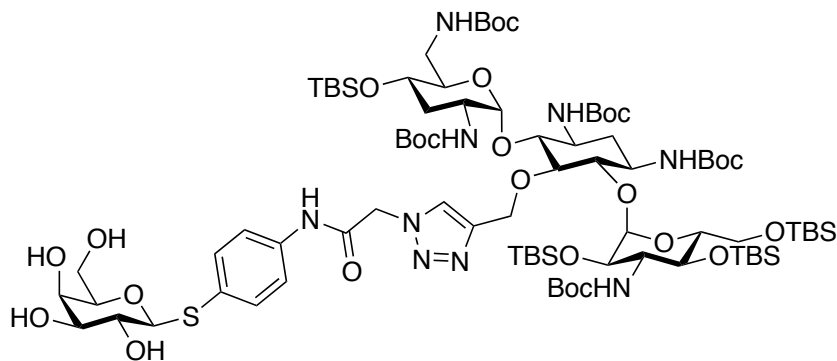
filtered off and washed with chilled water. Purification by MPLC (PE : EA, 5 - 20%) yielded the title compound as a white amorphous solid (1020 mg, 65% over two steps).

Propargylated Boc-/TBS-protected tobramycin **3**:



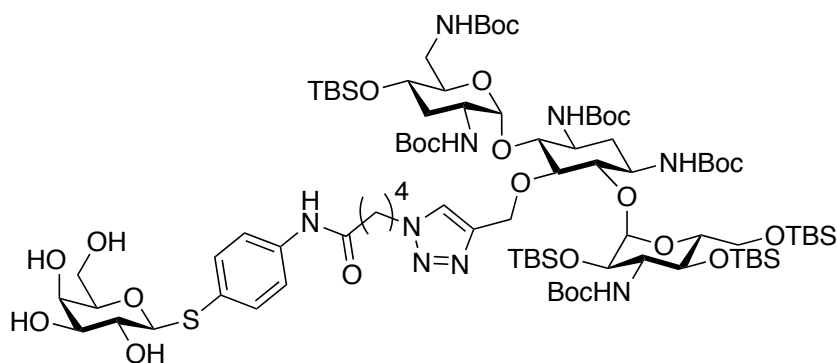
2 (880 mg, 0.62 mmol, 1 eq.), TBAHSO₄ (21 mg, 0.062 mmol, 10 mol%) and KOH (87 mg, 1.55 mmol, 2.5 eq.) were dissolved in dry toluene (10 mL). Propargylbromide (267 μ L, 80% in toluene, 2.48 mmol, 2.5 eq.) was added to the dispersion while stirring at r.t.. Reaction progress was monitored by TLC (PE : EA, 8 : 2) and further propargylbromide and KOH were added until full consumption of the starting material. The reaction was diluted with CH₂Cl₂ (50 mL) and washed twice with H₂O (50 mL) and satd. brine (50 mL). The organic phase was dried over Na₂SO₄ and the solvent was evaporated *in vacuo*. Purification by MPLC (PE : EA, 5 - 20%) gave the title compound as a white amorphous solid (830 mg, 91%).

LecA-targeted Boc-/TBS-protected tobramycin conjugate **6**:



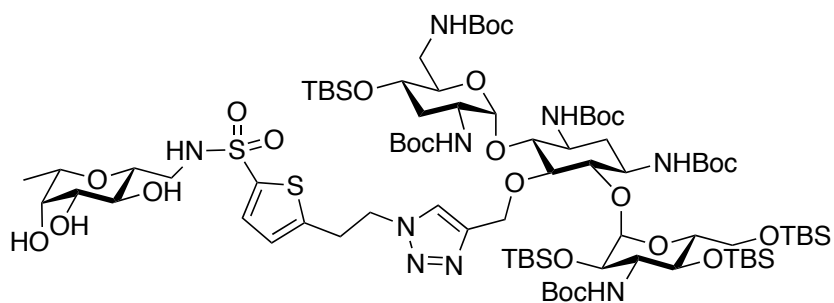
Azide **4** (23 mg, 0.062 mmol, 1 eq.) and alkyne **3** (100 mg, 0.068 mmol, 1.1 eq.) were dissolved in a degassed mixture of DMF/DIPEA (8 : 2, 3 mL) and heated to 45 °C. CuSO₄ (68 μ L of a 100 mM aqueous solution; 0.0068 mmol, 10 mol%) and sodium ascorbate (136 μ L of a 100 mM aqueous solution; 0.0136 mmol, 20 mol%) were added and the reaction was stirred for three days. After evaporation of the solvents *in vacuo*, the product was purified by MPLC (CH₂Cl₂ : MeOH, 1 - 20%) and obtained as a white amorphous solid (106 mg, 93%)

LecA-targeted Boc-/TBS-protected tobramycin conjugate **7**:



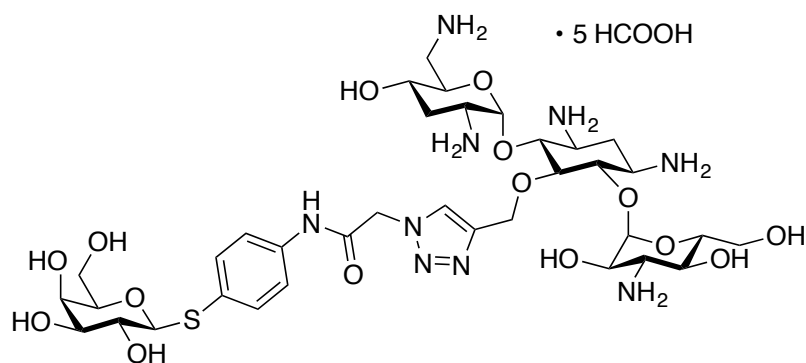
Azide **5** (25 mg, 0.061 mmol, 1 eq.) and alkyne **3** (100 mg, 0.068, 1.1 eq.) were dissolved in a degassed mixture of DMF/DIPEA (5 : 1, 1.2 mL). CuSO₄ (68 μL of a 100 mM aqueous solution; 0.0068 mmol, 11 mol%) and sodium ascorbate (136 μL of a 100 mM aqueous solution; 0.0136 mmol, 22 mol%) were added and the reaction was stirred for three days. After evaporation of the solvents *in vacuo*, the product was purified by MPLC (CH₂Cl₂ : MeOH, 1 - 20%) and obtained as a white amorphous solid (112 mg, 98%).

LecB-targeted Boc-/TBS-protected tobramycin conjugate **9**:



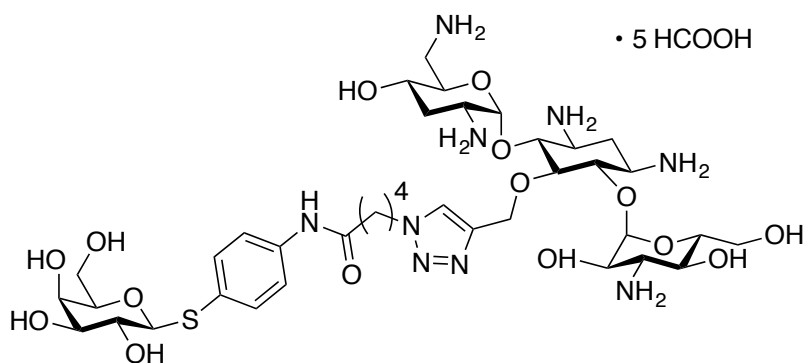
Azide **8** (50 mg, 0.13 mmol, 1 eq.) and alkyne **3** (209 mg, 0.143 mmol, 1.1 eq.) were dissolved in 1 mL degassed MeCN and heated to 55 °C. DIPEA (23 μL, 0.13 mmol, 1 eq.) and CuI (50 μL of a 50 mg/mL solution in a mixture of MeCN/H₂O [11 : 1], 2.5 μg, 13 μmol, 10 mol%) were added and the reaction was stirred for 18 h. After evaporation of the solvent *in vacuo*, the reaction was purified by MPLC (CH₂Cl₂ : MeOH, 1 - 10%). The product was obtained as a white amorphous solid (151 mg, 58%).

LecA-targeted tobramycin conjugate **10**:



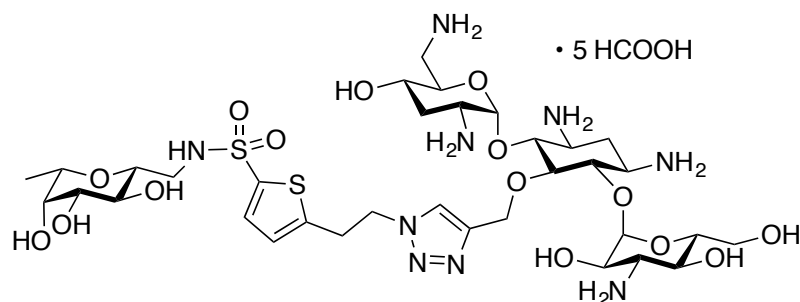
The title compound was synthesised from **6** (50 mg, 0.027 mmol) according to general procedure (i) and was obtained as a white amorphous solid (6 mg, 20%) after lyophilisation. ^1H NMR (500 MHz, $\text{H}_2\text{O}-d_2$) δ 8.42 (s, 5H, HCOO^-), 8.15 (s, 1H, triazole-H), 7.57 (d, $J = 8.7$ Hz, 2H, phenyl-H), 7.47 (d, $J = 8.7$ Hz, 2H, phenyl-H), 5.55 (d, $J = 2.9$ Hz, 1H, tobra-C1'-H), 5.47 (s, 2H, $\text{HNCO}-\text{CH}_2$ -triazole), 5.23 (d, $J = 3.5$ Hz, 1H, tobra-C1''-H), 5.17 (d, $J = 11.3$ Hz, 1H, triazole- CH_2 -tobra), 4.88 (d, $J = 11.4$ Hz, triazole- CH_2 -tobra), 4.71 (d, $J = 9.7$ Hz, 1H, Gal-C1-H), 4.17 – 4.06 (m, 2H, tobra-C5'-H + tobra-C4-H), 4.03 – 3.85 (m, 5H, Gal-C4-H + tobra-C5-H + tobra-C6-H + tobra-C2''-H + tobra-C5''-H), 4.03 – 3.51 (m, 7H, Gal-C5-H + Gal-C6-H' + Gal-C6-H + tobra-C4'-H + tobra-C2'-H + tobra-C6''-H + tobra-C4''-H), 3.66 (dd, $J = 3.3, 9.4$ Hz, 1H, Gal-C3-H), 3.64 – 3.52 (m, 4H, Gal-C2-H + tobra-C6''-H + tobra-C3''-H + tobra-C1-H), 3.51 – 3.40 (m, 1H, tobra-C3-H), 3.28 (d, $J = 6.2$ Hz, 2H, tobra-C6'-H), 2.46 (ddd, $J = 4.4, 12.7$ Hz, 1H, tobra-C2- H_e), 2.25 (ddd, $J = 4.1, 13.9$ Hz, 1H, tobra-C3'- H_e), 2.11 (ddd, 1H, tobra-C3'- H_a), 1.84 (ddd, $J = 12.7$ Hz, 1H, tobra-C2- H_a). ^{13}C NMR (126 MHz, $\text{H}_2\text{O}-d_2$) δ 170.90 (HCOO^-), 166.14, 143.63, 136.06, 132.29, 129.28, 126.39, 121.97, 101.07 (tobra-C1''), 93.04 (tobra-C1'), 88.04 (Gal-C1), 82.07, 81.55, 78.97, 76.76, 73.88, 73.64, 73.11, 69.05, 68.61, 68.37, 64.79, 64.09, 63.63, 60.92, 59.13, 54.70, 52.43, 49.75, 48.33, 47.38, 38.78, 28.84, 28.46.

LecA-targeted tobramycin conjugate **11**:

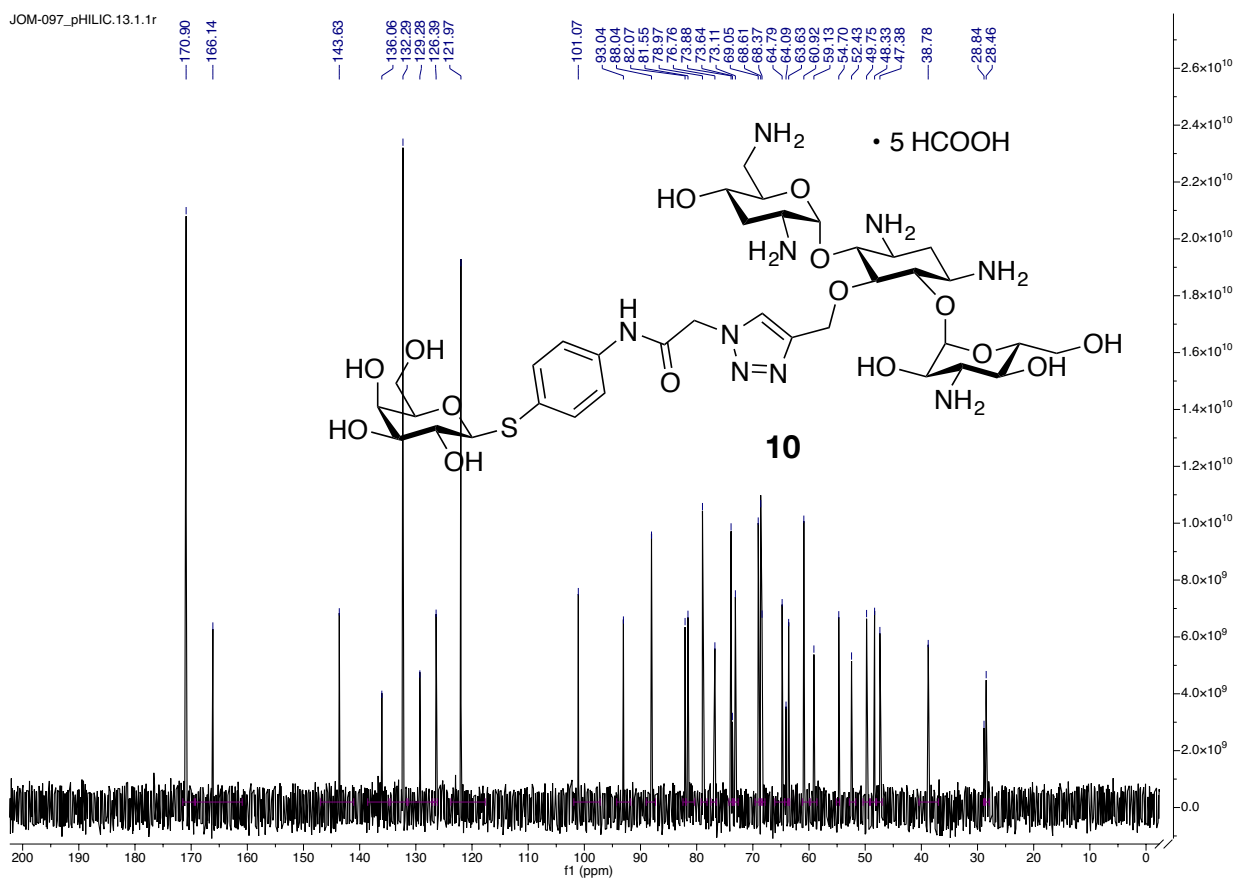
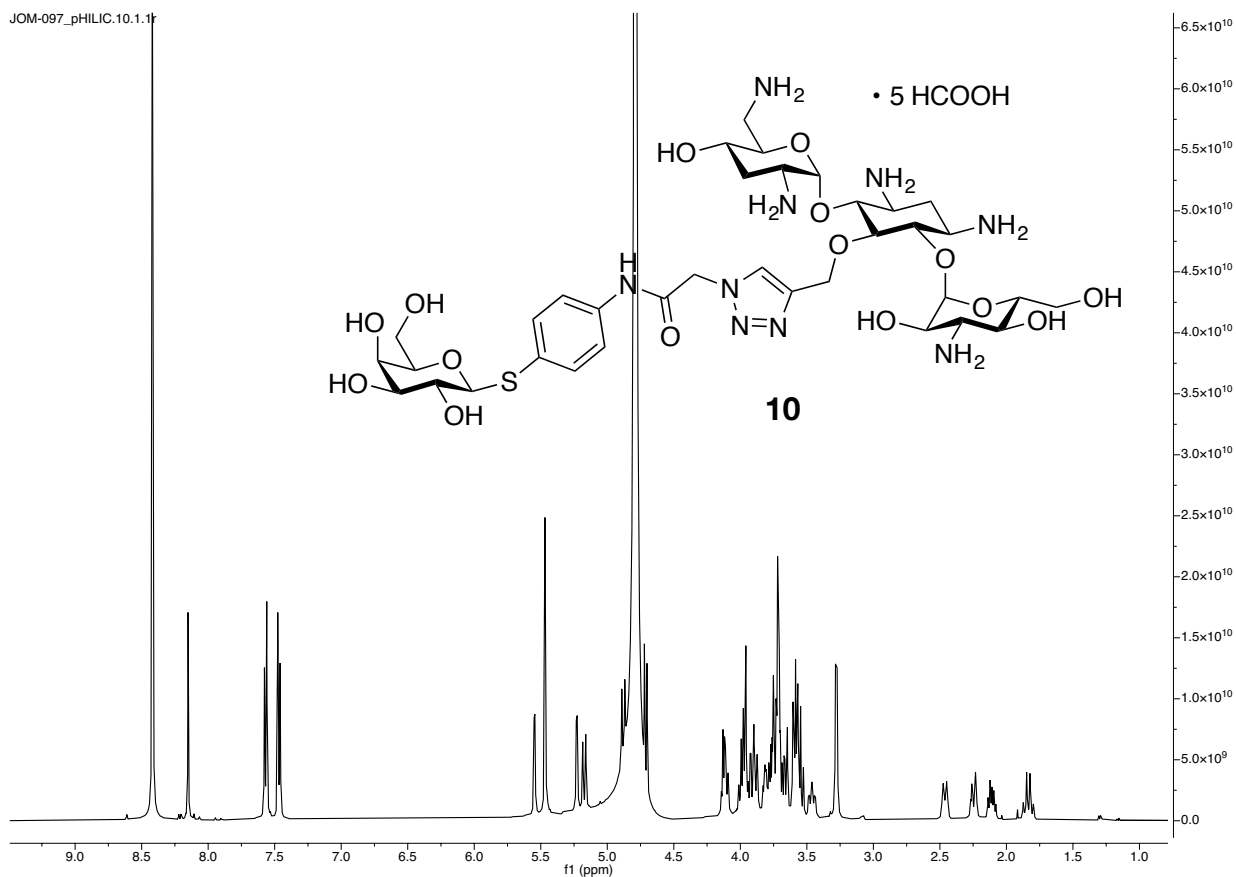


The title compound was synthesised from **7** (60 mg, 0.032 mmol) according to general procedure (i) and was obtained as a white amorphous solid (17 mg, 46%) after lyophilisation. ^1H NMR (500 MHz, $\text{H}_2\text{O}-d_2$) δ 8.41 (s, 5H, HCOO^-), 8.06 (s, 1H, triazole-H), 7.54 (d, $J = 8.7$ Hz, 2H, phenyl-H), 7.40 (d, $J = 8.7$ Hz, 2H, phenyl-H), 5.56 (d, $J = 2.9$ Hz, 1H, tobra-C1'-H), 5.19 (d, $J = 3.5$ Hz, 1H, tobra-C1"-H), 5.10 (d, $J = 11.2$ Hz, 1H, triazole- CH_2 -tobra), 4.83 (s, 1H, triazole- CH_2' -tobra), 4.70 (d, $J = 9.8$ Hz, 1H, Gal-C1-H), 4.48 (t, $J = 6.7$ Hz, 2H, R- CH_2 -triazole), 4.17 – 4.06 (m, 2H, tobra-C5'-H + tobra-C4-H), 4.00 – 3.88 (m, 4H, Gal-C4-H, tobra-C2"-H + tobra-C5"-H + tobra-C5-H), 3.85 (ddd, $J = 9.9, 2.4$ Hz, 1H, tobra-C5"-H), 3.82 – 3.68 (m, 7H, tobra-C4'-H + tobra-C4"-H + tobra-C6"-H + tobra-C2'-H + Gal-C5-H + Gal-C6-H + Gal-C6-H'), 3.66 (dd, $J = 9.4, 3.4$ Hz, 1H, Gal-C3-H), 3.63 – 3.44 (m, 5H, tobra-C3-H + tobra-C6"-H + tobra-C3"-H + tobra-C1-H + Gal-C2-H), 3.32 – 3.20 (m, 2H, tobra-C6'-H), 2.51 – 2.45 (m, 1H, tobra-C2- H_e), 2.43 (t, $J = 7.3$ Hz, 2H, $\text{HNCO}-\text{CH}_2$ -R), 2.24 (ddd, $J = 13.9, 4.1$ Hz, 1H), 2.11 (ddd, $J = 13.8, 7.9$ Hz, 1H, tobra-C3'- H_a), 1.95 (tt, $J = 12.7, 6.4$ Hz, 1H, linker- CH_2 -), 1.85 (ddd, $J = 12.6$ Hz, 1H, tobra-C2'- H_a), 1.68 – 1.53 (m, 2H, linker- CH_2 -). ^{13}C NMR (126 MHz, $\text{H}_2\text{O}-d_2$) δ 174.89, 170.86 (HCOO^-), 143.39, 136.58, 132.23, 128.79, 124.78, 122.25, 101.11 (tobra-C1"), 93.11 (tobra-C1'), 88.09 (Gal-C1), 82.05, 81.45, 78.96, 76.60, 73.89, 73.50, 73.10, 69.06, 68.61, 68.36, 64.73, 64.15, 63.67, 60.93, 59.04, 54.70, 50.10, 49.74, 48.32, 47.41, 38.84, 35.47, 28.71, 28.65, 28.46, 21.91.

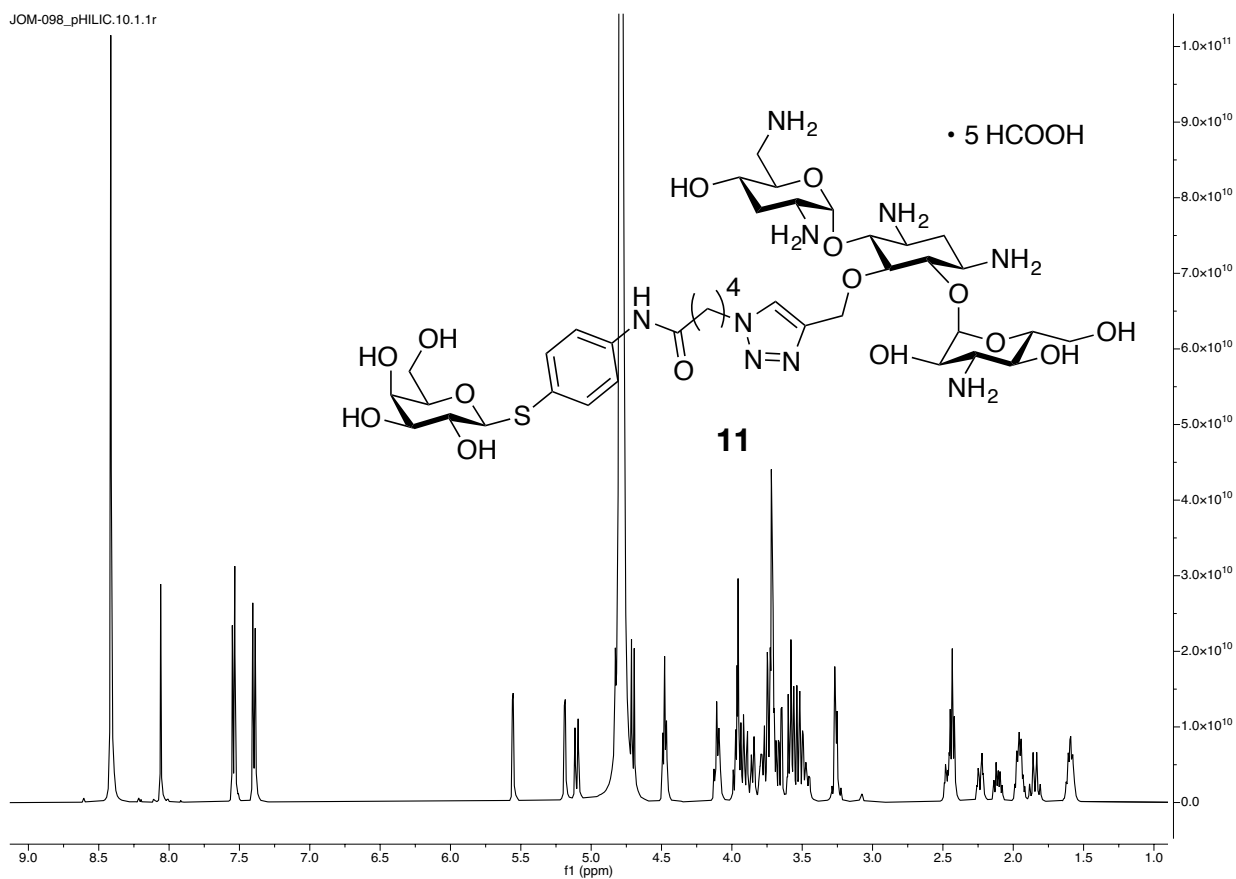
LecB-targeted tobramycin conjugate **12**:



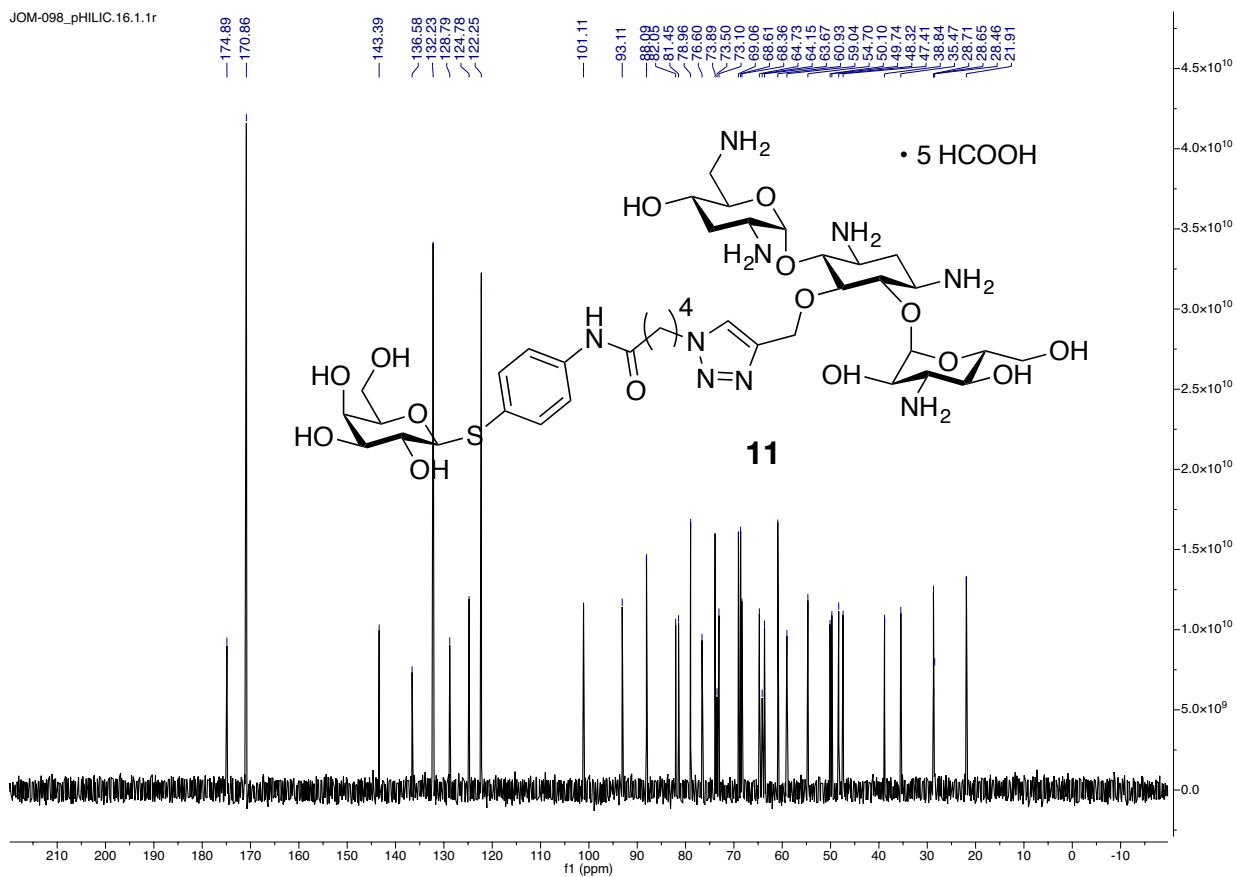
The title compound was synthesised from **9** (100 mg, 0.064 mmol) according to general procedure (i) and was obtained as a white amorphous solid (42 mg, 58%) after lyophilisation. ¹H NMR (500 MHz, H₂O-*d*₂) δ 8.42 (s, 5H, HCOO⁻), 7.84 (s, 1H, triazole-H), 7.51 (d, *J* = 3.8 Hz, 1H, thiophene-H), 6.91 (d, *J* = 3.9 Hz, 1H, thiophene-H), 5.51 (d, *J* = 3.0 Hz, 1H, tobra-C1'-H), 5.14 (d, *J* = 3.5 Hz, 1H, tobra-C1"-H), 5.06 (d, *J* = 11.0 Hz, 1H, triazole-CH₂-tobra), 4.76 – 4.66 (m, 3H, triazole-CH₂-tobra + thiophene-CH₂-CH₂-triazole), 4.13 – 4.05 (m, 1H, hybrid-C1-H), 4.00 (dd, *J* = 9.4 Hz, 1H, tobra-C4-H), 3.95 – 3.88 (m, 3H, tobra-C5-H + tobra-C2'-H + tobra-C5"-H), 3.87 – 3.80 (m, 2H, tobra-C4'-H + hybrid-C2-H), 3.77 – 3.70 (m, 4H, tobra-C6"-H + tobra-C2'-H + hybrid-C3-H + hybrid-C4-H), 3.59 – 3.41 (m, 7H, thiophene-CH₂-CH₂-triazole + hybrid-C5-H + tobra-C6"-H + tobra-C3"-H + tobra-C1-H + tobra-C6-H), 3.41 – 3.36 (m, 2H, tobra-C3-H + tobra-C4"-H), 3.35 – 3.30 (m, 2H, tobra-C6'-H + hybrid-C7-H), 3.27 (dd, *J* = 13.7, 8.4 Hz, 1H, hybrid-C7-H), 3.19 (ddd, *J* = 9.8, 7.8, 2.3 Hz, 1H, tobra-C5'-H), 3.04 (dd, *J* = 13.7, 7.7 Hz, 1H, tobra-C6'-H), 2.43 (ddd, *J* = 12.7, 4.4 Hz, 1H, tobra-C2-H_e), 2.27 (ddd, *J* = 13.6, 4.1 Hz, 1H, tobra-C3'-H_e), 2.12 (ddd, *J* = 13.5, 8.4 Hz, 1H, tobra-C3'-H_a), 1.78 (ddd, *J* = 12.6 Hz, 1H, tobra-C2-H_a), 1.14 (d, *J* = 6.4 Hz, 3H, hybrid-C6-H). ¹³C NMR (126 MHz, H₂O-*d*₂) δ 170.92 (HCOO⁻), 147.50, 143.55, 137.06, 133.04, 127.42, 125.53, 101.00 (tobra-C1"), 93.24 (tobra-C1'), 82.21, 81.66, 77.38, 77.18, 74.19, 73.88, 73.14, 72.98, 71.63, 68.42, 68.04, 64.83, 64.19, 63.92, 59.20, 54.74, 51.22, 49.70, 48.38, 47.57, 44.04, 39.15, 29.99, 29.32, 28.70, 15.71.

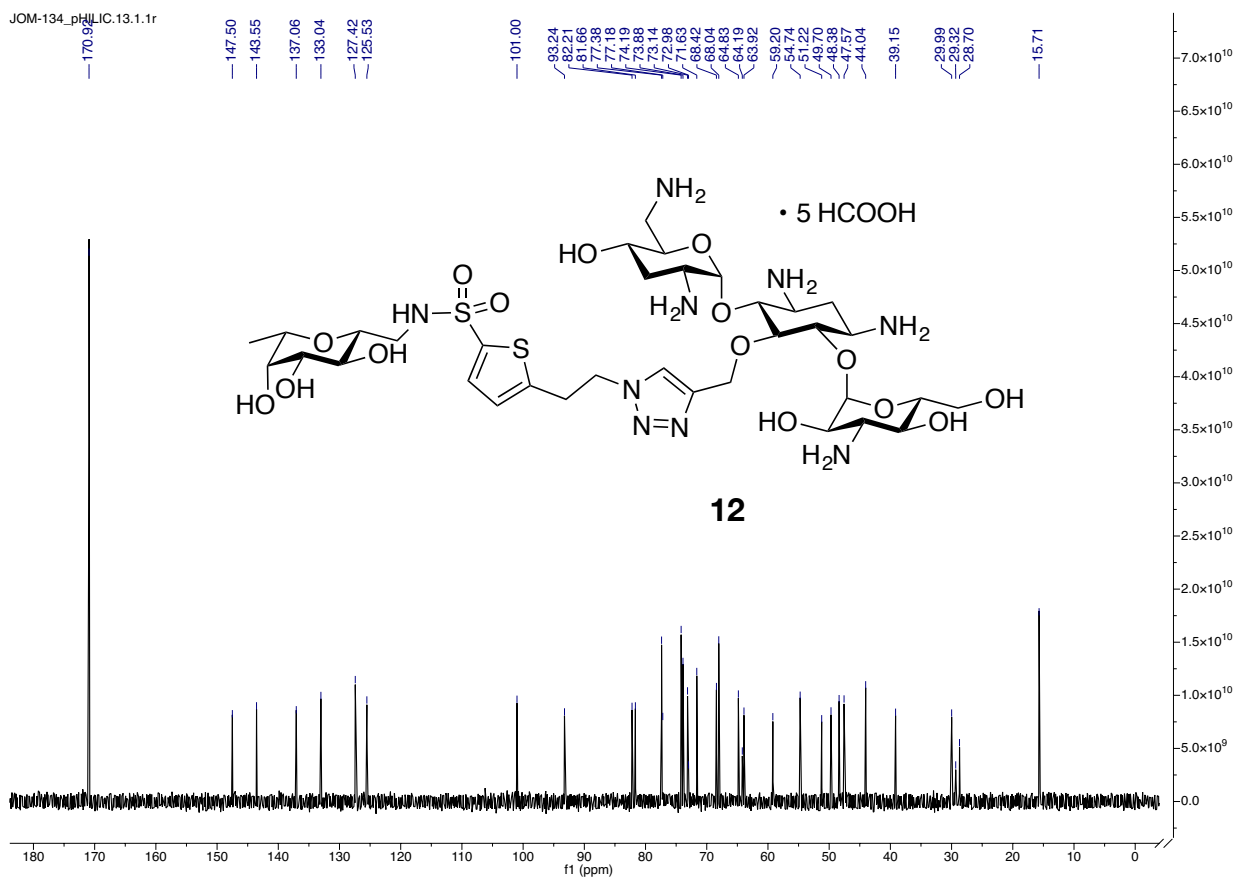
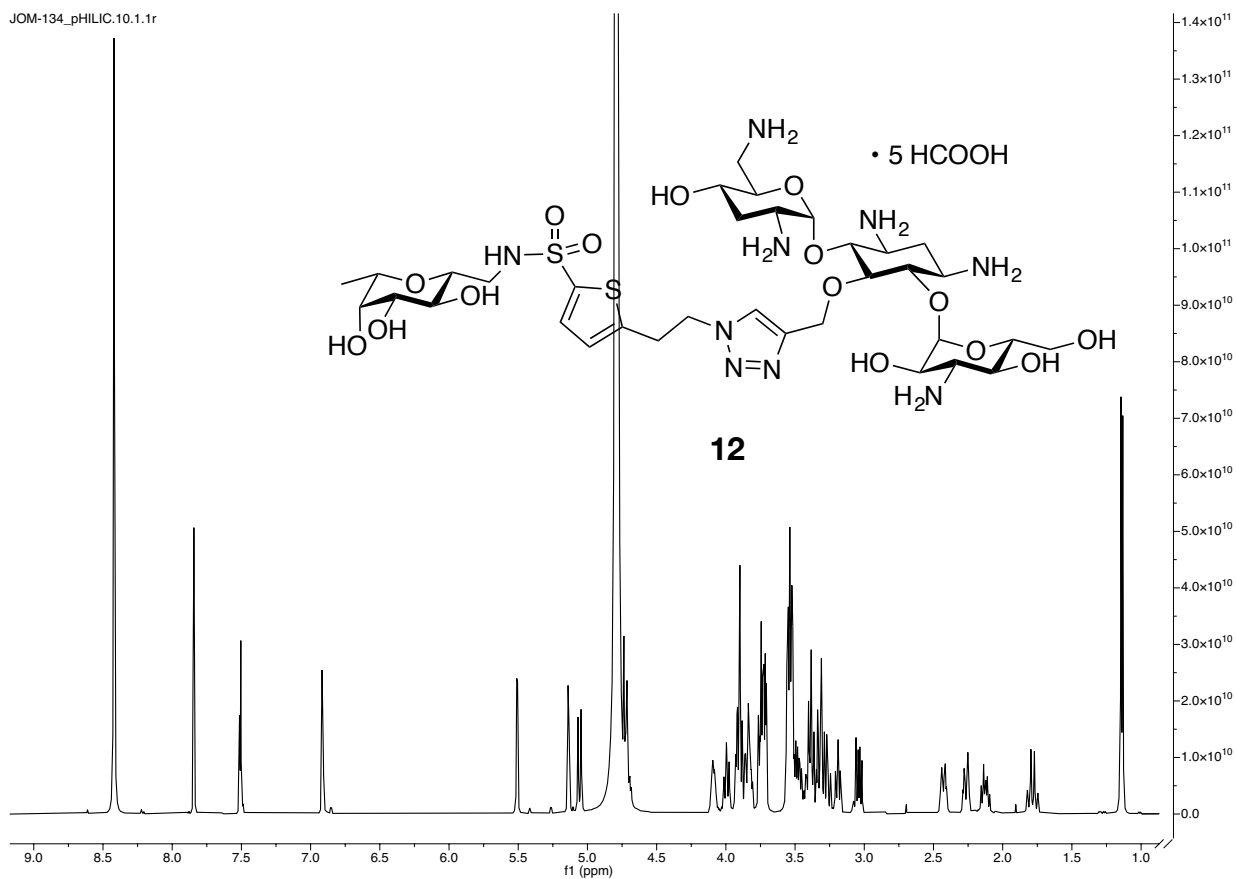


JOM-098_pHILIC.10.1.1r



JOM-098_pHILIC.16.1.1r





5.3. Supporting Information for Chapter 3.3

Chemical Synthesis

Commercial chemicals and solvents were used without further purification. Deuterated solvents were purchased from Eurisotop (Saarbrücken, Germany). Ciprofloxacin was purchased from Sigma-Aldrich (purity $\geq 98\%$, HPLC, Merck KGaA, Darmstadt, Germany), and ciprofloxacin · HCl was purchased from Cayman Chemical (Ann Arbor, Michigan, USA). Thin layer chromatography (TLC) was performed on Silica Gel 60 coated aluminum sheets containing a fluorescence indicator (Merck KGaA, Darmstadt, Germany) and developed under UV light (254 nm) and aqueous KMnO₄ solution or a molybdate solution (a 0.02 M solution of ammonium cerium sulfate dihydrate and ammonium molybdate tetrahydrate in aqueous 10% H₂SO₄) or ninhydrin solution (0.6 g ninhydrin in 200 mL n-BuOH and 6 mL AcOH). Self-packed Silica Gel 60 columns (60 Å, 400 mesh particle size, Fluka, for normal-phase liquid chromatography) or Chromabond Flash RS15 C18 ec columns (Macherey-Nagel, Düren, Germany, for reversed-phase liquid chromatography), were used on a Teledyne Isco Combiflash Rf200 system for preparative medium pressure liquid chromatography (MPLC). Nuclear magnetic resonance (NMR) spectroscopy was performed on a Bruker Avance III 500 UltraShield spectrometer at 500 MHz (¹H) or 126 MHz (¹³C). Chemical shifts are given in parts per million (ppm) and were calibrated on residual solvent peaks as an internal standard. Multiplicities were specified as s (singlet), d (doublet), t (triplet), q (quartet), or m (multiplet). The signals were assigned with the help of ¹H,¹H COSY, and DEPT-135-edited ¹H,¹³C HSQC experiments. Assignment numbering of the C-glycoside atoms and groups corresponds to the numbering in fucose. Assignment numbering of the galactoside atoms and groups corresponds to the numbering in galactose. Assignment numbering of the fluoroquinolone atoms and groups corresponds to the numbering in ciprofloxacin (cipro).^[183] If not stated otherwise, the purity of the final

compounds was further analyzed by HPLC-UV, and all UV active compounds had a purity of at least 95%. Chromatographic separation was performed on a Dionex Ultimate 3000 HPLC (Thermo Scientific, Germany) with UV detection at 254 nm using a RP-18 column (100/2 Nucleoshell RP18plus, 2.7 μm , from Macherey-Nagel, Germany) as a stationary phase. LCMS-grade distilled MeCN and double distilled H₂O were used as mobile phases containing formic acid (0.1% v/v). In a gradient run, an initial concentration of 5% MeCN in H₂O was increased to 95% during 7 min at a flow rate 600 $\mu\text{L}/\text{min}$. The injection volume was 4 μL of 1 mM compound in H₂O/DMSO = 100:1. Mass spectra were obtained on a Bruker amaZon SL spectrometer and data were analysed using DataAnalysis from Bruker. UPLC-HRMS for key compounds were obtained after chromatographic separation using a RP-18 column (EC 150/2 Nucleodur C18 Pyramid, 3 μm , from Macherey-Nagel, Germany) and a Q Exactive Focus Orbitrap spectrometer (Thermo Scientific, Germany). The data was analyzed using Xcalibur data acquisition and interpretation software (Thermo Scientific, Germany).

Methyl 4-mercaptobenzoate (**5**): **5** was synthesised according to the protocol from Novoa *et al.*^[142]: 4-mercapto benzoic acid (5.2 g, 34 mmol, 1 eq.) was dissolved in 50 mL dry MeOH (purged with Ar) and treated to 6 drops conc. H₂SO₄. The mixture was refluxed for three days. After cooling to room temperature, the pH was adjusted to 5 using NaOMe (1 M in MeOH) and the solution was loaded on silica *in vacuo*. The product was eluted with CH₂Cl₂. After evaporation of the solvent, the product (4.8 g, 80%, 93% purity determined by ¹H-NMR) was used without further purification. ¹H NMR (500 MHz, CHCl₃-*d*) δ 7.89 (d, J = 8.4 Hz, 2H, Ar-H), 7.29 (d, J = 8.4 Hz, 2H, Ar-H), 3.90 (s, 3H, COOMe), 3.62 (s, 1H, SH).

p-Methylbenzoyl 2,3,4,6-Tetra-*O*-acetyl- β -D-thiogalactopyranoside (**6**): **6** was synthesised according to a previously reported protocol from Novoa *et al.*^[142]: β -D-Galactose

pentaacetate (3 g, 7.7 mmol, 1 eq.) was dissolved in 20 mL dry CH₂Cl₂ in a heat-dried flask under a N₂ atmosphere. The solution was cooled on ice and BF₃ • Et₂O (3.8 mL, 30.7 mmol, 4 eq.) was added dropwise under vigorous stirring. A solution of **5** (3 eq., 0.4 M) was added dropwise to the reaction. The reaction was allowed to warm to r.t. and stirred over night. After the reaction was quenched with ice water, the organic phase was subsequently washed with satd. aqueous NaHCO₃ (2x), water (2x) and satd. brine (2x). The combined organic layers were dried over Na₂SO₄ and the solvent was evaporated *in vacuo*. After purification by MPLC (SiO₂, EtOAc in toluene, 5-30%), the title compound was crystallised from a mixture of EtOAc in hexane (1:1) and obtained as white crystals (2.2 g, 58%). ¹H NMR (500 MHz, MeOH-*d*₄) δ 7.96 (d, J = 8.5 Hz, 2H, Ar-H), 7.58 (d, J = 8.5 Hz, 2H, Ar-H), 5.46 (dd, J = 2.9, 1.1 Hz, 1H, glyco-H-4), 5.26 – 5.17 (m, 2H, glyco-H2, glyco-H-3), 5.15 (dd, J = 8.7, 1.4 Hz, 1H, glyco-H-1), 4.25 (td, J = 6.4, 1.2 Hz, 1H, glyco-H-5), 4.16 (d, J = 6.0 Hz, 2H, glyco-H6), 3.90 (s, 3H, COOCH₃), 2.14 (s, 3H, Ac-CH₃), 2.05 (s, 3H, Ac-CH₃), 2.03 (s, 3H, Ac-CH₃), 1.94 (s, 3H, Ac-CH₃). ¹³C NMR (126 MHz, MeOH-*d*₄) δ 172.03 (C=O), 171.88 (C=O), 171.36 (C=O), 171.18 (C=O), 168.01 (C=OOMe), 141.30 (Ar-C), 131.07 (Ar-C), 130.85 (Ar-C), 129.99 (Ar-C), 85.58 (glyco-C-1), 75.60 (glyco-C-5), 73.25 (glyco-C-2), 69.02 (glyco-C-2), 68.41 (glyco-C-4), 63.01 (glyco-C-3), 52.71 (COOCH₃), 20.63 (Ac-CH₃), 20.60 (Ac-CH₃), 20.48 (2x Ac-CH₃). LR-MS: *m/z* = 521.1 [M+Na]⁺.

p-benzoyl-β-D-thiogalactopyranoside (**7**): **6** (1 g, 2.0 mmol, 1 eq.) was dispersed in 20 mL dry MeOH. A solution of NaOMe (300 μL, 1 M, 1.5 eq.) in MeOH was added dropwise while cooling on ice. The reaction was allowed to warm to r.t. and stirred for 30 min. A solution of LiOH (50 mg, 2 mmol, 1 eq.) in 3 mL water was added to the reaction. After 1 h, the pH was adjusted to pH = 4 with Amberlite IR-120 H⁺ exchange resin while cooling on ice. The resin was removed by filtration and the solvent was evaporated *in vacuo*. The title

compound was obtained as a white amorphous solid (630 mg, quant.) containing approximately 17% NaOAc as an impurity, determined by ^1H NMR. ^1H NMR (500 MHz, MeOH- d_4) δ 7.88 (d, J = 8.5 Hz, 2H, Ar-H), 7.51 (d, J = 8.4 Hz, 2H, Ar-H), 4.70 (d, J = 9.8 Hz, 1H, glyco-H-1), 3.94 (dd, J = 3.3, 1.0 Hz, 1H, glyco-H-4), 3.77 (dd, J = 11.5, 6.8 Hz, 1H, glyco-H-6), 3.72 (dd, J = 11.5, 5.3 Hz, 1H, glyco-H-6), 3.68 – 3.58 (m, 2H, glyco-H-2, glyco-H-5), 3.54 (dd, J = 9.2, 3.4 Hz, 1H, glyco-H-3). ^{13}C NMR (126 MHz, MeOH)- d_4 δ 174.26 (COOH), 139.62 (Ar-C), 136.33 (Ar-C), 130.78 (Ar-CH), 130.10 (Ar-CH), 89.51 (glyco-C-1), 80.55 (glyco-C-5), 76.27 (glyco-C-3), 70.95 (glyco-C-2), 70.42 (glyco-C-4), 62.56 (glyco-C-6). LR-MS: m/z = 315.1 [M-H].

Bn-protected, LecA-targeted peptide linker (**9**): **7** (316 mg, 1 mmol, 1 eq.), **8** (590 mg, 1.3 mmol, 1.3 eq.) and TBTU (414 mg, 1.3 mmol, 1.3 eq.) were dissolved in 10 mL dry DMF. DIPEA (360 μL , 2 mmol, 2 eq.) was added dropwise and the reaction was stirred for 1 h at room temperature. The solvent was evaporated *in vacuo* and the reaction was purified by MPLC (MeCN in EtOH/ H_2O (1:1) 5-15%). The title compound was obtained as a white amorphous solid (420 mg, 58%), approximately 15% contaminated with coupling reagent side products, determined by ^1H -NMR. ^1H NMR (500 MHz, MeOH- d_4) δ 8.33 (d, J = 7.1 Hz, 1H, NH), 7.98 (d, J = 8.1 Hz, 1H, NH), 7.88 – 7.81 (m, 2H, glyco-Ar-H), 7.65 – 7.55 (m, 2H, glyco-Ar-H), 7.39 – 7.25 (m, 5H, Bn), 5.16 (d, J = 12.3 Hz, 2H, Bn), 5.12 (d, J = 12.3 Hz, 1H, Bn), 4.72 (d, J = 9.7 Hz, 1H, glyco-H-1), 4.49 – 4.37 (m, 2H, Ala- C_α -H, Ala'- C_α -H, Leu- C_α -H), 3.95 (d, J = 16.9 Hz, 1H, Gly- C_α -H), 3.92 (dd, J = 3.4, 0.9 Hz, 1H, glyco-H-4), 3.79 (d, J = 17.0 Hz, 1H, Gly- C_α -H), 3.79 – 3.68 (m, 2H, glyco-H-6), 3.66 (t, J = 9.4 Hz, 1H, glyco-H-2), 3.62 (ddd, J = 6.7, 5.1, 1.1 Hz, 1H, glyco-H-5), 3.52 (dd, J = 9.1, 3.3 Hz, 1H, glyco-H-3), 1.74 – 1.50 (m, 3H, Leu-CH, Leu- CH_2), 1.48 (d, J = 7.2 Hz, 3H, Ala- CH_3), 1.41 (d, J = 7.3 Hz, 3H, Ala'- CH_3), 0.84 (d, J = 6.0 Hz, 3H, Leu- CH_3), 0.80 (d, J = 5.9 Hz, 3H, Leu- CH_3). ^{13}C NMR (126 MHz, MeOH- d_4) δ 176.17 (CONH), 174.63 (CONH), 173.76

(CONH), 171.59 (CONH), 169.71 (COOBn), 142.01 (Ar-C), 137.26 (Ar-C), 132.53 (Ar-C), 130.03 (Ar-C), 129.59 (Ar-C), 129.30 (Ar-C), 129.24 (Ar-C), 129.15 (Ar-C), 89.04 (glyco-C-1), 80.76 (glyco-C-5), 76.31 (glyco-C-3), 70.90 (glyco-C-2), 70.41 (glyco-C-4), 67.93, 62.65 (glyco-C-6), 52.93 (Leu-C α), 52.00 (Ala-C α), 49.70 (Leu-C α), 43.75 (Gly-C α), 41.73 (Leu-CH), 25.64 (Leu-CH $_2$), 23.44 (Leu-CH $_3$), 21.77 (Leu-CH $_3$), 17.27 (Ala'-CH $_3$), 17.22 (Ala-CH $_3$). LR-MS: $m/z = 719.3 [M+H]^+$.

LecA-targeted peptide linker (**10**): **9** (116 mg, 0.16 mmol, 1 eq.) was dissolved DMF (2 mL) at 50 °C. LiOH (35 mg, 9 eq.) was dissolved in 1 mL H $_2$ O and added stepwise over three days until full turnover was observed. The reaction was neutralised with Amberlite IR-120 H $^+$ exchange resin. After filtration, the solvent was removed via lyophilisation. The product was purified by preparative HPLC (MeCN:H $_2$ O, 5-30%, 0.1% formic acid) and obtained as a white amorphous solid (49 mg, 49 %). ^1H NMR (500 MHz, DMSO- d_6) δ 12.44 (br s, 1H, COOH), 8.60 (d, $J = 6.6$ Hz, 1H, NH), 8.25 (t, $J = 5.8$ Hz, 1H, NH), 8.16 (d, $J = 7.1$ Hz, 1H, NH), 7.84 (d, $J = 8.5$ Hz, 2H, Ar-H), 7.76 (d, $J = 8.5$ Hz, 1H, NH), 7.50 (d, $J = 8.5$ Hz, 2H, Ar-H), 5.21 (d, $J = 6.1$ Hz, 1H, OH), 4.91 (br s, 1H, OH), 4.71 (d, $J = 9.6$ Hz, 1H, glyco-H-1), 4.66 (br s, 1H, OH), 4.52 (d, $J = 4.4$ Hz, 1H, OH), 4.45 – 4.31 (m, 2H, Ala-C α -H), 4.16 (dq, $J = 7.3, 7.3$ Hz, 1H, Ala-C α -H), 3.76 – 3.60 (m, 3H, Gly-CH $_2$, glyco-H-4), 3.57 – 3.42 (m, 4H, glyco-H-6, glyco-H-2, glyco-H-5), 3.38 (dd, $J = 9.5, 3.1$ Hz, 1H, glyco-H-3), 1.56 (dh, $J = 13.3, 6.5$ Hz, 1H, Leu-CH), 1.51 – 1.41 (m, 2H, Leu-CH $_2$), 1.34 (d, $J = 7.2$ Hz, 3H, Ala-CH $_3$), 1.27 (d, $J = 7.3$ Hz, 3H, Ala-CH $_3$), 0.82 (d, $J = 2.5$ Hz, 3H, Leu-CH $_3$), 0.80 (d, $J = 2.6$ Hz, 3H, Leu-CH $_3$). ^{13}C NMR (126 MHz, DMSO- d_6) δ 174.04 (NHC=O), 173.03 (NHC=O), 171.73 (NHC=O), 168.51 (NHC=O), 165.95 (COOH), 140.30 (Ar-C), 130.82 (Ar-C), 128.06 (Ar-C), 127.53 (Ar-C), 86.63 (glyco-C-1), 79.32 (glyco-C-5), 74.68 (glyco-C-3), 69.16 (glyco-C-2), 68.41 (glyco-C-4), 60.62 (glyco-C-6), 50.43 (Leu-C α), 49.55 (Ala-C α),

47.50 (Ala-C α), 42.17 (Gly-C α), 40.91 (Leu-CH $_2$), 23.94 (Leu-CH), 23.14 (Leu-CH $_3$), 21.62 (Leu-CH $_3$), 17.52 (Ala-CH $_3$), 17.00 (Ala-CH $_3$). LR-MS: m/z = 629.2 [M+H] $^+$.

N- β -L-Fucopyranosylmethyl-2-(*p*-carboxybenzyl-methyl)-sulfonamide (**13**): **11** (400 mg, 2.26 mmol, 1 eq.) was dissolved in dry DMF (15 mL) and K $_2$ CO $_3$ (625 mg, 4.52 mmol, 2 eq.) was added while cooling on ice. Sulfonylchloride **12** (970 mg, 4.13 mmol, 1.8 eq.) was dissolved in dry DMF (5 mL) and added dropwise to the starting material. The ice bath was removed and the reaction was stirred at room temperature over night. The reaction was quenched with MeOH (1 mL) and neutralised to pH 7 with HCl (1 M) while cooling on ice. The solvent was removed *in vacuo* and the reaction was purified by MPLC (SiO $_2$, MeOH in CH $_2$ Cl $_2$, 1-10%). The title compound was obtained as a white amorphous solid (228 mg, 27 %). 1 H NMR (500 MHz, DMSO-*d* $_6$) δ 8.13 (d, J = 8.4 Hz, 2H, Ar-H), 7.94 (d, J = 8.5 Hz, 2H, Ar-H), 7.81 (br s, 1H, -NH SO_2 -), 4.78 (d, J = 5.3 Hz, 1H, OH), 4.59 (d, J = 5.7 Hz, 1H, OH), 4.26 (d, J = 5.4 Hz, 1H, OH), 3.89 (s, 3H, COOCH $_3$), 3.39 – 3.35 (m, 1H, glyco-H-4), 3.29 (q, J = 6.2 Hz, 1H, glyco-H-5), 3.24 (d, J = 13.4 Hz, 1H, linker-CH $_2$ -), 3.18 (ddd, J = 9.0, 5.7, 3.2 Hz, 1H, glyco-H-3), 3.11 (td, J = 9.2, 4.7 Hz, 1H, glyco-H-1), 2.96 (td, J = 8.8, 2.2 Hz, 1H, glyco-H-2), 2.78 – 2.68 (m, 1H, linker-CH $_2$ -), 1.01 (d, J = 6.4 Hz, 6H, glyco-H-6). 13 C NMR (126 MHz, DMSO-*d* $_6$) δ 165.28 (C=O), 145.10 (Ar-C), 132.63 (Ar-C), 129.88 (Ar-C), 126.89 (Ar-C), 78.33 (glyco-C-2), 74.58 (glyco-C-3), 73.57 (glyco-C-5), 71.51 (glyco-C-4), 68.22 (glyco-C-1), 52.61 (COOCH $_3$), 44.56 (linker-CH $_2$ -), 16.86 (glyco-C-6). LR-MS: m/z = 376.1 [M+H] $^+$.

N- β -L-Fucopyranosylmethyl-2-(*p*-carboxybenzyl)-sulfonamide (**14**): **13** (224 mg, 0.60 mmol, 1 eq.) was dissolved in a mixture of THF, MeOH and H $_2$ O (3:1:1, 7 mL) and LiOH (72 mg, 3 mmol, 5 eq.) was added. The reaction was stirred over night at room temperature until disappearance of the starting material. After neutralisation with Amberlite IR-120 H $^+$ to pH 7, the solvents were removed *in vacuo*. The title compound was obtained

after lyophilisation as white powder (206 mg, 95 %). ^1H NMR (500 MHz, $\text{H}_2\text{O}-d_2$) δ 8.19 (d, $J = 8.6$ Hz, 1H, Ar-H), 7.99 (d, $J = 8.5$ Hz, 1H, Ar-H), 3.69 (d, $J = 3.3$ Hz, 1H, glyco-H-2), 3.49 (dd, $J = 9.6, 3.4$ Hz, 1H, glyco-H-1), 3.44 (q, $J = 6.5$ Hz, 1H, glyco-H-5), 3.42 – 3.37 (m, 2H, glyco-linker- CH_2 -, glyco-H-4), 3.20 – 3.05 (m, 2H, glyco-linker- CH_2 -, glyco-H-3), 1.10 (d, $J = 6.5$ Hz, 3H, glyco-H-6). ^{13}C NMR (126 MHz, $\text{H}_2\text{O}-d_2$) δ 169.46 (COOH), 142.73 (Ar-C), 134.86 (s, Ar-C), 130.49 (Ar-C), 126.84 (Ar-C), 77.43 (glyco-C-3), 74.11 (glyco-C-1), 73.92 (glyco-C-5), 71.66 (glyco-C-2), 68.03 (glyco-C-4), 43.92 (linker- CH_2 -), 15.65 (glyco-C-6).

Bn-protected LecB-targeted peptide linker **15**: **14** (200 mg, 0.55 mmol, 1 eq.), **8** (302 mg, 0.66 mg, 1.2 eq.) and TBTU (267 mg, 0.83 mmol, 1.5 eq.) were dissolved in dry DMF (10 mL). DIPEA (288 μL , 1.65 mmol, 3 eq.) was added dropwise and the reaction was stirred for 1 h. The solvent was evaporated *in vacuo* and the reaction was purified by RP-MPLC (C18-phase, MeCN in Water, 10-35%, 0.1% formic acid). After lyophilisation, the title compound was isolated as a white powder (336 mg, 80%). ^1H NMR (500 MHz, MeOH- d_4) δ 8.06 (d, $J = 8.5$ Hz, 2H, ArH), 7.95 (d, $J = 8.4$ Hz, 2H, ArH), 7.41 – 7.27 (m, 5H, Bn), 5.17 (d, $J = 12.3$ Hz, 1H, Bn- CH_2 -), 5.12 (d, $J = 12.3$ Hz, 1H, Bn- CH_2 -), 4.49 – 4.40 (m, 3H, Ala-C α -H, Ala'-C α -H, Leu-C α -H), 3.97 (d, $J = 16.8$ Hz, 1H, Gly-C α -H), 3.79 (d, $J = 16.9$ Hz, 1H, Gly-C α -H), 3.58 (dd, $J = 2.9, 0.7$ Hz, 1H, glyco-H-4), 3.44 (qd, $J = 6.4, 1.1$ Hz, 1H, glyco-H-5), 3.41 – 3.36 (m, 2H, glyco-H-3, glyco-H-1), 3.34 (dd, $J = 8.3, 2.9$ Hz, 1H, linker- CH_2 -), 3.11 (ddd, $J = 9.0, 7.1, 2.4$ Hz, 1H, glyco-H-2), 3.04 (dd, $J = 12.9, 7.1$ Hz, 1H, linker- CH_2 -), 1.68 – 1.52 (m, 3H, Leu-CH, Leu- CH_2), 1.50 (d, $J = 7.2$ Hz, 3H, Ala'- CH_3), 1.41 (d, $J = 7.4$ Hz, 3H, Ala'- CH_3), 1.17 (d, $J = 6.4$ Hz, 3H, glyco-C6-H), 0.84 (d, $J = 5.9$ Hz, 3H, Leu- CH_3), 0.78 (d, $J = 6.0$ Hz, 3H, Leu- CH_3). ^{13}C NMR (126 MHz, MeOH- d_4) δ 175.85 (CONH), 174.62 (COOBn), 173.76 (CONH), 171.53 (CONH), 168.83 (CONH), 145.04 (Ar-C), 138.56 (Ar-C), 137.25 (Bn-C), 129.59 (Bn-C), 129.51 (Ar-C), 129.32 (Bn-C), 129.25

(Bn-C), 128.10 (Ar-C), 79.61 (glyco-C-2), 76.33 (glyco-C-3), 75.52 (glyco-C-5), 73.56 (glyco-C-4), 69.62 (glyco-C-1), 67.93 (Bn-CH₂), 52.88 (Ala-C α), 52.04 (Ala'-C α), 49.67 (Leu-C α), 45.55 (linker-CH₂-), 43.72 (Gly-C α), 41.75 (Leu-CH₂), 25.63 (Leu-CH), 23.44 (Leu-CH₃), 21.78 (Leu-CH₃), 17.24 (Ala-CH₃), 17.21 (Ala'-CH₃), 17.10 (glyco-C6-H). LR-MS: $m/z = 764.2$ [M+H]⁺.

LecB-targeted peptide linker **16**: **15** (300 mg, 0.39 mmol, 1 eq.) was dissolved in MeOH (4 mL). Pd/C (10% m/m, 41 mg, 10 mol%) was added and the atmosphere was changed to H₂ (1 atm.). The reaction was stirred at room temperature for 16 h until full transformation of the starting material. Pd/C was removed by centrifugation (17600 rcf, 10 min) and the solvent was removed *in vacuo*. The title compound was obtained as a white amorphous solid (250 mg, 95 %). ¹H NMR (500 MHz, MeOH-*d*₄) δ 8.87 (d, $J = 5.5$ Hz, 1H, NH), 8.56 (t, $J = 5.9$ Hz, 1H, NH), 8.22 (d, $J = 7.2$ Hz, 1H, NH), 8.07 (d, $J = 8.5$ Hz, 2H, Ar-H), 7.98 (s, 1H, NH), 7.96 (d, $J = 8.6$ Hz, 2H, Ar-H), 4.56 – 4.43 (m, 2H, Leu-C α -H, Ala-C α -H), 4.37 (qd, $J = 7.3, 2.3$ Hz, 1H, Ala-C α -H), 3.99 (d, $J = 17.0$ Hz, 1H, Gly-C α -H), 3.81 (d, $J = 16.8$ Hz, 1H, Gly-C α -H), 3.59 (d, $J = 2.9$ Hz, 1H, glyco-H-4), 3.44 (q, $J = 6.6$ Hz, 1H, glyco-H-5), 3.41 – 3.32 (m, 3H, glyco-H-3, glyco-H-1, linker-CH₂-), 3.11 (ddd, $J = 9.0, 7.2, 2.4$ Hz, 1H, glyco-H-2), 3.03 (dd, $J = 12.9, 7.2$ Hz, 1H, linker-CH₂-), 1.74 – 1.58 (m, 3H, Leu-CH, Leu-CH₂), 1.51 (d, $J = 7.2$ Hz, 3H, Ala-CH₃), 1.41 (d, $J = 7.3$ Hz, 3H, Ala'-CH₃), 1.17 (d, $J = 6.6$ Hz, 3H, glyco-H-6), 0.88 (d, $J = 6.3$ Hz, 3H, Leu-CH₃), 0.82 (d, $J = 6.3$ Hz, 3H, Leu-CH₃). ¹³C NMR (126 MHz, MeOH-*d*₄) δ 175.85 (CONH), 175.80 (COOH), 174.44 (CONH), 171.55 (CONH), 168.85 (CONH), 145.04 (Ar-C), 138.56 (Ar-C), 129.51 (Ar-C), 128.11 (Ar-C), 79.62 (glyco-C-2), 76.32 (glyco-C-3), 75.52 (glyco-C-5), 73.56 (glyco-C-4), 69.63 (glyco-C-1), 52.96 (Ala-C α), 52.03 (Ala'-C α), 49.85 (Leu-C α), 45.55 (linker-CH₂-), 43.72 (Gly-C α), 41.73 (Leu-CH₂), 25.65 (Leu-CH), 23.46 (Leu-CH₃), 21.81 (Leu-CH₃), 17.61 (Ala-CH₃), 17.23 (Ala'-CH₃), 17.09 (glyco-C6-H). LR-MS: $m/z = 674.2$ [M+H]⁺.

Boc-protected Leu-Ala-ciprofloxacin-conjugate **18**: Dipeptide **17** (100 mg, 0.33 mmol, 1 eq.) and NMM (36 μ L, 0.33 mmol, 1 eq.) were dissolved in 3 mL. The solution was cooled to -20 °C with a cooling bath (ice, sodium chloride) and lbcf (43 μ L, 0.33 mmol, 1 eq.) was added dropwise under vigorous stirring. The reaction was stirred for 20 min. This solution was then added dropwise to a dispersion of Ciprofloxacin (119 mg, 0.36 mmol, 1.1 eq.) and NMM (51 μ L, 0.46 mmol, 1.4 eq.) in dry THF (4 mL) via a transfer channel. The reaction was allowed to warm to r.t. and stirred for 2.5 h. The reaction was poured on ice-water (20 mL) and acidified with aqueous HCl (1 M) to pH = 4. The aqueous phase was extracted with CH₂Cl₂ (3 x 20 mL). The combined organic layers were washed with satd. aqueous NH₄Cl and dried over Na₂SO₄. The solvent was removed *in vacuo* and the product was purified by MPLC (CHCl₃/PE (9 : 1) : MeOH, 1 - 10 %), yielding the product as a beige amorphous solid (50 mg, 25 %). ¹H NMR (500 MHz, CHCl₃-*d*) δ 8.78 (s, 1H, cipro-C2-H), 8.05 (d, J = 12.6 Hz, 1H, cipro-C5-H), 7.45 (d, J = 5.3 Hz, 1H, cipro-C8-H), 7.01 (d, J = 7.0 Hz, 1H, Ala-NH), 5.03 – 4.89 (m, 1H, Ala-C α -H), 4.88 – 4.83 (m, 1H, Leu-NH), 4.14 (s, 1H, Leu-C α -H), 4.09 – 3.98 (m, 1H, piperazine-C-H), 3.95 – 3.80 (m, 1H, piperazine-C-H), 3.74 – 3.67 (m, 2H, 2x piperazine-C-H), 3.56 (s, 1H, *cPr*-H), 3.39 (s, 3H, 3x piperazine-C-H), 3.30 – 3.15 (m, 1H, piperazine-C-H), 1.75 – 1.59 (m, 2H, Leu-CH₂ + Leu-CH-CH₃CH₃), 1.44 (s, 12H, *cPr*-CH₂ + Boc-CH₃ + Leu-CH₂), 1.37 (d, J = 6.6 Hz, 3H, Ala-CH₃), 1.21 (s, 2H, *cPr*-CH₂), 1.00 – 0.81 (m, 6H, Leu-CH₃). ¹³C NMR (126 MHz, CDCl₃-*d*) δ 177.21 (cipro-C4=O), 172.07 (C=O), 170.77 (C=O), 166.99 (cipro-COOH), 155.69 (carbamate-C=O), 153.77 (d, J = 251.8 Hz, cipro-C-6), 147.85 (cipro-C-2), 145.13 (cipro-C-7), 139.09 (cipro-C-8a), 120.85 (d, J = 7.8 Hz, cipro-C-4a), 112.92 (d, J = 23.2 Hz, cipro-C-5), 108.45 (cipro-C-3), 105.71 (cipro-C-8), 80.34 (Boc), 53.40 (Leu-C α), 50.16 (piperazine-C), 49.84 (piperazine-C), 45.27 (piperazine-C), 45.07 (Leu-C α), 41.91

(piperazine-C), 41.57 (Leu-CH₂), 35.54 (cPr-CH), 28.42 (Boc-CH₃), 24.92 (Leu-CH-CH₃CH₃), 23.20 (Leu-CH₃), 21.89 (Leu-CH₃), 18.96 (Ala-CH₃), 8.46 (cPr-CH₂).

Leu-Ala-ciprofloxacin-conjugate **19**: Boc-Protected conjugate **18** (43 mg, 0.07 mmol, 1 eq.) was dissolved in 3 mL HCl in dioxane (4 M) while cooling on ice. The ice bath was removed and the reaction was stirred at r.t. for 4 h. The solvent was evaporated *in vacuo* and the residue was dissolved in 1 mL MeOH. The product was precipitated with ice-cold Et₂O (20 mL) and the resulting precipitate was washed three times with ice-cold Et₂O. The precipitate was dried *in vacuo* and obtained as a yellow solid (30 mg, 78 %). ¹H NMR (500 MHz, DMSO-*d*6) δ 15.17 (s, 1H, cipro-COOH), 8.85 (d, J = 7.5 Hz, 1H, Ala-NH), 8.67 (s, 1H, cipro-C2-H), 8.27 (s, 1H, Leu-NH₃⁺), 7.93 (d, J = 13.1 Hz, 1H, cipro-C5-H), 7.58 (d, J = 7.2 Hz, 1H, cipro-C8-H), 4.92 – 4.82 (m, 1H, Ala-C_α-H), 3.82 (s, 2H, Leu-C_α-H + cPr-CH), 3.78 – 3.73 (m, 2H, 2x piperazine-C-H), 3.73 – 3.69 (m, 2H, 2x piperazine-C-H), 1.68 (dp, J = 13.2, 6.6 Hz, 1H, Leu-CH-CH₃CH₃), 1.59 – 1.49 (m, 2H, Leu-CH₂), 1.32 (d, J = 6.3 Hz, 2H, cPr-CH₂), 1.28 (d, J = 6.9 Hz, 2H, Ala-CH₃), 1.19 (s, 2H, cPr-CH₂), 0.91 (d, J = 6.5 Hz, 3H, Ala-CH₃), 0.89 (d, J = 6.5 Hz, 3H, Ala-CH₃). ¹³C NMR (126 MHz, DMSO-*d*6) δ 176.39 (cipro-C4), 169.95 (C=O), 168.29 (C=O), 165.92 (cipro-COOH), 152.96 (d, J = 249.3 Hz, cipro-C6), 148.15 (cipro-C2), 144.80 (d, J = 10.1 Hz, cipro-C7), 139.15 (cipro-C8a), 118.92 (d, J = 7.6 Hz, cipro-C4a), 111.08 (d, J = 23.0 Hz, cipro-C5), 106.79 (cipro-C3), 106.71 (d, J = 2.7 Hz, cipro-C8), 50.62 (Leu-C_α), 49.70 (piperazine-C), 49.19 (piperazine-C), 44.65 (piperazine-C), 44.57 (Ala-C_α), 41.21 (piperazine-C), 40.23 (Leu-CH₂), 35.94 cPr-CH, 23.53 (Leu-CH-CH₃CH₃), 22.68 (Leu-CH₃), 22.04 (Leu-CH₃), 17.75 (Ala-CH₃), 7.64 (cPr-CH₂). HR-MS calcd [C₂₆H₃₅FN₅O₅]⁺: 516.2617, found 516.2610.

(*N*-Boc)-ciprofloxacin-benzylester (**20**): Ciprofloxacin (**1**) (1000 mg, 3.02 mmol, 1 eq.) and KHCO₃ (1511 mg, 15.1 mmol, 5 eq.) and Boc₂O (775 μL, 3.62 mmol, 1.2 eq.) were dispersed in 12 mL dry DMF. The reaction was heated to 40 °C and stirred for 2 h. Then,

BnBr (430 μ L, 3.62 mmol, 1.2 eq.) was added and the reaction was heated to 120 °C and stirred for 90 min. The reaction was allowed to cool to r.t. and poured on 100 mL ice cold water. The precipitate was filtered off and dried *in vacuo*. The product was obtained as a beige amorphous solid (1.36 g, 86 %). No NMR measured due to solubility issues: the sample degraded in CDCl₃ and was not soluble in other common solvents. LR-MS: $m/z = 522.3 [M+H]^+$.

Ciprofloxacin-benzylester • HCl (**21**): **20** (500 mg, 0.96 mmol, 1 eq.) was partially dissolved in 2 mL CH₂Cl₂ and cooled with an ice-bath. 10 mL HCl in dioxane (4 N) was added slowly under vigorous stirring and the reaction was allowed to warm to r.t. and stirred for 1 h. The solvent was evaporated *in vacuo* and the product was obtained as a yellow solid (448 mg, quant.). ¹H NMR (500 MHz, DMSO-*d*₆) δ 9.54 (s, 2H, piperazine-NH₂⁺), 8.48 (s, 1H, cipro-C2-H), 7.81 (d, $J = 13.2$ Hz, 1H, cipro-C5-H), 7.51 – 7.46 (m, 3H, cipro-C8-H + Bn-Ar), 7.42 – 7.37 (m, 2H, Bn-Ar), 7.35 – 7.30 (m, 1H, Bn-Ar), 5.27 (s, 2H, Bn-CH₂-), 3.73 – 3.64 (m, 1H, cPr-CH), 3.52 – 3.45 (m, 4H, 4x piperazine-C-H), 3.30 (s, 4H, 4x piperazine-C-H), 1.25 (dd, $J = 6.9$ Hz, 2H, cPr-CH₂), 1.15 – 1.04 (m, 2H, cPr-CH₂). ¹³C NMR (126 MHz, DMSO-*d*₆) δ 172.05 (C=O), 164.96 (COOBn), 152.94 (d, $J = 246.5$ Hz, cipro-C6), 149.06 (cipro-C2), 143.28 (d, $J = 10.9$ Hz, cipro-C7), 138.50 (cipro-C8a), 137.10 (Bn), 128.86 (Bn), 128.25 (Bn), 128.09 (Bn), 123.03 (d, $J = 6.3$ Hz, cipro-C4a), 112.30 (d, $J = 22.7$ Hz, cipro-C5), 109.42 (cipro-C3), 107.19 (cipro-C8), 65.73 (piperazine-C), 46.93 (piperazine-C), 46.90 (piperazine-C), 43.01 (piperazine-C), 35.39 (cPr-CH), 8.05 (cPr-CH₂). LR-MS: $m/z = 422.1 [M+H]^+$.

LecA-targeted ciprofloxacin-prodrug **22**: The title compound was synthesised in two chemical steps: First, **10** (31 mg, 0.049 mmol, 1 eq.), **21** (34 mg, 0.074 mmol, 1.5 eq.) and TBTU (24 mg, 0.074 mmol, 1.5 eq.) were dissolved in 1 mL dry DMF. DIPEA (17 μ L, 0.098 mmol, 2 eq.) was added dropwise and the reaction was stirred for 1 h. After evaporation of

the solvent, the residue was taken up in 1.5 mL MeOH/DMF (2:1). Pd black (10 mg, 0.05 mmol, 1 eq.) was added and the reaction was stirred under H₂ atmosphere for 6 d. Afterwards, the reaction was filtered over celite and further purified by preparative HPLC (MeCN:H₂O, 20-33%, 0.1% formic acid). The title compound was obtained as a beige amorphous solid (10 mg, 22% over 2 chemical steps). ¹H NMR (500 MHz, MeOH-*d*₄) δ 8.79 (s, 1H, cipro-H-2), 7.91 (d, J = 13.0 Hz, 1H, cipro-H-5), 7.81 (d, J = 8.1 Hz, 2H, Ar-H), 7.61 (d, J = 6.8 Hz, 1H, cipro-C8-H), 7.54 (d, J = 8.0 Hz, 2H, Ar-H), 4.92 – 4.87 (m, 1H, Ala-C_α-H), 4.72 (d, J = 9.7 Hz, 1H, glyco-H-1), 4.48 (dd, J = 10.7, 3.8 Hz, 1H, Leu-C_α-H), 4.40 (q, J = 6.0 Hz, 1H, Ala-C_α-H), 4.06 – 3.88 (m, 4H, 2x piperazine-CH, Gly-CH, glyco-H-4), 3.83 – 3.59 (m, 8H, 2x piperazine-CH, Gly-CH, cPr-CH, glyco-H6, glyco-H-2, glyco-H-5), 3.53 (dd, J = 9.2, 3.4 Hz, 1H, glyco-H-3), 3.43 (s, 3H, piperazine-CH₂, piperazine-CH), 1.77 – 1.66 (m, 1H, Leu-CH₂), 1.67 – 1.57 (m, 2H, Leu-CH₂, Leu-CH), 1.48 (d, J = 7.1 Hz, 3H, Ala-CH₃), 1.42 (d, J = 6.3 Hz, 2H, cPr-CH₂), 1.36 (d, J = 6.8 Hz, 3H, Ala-CH₃), 1.27 – 1.18 (m, 2H, cPr-CH₂), 0.87 (d, J = 5.7 Hz, 3H, Leu-CH₃), 0.82 (d, J = 5.8 Hz, 3H, Leu-CH₃). ¹³C NMR (126 MHz, MeOH-*d*₄) δ 177.03 (C=O), 174.85 (C=O), 172.80 (C=O), 171.14 (C=O), 170.36 (C=O), 168.31 (C=O), 168.26 (C=O), 153.70 (d, J = 250.0 Hz, cipro-C-6), 148.03 (cipro-C), 145.50 (d, J = 10.1 Hz, cipro-C-7), 140.79 (cipro-C), 139.38 (Ar-C), 130.87 (Ar-C), 128.35 (Ar-C), 127.77 (Ar-C), 119.59 (d, J = 8.1 Hz, cipro-C-4a), 111.15 (d, J = 23.5 Hz, cipro-C-5), 106.80 (cipro-C), 106.31 (d, J = 2.7 Hz, cipro-C-8), 87.53 (glyco-C-1), 79.38 (glyco-C-5), 74.86 (glyco-C-3), 69.47 (glyco-C-2), 68.99 (glyco-C-4), 61.26 (glyco-C-6), 51.70 (Leu-C_α), 50.77 (Ala-C_α), 49.66 (d, J = 3.7 Hz, piperazine-C), 49.28 (d, J = 2.6 Hz, piperazine-C), 45.25 (Ala-C_α), 45.08 (Gly-C_α), 42.49 (piperazine-C), 41.80 (piperazine-C), 40.17 (Leu-CH₂), 35.67 (cPr-CH), 24.31 (Leu-CH), 22.16 (Leu-CH₃), 20.18 (Leu-CH₃), 16.40 (Ala-CH₃), 15.87 (Leu-CH₃), 7.24 (cPr-CH₂), 7.17 (cPr-CH₂). HR-MS calcd [C₄₄H₅₇FN₇O₁₃S]⁺: 942.3714, found 942.3689.

LecB-targeted ciprofloxacin-prodrug-benzylester (**23**): **16** (70 mg, 0.10 mmol, 1 eq.), **21** (55 mg, 0.12 mg, 1.2 eq.) and TBTU (48 mg, 0.15 mmol, 1.5 eq.) were dissolved in dry DMF (2 mL). DIPEA (52 μ L, 0.3 mmol, 3 eq.) was added dropwise and the reaction was stirred for 1 h. The solvent was evaporated *in vacuo* and the reaction was purified by pHPLC (MeCN in Water, 25-40%, 0.1% formic acid). After lyophilisation, the title compound was isolated as an off-white powder (90 mg, 84%). ^1H NMR (500 MHz, MeOH-*d*₄) δ 8.65 (s, 1H, cipro-H-2), 8.04 (d, J = 8.5 Hz, 2H, glyco-Ar-H), 7.93 (d, J = 8.5 Hz, 2H, glyco-Ar-H), 7.88 (d, J = 13.3 Hz, 1H, cipro-H-5), 7.52 (d, J = 7.2 Hz, 1H, cipro-H-8), 7.48 (d, J = 7.4 Hz, 2H, Bn-Ar), 7.42 – 7.35 (m, 2H, Bn-Ar), 7.34 – 7.29 (m, 1H, Bn-Ar), 5.33 (s, 2H, Bn-CH₂), 4.92 – 4.88 (m, 1H, Ala-C α -H), 4.49 – 4.42 (m, 2H, Leu-C α -H, Ala'-C α -H), 4.00 (d, J = 16.8 Hz, 1H, Gly-C α -H), 3.94 – 3.84 (m, 2H, 2x piperazine-H), 3.78 (d, J = 16.8 Hz, 1H, glycin-C α -H), 3.77 – 3.70 (m, 1H, piperazine-H), 3.70 – 3.61 (m, 2H, cPr-CH, piperazine-H), 3.58 (d, J = 2.9 Hz, 1H, glyco-H-4), 3.43 (q, J = 6.2 Hz, 1H, glyco-H-5), 3.40 – 3.34 (m, 4H, 3x piperazine-H, glyco-H-3, glyco-H-1), 3.34 – 3.27 (m, 1H, glyco-linker-CH₂), 3.28 – 3.22 (m, 1H, piperazine-H), 3.10 (ddd, J = 9.0, 7.1, 2.4 Hz, 1H, glyco-H-2), 3.02 (dd, J = 12.9, 7.1 Hz, 1H, glyco-linker-CH₂-), 1.76 – 1.56 (m, 3H, Leu-CH, Leu-CH₂), 1.50 (d, J = 7.2 Hz, 3H, Ala-CH₃), 1.35 (d, J = 6.9 Hz, 3H, Ala-CH₃), 1.34 – 1.25 (m, 2H, cPr-CH₂), 1.16 (d, J = 6.5 Hz, 3H, glyco-H-6), 1.14 – 1.06 (m, 2H, cPr-CH₂), 0.87 (d, J = 5.8 Hz, 3H, Leu-CH₃), 0.82 (d, J = 5.7 Hz, 3H, Leu-CH₃). ^{13}C NMR (126 MHz, MeOH-*d*₄) δ 175.83 (CONH), 175.43 (cipro-C=O), 174.11 (CONH), 172.55 (CONH), 171.68 (CONH), 165.93 (COOBn), 154.88 (d, J = 248.4 Hz, cipro-C-6), 150.13 (cipro-Ar-C), 145.93 (d, J = 10.6 Hz, cipro-C-7), 145.06 (Ar-C), 139.87 (Ar-C), 138.52 (Ar-C), 137.93 (Ar-C), 129.56 (glyco-Ar-C), 129.53 (Bn-Ar), 129.24 (Bn-Ar), 129.15 (Bn-Ar), 128.08 (glyco-Ar-C), 123.70 (d, J = 6.5 Hz, cipro-C-4a), 113.18 (d, J = 24.3 Hz, cipro-C-5), 110.28 (Ar-C), 107.58 (d, J = 2.9 Hz, cipro-C-8), 79.62 (glyco-C-2), 76.33 (glyco-C-3), 75.51 (glyco-C-5), 73.55 (glyco-

C-4), 69.62 (glyco-C-1), 67.16 (Bn), 53.11 (Leu-Ca), 52.13 (Ala-Ca), 51.25 (piperazine-C), 50.78 (piperazine-C), 46.58 (piperazine-C), 45.55 (glyco-linker-CH₂), 43.89 (Gly-Ca), 43.22 (piperazine-C), 41.60 (Leu-CH₂), 36.38 (cPr-CH), 25.74 (Leu-CH), 23.53 (Leu-CH₃), 21.63 (Leu-CH₃), 17.87 (Ala-CH₃), 17.23 (Ala-CH₃), 17.11 (glyco-C-6), 8.60 (cPr-CH₂), 8.54 (cPr-CH₂). LR-MS: $m/z = 539.2 [M+2H]^{2+}$.

LecB-targeted ciprofloxacin-prodrug **25: 23** (57 mg, 0.052 mmol, 1 eq.) was dissolved in MeOH (1 mL). Pd/C (10% m/m, 5 mg, 10 mol%) was added and the atmosphere was changed to H₂ (1 atm.). The reaction was stirred at room temperature for 24 h until full consumption of the starting material. Pd/C was removed by centrifugation (17600 rcf, 10 min) and the solvent was removed *in vacuo*. After purification by pHPLC (MeCN in Water, 22-35%, 0.1% formic acid), the title compound was obtained as an off-white amorphous solid (38 mg, 74%). ¹H NMR (500 MHz, MeOH-*d*₄) δ 8.60 (s, 1H, FQ-H-2), 8.05 (d, J = 8.0 Hz, 2H, glyco-Ar-H), 7.94 (d, J = 8.0 Hz, 2H, glyco-Ar-H), 7.72 (d, J = 14.1 Hz, 1H, FQ-H-5), 7.05 (s, 1H, FQ-H-8), 4.47 (s, 1H, piperazine-H), 4.41 (q, J = 7.3 Hz, 1H, Ala-Ca-H), 4.36 – 4.23 (m, 2H, Ala'-Ca-H), 3.97 – 3.77 (m, 3H, 2x piperazine-H, Gly-Ca-H), 3.74 – 3.61 (m, 4H, 2x piperazine-H, Gly-Ca-H, cPr-CH), 3.58 (d, J = 1.9 Hz, 1H, glyco-H-4), 3.44 (q, J = 6.4 Hz, 1H, glyco-H-5), 3.41 – 3.27 (m, 4H, glyco-H-3, glyco-H-1, piperazine-H, glyco-linker-CH₂-), 3.10 (ddd, J = 8.9, 7.5, 2.4 Hz, 1H, glyco-H-2), 3.02 (dd, J = 12.9, 7.1 Hz, 1H, glyco-linker-CH₂-), 2.34 – 2.22 (m, 1H, piperazine-H), 2.21 – 2.10 (m, 1H, piperazine-H), 1.78 – 1.69 (m, 1H, Leu-CH), 1.69 – 1.56 (m, 2H, Leu-CH₂), 1.51 (d, J = 7.1 Hz, 3H, Ala-CH₃), 1.44 – 1.35 (m, 5H, Ala'-CH₃, cPr-CH₂), 1.18 (s, 2H, cPr-CH₂), 1.16 (d, J = 6.5 Hz, 3H, glyco-C-6), 0.86 (d, J = 4.6 Hz, 3H, Leu-CH₃), 0.85 (d, J = 4.6 Hz, 3H, Leu-CH₃). ¹³C NMR (126 MHz, MeOH-*d*₄) δ 177.54 (d, J = 2.3 Hz, FQ-C=O), 176.27 (CONH), 175.08 (CONH), 174.75 (CONH), 172.35 (CONH), 170.05 (CONH), 169.06 (COOH), 152.04 (d, J = 247.5 Hz, cipro-C-6), 148.59 (cipro-C-2), 145.13 (Ar-C), 143.54 (d, J = 12.1

Hz, cipro-C-7), 141.38 (Ar-C), 138.36 (Ar-C), 129.54 (glyco-Ar-C), 128.11 (glyco-Ar-C), 111.96 (d, J = 23.9 Hz, cipro-C-5), 101.66 (cipro-C-8), 79.62 (glyco-C-2), 76.33 (glyco-C-3), 75.52 (glyco-C-5), 73.55 (glyco-C-4), 69.61 (glyco-C-1), 56.00 (d, J = 6.4 Hz, piperazine-C), 53.88 (Leu-C α), 52.48 (Ala-C α), 50.93 (piperazine-C), 50.84 (Ala'-CH₃), 49.24 (extracted from HSQC, piperazine-C) 45.55 (glyco-linker-CH₂), 44.20 (Gly-C α), 41.19 (Leu-CH₂), 36.80 (cPr-CH), 31.80 (piperazine-C), 25.81 (Leu-CH), 23.53 (Leu-CH₃), 21.56 (Leu-CH₃), 17.85 (Ala-CH₃), 17.27 (Ala'-CH₃), 17.11 (glyco-C-6), 8.49 (cPr-CH₂), 8.46 (cPr-CH₂). HR-MS calcd [C₄₅H₆₀FN₈O₁₄S]⁺: 987.3928, found 987.3908.

(S)-7-(3-Tertbutoxycarbonylamino-1-pyrrolidinyl)-1-cyclopropyl-6-fluoro-1,4-dihydro-4-oxo-1,8-naphthyridine-3-carboxylic acid (**28**): 7-chloro-1-cyclopropyl-6-fluoro-4-oxo-1,4-dihydroquinoline-3-carboxylic acid (**26**, 500 mg, 1.78 mmol, 1 eq.) and (S)-3-(Boc-amino)-pyrrolidine (**27**, 995 mg, 5.34 mmol, 3 eq.) were dispersed in 10 mL dry pyridine. The mixture was heated with an oil bath to 160 °C and refluxed over night. After cooling to room temperature, the solvent was evaporated *in vacuo* and purified by NP-MPLC (CH₂Cl₂ : n-Hex (70 : 28) : MeOH, 2 - 5%). The product was obtained as a beige amorphous solid (383 mg, 50 %). ¹H NMR (500 MHz, DMSO-*d*₆) δ 15.54 (s, 1H, COOH), 8.56 (s, 1H, Ar4H-2), 7.78 (d, J = 14.1 Hz, 1H, ArH-5), 7.30 (d, J = 6.7 Hz, 1H, BocNH), 7.03 (d, J = 7.6 Hz, 1H, ArH-8), 4.17 (q, J = 6.3 Hz, 1H, aminopyrrolidine-H), 3.86 – 3.77 (m, 1H, aminopyrrolidine-H), 3.77 – 3.67 (m, 2H, aminopyrrolidine-H, cPr-CH), 3.64 – 3.56 (m, 1H, aminopyrrolidine-H), 3.44 (dt, J = 10.7, 3.9 Hz, 1H, aminopyrrolidine-H), 2.15 (dq, J = 13.3, 7.1 Hz, 1H, aminopyrrolidine-H), 1.93 (dq, J = 12.6, 6.0 Hz, 1H, aminopyrrolidine-H), 1.39 (s, 9H, Boc-CH₃), 1.34 – 1.25 (m, 2H, cPr-CH₂), 1.18 – 1.10 (m, 2H, cPr-CH₂). ¹³C NMR (126 MHz, DMSO-*d*₆) δ 175.87 (d, J = 3.3 Hz, C-4), 166.32 (COOH), 155.29 (Boc-C=O), 149.96 (d, J = 246.3 Hz, C-6), 147.44 (C), 141.65 (d, J = 11.6 Hz, C-7), 139.83 (C), 114.42 (d, J = 7.0 Hz, C-4a), 110.71 (d, J = 22.6 Hz, C-5), 106.17 (C), 100.43 (d, J = 5.7 Hz, C-8),

78.04 (Boc-C), 55.18 (d, J = 6.8 Hz, aminopyrrolidine-C), 49.84 (aminopyrrolidine-C), 48.15 (d, J = 3.8 Hz, aminopyrrolidine-C), 35.74 (cPr-C), 30.43 (aminopyrrolidine-C), 28.28 (Boc-CH₃), 7.59 (cPr-CH₂), 7.53 (cPr-CH₂). LR-MS: $m/z = 432.2$ [M+H]⁺.

(S)-7-(3-Amino-1-pyrrolidinyl)-1-cyclopropyl-6-fluoro-1,4-dihydro-4-oxo-1,8-naphthyridine-3-carboxylic acid • HCl (**28**) (59 mg, 0.14 mmol, 1 eq.) was dissolved in 3 mL HCl in dioxane (4 N) while cooling on ice. The reaction was allowed to warm to r.t. and stirred for 90 min until full consumption of the starting material. After the solvent was evaporated *in vacuo*, the remaining solid was taken up in 2 mL MeOH and the product was precipitated with Et₂O. The precipitate was first washed three times with Et₂O, then dried *in vacuo* and the product was obtained as a yellow amorphous solid (m = 45 mg, 86 %). ¹H NMR (500 MHz, DMSO-*d*₆) δ 15.46 (s, 1H, COOH), 8.60 (s, 1H, H-2), 8.33 (s, 3H, NH₃⁺), 7.86 (d, J = 14.2 Hz, 1H, H-5), 7.10 (d, J = 7.6 Hz, 1H, H-8), 4.10 – 3.88 (m, 2H, aminopyrrolidine-CH + cPr-CH), 3.88 – 3.69 (m, 3H, aminopyrrolidine-CH₂, aminopyrrolidine-CH), 3.69 – 3.61 (m, 1H, aminopyrrolidine-CH), 2.34 (ddt, J = 14.0, 8.0, 7.5 Hz, 1H, aminopyrrolidine-CH), 2.15 (ddt, J = 12.2, 7.8, 4.5 Hz, 1H, aminopyrrolidine-CH), 1.34 – 1.27 (m, 2H, cPr-CH₂), 1.23 – 1.11 (m, 2H, cPr-CH₂). ¹³C NMR (126 MHz, H₂O-*d*₂) δ 173.95 (d, C-4), 169.31 (C), 150.05 (d, J = 249.4 Hz, C-6), 147.02 (C), 141.31 (d, J = 11.0 Hz, C-7), 139.14 (C), 113.20 (d, J = 7.1 Hz, C-4a), 109.51 (d, J = 23.2 Hz, C-5), 104.62 (C), 100.57 (C-8), 52.62 (d, J = 7.8 Hz, aminopyrrolidine-C), 50.11 (aminopyrrolidine-C), 47.27 (d, J = 3.2 Hz, aminopyrrolidine-C), 35.79 (cPr-CH), 28.36 (aminopyrrolidine-C), 7.18 (2x cPr-CH₂). HR-MS calcd [C₁₇H₁₉FN₃O₃]⁺: 332.1405, found 332.1397.

(S)-7-(3-Tertbutoxycarbonylamino-1-pyrrolidinyl)-1-cyclopropyl-6-fluoro-1,4-dihydro-4-oxo-1,8-naphthyridine-3-carboxylic acid benzyl ester (**29**): **28** (364 mg, 0.84 mmol, 1 eq.) and freshly ground KHCO₃ were dried on high vacuum for 15 min. After dispersion in 10

mL dry DMF, BnBr (150 μ L, 1.26 mmol, 1.5 eq.) was added and the reaction was heated to 110 °C. Full conversion was achieved after 60 min and the reaction was allowed to cool to r.t.. The solvent was reduced *in vacuo* and diluted with CH₂Cl₂. The organic phase was washed with water, KHSO₄ (1 M) and satd. brine. The combined organic layers were dried over Na₂SO₄ and the solvent was evaporated *in vacuo*, giving the title compound as a white amorphous solid (217 mg, 50%). ¹H NMR (500 MHz, DMSO-*d*₆) δ 8.40 (s, 1H, H-2), 7.68 (d, J = 14.5 Hz, 1H, H-5), 7.51 – 7.46 (m, 2H, Bn-Ar), 7.42 – 7.36 (m, 2H, Bn-Ar), 7.36 – 7.29 (m, 1H, Bn-Ar), 7.28 (d, J = 6.7 Hz, 1H, NH), 6.94 (d, J = 7.6 Hz, 1H, H-8), 5.25 (s, 2H, Bn-CH₂-), 4.23 – 4.08 (m, 1H, aminopyrrolidine-CH), 3.78 – 3.71 (m, 1H, aminopyrrolidine-CH), 3.69 – 3.62 (m, 1H, aminopyrrolidine-CH), 3.59 (tt, J = 7.2, 4.0 Hz, 1H, cPr-CH), 3.56 – 3.49 (m, 1H, aminopyrrolidine-CH), 3.43 – 3.36 (m, 1H, aminopyrrolidine-CH), 2.13 (dddd, J = 13.5, 6.9, 6.9, 6.9 Hz, 1H, aminopyrrolidine-CH), 1.91 (dddd, J = 12.5, 6.2, 6.2, 6.2 Hz, 1H, aminopyrrolidine-CH), 1.39 (s, 9H, Boc-CH₃), 1.25 – 1.20 (m, 2H, cPr-CH₂), 1.09 – 1.03 (m, 2H, cPr-CH₂). ¹³C NMR (126 MHz, DMSO-*d*₆) δ 171.51 (d, J = 2.0 Hz, C-4), 164.77 (COOBn), 155.29 (Boc-C=O), 149.47 (d, J = 242.8 Hz, C-6), 148.15 (C), 140.37 (d, J = 11.8 Hz, C-7), 138.64 (C), 136.79 (Bn-C), 128.42 (Bn-C), 127.77 (Bn-C), 127.62 (Bn-C), 117.82 (d, J = 5.9 Hz, C-4a), 111.54 (d, J = 22.8 Hz, C-5), 108.53 (C), 100.53 (d, J = 5.3 Hz, C-8), 77.98 (Boc-C), 65.14 (Bn-CH₂), 55.09 (d, J = 5.0 Hz, aminopyrrolidine-C), 49.85 (aminopyrrolidine-C), 47.98 (d, J = 4.7 Hz, aminopyrrolidine-C), 34.73 (cPr-CH), 30.47 (aminopyrrolidine-C), 28.28 (Boc-CH₃), 7.57 (cPr-CH₂), 7.52 (cPr-CH₂). LR-MS: *m/z* = 522.2 [M+H]⁺.

(S)-7-(3-Amino-1-pyrrolidinyl)-1-cyclopropyl-6-fluoro-1,4-dihydro-4-oxo-1,8-naphthyridine-3-carboxylic acid benzyl ester • HCl (**30**): **29** (187 mg, 0.36 mmol, 1 eq.) was dissolved in 4 mL HCl in dioxane (4 N) while cooling on ice. The reaction was allowed to warm to r.t. and stirred for 1 h until full consumption of the starting material. After the

solvent was evaporated *in vacuo*, the remaining solid was taken up in 2 mL MeOH and the product was precipitated with Et₂O. The precipitate was first washed three times with Et₂O, then dried *in vacuo* and the product was obtained as a yellow amorphous solid (160 mg, 97 %). ¹H NMR (500 MHz, MeOH-*d*₄) δ 8.85 (s, 1H, H-2), 7.81 (d, J = 14.1 Hz, 1H, H-5), 7.53 (d, J = 7.0 Hz, 2H, Bn-H), 7.47 – 7.32 (m, 3H, Bn-H), 6.96 (d, J = 7.3 Hz, 1H, H-8), 5.49 (d, J = 8.4 Hz, 1H, Bn-CH₂), 5.39 (d, J = 12.1 Hz, 1H, Bn-CH₂), 4.18 – 4.07 (m, 2H, aminopyrrolidine-CH + aminopyrrolidine-CH), 4.05 – 3.98 (m, 1H, aminopyrrolidine-CH), 3.81 – 3.67 (m, 3H, aminopyrrolidine-CH₂ + *c*Pr-CH), 2.50 (dddd, 1H, aminopyrrolidine-CH), 2.27 (dddd, J = 16.0, 5.8, 3.0 Hz, 1H, aminopyrrolidine-CH), 1.49 – 1.30 (m, 2H, *c*Pr-CH₂), 1.23 – 1.07 (m, 2H, *c*Pr-CH₂). ¹³C NMR (126 MHz, MeOH-*d*₄) δ 171.63 (d, J = 3.6 Hz, C-4), 167.13 (COOBn), 152.61 (d, J = 250.1 Hz, C-6), 149.77 (C), 144.39 (d, J = 12.0 Hz, C-7), 141.62 (C), 136.83 (Bn-C), 129.92 (Bn-C), 129.84 (Bn-C), 129.79 (Bn-C), 115.09 (d, J = 8.2 Hz, C-4a), 112.27 (d, J = 24.7 Hz, C-5), 106.16 (C), 101.91 (d, J = 5.9 Hz, C-8), 68.76 (Bn-CH₂), 54.92 (d, J = 9.2 Hz, aminopyrrolidine-C), 51.82 (d, J = 3.0 Hz, aminopyrrolidine-C), 48.68 (aminopyrrolidine-C, extracted from ¹H-¹³C-HSQC) 38.04 (*c*Pr-CH), 29.90 (aminopyrrolidine-C), 8.69 (2x *c*Pr-CH₂). LR-MS: *m/z* = 422.2 [M+H]⁺.

benzyl 7-((S)-3-((S)-2-((S)-2-((tert-butoxycarbonyl)amino)-4-methylpentanamido)propanamido)pyrrolidin-1-yl)-1-cyclopropyl-6-fluoro-4-oxo-1,4-dihydroquinoline-3-carboxylate (**31**): **30** (55 mg, 0.12 mmol, 1 eq.), dipeptide **17** (54 mg, 0.18 mmol, 1.5 eq.) and DIPEA (100 μL, 0.6 mmol, 5 eq.) were dissolved in 900 μL dry DMF. TBTU (77 mg, 0.24 mmol, 2 eq.) was added and the reaction was heated to 40° C. Reaction progress was monitored by TLC (CH₂Cl₂ : MeOH, 95 : 5) and full turnover was achieved after 1 h. The reaction concentrated *in vacuo* and diluted with CH₂Cl₂. The organic phase was washed with KHSO₄ (1 M), aqueous satd. NaHCO₃ and satd. brine. The combined organic layers were dried over Na₂SO₄ and the solvent was evaporated *in*

vacuo. After purification via NP-MPLC (CH₂Cl₂ : MeOH, 1 - 5%), the title compound was obtained as a beige amorphous solid (63 mg, 74%). ¹H NMR (500 MHz, Acetone-*d*₆) δ 8.47 (s, 1H, FQ-H-2), 8.21 (d, J = 7.0 Hz, 1H, NH), 7.62 – 7.51 (m, 3H, Bn-H, FQ-H-5), 7.47 – 7.38 (m, 2H, Bn-H), 7.37 – 7.31 (m, 1H, Bn-H), 6.73 (d, J = 7.5 Hz, 1H, FQ-H-8), 6.25 (d, J = 8.1 Hz, 1H, NH), 5.35 (d, J = 12.6 Hz, 1H, Bn-CH₂-), 5.26 (d, J = 12.6 Hz, 1H, Bn-CH₂-), 4.57 – 4.52 (m, 1H, aminopyrrolidine-H), 4.48 (dq, J = 7.2, 7.1 Hz, 1H, Ala-C_α-H), 4.09 – 4.00 (m, 1H, Leu-C_α-H), 3.92 (ddd, J = 10.3, 6.0, 3.8 Hz, 1H, aminopyrrolidine-H), 3.62 (dt, J = 9.7, 3.1 Hz, 1H, aminopyrrolidine-H), 3.56 – 3.46 (m, 1H, aminopyrrolidine-H), 3.45 – 3.37 (m, 2H, aminopyrrolidine-H, *c*Pr-CH), 2.24 – 2.11 (m, 1H, aminopyrrolidine-H), 2.03 – 1.96 (m, 1H, aminopyrrolidine-H), 1.65 (ddd, J = 13.1, 13.1, 6.6 Hz, 1H, Leu-CH₂), 1.57 – 1.49 (m, 2H, Leu-CH₂, Leu-CH), 1.40 (s, 9H, Boc-CH₃), 1.33 (d, J = 7.1 Hz, 3H, Ala-CH₃), 1.26 – 1.20 (m, 1H, *c*Pr-CH₂), 1.20 – 1.09 (m, 2H, *c*Pr-CH₂), 1.00 – 0.93 (m, 1H, *c*Pr-CH₂), 0.85 (d, J = 6.6 Hz, 3H, Leu-CH₃), 0.80 (d, J = 6.5 Hz, 3H, Leu-CH₃). ¹³C NMR (126 MHz, Acetone-*d*₆) δ 172.11 (d, J = 4.6 Hz, FQ-C=O), 171.85 (C=O), 171.78 (C=O) 164.70 (COOBn), 155.69 (Boc-C=O), 149.71 (d, J = 240.1 Hz, FQ-C-6), 147.77 (FQ-C), 140.87 (d, J = 11.6 Hz, (FQ-C-7), 138.53 (FQ-C), 137.13 (Bn-C), 128.42 (Bn-C), 128.18 (Bn-C), 127.87 (Bn-C), 118.04 (d, J = 9.4 Hz, FQ-C-4a), 111.94 (d, J = 22.3 Hz, FQ-C-5), 109.01 (FQ-C), 100.34 (FQ-C-8), 78.46 (Boc-C), 65.43 (Bn-CH₂), 55.12 (aminopyrrolidine-C), 53.35 (Leu-C_α), 49.65 (aminopyrrolidine-C), 48.77 (Ala-C_α), 47.44 (Leu-C_α), 40.69 (Leu-CH₂), 34.43 (*c*Pr-CH), 31.18 (aminopyrrolidine-C), 27.68 (Boc-CH₃), 24.50 (Leu-CH), 22.58 (Leu-CH₃), 20.91 (Leu-CH₃), 18.24 (Ala-CH₃), 7.51 (*c*Pr-CH₂), 7.43 (*c*Pr-CH₂). LR-MS: *m/z* = 706.4 [M+H]⁺.

7-((*S*)-3-((*S*)-2-((*S*)-2-amino-4-methylpentanamido)propanamido)pyrrolidin-1-yl)-1-cyclopropyl-6-fluoro-4-oxo-1,4-dihydroquinoline-3-carboxylic acid (**35**): The title compound was synthesized from **31** over two chemical steps. **31** (60 mg, 0.09 mmol, 1 eq.) was dissolved in MeOH (1 mL) and Pd (5 mg, 0.05 mmol, 0.5 eq.) was added. The reaction was stirred under H₂ atmosphere (1 atm) over night at room temperature. The Palladium was removed via centrifugation (17,600 rcf, 5 min) and the solvent was evaporated *in vacuo*. Residual solid was dissolved in HCl in dioxane (4 N) while cooling on ice. The reaction was allowed to warm to room temperature. After disappearance of the starting material (1 h), the solvent was evaporated *in vacuo*. The remaining solid was taken up in 2 mL MeOH and the product was precipitated with Et₂O. The precipitate was isolated by decantation and further purified by preparative HPLC (H₂O : MeCN, 15 - 30 %, 0.1 % formic acid). After lyophilisation, the product was obtained as an off-white solid (28 mg, 61 %). ¹H NMR (500 MHz, MeOH-*d*₄) δ 8.53 (s, 0.5 H, HCOOH), 8.49 (s, 1H, FQ-H-2), 7.64 (d, J = 14.1 Hz, 1H, FQ-H-5), 6.99 (d, J = 7.3 Hz, 1H, FQ-H-8), 4.52 (s, 1H, Leu-C_α-H), 4.40 (q, J = 6.2 Hz, 1H, Ala-C_α-H), 4.00 – 3.84 (m, 1H, aminopyrrolidine-H), 3.84 – 3.74 (m, 1H, aminopyrrolidine-H), 3.74 – 3.55 (m, 4H, cPr-CH, 3x aminopyrrolidine-H), 2.38 – 2.25 (m, 1H, aminopyrrolidine-H), 2.20 – 2.07 (m, 1H, aminopyrrolidine-H), 1.82 – 1.71 (m, 1H, Leu-CH), 1.68 (ddd, J = 13.9, 8.1, 5.8 Hz, 1H, Leu-CH₂), 1.53 (ddd, J = 14.0, 8.3, 6.1 Hz, 1H, Leu-CH₂), 1.40 (d, J = 7.0 Hz, 3H, Ala-CH₃), 1.37 (s, 2H, cPr-CH₂), 1.20 (s, 2H, cPr-CH₂), 1.00 (d, J = 6.5 Hz, 3H, Leu-CH₃), 0.98 (d, J = 6.5 Hz, 3H, Leu-CH₃). ¹³C NMR (126 MHz, MeOH-*d*₄) δ 177.28 (d, J = 2.8 Hz, FQ-C-4), 174.73 (FQ-COOH), 173.91 (HCOOH), 170.09 (C=O), 169.91 (C=O), 151.97 (d, J = 247.4 Hz, FQ-C-6), 148.41 (C), 143.39 (d, J = 11.8 Hz, FQ-C-7), 141.24 (C), 116.00 (d, J = 7.3 Hz, FQ-C-4a), 111.77 (d, J = 23.5 Hz, FQ-C-5), 107.33 (C), 101.55 (d, J = 5.9 Hz, FQ-C-8), 55.98 (d, J = 7.1 Hz, aminopyrrolidine-C), 53.56 (aminopyrrolidine-C), 50.93 (d, J = 1.8 Hz, aminopyrrolidine-C),

50.49 (cPr-CH), 43.46 (Leu-CH₂), 36.72 (cPr-CH), 31.88 (aminopyrrolidine-C), 25.56 (Leu-CH), 23.32 (Leu-CH₃), 22.27 (Leu-CH₃), 18.27 (Ala-CH₃), 8.39 (2x cPr-CH₂). HR-MS calcd [C₂₆H₃₅FN₅O₅]⁺: 516.2617, found 516.2610.

LecA-targeted aminopyrrolidine-RQ-prodrug **36**: The title compound was synthesised in two chemical steps: First, **10** (31 mg, 0.049 mmol, 1 eq.), **30** (34 mg, 0.074 mmol, 1.5 eq.) and TBTU (24 mg, 0.074 mmol, 1.5 eq.) were dissolved in 1 mL dry DMF. DIPEA (27 μ L, 0.16 mmol, 3.2 eq.) was added dropwise and the reaction was stirred for 1 h. After evaporation of the solvent, the residue was taken up in MeOH (2 mL). Pd black (10 mg, 0.05 mmol, 1 eq.) was added and the reaction was stirred under H₂ atmosphere for 2 d. Afterwards, the reaction was filtered over celite and further purified by preparative HPLC (MeCN : H₂O, 20-33%, 0.1% formic acid). The title compound was obtained as a beige amorphous solid (22 mg, 48% over 2 chemical steps). ¹H NMR (500 MHz, MeOH-*d*₄) δ 8.60 (s, 1H, FQ-H-2), 7.82 (d, J = 8.2 Hz, 2H, Ar-H), 7.71 (d, J = 14.2 Hz, 1H, FQ-H-5), 7.56 (d, J = 8.3 Hz, 2H, Ar-H), 7.04 (d, J = 7.4 Hz, 1H, FQ-H-8), 4.71 (d, J = 9.8 Hz, 1H, glyco-H-1), 4.54 – 4.44 (m, 1H, aminopyrrolidine-CH), 4.36 (q, J = 7.2 Hz, 1H, Ala-C α -H), 4.33 – 4.25 (m, 2H, Ala-C α -H, Leu-C α -H), 3.91 (d, J = 3.5 Hz, 1H, glyco-H-4), 3.90 – 3.59 (m, 11H, cPr-CH, 2x aminopyrrolidine-CH₂, Gly-CH₂, glyco-H-2, glyco-H-5, glyco-H-6), 3.52 (dd, J = 9.2, 3.3 Hz, 1H, glyco-H-3), 2.37 – 2.20 (m, 1H, aminopyrrolidine-H), 2.20 – 2.10 (m, 1H, aminopyrrolidine-H), 1.75 (ddd, J = 14.6, 11.2, 3.6 Hz, 1H, Leu-CH₂), 1.70 – 1.56 (m, 2H, Leu-CH₂ + Leu-CH), 1.49 (d, J = 7.2 Hz, 3H, Ala-CH₃), 1.41 (d, J = 7.2 Hz, 3H, Ala-CH₃), 1.38 (d, J = 7.1 Hz, 2H, cPr-CH₂), 1.30 – 1.14 (m, 2H, cPr-CH₂), 0.87 (d, J = 6.2 Hz, 3H, Leu-CH₃), 0.85 (d, J = 6.2 Hz, 3H, Leu-CH₃). ¹³C NMR (126 MHz, MeOH-*d*₄) δ 177.52 (d, J = 2.8 Hz, FQ-C=O), 176.71 (C=O), 175.15 (C=O), 174.86 (C=O), 172.46 (C=O), 170.07 (C=O), 169.97 (C=O), 152.04 (d, J = 247.4 Hz, FQ-C-6), 148.62 (FQ-C), 143.56 (d, J = 11.9 Hz, FQ-C-7), 142.33 (FQ-C), 141.38 (Ar-C), 132.15 (Ar-C), 129.81 (Ar-

C), 129.18 (Ar-C), 116.06 (d, J = 6.5 Hz, FQ-C-4a), 111.92 (d, J = 23.6 Hz, FQ-C-5), 107.34 (FQ-C), 101.64 (d, J = 5.9 Hz, FQ-C-8), 88.88 (glyco-C-1), 80.79 (glyco-C-5), 76.26 (glyco-C-3), 70.85 (glyco-C-2), 70.39 (glyco-C-4), 62.67 (glyco-C-6), 55.95 (d, J = 5.3 Hz, aminopyrrolidine-C), 53.91 (Leu-C α), 52.60 (Ala-C α), 50.94 (aminopyrrolidine-C, Ala-C α), 44.21 (Gly-C α), 41.12 (Leu-CH $_2$), 36.82 (cPr-CH), 31.81 (aminopyrrolidine-C), 25.79 (Leu-CH), 23.55 (Leu-CH $_3$), 21.50 (Leu-CH $_3$), 17.78 (Ala-CH $_3$), 17.25 (Ala-CH $_3$), 8.49 (cPr-CH $_2$), 8.47 (cPr-CH $_2$). HR-MS calcd [C $_{44}$ H $_{57}$ FN $_7$ O $_{13}$ S] $^+$: 942.3714, found 942.3694.

LecB-targeted aminopyrrolidine-FQ-prodrug benzyl ester **33**: **16** (70 mg, 0.10 mmol, 1 eq.), **30** (55 mg, 0.12 mg, 1.2 eq.) and TBTU (48 mg, 0.15 mmol, 1.5 eq.) were dissolved in dry DMF (2 mL). DIPEA (52 μ L, 0.3 mmol, 3 eq.) was added dropwise and the reaction was stirred for 1 h. The solvent was evaporated *in vacuo* and the reaction was purified by preparative HPLC (MeCN : H $_2$ O, 25-40%, 0.1% formic acid). After lyophilisation, the title compound was isolated as an off-white powder (53 mg, 49%). 1 H NMR (500 MHz, MeOH-*d* $_4$) δ 8.56 (s, 1H, FQ-H-2), 8.04 (d, J = 8.2 Hz, 2H, glyco-Ar-H), 7.93 (d, J = 8.3 Hz, 2H, glyco-Ar-H), 7.75 (d, J = 14.5 Hz, 1H, FQ-H-5), 7.47 (d, J = 7.2 Hz, 2H, Bn), 7.39 – 7.34 (m, 2H, Bn), 7.34 – 7.29 (m, 1H, Bn), 6.98 (d, J = 7.5 Hz, 1H, FQ-H-8), 5.31 (s, 2H, Bn), 4.47 – 4.38 (m, 2H, Ala-C α -H, aminopyrrolidine-H), 4.36 – 4.26 (m, 2H, Ala-C α -H, Leu-C α -H), 3.91 – 3.82 (m, 1H, aminopyrrolidine-H), 3.79 (d, J = 16.7 Hz, 1H, Gly-C α -H), 3.80 – 3.74 (m, 1H, aminopyrrolidine-H), 3.66 (d, J = 16.7 Hz, 1H, Gly-C α -H), 3.64 – 3.59 (m, 1H, aminopyrrolidine-H), 3.58 (d, J = 2.8 Hz, 1H, glyco-H-4), 3.58 – 3.51 (m, 2H, cPr-CH, aminopyrrolidine-H), 3.43 (dq, J = 6.5, 0.5 Hz, 1H, glyco-H-5), 3.40 – 3.35 (m, 2H, glyco-H-3, glyco-H-1), 3.34 – 3.27 (m, 1H, linker-CH $_2$ -), 3.10 (ddd, J = 9.0, 7.1, 2.4 Hz, 1H, glyco-H-2), 3.02 (dd, J = 12.9, 7.1 Hz, 1H, linker-CH $_2$ -), 2.35 – 2.20 (m, 1H, aminopyrrolidine-H), 2.15 – 2.07 (m, 1H, aminopyrrolidine-H), 1.81 – 1.69 (m, 1H, Leu-CH), 1.69 – 1.55 (m, 2H, Leu-CH $_2$), 1.50 (d, J = 7.2 Hz, 3H, Leu-CH $_3$), 1.39 (d, J = 7.2 Hz,

3H, Leu-CH₃), 1.33 – 1.28 (m, 1H, *c*Pr-CH₂), 1.16 (d, J = 6.4 Hz, 3H, glyco-H-6), 1.12 – 1.05 (m, 2H, *c*Pr-CH₂), 0.85 (d, J = 6.4 Hz, 3H, Leu-CH₃), 0.84 (d, J = 6.3 Hz, 3H, Leu-CH₃). ¹³C NMR (126 MHz, MeOH-*d*₄) δ 176.30 (CONH), 175.32 (d, J = 2.7 Hz, FQ-C=O), 175.05 (CONH), 174.75 (CONH), 172.38 (CONH), 169.09 (CONH), 166.10 (COOBn), 151.73 (d, J = 244.9 Hz, FQ-C-6), 149.61 (FQ-Ar-C), 145.13 (Ar-C), 142.67 (d, J = 12.0 Hz, FQ-C-7), 140.44 (Ar-C), 138.34 (Ar-C), 138.00 (Ar-C), 129.56 (glyco-Ar-C), 129.53 (Bn-Ar-C), 129.25 (Bn-Ar-C), 129.13 (Bn-Ar-C), 128.10 (glyco-Ar-C), 119.19 (d, J = 6.7 Hz, FQ-C-4a), 112.91 (d, J = 23.1 Hz, FQ-C-5), 109.81 (Ar-C), 101.62 (d, J = 5.1 Hz, FQ-C-8), 79.62 (glyco-C-2), 76.32 (glyco-C-3), 75.51 (glyco-C-5), 73.54 (glyco-C-4), 69.60 (glyco-C-1), 67.07 (Bn), 55.94 (d, J = 6.7 Hz, aminopyrrolidine-C), 53.94 (Leu-C_α), 52.54 (Ala-C_α), 50.87 (d, J = 1.8 Hz, aminopyrrolidine-C), 50.76 (Ala-C_α), 48.84 (aminopyrrolidine-C, extracted from ¹H-¹³C-HSQC) 45.55 (glyco-linker-CH₂-), 44.19 (Gly-C_α), 41.16 (Leu-CH₂), 36.18 (*c*Pr-CH), 31.88 (aminopyrrolidine-C), 25.80 (Leu-CH), 23.52 (Leu-CH₃), 21.53 (Leu-CH₃), 17.88 (Ala-CH₃), 17.26 (Ala-CH₃), 17.11 (glyco-C-6), 8.51 (*c*Pr-CH₂), 8.49 (*c*Pr-CH₂). LR-MS: *m/z* = 539.2 [M+2H]²⁺.

LecB-targeted aminopyrrolidine-FQ-prodrug **37**: **33** (40 mg, 0.037 mmol, 1 eq.) was dissolved in MeOH (1 mL). Pd/C (10% m/m, 4 mg, 10 mol%) was added and the atmosphere was changed to H₂ (1 atm.). The reaction was stirred at room temperature for 24 h until full consumption of the starting material. Pd/C was removed by centrifugation (17600 rcf, 10 min) and the solvent was removed *in vacuo*. After purification by pHPLC (MeCN in Water, 22-35%, 0.1% formic acid), the title compound was obtained as an off-white amorphous solid (15 mg, 41%). ¹H NMR (500 MHz, MeOH-*d*₄) δ 8.78 (s, 1H, FQ-H-2), 8.05 (d, J = 8.1 Hz, 2H, glyco-Ar-H), 7.93 (d, J = 8.3 Hz, 2H, glyco-Ar-H), 7.90 (d, J = 13.1 Hz, 1H, FQ-H-5), 7.61 (d, J = 7.2 Hz, 1H, FQ-H-8), 4.90 (q, J = 6.9 Hz, 1H, Ala-C_α-H), 4.54 – 4.37 (m, 2H, Ala'-C_α-H, Leu-C_α-H), 4.00 (d, J = 16.9 Hz, 1H, Gly-C_α-H), 3.96 – 3.84

(m, 2H, 2x aminopyrrolidine-H), 3.83 – 3.72 (m, 2H, aminopyrrolidine-H, Gly-C α -H), 3.72 – 3.63 (m, 1H, aminopyrrolidine-H), 3.58 (d, J = 2.9 Hz, 1H, glyco-H-4), 3.50 – 3.27 (m, 7H, 3x aminopyrrolidine-H, glyco-H-5, glyco-H-1, glyco-H-3, glyco-linker-CH₂-), 3.10 (ddd, J = 9.0, 7.1, 2.4 Hz, 1H, glyco-H-2), 3.02 (dd, J = 12.9, 7.2 Hz, 1H, glyco-linker-CH₂-), 1.78 – 1.57 (m, 3H, Leu-CH, Leu-CH₂), 1.50 (d, J = 7.1 Hz, 3H, Ala-CH₃), 1.42 (d, J = 6.9 Hz, 2H, cPr-CH₂), 1.36 (d, J = 6.8 Hz, 3H, Ala'-CH₃), 1.26 – 1.20 (m, 2H, cPr-CH₂), 1.16 (d, J = 6.4 Hz, 3H, glyco-H-6), 0.87 (d, J = 5.6 Hz, 3H, Leu-CH₃), 0.83 (d, J = 5.6 Hz, 3H, Leu-CH₃). ¹³C NMR (126 MHz, MeOH-*d*₄) δ 178.37 (d, J = 2.0 Hz, FQ-C=O), 175.82 (CONH), 174.14 (CONH), 172.57 (CONH), 171.68 (CONH), 169.67 (CONH), 168.86 (COOH), 155.08 (d, J = 250.0 Hz, FQ-C-6), 149.36 (FQ-C-2), 146.84 (d, J = 9.9 Hz, FQ-C-7), 145.06 (Ar-C), 140.78 (Ar-C), 138.51 (Ar-C), 129.53 (glyco-Ar-C), 128.08 (glyco-Ar-C), 121.07 (d, J = 7.0 Hz, FQ-C-4a), 112.56 (d, J = 23.4 Hz, FQ-C-5), 107.68 (Ar-C), 79.62 (glyco-C-2), 76.33 (glyco-C-3), 75.52 (glyco-C-5), 73.55 (glyco-C-4), 69.61 (glyco-C-1), 53.12 (Leu-C α), 52.12 (Ala-C α), 51.06 (aminopyrrolidine-C), 50.67 (d, J = 3.8 Hz, aminopyrrolidine-C), 46.60 (Ala'-C α), 46.46 (aminopyrrolidine-C), 45.55 (glyco-linker-CH₂-), 43.91 (Gly-C α), 43.17 (aminopyrrolidine-C), 41.61 (Leu-CH₂), 37.02 (cPr-CH), 25.74 (Leu-CH), 23.54 (Leu-CH₃), 21.63 (Leu-CH₃), 17.85 (Ala-CH₃), 17.26 (Ala'-CH₃), 17.10 (glyco-C-6), 8.61 (cPr-CH₂), 8.56 (cPr-CH₂). HR-MS calcd [C₄₅H₆₀FN₈O₁₄S]⁺: 987.3928, found 987.3903.

(S)-7-(3-(hydroxymethyl)-1-pyrrolidinyl)-1-cyclopropyl-6-fluoro-1,4-dihydro-4-oxo-1,8-naphthyridine-3-carboxylic acid (**39**): 7-chloro-1-cyclopropyl-6-fluoro-4-oxo-1,4-dihydroquinoline-3-carboxylic acid (**26**, 1000 mg, 3.55 mmol, 1 eq.) was dispersed in dry pyridine (10 mL) and heated to 80 °C to fully dissolve. L- β -prolinol (**38**, 732 μ L, 7.1 mmol, 2 eq.) was added and the temperature was increased to 140 °C. The reaction was refluxed over night. After cooling to room temperature, the product precipitated from the reaction and was isolated by filtration. The precipitate was washed with ice-cold MeOH and

obtained as a yellow solid (750 mg, 62%). ^1H NMR (500 MHz, $\text{MeOH-}d + \text{CHCl}_3\text{-}d$, 1:1) δ 8.78 (s, 1H, FQ-H-2), 7.87 (d, $J = 13.9$ Hz, 1H, FQ-H-5), 7.03 (d, $J = 7.3$ Hz, 1H, FQ-H-8), 3.88 – 3.76 (m, 2H, 2x pyrrolidinyl-methanol-H), 3.76 – 3.67 (m, 3H, 2x pyrrolidinyl-methanol-H, *cPr*-CH), 3.60 (dd, $J = 10.8, 7.2$ Hz, 1H, pyrrolidinyl-methanol-H), 3.51 (ddd, $J = 10.1, 7.4, 2.1$ Hz, 2H, 2x pyrrolidinyl-methanol-H), 2.59 (hept, $J = 7.2$ Hz, 1H, pyrrolidinyl-methanol-H), 2.18 (dtd, $J = 11.9, 7.1, 4.5$ Hz, 1H, pyrrolidinyl-methanol-H), 1.88 (dq, $J = 12.6, 8.2$ Hz, 1H, pyrrolidinyl-methanol-H), 1.45 (q, $J = 6.8$ Hz, 2H, *cPr*- CH_2), 1.21 (q, $J = 6.6$ Hz, 2H, *cPr*- CH_2). ^{13}C NMR (126 MHz, $\text{MeOH-}d + \text{CHCl}_3\text{-}d$, 1:1) δ 173.16 (FQ-C=O), 169.65 (COOH), 152.06 (d, $J = 252.5$ Hz, FQ-C-6), 148.01 (FQ-C-2), 144.44 (d, $J = 15.8$ Hz, FQ-C-7), 141.51 (FQ-C), 128.36 (FQ-C), 111.48 (d, $J = 24.1$ Hz, FQ-C-5), 105.36 (d, $J = 2.6$ Hz, FQ-C-8), 100.04 (d, $J = 6.3$ Hz, FQ-C-4a), 63.69 (pyrrolidinyl-methanol-C), 53.78 (d, $J = 5.7$ Hz, pyrrolidinyl-methanol-C), 50.71 (d, $J = 6.6$ Hz, pyrrolidinyl-methanol-C), 41.38 (d, $J = 1.9$ Hz, pyrrolidinyl-methanol-C), 37.18 (s, *cPr*-CH), 28.25 (pyrrolidinyl-methanol-C), 8.47 (*cPr*- CH_2). LR-MS: $m/z = 347.2$ [$\text{M}+\text{H}$] $^+$.

(*S*)-7-(3-(hydroxymethyl)-1-pyrrolidinyl)-1-cyclopropyl-6-fluoro-1,4-dihydro-4-oxo-1,8-naphthyridine-3-carboxylic acid methyl ester (**40**): **39** (500 mg, 1.44 mmol, 1 eq.) and (*R/S*)-camphor-10-sulfonic acid (668 mg, 2.88 mmol, 2 eq.) were dried on high vacuum and subsequently dissolved in dry MeOH (15 mL). The reaction was refluxed until a clear solution was obtained (72 h). After cooling to room temperature, the solvent was evaporated *in vacuo*. The residual solid was dissolved in CH_2Cl_2 (10 mL) and the organic phase was washed with satd. aqueous NaHCO_3 (3 x) and satd. brine (2 x) and dried over Na_2SO_4 . After evaporation of the solvent, the product was obtained as a yellow solid (510 mg 96%), containing 4 % of the starting material as an impurity, determined by ^1H -NMR. ^1H NMR (500 MHz, $\text{DMSO-}d_6$) δ 8.35 (s, 1H, FQ-H-2), 7.64 (d, $J = 14.6$ Hz, 1H, FQ-H-5), 6.94 (d, $J = 7.6$ Hz, 1H, FQ-H-8), 4.80 (t, $J = 5.2$ Hz, 1H, OH), 3.72 (s, 3H, COOMe), 3.66

– 3.52 (m, 4H, 3x pyrrolidiny-methanol-H, cPr-CH), 3.49 (td, J = 10.8, 5.0 Hz, 1H, pyrrolidiny-methanol-H), 3.46 – 3.39 (m, 1H, pyrrolidiny-methanol-H), 3.35 – 3.30 (m, 1H, pyrrolidiny-methanol-H), 2.44 (p, J = 7.0 Hz, 1H, pyrrolidiny-methanol-H), 2.04 (dtd, J = 11.8, 7.1, 4.8 Hz, 1H, pyrrolidiny-methanol-H), 1.76 (dq, J = 11.8, 7.7 Hz, 1H, pyrrolidiny-methanol-H), 1.27 – 1.20 (m, 1H, cPr-CH₂), 1.11 – 1.02 (m, 1H, cPr-CH₂). ¹³C NMR (126 MHz, DMSO-*d*₆) δ 171.46 (FQ-C=O), 165.20 (COOMe), 149.43 (d, J = 242.8 Hz, FQ-C-6), 147.93 (FQ-C-2), 140.48 (d, J = 11.3 Hz, FQ-C-7), 138.63 (FQ-C), 117.62 (d, J = 5.5 Hz, FQ-C-4a), 111.44 (d, J = 22.5 Hz, FQ-C-5), 108.57 (FQ-C), 100.47 (d, J = 5.3 Hz, FQ-C-8), 62.55 (pyrrolidiny-methanol-C), 52.50 (d, J = 5.4 Hz, pyrrolidiny-methanol-C), 51.24 (COOCH₃), 49.23 (d, J = 5.3 Hz, pyrrolidiny-methanol-C), 40.68 (d, J = 1.7 Hz, pyrrolidiny-methanol-C), 34.63 (cPr-CH), 27.46 (pyrrolidiny-methanol-C), 7.53 (cPr-CH₂). LR-MS: *m/z* = 361.2 [M+H]⁺.

(*S*)-7-(3-(azidomethyl)-1-pyrrolidiny)-1-cyclopropyl-6-fluoro-1,4-dihydro-4-oxo-1,8-naphthyridine-3-carboxylic acid methyl ester (**41**): **40** (400 mg, 1.1 mmol, 1 eq.) and PPh₃ (577 mg, 2.2 mmol, 2 eq.) were dispersed in dry THF (10 mL) at room temperature. DIAD (473 μL, 2.2 mmol, 2 eq.) was added dropwise under vigorous stirring, resulting in a clear solution. Afterwards, DPPA (432 μL, 2.2 mmol, 2 eq.) was added dropwise, which resulted in a precipitation after 10 min. The reaction was stirred for 1 h and subsequently quenched with MeOH. After evaporation of the solvent *in vacuo*, the product was purified via NP-MPLC (CH₂Cl₂/PE (9/5) : EtOH, 1 - 5%), yielding the title compound as an off-white solid (277 mg, 65 %). ¹H NMR (500 MHz, MeOH-*d*₄) δ 8.46 (s, 1H, FQ-H-2), 7.64 (d, J = 14.7 Hz, 1H, FQ-H-5), 6.89 (d, J = 7.6 Hz, 1H, FQ-H-8), 3.82 (s, 3H, COOCH₃) 3.71 (ddd, J = 10.3, 7.3, 3.1 Hz, 1H, azidomethylpyrrolidine-H), 3.65 (ddq, J = 10.8, 7.6, 3.5 Hz, 1H, azidomethylpyrrolidine-H), 3.62 – 3.55 (m, 1H, azidomethylpyrrolidine-H), 3.55 – 3.50 (m, 2H, azidomethylpyrrolidine-H, cPr-CH), 3.47 (dd, J = 12.3, 7.3 Hz, 1H,

azidomethylpyrrolidine-H), 3.35 (ddd, J = 10.2, 7.4, 2.7 Hz, 1H, azidomethylpyrrolidine-H), 2.61 (hept, J = 7.2 Hz, 1H, azidomethylpyrrolidine-H), 2.20 (dtd, J = 11.6, 7.0, 4.1 Hz, 1H, azidomethylpyrrolidine-H), 1.84 (dq, J = 12.4, 8.2 Hz, 1H, azidomethylpyrrolidine-H), 1.40 – 1.24 (m, 2H, cPr-CH₂), 1.20 – 1.06 (m, 2H, cPr-CH₂). ¹³C NMR (126 MHz, MeOH-d₄) δ 175.19 (FQ-C=O), 166.90 (COOMe), 151.68 (d, J = 244.4 Hz, FQ-C-6), 149.64 (FQ-C-2), 142.60 (d, J = 11.8 Hz, FQ-C-7), 140.45 (FQ-C), 119.15 (d, J = 6.4 Hz, FQ-C-4a), 112.85 (d, J = 23.1 Hz, FQ-C-5), 109.77 (FQ-C), 101.46 (d, J = 5.4 Hz, FQ-C-8), 54.73 (azidomethylpyrrolidine-C), 54.24 (d, J = 6.2 Hz, azidomethylpyrrolidine-C), 52.01 (COOCH₃), 50.46 (d, J = 5.6 Hz, azidomethylpyrrolidine-C), 39.86 (azidomethylpyrrolidine-C), 36.11 (cPr-CH), 29.77 (azidomethylpyrrolidine-C), 8.44 (cPr-CH₂). LR-MS: m/z = 385.2 [M+H]⁺.

(S)-7-(3-(azidomethyl)-1-pyrrolidinyl)-1-cyclopropyl-6-fluoro-1,4-dihydro-4-oxo-1,8-naphthyridine-3-carboxylic acid • HCl (**42**): **41** (150 mg, 0.39 mmol, 1 eq.) and Pd/C (10 % m/m, 42 mg, 10 mol%) were stirred in MeOH (10 mL) under H₂-atmosphere (1 atm) over night. The reaction was filtered over celite and concentrated *in vacuo*. HCl in dioxane (4 N, 100 μL) was mixed with 40 mL Et₂O and carefully added to the solution of product in MeOH while stirring on ice, yielding the title compound as a yellow solid (120 mg, 78%) ¹H NMR (500 MHz, H₂O-d₂) δ 8.34 (s, 1H, FQ-H-2), 7.27 (d, J = 14.6 Hz, 1H, FQ-H-5), 6.54 (d, J = 7.4 Hz, 1H, FQ-H-8), 3.82 (s, 3H, COOCH₃), 3.69 – 3.60 (m, 1H, aminomethylpyrrolidine-H), 3.55 – 3.40 (m, 2H, aminomethylpyrrolidine-H, cPr-CH), 3.30 (s, 1H), 3.25 – 3.08 (m, 3H, 3x aminomethylpyrrolidine-H), 2.72 – 2.58 (m, 1H, aminomethylpyrrolidine-H), 2.35 – 2.20 (m, 1H, aminomethylpyrrolidine-H), 1.94 – 1.64 (m, 1H, aminomethylpyrrolidine-H), 1.25 (d, J = 5.6 Hz, 2H, cPr-CH₂), 0.98 (s, 2H, cPr-CH₂). ¹³C NMR (126 MHz, H₂O-d₂) δ 173.63 (FQ-C=O), 166.68 (COOCH₃), 149.62 (d, J = 245.1 Hz, FQ-C-6), 148.66 (FQ-C-2), 140.59 (d, J = 11.7 Hz, FQ-C-7), 138.43 (FQ-C), 116.50 (d,

J = 6.5 Hz, FQ-C-4a), 110.83 (d, J = 23.6 Hz, FQ-C-5), 107.09 (FQ-C), 99.97 (d, J = 5.4 Hz, FQ-C-8), 52.65 (d, J = 5.8 Hz, aminomethylpyrrolidine-C), 51.90 (COOCH₃), 48.98 (d, J = 6.0 Hz, aminomethylpyrrolidine-C), 41.69 (aminomethylpyrrolidine-C), 36.30 (cPr-CH), 35.01 (aminomethylpyrrolidine-C), 28.55 (aminomethylpyrrolidine-C), 7.13 (cPr-CH₂). LR-MS: *m/z* = 360.2 [M+H]⁺.

(S)-7-(3-(aminomethyl)-1-pyrrolidinyl)-1-cyclopropyl-6-fluoro-1,4-dihydro-4-oxo-1,8-naphthyridine-3-carboxylic acid (**3**): Methyl ester **42** (39 mg, 0.1 mmol, 1 eq.) was dissolved in a mixture of THF, MeOH and H₂O (3/1/1) at room temperature. LiOH (13 mg, 0.5 mmol, 5 eq.) was added and the reaction was stirred over night until full transformation. After evaporation of the solvent *in vacuo*, the product was purified by pHPLC (MeCN in Water, 10-25%, 0.1% formic acid), yielding the title compound as an off-white amorphous solid (15 mg, 43%). ¹H NMR (500 MHz, H₂O-*d*₂) δ 8.31 (s, 1H, FQ-H-2), 6.93 (d, J = 13.8 Hz, 1H, FQ-H-5), 6.56 (d, J = 7.4 Hz, 1H, FQ-H-8), 3.75 – 3.67 (m, 1, aminomethylpyrrolidine-H), 3.63 – 3.51 (m, 1H, aminomethylpyrrolidine-H), 3.54 – 3.48 (m, 1H, aminomethylpyrrolidine-H), 3.42 (s, 1H, aminomethylpyrrolidine-H), 3.29 – 3.12 (m, 3H, cPr-CH, aminomethylpyrrolidine-CH₂), 2.69 (dt, J = 14.2, 5.8 Hz, 1H, aminomethylpyrrolidine-H), 2.35 – 2.23 (m, 1H, aminomethylpyrrolidine-H), 1.89 – 1.75 (m, 1H, aminomethylpyrrolidine-H), 1.35 (d, J = 6.2 Hz, 2H, cPr-CH₂), 1.08 (s, 2H, cPr-CH₂). ¹³C NMR (126 MHz, H₂O-*d*₂) δ 173.86 (d, J = 3.5 Hz, FQ-C=O), 169.38 (COOH), 149.71 (d, J = 249.2 Hz, FQ-C-6), 146.83 (FQ-C), 141.48 (d, J = 11.1 Hz, FQ-C-7), 139.22 (FQ-C), 112.55 (d, J = 7.3 Hz, FQ-C-4a), 109.34 (d, J = 23.5 Hz, FQ-C-5), 104.99 (d, J = 3.5 Hz, FQ-C-8a), 99.64 (d, J = 5.6 Hz, FQ-C-8), 52.70 (d, J = 6.8 Hz, aminomethylpyrrolidine-C), 49.19 (d, J = 4.9 Hz, aminomethylpyrrolidine-C), 41.51 (aminomethylpyrrolidine-C), 36.32 (aminomethylpyrrolidine-C), 35.72 (cPr-CH), 28.39 (aminomethylpyrrolidine-C), 7.22 (cPr-CH₂). HR-MS calcd [C₁₈H₂₁FN₃O₃]⁺: 346.1561, found 346.1555.

1-cyclopropyl-6-fluoro-7-((*R*)-3-((4*S*,7*S*)-7-isobutyl-4,11,11-trimethyl-3,6,9-trioxo-10-oxa-2,5,8-triazadodecyl)pyrrolidin-1-yl)-4-oxo-1,4-dihydroquinoline-3-carboxylic acid methyl ester (**43**): **42** (50 mg, 0.13 mmol, 1 eq.), **17** (48 mg, 0.16 mmol, 1.2 eq.) and TBTU (51 mg, 0.16 mmol, 1.2 eq.) were dissolved in dry DMF (1.5 mL) and cooled on ice. DIPEA (45 μ L, 0.26 mmol, 2 eq.) was added dropwise and the reaction was allowed to warm to room temperature. After 16 h, the solvent was concentrated *in vacuo* and diluted with CH₂Cl₂ (20 mL). The organic phase was washed with aqueous KHSO₄ (1 M, 2x), neutralised with aqueous satd. NaHCO₃ (1x), washed with satd. brine (2x) and dried over Na₂SO₄. After purification via NP-MPLC (CH₂Cl₂ : MeOH, 1 - 10%), the title compound was obtained as a white solid (42 mg, 50 %). The compound was directly used for global deprotection without NMR-spectroscopic characterisation. LR-MS: *m/z* = 630.4 [M+H]⁺.

1-cyclopropyl-6-fluoro-7-((*R*)-3-((4*S*,7*S*)-7-isobutyl-4,11,11-trimethyl-3,6,9-trioxo-10-oxa-2,5,8-triazadodecyl)pyrrolidin-1-yl)-4-oxo-1,4-dihydroquinoline-3-carboxylic acid (**47**):

The title compound was synthesised over two chemical steps: **43** (42 mg, 0.065 mmol, 1 eq.) and LiOH (7.8 mg, 0.325 mmol, 5 eq.) were dissolved in a mixture of THF/H₂O/MeOH (5/5/1, 1.5 mL) and stirred at room temperature until full consumption of the starting material (3 h). The reaction was diluted with MeOH (5 mL) and neutralised with Amberlite IR-120 H⁺ exchange resin. After evaporation of the solvent, the residuum (35 mg, 86%) was dissolved in a mixture of dioxane/MeOH (8/2, 1 mL). While cooling on ice, HCl in dioxane (4 N, 2 mL) was added dropwise. The reaction was allowed to warm to r.t. and stirred until full consumption of the starting material (1 h). After removal of the solvent *in vacuo*, the product was purified via preparative HPLC (H₂O : MeCN, 18 - 30%, 0.1% formic acid). The title compound was obtained as a white solid (16 mg, 46 % over two steps). ¹H NMR (500 MHz, MeOH-*d*₄) δ 9.01 (s, 1H, FQ-H-2), 7.96 (d, *J* = 13.9 Hz, 1H, FQ-H-5), 7.23 (d, *J* = 7.4 Hz, 1H, FQ-H-8), 4.40 (q, *J* = 7.1 Hz, 1H, Ala-C α -H), 4.04 – 3.83

(m, 4H, *cPr*-CH, Ala-C α -H, Leu-C α -H, aminomethylpyrrolidine-H), 3.81 – 3.70 (m, 1H, aminomethylpyrrolidine-H), 3.61 – 3.53 (m, 1H, aminomethylpyrrolidine-H), 3.36 (d, *J* = 6.9 Hz, 2H, aminomethylpyrrolidine-CH $_2$), 2.63 (tt, *J* = 7.1, 7.1 Hz, 1H, aminomethylpyrrolidine-H), 2.38 – 2.09 (m, 1H, aminomethylpyrrolidine-H), 1.97 – 1.84 (m, 1H, aminomethylpyrrolidine-H), 1.83 – 1.72 (m, 2H, Leu-CH $_2$, Leu-CH), 1.72 – 1.63 (m, 1H, Leu-CH $_2$), 1.53 – 1.48 (m, 2H, *cPr*-CH $_2$), 1.42 (d, *J* = 7.1 Hz, 3H, Ala-CH $_3$), 1.34 – 1.24 (m, 2H, *cPr*-CH $_2$), 1.02 (d, *J* = 6.2 Hz, 3H, Leu-CH $_3$), 1.00 (d, *J* = 6.1 Hz, 3H, Leu-CH $_3$). ^{13}C NMR (126 MHz, MeOH-*d* $_4$) δ 174.81 (C=O), 171.62 (d, *J* = 4.2 Hz, FQ-C=O), 170.69 (C=O), 170.36 (COOH), 153.15 (d, *J* = 252.6 Hz, FQ-C-6), 149.44 (FQ-C-2), 145.64 (d, *J* = 12.1 Hz, FQ-C-7), 142.75 (FQ-C), 112.62 (d, *J* = 8.4 Hz, FQ-C-4a), 111.28 (d, *J* = 24.9 Hz, FQ-C-5), 104.76 (FQ-C), 101.14 (d, *J* = 6.3 Hz, FQ-C-8), 55.03 (d, *J* = 6.5 Hz, aminomethylpyrrolidine-C), 52.84 (Ala-C α), 51.17 (d, *J* = 5.9 Hz, aminomethylpyrrolidine-C), 50.74 (Ala-C α), 42.15 (aminomethylpyrrolidine-C), 41.66 (Leu-CH $_2$), 40.25 (aminomethylpyrrolidine-C), 38.49 (*cPr*-CH), 29.67 (aminomethylpyrrolidine-C), 25.35 (Leu-CH), 23.18 (Leu-CH $_3$), 22.07 (Leu-CH $_3$), 18.30 (Ala-CH $_3$), 8.64 (*cPr*-CH $_2$). HR-MS calcd [C $_{27}$ H $_{37}$ FN $_5$ O $_5$] $^+$: 530.2773, found 530.2766.

LecA-targeted aminomethylpyrrolidine-FQ-Prodrug **48**: The title compound was synthesised in two chemical steps: First, **10** (27 mg, 0.049 mmol, 1 eq.), **42** (30 mg, 0.076 mmol, 1.8 eq.) and TBTU (21 mg, 0.065 mmol, 1.8 eq.) were dissolved in 2 mL dry DMF. DIPEA (15 μL , 0.086 mmol, 2 eq.) was added dropwise and the reaction was stirred for 1 h. After evaporation of the solvent, the residue was taken up in 1 mL H $_2$ O/THF (1:1). LiOH (10 mg, 0.4 mmol, 10 eq.) was dissolved in 1 mL water and added stepwise to the reaction until a full transformation was observed (3 h). Afterwards, the reaction was neutralised with Amberlite IR-120 H $^+$ exchange resin and further purified by preparative HPLC (MeCN:H $_2$ O, 20-33%, 0.1% formic acid). The title compound was obtained as a beige amorphous solid

(33 mg, 70% over 2 chemical steps). ^1H NMR (500 MHz, MeOH-*d*4) δ 8.65 (s, 1H, FQ-H-2), 7.79 (d, $J = 8.0$ Hz, 2H, Ar-H), 7.72 (d, $J = 14.2$ Hz, 1H, FQ-H-5), 7.52 (d, $J = 8.0$ Hz, 2H, Ar-H), 7.02 (d, $J = 7.2$ Hz, 1H, FQ-H-8), 4.71 (d, $J = 9.8$ Hz, 1H, glyco-H-1), 4.43 – 4.32 (m, 2H, Ala-C $_{\alpha}$ -H, Leu-C $_{\alpha}$ -H), 4.29 (q, $J = 7.3$ Hz, 1H, Ala-C $_{\alpha}$ -H), 3.97 – 3.89 (m, 2H, glyco-H-4, Gly-CH), 3.82 – 3.58 (m, 9H, Gly-CH, 3x aminomethylpyrrolidine-H, *c*Pr-CH, glyco-H-6, glyco-H-2, glyco-H-5), 3.52 (dd, $J = 9.2, 3.3$ Hz, 1H, glyco-H-3), 3.47 – 3.33 (m, 2H, 2x aminomethylpyrrolidine-H), 3.29 – 3.22 (m, 1H, aminomethylpyrrolidine-H), 2.60 (tt, $J = 13.4, 6.6$ Hz, 1H, aminomethylpyrrolidine-H), 2.18 (td, $J = 12.0, 6.2$ Hz, 1H, aminomethylpyrrolidine-H), 1.86 – 1.71 (m, 1H, aminomethylpyrrolidine-H, Leu-CH $_2$), 1.71 – 1.58 (m, 2H, Leu-CH $_2$, Leu-CH), 1.49 (d, $J = 7.3$ Hz, 3H, Ala-CH $_3$), 1.42 (d, $J = 7.2$ Hz, 3H, Ala-CH $_3$), 1.39 – 1.36 (m, 2H, *c*Pr-CH $_2$), 1.18 (s, 2H, *c*Pr-CH $_2$), 0.88 (d, $J = 5.5$ Hz, 6H, 2x Leu-CH $_3$). ^{13}C NMR (126 MHz, MeOH-*d*4) δ 177.62 (C=O), 176.64 (C=O), 175.27 (C=O), 174.88 (C=O), 172.68 (C=O), 170.26 (C=O), 169.79 (C=O), 152.02 (d, $J = 248.5$ Hz, FQ-C-6), 148.66 (FQ-C), 142.31 (FQ-C), 141.49 (Ar-C), 132.09 (Ar-C), 129.69 (Ar-C), 129.13 (Ar-C), 111.98 (d, $J = 23.3$ Hz, FQ-C-5), 101.44 (d, $J = 6.1$ Hz, FQ-C-8), 88.86 (glyco-C-1), 80.79 (glyco-C-5), 76.26 (glyco-C-3), 70.85 (glyco-C-2), 70.40 (glyco-C-4), 62.68 (glyco-C-6), 54.49 (d, $J = 5.9$ Hz, aminomethylpyrrolidine-C), 53.94 (Leu-C $_{\alpha}$), 52.42 (Ala-C $_{\alpha}$), 51.07 (Ala-C $_{\alpha}$), 50.67 (d, $J = 6.2$ Hz, aminomethylpyrrolidine-C), 44.22 (Gly-C $_{\alpha}$), 42.42 (aminomethylpyrrolidine-C), 41.16 (Leu-CH $_2$), 40.00 (aminomethylpyrrolidine-C), 36.85 (*c*Pr-CH), 29.90 (aminomethylpyrrolidine-C), 25.80 (Leu-CH), 23.57 (Leu-CH $_3$), 21.49 (Leu-CH $_3$), 17.66 (Ala-CH $_3$), 17.31 (Ala-CH $_3$), 8.53 (*c*Pr-CH $_2$), 8.49 (*c*Pr-CH $_2$). HR-MS calcd [C $_{45}$ H $_{59}$ FN $_7$ O $_{13}$ S] $^+$: 956.3870, found 956.3852.

LecB-targeted aminomethylpyrrolidine-FQ-Prodrug methyl ester **45: 16** (70 mg, 0.10 mmol, 1 eq.), **42** (48 mg, 0.12 mg, 1.2 eq.) and TBTU (48 mg, 0.15 mmol, 1.5 eq.) were dissolved in dry DMF (2 mL). DIPEA (64 μL , 0.36 mmol, 3.6 eq.) was added dropwise and the

reaction was stirred for 1 h. The solvent was evaporated *in vacuo* and the reaction was purified by pHPLC (MeCN : Water, 25-40%, 0.1% formic acid). After lyophilisation, the title compound was isolated as an off-white powder (73 mg, 72%). ¹H NMR (500 MHz, MeOH-*d*₄) δ 8.55 (s, 1H, FQ-H-2), 8.02 (d, J = 8.5 Hz, 2H, glyco-Ar-H), 7.91 (d, J = 8.5 Hz, 2H, glyco-Ar-H), 7.75 (d, J = 14.6 Hz, 1H, FQ-H-5), 6.98 (d, J = 7.5 Hz, 1H, FQ-H-8), 4.43 (q, J = 7.1 Hz, 1H, Ala-Cα-H), 4.36 – 4.26 (m, 2H, Ala'-Cα-H, Leu-Cα), 3.95 (d, J = 16.6 Hz, 1H, Gly-Cα-H), 3.83 (s, 3H, COOCH₃), 3.79 (d, J = 16.6 Hz, 1H, Gly-Cα-H), 3.74 – 3.65 (m, 2H, 2x aminomethylpyrrolidine-H), 3.64 – 3.54 (m, 3H, cPr-CH, glyco-H-4, aminomethylpyrrolidine-H), 3.44 (q, J = 6.5 Hz, 1H, glyco-H-5), 3.41 – 3.35 (m, 4H, glyco-H-1, glyco-H-3, 2x aminomethylpyrrolidine-H), 3.35 – 3.28 (m, 1H, glyco-linker-CH₂), 3.25 (dd, J = 13.6, 7.5 Hz, 1H, aminomethylpyrrolidine-H), 3.10 (ddd, J = 9.0, 7.1, 2.5 Hz, 1H, glyco-H-2), 3.02 (dd, J = 12.9, 7.1 Hz, 1H, glyco-linker-CH₂-), 2.68 – 2.52 (m, 1H, aminomethylpyrrolidine-H), 2.32 – 2.10 (m, 1H, aminomethylpyrrolidine-H), 1.85 – 1.76 (m, 1H, aminomethylpyrrolidine-H), 1.76 – 1.58 (m, 3H, Leu-CH, Leu-CH₂), 1.50 (d, J = 7.2 Hz, 3H, Ala-CH₃), 1.41 (d, J = 7.2 Hz, 3H, Ala'-CH₃), 1.37 – 1.29 (m, 2H, cPr-CH₂), 1.16 (d, J = 6.4 Hz, 3H, glyco-H-6), 1.14 – 1.04 (m, 2H, cPr-CH₂), 0.88 (d, J = 4.0 Hz, 3H, Leu-CH₃), 0.87 (d, J = 4.1 Hz, 3H, Leu-CH₃). ¹³C NMR (126 MHz, MeOH-*d*₄) δ 176.22 (CONH), 175.30 (d, J = 2.7 Hz, FQ-C=O), 175.17 (CONH), 174.76 (CONH), 172.58 (CONH), 168.94 (CONH), 166.97 (COOMe), 151.72 (d, J = 244.6 Hz, FQ-C-6), 149.61 (Ar-C), 145.07 (Ar-C), 142.80 (d, J = 12.0 Hz, FQ-C-7), 140.51 (Ar-C), 138.35 (Ar-C), 129.50 (glyco-Ar-C), 128.07 (glyco-Ar-C), 118.97 (d, J = 6.4 Hz, FQ-C-4a), 112.82 (d, J = 23.3 Hz, FQ-C-5), 109.75 (Ar-C), 101.40 (d, J = 5.4 Hz, FQ-C-8), 79.63 (glyco-C-2), 76.33 (glyco-C-3), 75.51 (glyco-C-5), 73.54 (glyco-C-4), 69.61 (glyco-C-1), 54.47 (d, J = 5.9 Hz, aminopyrrolidine-C), 53.93 (Leu-Cα), 52.35 (Ala-Cα), 52.04 (aminopyrrolidine-C), 50.96 (Ala'-Cα), 50.53 (d, J = 6.2 Hz, aminopyrrolidine-C), 45.55 (glyco-linker-CH₂), 44.23 (Gly-Cα), 42.61

(aminopyrrolidine-C), 41.20 (Leu-CH₂), 40.01 (aminopyrrolidine-C), 36.17 (cPr-CH), 29.93 (RHNCH₂-aminopyrrolidine), 25.81 (Leu-CH), 23.56 (Leu-CH₃), 21.54 (Leu-CH₃), 17.77 (Ala-CH₃), 17.31 (Ala-CH₃), 17.11 (glyco-C-6), 8.53 (cPr-CH₂), 8.50 (cPr-CH₂). LR-MS: $m/z = 508.2 [M+2H]^{2+}$.

LecB-targeted aminomethylpyrrolidine-FQ-Prodrug methyl ester **49: 45** (50 mg, 0.049 mmol, 1 eq.) was dissolved in a mixture of THF, MeOH and H₂O (3:1:1, 1mL) and LiOH (9 mg, 0.368 mmol, 7.5 eq.) was added. The reaction was stirred over night at room temperature until disappearance of the starting material. After neutralisation with Amberlite IR-120 H⁺ to pH 7, the solvents were removed *in vacuo*. The title compound was obtained after lyophilisation as an off-white powder (47 mg, 96 %). ¹H NMR (500 MHz, MeOH-*d*₄) δ 8.64 (s, 1H, FQ-H-2), 8.03 (d, J = 8.1 Hz, 2H, glyco-Ar-H), 7.91 (d, J = 8.1 Hz, 2H, glyco-Ar-H), 7.69 (d, J = 14.2 Hz, 1H, FQ-H-5), 7.03 (d, J = 7.4 Hz, 1H, FQ-H-8), 4.43 (q, J = 7.1 Hz, 1H, Ala-C α -H), 4.34 (dd, J = 10.6, 4.2 Hz, 1H, Leu-C α -H), 4.30 (q, J = 7.2 Hz, 1H, Ala-C α -H), 3.95 (d, J = 16.6 Hz, 1H, Gly-C α -H), 3.79 (d, J = 16.6 Hz, 1H, Gly-C α -H), 3.77 – 3.60 (m, 4H, 3x aminomethylpyrrolidine-H, cPr-CH), 3.58 (d, J = 1.9 Hz, 1H, glyco-H-4), 3.49 – 3.22 (m, 7H, 3x aminomethylpyrrolidine-H, glyco-H-3, glyco-H-5, glyco-H-1, glyco-linker-CH₂), 3.10 (ddd, J = 9.0, 7.0, 2.6 Hz, 1H, glyco-H-2), 3.02 (dd, J = 12.9, 7.1 Hz, 1H, glyco-linker-CH₂), 2.67 – 2.55 (m, 1H, aminomethylpyrrolidine-H), 2.23 – 2.13 (m, 1H, aminopyrrolidine-H), 1.82 (ddd, J = 12.2, 7.8 Hz, 1H, aminopyrrolidine-H), 1.77 – 1.58 (m, 3H, Leu-CH, Leu-CH₂), 1.50 (d, J = 7.1 Hz, 3H, Ala-CH₃), 1.41 (d, J = 7.2 Hz, 3H, Ala-CH₃), 1.39 – 1.37 (m, 2H, cPr-CH₂), 1.20 – 1.18 (m, 2H, cPr-CH₂), 1.16 (d, J = 6.4 Hz, 3H, glyco-H-6), 0.88 (d, J = 5.0 Hz, 3H, Leu-CH₃), 0.87 (d, J = 5.2 Hz, 3H, Leu-CH₃). ¹³C NMR (126 MHz, MeOH-*d*₄) δ 177.58 (d, J = 2.8 Hz, FQ-C=O), 176.19 (CONH), 175.21 (CONH), 174.78 (CONH), 172.56 (CONH), 170.13 (CONH), 168.92 (COOH), 151.98 (d, J = 247.3 Hz, FQ-C-6), 148.61 (FQ-C-2), 145.07 (Ar-C), 143.64 (d, J = 11.2 Hz FQ-C-7), 141.45 (Ar-

C), 138.34 (Ar-C), 129.50 (glyco-Ar-C), 128.08 (glyco-Ar-C), 111.95 (d, J = 23.5 Hz, FQ-C-5), 101.44 (d, J = 6.0 Hz, FQ-C-8), 79.63 (glyco-C-2), 76.33 (glyco-C-3), 75.52 (glyco-C-5), 73.55 (glyco-C-4), 69.61 (glyco-C-1), 54.51 (d, J = 5.6 Hz, aminomethylpyrrolidine-C), 53.92 (Leu-C α), 52.33 (Ala-C α), 50.98 (Ala-C α), 50.64 (d, J = 6.3 Hz, aminopyrrolidine-C), 45.55 (glyco-linker-CH₂), 44.22 (Gly-C α), 42.46 (aminomethylpyrrolidine-C), 41.22 (Leu-CH₂), 40.00 (aminomethylpyrrolidine-C), 36.80 (cPr-CH), 29.89 (aminomethylpyrrolidine-C), 25.81 (Leu-CH), 23.56 (Leu-CH₃), 21.56 (Leu-CH₃), 17.76 (Ala-CH₃), 17.31 (Ala'-CH₃), 17.11 (glyco-C-6), 8.51 (cPr-CH₂), 8.48 (cPr-CH₂). HR-MS calcd [C₄₆H₆₂FN₈O₁₄S]⁺: 1001.4085, found 1001.4063.

Competitive binding assays

LecA (according to Joachim *et al.*^[94]): A serial dilution of the test compounds was prepared in TBS/Ca (8.0 g/L NaCl, 2.4 g/L Tris, 0.19 g/L KCl, 0.15 g/L CaCl₂ • 2 H₂O), with 30% DMSO as co-solvent. A concentrated solution of LecA was diluted in TBS/Ca together with the fluorescent reporter ligand (N-(fluorescein-5-yl)-N'-(β-d-(m-aminophenyl)-galactopyranosyl)-thiocarbamide) to yield concentrations of 40 μM and 20 nM, respectively. 10 μL of this mix was added to 10 μL serial dilutions of the test compounds in a black 384-well microtiter plates (Greiner Bio-One, Germany, cat. no. 781900) in triplicates. After centrifugation (2680 rcf, 1 min, r.t.), the reactions were incubated for 30 - 60 min at r.t. in a humidity chamber. Fluorescence (excitation 485 nm, emission 535 nm) was measured in parallel and perpendicular to the excitation plane on a PheraStar FS plate reader (BMG Labtech GmbH, Germany). The measured intensities were reduced by the values of only LecA in TBS/Ca and fluorescence polarization was calculated. The data were analyzed with the MARS Data Analysis Software (BMG Labtech GmbH, Germany) and fitted according to the four parameter variable slope model. Bottom and top plateaus were fixed according to the control compounds in each assay ((p-nitrophenyl)-β-d-galactoside) and the data was reanalyzed with these values fixed. A minimum of three independent measurements on three plates was performed for each inhibitor.

LecB (LecB_{PAO1} according to Hauck *et al.*^[174] and LecB_{PA14} according to Sommer *et al.*^[28]): A serial dilution of the test compounds was prepared in TBS/Ca, with 20% DMSO as co-solvent. A concentrated solution of LecB PAO1 or PA14 was diluted in TBS/Ca together with the fluorescent reporter ligand (N-(fluorescein-5-yl)-N'-(α-l-fucopyranosyl ethylen)-thiocarbamide) to yield concentrations of 300 nM and 20 nM, respectively. 10 μL of this mix was added to 10 μL serial dilutions of the test compounds in a black 384-well microtiter plates (Greiner Bio-One, Germany, cat. no. 781900) in triplicates. After centrifugation

(2680 rcf, 1 min, r.t.), the reactions were incubated for 4 - 8 h at r.t. in a humidity chamber. Fluorescence was measured and analyzed as for LecA. Bottom and top plateaus were fixed according to the control compound in each assay (l-fucose) and the data were reanalyzed with these values fixed. A minimum of three independent measurements on three plates was performed for each inhibitor.

Bacterial strain list

Pseudomonas aeruginosa PA14 wt (DSM 19882) was obtained from the German Collection of Microorganisms and Cell Cultures (DSMZ).

Prodrug activation assay

P. aeruginosa PA14 was streaked on LB-agar plates (1% agar) from glycerol stocks and incubated at 37 °C over night. 2 - 5 colonies were picked and dispersed in 10 mL LB (10 g/L trypton, 10 g/L NaCl, 5g/L yeast extracts). This dispersion was incubated over night at 37 °C, 180 rpm under high humidity. The culture was centrifuged (4000 rcf, r.t., 10 min) and the supernatant was filtered (0.22 µm pore size). 1 mL filtrate was mixed with 9 mL human plasma (BioIVT - West Sussex, United Kingdom, LiHep-treated, pooled, mixed gender) to result in the matrix for this experiment.

A 1 mM solution of the studied compound was prepared in PBS (150 mM NaCl, 2.6 mM KCl, 1.4 mM KH₂PO₄, 10 mM Na₂HPO₄, pH 7.4) with 20% DMSO. 50 µL of this solution was diluted in 950 µL matrix or human plasma (spiked with 10% LB) on ice. After brief vortex, 100 µL were immediately treated with 100 µL ice-cold MeCN (spiked with 1.5 µM diphenhydramine as internal standard). The rest of the solution was incubated at 37 °C and 500 rpm in an Eppendorf thermomixer. At various time points (30, 60, 120, 180 min), 100 µL sample were taken and treated as described above. After extensive vortexing, the samples were centrifuged (17600 rcf, 10 min, 10 °C) and the supernatant was analysed by HPLC-MS. The AUC of the parent drug and its cleavage products and the internal

standard was quantified using Compass QuantAnalysis quantification software. The relative AUC is calculated by $AUC(\text{compound})/AUC(\text{ISTD})$. Procaine was used as a positive control as it readily degrades in human plasma.

Antibiotic susceptibility (MIC assay)

The antibiotic activity of the reference compounds **1**, **2**, **3**, **19**, **35** and **47** was determined by broth micro-dilution assay based on the EUCAST guidelines, according to Wiegand, Hilpert and Hancock^[95]. Serial dilutions in sterile Müller-Hinton broth II (Fluka analytical, cat. no. 90922: 17.5 g/L casein acid hydrolysate, 3 g/L beef extract, 1.5 g/L starch, supplemented with 20 - 25 mg/L Ca^{2+} and 10 - 15 mg/L Mg^{2+} , pH 7.3) of the conjugates were prepared from 100 mM DMSO stocks (for ciprofloxacin (**1**) a 10 mM aqueous stock of ciprofloxacin • HCl was used), in sterile 96-well plates, yielding a concentration range from 128 $\mu\text{g}/\text{mL}$ - 0.125 $\mu\text{g}/\text{mL}$ (12.8 - 0.0125 for ciprofloxacin (**1**) and fluoroquinolones **2** and **3**). Bacterial strains were streaked on LB-agar plates (1% agar) from glycerol stocks and incubated at 37 °C over night. Colonies were picked from plate and dispersed in fresh Müller-Hinton broth II (MHB II) to yield a OD600 of 0.08 - 0.13. This dispersion was diluted 1 : 100 in fresh MHB II, which was then used for the assay to achieve a final inoculum of 5×10^5 CFU/mL. 50 μL inoculum was mixed with 50 μL of the serial dilution in the corresponding well of the 96-well plate.

For the measurement of the time- and matrix-dependent antibiotic activity of prodrugs **24**, **25**, **36**, **37**, **48** and **49**, a serial dilution in PBS with 20% DMSO was prepared in sterile 96-well plates, yielding a concentration range of 1 mM - 1.9 μM (100 μM - 0.19 μM for ciprofloxacin). The different matrices were prepared under sterile conditions: (i) 5 mL human plasma and 1 mL sterile filtrate from an *P. aeruginosa* PA14 overnight culture in LB were mixed with 4 mL PBS; (ii) 1 mL sterile filtrate from an *P. aeruginosa* PA14 overnight culture was diluted in 9 mL PBS; (iii) PBS only and (iv) 5 mL human plasma and 1 mL LB

were mixed with 4 mL PBS. 6 μL of each compound dilution series was diluted in 115 μL matrix (\approx 1:20 dilution) in a 96-well format at time point $T = -3$ h or $T = -10$ min. The plates prepared at $T = -3$ h were sealed with gas-permeable foil and incubated at 37 °C in a humid incubator. The other plates were kept at room temperature. At $T = 0$ h, 50 μL of each well was mixed with 50 μL inoculum (as described above) in double-concentrated MHBII in a sterile 96-well plate.

The plates were sealed with gas-permeable foil and incubated at 37 °C for 18 - 20 h in a humid incubator. Growth inhibition was assessed by visual inspection and given MIC values are the lowest concentration of antibiotic at which there was no visible growth.

***In vitro* ADMET**

Cytotoxicity

The epithelial cell line A549 (ATCC(R) CCL-185) was cultivated in Dulbecco's modified Eagle's medium (DMEM) with 10% heat-inactivated fetal calf serum (FCS) and 20 mM L-Glutamine at 37°C and 5% CO₂. A549 cells were seeded into a 96well-plate (Nunc, Roskilde, Denmark) and grown to 75% confluency. The following compounds were tested in the cell assay: **36**, **37** and **2**. Every compound was dissolved in DMSO and diluted in PBS (final DMSO concentration in the cell assay: 1%). Cells were incubated with the respective compound in concentrations ranging from 0.001-50 μM for 24 h at 37°C and 5% CO₂. Cells treated with vehicle only (DMSO diluted in PBS, final DMSO concentration in the cell assay: 1%) served as a negative control. Furthermore, pure medium (DMEM + 10% FCS) and completely damaged cells served as positive controls. To damage cells, cells were treated with 0.5% Triton X-100 1 h prior to addition of MTT (Sigma). After 24 h cells were washed twice with the respective medium. MTT diluted in PBS (stock solution 5 mg/ml) was added to the wells at a final concentration of 1 mg/ml. The cells were incubated for 4 h at 37°C and 5% CO₂. Medium was removed and 0.04 M HCl in 2-

propanol was added. The cells were incubated at room temperature for 15 min. Then supernatant was transferred to a 96well-plate. The samples were measured at 560 nm and at 670 nm as a reference wavelength on a Tecan Sunrise ELISAReader using Magellan software. Data was normalized using the following formula: $(A-B)/(C-B)$ with 'A' as the respective data point, 'B' as the value of the Triton X-100-treated control and 'C' as the vehicle control. The experiment was repeated at least three times. The error bars indicate the standard deviation.

Plasma stability assays

Each compound dissolved in DMSO was added to mouse plasma (pH 7.4, 37°C) or to human plasma (pH 7.4, 37°C) to yield a final concentration of 1 μ M. In addition, procaine and procainamide (dissolved in DMSO) were added to mouse plasma or to human plasma (pH 7.4, 37°C) to yield a final concentration of 1 μ M. Procaine served as positive control as it is unstable in mouse plasma. Procainamide served as negative control as it is stable in mouse plasma. The samples were incubated for 0 min, 15 min, 30 min, 60 min, 90 min, 120 min and 240 min at 37°C. At each time point, 10 μ l of the respective sample was extracted with 90 μ l acetonitrile and 1 μ l of caffeine as internal standard for 5 min at 2000 rpm on a MixMate® vortex mixer (Eppendorf). Acetonitrile and caffeine were dispensed using a Mantis Formulatrix®. The samples were centrifuged for 20 min at 2270 rcf at 4°C and the supernatants were transferred to 96-well Greiner V-bottom plates. Samples were analysed using HPLC-MS/MS analysis as described in the respective section. Peak areas of each compound and of the internal standard were analysed using the MultiQuant 3.0 software (AB Sciex). Peak areas of the respective compound were normalised to the internal standard peak area and to the respective peak areas at time point 0 min: $(C/D)/(A/B)$ with A: peak area of the compound at time point 0 min, B: peak area of the internal standard at time point 0 min, C: peak area of the compound at the

respective time point, D: peak area of the internal standard at the respective time point. Every experiment was repeated independently at least three times.

Microsomal stability assay

S9 liver microsomes (mouse and human, Thermo Fisher) were thawed slowly on ice. 20 mg/ml of microsomes, 2 μ l of a 100 μ M solution of every compound and 183 μ l of 100 mM phosphate buffer were incubated 5 min at 37°C in a water bath. Reactions were initiated using 10 μ l of 20 mM NADPH (Roth). Samples were incubated in three replicates at 37°C under gentle agitation at 150 rpm. At 0, 5, 15, 30, and 60 min, reactions were terminated by the addition of 180 μ l acetonitrile using a Mantis Formulatrix® dispenser. Samples were vortexed for 5 min using a Eppendorf MixMate® vortex mixer and centrifuged at 2270 rcf for 20 min at 4°C. The supernatants were transferred to 96-well Greiner V-bottom plates, sealed and analyzed according to the section HPLC-MS/MS analysis. Peak areas of the respective time point of the compounds were normalized to the peak area at time point 0 min. Then half-life was calculated using linear regression (Microsoft Excel®). Clint [μ l/min/mg protein] was calculated using the following formula:

$$\text{Clint} = 0.693 / (0.005 \times t_{1/2})$$

Cell accumulation assay

A549 cells were seed into 96well plates as described for the cytotoxicity assay. Cells were cultivated at 37°C and 5 % CO₂ until they reached 95 % confluency. Cells were treated with **2**, **36** or **37** at a final concentration of 10 μ g/ml or left untreated. Each condition was assayed in technical duplicates with two biological replicates. Cells were treated for 15 min, 30 min and 60 min. After incubation for the respective time point, cells were washed twice with pre-warmed PBS and were then lysed in MeOH and scratched from the surface. Supernatants from medium, wash fluids as well as the cell extracts were subjected to mass spectrometric analysis. For wash fluid and medium samples, calibration and QC samples were prepared using PBS as matrix and spiking the respective compounds into

the matrix. For cell extract samples, calibration and QC samples were prepared using MeOH as matrix. For calibration and QC samples compounds were dispensed using a Mantis(R) Formulatrix. Medium, wash fluid, cell extract samples as well as both calibration and QC samples were extracted using MeOH containing 12.5 ng/ml caffeine as internal standard for 10 min at 800 rpm on an Eppendorf(R) VortexMixMate and then centrifuged at 4000 rpm for 20 min at 4 °C. Supernatants were transferred to a Greiner V-bottom plate, sealed and subjected for HPLC-MS/MS analysis.

Plasma protein binding assay

Plasma protein binding was assessed using the rapid equilibrium device (RED) system from ThermoFisher. Compounds **2**, **36** or **37** were dissolved in DMSO. Naproxene served as control as it shows high plasma protein binding. Compounds were diluted in murine plasma (from CD-1 mice, pooled) or in human plasma (human donors, both genders, pooled) to a final concentration of 1 μ M. Dialysis buffer and plasma samples were added to the respective chambers according the manufacturer's protocol. The RED plate was sealed with a tape and incubated at 37°C for 2 hours at 800 rpm on an Eppendorf MixMate® vortex-mixer. Then samples were withdrawn from the respective chambers. To 25 μ l of each dialysis sample, 25 μ l of plasma and to 25 μ l of plasma sample, 25 μ l of dialysis buffer was added. Then 150 μ l ice-cold extraction solvent (MeCN/H₂O (90:10) containing 12.5 ng/ml caffeine as internal standard) was added. Samples were incubated for 30 min on ice. Then samples were centrifuged at 4°C at 2270 rcf for 10 min. Supernatants were transferred to Greiner V-bottom 96-well plates and sealed with a tape. Then samples were subjected to HPLC-MS/MS analysis as described in the section 'HPLC-MS/MS analysis'. The percentage of bound compound was calculated as follows:

$$f_u = (C_{\text{buffer chamber}} / C_{\text{plasma chamber}}) * 100$$

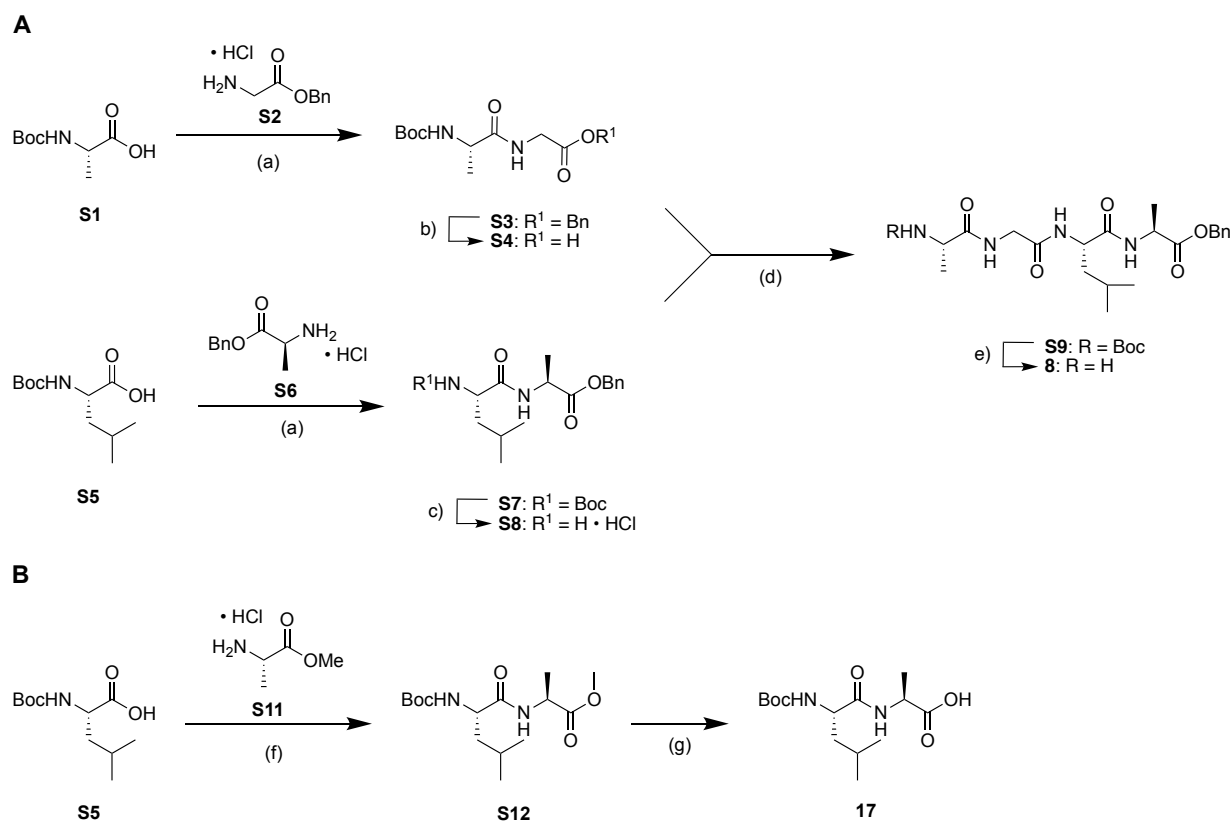
$$f_{\text{bound}} = 1 - f_u$$

HPLC-MS/MS analysis

| ID | Q1 mass [Da] | Q3 mass [Da] | Time [msec] | DP [volts] | CE [volts] | CXP [volts] |
|---------------------|--------------|--------------|-------------|------------|------------|-------------|
| 2 | 332.917 | 314.9 | 30 | 1 | 29 | 34 |
| | 332.917 | 272.2 | 30 | 1 | 27 | 14 |
| 36 | 940.206 | 778.2 | 30 | -300 | -48 | -37 |
| | 940.206 | 734.3 | 30 | -300 | -62 | -29 |
| 37 | 985.228 | 941.3 | 30 | -300 | -58 | -43 |
| | 985.228 | 527.2 | 30 | -300 | -70 | -23 |
| Naproxene | 231.106 | 185.1 | 50 | 80 | 19 | 10 |
| | 231.106 | 170.2 | 50 | 80 | 33 | 12 |
| Caffeine | 195.024 | 138.0 | 50 | 80 | 25 | 14 |
| | 195.024 | 110.0 | 50 | 80 | 31 | 18 |
| Procaine | 236.773 | 100.0 | 30 | 80 | 21 | 12 |
| | 236.773 | 120.0 | 30 | 80 | 31 | 14 |
| Procainamide | 235.744 | 163.0 | 30 | 80 | 21 | 18 |
| | 235.744 | 120.0 | 30 | 80 | 39 | 12 |

Cell samples as well as plasma stability, plasma protein binding and metabolic stability samples were analyzed using an Agilent 1290 Infinity II coupled to an AB Sciex 6500plus mass spectrometer. LC conditions were as follows: column: Agilent Zorbax Eclipse Plus C18, 50x2.1 mm, 1.8 μ m; temperature: 30°C; injection volume: 5 μ l per sample; flow rate: 700 μ l/min. Solvents: A: water + 0.1 % formic acid; solvent B: 95 % acetonitrile/5 % H₂O + 0.1 % formic acid. Gradient for **2**, **36** and **37**: 99 % A from 0 min until 1 min; 99 - 0 % A from 1.0 until 2.2 min, 0 % A until 3.2 min. Gradient for naproxene: 99 % A from 0 min until 1 min; 99 - 0 % A from 1.0 until 5.5 min, 0 % A until 6.0 min. Gradient for procaine and procaine: 99 % A from 0 min until 1.0 min, 99 - 0 % A from 1.0 until 3.5 min, 0 % A until 3.7 min. Mass transitions for controls and compounds are depicted in the table above.

CHEMICAL SYNTHESIS OF THE TETRAPEPTIDE LINKER **8** AND DIPEPTIDE BUILDING BLOCK **17**



Scheme S1. Chemical synthesis of tetrapeptide linker **8** and dipeptide building block **17**.^a

^aReagents and conditions: (a) EDC·HCl, HOBT, DIPEA, CH₂Cl₂, r.t., 6 - 24 h, 88% for **S3**, 98 % for **S7**; (b) Pd/C, H₂, THF, r.t., 16 h, quant.; (c) HCl, dioxane, r.t., 2 h, quant.; (d) EDC·HCl, HOBT, DIPEA, CH₂Cl₂, r.t., 2 h, 51%; (e) HCl, dioxane, r.t., 4 h, quant.; (f) EDC·HCl, HOBT, DIPEA, CH₂Cl₂, r.t., 3 h, 72%; (g) LiOH, THF/MeOH/H₂O (3:1:1), r.t., 1.5 h, 95%.

Tetrapeptide linker **8** was synthesised by conventional solution phase peptide synthesis (scheme S1, A). Boc-protected alanine (**S1**) and benzyl-protected glycine (**S2**) were coupled with EDC/HOBT to obtain dipeptide **S3** in high yields. **S3** was then benzyl-deprotected by hydrogenolysis towards **S4**. Boc-protected leucine (**S5**) was coupled to benzyl-protected alanine (**S6**) as described above. The resulting dipeptide **S7** was then boc-deprotected under acidic conditions to obtain compound **S8** in excellent yields. The

building blocks **S4** and **S8** were again coupled under activation with EDC/HOBt towards the bis-protected tetrapeptide **S9**. After acidic deprotection, the title compound **8** was obtained in quantitative yields.

The dipeptide linker **17** was synthesised by conventional solution phase peptide synthesis (Scheme S1, B). Boc-protected alanine (**S1**) and benzyl-protected glycine (**S2**) were coupled with EDC/HOBt to obtain dipeptide **S3** in high yields. **S3** was then benzyl-deprotected by hydrogenolysis towards **S4**.

S9:

^1H NMR (500 MHz, CDCl_3) δ 7.40 – 7.28 (m, 5H, Bn), 7.11 – 7.01 (m, 1H, NH), 6.99 (d, J = 6.6 Hz, 1H, NH), 6.89 (d, J = 7.6 Hz, 1H, NH), 5.19 (d, J = 12.3 Hz, 1H, Bn- CH_2), 5.13 (d, J = 12.3 Hz, 1H, Bn- CH_2), 4.60 (dq, J = 7.3, 7.3 Hz, 1H, Ala- C_α -H), 4.52 (td, J = 8.9, 5.4 Hz, 1H, Leu- C_α -H), 4.14 (dq, J = 6.9, 6.9 Hz, 1H, Ala- C_α -H), 4.02 (dd, J = 16.7, 5.9 Hz, 1H, Gly- CH_2), 3.89 (dd, J = 16.6, 5.1 Hz, 1H, Gly- CH_2), 1.74 – 1.58 (m, 2H, Leu-CH + Leu- CH_2), 1.57 – 1.49 (m, 1H, Leu- CH_2), 1.43 (s, Boc- CH_3), 1.40 (d, J = 7.3 Hz, 3H, Ala- CH_3), 1.35 (d, J = 7.1 Hz, 3H, Ala- CH_3), 0.90 (d, J = 6.5 Hz, 3H, Leu- CH_3), 0.88 (d, J = 6.4 Hz, 3H, Leu- CH_3). ^{13}C NMR (126 MHz, CDCl_3) δ 173.72 (C=O), 172.66 (C=O), 171.82 (C=O), 169.11 (C=O), 155.84 (Boc-C=O), 135.36 (Bn-C), 128.63 (Bn-C), 128.43 (Bn-C), 128.15 (Bn-C), 80.53 (Boc-C), 67.17 (Bn- CH_2), 52.00 (Ala- C_α), 50.63 (Leu- C_α), 48.18 (Ala- C_α), 43.25 (Gly- CH_2), 40.94 (Leu- CH_2), 28.35 (Boc- CH_3), 24.69 (Leu-CH), 22.84 (Leu- CH_3), 21.86 (Leu- CH_3), 18.17 (Ala- CH_3) 17.94 (Ala- CH_3). LR-MS: m/z = 521.32

17:

^1H NMR (500 MHz, $\text{MeOH-}d_4$) δ 7.48 – 7.11 (m, 5H, Bn-H), 5.17 (d, J = 12.3 Hz, 1H, Bn- CH_2), 5.12 (d, J = 12.3 Hz, 1H, Bn- CH_2), 4.43 (dq, J = 11.3, 3.1 Hz, 2H, 2x Ala- C_α -H), 4.07 – 3.85 (m, 3H, Leu- C_α -H + Gly- CH_2), 1.72 – 1.62 (m, 1H, Leu-CH), 1.59 – 1.45 (m, 1H, Leu- CH_2), 1.52 (d, J = 7.1 Hz, 3H, Ala- CH_3), 1.41 (d, J = 7.3 Hz, 3H, Ala- CH_3), 0.91 (d, J =

6.6 Hz, 3H, Leu-CH₃), 0.89 (d, J = 6.5 Hz, 3H, Leu-CH₃). ¹³C NMR (126 MHz, MeOH-d₄) δ 174.55 (C=O), 173.78 (C=O), 171.49 (C=O), 170.84 (C=O), 137.21 (Bn-C), 129.59 (Bn-C), 129.36 (Bn-C), 129.31 (Bn-C), 67.98 (Bn-CH₂), 52.87 (Ala-C_α), 50.26 (Leu-C_α), 49.63 (Ala-C_α) 43.11 (Gly-C_α), 42.21 (Leu-CH₂), 25.75 (Leu-CH), 23.43 (Leu-CH₃), 21.97 (Leu-CH₃), 17.39 (Ala-CH₃), 17.14 (Ala-CH₃). LR-MS: m/z = 421.26

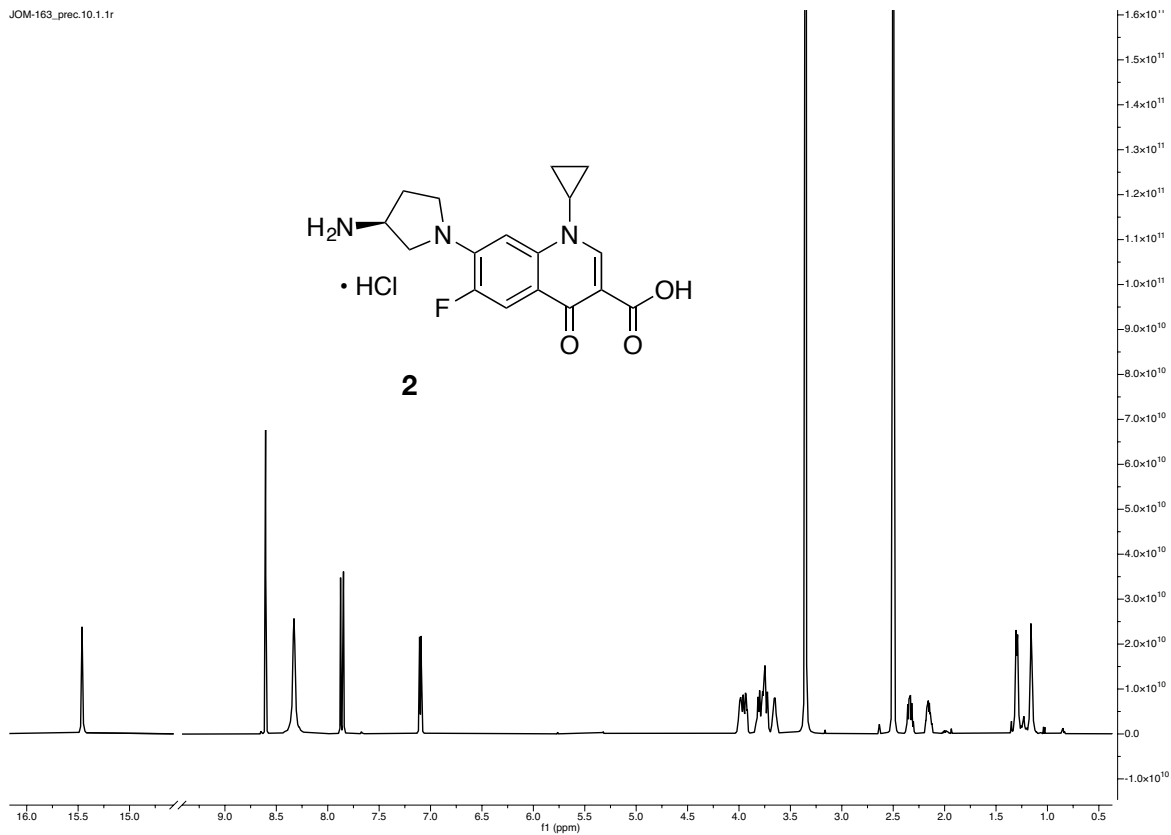
S12:

Boc-L-Leu • H₂O (1.82 g, 7.88 mmol, 1.1 eq.), EDC • HCl (2.06 g, 10.74 mmol, 1.5 eq.) and HOBT • H₂O (1.65 g, 10.74 mmol, 1.5 eq.) were dissolved in 60 mL dry DMF and stirred for 30 min at 4 °C. L-Ala-COOMe • HCl (1 g, 7.16 mmol, 1 eq.) and DIPEA (2.49 mL, 14.32 mmol, 2 eq.) were dispersed in 5 mL dry DMF and added to the activated acid. The ice-bath was removed and the reaction was allowed to warm to r.t.. Reaction progress was monitored by TLC (CH₂Cl₂ : MeOH, 95 : 5) and full turnover was achieved after 3 h. The reaction was concentrated *in vacuo* and diluted with 100 mL H₂O. The aqueous phase was extracted with CH₂Cl₂ (3x 100 mL) and the combined org. phases were washed with 100 mL aqueous HCl (0.2 M), half satd. brine (100 mL) and brine (100 mL). The organic phase was dried over Na₂SO₄ and solvent was evaporated *in vacuo*. The product was purified by MPLC (CH₂Cl₂ : MeOH, 1 - 10%) and obtained as a white amorphous solid (1.64 g, 72 %). ¹H NMR (500 MHz, CDCl₃) δ 6.67 (d, J = 7.5 Hz, 1, Ala-NH), 4.94 (d, J = 8.5 Hz, 1H, Leu-NH), 4.55 (dq, J = 7.2 Hz, 1H, Ala-C_α-H), 4.12 (dd, J = 9.1 Hz, 1H, Leu-C_α-H), 3.73 (s, 3H, Ala-COOCH₃), 1.74 – 1.60 (m, 2H, Leu-CHCH₃CH₃ + Leu-CH₂'), 1.51 – 1.45 (m, 1H, Leu-CH₂), 1.43 (s, 9H, Boc-CH₃), 1.39 (d, J = 7.2 Hz, 3H, Ala-CH₃), 0.94 (d, J = 4.9 Hz, 3H, Leu-CH₃), 0.92 (d, J = 4.8 Hz, 3H, Leu-CH₃). ¹³C NMR (126 MHz, CDCl₃) δ 173.32 (C=O), 172.35 (C=O), 155.82 (carbamate-C=O), 80.14 (Boc), 53.04 (Leu-C_α), 52.54 (Ala-C_α), 48.07 (Leu-C_α), 41.41 (Leu-CH₂), 28.40 (Boc-CH₃), 24.77 (Leu-CH), 23.05 (Leu-CH₃), 22.09 (Leu-CH₃), 18.33 (Ala-CH₃).

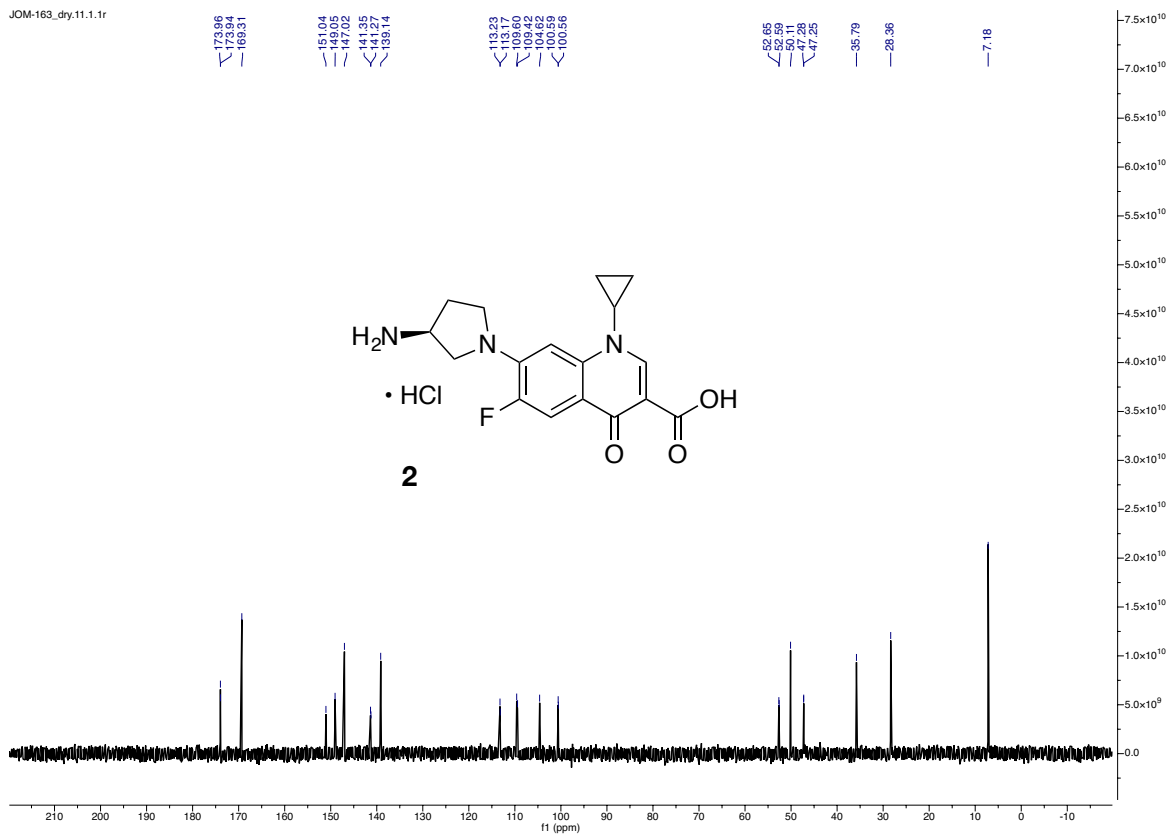
17: (acc. to Jiang *et al.* *JACS* **2003**, 7, 1877 - 1887)

Boc-Leu-Ala-COOBn (640 mg, 2.02 mmol, 1 eq.) was dissolved in 20 mL solvent mixture (THF/MeOH/H₂O, 3 : 1 : 1). LiOH (145.14 mg, 6.06 mmol, 3 eq.) was added and the reaction was stirred at r.t. for 1.5 h. The reaction was cooled to 4 °C with an ice bath and quenched with 1 M aqueous HCl to pH = 4. The reaction was diluted with EtOAc until the phases separated and the organic phase was collected. The organic phase was washed with satd. brine (pH = 4) and dried over Na₂SO₄. After evaporation of the solvent, the product was obtained as a white amorphous solid (578 mg, 95 %). ¹H NMR (500 MHz, MeOD-d₄) δ 8.16 (d, J = 7.4 Hz, 1H, Ala-NH), 4.39 (qd, J = 7.3, 5.1 Hz, 1H, Ala-C_α-H), 4.20 – 4.07 (m, 1H, Leu-C_α-H), 1.71 (dh, J = 13.0, 6.3 Hz, 1H, Leu-CHCH₃CH₃), 1.60 – 1.46 (m, 2H, Leu-CH₂), 1.44 (s, 9H, Boc-CH₃), 1.40 (d, J = 7.3 Hz, 3H, Ala-CH₃), 0.96 (d, J = 6.7 Hz, 3H, Leu-CH₃), 0.94 (d, J = 6.6 Hz, 1H, Leu-CH₃). ¹³C NMR (126 MHz, MeOH-d₄) δ 175.71 (C=O), 175.41 (C=O), 157.85 (Boc-C=O), 80.55 (Boc-C), 54.29 (Leu-C_α), 42.22 (Leu-CH₂), 28.70 (Boc-CH₃), 25.84 (Leu-CH), 23.47 (Ala-CH₃), 21.93 (Leu-CH₃), 17.78 (Ala-CH₃).

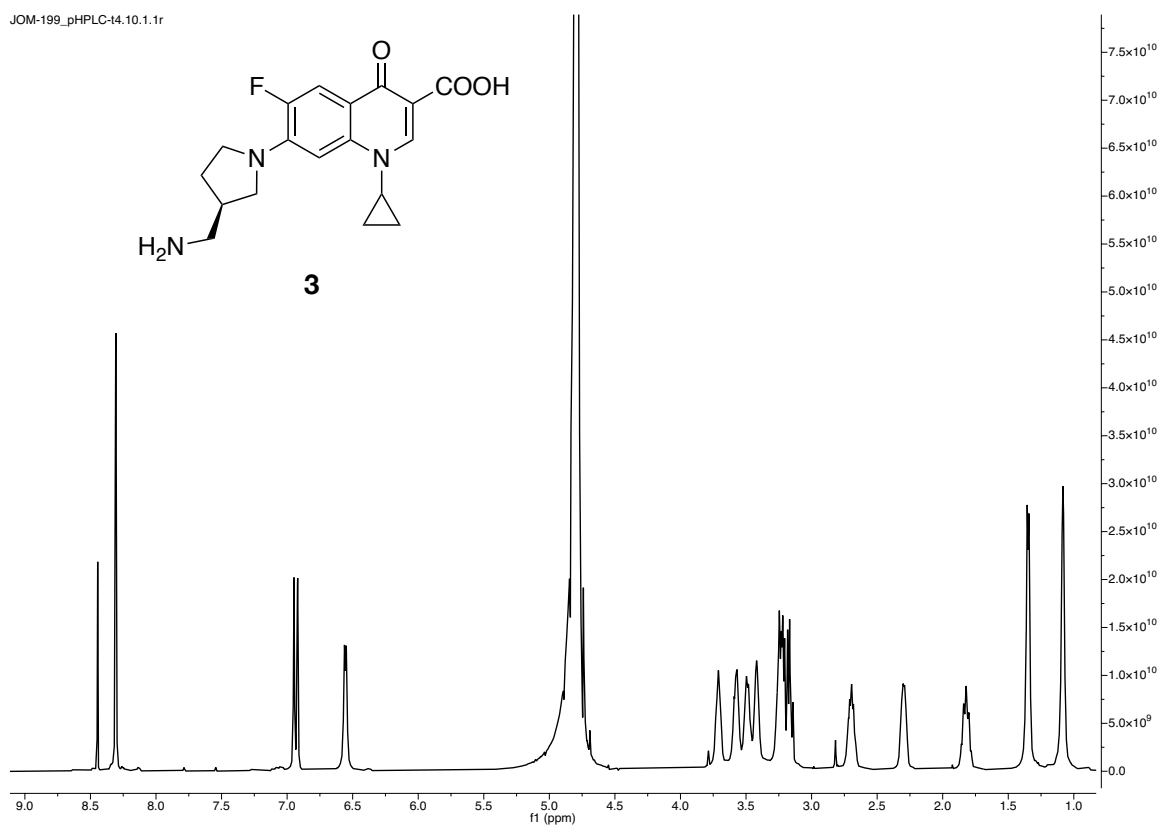
JOM-163_prec.10.1.1r



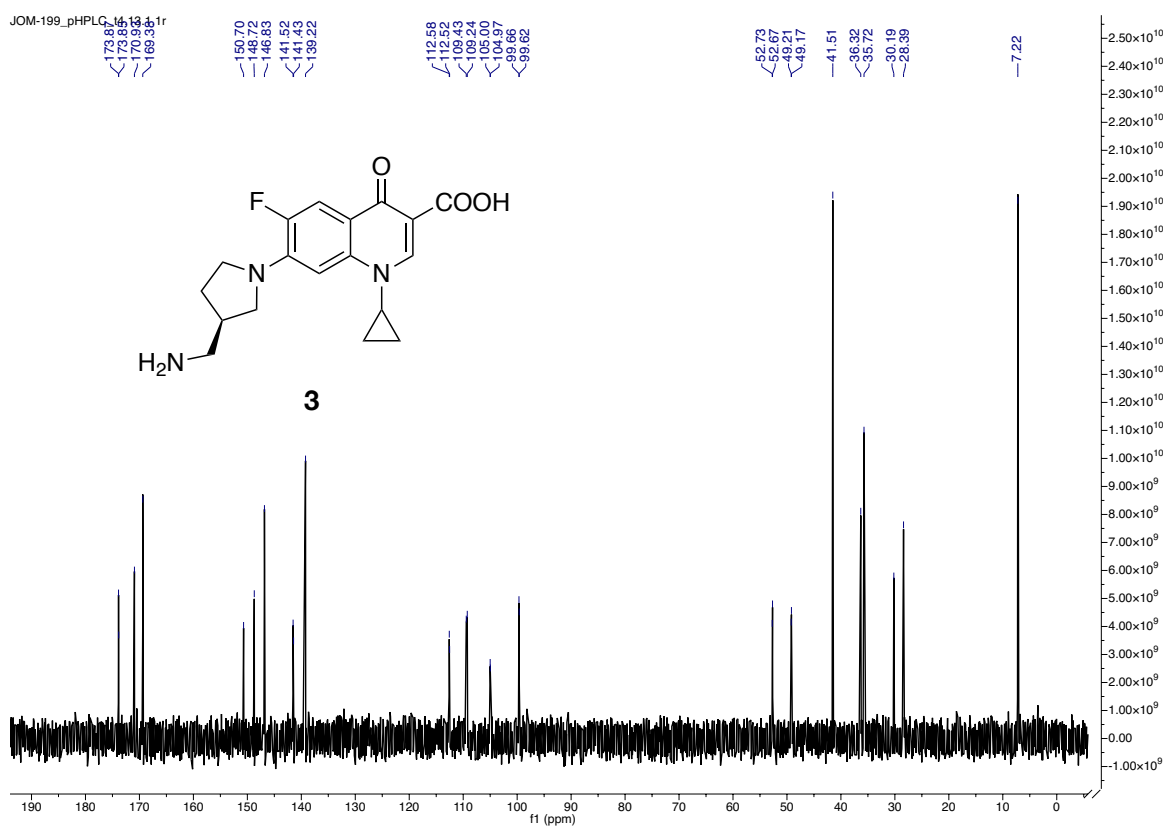
JOM-163_dry.11.1.1r



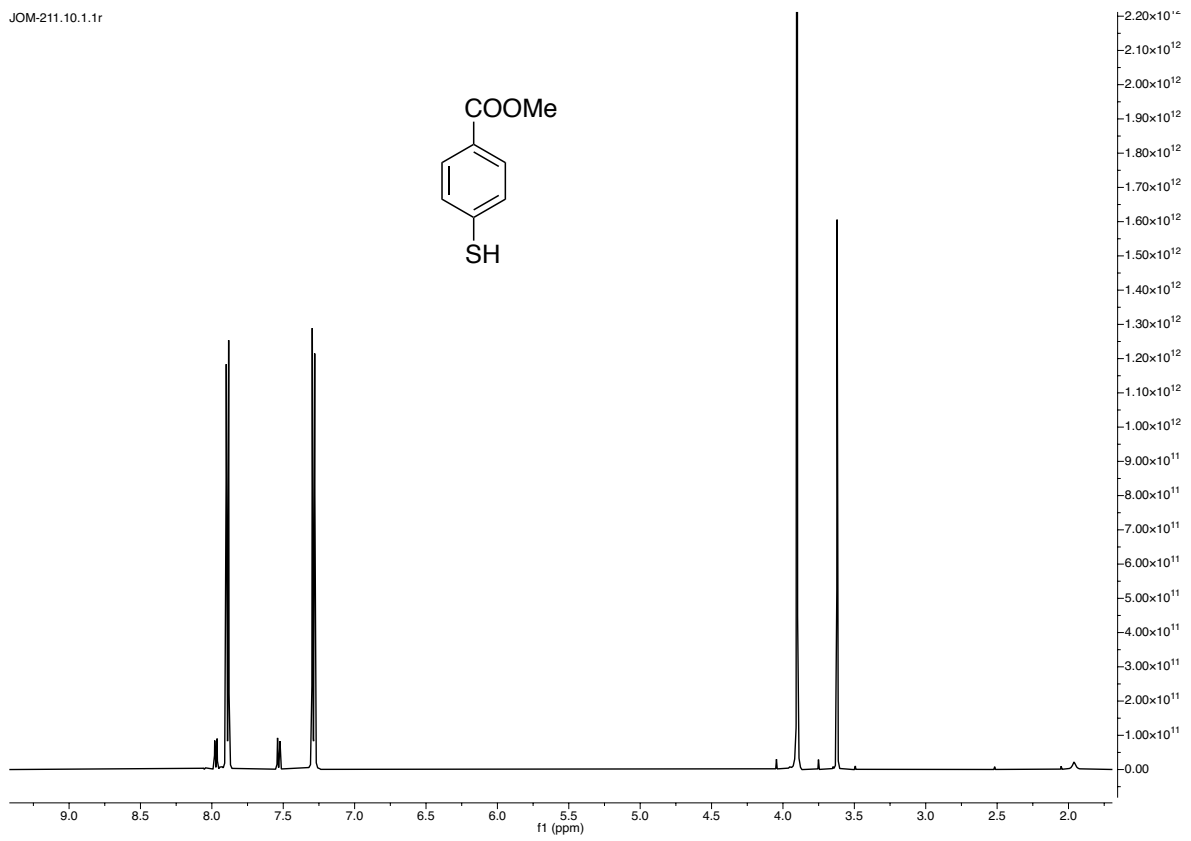
JOM-199_pHPLC-t4.10.1.1r



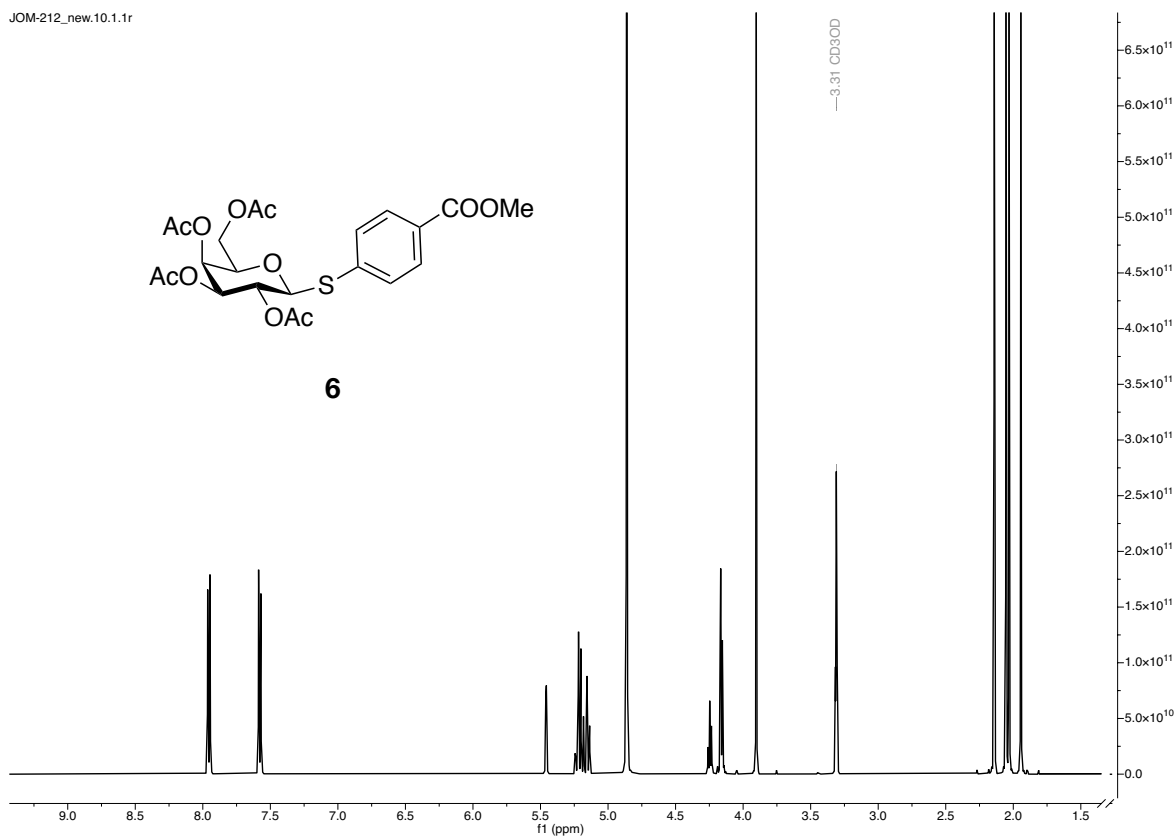
JOM-199_pHPLC-t4.10.1.1r



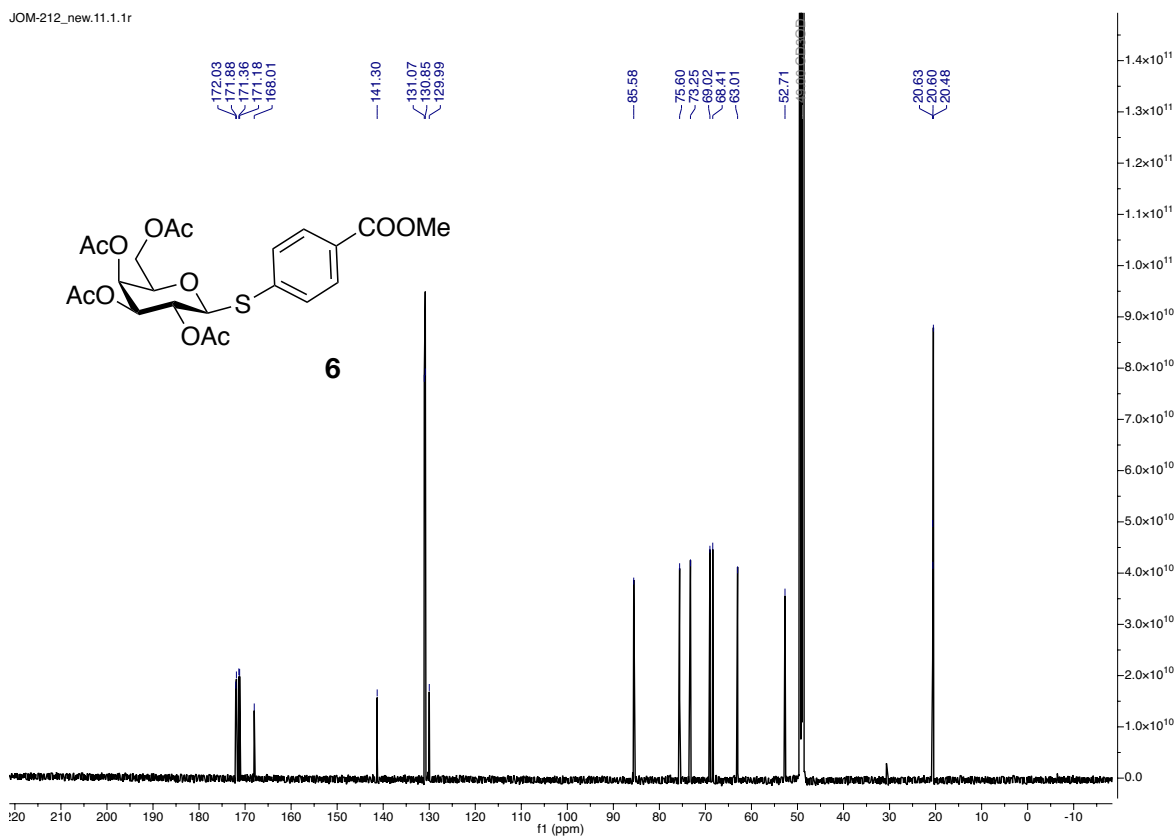
JOM-211.10.1.1r



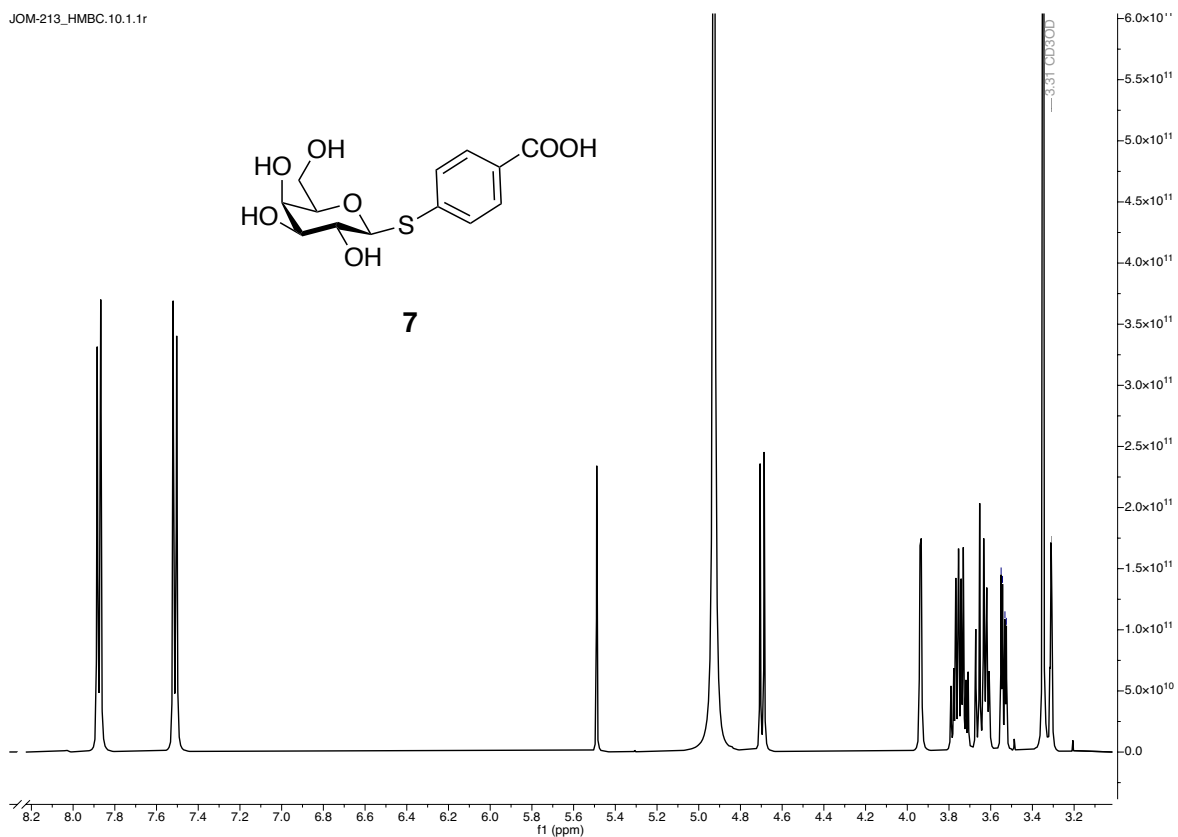
JOM-212_new.10.1.1r



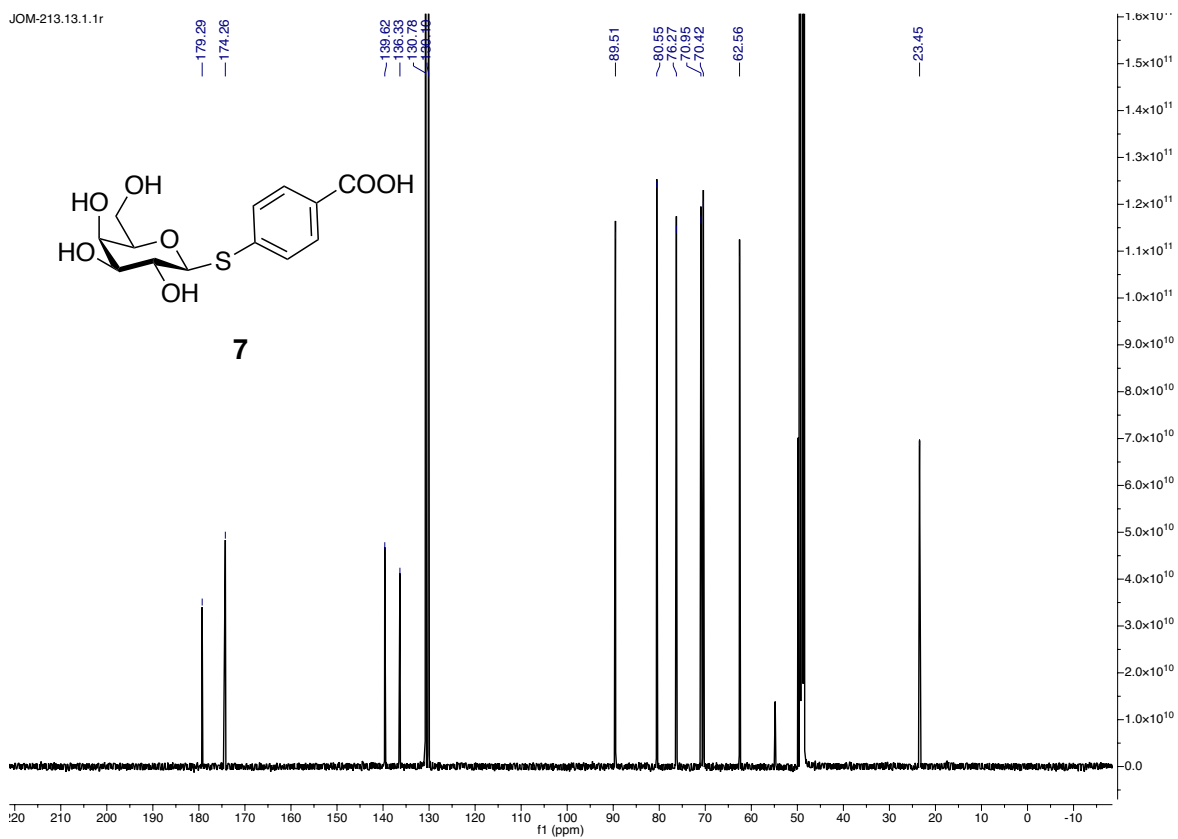
JOM-212_new.11.1.1r



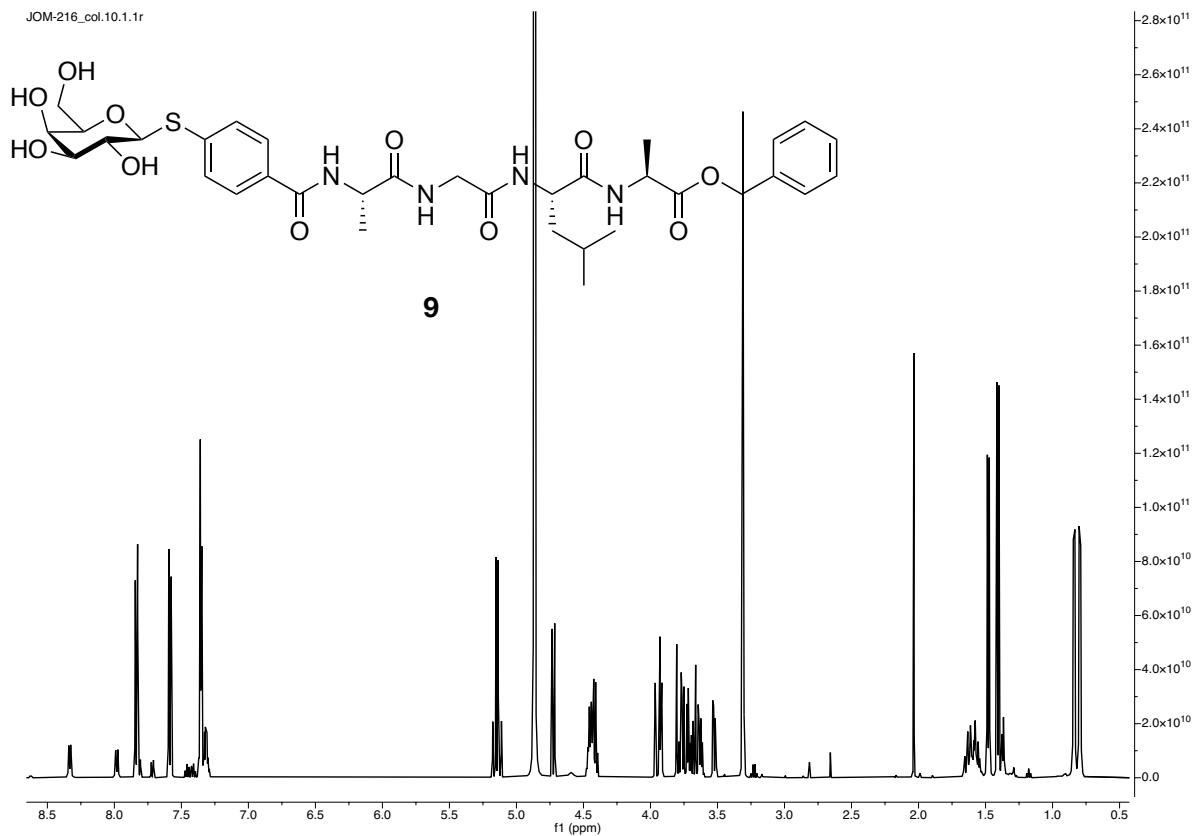
JOM-213_HMBC.10.1.1r



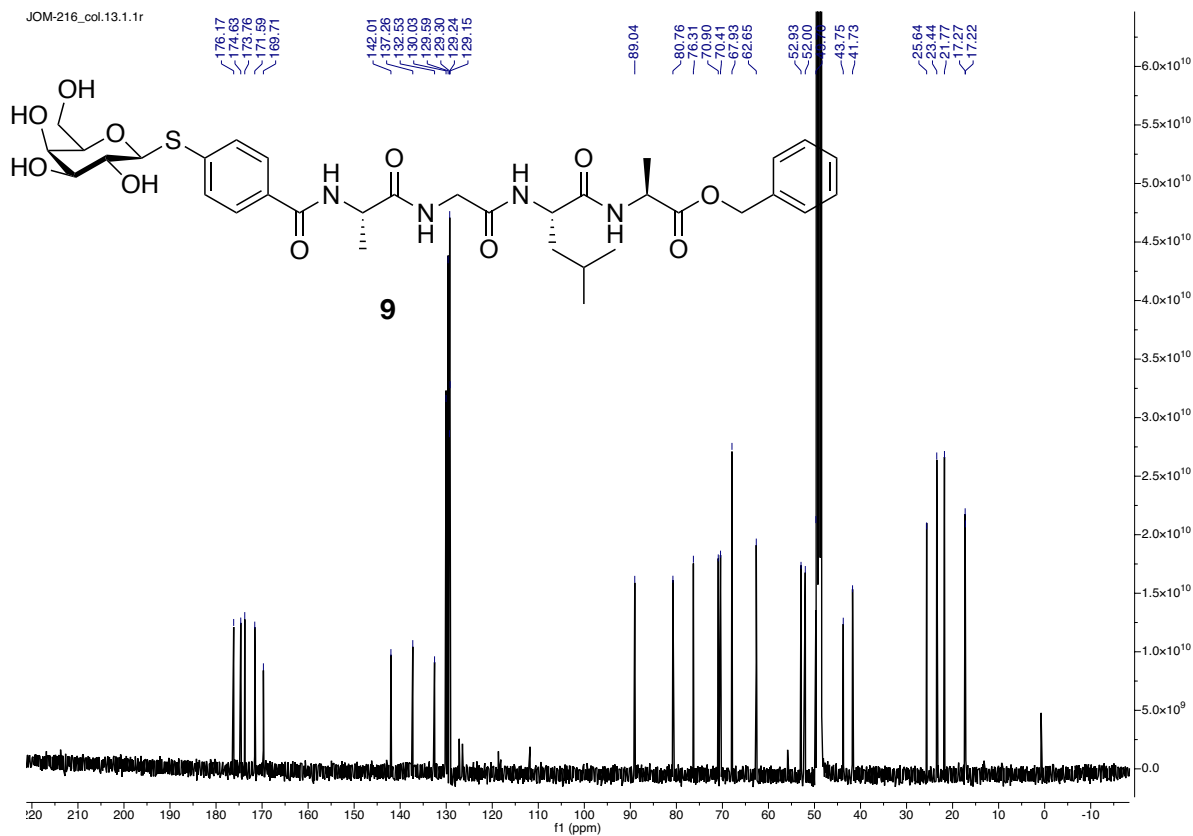
JOM-213.13.1.1r



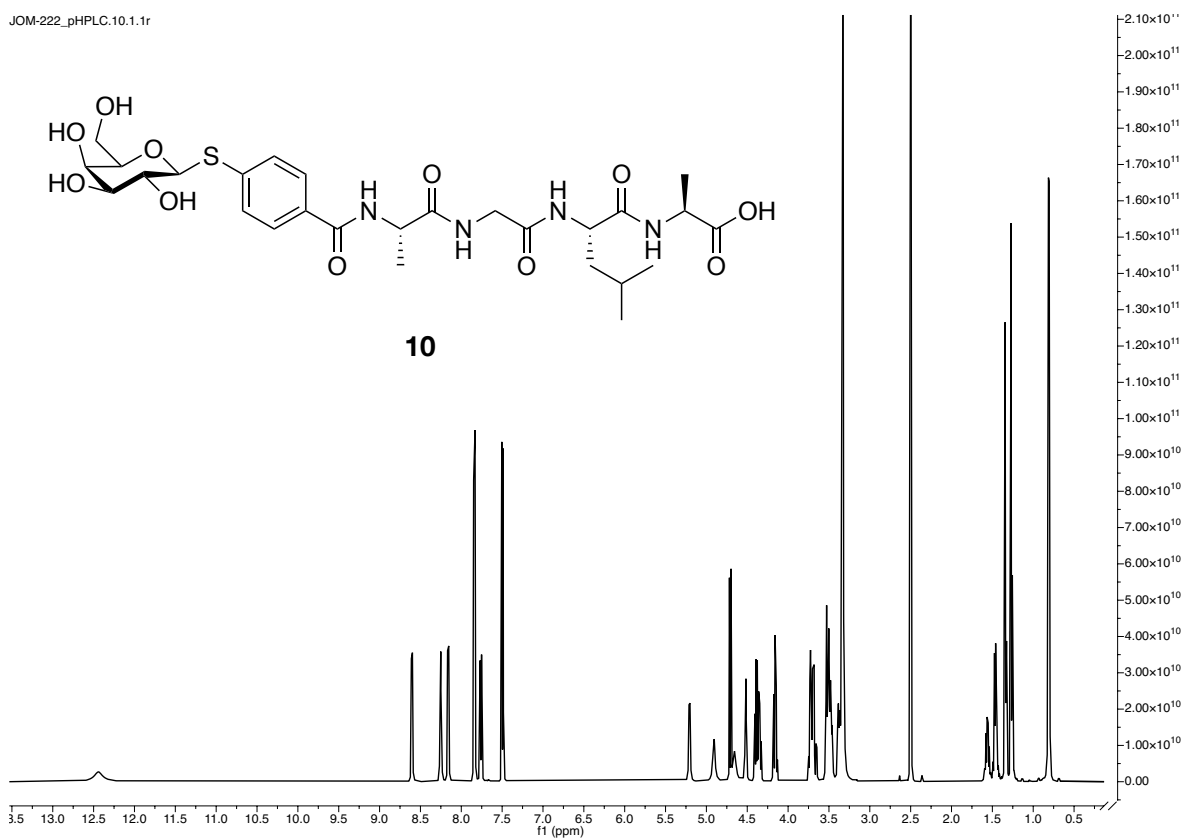
JOM-216_col.10.1.1r



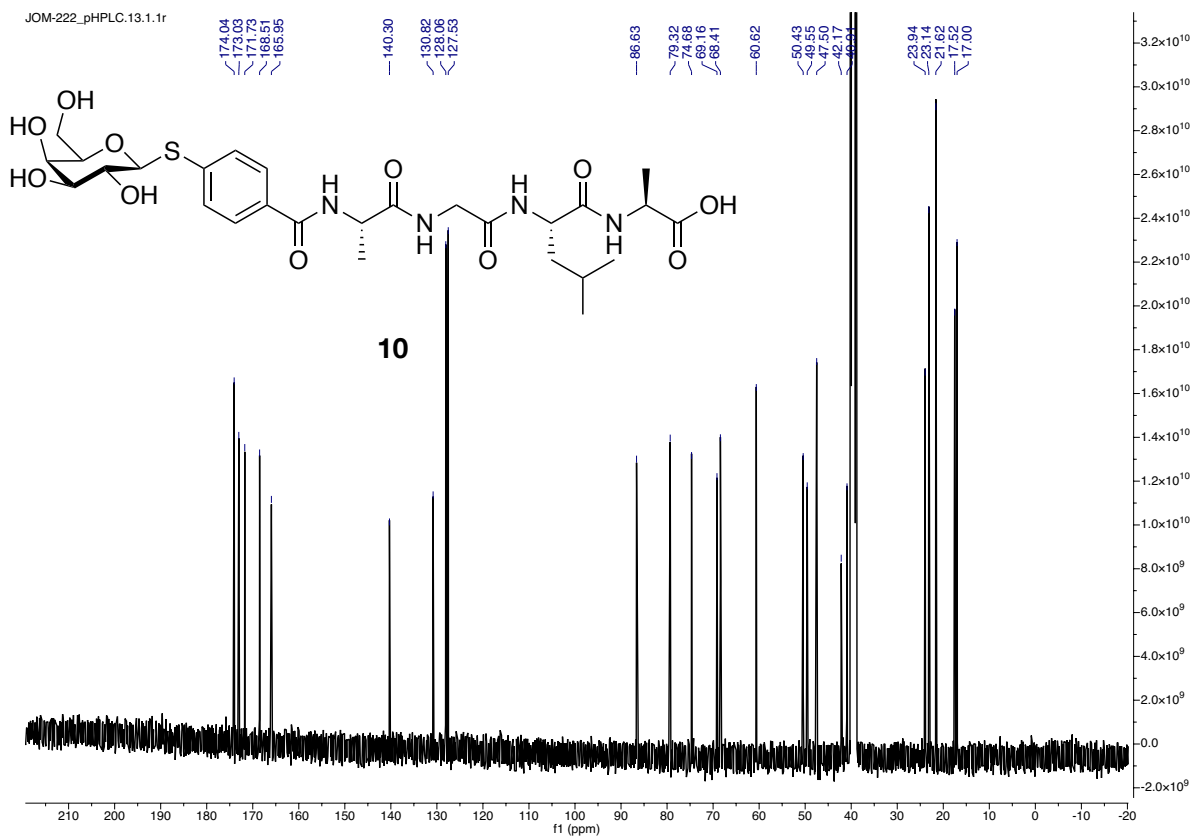
JOM-216_col.13.1.1r



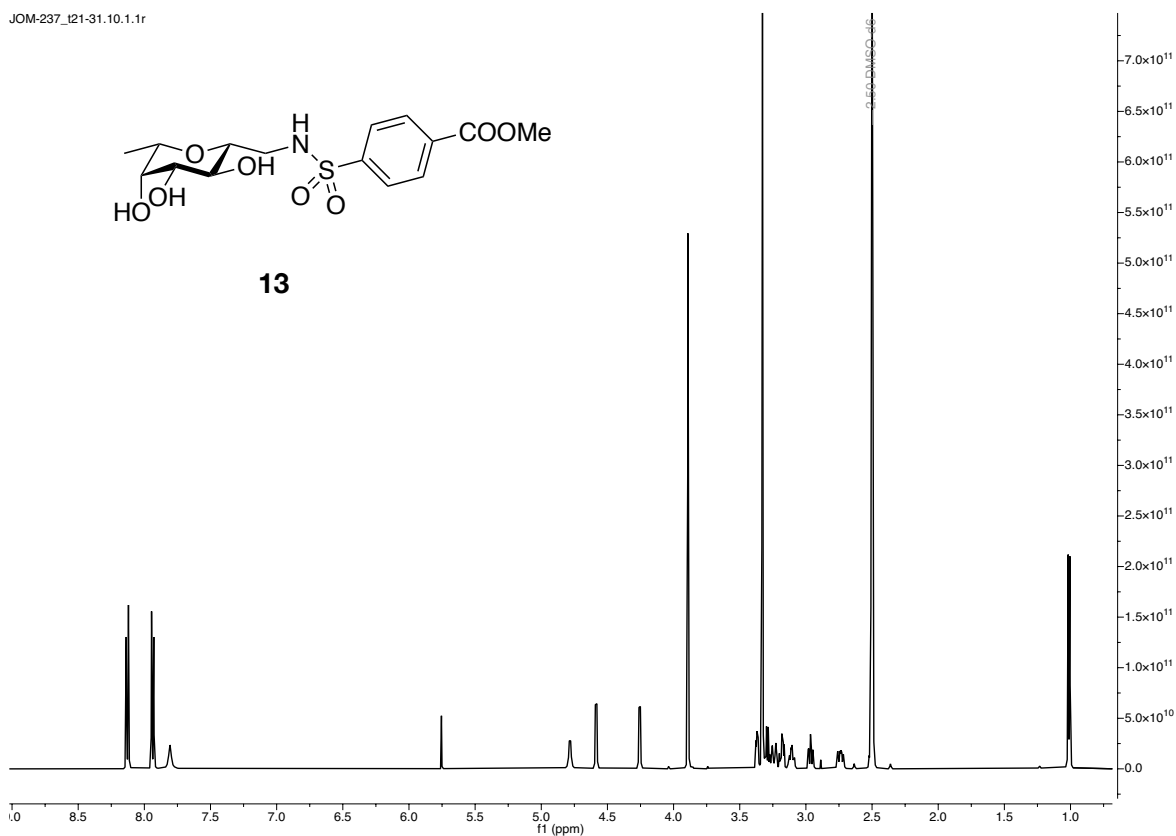
JOM-222_pHPLC.10.1.1r



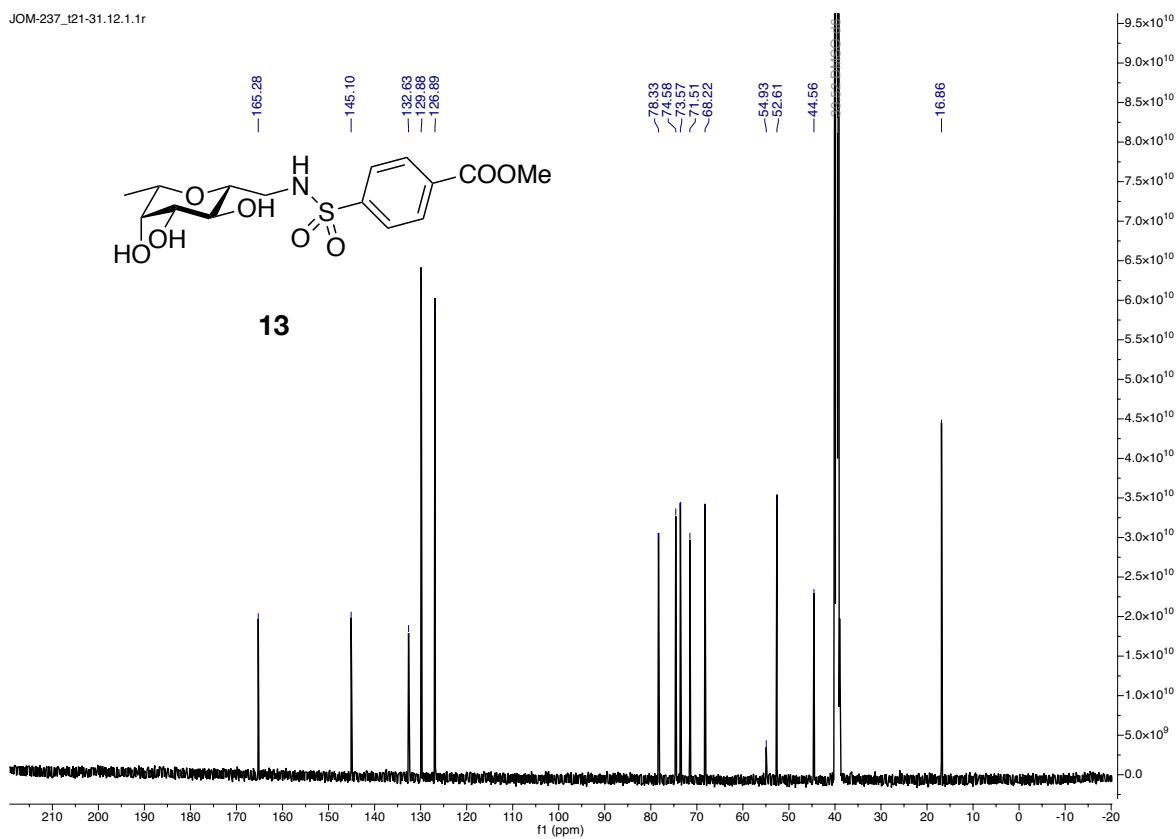
JOM-222_pHPLC.13.1.1r



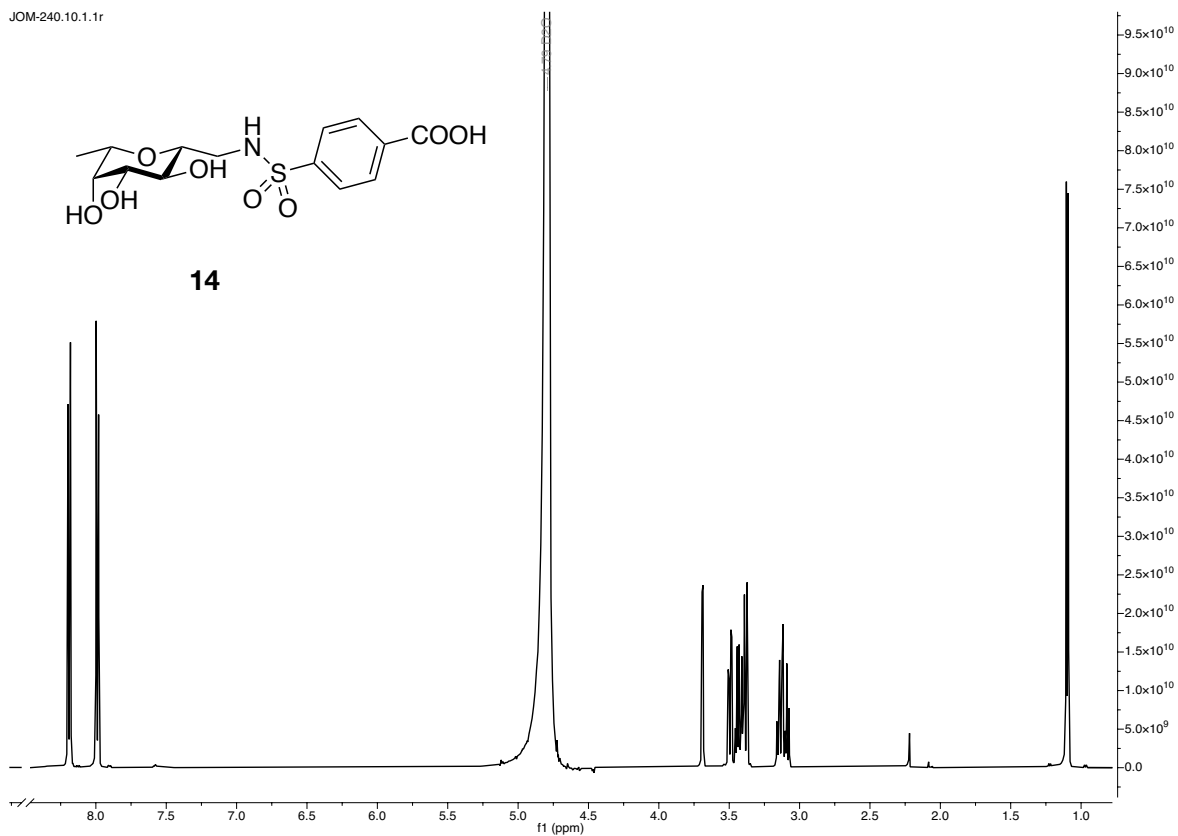
JOM-237_121-31.10.1.1r



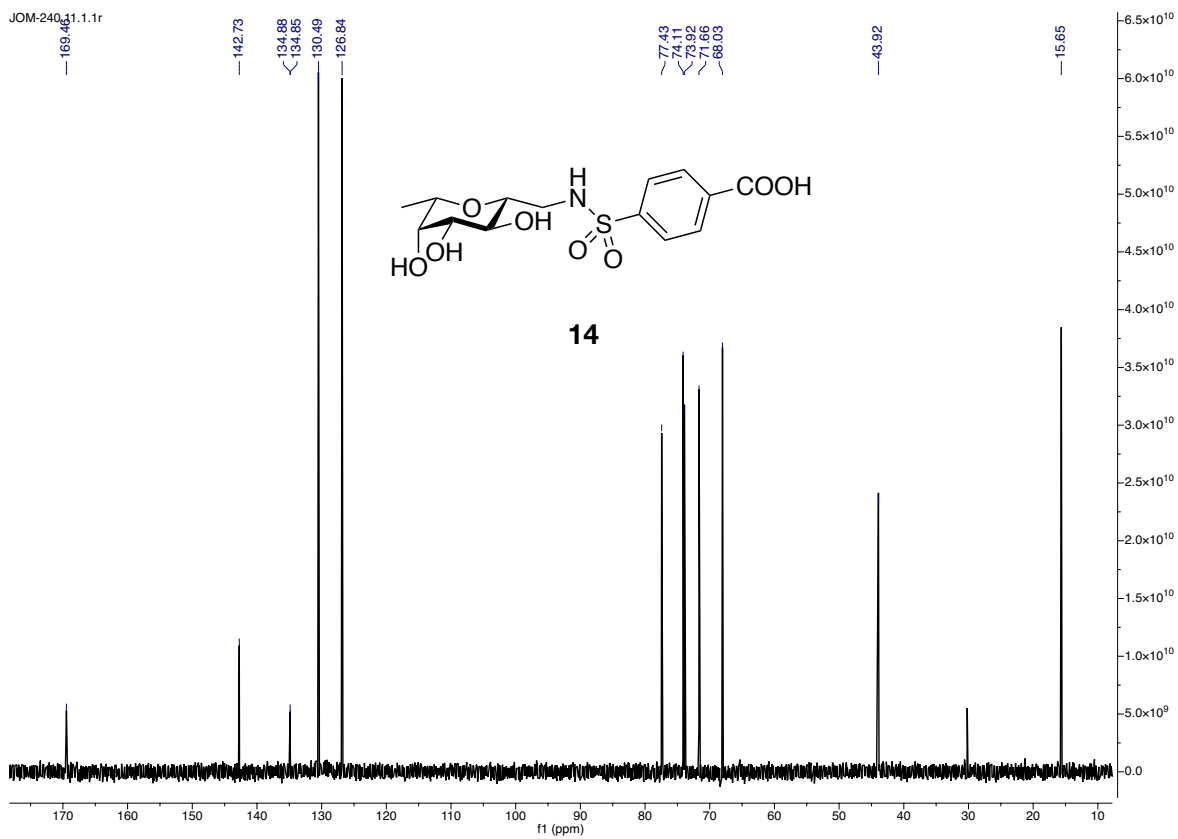
JOM-237_121-31.12.1.1r



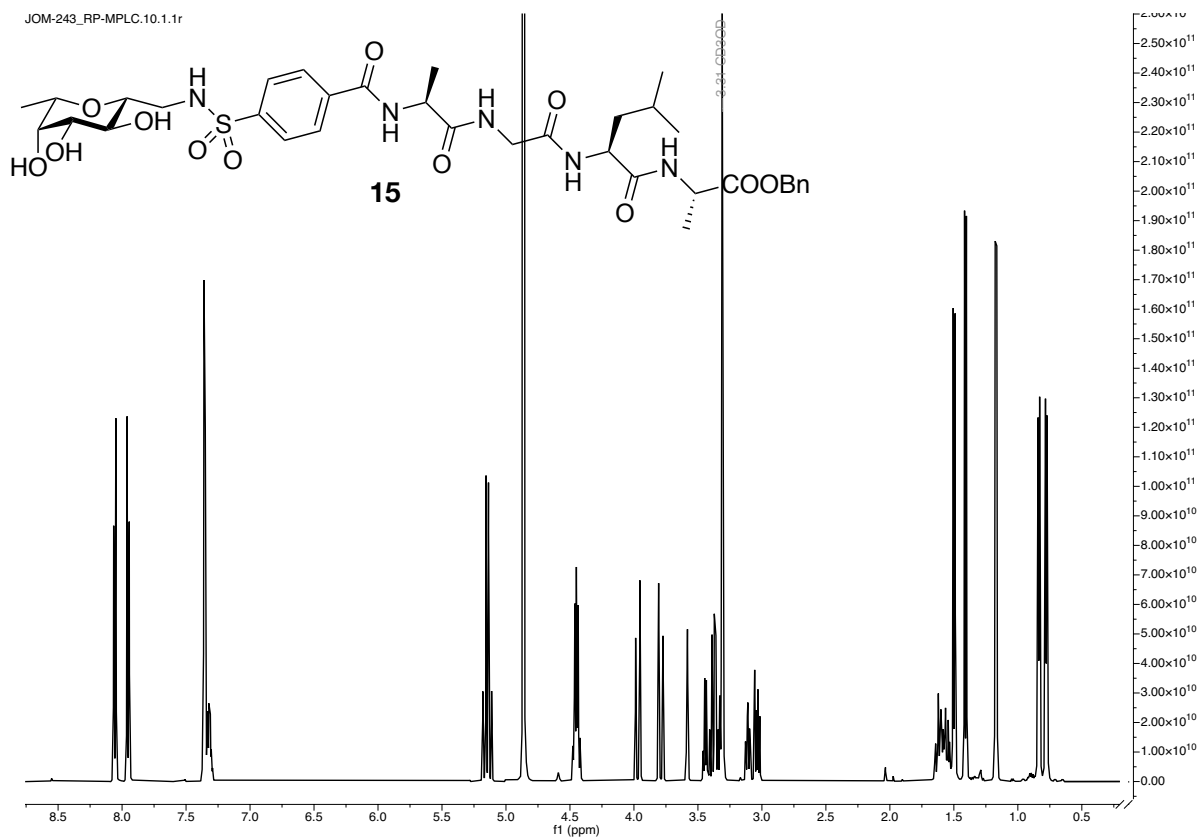
JOM-240.10.1.1r



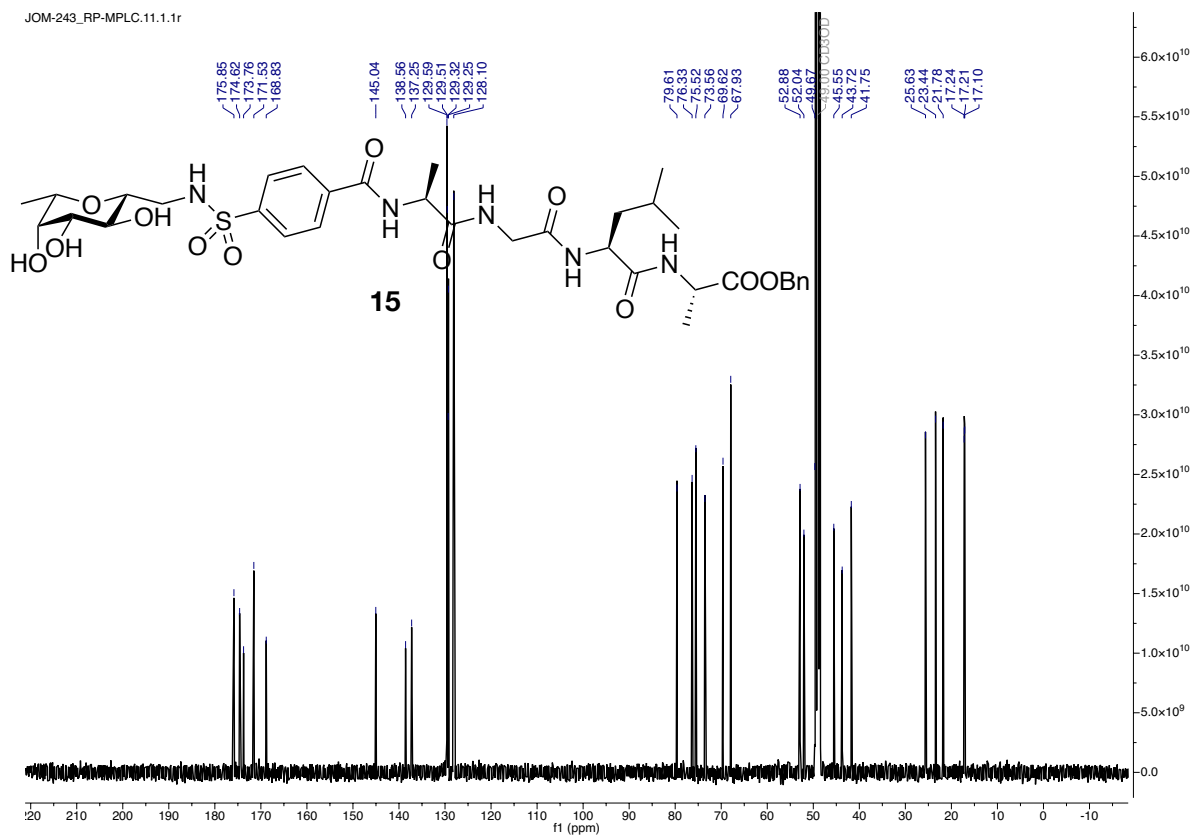
JOM-240.11.1.1r



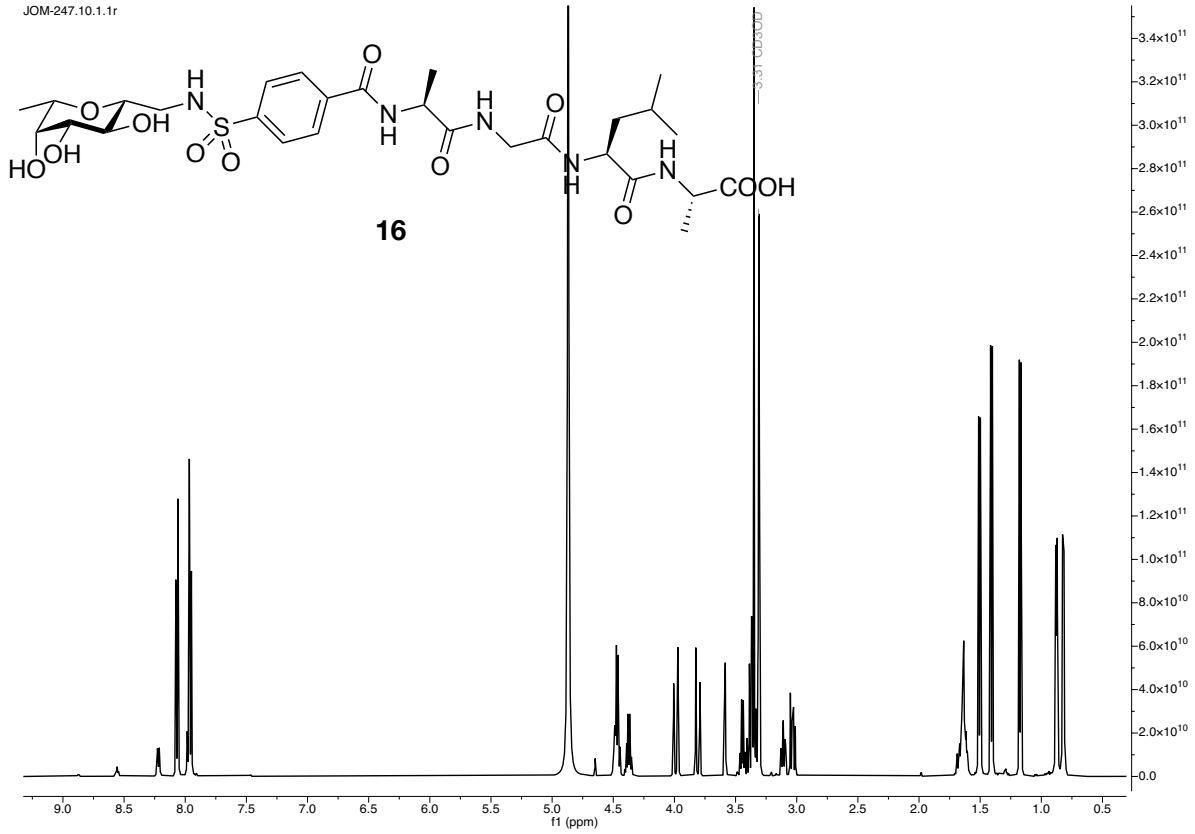
JOM-243_RP-MPLC.10.1.1r



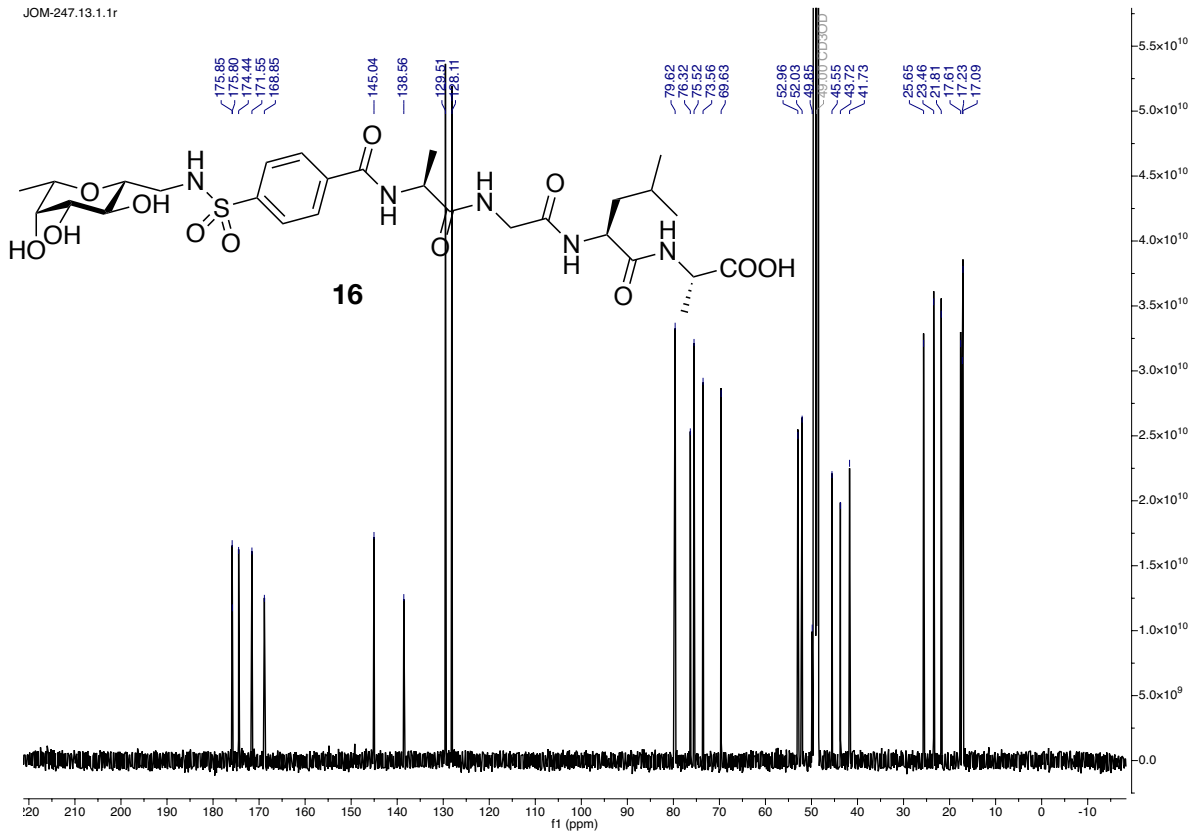
JOM-243_RP-MPLC.11.1.1r



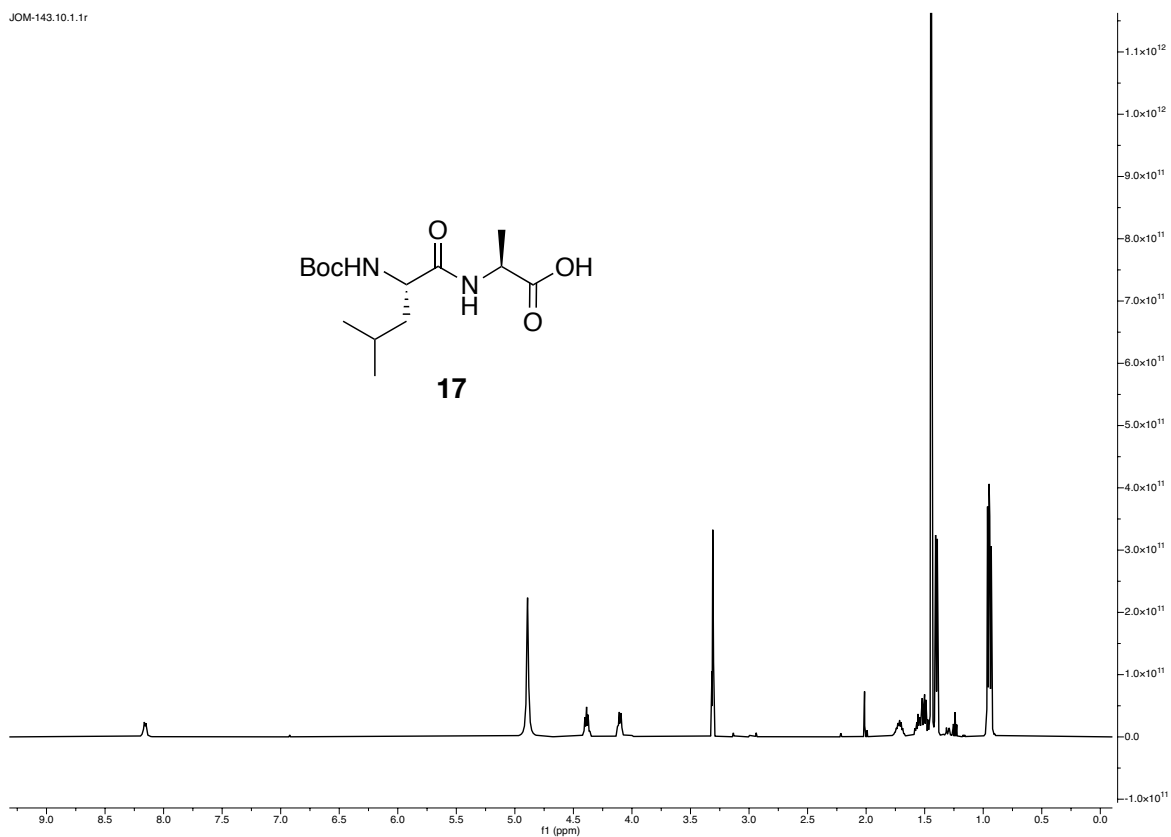
JOM-247.10.1.1r



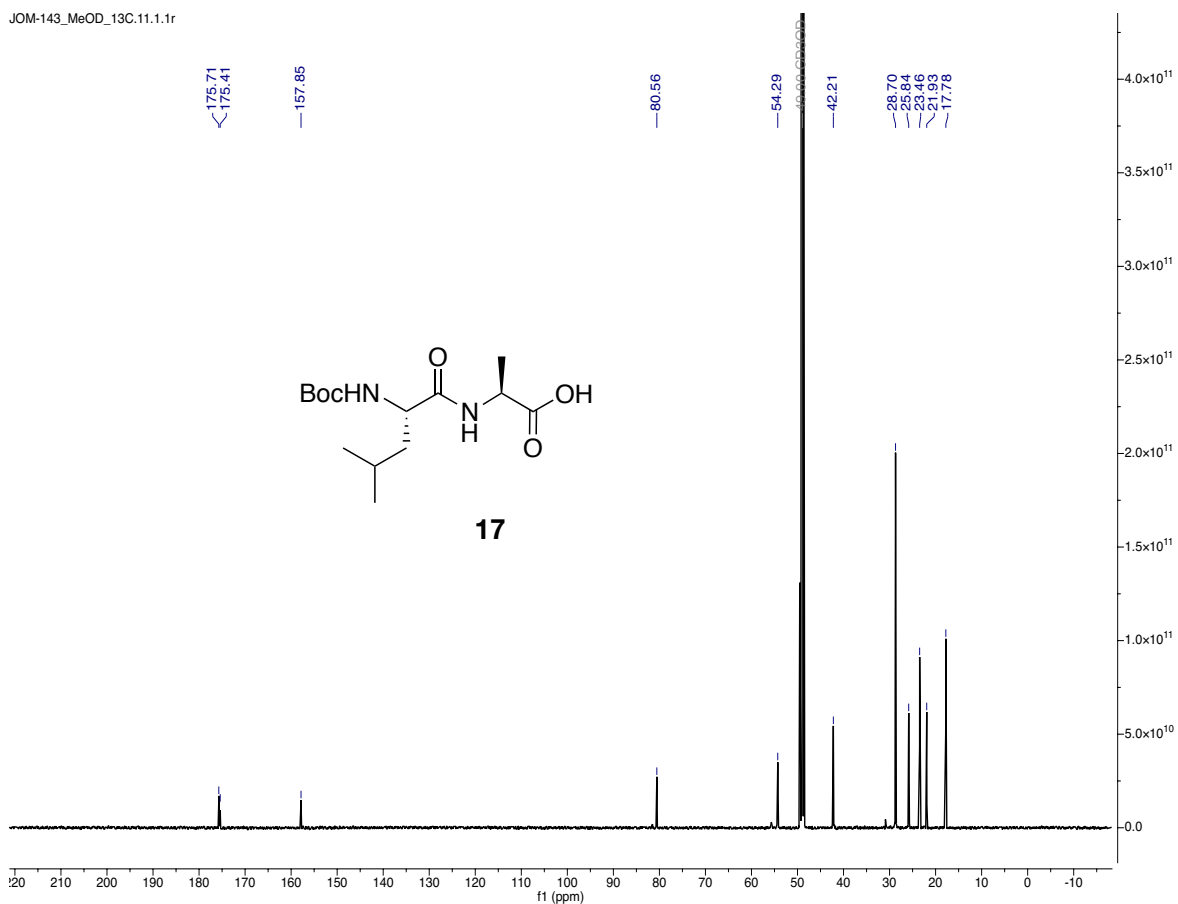
JOM-247.13.1.1r



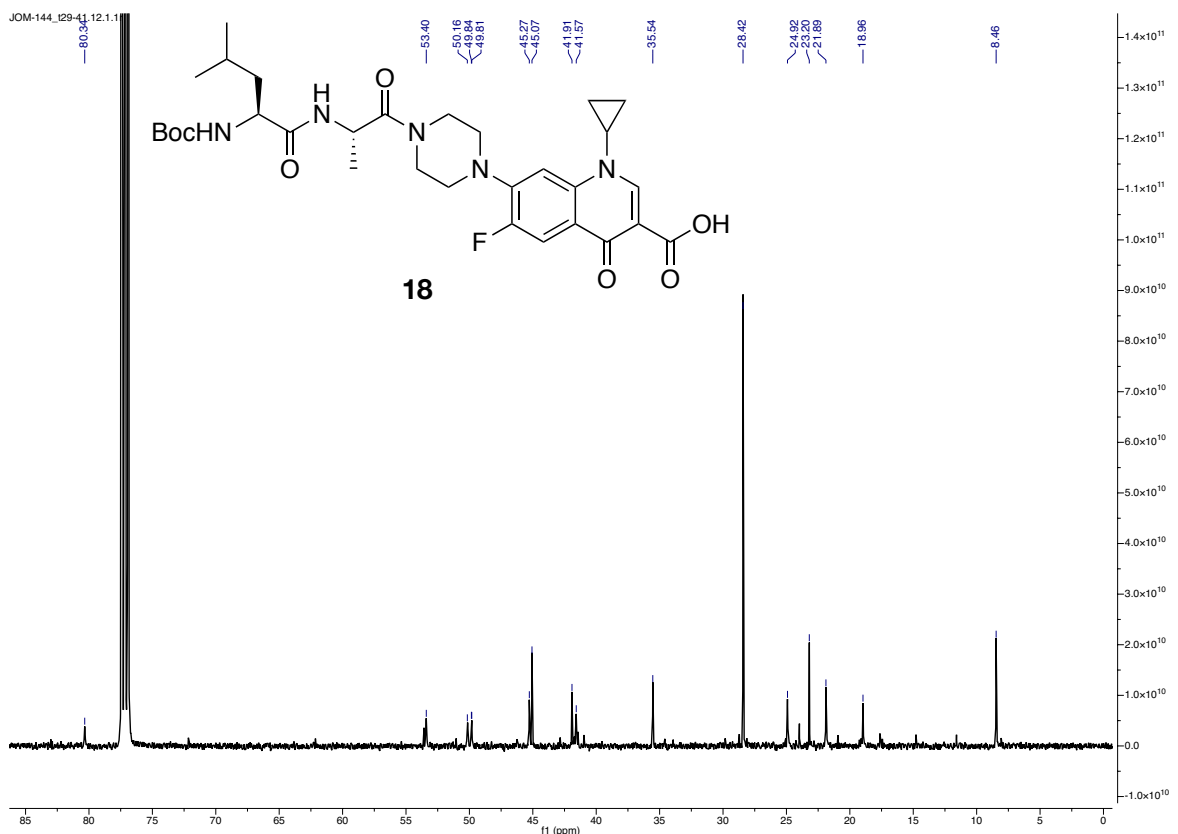
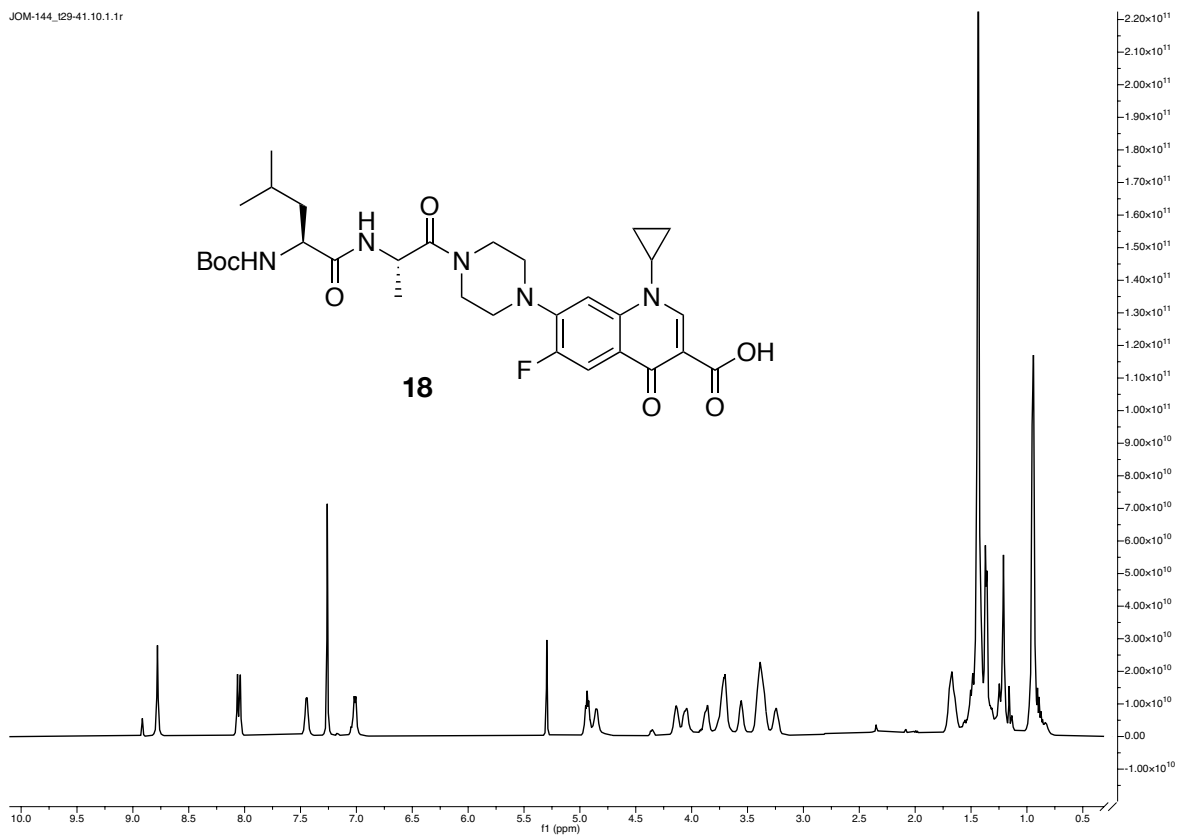
JOM-143.10.1.1r



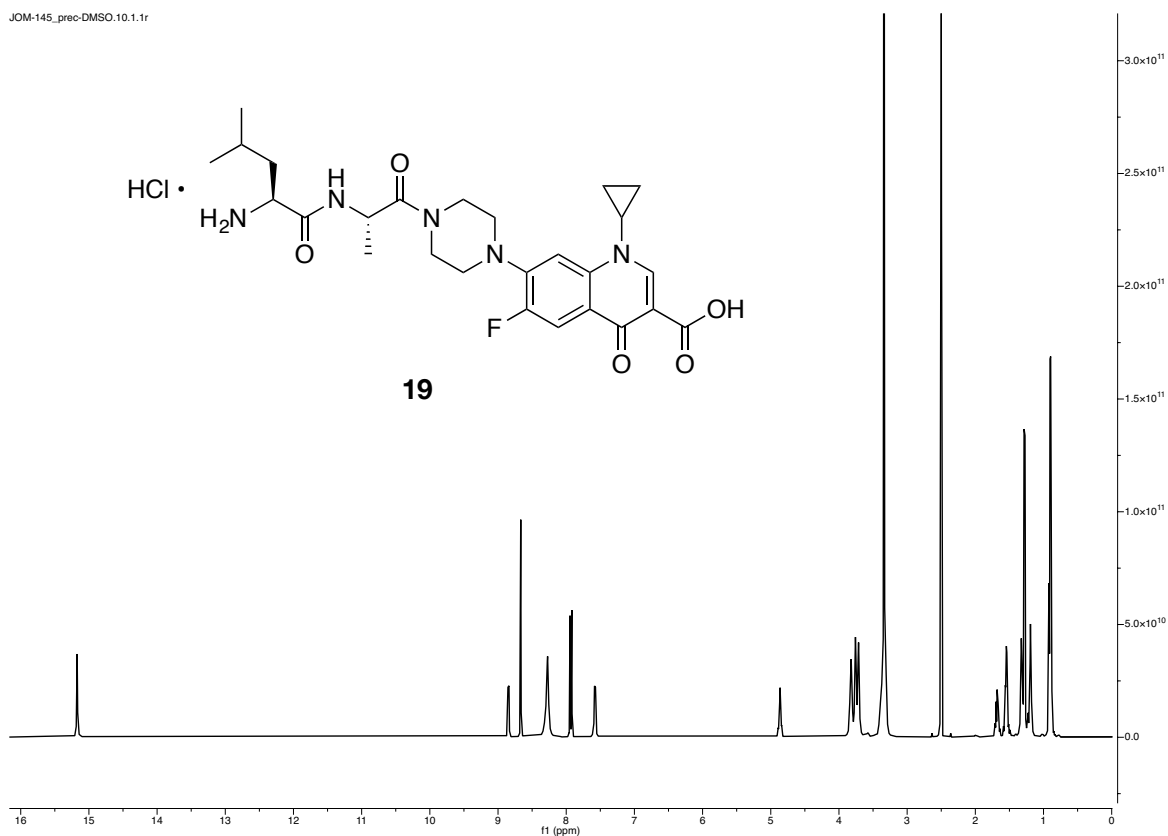
JOM-143_MeOD_13C.11.1.1r



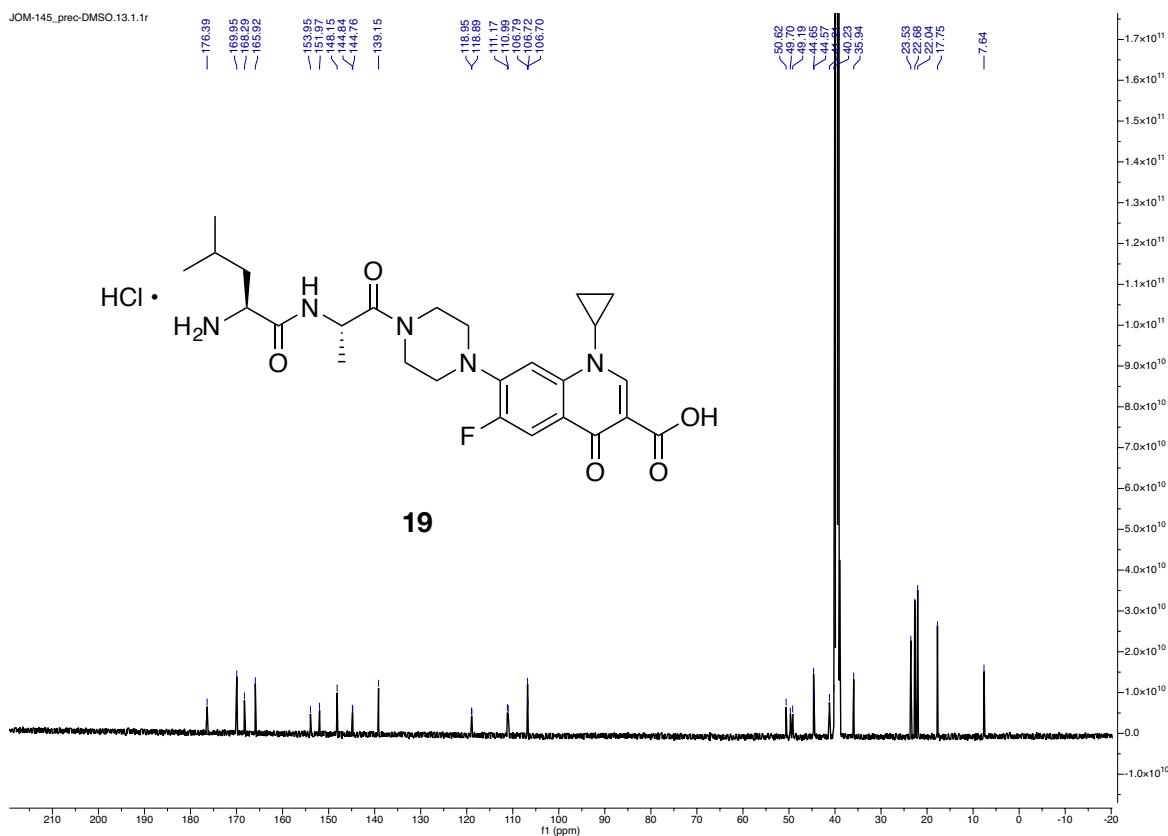
JOM-144_L29-41.10.1.1r



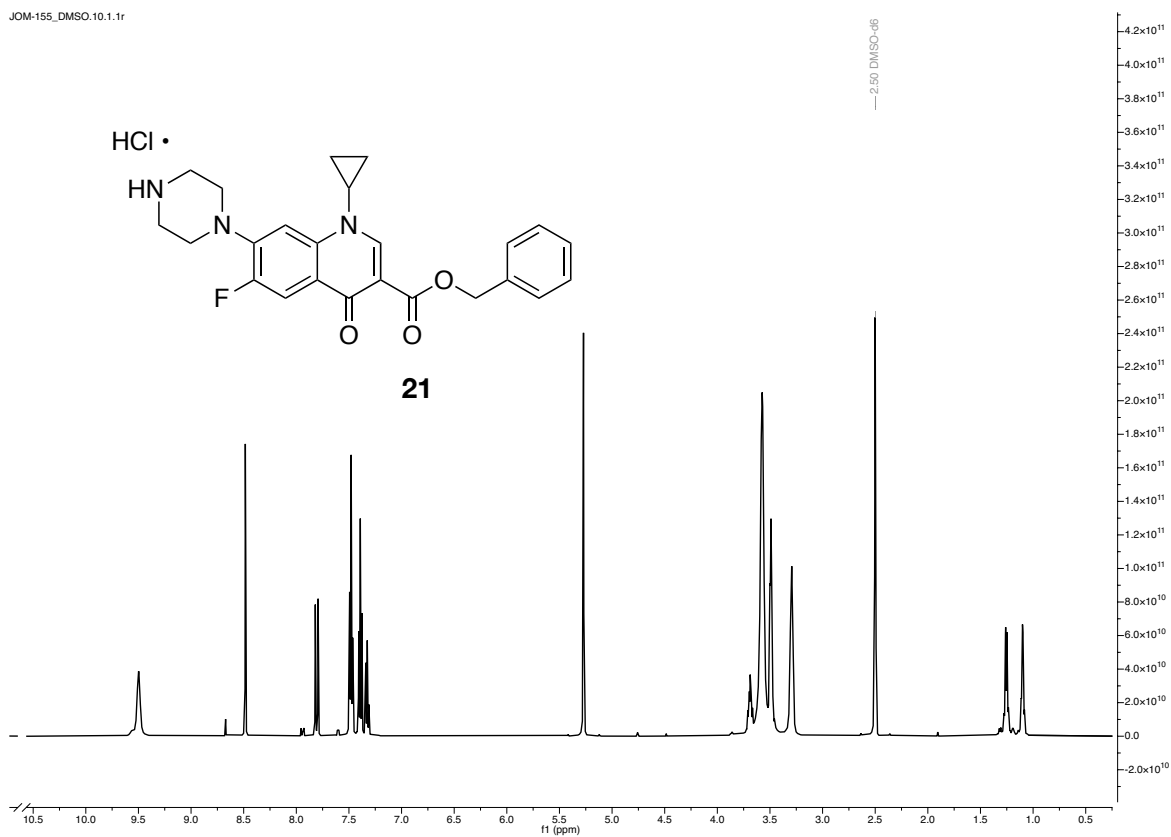
JOM-145_prec-DMSO.10.1.1r



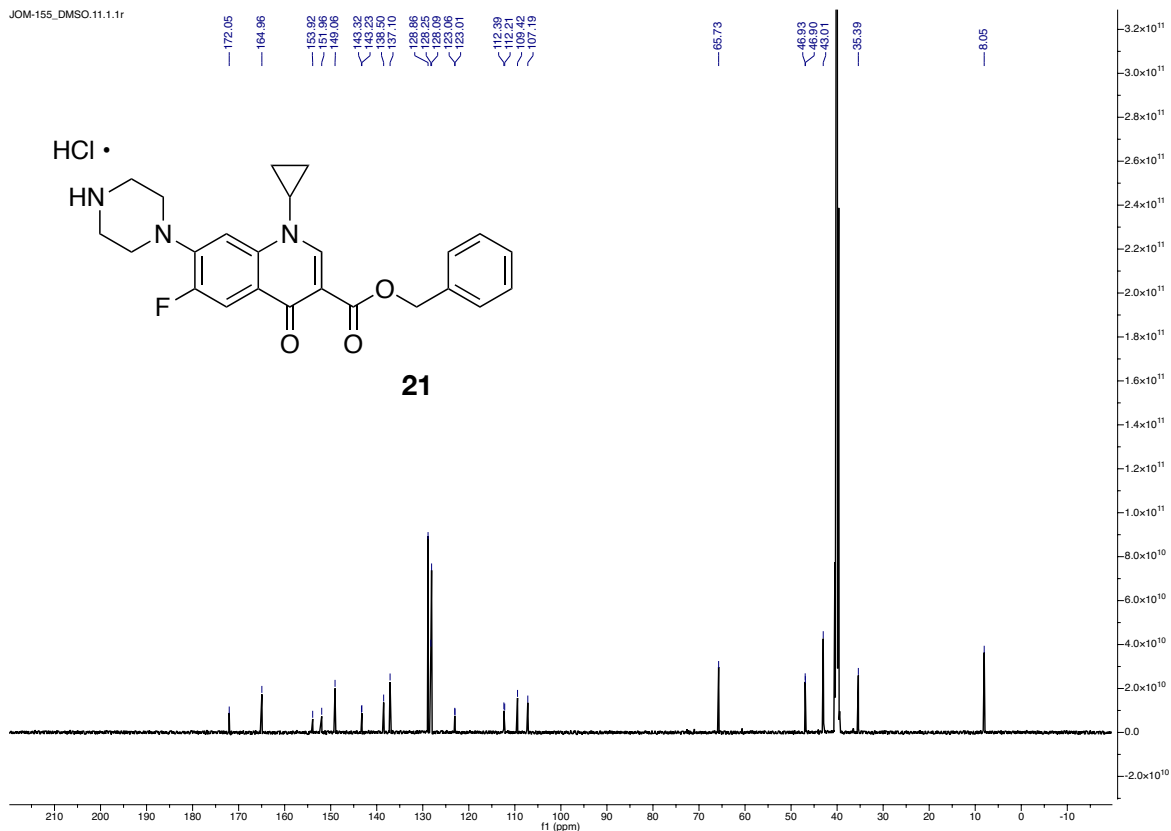
JOM-145_prec-DMSO.13.1.1r



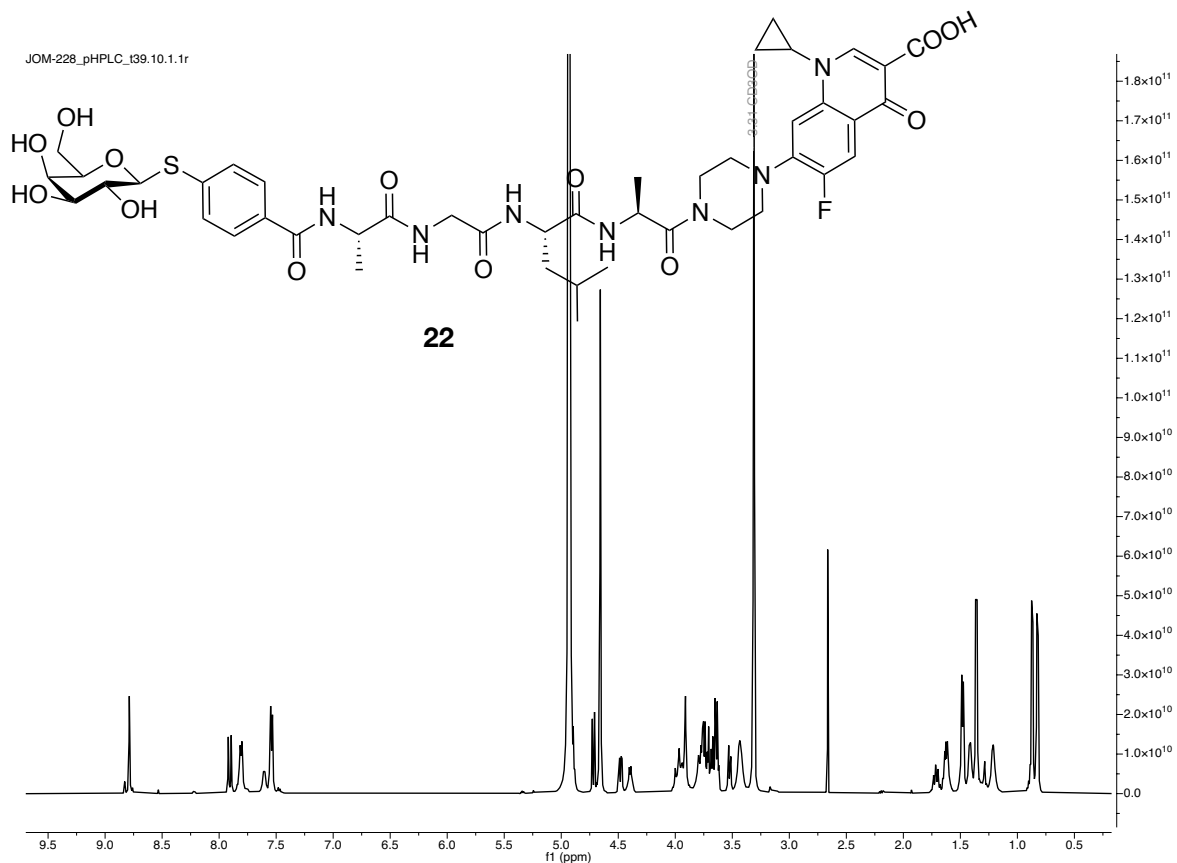
JOM-155_DMSO.10.1.1f



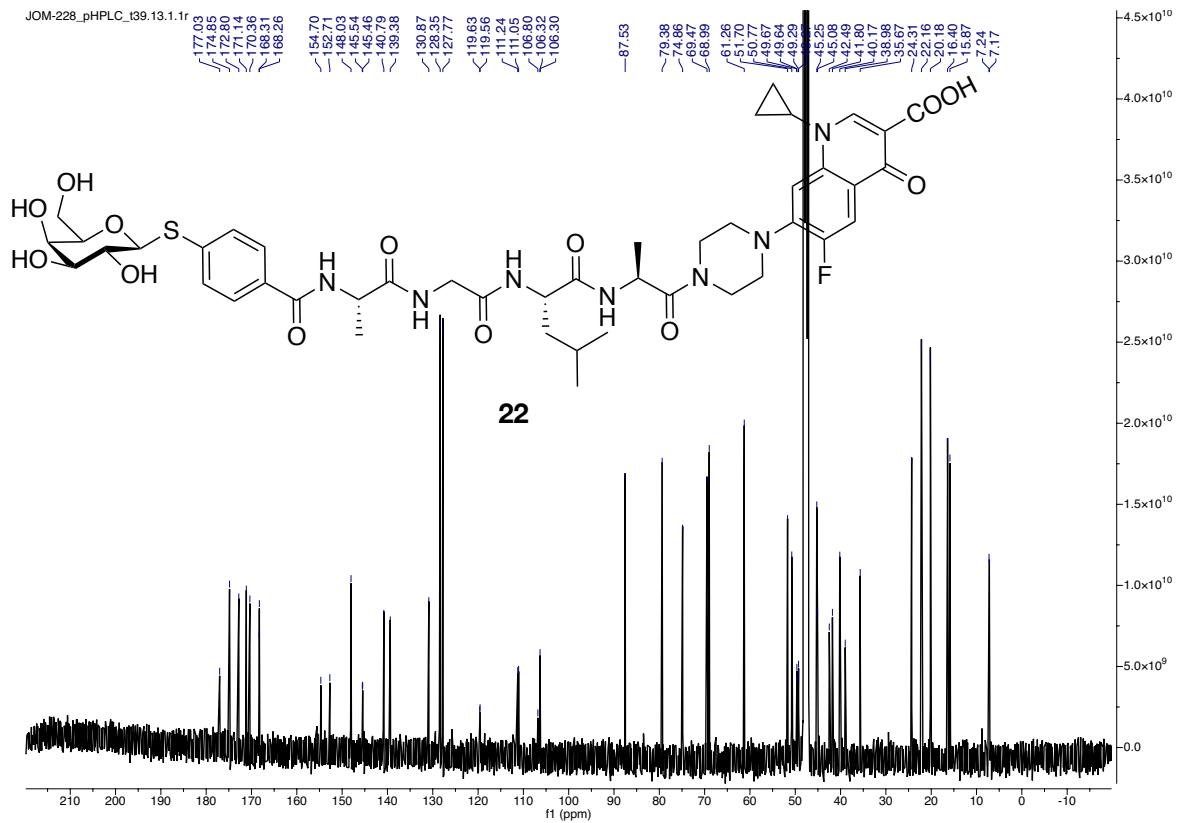
JOM-155_DMSO.11.1.1f



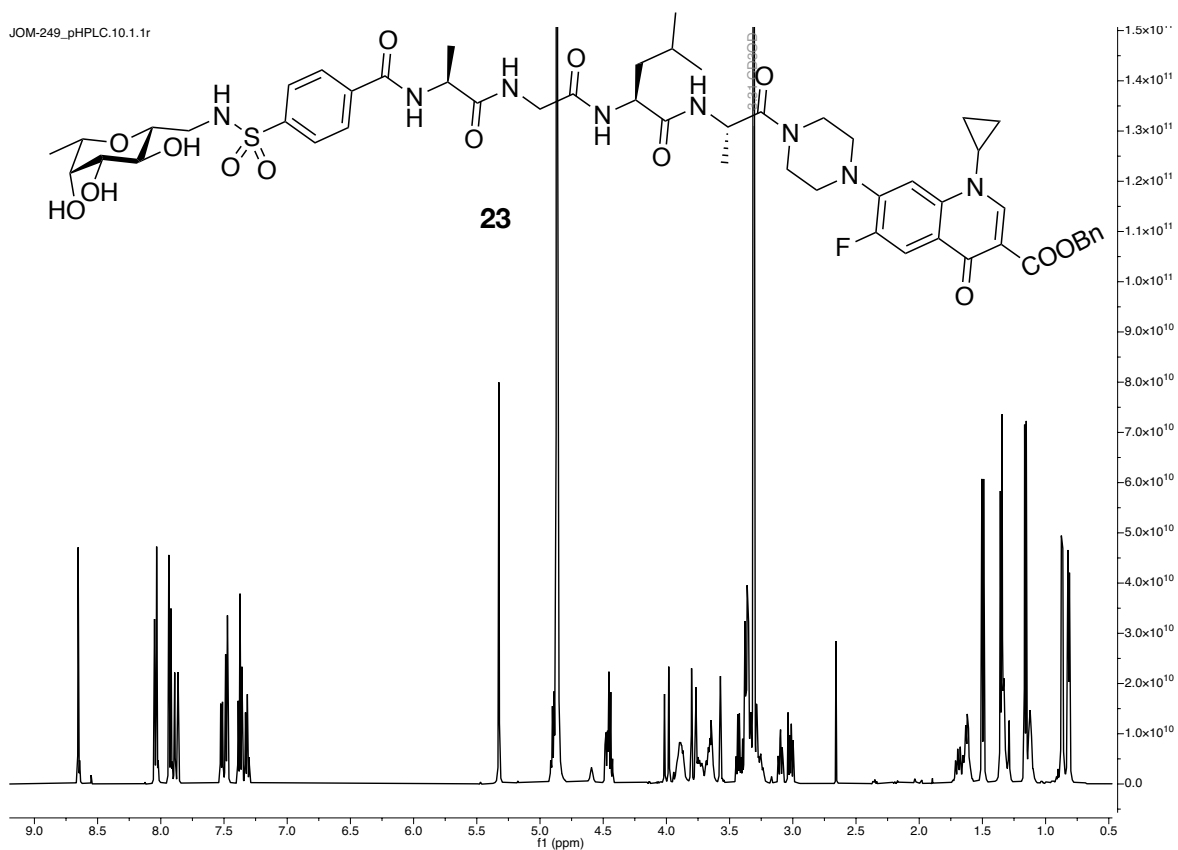
JOM-228_pHPLC_139.10.1.1r



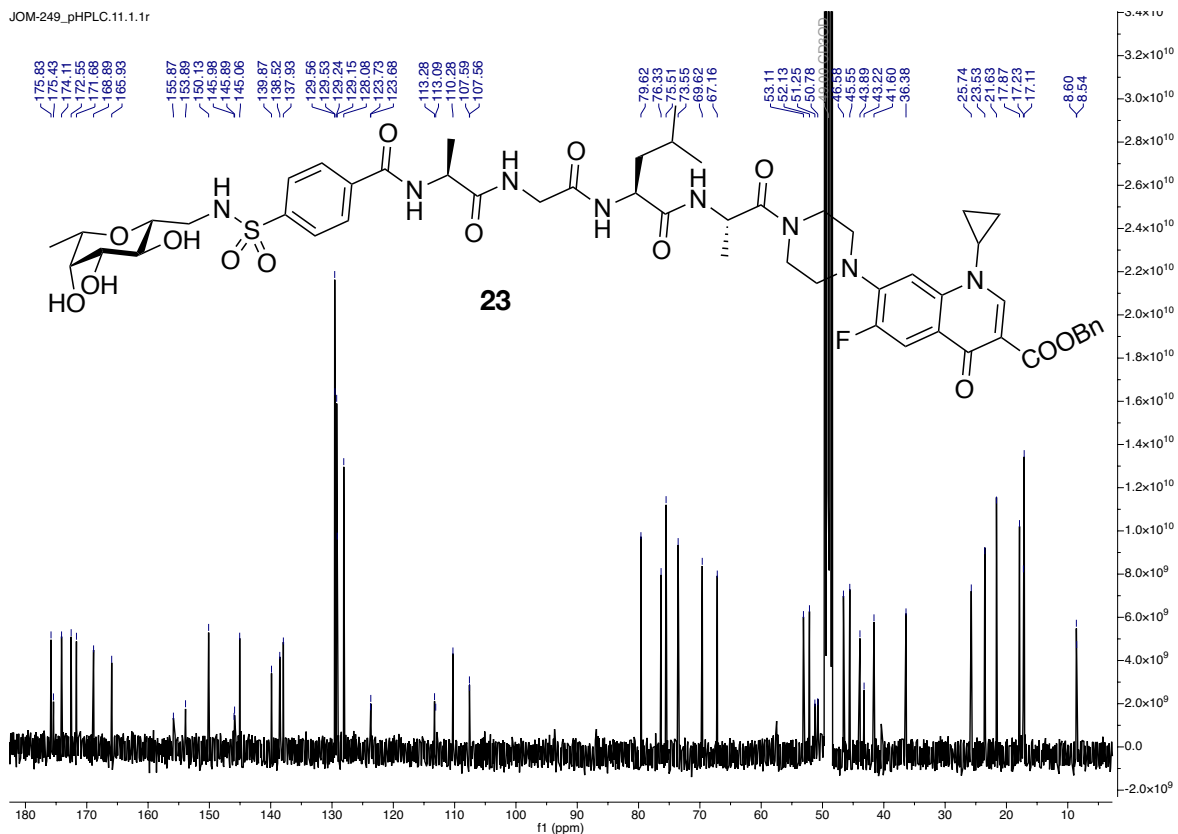
JOM-228_pHPLC_139.13.1.1r



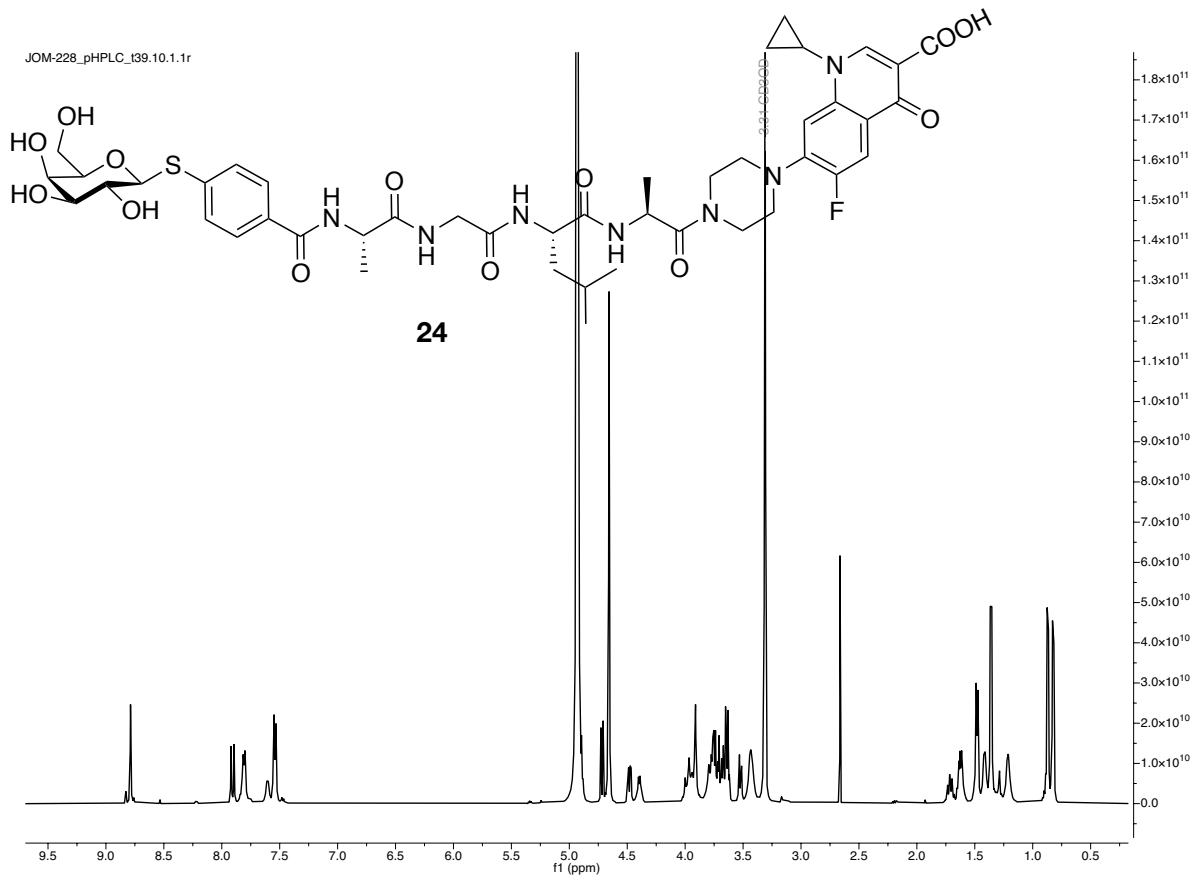
JOM-249_pHPLC.10.1.1r



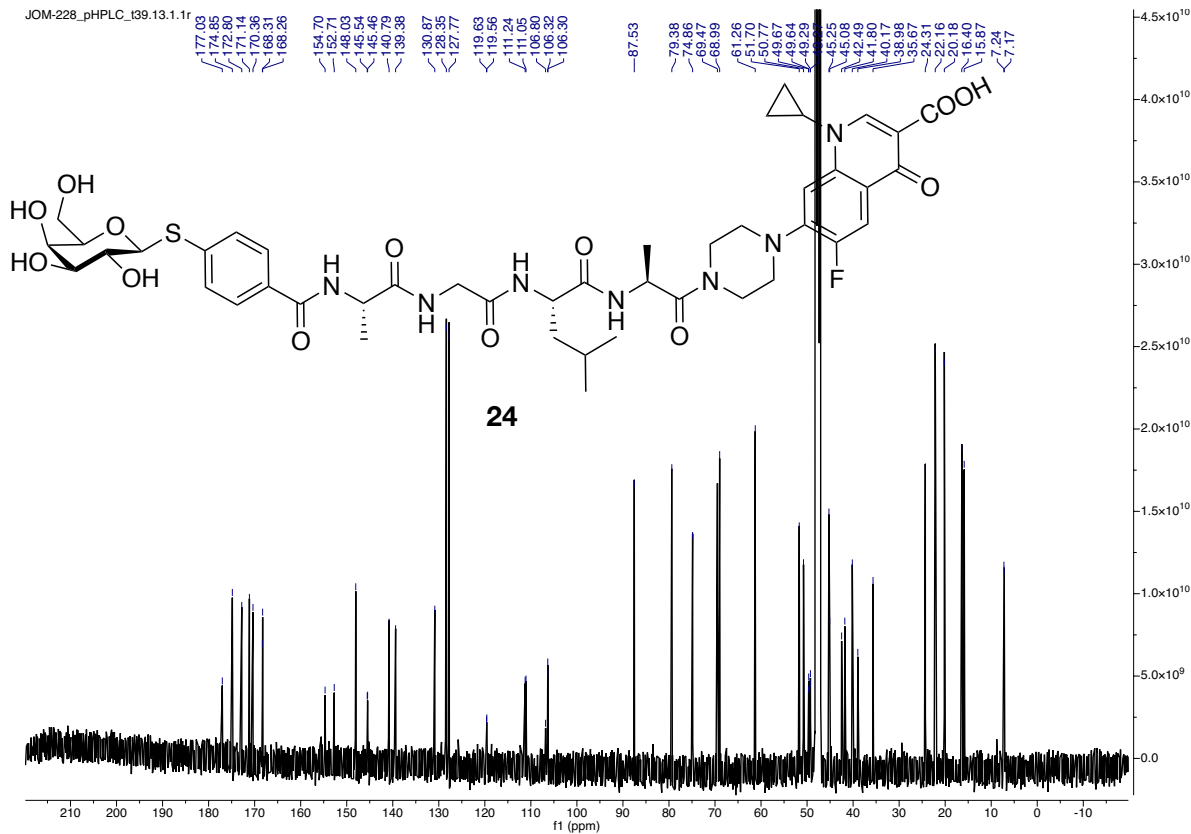
JOM-249_pHPLC.11.1.1r

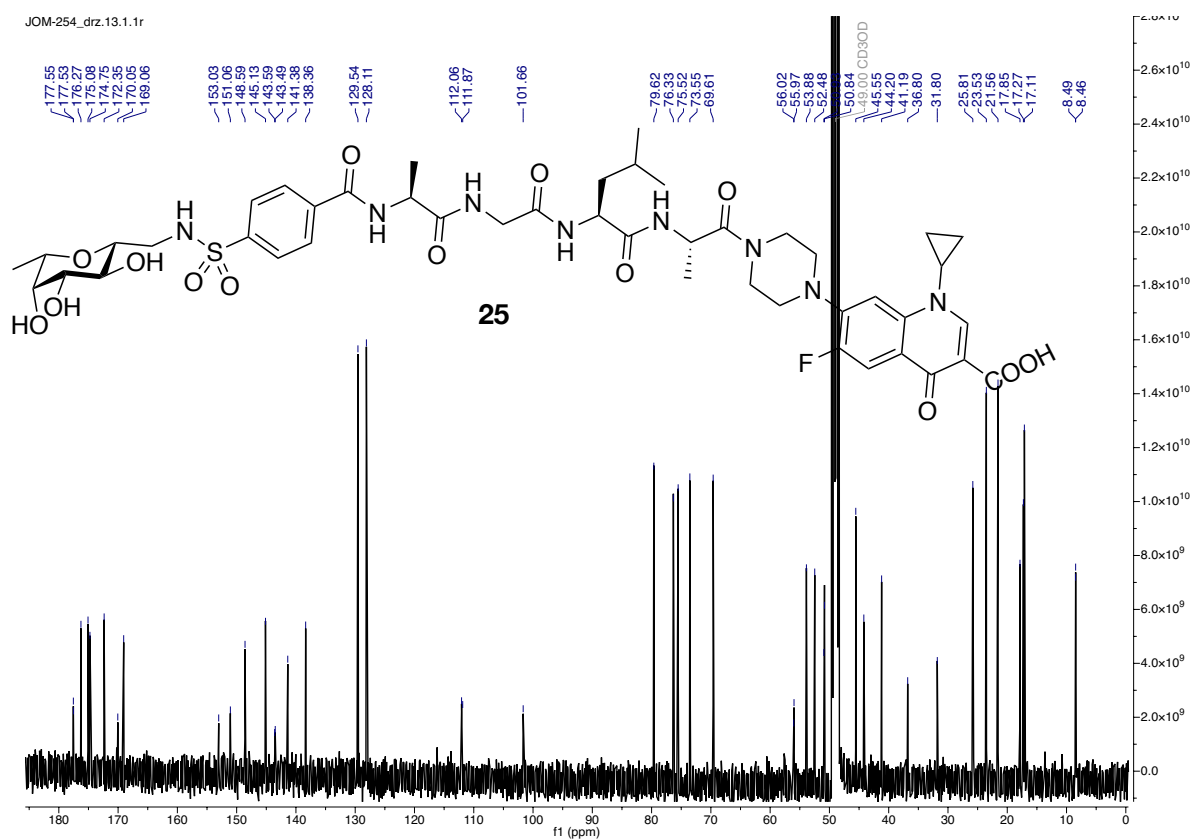
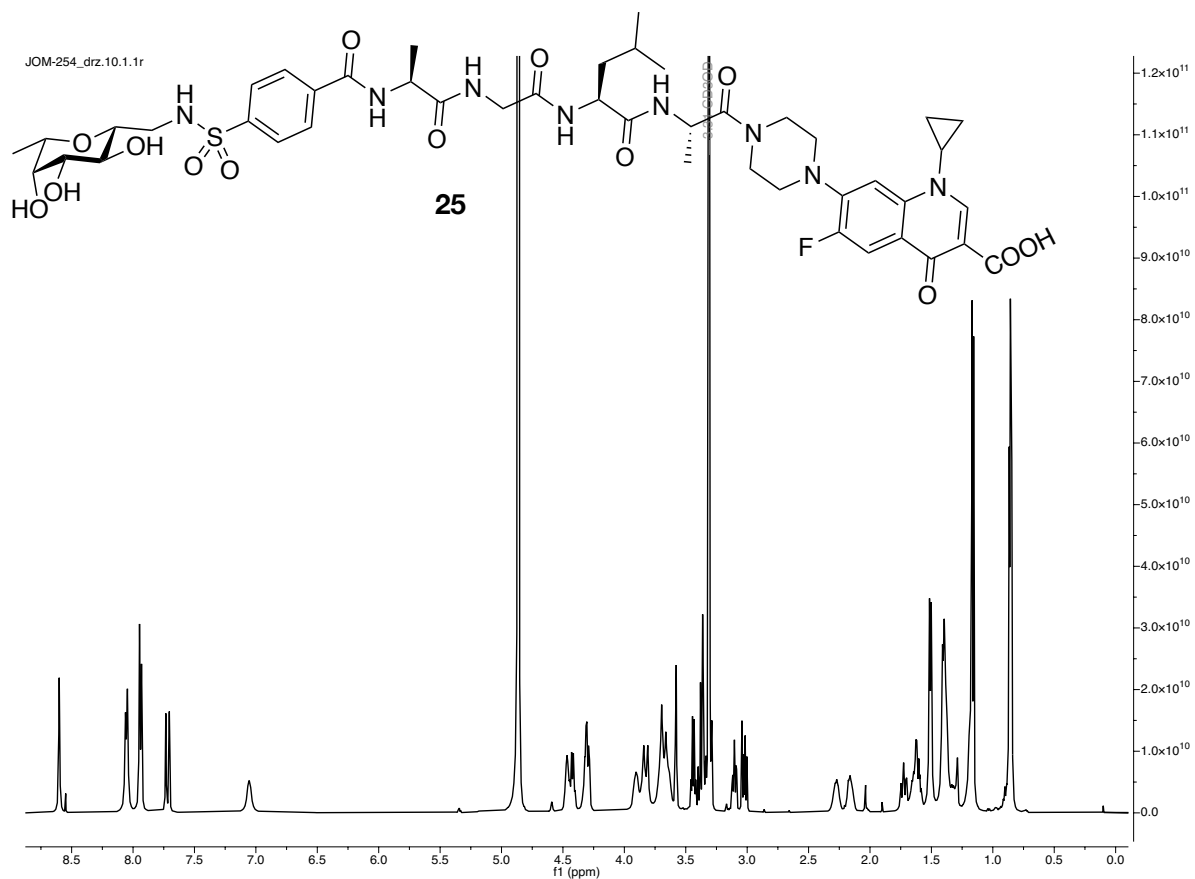


JOM-228_pHPLC_139.10.1.1r

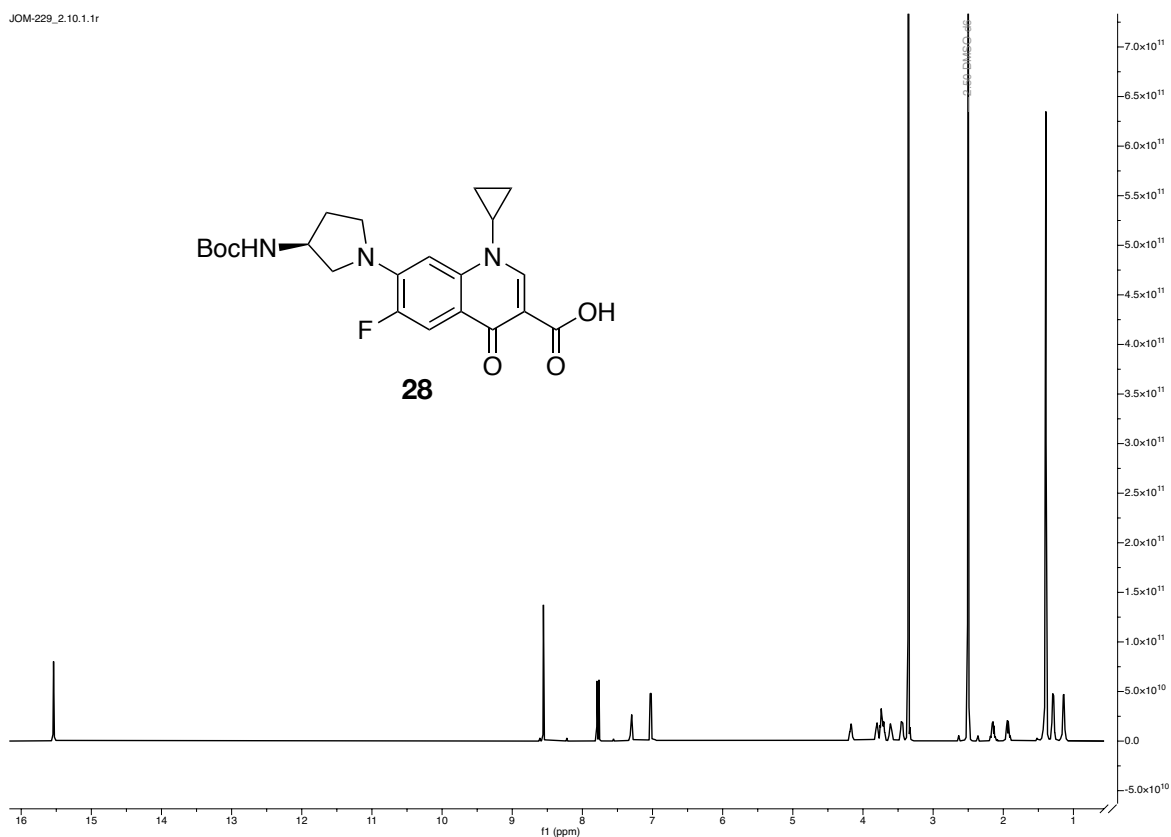


JOM-228_pHPLC_139.13.1.1r

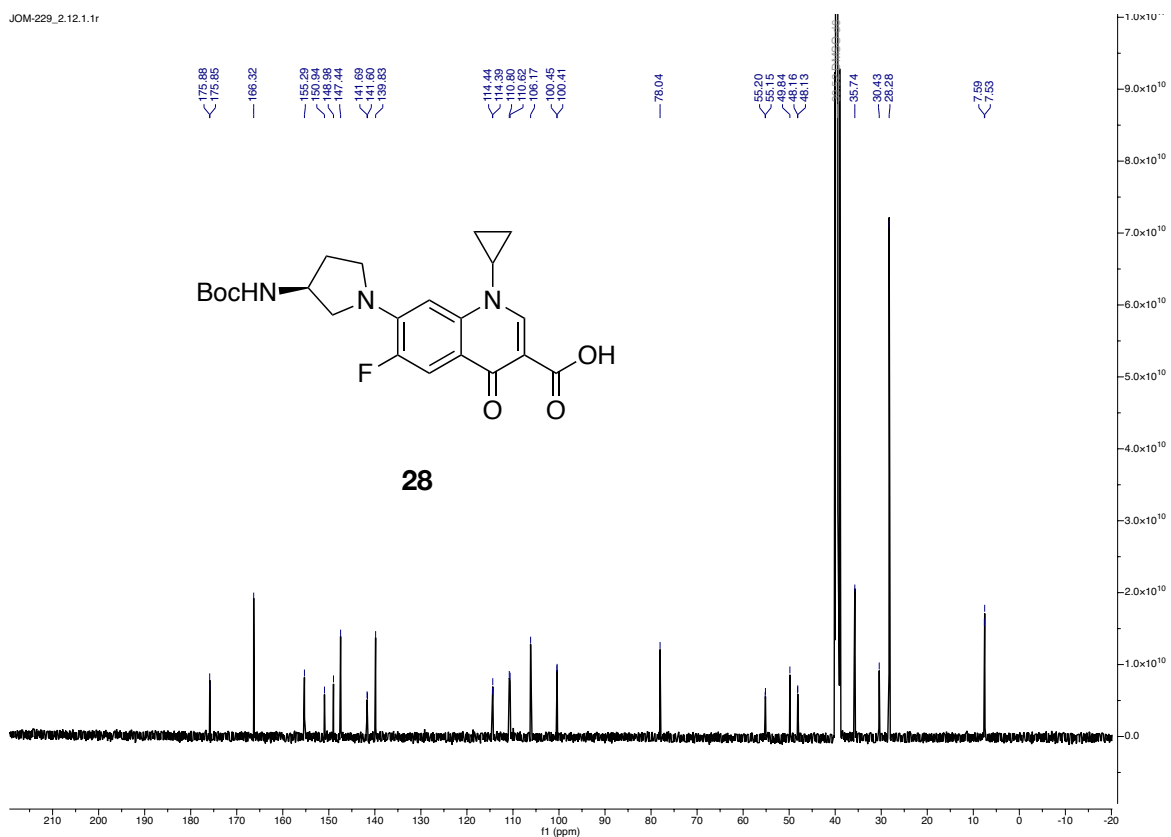




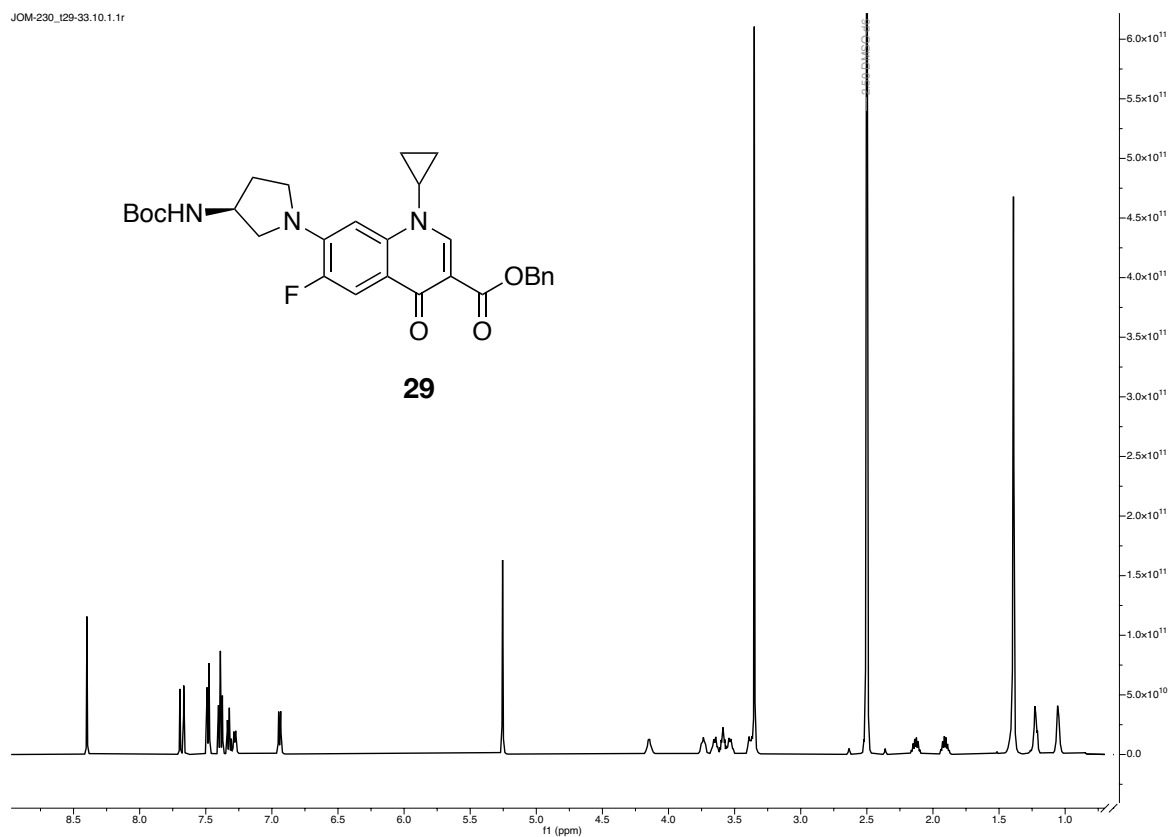
JOM-229_2.10.1.1r



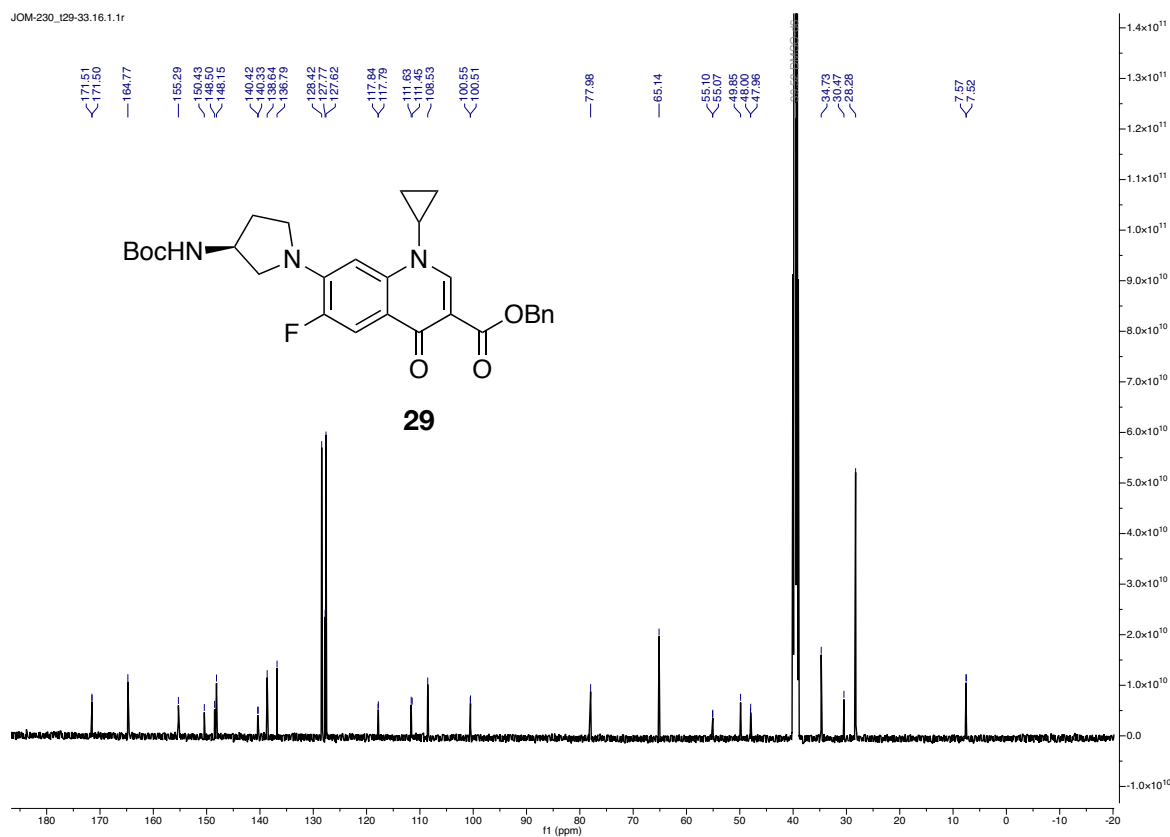
JOM-229_2.12.1.1r



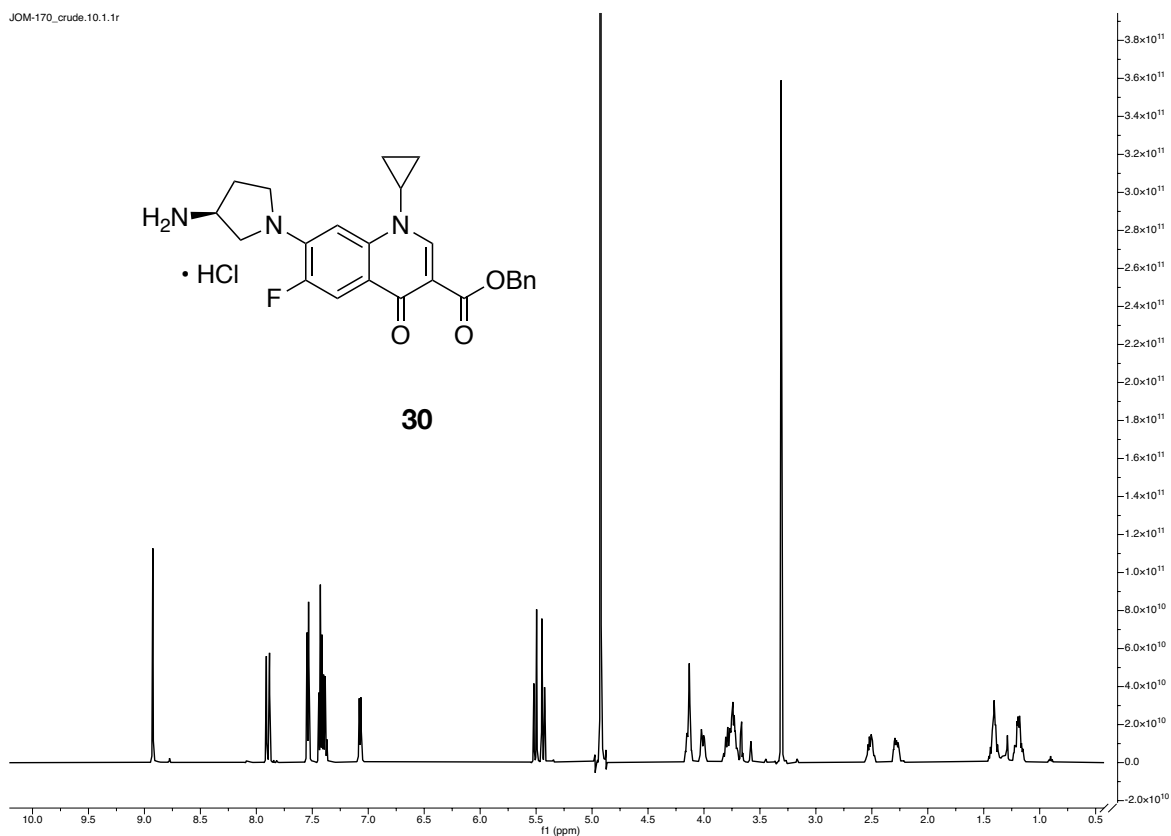
JOM-230_129-33.10.1.1r



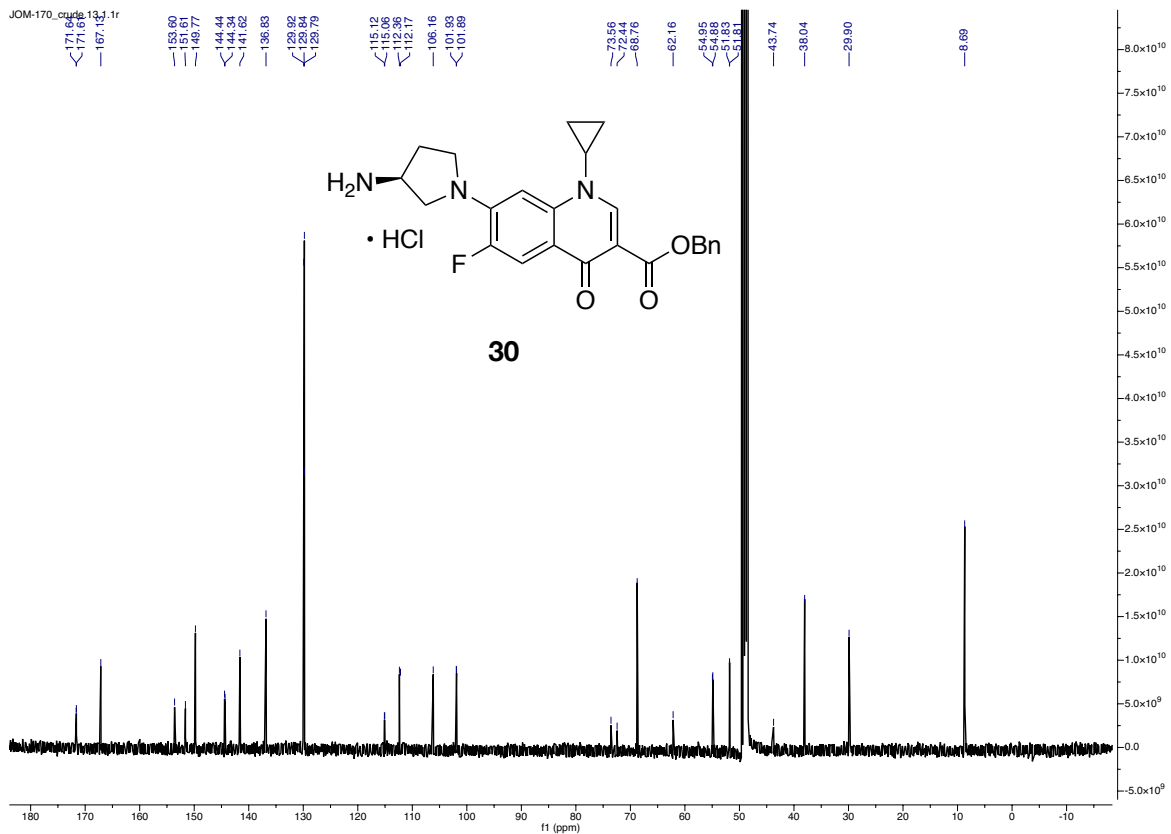
JOM-230_129-33.16.1.1r

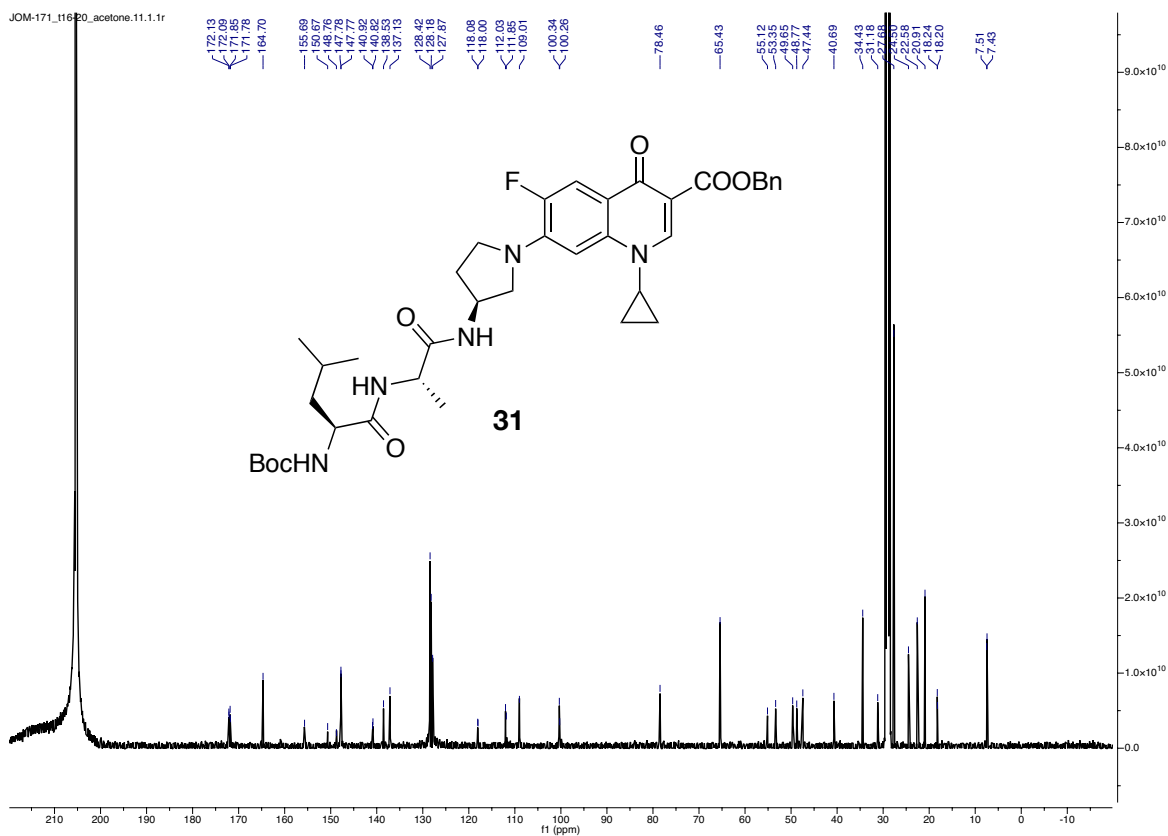
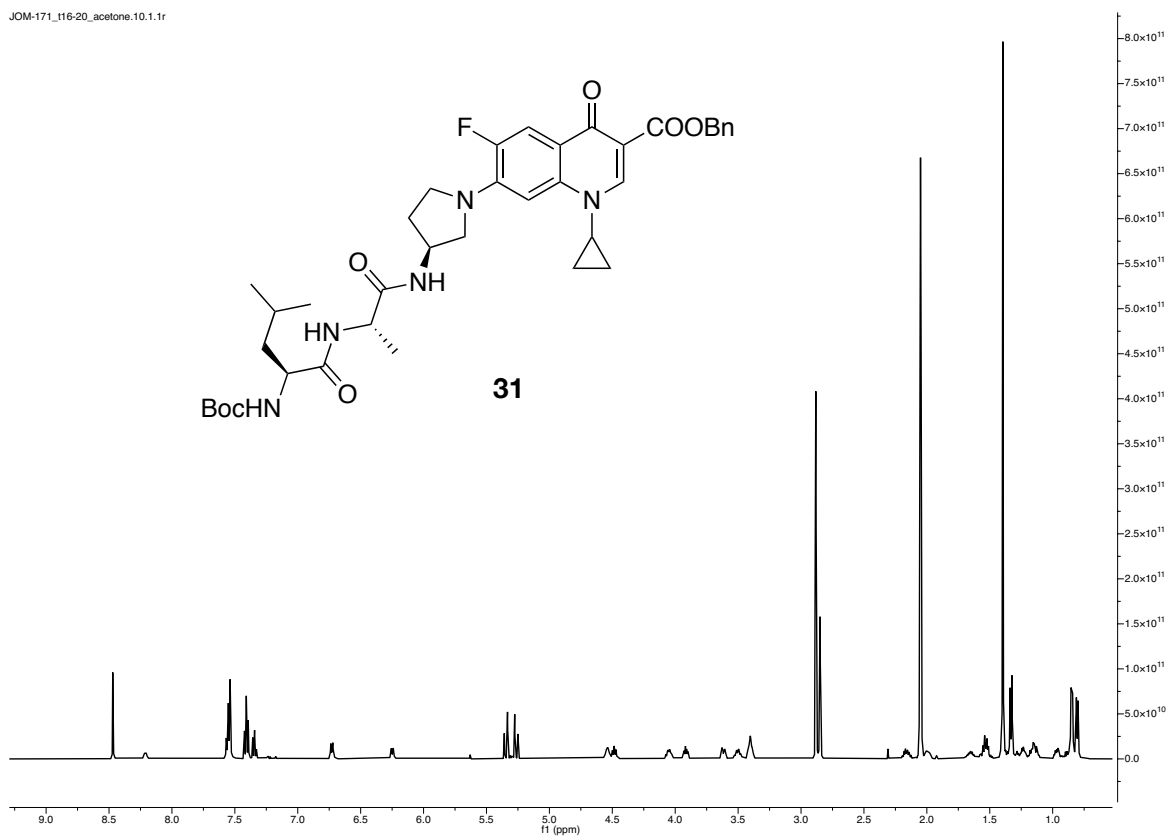


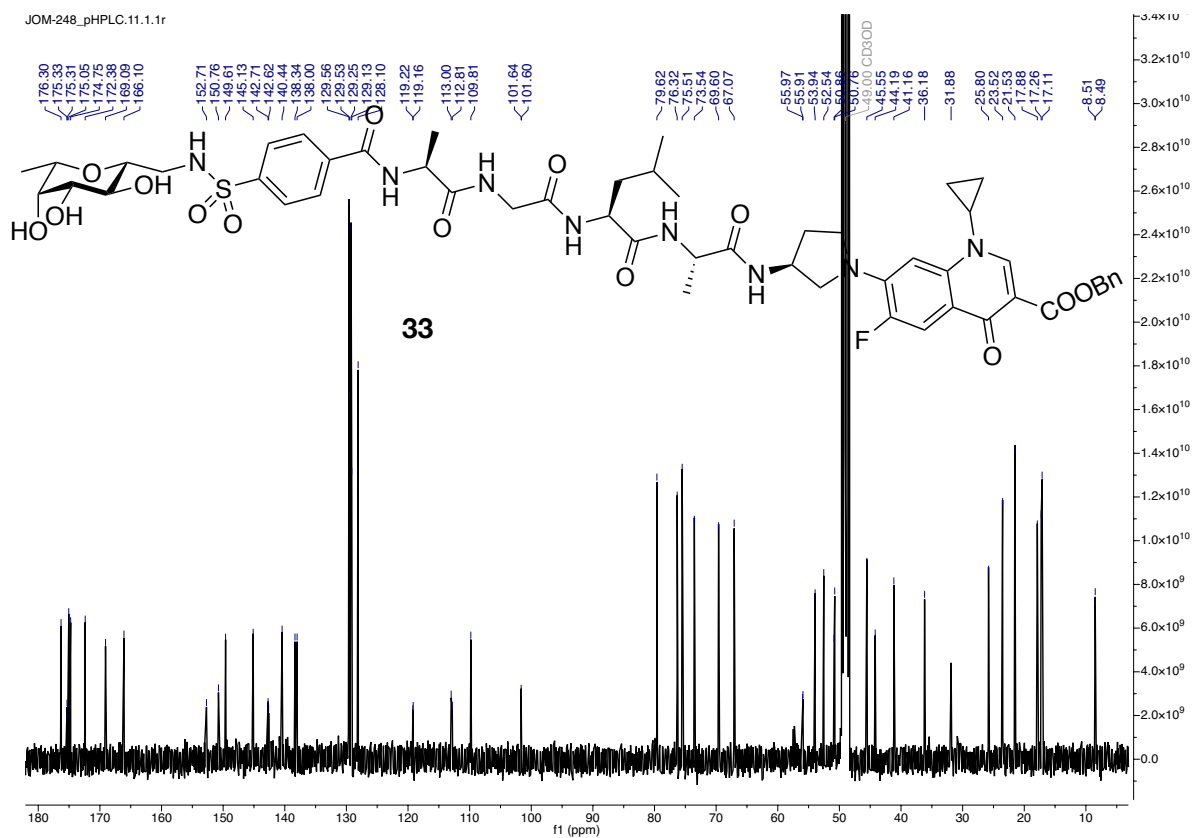
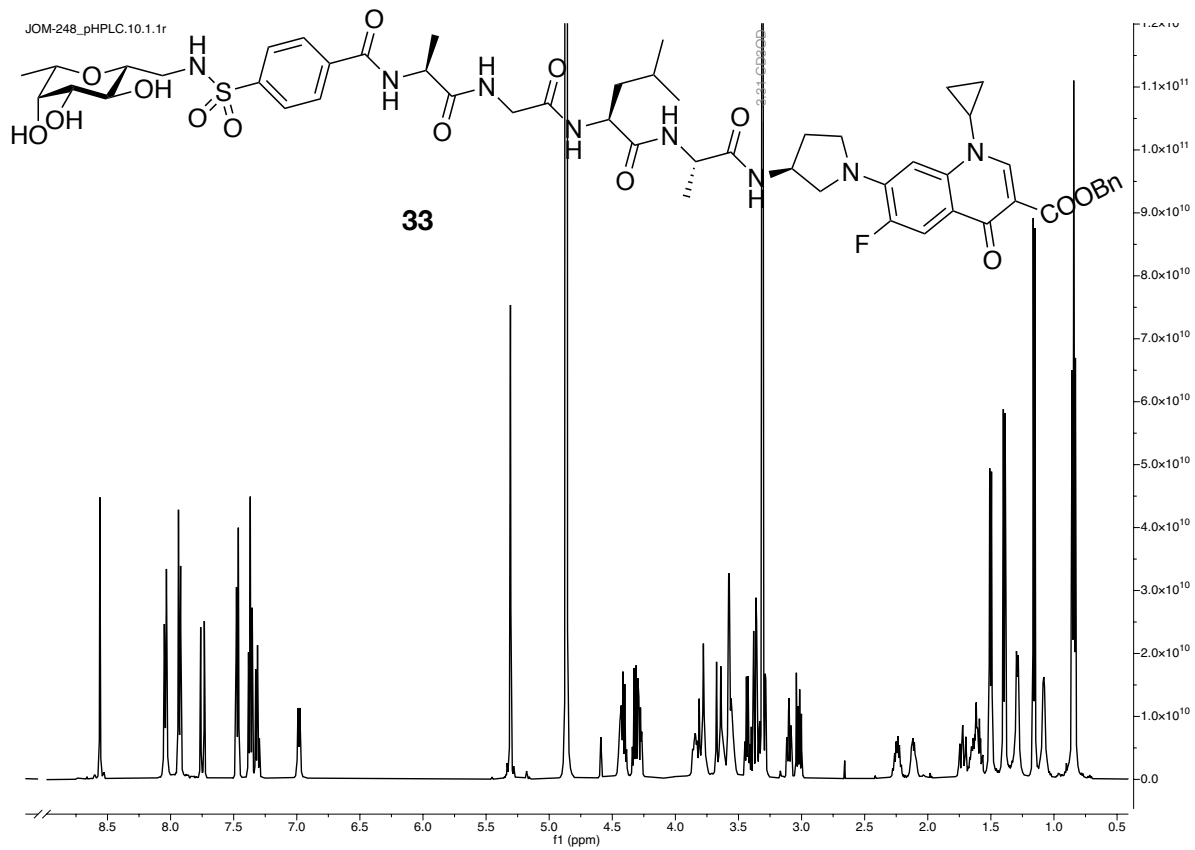
JOM-170_crude.10.1.1r



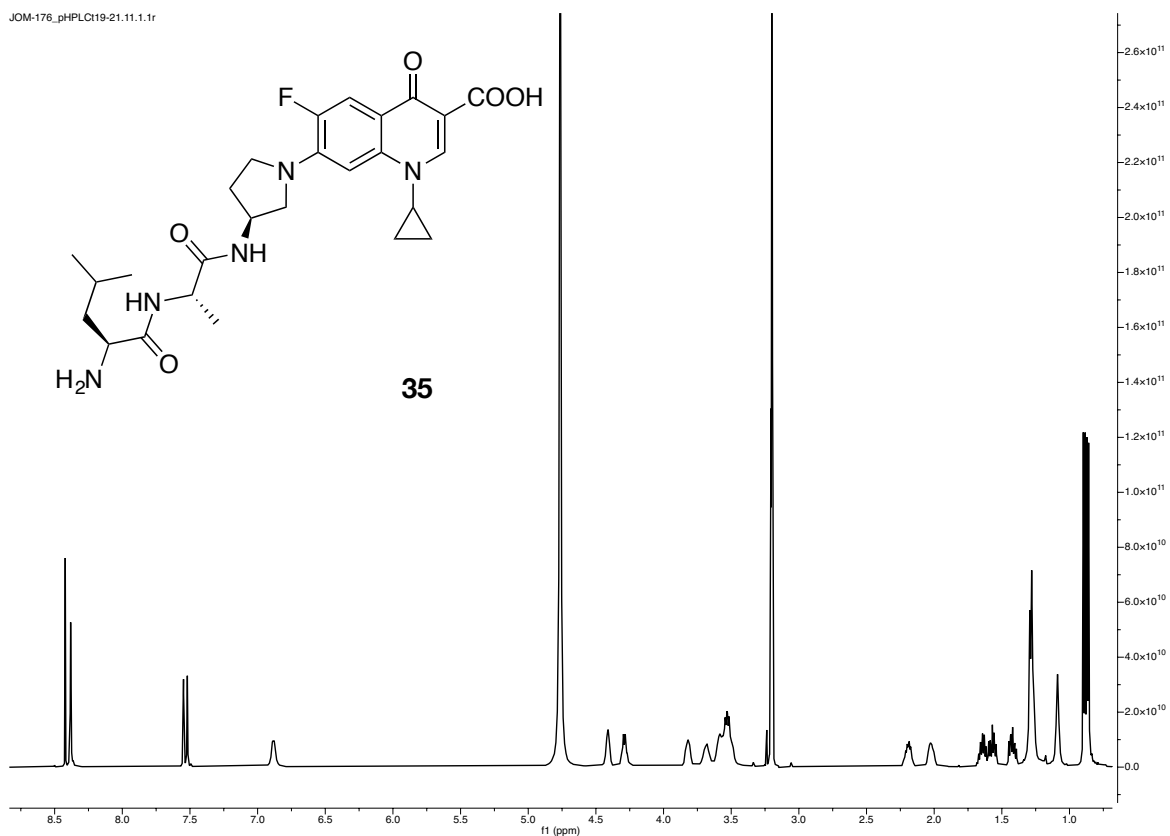
JOM-170_crude.13.1.1r



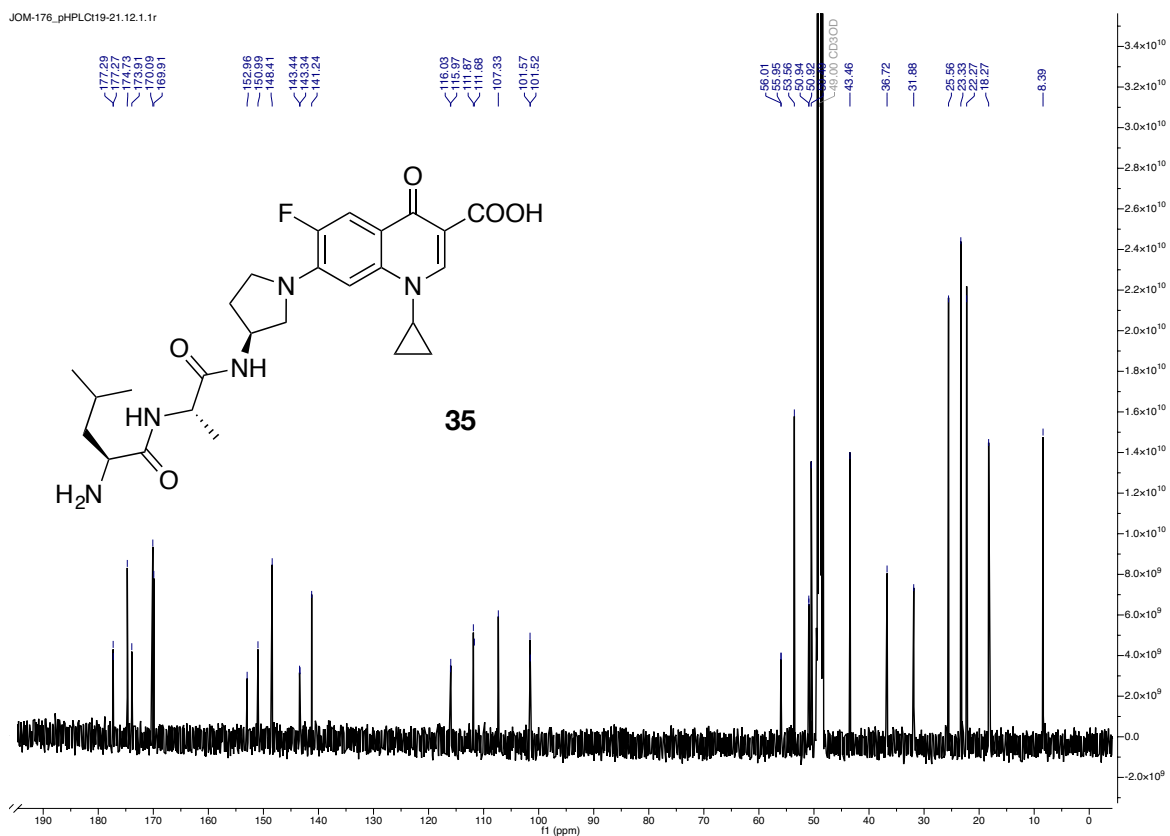




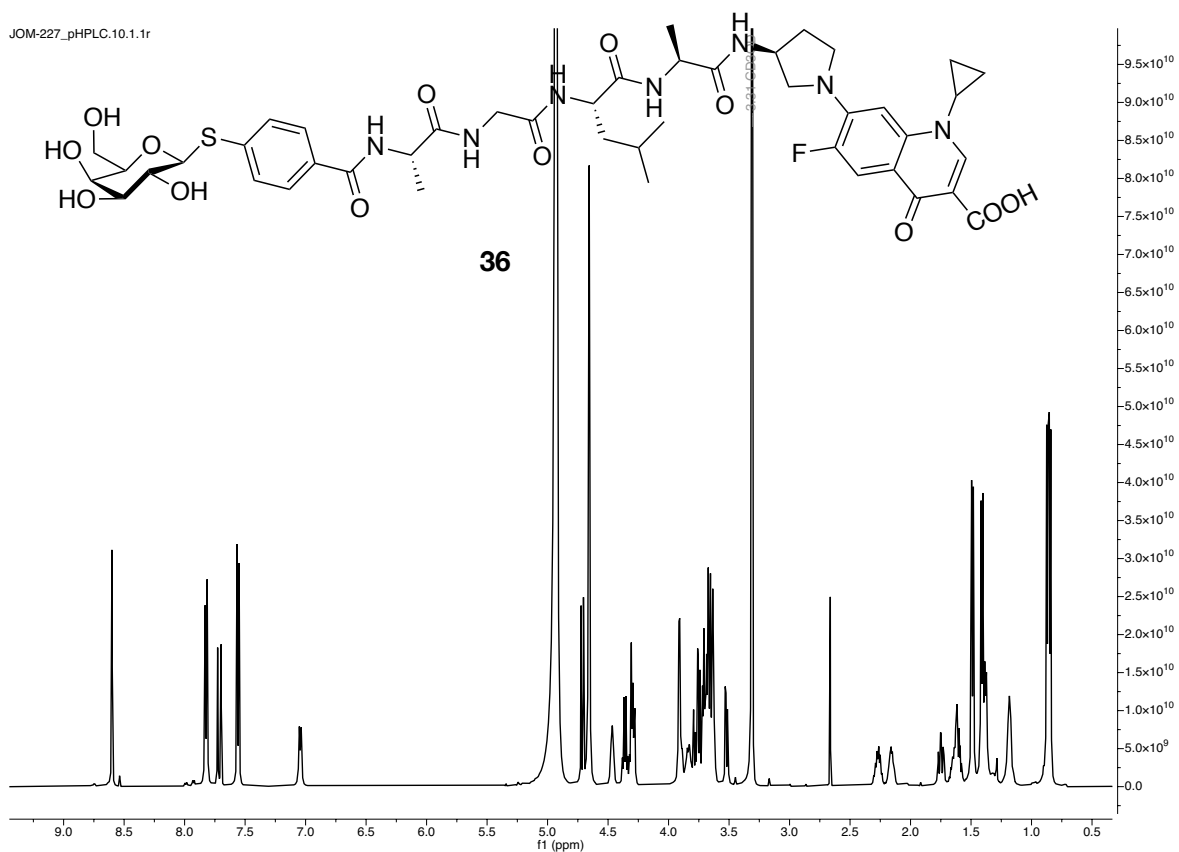
JOM-176_pHPLC19-21.11.1.1f



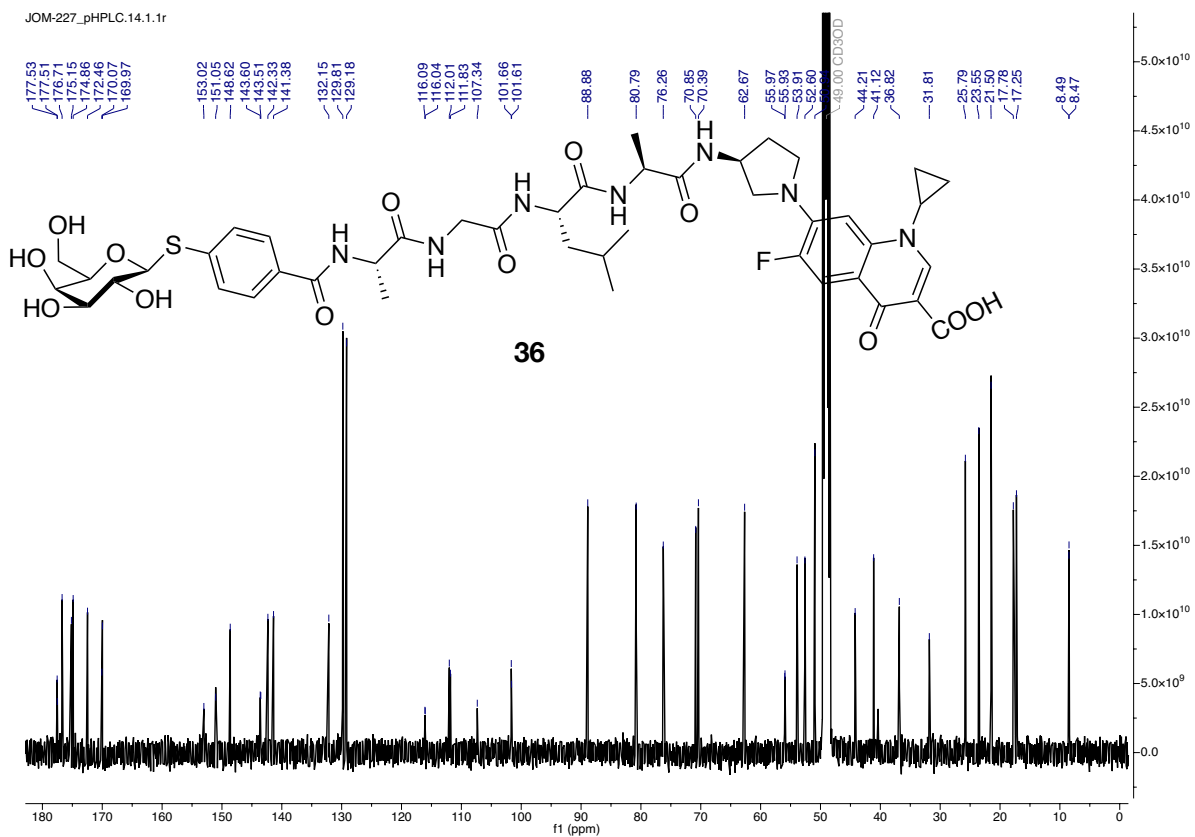
JOM-176_pHPLC19-21.12.1.1f

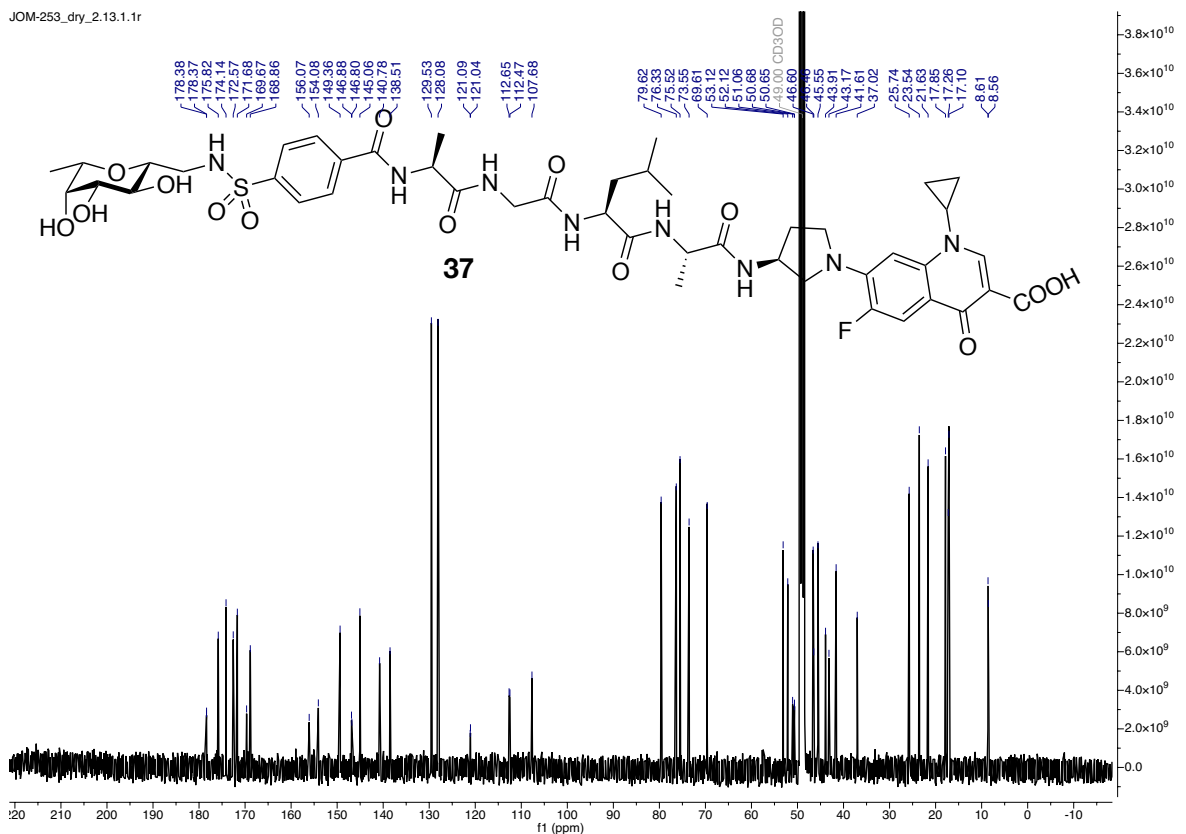
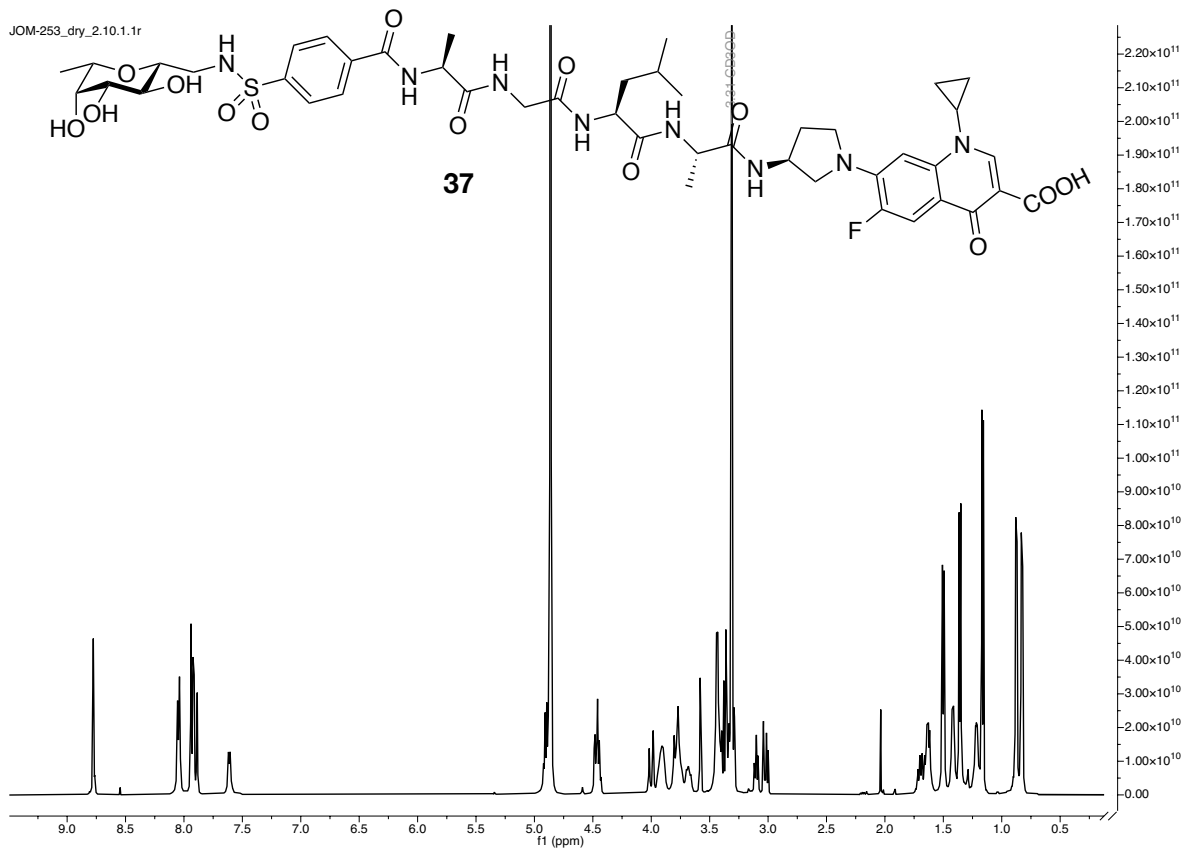


JOM-227_pHPLC.10.1.1r

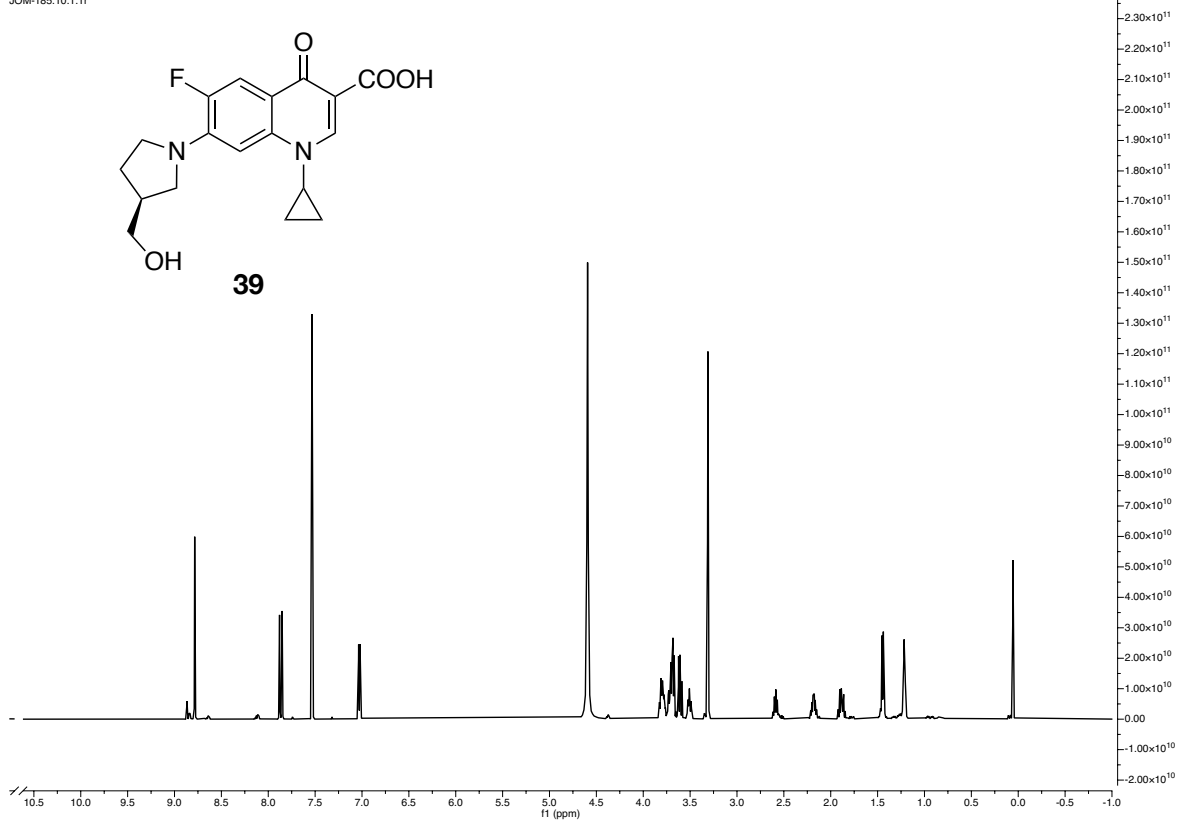


JOM-227_pHPLC.14.1.1r

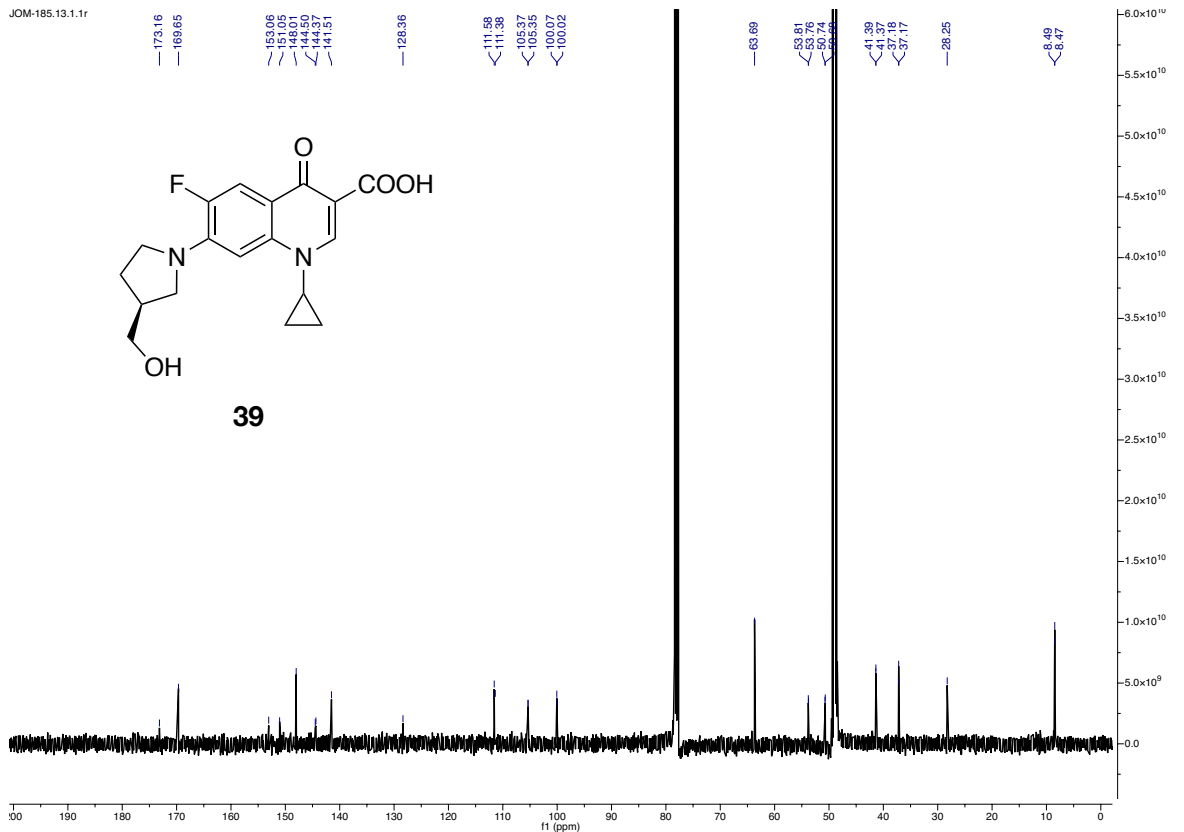




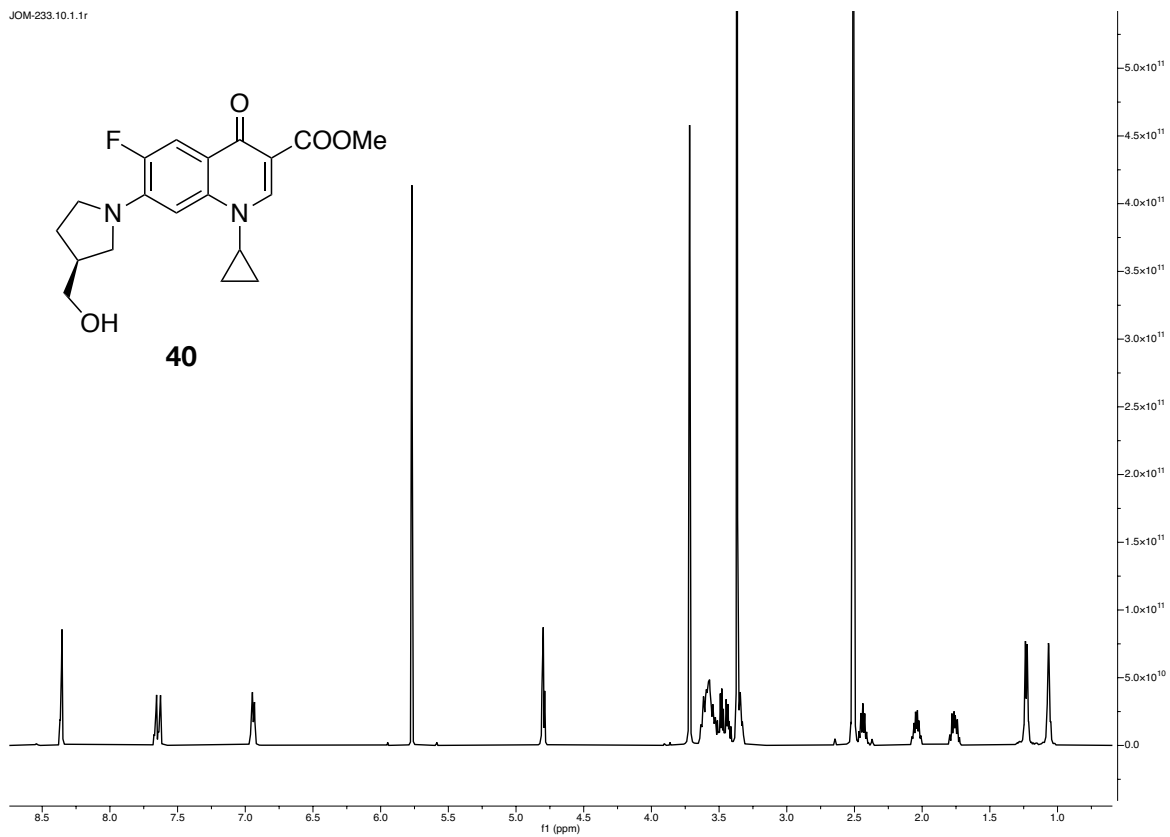
JOM-185.10.1.1r



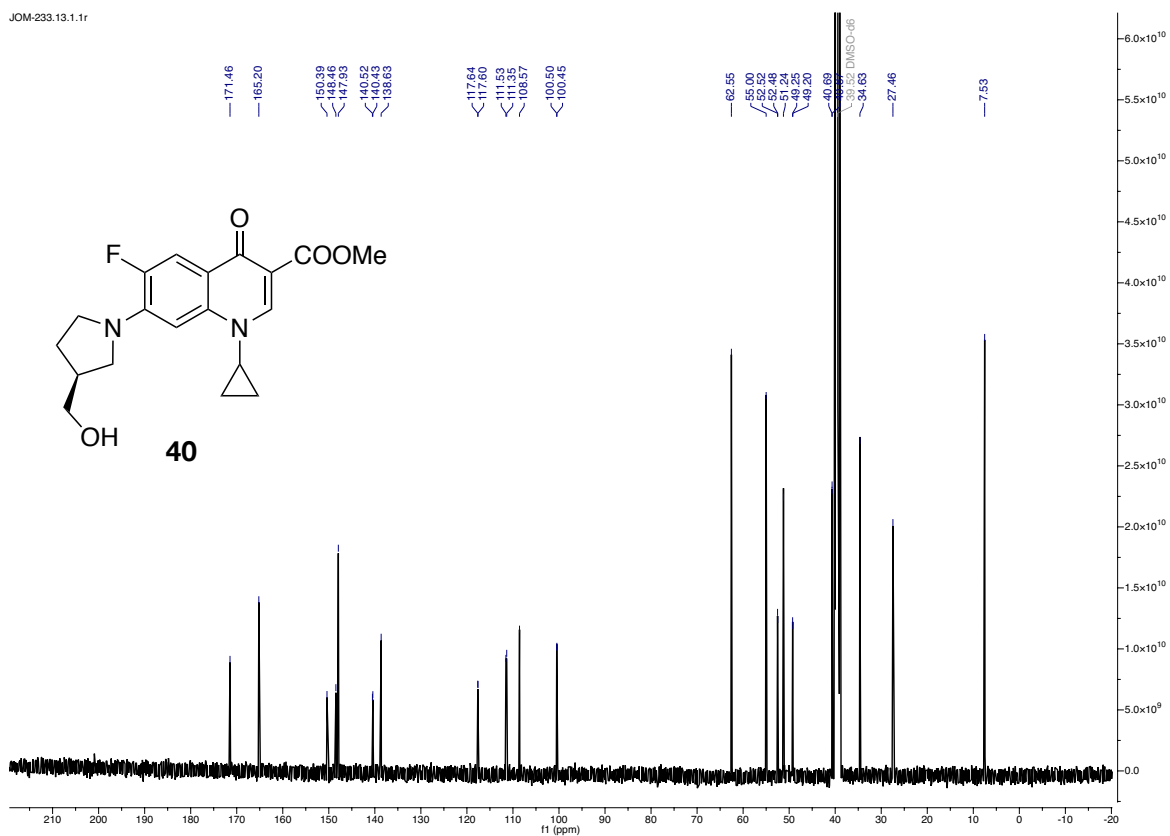
JOM-185.13.1.1r

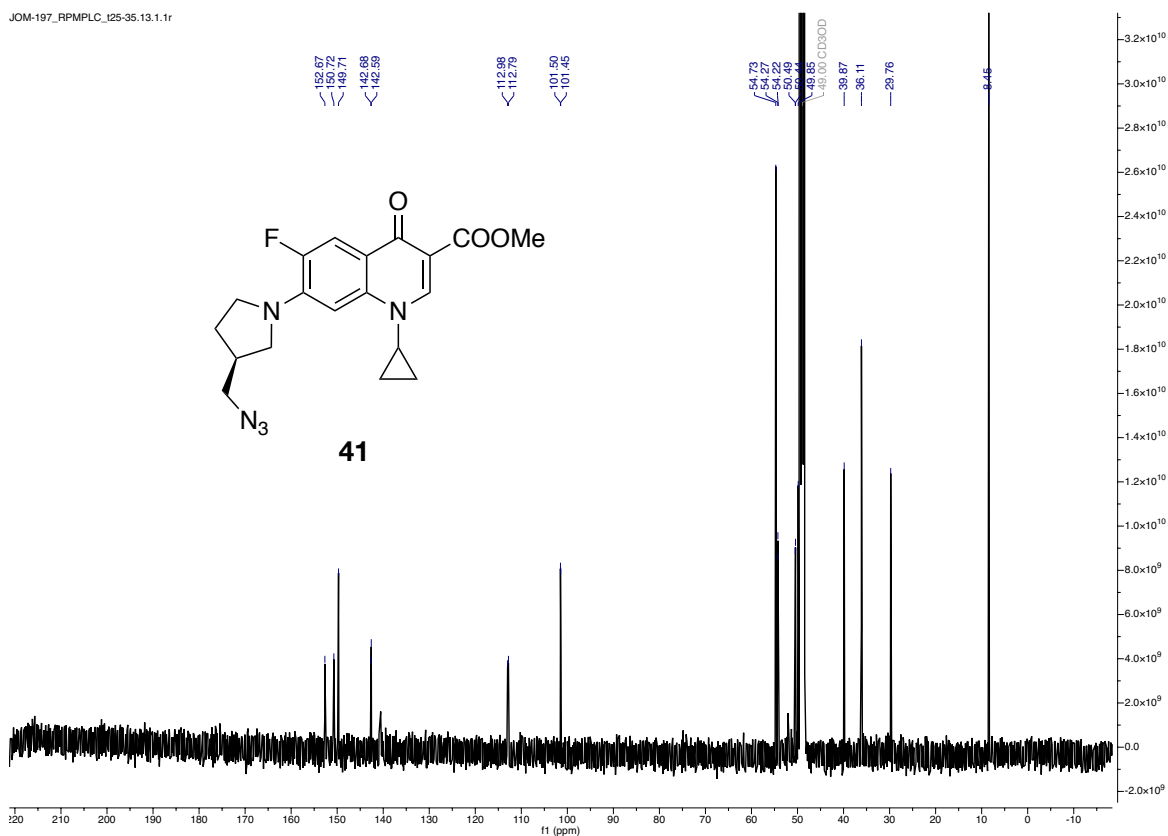
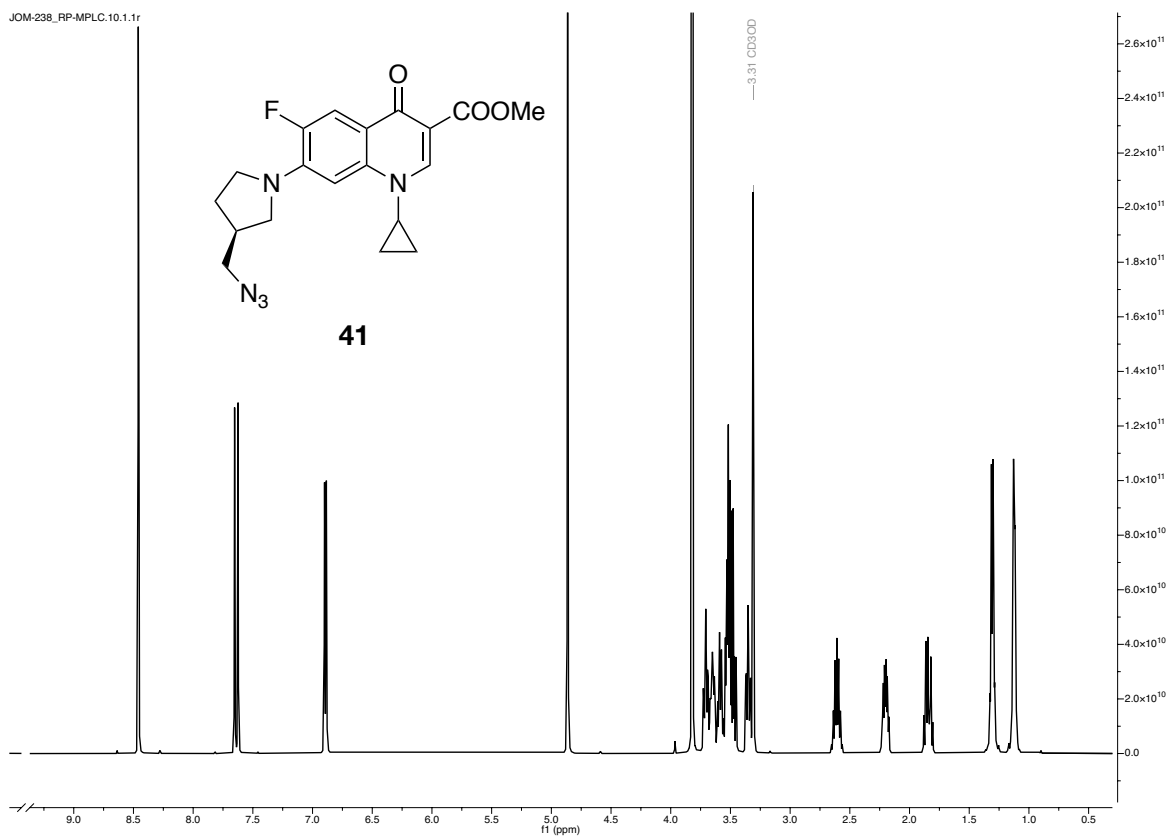


JOM-233.10.1.1f

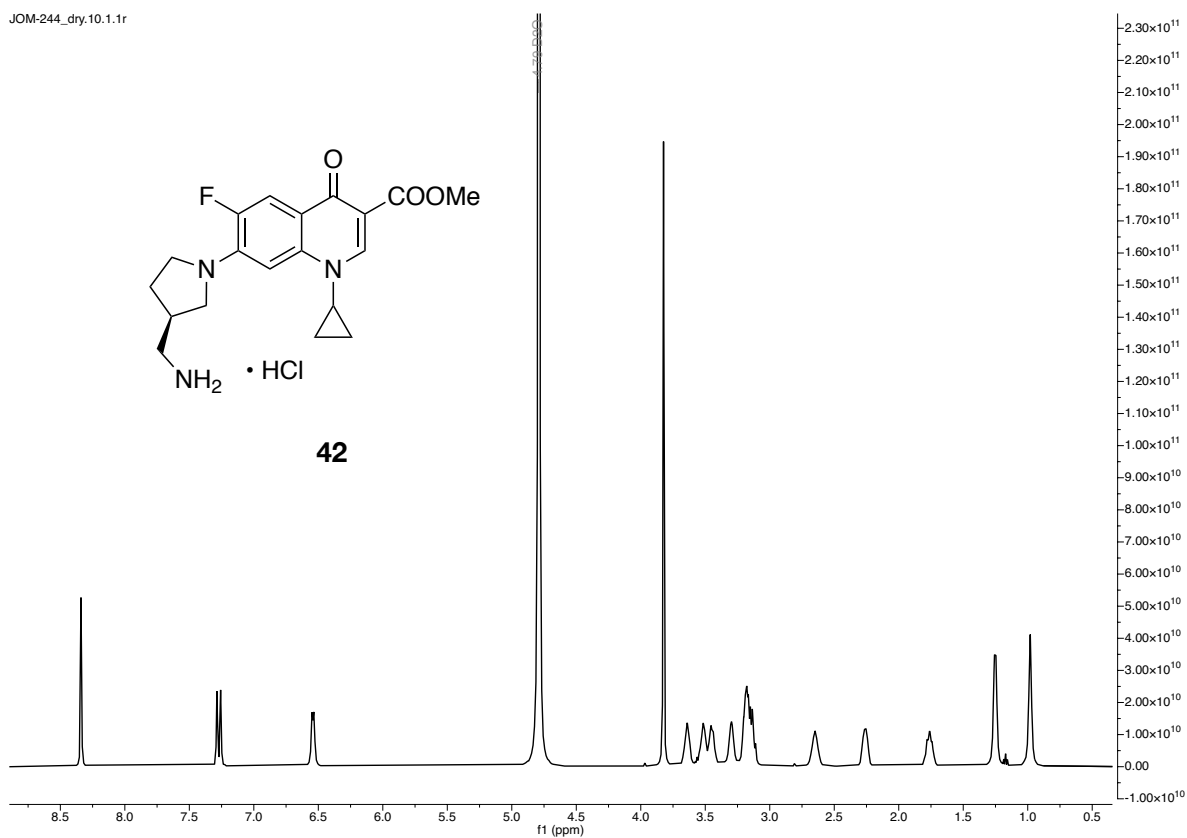


JOM-233.13.1.1f

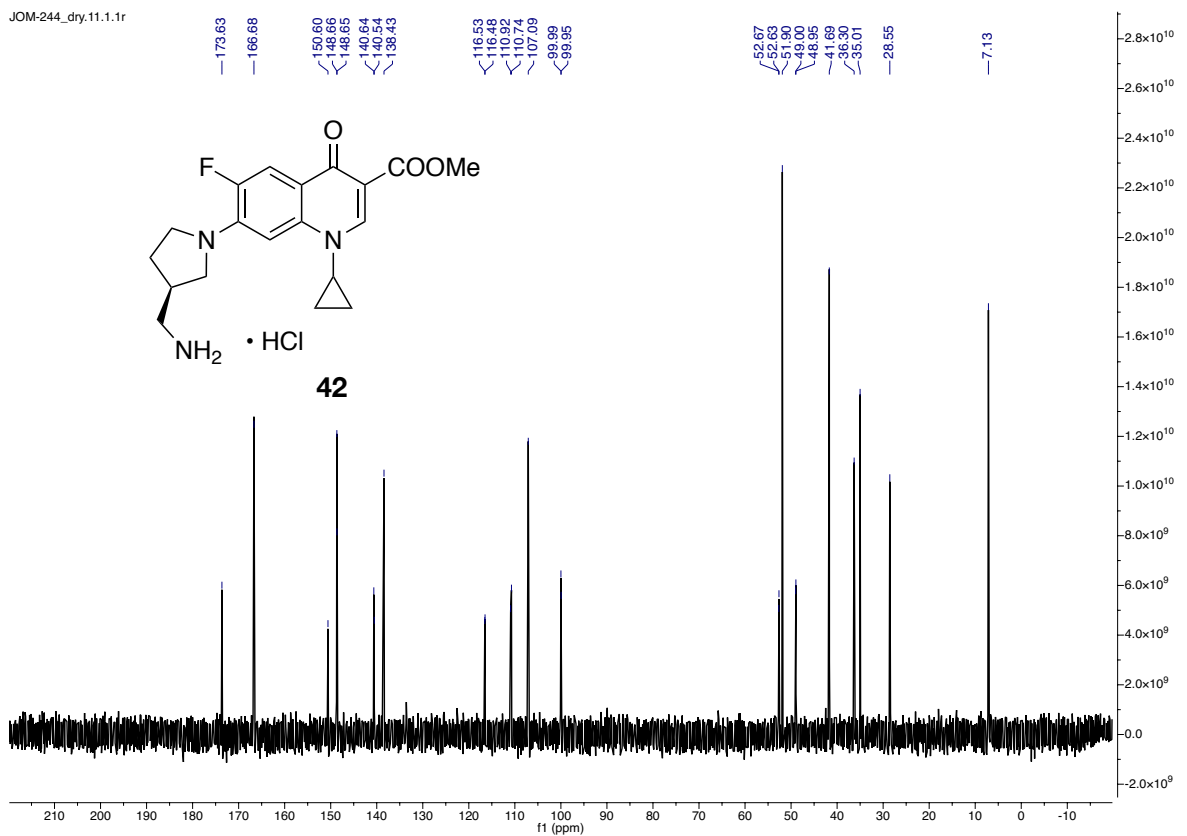


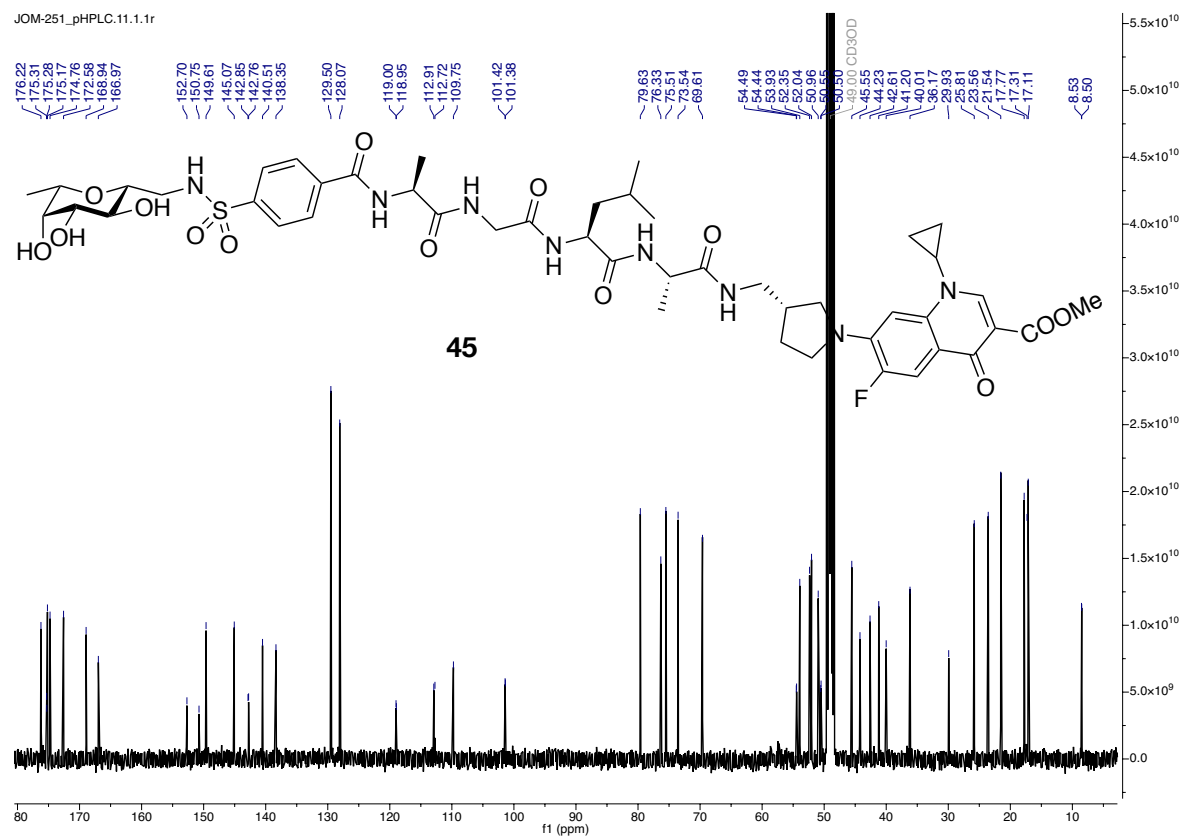
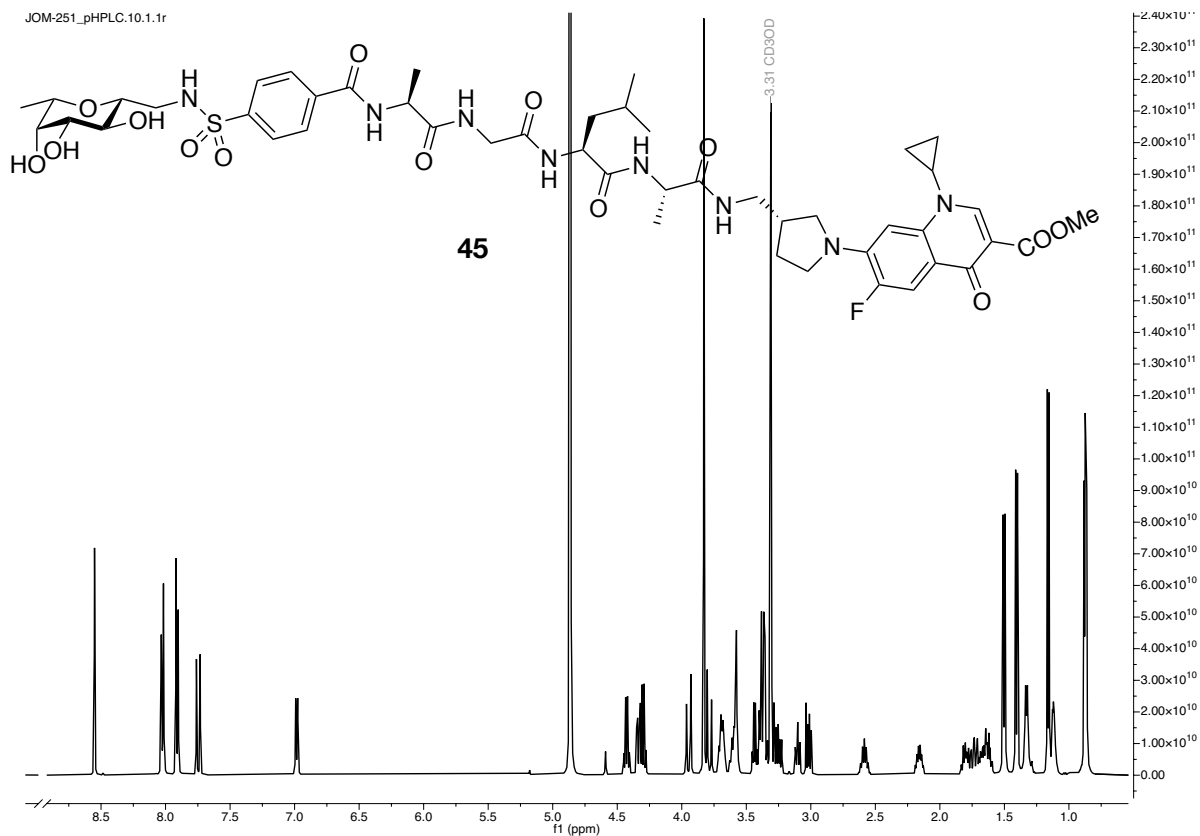


JOM-244_dry.10.1.1r

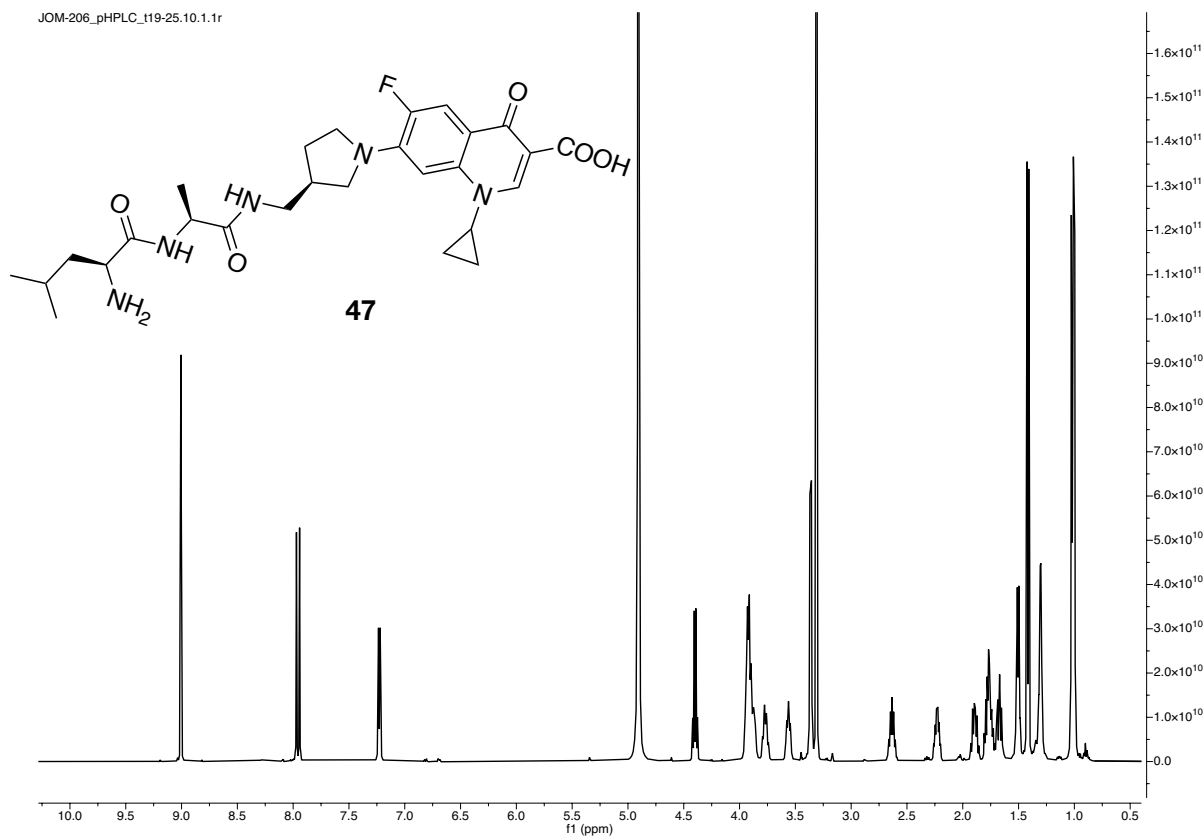


JOM-244_dry.11.1.1r

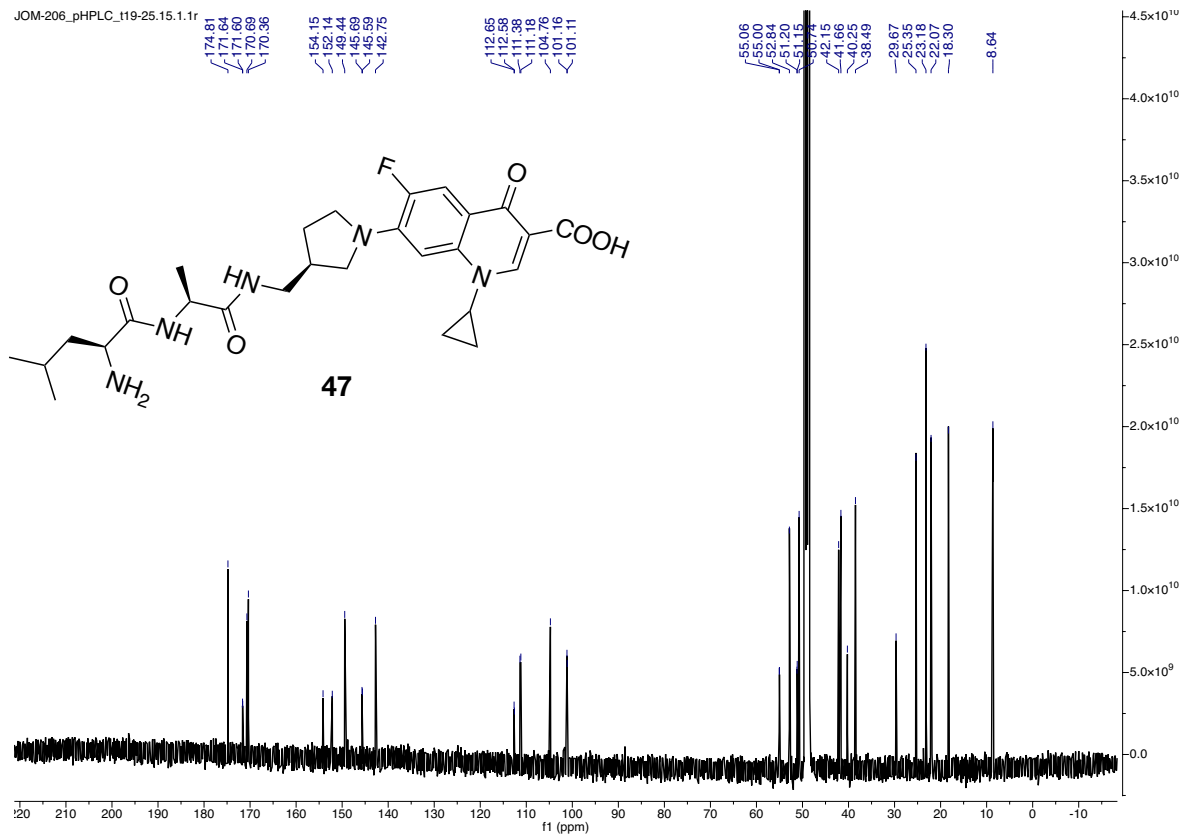


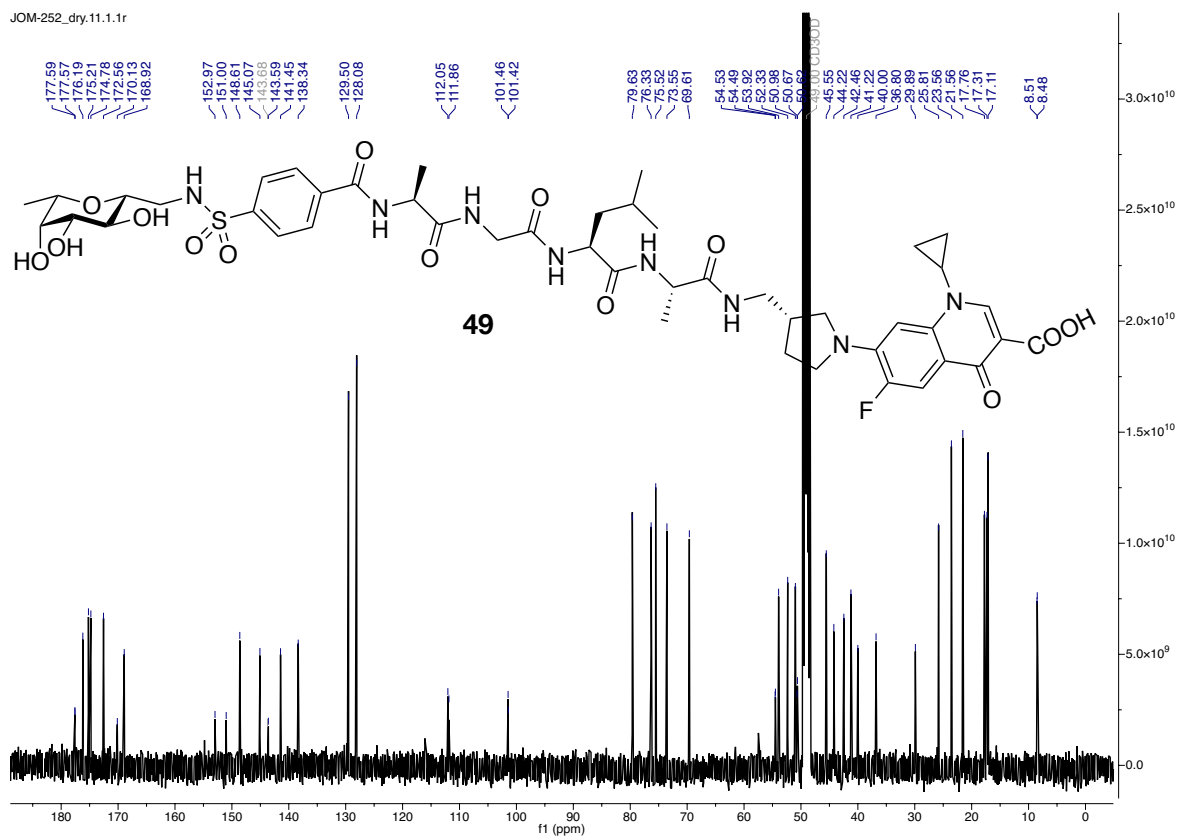
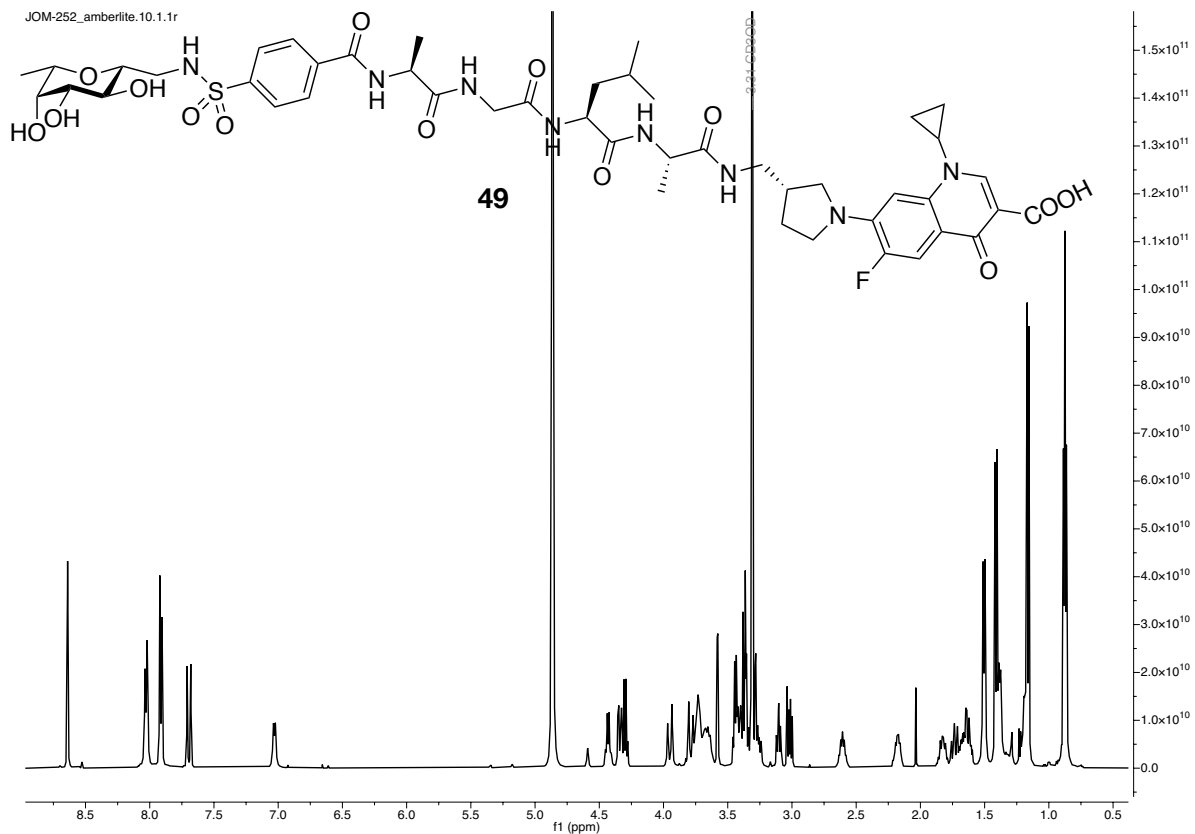


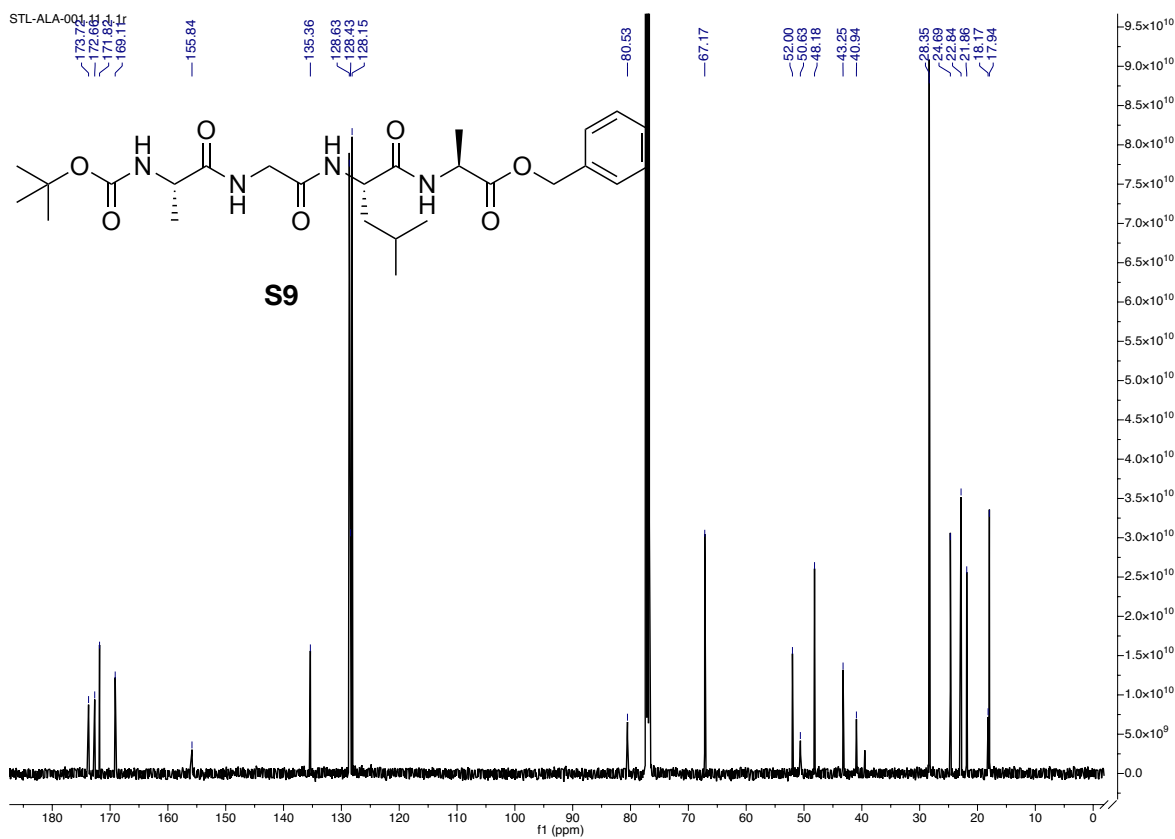
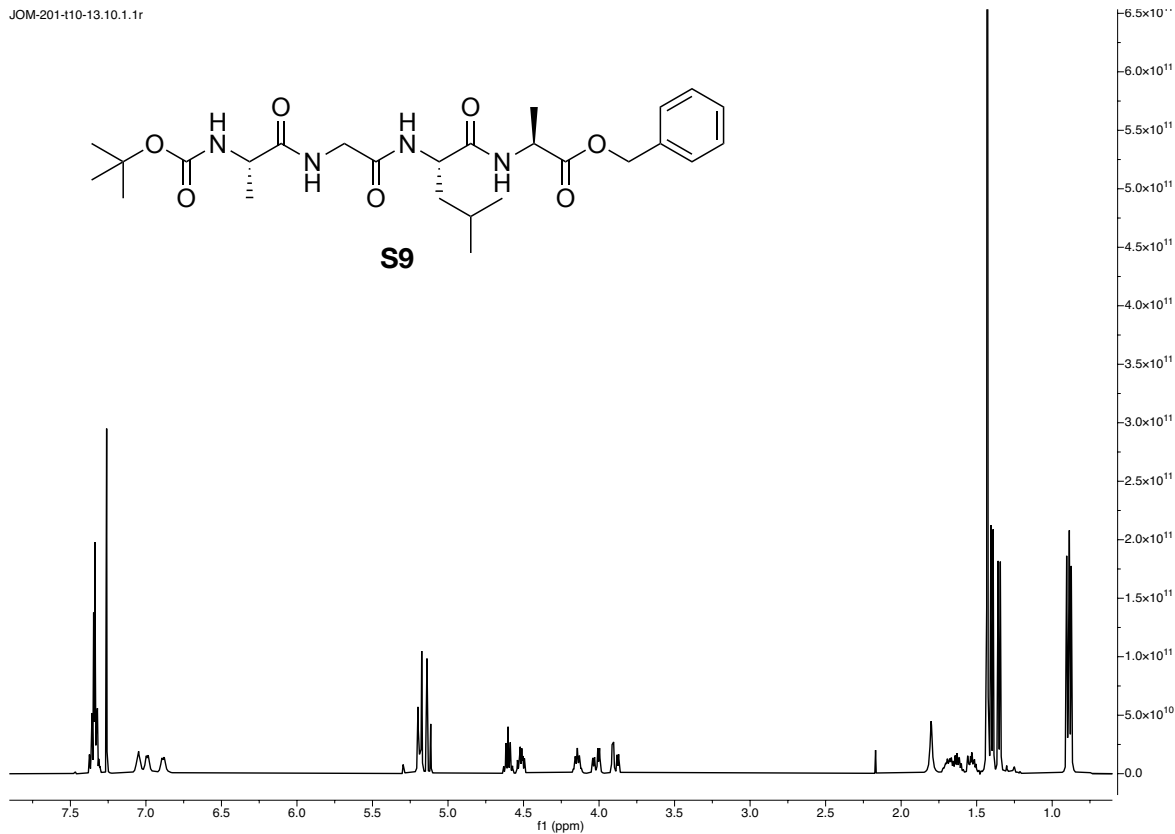
JOM-206_pHPLC_t19-25.10.1.1r



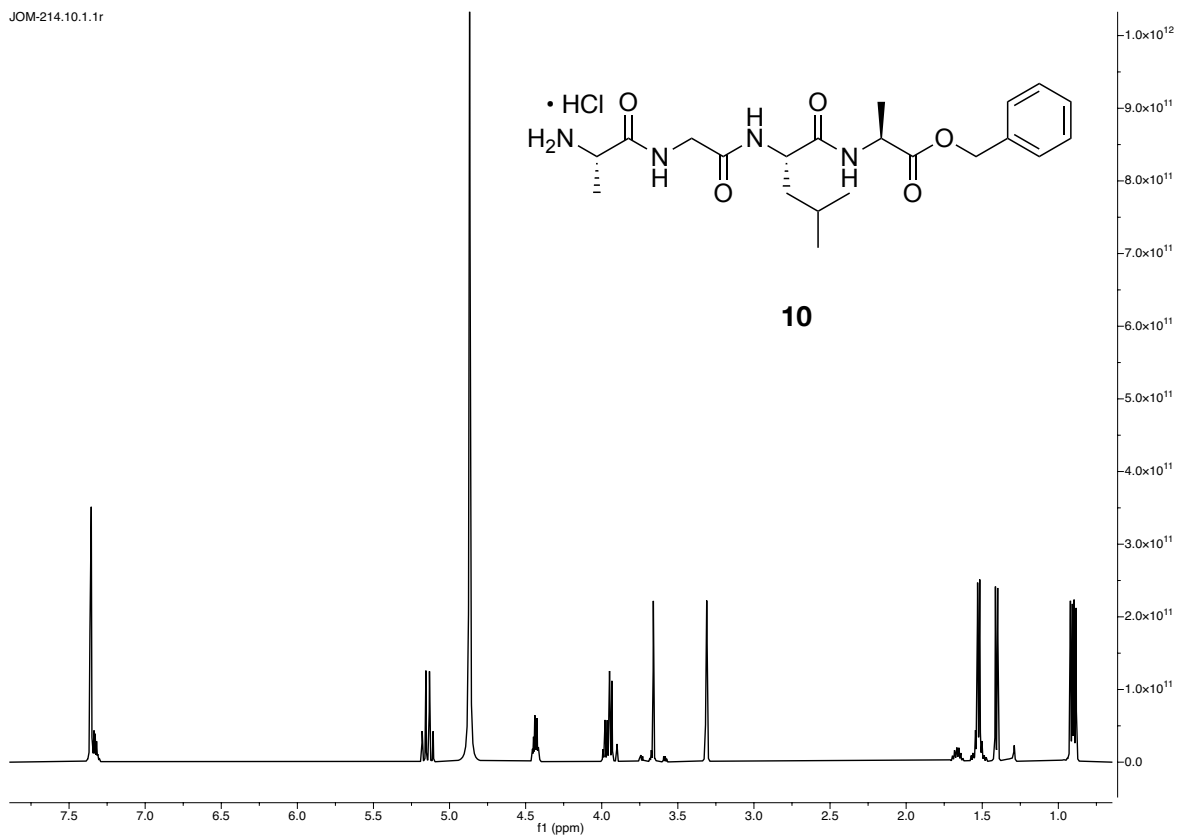
JOM-206_pHPLC_t19-25.15.1.1r



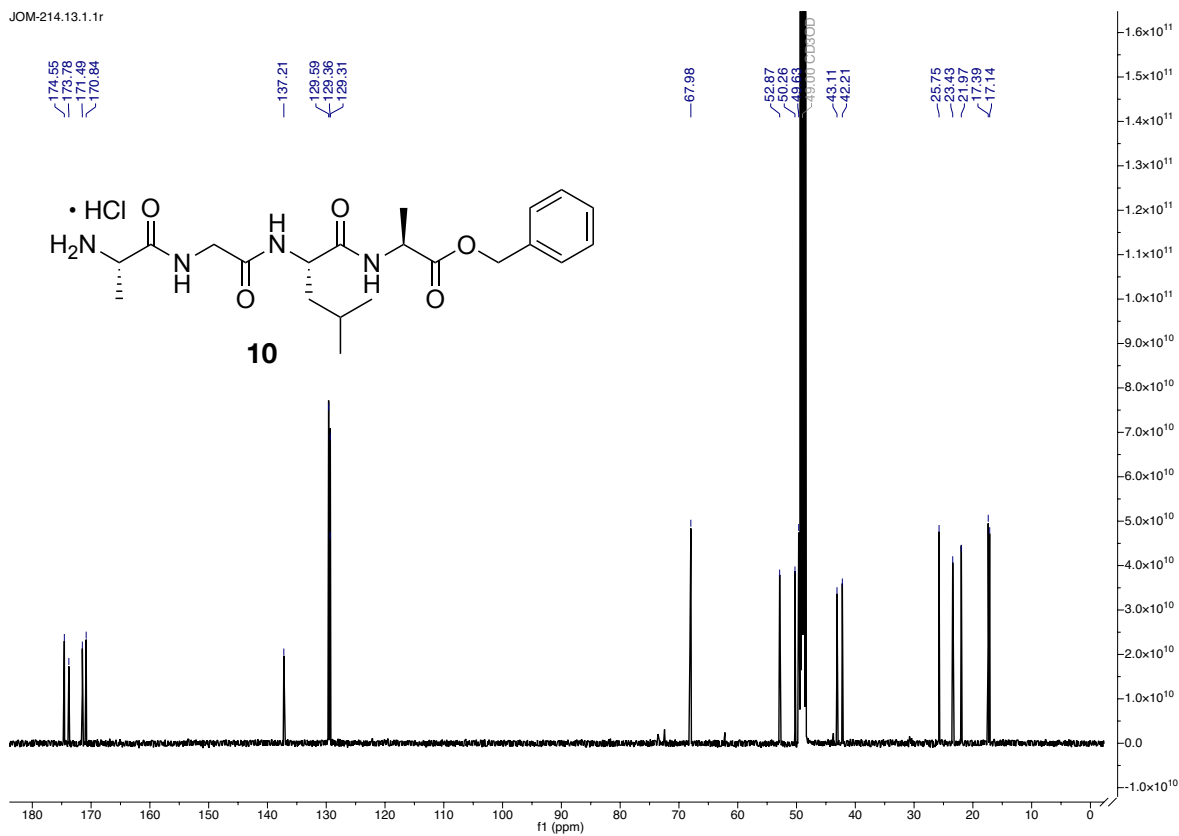




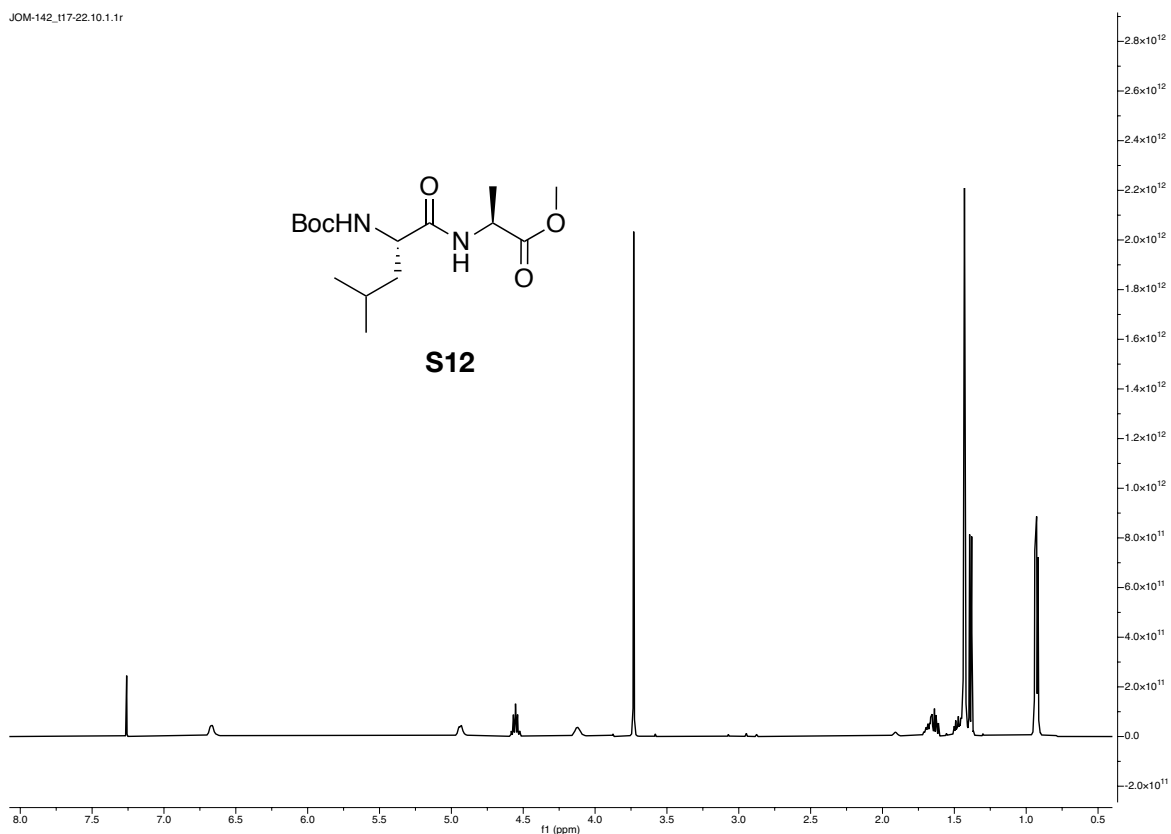
JOM-214.10.1.1r



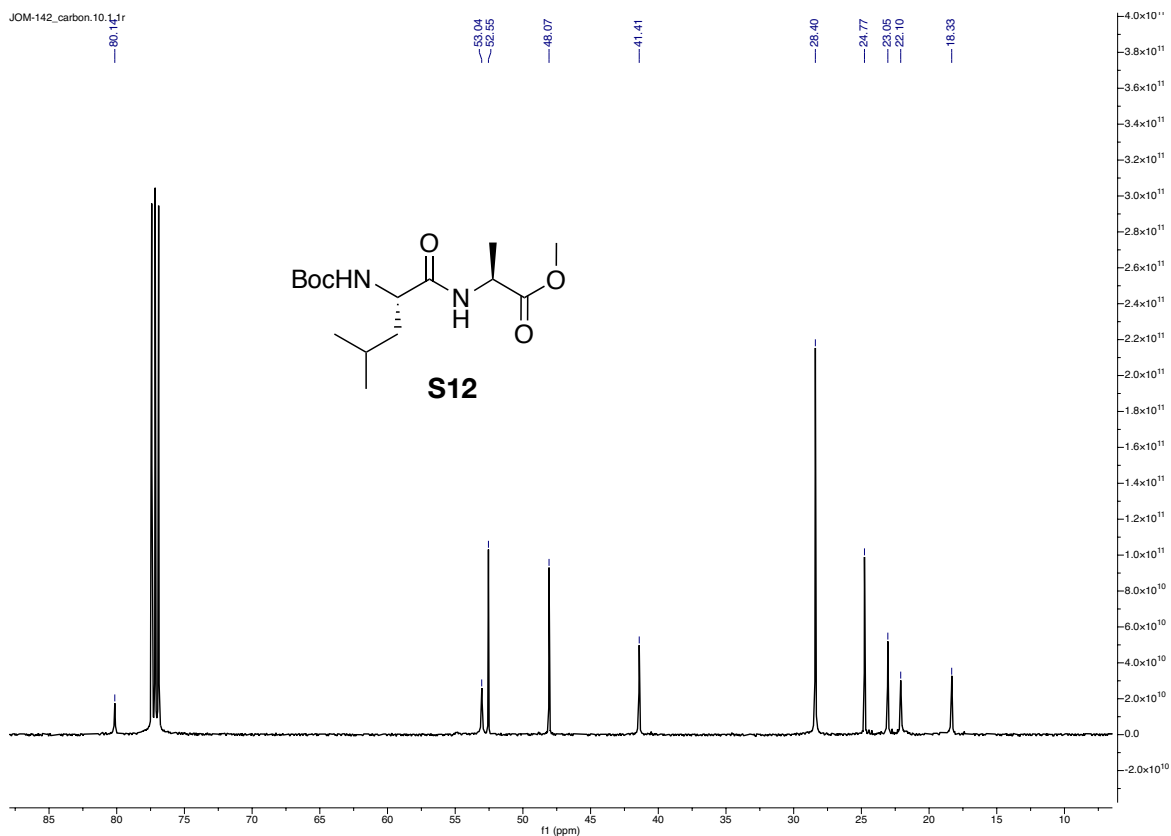
JOM-214.13.1.1r



JOM-142_117-22.10.1.1r



JOM-142_carbon.10.1.1r



STABILITY OF DIPEPTIDE-CONJUGATE **19** AND **35** IN PA14-FILTRATE (FIGURE S1)

The stability of the dipeptide conjugates that would result after LasB-mediated cleavage of the prodrugs **24/25** and **36/37** was measured in PA14-filtrate, without the addition of human blood plasma. In the presence PA14-filtrate and human blood plasma, the dipeptide conjugates are almost quantitatively metabolised within 2 h (figure 3 and figure S2). In PA14-filtrate alone however, only small fractions are metabolised after 2 h, compound **19** (ciprofloxacin based) reacting slower than compound **35** (aminopyrrolidine-based). Even after 24 h, no ciprofloxacin is released from compound **19** and only small amounts are released from compound **35** in PA14-filtrate.

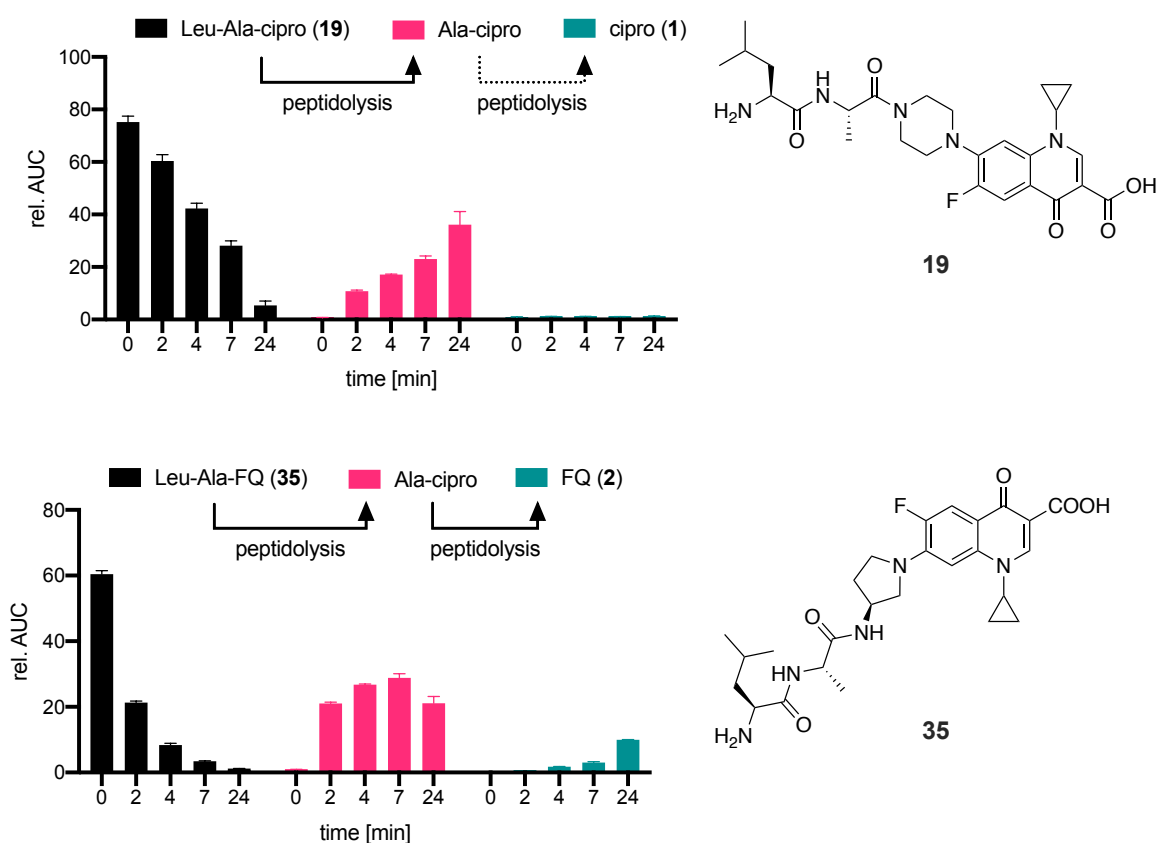


Figure S1. Stability of the dipeptide-conjugates **19** and **35** in PA14-filtrate without the addition of human blood plasma. The release of the free corresponding drugs by proteolysis was very slow compared to the presence of PA14-filtrate and human blood plasma. The experiment was performed in technical triplicates. The results are given as mean and standard deviation.

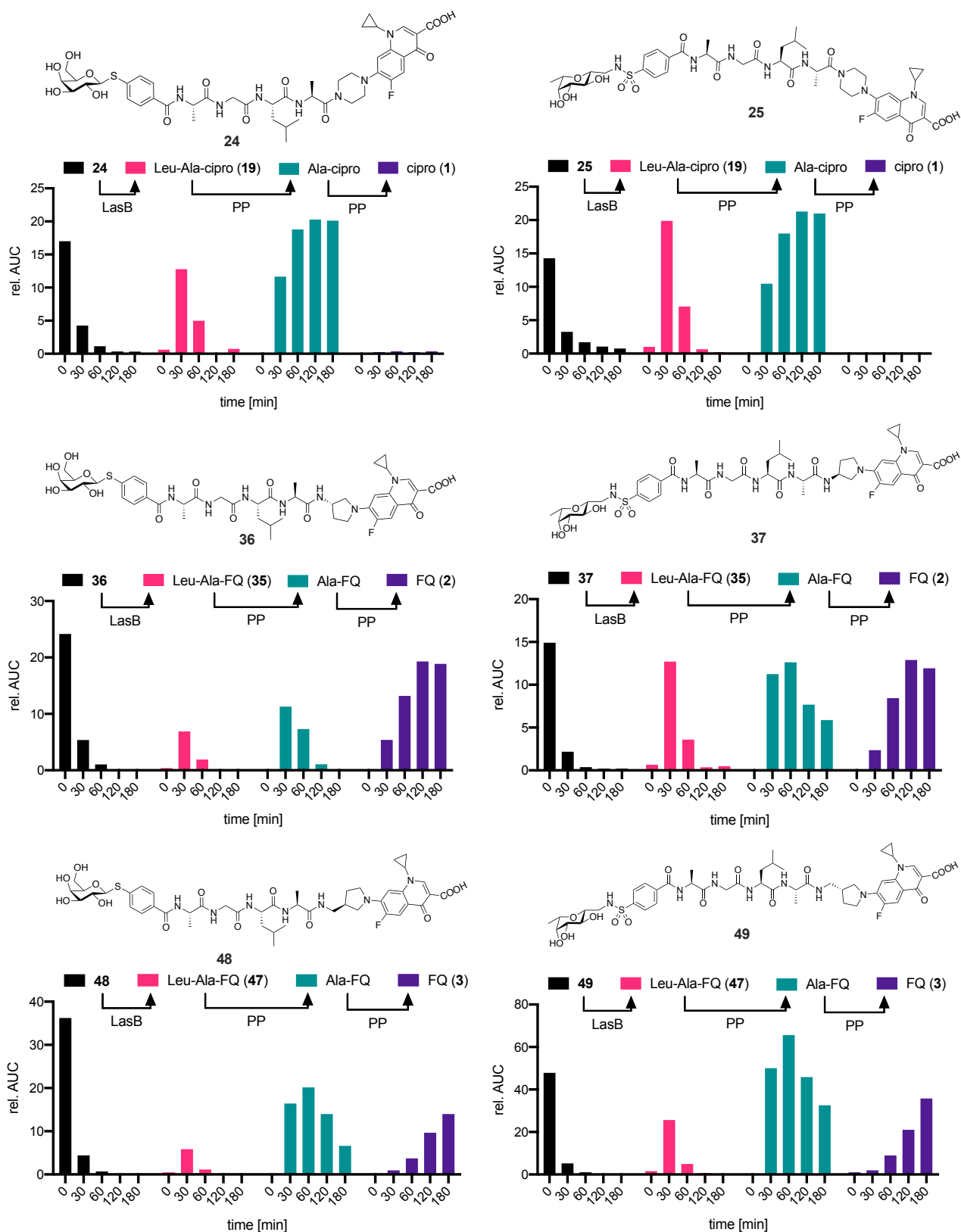


Figure S2. Biological replicates of the experiments shown in **Figure 3**. Activation of the lectin-targeted prodrugs in human blood plasma and PA14-filtrate. PP = plasma proteins.

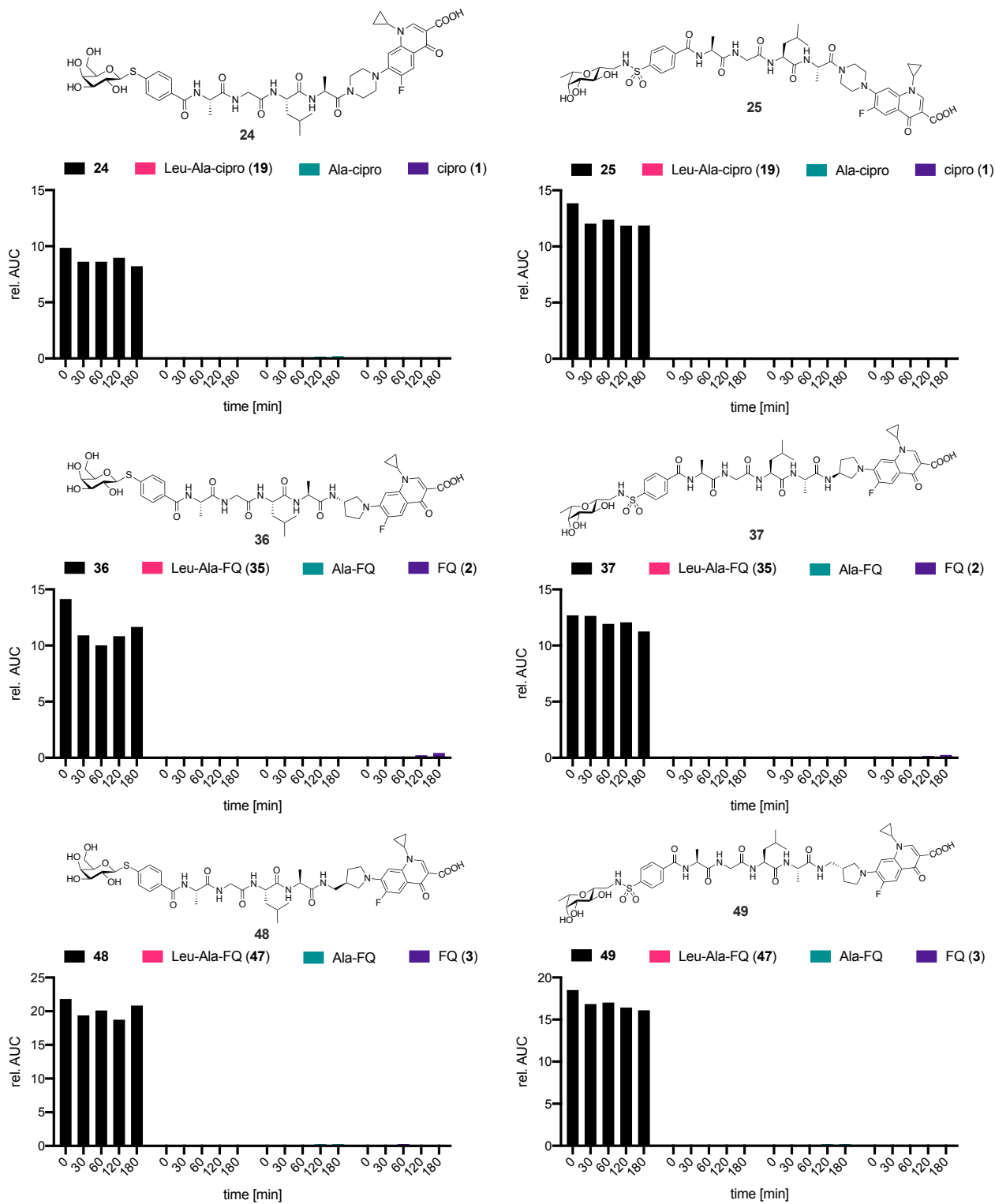


Figure S3. Biological replicates of the experiments shown in **Figure 4**. Stability of the lectin-targeted prodrugs in 50% human blood plasma spiked with 10% LB.

Table S2. Key compounds and intermediates as smiles.

| compound | SMILES |
|----------|---|
| 2 | <chem>O=C(O)C1=CN(C2=CC(N3CC[C@@H](N)C3)=C(F)C=C2C1=O)C4CC4.Cl</chem> |
| 3 | <chem>O=C1C(C(O)=O)=CN(C2CC2)C3=CC(N4C[C@@H](CN)CC4)=C(F)C=C31</chem> |
| 7 | <chem>O[C@@H]1[C@H](O)[C@@H](O)[C@H](SC2=CC=C(C(O)=O)C=C2)O[C@@H]1CO</chem> |
| 8 | <chem>N[C@@H](C)C(NCC(N[C@@H](CC(C)C)C(N[C@@H](C)C(OCC1=CC=CC=C1)=O)=O)=O)O.Cl</chem> |
| 10 | <chem>O[C@@H]1[C@H](O)[C@@H](O)[C@H](SC2=CC=C(C(N[C@@H](C)C(NCC(N[C@@H](CC(C)C)C(N[C@@H](C)C(O)=O)=O)=O)=O)C=C2)O[C@@H]1CO</chem> |
| 14 | <chem>C[C@H]1[C@@H](O)[C@@H](O)[C@H](O)[C@@H](CNS(C2=CC=C(C(O)=O)C=C2)(=O)=O)O1</chem> |
| 16 | <chem>C[C@H]1[C@@H](O)[C@@H](O)[C@H](O)[C@@H](CNS(C2=CC=C(C(N[C@@H](C)C(NCC(N[C@@H](CC(C)C)C(N[C@@H](C)C(O)=O)=O)=O)=O)C=C2)(=O)=O)O1</chem> |
| 17 | <chem>CC(C[C@H](NC(OC(C)C)C)C)C(N[C@H](C(O)=O)C)C=O</chem> |
| 19 | <chem>O=C(O)C1=CN(C2=CC(N3CCN(C([C@H](C)NC([C@H](CC(C)C)N)=O)=O)CC3)=C(F)C=C2C1=O)C4CC4.[HCl ·]</chem> |
| 21 | <chem>O=C(OCC1=CC=CC=C1)C2=CN(C3=CC(N4CCNCC4)=C(F)C=C3C2=O)C5CC5.[HCl ·]</chem> |
| 24 | <chem>O[C@@H]1[C@H](O)[C@@H](O)[C@H](SC2=CC=C(C(N[C@@H](C)C(NCC(N[C@@H](CC(C)C)C(N[C@@H](C)C(N(CC3)CCN3C4=C(F)C=C5C(N(C6CC6)C=C(C5=O)C(O)=O)=C4)=O)=O)=O)C=C2)O[C@@H]1CO</chem> |
| 25 | <chem>C[C@H]1[C@@H](O)[C@@H](O)[C@H](O)[C@@H](CNS(C2=CC=C(C(N[C@@H](C)C(NCC(N[C@@H](CC(C)C)C(N[C@@H](C)C(N(CC3)CCN3C4=C(F)C=C5C(N(C6CC6)C=C(C5=O)C(O)=O)=C4)=O)=O)=O)C=C2)(=O)=O)O1</chem> |
| 30 | <chem>O=C(OCC1=CC=CC=C1)C2=CN(C3=CC(N4CC[C@H](N)C4)=C(F)C=C3C2=O)C5CC5.Cl</chem> |
| 35 | <chem>O=C1C(C(O)=O)=CN(C2CC2)C3=CC(N4C[C@@H](NC([C@H](C)NC([C@H](CC(C)C)N)=O)=O)CC4)=C(F)C=C31</chem> |
| 36 | <chem>O[C@@H]1[C@H](O)[C@@H](O)[C@H](SC2=CC=C(C(N[C@@H](C)C(NCC(N[C@@H](CC(C)C)C(N[C@@H](C)C(N[C@H](C3)CCN3C4=C(F)C=C5C(N(C6CC6)C=C(C5=O)C(O)=O)=C4)=O)=O)=O)C=C2)O[C@@H]1CO</chem> |
| 37 | <chem>C[C@H]1[C@@H](O)[C@@H](O)[C@H](O)[C@@H](CNS(C2=CC=C(C(N[C@@H](C)C(NCC(N[C@@H](CC(C)C)C(N[C@@H](C)C(N[C@H](C3)CCN3C4=C(F)C=C5C(N(C6CC6)C=C(C5=O)C(O)=O)=C4)=O)=O)=O)C=C2)(=O)=O)O1</chem> |
| 40 | <chem>O=C1C(C(OC)=O)=CN(C2CC2)C3=CC(N4C[C@@H](CO)CC4)=C(F)C=C31</chem> |
| 41 | <chem>O=C1C(C(OC)=O)=CN(C2CC2)C3=CC(N4C[C@@H](CN=[N+]=[N-])CC4)=C(F)C=C31</chem> |
| 42 | <chem>O=C1C(C(OC)=O)=CN(C2CC2)C3=CC(N4C[C@@H](CN)CC4)=C(F)C=C31.Cl</chem> |
| 47 | <chem>O=C(N[C@@H](C)C(NC[C@H](C1)CCN1C2=C(F)C=C3C(N(C4CC4)C=C(C3=O)C(O)=O)=C2)=O)[C@@H](N)CC(C)C</chem> |
| 48 | <chem>O[C@@H]1[C@H](O)[C@@H](O)[C@H](SC2=CC=C(C(N[C@@H](C)C(NCC(N[C@@H](CC(C)C)C(N[C@@H](C)C(NC[C@H](C3)CCN3C4=C(F)C=C5C(N(C6CC6)C=C(C5=O)C(O)=O)=C4)=O)=O)=O)C=C2)O[C@@H]1CO</chem> |
| 49 | <chem>C[C@H]1[C@@H](O)[C@@H](O)[C@H](O)[C@@H](CNS(C2=CC=C(C(N[C@@H](C)C(NCC(N[C@@H](CC(C)C)C(N[C@@H](C)C(NC[C@H](C3)CCN3C4=C(F)C=C5C(N(C6CC6)C=C(C5=O)C(O)=O)=C4)=O)=O)=O)C=C2)(=O)=O)O1</chem> |

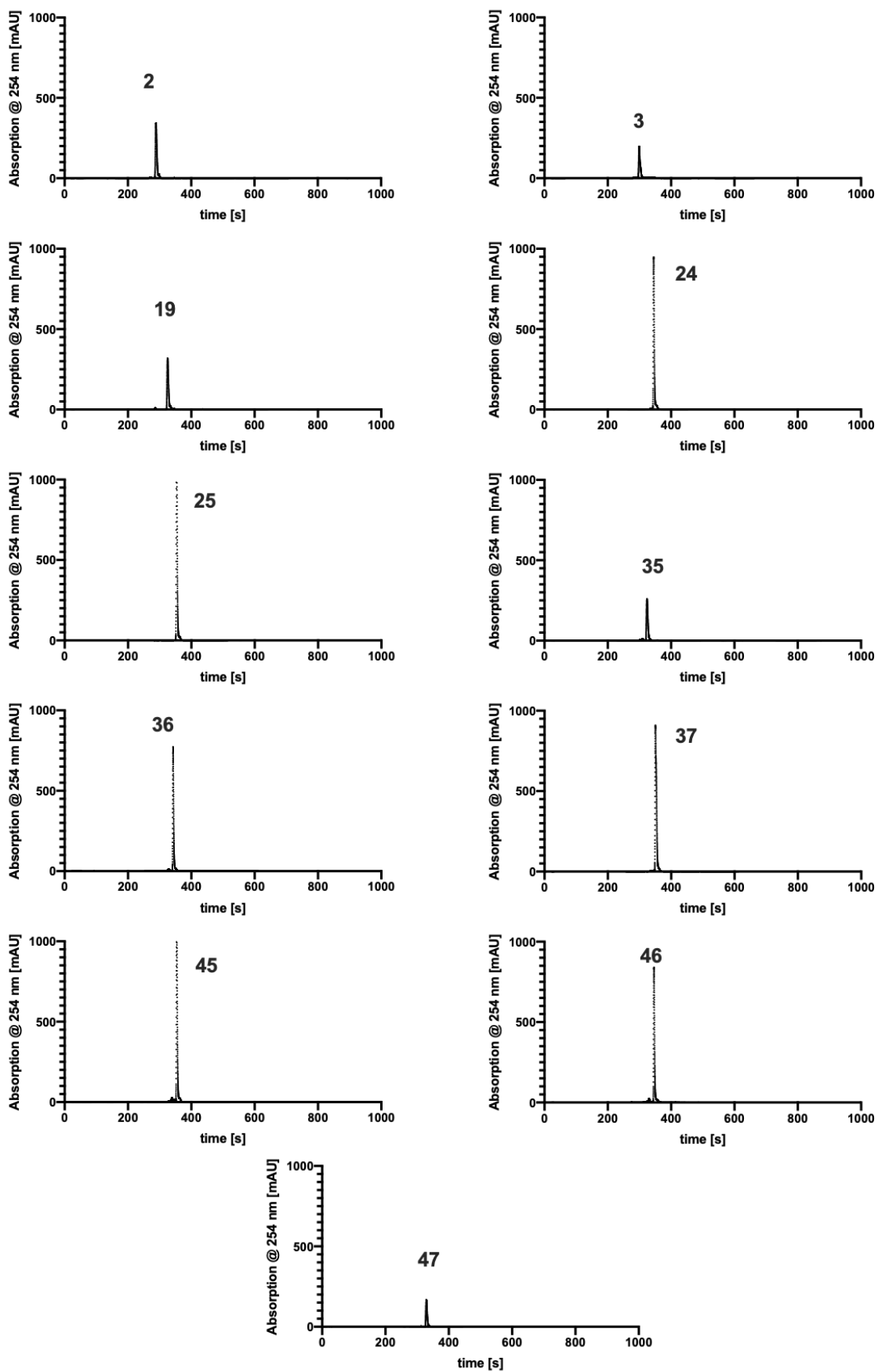
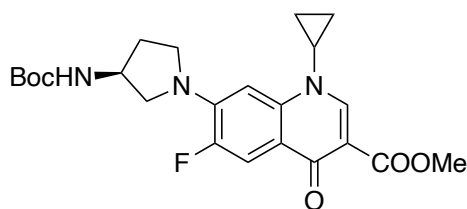


Figure S4. Purity of key compounds by HPLC-UV

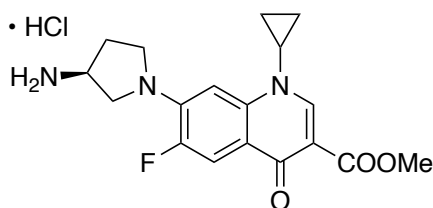
5.4. Supporting Information for Chapter 3.4

7-(3-(tert-butyloxycarbonyl)-amino)pyrrolidinyl-1-cyclopropyl-6-fluoro-4-oxo-1,4-dihydroquinoline-3-carboxylic acid methylester (**5**):



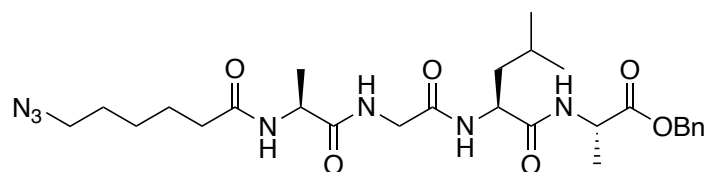
Boc-protected fluoroquinolone **4** (300 mg, 0.7 mmol, 1 eq.), TBTU (558 mg, 1.7 mmol, 2.5 eq.) and DMAP (8 mg, 0.1 mmol, 10 mol%) were dispersed in dry CH₂Cl₂ (7 mL). Methanol (422 μ l, 10.4 mmol, 15 eq.) and DIPEA (363 μ l, 2.1 mmol, 3 eq.) were subsequently added under vigorous stirring and reacted over night at r.t.. The reaction was diluted with CH₂Cl₂ and washed with aqueous satd. NaHCO₃, KHSO₄ (1 M) and satd. brine. After drying over NaSO₄ the solvent was evaporated *in vacuo* and the product was purified by NP-MPLC (CH₂Cl₂/MeOH, 1 - 11%). The product was obtained as a beige amorphous solid (194 mg, 63%). ¹H NMR (500 MHz, DMSO-*d*₆) δ 8.37 (s, 1H, FQ-H-2), 7.67 (d, *J* = 14.5 Hz, 1H, FQ-H-5), 7.28 (d, *J* = 6.7 Hz, 1H, Boc-NH), 6.94 (d, *J* = 7.8 Hz, 1H, FQ-H-8), 4.15 (q, *J* = 5.5 Hz, 1H, aminopyrrolidine-CH), 3.74 (d, *J* = 6.7 Hz, 1H, aminopyrrolidine-CH), 3.71 (s, 3H, COOCH₃), 3.65 (q, *J* = 7.4 Hz, 1H, aminopyrrolidine-CH), 3.58 (m, 1H, cPr-CH), 3.53 (m, 1H, aminopyrrolidine-CH), 3.48 (m, 1H, aminopyrrolidine-CH), 2.13 (m, 1H, aminopyrrolidine-CH), 1.91 (m, 1H, aminopyrrolidine-CH), 1.39 (s, 9H, Boc-CH₃), 1.23 (m, 2H, cPr-CH₂), 1.05 (m, 2H, cPr-CH₂). ¹³C-NMR (126 MHz, DMSO-*d*₆) δ 171.42 (C=O), 165.15 (C=O), 155.26 (Boc-C=O), 149.42 (d, *J* = 243.6 Hz, FQ-C-6), 147.87 (FQ-C-2), 140.34 (d, *J* = 11.9 Hz, FQ-C-7), 138.60 (FQ-C-8a), 117.76 (d, *J* = 5.5 Hz, FQ-C-4a), 111.44 (d, *J* = 23.0 Hz, FQ-C-5), 108.64 (FQ-C), 100.48 (d, *J* = 5.5 Hz, FQ-C-8), 77.94 (Boc-C), 55.06 (d, *J* = 5.1 Hz, aminopyrrolidine-C), 51.17 (COOCH₃), 49.82 (aminopyrrolidine-C), 47.93 (d, *J* = 5.2 Hz, aminopyrrolidine-C), 34.60 (cPr-CH), 30.42 (aminopyrrolidine-C), 28.23 (Boc-CH₃), 7.52 (cPr-CH₂), 7.47 (cPr-CH₂). LR-MS: *m/z* = 446.2, [M+H]⁺.

7-aminopyrrolidinyl-1-cyclopropyl-6-fluoro-4-oxo-1,4-dihydroquinoline-3-carboxylic acid (6):



5 (116 mg, 0.26 mmol, 1 eq.) was dispersed in dioxane (5 mL) and HCl (5.15 mL, 4 M in dioxane, 20.5 mmol, 79 eq.) was added dropwise while cooling on ice. The reaction was allowed to warm to r.t. and stirred for 22 h. The consumption of the starting material was monitored by TLC (CH₂Cl₂ : MeOH, 95 : 5). After evaporation of the solvent *in vacuo*, the product was obtained as a yellow amorphous solid (269 mg, quant.). ¹H NMR (500 MHz, MeOH-*d*₄) δ 9.10 (s, 1H, FQ-H-2), 8.07 (d, J = 14.0 Hz, 1H, FQ-H-5), 7.32 (d, J = 7.4 Hz, 1H, FQ-H-8), 4.24 – 4.12 (m, 2H, aminopyrrolidine-CH₂), 4.06 (s, 3H, COOCH₃), 4.04 – 3.96 (m, 3H, aminopyrrolidine-CH₂ + cPr-CH), 3.90 (m, 1H, aminopyrrolidine-H), 2.56 (m, 1H, aminopyrrolidine-H), 2.31 (m, 1H, aminopyrrolidine-H), 1.52 (m, 2H, cPr-CH₂), 1.32 (m, 2H, cPr-CH₂). ¹³C NMR (126 MHz, MeOH-*d*₄) δ 170.40 (d, J = 4.4 Hz, C=O), 168.24 (C=O), 153.20 (d, J = 252.1 Hz, FQ-C-6), 149.95 (FQ-C-2), 145.14 (d, J = 12.8 Hz, FQ-C-7), 142.35 (FQ-C-8a), 113.88 (d, J = 8.7 Hz, FQ-C-4a), 111.84 (d, J = 24.8 Hz, FQ-C-5), 105.30 (FQ-C), 102.14 (d, J = 6.4 Hz, FQ-C-8), 54.91 (aminopyrrolidine-C), 54.83 (aminopyrrolidine-C), 53.84 (COOCH₃), 51.58 (d, J = 2.7 Hz, aminopyrrolidine-C), 38.73 (cPr-CH), 29.99 (aminopyrrolidine-C), 8.75 (cPr-CH₂), 8.71 (cPr-CH₂). LR-MS: m/z = 346.2, [M+H]⁺.

Benzyl-protected alkyl-peptide linker **9**:

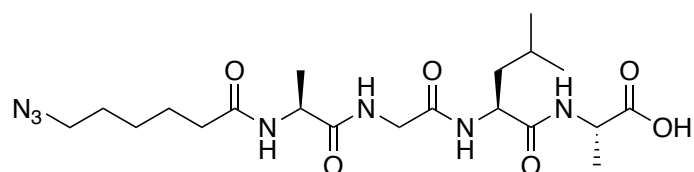


7 (500 mg, 1.09 mmol, 1 eq.), TBTU (700 mg, 2.18 mmol, 2 eq.) and ω-Azido-hexanoic acid (160 μL, 1.09 mmol, 1 eq.) were dissolved in dry CH₂Cl₂ (10 mL). DIPEA (571 μL, 3.27 mmol, 3 eq.) was added dropwise at r.t.. Upon the addition of base, a gel formed, which was redissolved by addition of dry DMF (3 mL). The reaction was stirred over night at r.t. and then diluted with CH₂Cl₂ (90 mL). The organic phase was washed with KHSO₄ (1 M), aqueous satd. NaHCO₃ and brine. After drying over Na₂SO₄, the solvent was evaporated

in vacuo and the product was purified by NP-MPLC (CH₂Cl₂ : MeOH/EtOH (1:1), 1-10%) to yield a white amorphous solid (407 mg, 68%). ¹H NMR (500 MHz, MeOH-*d*₄) δ 7.39 – 7.28 (m, 5H, Ar-H), 5.17 (d, J = 12.3 Hz, 1H, Bn-CH₂), 5.13 (d, J = 12.3 Hz, 1H, Bn-CH₂), 4.51 – 4.40 (m, 2H, Leu-Cα-H, Ala-Cα-H), 4.23 (q, J = 7.1 Hz, 1H, Ala-Cα-H), 3.90 (d, J = 16.8 Hz, 1H, Gly-CH₂), 3.79 (d, J = 16.8 Hz, 1H, Gly-CH₂), 3.28 (d, J = 6.8 Hz, 2H, linker-CH₂), 2.26 (t, J = 7.6 Hz, 2H, linker-CH₂), 1.85 – 1.50 (m, 7H, Leu-CH, Leu-CH₂, linker-CH₂, linker-CH₂), 1.41 (m, 5H, Ala-CH₃, linker-CH₂), 1.35 (d, J = 7.1 Hz, 3H, Ala-CH₃), 0.91 (d, J = 6.4 Hz, 3H, Leu-CH₃), 0.88 (d, J = 6.4 Hz, 3H, Leu-CH₃). ¹³C NMR (126 MHz, MeOH-*d*₄) δ 176.08 (C=O), 176.01 (C=O), 174.59 (C=O), 173.75 (C=O), 171.47 (C=O), 137.27 (Ar-C), 129.57 (Ar-C), 129.29 (Ar-C), 129.23 (Ar-C), 67.91 (Bn-CH₂), 52.96 (Ala-Cα), 52.27 (linker-CH₂), 51.11 (Ala-Cα), 49.67 (Leu-Cα), 43.61 (Gly-Cα), 41.82 (Leu-CH₂), 36.41 (linker-CH₂), 29.64 (linker-CH₂), 27.40 (linker-CH₂), 26.21 (linker-CH₂), 25.71 (Leu-CH), 23.52 (Leu-CH₃), 21.85 (Leu-CH₃), 17.44 (Ala-CH₃), 17.22 (Ala-CH₃).

LR-MS: 560.4 [M+H]⁺.

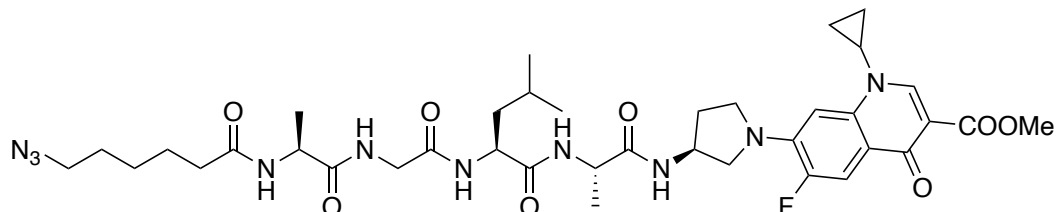
alkyl-peptide linker **10** (= **2**):



9 (400 mg, 0.85 mmol, 1 eq.) was dissolved in a mixture of THF/MeOH/H₂O (8 mL, 3:2:2) at r.t.. LiOH (61 mg, 2.55 mmol, 3 eq.) was dissolved in H₂O (1 mL) and added dropwise to the starting material. The reaction was stirred at room temperature until disappearance of the starting material (10 min), monitored by TLC (CH₂Cl₂, MeOH 95:5). The reaction was cooled on ice and neutralised with Amberlite IR120/H⁺. After filtration of the ion exchange resin, solvent was removed *in vacuo*. The product was purified by NP-MPLC (CH₂Cl₂ : MeOH, 1-10%) and obtained as a white amorphous solid (234 mg, 59%). ¹H NMR (500 MHz, MeOH-*d*₄) 4.46 (dd, J = 9.1, 5.5 Hz, 1H, Leu-Cα-H), 4.38 (q, J = 7.3 Hz, 1H, Ala-Cα-H), 4.27 (q, J = 7.1 Hz, 1H, Ala-Cα-H), 3.93 (d, J = 16.7 Hz, 1H, Gly-Cα-H), 3.81 (d, J = 16.7 Hz, 1H, Gly-Cα-H), 3.28 (t, J = 6.8 Hz, 1H, linker-CH₂), 2.26 (t, J = 7.6 Hz, 1H, linker-CH), 1.82 – 1.54 (m, 7H, Leu-CH, Leu-CH₂, 2x linker-CH₂), 1.48 – 1.41 (m, 1H, linker-CH), 1.40 (d, J = 7.3 Hz, 3H, Ala-CH₃), 1.36 (d, J = 7.2 Hz, 3H, Ala-CH₃), 0.95 (d, J = 6.1 Hz, 3H, Leu-CH₃), 0.92 (d, J = 6.1 Hz, 3H, Leu-CH₃). ¹³C NMR (126 MHz, MeOH-*d*₄) δ 176.53 (C=O), 176.26 (C=O), 176.06 (C=O), 174.31 (C=O), 171.74 (C=O), 53.26 (Ala-Cα), 52.28 (linker-CH₂), 51.19 (linker-CH₂), 49.87 (Leu-Cα), 43.66 (Gly-Cα), 41.73 (Leu-CH₂),

36.41 (linker-CH₂), 29.64 (linker-CH₂), 27.41 (linker-CH₂), 26.25 (linker-CH₂), 25.77 (Leu-CH), 23.56 (Leu-CH₃), 21.81 (Leu-CH₃), 17.78 (Ala-CH₃), 17.38 (Ala-CH₃). LRMS: 470.3 [M+H]⁺.

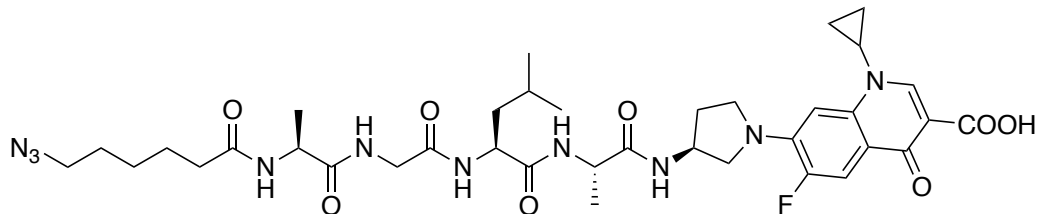
Methyl-protected alkyl-peptidyl fluoroquinolone building block **11**:



10 (70 mg, 0.15 mmol, 1 eq.), **6** (69 mg, 0.18 mg, 1.2 eq.) and TBTU (96 mg, 0.3 mmol, 2 eq.) were dissolved in dry DMF (2 mL). DIPEA (79 μ L, 0.45 mmol, 3 eq.) was added dropwise and the reaction was stirred for 4 h, monitored by TLC. The reaction was diluted with CH₂Cl₂ (25 mL) and the organic phase was washed with KHSO₄ (1 M), aqueous satd. NaHCO₃ and brine. After evaporation of the solvent, the product was purified by NP-MPLC (CH₂Cl₂ : MeOH, 1-10%). The combined elution fractions were further purified by precipitation from MeOH with Et₂O and the product was isolated as a beige amorphous solid (65 mg, 54%, 90% purity according to ¹H-NMR). ¹H NMR (500 MHz, MeOH-*d*₄) δ 8.58 (s, 1H, FQ-H-2), 7.78 (d, *J* = 14.6 Hz, 1H, FQ-H-5), 7.03 (d, *J* = 7.6 Hz, 1H, FQ-H-8), 4.53 – 4.43 (m, 1H, aminopyrrolidine-CH), 4.37 – 4.22 (m, 2H, Ala-C α , Leu-C α), 4.16 (q, *J* = 7.2 Hz, 1H, Ala-C α), 3.94 – 3.84 (m, 1H, aminopyrrolidine-CH), 3.84 (s, 3H, COOMe), 3.84 – 3.77 (m, 1H, aminopyrrolidine-CH), 3.72 (d, *J* = 16.6 Hz, 1H, Gly-CH₂), 3.69 – 3.66 (m, 1H, aminopyrrolidine-CH), 3.63 (d, *J* = 16.6 Hz, 1H, Gly-CH₂), 3.61 – 3.54 (m, 2H, cPr-CH, aminopyrrolidine-CH), 3.28 (t, *J* = 6.9 Hz, 2H, linker-CH₂), 2.36 – 2.19 (m, 3H, linker-CH₂, aminopyrrolidine-CH), 2.14 (dt, *J* = 12.7, 2.9 Hz, 1H, aminopyrrolidine-CH), 1.90 – 1.49 (m, 7H, Leu-CH, Leu-CH₂, linker-CH₂, linker-CH₂), 1.45 – 1.38 (m, 5H, Ala-CH₃, linker-CH₂), 1.36 (d, *J* = 7.2 Hz, 3H, Ala-CH₃), 1.34 – 1.27 (m, 2H, cPr-CH₂), 1.13 (dd, *J* = 9.0, 3.8 Hz, 2H, cPr-CH₂), 0.94 (d, *J* = 6.3 Hz, 3H, Leu-CH₃), 0.87 (d, *J* = 6.3 Hz, 3H, Leu-CH₃). ¹³C NMR (126 MHz, MeOH-*d*₄) δ 176.64 (C=O), 176.48 (C=O), 175.29 (C=O), 175.11 (C=O), 174.83 (C=O), 172.44 (C=O), 166.99 (C=O), 151.79 (d, *J* = 244.8 Hz, FQ-C-6), 149.68 (FQ-C), 142.73 (d, *J* = 11.5 Hz, FQ-C-7), 140.51 (FQ-C), 119.20 (d, *J* = 6.1 Hz, FQ-C-8a), 112.90 (d, *J* = 23.0 Hz, FQ-C-4a), 109.80 (FQ-C), 101.59 (d, *J* = 5.4 Hz, FQ-C-8), 55.95 (d, *J* = 6.0 Hz, aminopyrrolidine-C), 54.09 (Leu-C α), 52.28 (linker-CH₂), 52.07 (COOMe), 51.85 (Ala-C α), 50.86 (aminopyrrolidine-C), 50.81 (Ala-C α), 44.13 (Gly-CH₂), 41.16 (Leu-CH₂), 36.33 (linker-CH₂), 36.16 (cPr-CH), 31.89 (aminopyrrolidine-C), 29.67

(linker-CH₂), 27.45 (linker-CH₂), 26.12 (linker-CH₂), 25.88 (Leu-CH), 23.55 (Leu-CH₃), 21.58 (Leu-CH₃), 17.80 (Ala-CH₃), 17.36 (Ala-CH₃), 8.53 (cPr-CH₂), 8.50 (cPr-CH₂). LR-MS: 797.6 [M+H]⁺.

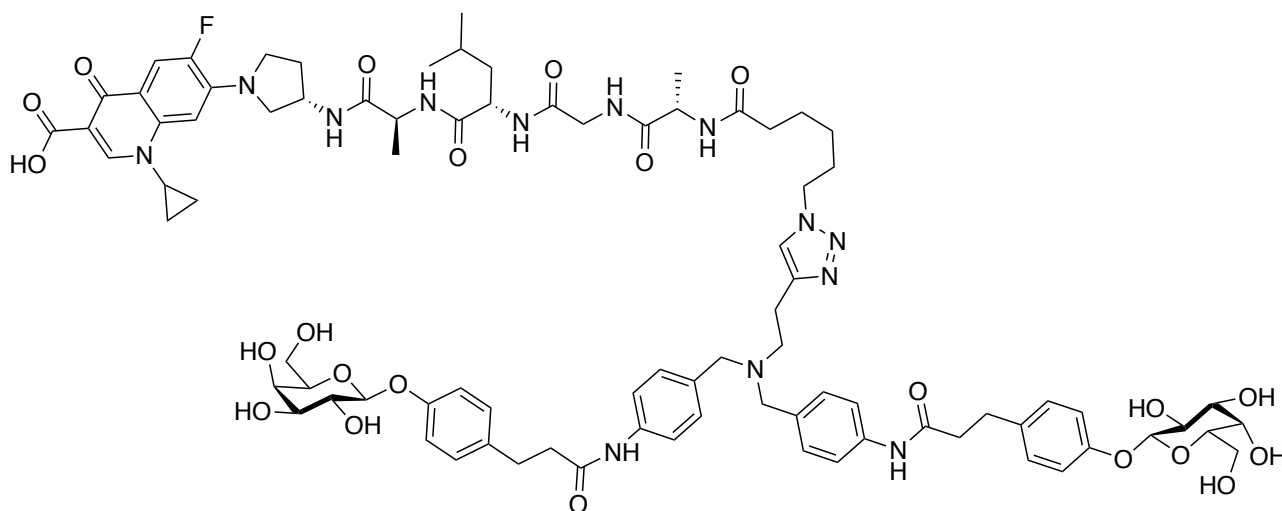
alkyl-peptidyl fluoroquinolone building block **12**:



11 (31 mg, 0.039 mmol, 1 eq.) was dissolved in a mixture of THF/MeOH/H₂O (1 mL, 3:1:1) at r.t.. LiOH (4 mg, 0.16 mmol, 4 eq.) was added to the starting material at room temperature and the reaction was stirred at room temperature until disappearance of the starting material (24 h), monitored by TLC (CH₂Cl₂ : MeOH 90 : 10, 1% NH₄OH). The reaction was cooled on ice and neutralised with Amberlite IR120/H⁺. After filtration of the ion exchange resin, the solvent was evaporated *in vacuo*. The product was obtained as a beige amorphous solid (30 mg, 98 %). ¹H NMR (500 MHz, DMSO-*d*₆) δ 15.52 (s, 1H, COOH), 8.58 (s, 1H, FQ-H-2), 8.30 – 8.22 (m, 1H, Ar-H), 8.16 (d, J = 6.5 Hz, 1H, NH), 8.01 (d, J = 6.7 Hz, 1H, NH), 7.96 (d, J = 7.4 Hz, 1H, NH), 7.87 (d, J = 7.8 Hz, 1H, NH), 7.81 (d, J = 14.1 Hz, 1H, FQ-H), 7.06 (d, J = 7.5 Hz, 1H, FQ-H), 4.42 – 4.34 (m, 1H, aminopyrrolidine-CH), 4.29 – 4.09 (m, 3H, Ala-Cα-H, Ala-Cα-H, Leu-Cα-H), 3.85 (br s, 1H, aminopyrrolidine-CH), 3.78 – 3.72 (m, 2H, cPr-CH, aminopyrrolidine-CH), 3.71 – 3.56 (m, 3H, Gly-CH₂ aminopyrrolidine-CH), 3.48 – 3.43 (m, 1H, aminopyrrolidine-CH), 3.30 (t, J = 6.9 Hz, 2H, linker-CH₂), 2.38 – 2.10 (m, 3H, linker-CH₂, aminopyrrolidine-CH), 2.03 – 1.89 (m, 1H, aminopyrrolidine-CH), 1.68 – 1.42 (m, 7H, Leu-CH₂, Leu-CH, Linker-CH₂, Linker-CH₂), 1.36 – 1.25 (m, 4H, cPr-CH₂, linker-CH₂), 1.23 (d, J = 7.2 Hz, 3H, Ala-CH₃), 1.20 (d, J = 7.1 Hz, 3H, Ala-CH₃), 1.18 – 1.10 (m, 2H, cPr-CH₂), 0.86 (d, J = 6.5 Hz, 3H, Leu-CH₃), 0.81 (d, J = 6.5 Hz, 3H, Leu-CH₃). ¹³C NMR (126 MHz, DMSO-*d*₆) δ 175.86 (C=O), 173.29 (C=O), 172.47 (C=O), 172.19 (C=O), 171.59 (C=O), 169.22 (C=O), 166.30 (C=O), 149.96 (d, J = 246.5 Hz, FQ-C-6), 147.44 (Ar-C), 141.62 (d, J = 11.2 Hz, FQ-C-7), 139.81 (Ar-C), 110.74 (d, J = 22.9 Hz, FQ-C-4a), 100.50 (d, J = 5.3 Hz, FQ-C-8), 69.80 (Gly-Cα), 54.97 (aminopyrrolidine-C), 51.31 (Leu-Cα), 50.53 (linker-CH₂), 48.81 (Ala-Cα), 48.67 (aminopyrrolidine-C), 48.38 (Ala-Cα), 48.01 (aminopyrrolidine-C), 42.30 (Gly-Cα), 40.43 (Leu-CH₂), 35.69 (cPr-CH), 34.85 (linker-CH₂), 30.37 (aminopyrrolidine-C), 28.03 (linker-CH₂), 25.82 (linker-CH₂), 24.56 (linker-CH₂), 24.08 (Leu-CH), 23.03 (Leu-CH₃), 21.44 (Leu-

CH₃), 17.87 (Ala-CH₃), 17.70 (Ala-CH₃), 7.57 (cPr-CH₂), 7.51 (cPr-CH₂). LR-MS: 783.5 [M+H]⁺

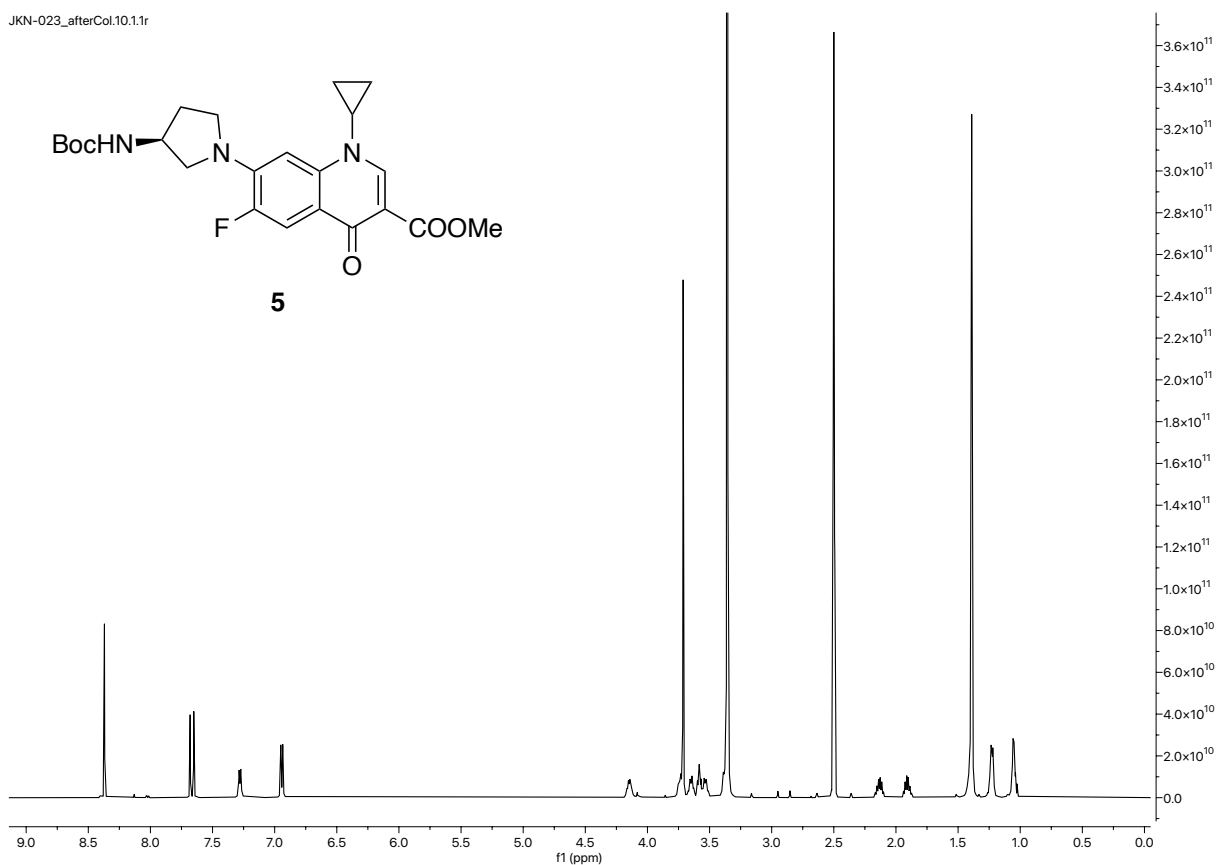
bivalent LecA-targeted prodrug **13**:



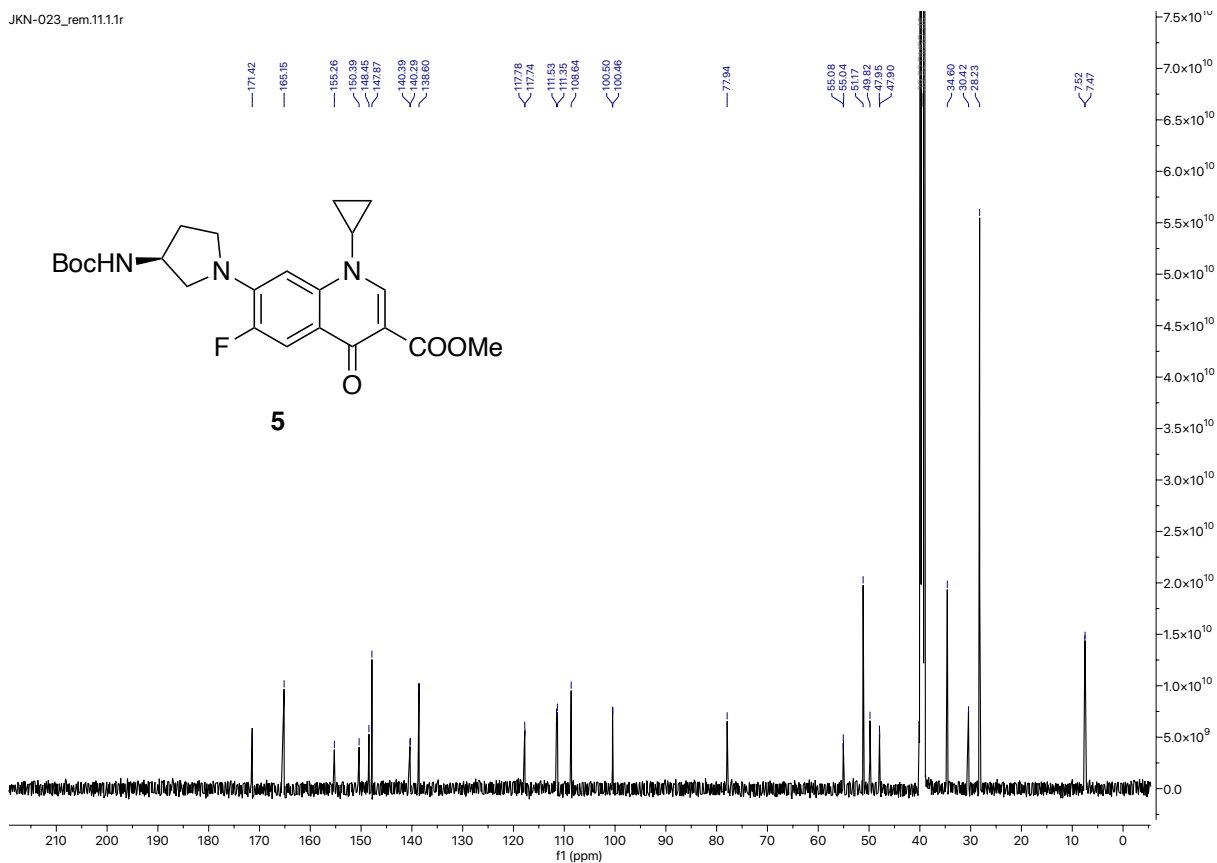
1 (10 mg, 11 μ mol, 1 eq.), **12** (8.7 mg, 11 μ mol, 1 eq.) and DIPEA (2 μ L, 11 μ mol, 1 eq.) were dissolved in dry DMF (400 μ L). CuSO₄ (56 μ L of a 100 mM solution in H₂O, 5.5 μ mol, 50 mol%) and sodium ascorbate (66 μ L of a 100 mM solution in H₂O, 6.6 μ mol, 60 mol%) were added and the reaction was stirred at r.t. for 24 h. The solvent was evaporated *in vacuo* and purified by preparative HPLC (MeCN : H₂O, 21 - 35%). The product was obtained as a white amorphous solid (8 mg, 43%). ¹H NMR (500 MHz, DMSO-*d*₆) δ 15.52 (s, 1H, COOH), 9.86 (s, 2H, glyco-probe-NH), 8.58 (s, 1H, FQ-H-2), 8.21 (t, J = 5.5 Hz, 1H, NH), 8.09 (d, J = 6.4 Hz, 1H, NH), 7.97 (d, J = 6.7 Hz, 1H, NH), 7.91 (d, J = 7.5 Hz, 1H, NH), 7.84 (d, J = 7.6 Hz, 1H, NH), 7.81 (d, J = 14.1 Hz, 1H, FQ-H-5), 7.69 (s, 1H, triazole-H), 7.51 (d, J = 8.1 Hz, 4H, Ar-H), 7.20 (d, J = 8.3 Hz, 4H, Ar-H), 7.14 (d, J = 8.5 Hz, 4H, Ar-H), 7.05 (d, J = 7.6 Hz, 1H, FQ-H-8), 6.93 (d, J = 8.6 Hz, 4H, Ar-H), 5.11 (br s, 2H, OH), 4.83 (br s, 2H, OH), 4.75 (d, J = 7.7 Hz, 2H, Gal-H-1), 4.62 (br s, 2H, OH), 4.47 (br s, 2H, OH), 4.40 – 4.31 (m, 1H, aminopyrrolidine-CH), 4.27 – 4.12 (m, 5H, linker-CH₂, Ala-C α -H, Ala-C α -H, Leu-C α -H), 3.90 – 3.79 (m, 1H, aminopyrrolidine-CH), 3.80 – 3.71 (m, 2H, cPr-CH, aminopyrrolidine-CH), 3.68 (d, J = 3.3 Hz, 2H, Gal-H-4), 3.67 – 3.57 (m, 3H, Gly-CH₂, aminopyrrolidine-CH), 3.58 – 3.35 (m, 13H, Gal-H-2, Gal-H-3, Gal-H-5, Gal-H-6, aminopyrrolidine-CH₂, aminopyrrolidine-CH), 2.83 (t, J = 7.7 Hz, 4H, CH₂-CH₂-N), 2.78 (t, J = 7.6 Hz, 2H, triazole-CH₂-CH₂-N), 2.64 – 2.59 (m, 2H, triazole-CH₂-CH₂-N), 2.56 (t, J = 7.8 Hz, 4H, CH₂-CH₂-CONH), 2.23 – 2.13 (m, 1H, aminopyrrolidine-CH), 2.13 – 2.06 (m, 2H, linker-CH₂), 2.01 – 1.92 (m, 1H, aminopyrrolidine-CH), 1.79 – 1.70 (m, 2H, linker-CH₂), 1.64 – 1.54 (m, 1H, Leu-CH), 1.50 (d, J = 7.2 Hz, 2H, linker-CH₂), 1.48 – 1.40 (m, 2H, Leu-

CH₂), 1.28 (d, J = 7.3 Hz, 2H, cPr-CH₂), 1.21 (d, J = 7.1 Hz, 3H, Ala-CH₃), 1.18 (d, J = 7.2 Hz, 3H, Ala-CH₃), 1.17 – 1.10 (m, 4H, cPr-CH₂ + linker-CH₂), 0.84 (d, J = 6.6 Hz, 6H, Leu-CH₃), 0.79 (d, J = 6.4 Hz, 3H, Leu-CH₃). ¹³C NMR (126 MHz, DMSO-*d*₆) δ 175.89 (d, J = 2.7 Hz, FQ-C-4), 173.26 (C=O), 172.41 (C=O), 172.14 (C=O), 171.56 (C=O), 170.31 (C=O), 169.17 (C=O), 166.26 (COOH), 155.84 (glyco-probe-Ar), 149.96 (d, J = 246.1 Hz, FQ-C-6), 147.46 (FQ-C), 145.00 (triazole-C), 141.61 (d, J = 11.5 Hz, FQ-C-7), 139.82 (FQ-C), 137.96 (glyco-probe-Ar), 134.34 (glyco-probe-Ar), 133.80 (glyco-probe-Ar), 129.03 (glyco-probe-Ar), 128.84 (glyco-probe-Ar), 121.84 (triazole-C), 118.87 (glyco-probe-Ar), 116.19 (glyco-probe-Ar), 114.52 (d, J = 6.2 Hz, FQ-C-4a), 110.75 (d, J = 23.0 Hz, FQ-C-5), 106.20 (FQ-C), 101.13 (Gal-C-1), 100.50 (d, J = 5.5 Hz, FQ-C-8), 75.44 (Gal-C-5), 73.31 (Gal-C-3), 70.30 (Gal-C-3), 68.14 (Gal-C-4), 60.39 (Gal-C-6), 56.73 (Ar-CH₂-N), 54.93 (aminopyrrolidine-CH₂), 52.39 (triazole-CH₂-CH₂-N), 51.23 (Leu-Cα), 48.98 (linker-CH₂), 48.73 (Ala-Cα), 48.64 (aminopyrrolidine-C), 48.31 (Ala-Cα), 48.02 (d, J = 5.2 Hz, aminopyrrolidine-C), 42.26 (Gly-CH₂), 40.45 (Leu-CH₂), 38.25 (CH₂-CH₂-CONH), 35.69 (cPr-CH), 34.78 (linker-CH₂), 30.35 (aminopyrrolidine-C), 30.09 (CH₂-CH₂-CONH), 29.56 (linker-CH₂), 25.55 (linker-CH₂), 24.41 (linker-CH₂), 24.06 (Leu-CH), 23.02 (Leu-CH₃), 22.91 (triazole-CH₂-CH₂-N), 21.43 (Leu-CH₃), 17.86 (Ala-CH₃), 17.73 (Ala-CH₃), 7.56 (cPr-CH₂), 7.49 (cPr-CH₂). HRMS calcd [C₈₅H₁₁₀FN₁₃O₂₂]²⁺: 841.8931 found: 841.8925.

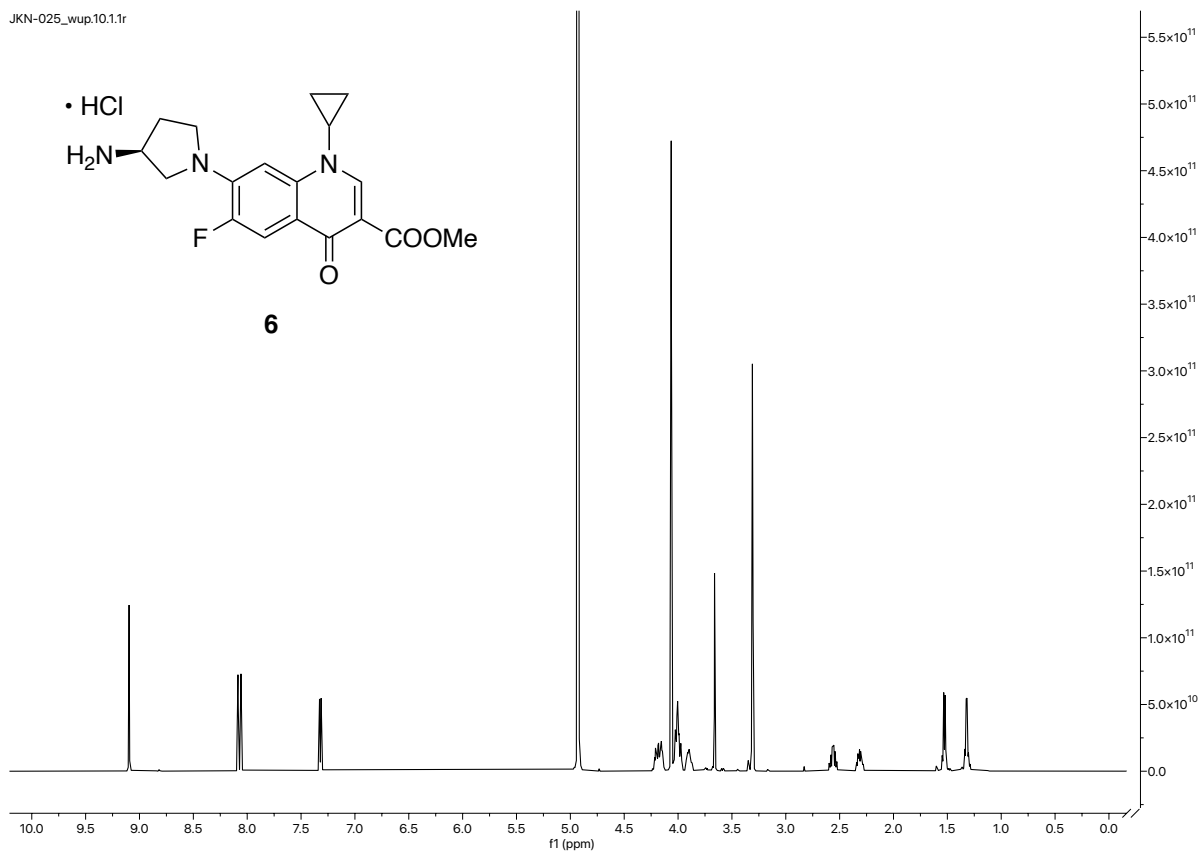
JKN-023_afterCol.10.1.1r



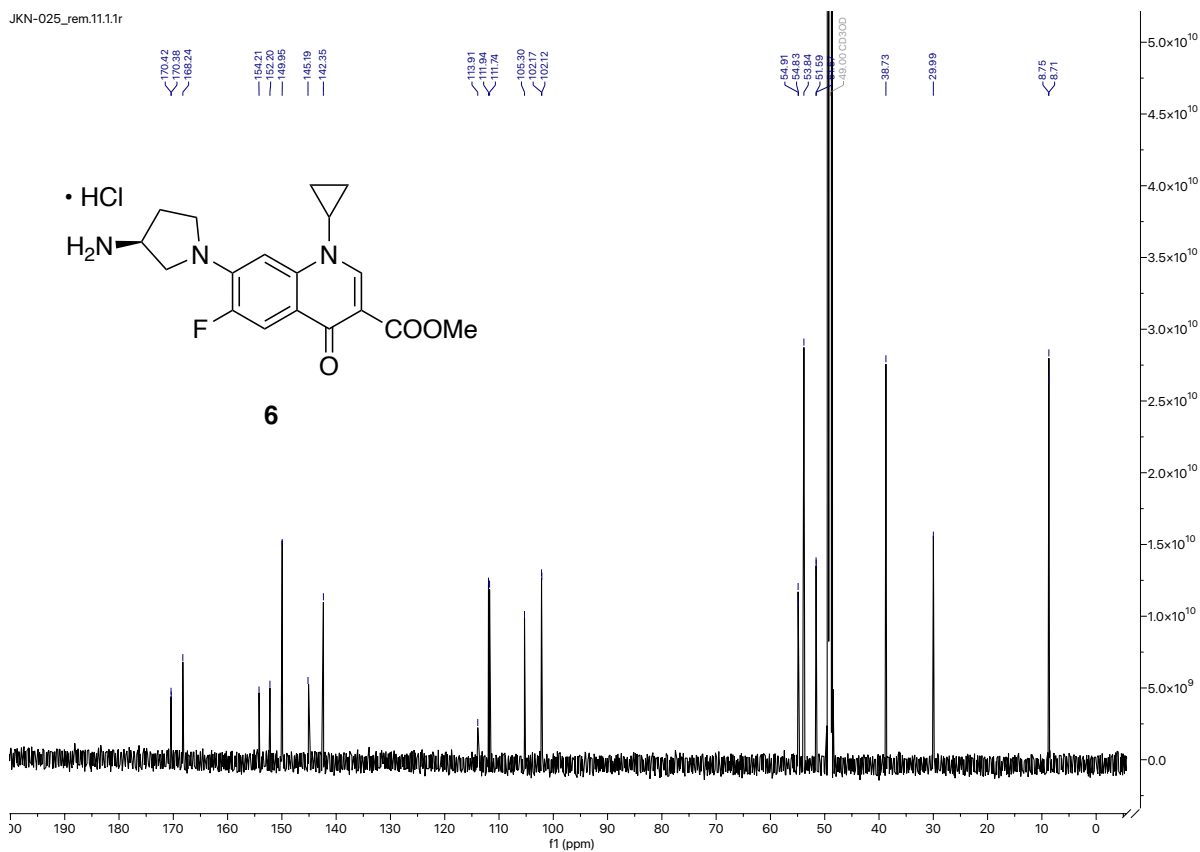
JKN-023_rem.111.1r



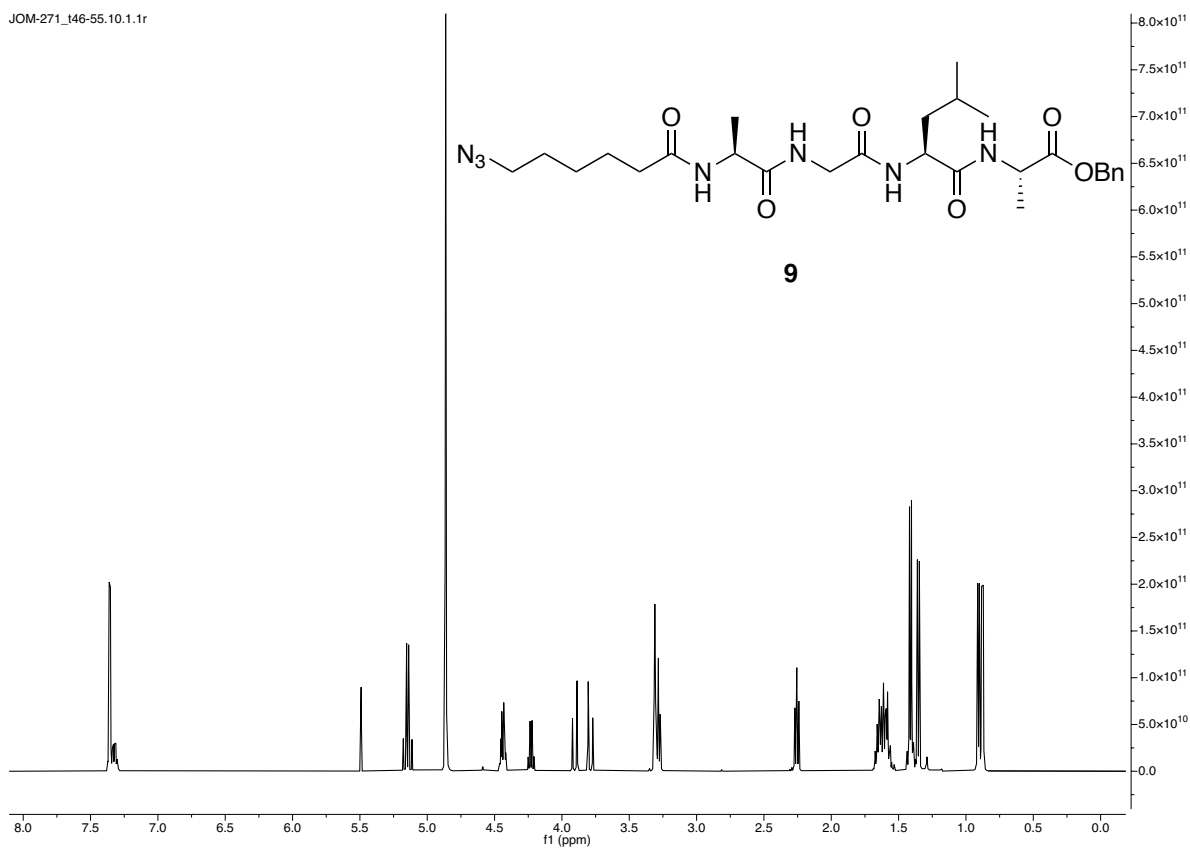
JKN-025_wup.10.1.1r



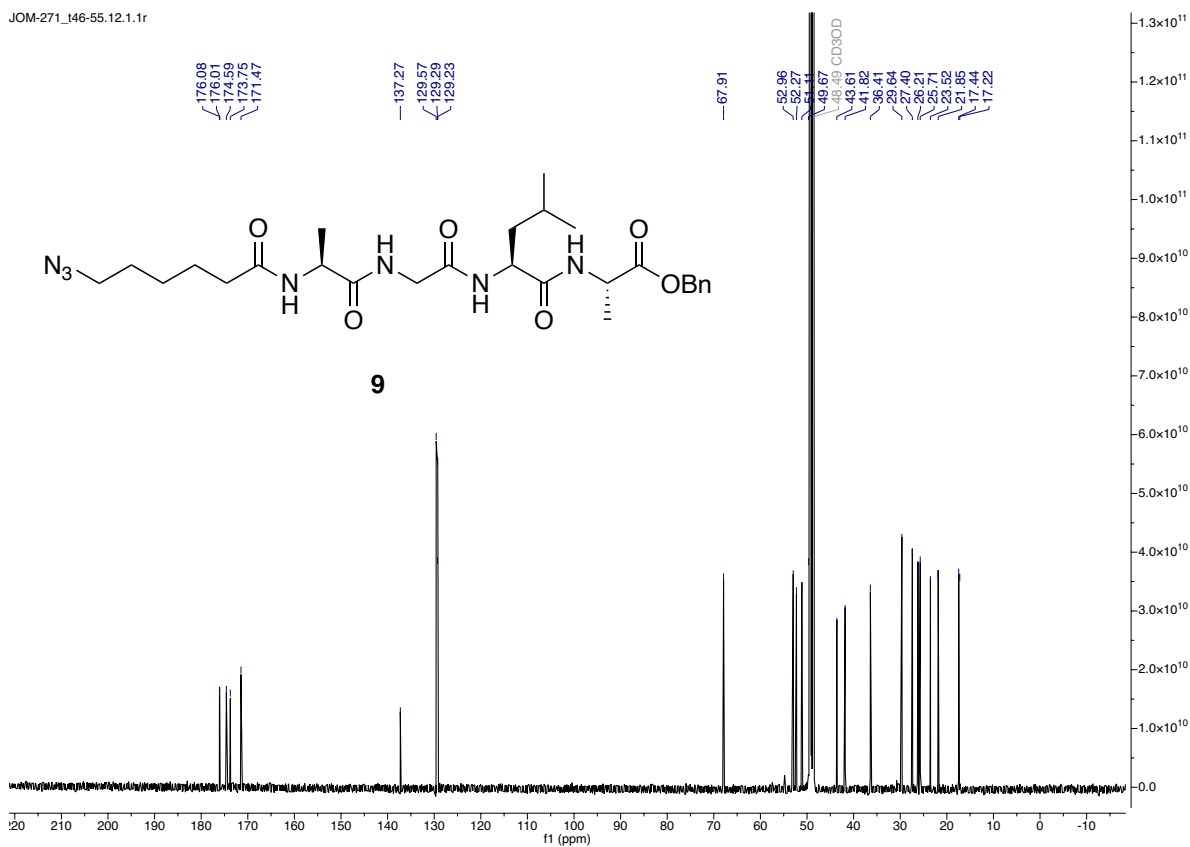
JKN-025_rem.11.1.1r

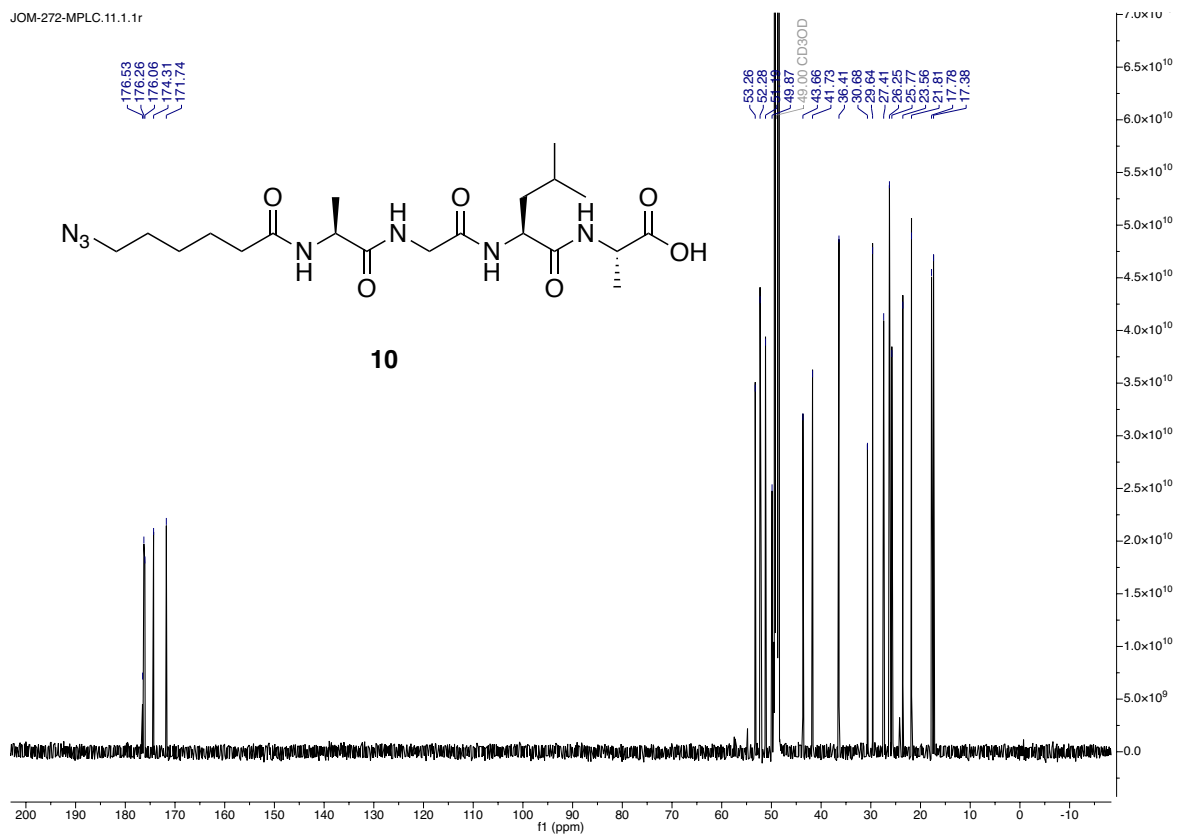
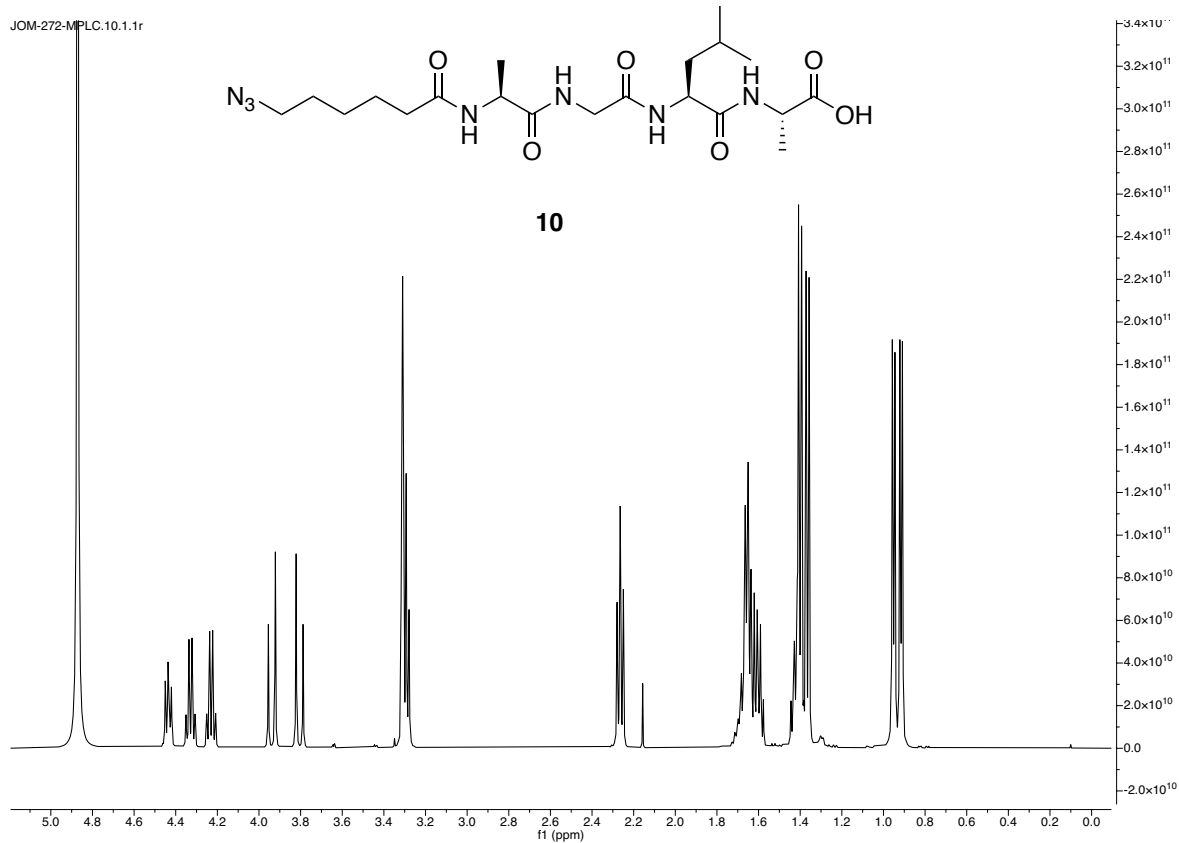


JOM-271_146-55.10.1.1r

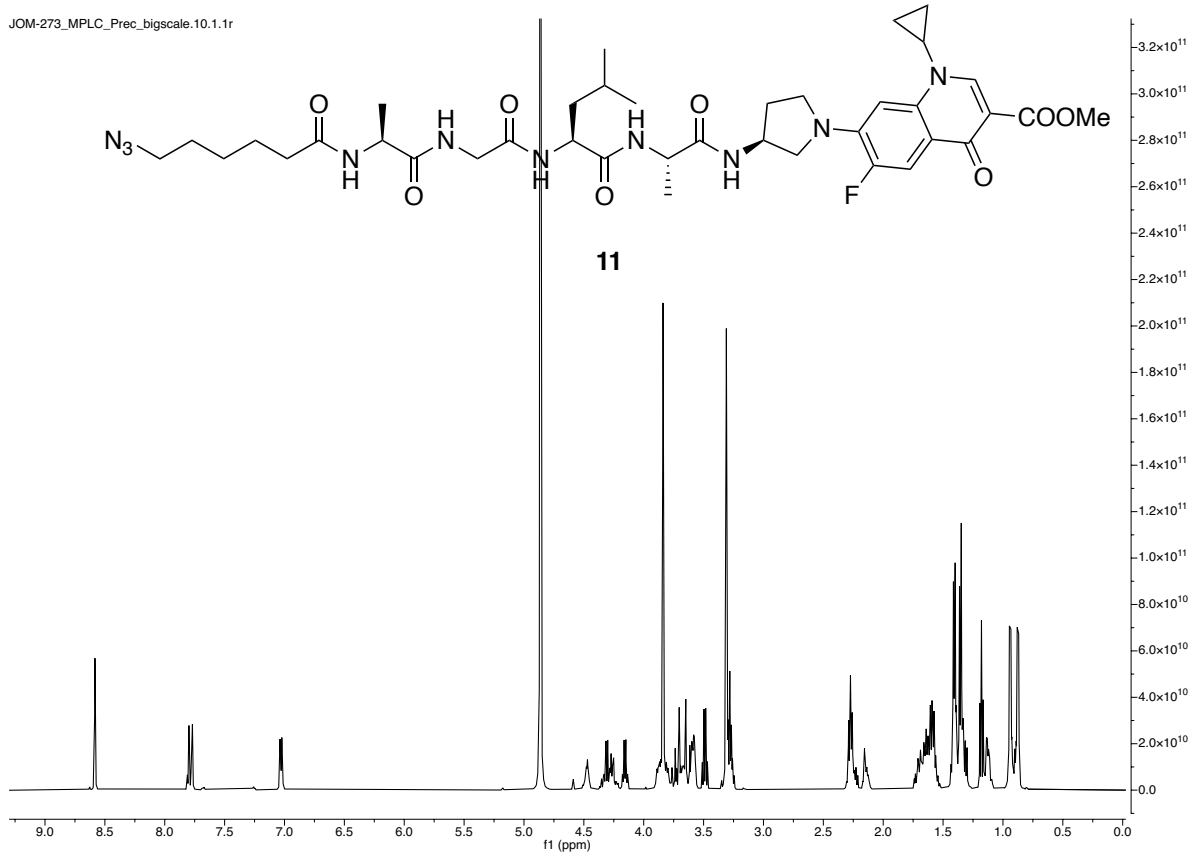


JOM-271_146-55.12.1.1r

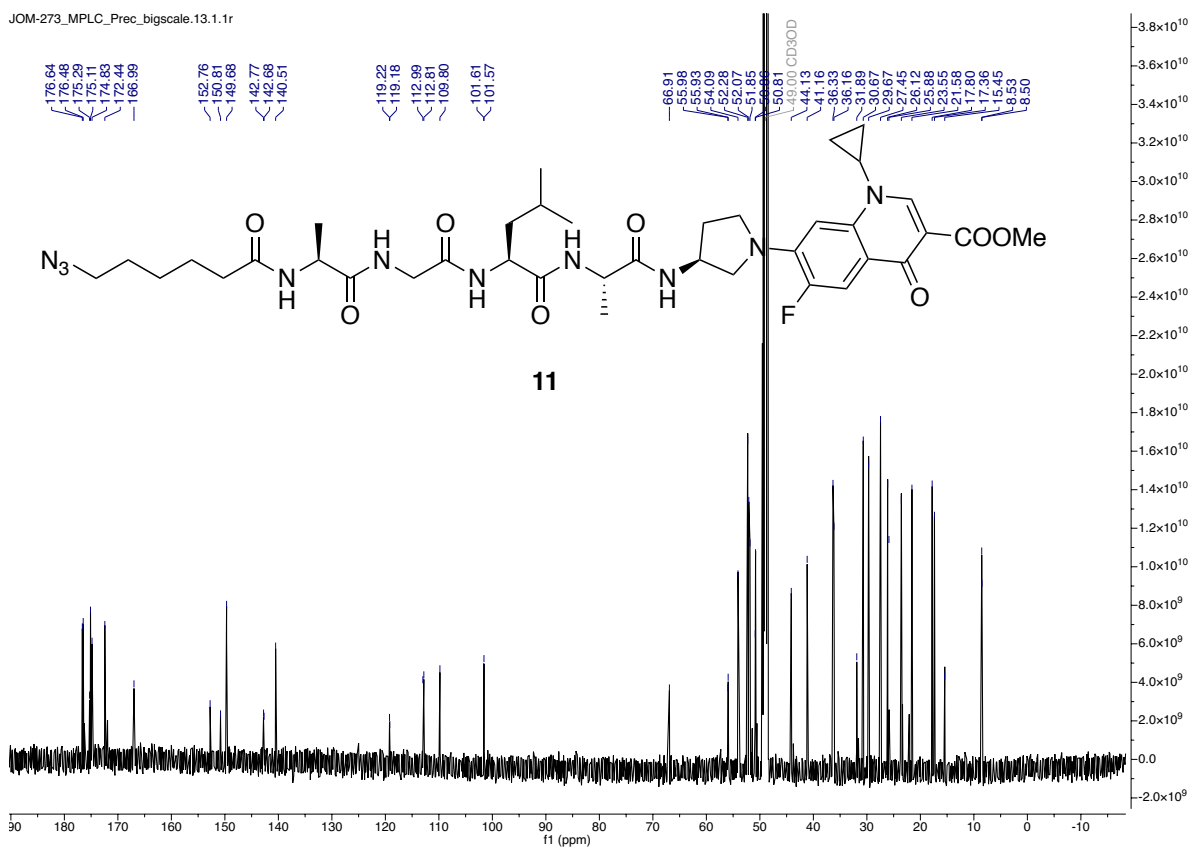




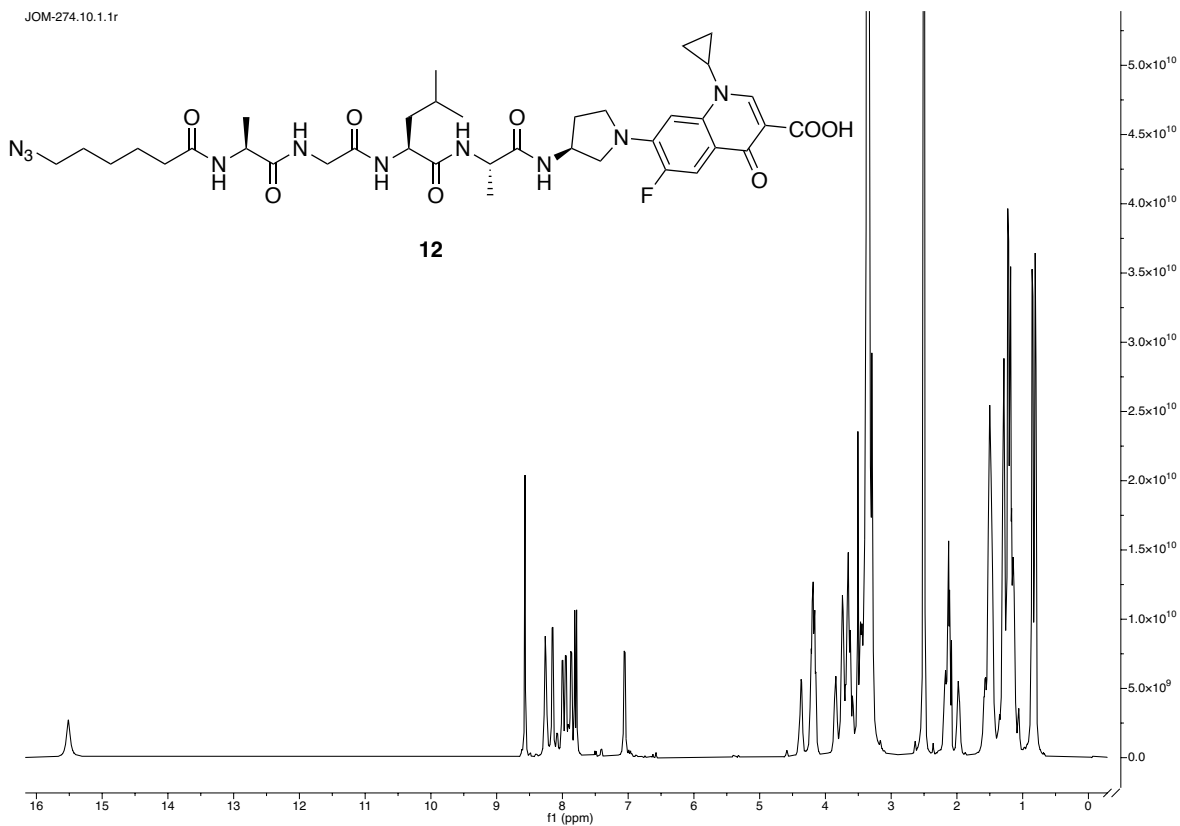
JOM-273_MPLC_Prec_bigscale.10.1.1r



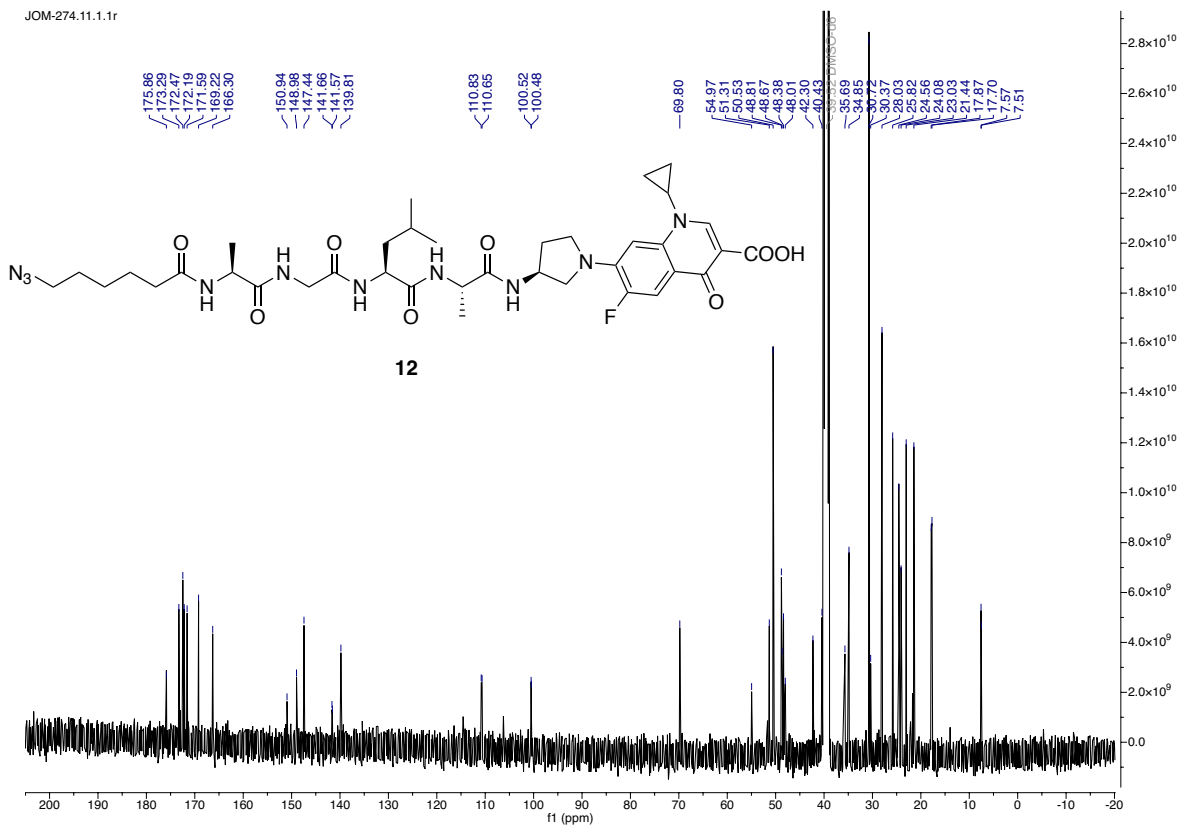
JOM-273_MPLC_Prec_bigscale.13.1.1r

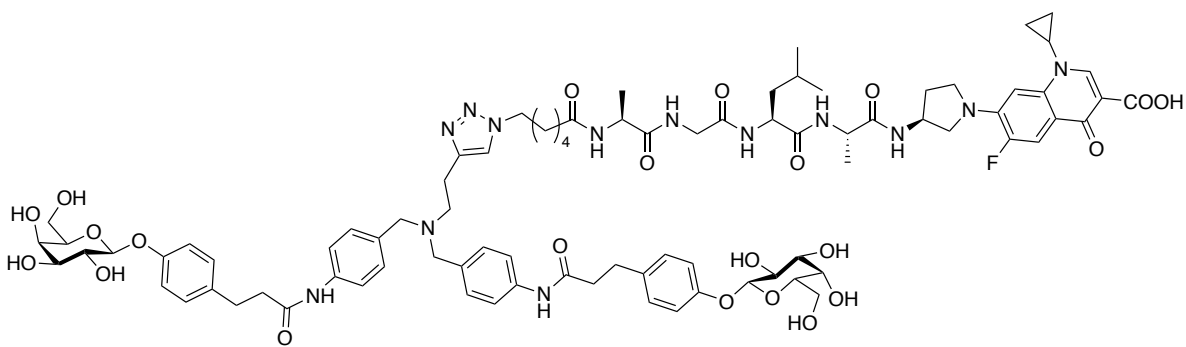
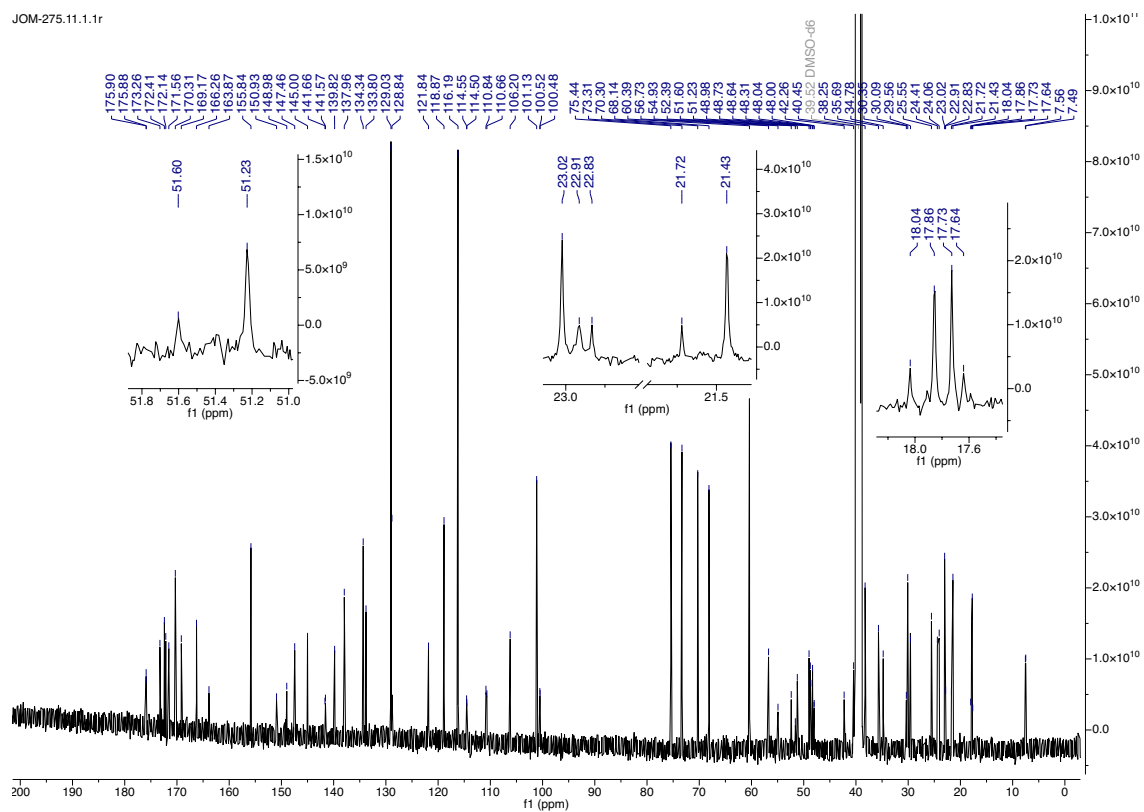


JOM-274.10.1.1r



JOM-274.11.1.1r





13

5.5. Supporting Information for Chapter 3.5

Materials and Methods

Bromelain was kindly obtained from Ursapharm (Saarbrücken, Germany).

Preparation of D-mannose sepharose

D-man sepharose was synthesised according to the protocol of Fornstedt and Porath^[171]: Sepharose CL-6B (15 mL) was suspended in Na₂CO₃-buffer (500 mM, pH 11, 15 mL). Divinylsulfone (1.5 mL) was added and the suspension was stirred at room temperature for 70 min. After filtration over fritted glass (40 - 100 µm pore size), the activated sepharose was extensively washed with demineralised water and resuspended in 15 mL D-mannose solution (20 %m/v, 500 mM Na₂CO₃, pH 10). The reaction was stirred over night at room temperature. The suspension was again filtered over fritted glass (40 - 100 µm pore size) and extensively washed with demineralised water. Subsequently, the activated sepharose was quenched with β-mercapto ethanol (300 µL) in NaHCO₃-buffer (15 mL, 500 mM NaHCO₃, pH 8.5) for 120 min. The product was recovered as described above and filled into 5 mL plastic columns for affinity chromatography.

Isolation of Acm-JRL from bromelain

Acm-JRL was isolated in analogy to the protocol of Azarkan *et al.*^[166] Bromelain powder (28 g) was suspended in an erlenmeyer flask with buffer (400 mL, 100 mM NaOAc pH 5, 1 mM EDTA, 20 mM methyl methanethiosulfonate) and stirred for 60 min at room temperature. After centrifugation (30,000 rcf, 30 min, 4°C), the supernatant was dialysed twice for 1 h against 4 L TBS (150 mM NaCl, 50 mM tris pH 7.4).

The solution was loaded on a D-mannose sepharose column pre-equilibrated with the dialysis buffer for affinity chromatography. After extensive washing, the lectin was eluted with 1 M D-mannose in buffer. The eluted fractions were pooled and dialysed against TBS (5 x > 3 h against 2 L). The yield (31 mg) was determined by UV-absorption at 280 nm (MW = 15.34 kDa, $\epsilon_{\text{calc}} = 19940 \text{ M}^{-1} \times \text{cm}^{-1}$).

Intact protein mass determination

Intact protein mass measurements for were performed on a Dionex Ultimate 3000 RSLC system using an Aeris Widepore XB C8, 150 x 2.1 mm, 3.6 µm dp column (Phenomenex, USA). Separation of 2 µl sample was achieved by a linear gradient from (A) H₂O + 0.1 % FA to (B) ACN + 0.1 % FA at a flow rate of 300 µl/min and 45 °C. The gradient was initiated by a 1 min isocratic step at 2 % B, followed by an increase to 75 % B in 10 min to end up with a 3 min step at 75 % B before re-equilibration with initial conditions. UV

spectra were recorded by a DAD in the range from 200 to 600 nm. The LC flow was split to 37.5 $\mu\text{L}/\text{min}$ before entering the maXis 4G hr - ToF mass spectrometer (Bruker Daltonics, Bremen, Germany) using the standard Bruker ESI source. In the source region, the temperature was set to 200 $^{\circ}\text{C}$, the capillary voltage was 4000 V, the dry-gas flow was 5.0 l/min and the nebulizer was set to 1.0 bar. Mass spectra were acquired in positive ionization mode ranging from 150 – 2500 m/z at 2.0 Hz scan rate. Protein masses were deconvoluted by using the Maximum Entropy algorithm (Copyright 1991 - 2004 Spectrum Square Associates, Inc.).

Dynamic light scattering

Dynamic light scattering (DLS) measurements were performed on a Zetasizer Nano-ZS (Malvern Instruments, UK). Solutions were filtered with a syringe filter (0.22 μm) before measurements. Acm-JRL (14 μM) was measured in TBS (150 mM NaCl, 50 mM tris pH 7.4) was measured at 25 $^{\circ}\text{C}$.

Differential scanning fluorimetry

20 μL of a solution containing Acm-JRL (20 μM), carbohydrate (10 mM) and SyproOrange (final concentration 10x of a 5000x stock in DMSO, Sigma-Aldrich, Germany) in TBS (150 mM NaCl, 50 mM tris pH 7.4) was added to a white semi-skirted 96-well plate (Thermo Fisher) in triplicates. Described Final concentrations of protein and dye were screened to obtain high signal intensity and well defined curves. Protein without carbohydrate (only buffer) was used as negative control. The melting curve measurements were performed and analysed on a real time PCR instrument (StepOnePlus, Applied Biosystems).

Reporter ligand displacement assay

The assay was performed in analogy to the protocol from Joachim *et al.*^[94]: A serial dilution of the test compounds was prepared in TBS (150 mM NaCl, 50 mM tris pH 7.4). A concentrated solution of Acm-JRL was diluted in TBS together with the fluorescent reporter ligand *N*-(fluorescein-5-yl)-*N'*-(α -L-fucopyranosyl ethylene)thiocarbamide to yield concentrations of 40 μM and 20 or 200 nM, respectively. A 10 μL solution of this mix was added to 10 μL serial dilutions of the test compounds in a black 384-well microtiter plates (Greiner Bio-One, Germany, cat. no. 781900) in triplicates. After centrifugation (2680 rcf, 1 min, r.t.), the reactions were incubated for 60 min at r.t. under high humidity. Fluorescence (excitation 485 nm, emission 535 nm) was measured in parallel and perpendicular to the excitation plane on a PheraStar FS plate reader (BMG Labtech GmbH, Germany). The measured intensities were reduced by the values of only Acm-JRL in TBS, and fluorescence polarisation was calculated. The data were analysed with the MARS Data

Analysis Software (BMG Labtech GmbH, Germany) and fitted according to the four-parameter variable slope model. Bottom and top plateaus were fixed according to the highest concentration of mannoside, and the data was reanalysed with these values fixed.

Fluorescent labelling of Acm-JRL and glycan array analysis

For FITC: A concentrated solution of Acm-JRL (0.12 μmol) was diluted in Na_2CO_3 -buffer (100 mM, pH 9.3) and concentrated (vivaspin, 10,000 MWCO) to yield a final protein concentration of 78 μM (1.8 mg in 1.5 mL). FITC (Merck, Darmstadt, Germany, 95 μL of a 7.7 mM solution in carbonate buffer pH 9.3, 0.73 μmol , 6.2 eq.) was added and incubated for 1 h at r.t.. The reaction was quenched with ethanolamine (1 μmol , 8.3 eq.) for 1 h at r.t.. The reaction was first purified by filtration (vivaspin, 10000 MWCO), then as described above for unlabelled Acm-JRL. The protein concentration and degree of labelling (DOL) was calculated according to the manufacturers protocol (Thermo Scientific, Rockford, USA):

$$c = \frac{A_{280\text{nm}} - A_{495\text{nm}} * k}{\epsilon^{280\text{nm}}}$$

$$DOL = \frac{A_{495\text{nm}}}{\epsilon_{FITC}^{495\text{nm}} * c}$$

$A_{280\text{nm}}$

Absorption of labeled protein at 280 nm

$A_{495\text{nm}}$

Absorption of labeled protein at 495 nm

$\epsilon^{280\text{nm}}$

extinction coefficient of unlabelled protein at 280 nm

$k = 0.3$

correction factor for FITC

$$\epsilon_{FITC}^{495\text{nm}} = 68000 \frac{l}{\text{mol} * \text{cm}}$$

extinction coefficient of FITC at 495 nm

for NHS-activated Cy3: A concentrated solution of Acm-JRL (0.24 μmol) was diluted in PBS pH 8.4 and concentrated (vivaspin, 10,000 MWCO) to yield a final protein concentration of 293 μM (4.5 mg in 1.5 mL). NHS-activated Cy3 (Lumiprobe, Hannover, Germany, 75 μL of a 29 mM solution in DMSO, 2.2 μmol , 9 eq.) was added and incubated for 5 h at r.t.. The reaction was first purified by filtration (vivaspin, 10,000 MWCO), then as described above for unlabelled Acm-JRL. The protein concentration and degree of labelling (DOL) was calculated as described above.

$k = 0.08$

correction factor for Cy3

$$\epsilon_{Cy3}^{550\text{nm}} = 150000 \frac{l}{\text{mol} * \text{cm}}$$

extinction coefficient of Cy3 at 550 nm

FITC-labeled Acm-JRL was tested by the National Center for Functional Glycomics (NCFG, Boston, MA, USA) on the CFG glycan microarray version 5.5 containing 585 printed glycans in replicates of 6. Standard procedures of NCFG (details see https://ncfg.hms.harvard.edu/files/ncfg/files/protocol-direct_glycan_binding_assay-cfg_slides.docx) were run at 5 and 50 µg/ml protein based on the protocol by Blixt *et al.* [185]. Raw-data will be shared online on the CFG website.

Cy3-labelled Acm-JRL was tested in-house on a glycan microarray slide from Semiotik LLC (Moscow, Russia) containing 610 printed glycans in replicates of 6. Standard procedures were run at 20, 200 and 400 µg/mL based on the protocol by Olivera-Ardid *et al.* [186]. Fluorescence intensity was measured at 565 nm upon excitation at 520 nm on a Sapphire Biomolecular imager (azure biosystems, Dublin, CA, USA) at 10 µm resolution. Scan data was processed with ScanArray software (Perkin Elmer, Waltham, MA, USA), using OSPS090418_full.360.80 um.gal (kindly provided by Semiotik) for dot-glycan assignment. Raw data (dot mean fluorescence intensity) was processed by GraphPad Prism 8 (Graph Pad Software, San Diego, CA, USA). Processed data in table format is provided on the following pages.

Protease activity assay

Purified Acm-JRL was used and adjusted to $A_{280\text{nm}} = 1$. 2 mg bromelain powder were suspended in 2 mL buffer (100 mM KCl, 5 mM KOAc, 5 mM HOAc, pH 4.6) and incubated at 37°C, 500 rpm on an Themomixer (Eppendorf, Hamburg, Germany) for 10 min. After centrifugation (17600 rcf, 10 min, r.t.) the supernatant was isolated and adjusted to $A_{280\text{nm}} = 1$. 4 µL protein was diluted in 200 µL buffer. Z-Lys-ONP (Merck, Darmstadt, Germany, 4 µL from a 25 mM solution in H₂O/MeCN 1:1) was added and absorption at 340 nm was measured on a CLARIOstar microplate reader (BMG Labtech, Ortenberg, Germany) for 300 s (5 s interval). Blank controls without enzyme and substrate were performed for background subtraction. Data was analysed by using GraphPad Prism 8 (Graph Pad Software, San Diego, CA, USA).

Table S1. Row number assignment for Semiotic glycan ID.

saccharide nomenclature, row number, SGID

| | | | | | |
|----------------------------------|----|----|---|-----|-----|
| Fuca-sp3 | 1 | 1 | Gal α 1-3Gal β -sp3 | 61 | 76 |
| Gal α -sp3 | 2 | 2 | Gal α 1-3GalNAc β -sp3 | 62 | 77 |
| Gal β -sp3 | 3 | 3 | Gal α 1-3GalNAc α -sp3 | 63 | 78 |
| GalNAc α 1-OSer | 4 | 4 | Gal α 1-3GlcNAc β -sp3 | 64 | 80 |
| GalNAc α -sp3 | 5 | 5 | Gal α 1-4GlcNAc β -sp3 | 65 | 81 |
| GalNAc β -sp3 | 6 | 6 | Gal α 1-4GlcNAc β -sp8 | 66 | 82 |
| Glc α -sp3 | 7 | 7 | Gal α 1-6Glc β -sp4 | 67 | 83 |
| Glc β -sp3 | 8 | 9 | Gal β 1-2Gal β -sp3 | 68 | 84 |
| GlcNAc β -sp3 | 9 | 10 | Gal β 1-3GlcNAc β -sp3 | 69 | 85 |
| GlcNAc β -sp2 | 10 | 11 | Gal β 1-3GlcNAc β -sp2 | 70 | 86 |
| GlcNAc β -sp8 | 11 | 13 | Gal β 1-3Gal β -sp3 | 71 | 87 |
| GlcN(Gc) β -sp4 | 12 | 14 | Gal β 1-3GalNAc β -sp3 | 72 | 88 |
| HOCH2(HOCH)4CH2NH2 | 13 | 15 | Gal β 1-3GalNAc α -sp3 | 73 | 89 |
| Man α -sp3 | 14 | 16 | Gal β 1-4Glc β -sp2 | 74 | 92 |
| Man α -sp4 | 15 | 17 | Gal β 1-4Glc β -sp4 | 75 | 93 |
| Man β -sp4 | 16 | 18 | Gal β 1-4Gal β -sp4 | 76 | 94 |
| ManNAc β -sp4 | 17 | 19 | Gal β 1-4GlcNAc β -sp2 | 77 | 96 |
| Rha α -sp3 | 18 | 20 | Gal β 1-4GlcNAc β -sp3 | 78 | 97 |
| Gal β -sp4 | 19 | 21 | Gal β 1-4GlcNAc β -sp5 | 79 | 98 |
| GlcNAc β -sp4 | 20 | 22 | Gal β 1-4GlcNAc β -sp8 | 80 | 99 |
| GalNAc β -sp4 | 21 | 23 | Gal β 1-6Gal β -sp4 | 81 | 100 |
| GlcNAc α -sp3 | 22 | 24 | GalNAc α 1-3GalNAc β -sp3 | 82 | 101 |
| GalNAc β -sp10 | 23 | 25 | GalNAc α 1-3Gal β -sp3 | 83 | 102 |
| Rha β -sp4 | 24 | 26 | GalNAc α 1-3GalNAc α -sp3 | 84 | 103 |
| Xyl β -sp4 | 25 | 28 | GalNAc β 1-3Gal β -sp3 | 85 | 104 |
| Fuc β -sp4 | 26 | 29 | GalNAc β 1-3GalNAc β -sp3 | 86 | 105 |
| Glc β -sp4 | 27 | 30 | GalNAc β 1-4GlcNAc β -sp3 | 87 | 106 |
| L-Ara α -sp4 | 28 | 31 | GalNAc β 1-4GlcNAc β -sp2 | 88 | 107 |
| GalNGc β -sp3 | 29 | 32 | Glc α 1-4Glc β -sp3 | 89 | 110 |
| Glc-2-NH2 | 30 | 33 | Glc β 1-4Glc β -sp4 | 90 | 111 |
| L-Glc β -sp4 | 31 | 34 | Glc β 1-6Glc β -sp4 | 91 | 112 |
| 3-O-Su-Gal β -sp3 | 32 | 37 | GlcNAc β 1-3GalNAc α -sp3 | 92 | 113 |
| 3-O-Su-GalNAc β -sp3 | 33 | 38 | GlcNAc β 1-3Man β -sp4 | 93 | 114 |
| 6-O-Su-GalNAc α -sp3 | 34 | 41 | GlcNAc β 1-4GlcNAc β -sp3 | 94 | 116 |
| 6-O-Su-GlcNAc β -sp3 | 35 | 43 | GlcNAc β 1-4GlcNAc β -sp4 | 95 | 117 |
| GlcA α -sp3 | 36 | 44 | GlcNAc β 1-6GalNAc α -sp3 | 96 | 118 |
| GlcA β -sp3 | 37 | 45 | Man α 1-4Man β -sp4 | 97 | 121 |
| 6-H2PO3Glc β -sp4 | 38 | 46 | Man α 1-6Man β -sp4 | 98 | 122 |
| 6-H2PO3Man α -sp3 | 39 | 47 | Man β 1-4GlcNAc β -sp4 | 99 | 123 |
| Neu5Ac α -sp3 | 40 | 48 | 6-Bn-Gal β 1-4GlcNAc β -sp2 | 100 | 125 |
| Neu5Ac α -sp9 | 41 | 49 | 6-Bn-Gal α 1-4(6-Bn)GlcNAc β -sp3 | 101 | 126 |
| Neu5Ac β -sp3 | 42 | 50 | Gal β 1-4Glc β -sp4-Trp | 102 | 128 |
| Neu5Ac β -sp9 | 43 | 51 | Gal β 1-3(6-O-Bn)GlcNAc β -sp3 | 103 | 129 |
| Neu5Gc α -sp3 | 44 | 52 | (6-O-Bn-Gal β 1)-3GlcNAc β -sp2 | 104 | 130 |
| Neu5Gc β -sp3 | 45 | 53 | (6-O-Bn-Gal β 1)-3(6-O-Bn)GlcNAc β -sp3 | 105 | 131 |
| 3-O-Su-GlcNAc β -sp3 | 46 | 55 | Gal β 1-3GalNAc α -sp5 | 106 | 132 |
| D-Rib β -sp4 | 47 | 57 | Gal β 1-4Glc β -sp4-Ala | 107 | 133 |
| Fuc β -sp3 | 48 | 58 | Gal β 1-4Glc β -sp4-Asn | 108 | 135 |
| α Kdo-5-phosphate-sp11 | 49 | 59 | Gal β 1-4Glc β -sp4-Ile | 109 | 136 |
| 6-O-Su-Gal β -sp3 | 50 | 60 | Gal β 1-4Glc β -sp4-Nle | 110 | 137 |
| 3-O-Su-GalNAc α -sp3 | 51 | 61 | Gal β 1-4Glc β -sp4-Val | 111 | 138 |
| GlcA β -sp2 | 52 | 62 | Gal β 1-4GlcNAc α -sp3 | 112 | 139 |
| 4-O-Su-GlcNAc β -sp2 | 53 | 63 | Gal α 1-3GalNAc(fur) β -sp3 | 113 | 140 |
| 4-O-Su-Gal β -sp3 | 54 | 64 | GlcNAc α 1-3GalNAc β -sp3 | 114 | 142 |
| 4-O-Su-GalNAc α -sp3 | 55 | 65 | Fuca1-2(3-O-Su)Gal β -sp3 | 115 | 143 |
| 4-O-Su-GalNAc β -sp3 | 56 | 66 | Gal β 1-3(6-O-Su)GlcNAc β -sp2 | 116 | 144 |
| Fuca1-2Gal β -sp3 | 57 | 71 | Gal β 1-3(6-O-Su)GlcNAc β -sp3 | 117 | 145 |
| Fuca1-3GlcNAc β -sp3 | 58 | 72 | Gal β 1-4(6-O-Su)Glc β -sp2 | 118 | 146 |
| Fuca1-4GlcNAc β -sp3 | 59 | 73 | GlcNAc β 1-4(6-O-Su)GlcNAc β -sp2 | 119 | 149 |
| Gal α 1-2Gal β -sp3 | 60 | 75 | 3-O-Su-Gal β 1-3GalNAc α -sp3 | 120 | 150 |

| | | | | | |
|--|-----|-----|---------------------------------------|-----|-----|
| 6-O-Su-Galβ1-3GalNAcα-sp3 | 121 | 151 | Fucβ1-2Galβ1-3GlcNAcβ-sp3 | 181 | 230 |
| 6-O-Su-Galβ1-4Glcβ-sp2 | 122 | 153 | Galβ1-4GlcNAcβ1-3GalNAcα-sp3 | 182 | 231 |
| 3-O-Su-Galβ1-3GlcNAcβ-sp3 | 123 | 154 | Galβ1-4GlcNAcβ1-6GalNAcα-sp3 | 183 | 232 |
| 3-O-Su-Galβ1-4GlcNAcβ-sp2 | 124 | 156 | Galβ1-3(Fuca1-4)GlcNAcβ-sp3 | 184 | 233 |
| 4-O-Su-Galβ1-4GlcNAcβ-sp2 | 125 | 158 | Galβ1-4(Fuca1-3)GlcNAcβ-sp3 | 185 | 234 |
| 4-O-Su-Galβ1-4GlcNAcβ-sp3 | 126 | 159 | GalNAcα1-3(Fuca1-2)Galβ-sp3 | 186 | 235 |
| 6-O-Su-Galβ1-3GlcNAcβ-sp2 | 127 | 160 | GalNAcα1-3(Fuca1-2)Galβ-sp5 | 187 | 236 |
| 6-O-Su-Galβ1-3GlcNAcβ-sp3 | 128 | 161 | GalNHα1-3(Fuca1-2)Galβ-OCH2CH2CH2NHAc | 188 | 237 |
| 6-O-Su-Galβ1-4GlcNAcβ-sp2 | 129 | 162 | GalNAcβ1-3(Fuca1-2)Galβ-sp3 | 189 | 239 |
| GlcAβ1-3GlcNAcβ-sp3 | 130 | 164 | (Glcα1-4)3β-sp4 | 190 | 240 |
| GlcAβ1-3Galβ-sp3 | 131 | 165 | (Glcα1-6)3β-sp4 | 191 | 241 |
| GlcAβ1-6Galβ-sp3 | 132 | 166 | GlcNAc1αa1-3Galβ1-4GlcNAcβ-sp2 | 192 | 242 |
| GlcNAcβ1-4-[HOOC(CH3)CH]-3-O-GlcNAcβ-sp4 | 133 | 167 | GlcNAcα1-3Galβ1-4GlcNAcβ-sp3 | 193 | 243 |
| GlcNAcβ1-4Mur-L-Ala-D-i-Gln-Lys | 134 | 168 | GlcNAcα1-6Galβ1-4GlcNAcβ-sp2 | 194 | 245 |
| Neu5Acα2-3Galβ-sp3 | 135 | 169 | GlcNAcβ1-2Galβ1-3GalNAcα-sp3 | 195 | 246 |
| Neu5Acα2-6Galβ-sp3 | 136 | 170 | GlcNAcβ1-3Galβ1-3GalNAcα-sp3 | 196 | 247 |
| Neu5Acα2-3GalNAcα-sp3 | 137 | 171 | GlcNAcβ1-3Galβ1-4GlcNAcβ-sp2 | 197 | 249 |
| Neu5Acα2-6GalNAcα-sp3 | 138 | 172 | GlcNAcβ1-3Galβ1-4GlcNAcβ-sp3 | 198 | 250 |
| Neu5Acβ2-6GalNAcα-sp3 | 139 | 173 | GlcNAcβ1-4Galβ1-4GlcNAcβ-sp2 | 199 | 251 |
| Neu5Gca2-6GalNAcα-sp3 | 140 | 174 | GlcNAcβ1-4GlcNAcβ1-4GlcNAcβ-sp4 | 200 | 252 |
| 3-O-Su-Galβ1-4(6-O-Su)GlcNAcβ-sp3 | 141 | 177 | GlcNAcβ1-6Galβ1-4GlcNAcβ-sp2 | 201 | 253 |
| 6-O-Su-Galβ1-4(6-O-Su)Glcβ-sp2 | 142 | 178 | GlcNAcβ1-6(Galβ1-3)GalNAcα-sp3 | 202 | 254 |
| 6-O-Su-Galβ1-3(6-O-Su)GlcNAcβ-sp2 | 143 | 179 | GlcNAcβ1-6(GlcNAcβ1-3)GalNAcα-sp3 | 203 | 255 |
| 6-O-Su-Galβ1-4(6-O-Su)GlcNAcβ-sp2 | 144 | 180 | GlcNAcβ1-6(GlcNAcβ1-4)GalNAcα-sp3 | 204 | 256 |
| 3,4-O-Su2-Galβ1-4GlcNAcβ-sp3 | 145 | 181 | Manα1-6(Manα1-3)Manβ-sp4 | 205 | 258 |
| 3,6-O-Su2-Galβ1-4GlcNAcβ-sp2 | 146 | 182 | Galβ1-4(Galβ1-3)GlcNAcβ-sp3 | 206 | 259 |
| 4,6-O-Su2-Galβ1-4GlcNAcβ-sp2 | 147 | 183 | Galβ1-3(Fucβ1-4)GlcNAcβ-sp3 | 207 | 260 |
| 4,6-O-Su2-Galβ1-4GlcNAcβ-sp3 | 148 | 184 | (GalNAcβ-PEG2)3β-DD | 208 | 263 |
| Neu5Acα2-8Neu5Acα2-sp9 | 149 | 187 | Galβ1-4Galβ1-4GlcNAcβ-sp3 | 209 | 264 |
| Neu5Acα2-8Neu5Acβ-sp9 | 150 | 188 | Galα1-4Galβ1-4GlcNAcβ-sp3 | 210 | 266 |
| 3,6-O-Su2-Galβ1-4(6-O-Su)GlcNAcβ-sp2 | 151 | 189 | GlcNAcβ1-3Galβ1-3GlcNAcβ-sp3 | 211 | 267 |
| Galβ1-4-(6-P)GlcNAcβ-sp2 | 152 | 190 | GlcNAcβ1-4(Fuca1-6)GlcNAcβ-sp3 | 212 | 268 |
| 6-P-Galβ1-4GlcNAcβ-sp2 | 153 | 191 | Neu5Acα2-3Galβ1-4Glcβ-sp4-Cit | 213 | 272 |
| GalNAcβ1-4(6-O-Su)GlcNAcβ-sp3 | 154 | 192 | Fucβ1-2Galβ1-4GlcNAcβ-sp3 | 214 | 273 |
| 3-O-Su-GalNAcβ1-4GlcNAcβ-sp3 | 155 | 193 | GalNAcα1-3Galβ1-4GlcNAcβ-sp3 | 215 | 274 |
| 6-O-Su-GalNAcβ1-4GlcNAcβ-sp3 | 156 | 194 | GalNAcβ1-3Galβ1-4GlcNAcβ-sp3 | 216 | 275 |
| 6-O-Su-GalNAcβ1-4-(3-O-Ac)GlcNAcβ-sp3 | 157 | 195 | GlcNAcβ1-4Galβ1-4GlcNAcβ-sp3 | 217 | 276 |
| 3-O-Su-GalNAcβ1-4(3-O-Su)-GlcNAcβ-sp3 | 158 | 196 | GalNGca1-3(Fuca1-2)Galβ-sp3 | 218 | 277 |
| 3,6-O-Su2-GalNAcβ1-4-GlcNAcβ-sp3 | 159 | 197 | GalNAcα1-3GalNAcβ1-3Galβ-sp3 | 219 | 278 |
| 4,6-O-Su2-GalNAcβ1-4GlcNAcβ-sp3 | 160 | 198 | Galβ1-3GlcNAcα1-3GalNAcα-sp3 | 220 | 279 |
| 4,6-O-Su2-GalNAcβ1-4-(3-O-Ac)GlcNAcβ-sp3 | 161 | 199 | Fuca1-2Galβ1-3GalNAcβ-sp3 | 221 | 281 |
| 4-O-Su-GalNAcβ1-4GlcNAcβ-sp3 | 162 | 200 | Galβ1-3Galβ1-4GlcNAcβ-sp3 | 222 | 282 |
| 6-O-Su-GalNAcβ1-4(6-O-Su)GlcNAcβ-sp3 | 163 | 202 | 3-O-Su-Galβ1-3(Fuca1-4)GlcNAcβ-sp3 | 223 | 287 |
| Galβ1-4(6-O-Su)GlcNAcβ-sp2 | 164 | 203 | 3-O-Su-Galβ1-4(Fuca1-3)GlcNAcβ-sp3 | 224 | 288 |
| 4-O-Su-GalNAcβ1-4GlcNAcβ-sp2 | 165 | 204 | Neu5Acα2-6(Galβ1-3)GalNAcα-sp3 | 225 | 289 |
| Neu5Acα2-6GalNAcβ-sp3 | 166 | 205 | Neu5Acα2-6(Galα1-3)GalNAcα-sp3 | 226 | 290 |
| Neu5Gca2-3Galβ-sp3 | 167 | 206 | Neu5Acβ2-6(Galβ1-3)GalNAcα-sp3 | 227 | 291 |
| Galβ1-3GlcNAcβ-sp4 | 168 | 208 | Neu5Acα2-3Galβ1-3GalNAcα-sp3 | 228 | 292 |
| αKdo-(2→8)-αKdo-sp11 | 169 | 211 | Neu5Acα2-3Galβ1-4Glcβ-sp3 | 229 | 293 |
| \$delta\$GlcAβ1-3Galβ-sp3 | 170 | 214 | Neu5Acα2-3Galβ1-4Glcβ-sp4 | 230 | 294 |
| Fuca1-2Galβ1-3GlcNAcβ-sp3 | 171 | 215 | Neu5Acα2-6Galβ1-4Glcβ-sp2 | 231 | 295 |
| Fuca1-2Galβ1-4GlcNAcβ-sp3 | 172 | 216 | Neu5Acβ2-6Galβ1-4Glcβ-sp2 | 232 | 297 |
| Fuca1-2Galβ1-3GalNAcα-sp3 | 173 | 217 | Neu5Acα2-3Galβ1-4GlcNAcβ-sp3 | 233 | 298 |
| Fuca1-2Galβ1-4Glcβ-sp4 | 174 | 219 | Neu5Acα2-3Galβ1-3GlcNAcβ-sp3 | 234 | 299 |
| Galα1-3Galβ1-4GlcNAcβ-sp3 | 175 | 222 | Neu5Acα2-6Galβ1-4GlcNAcβ-sp3 | 235 | 300 |
| Galα1-4Galβ1-4Glcβ-sp2 | 176 | 223 | Neu5Acβ2-6Galβ1-4GlcNAcβ-sp3 | 236 | 302 |
| Galα1-4Galβ1-4GlcNAcβ-sp2 | 177 | 225 | Neu5Gca2-3Galβ1-4GlcNAcβ-sp3 | 237 | 303 |
| Galα1-3(Fuca1-2)Galβ-sp3 | 178 | 226 | Neu5Gca2-6Galβ1-4GlcNAcβ-sp3 | 238 | 304 |
| Galα1-3(Fuca1-2)Galβ-sp5 | 179 | 227 | Neu5Gcβ2-6Galβ1-4GlcNAcβ-sp3 | 239 | 305 |
| Galβ1-3Galβ1-4GlcNAcβ-sp4 | 180 | 229 | Neu5Acα2-6(Neu5Acα2-3)GalNAcα-sp3 | 240 | 309 |

| | | | | | |
|--|-----|-----|---------------------------------------|-----|-----|
| 6-O-Su-Galβ1-3GalNAcα-sp3 | 121 | 151 | Fucβ1-2Galβ1-3GlcNAcβ-sp3 | 181 | 230 |
| 6-O-Su-Galβ1-4Glcβ-sp2 | 122 | 153 | Galβ1-4GlcNAcβ1-3GalNAcα-sp3 | 182 | 231 |
| 3-O-Su-Galβ1-3GlcNAcβ-sp3 | 123 | 154 | Galβ1-4GlcNAcβ1-6GalNAcα-sp3 | 183 | 232 |
| 3-O-Su-Galβ1-4GlcNAcβ-sp2 | 124 | 156 | Galβ1-3(Fuca1-4)GlcNAcβ-sp3 | 184 | 233 |
| 4-O-Su-Galβ1-4GlcNAcβ-sp2 | 125 | 158 | Galβ1-4(Fuca1-3)GlcNAcβ-sp3 | 185 | 234 |
| 4-O-Su-Galβ1-4GlcNAcβ-sp3 | 126 | 159 | GalNAcα1-3(Fuca1-2)Galβ-sp3 | 186 | 235 |
| 6-O-Su-Galβ1-3GlcNAcβ-sp2 | 127 | 160 | GalNAcα1-3(Fuca1-2)Galβ-sp5 | 187 | 236 |
| 6-O-Su-Galβ1-3GlcNAcβ-sp3 | 128 | 161 | GalNHα1-3(Fuca1-2)Galβ-OCH2CH2CH2NHAc | 188 | 237 |
| 6-O-Su-Galβ1-4GlcNAcβ-sp2 | 129 | 162 | GalNAcβ1-3(Fuca1-2)Galβ-sp3 | 189 | 239 |
| GlcAβ1-3GlcNAcβ-sp3 | 130 | 164 | (Glcα1-4)3β-sp4 | 190 | 240 |
| GlcAβ1-3Galβ-sp3 | 131 | 165 | (Glcα1-6)3β-sp4 | 191 | 241 |
| GlcAβ1-6Galβ-sp3 | 132 | 166 | GlcNAc1αa1-3Galβ1-4GlcNAcβ-sp2 | 192 | 242 |
| GlcNAcβ1-4-[HOOC(CH3)CH]-3-O-GlcNAcβ-sp4 | 133 | 167 | GlcNAcα1-3Galβ1-4GlcNAcβ-sp3 | 193 | 243 |
| GlcNAcβ1-4Mur-L-Ala-D-i-Gln-Lys | 134 | 168 | GlcNAcα1-6Galβ1-4GlcNAcβ-sp2 | 194 | 245 |
| Neu5Acα2-3Galβ-sp3 | 135 | 169 | GlcNAcβ1-2Galβ1-3GalNAcα-sp3 | 195 | 246 |
| Neu5Acα2-6Galβ-sp3 | 136 | 170 | GlcNAcβ1-3Galβ1-3GalNAcα-sp3 | 196 | 247 |
| Neu5Acα2-3GalNAcα-sp3 | 137 | 171 | GlcNAcβ1-3Galβ1-4GlcNAcβ-sp2 | 197 | 249 |
| Neu5Acα2-6GalNAcα-sp3 | 138 | 172 | GlcNAcβ1-3Galβ1-4GlcNAcβ-sp3 | 198 | 250 |
| Neu5Acβ2-6GalNAcα-sp3 | 139 | 173 | GlcNAcβ1-4Galβ1-4GlcNAcβ-sp2 | 199 | 251 |
| Neu5Gca2-6GalNAcα-sp3 | 140 | 174 | GlcNAcβ1-4GlcNAcβ1-4GlcNAcβ-sp4 | 200 | 252 |
| 3-O-Su-Galβ1-4(6-O-Su)GlcNAcβ-sp3 | 141 | 177 | GlcNAcβ1-6Galβ1-4GlcNAcβ-sp2 | 201 | 253 |
| 6-O-Su-Galβ1-4(6-O-Su)Glcβ-sp2 | 142 | 178 | GlcNAcβ1-6(Galβ1-3)GalNAcα-sp3 | 202 | 254 |
| 6-O-Su-Galβ1-3(6-O-Su)GlcNAcβ-sp2 | 143 | 179 | GlcNAcβ1-6(GlcNAcβ1-3)GalNAcα-sp3 | 203 | 255 |
| 6-O-Su-Galβ1-4(6-O-Su)GlcNAcβ-sp2 | 144 | 180 | GlcNAcβ1-6(GlcNAcβ1-4)GalNAcα-sp3 | 204 | 256 |
| 3,4-O-Su2-Galβ1-4GlcNAcβ-sp3 | 145 | 181 | Manα1-6(Manα1-3)Manβ-sp4 | 205 | 258 |
| 3,6-O-Su2-Galβ1-4GlcNAcβ-sp2 | 146 | 182 | Galβ1-4(Galβ1-3)GlcNAcβ-sp3 | 206 | 259 |
| 4,6-O-Su2-Galβ1-4GlcNAcβ-sp2 | 147 | 183 | Galβ1-3(Fucβ1-4)GlcNAcβ-sp3 | 207 | 260 |
| 4,6-O-Su2-Galβ1-4GlcNAcβ-sp3 | 148 | 184 | (GalNAcβ-PEG2)3β-DD | 208 | 263 |
| Neu5Acα2-8Neu5Acα2-sp9 | 149 | 187 | Galβ1-4Galβ1-4GlcNAcβ-sp3 | 209 | 264 |
| Neu5Acα2-8Neu5Acβ-sp9 | 150 | 188 | Galα1-4Galβ1-4GlcNAcβ-sp3 | 210 | 266 |
| 3,6-O-Su2-Galβ1-4(6-O-Su)GlcNAcβ-sp2 | 151 | 189 | GlcNAcβ1-3Galβ1-3GlcNAcβ-sp3 | 211 | 267 |
| Galβ1-4-(6-P)GlcNAcβ-sp2 | 152 | 190 | GlcNAcβ1-4(Fuca1-6)GlcNAcβ-sp3 | 212 | 268 |
| 6-P-Galβ1-4GlcNAcβ-sp2 | 153 | 191 | Neu5Acα2-3Galβ1-4Glcβ-sp4-Cit | 213 | 272 |
| GalNAcβ1-4(6-O-Su)GlcNAcβ-sp3 | 154 | 192 | Fucβ1-2Galβ1-4GlcNAcβ-sp3 | 214 | 273 |
| 3-O-Su-GalNAcβ1-4GlcNAcβ-sp3 | 155 | 193 | GalNAcα1-3Galβ1-4GlcNAcβ-sp3 | 215 | 274 |
| 6-O-Su-GalNAcβ1-4GlcNAcβ-sp3 | 156 | 194 | GalNAcβ1-3Galβ1-4GlcNAcβ-sp3 | 216 | 275 |
| 6-O-Su-GalNAcβ1-4-(3-O-Ac)GlcNAcβ-sp3 | 157 | 195 | GlcNAcβ1-4Galβ1-4GlcNAcβ-sp3 | 217 | 276 |
| 3-O-Su-GalNAcβ1-4(3-O-Su)-GlcNAcβ-sp3 | 158 | 196 | GalNGca1-3(Fuca1-2)Galβ-sp3 | 218 | 277 |
| 3,6-O-Su2-GalNAcβ1-4-GlcNAcβ-sp3 | 159 | 197 | GalNAcα1-3GalNAcβ1-3Galβ-sp3 | 219 | 278 |
| 4,6-O-Su2-GalNAcβ1-4GlcNAcβ-sp3 | 160 | 198 | Galβ1-3GlcNAcα1-3GalNAcα-sp3 | 220 | 279 |
| 4,6-O-Su2-GalNAcβ1-4-(3-O-Ac)GlcNAcβ-sp3 | 161 | 199 | Fuca1-2Galβ1-3GalNAcβ-sp3 | 221 | 281 |
| 4-O-Su-GalNAcβ1-4GlcNAcβ-sp3 | 162 | 200 | Galβ1-3Galβ1-4GlcNAcβ-sp3 | 222 | 282 |
| 6-O-Su-GalNAcβ1-4(6-O-Su)GlcNAcβ-sp3 | 163 | 202 | 3-O-Su-Galβ1-3(Fuca1-4)GlcNAcβ-sp3 | 223 | 287 |
| Galβ1-4(6-O-Su)GlcNAcβ-sp2 | 164 | 203 | 3-O-Su-Galβ1-4(Fuca1-3)GlcNAcβ-sp3 | 224 | 288 |
| 4-O-Su-GalNAcβ1-4GlcNAcβ-sp2 | 165 | 204 | Neu5Acα2-6(Galβ1-3)GalNAcα-sp3 | 225 | 289 |
| Neu5Acα2-6GalNAcβ-sp3 | 166 | 205 | Neu5Acα2-6(Galα1-3)GalNAcα-sp3 | 226 | 290 |
| Neu5Gca2-3Galβ-sp3 | 167 | 206 | Neu5Acβ2-6(Galβ1-3)GalNAcα-sp3 | 227 | 291 |
| Galβ1-3GlcNAcβ-sp4 | 168 | 208 | Neu5Acα2-3Galβ1-3GalNAcα-sp3 | 228 | 292 |
| αKdo-(2→8)-αKdo-sp11 | 169 | 211 | Neu5Acα2-3Galβ1-4Glcβ-sp3 | 229 | 293 |
| \$delta\$GlcAβ1-3Galβ-sp3 | 170 | 214 | Neu5Acα2-3Galβ1-4Glcβ-sp4 | 230 | 294 |
| Fuca1-2Galβ1-3GlcNAcβ-sp3 | 171 | 215 | Neu5Acα2-6Galβ1-4Glcβ-sp2 | 231 | 295 |
| Fuca1-2Galβ1-4GlcNAcβ-sp3 | 172 | 216 | Neu5Acβ2-6Galβ1-4Glcβ-sp2 | 232 | 297 |
| Fuca1-2Galβ1-3GalNAcα-sp3 | 173 | 217 | Neu5Acα2-3Galβ1-4GlcNAcβ-sp3 | 233 | 298 |
| Fuca1-2Galβ1-4Glcβ-sp4 | 174 | 219 | Neu5Acα2-3Galβ1-3GlcNAcβ-sp3 | 234 | 299 |
| Galα1-3Galβ1-4GlcNAcβ-sp3 | 175 | 222 | Neu5Acα2-6Galβ1-4GlcNAcβ-sp3 | 235 | 300 |
| Galα1-4Galβ1-4Glcβ-sp2 | 176 | 223 | Neu5Acβ2-6Galβ1-4GlcNAcβ-sp3 | 236 | 302 |
| Galα1-4Galβ1-4GlcNAcβ-sp2 | 177 | 225 | Neu5Gca2-3Galβ1-4GlcNAcβ-sp3 | 237 | 303 |
| Galα1-3(Fuca1-2)Galβ-sp3 | 178 | 226 | Neu5Gca2-6Galβ1-4GlcNAcβ-sp3 | 238 | 304 |
| Galα1-3(Fuca1-2)Galβ-sp5 | 179 | 227 | Neu5Gcβ2-6Galβ1-4GlcNAcβ-sp3 | 239 | 305 |
| Galβ1-3Galβ1-4GlcNAcβ-sp4 | 180 | 229 | Neu5Acα2-6(Neu5Acα2-3)GalNAcα-sp3 | 240 | 309 |

| | | |
|---|-----|-----|
| Neu5Aca2-3Galβ1-4GlcNAcβ-O(CH2)3NH-amide-Neu5Aca2-3Galβ1-4GlcNAcβ-sp3 | 241 | 310 |
| Neu5Aca2-3Galβ1-4-(6-O-Su)GlcNAcβ-sp3 | 242 | 315 |
| Fuca1-2(6-Su)Galβ1-4GlcNAcβ-sp3 | 243 | 316 |
| Neu5Aca2-6Galβ1-4-(6-O-Su)GlcNAcβ-sp3 | 244 | 318 |
| Neu5Aca2-3-(6-O-Su)Galβ1-4GlcNAcβ-sp3 | 245 | 319 |
| 4-O-Su-Neu5Aca2-3-(6-O-Su)Galβ1-4GlcNAcβ-sp3 | 246 | 320 |
| (Neu5Aca2-8)3-sp3 | 247 | 321 |
| (Neu5Aca2-8)3β-sp3 | 248 | 322 |
| Neu5Aca2-6Galβ1-3GlcNAcβ-sp3 | 249 | 323 |
| Neu5Aca2-6Galβ1-3(6-O-Su)GlcNAcβ-sp3 | 250 | 324 |
| Neu5Aca2-3Galβ1-4Glcβ-sp4-Nle | 251 | 327 |
| Neu5Aca2-3Galβ1-4Glcβ-sp4-Phe | 252 | 328 |
| Neu5Aca2-3Galβ1-4Glcβ-sp4-Trp | 253 | 329 |
| Neu5Gca2-3Galβ1-3GlcNAcβ-sp3 | 254 | 331 |
| Neu5Gca2-3Galβ1-4-(6-O-Su)GlcNAcβ-sp3 | 255 | 334 |
| Neu5Aca2-3Galβ1-3-(6-O-Su)GlcNAcβ-sp3 | 256 | 335 |
| GalNAca1-4Galβ1-4GlcNAcβ-sp3 | 257 | 337 |
| Neu5Aca2-6Galβ1-3GalNAca-sp3 | 258 | 338 |
| Gala1-3(Neu5Acβ2-6)GalNAcβ-sp3 | 259 | 340 |
| Neu5Aca2-3(6-O-Su)Galβ1-3GalNAca-sp3 | 260 | 342 |
| Neu5Acβ2-3Galβ1-4GlcNAcβ-sp3 | 261 | 344 |
| Neu5Aca2-3Galβ1-3(6-O-Su)GalNAca-sp3 | 262 | 345 |
| Neu5Aca2-3-(6-O-Su)Galβ1-4(6-O-Su)GlcNAcβ-sp3 | 263 | 346 |
| Neu5Gca2-3Galβ1-4Glcβ-sp3 | 264 | 350 |
| Gala1-3(Fuca1-2)Galβ1-3GlcNAcβ-sp3 | 265 | 359 |
| Gala1-3(Fuca1-2)Galβ1-4GlcNAcβ-sp3 | 266 | 360 |
| Gala1-3(Fuca1-2)Galβ1-4GlcNAcβ-sp2 | 267 | 361 |
| Gala1-3(Fuca1-2)Galβ1-3GalNAca-sp3 | 268 | 362 |
| Gala1-3(Fuca1-2)Galβ1-3GalNAcβ-sp3 | 269 | 363 |
| Gala1-3Galβ1-4(Fuca1-3)GlcNAcβ-sp3 | 270 | 364 |
| Gala1-4(Fuca1-2)Galβ1-4GlcNAcβ-sp3 | 271 | 365 |
| GalNAca1-3(Fuca1-2)Galβ1-3GlcNAcβ-sp3 | 272 | 366 |
| GalNAca1-3(Fuca1-2)Galβ1-4GlcNAcβ-sp3 | 273 | 368 |
| GalNAca1-4(Fuca1-2)Galβ1-4GlcNAcβ-sp3 | 274 | 369 |
| GalNAcβ1-3(Fuca1-2)Galβ1-4GlcNAcβ-sp3 | 275 | 370 |
| Fuca1-2Galβ1-3(Fuca1-4)GlcNAcβ-sp3 | 276 | 371 |
| Fuca1-2Galβ1-4(Fuca1-3)GlcNAcβ-sp3 | 277 | 372 |
| Gala1-3Galβ1-4GlcNAcβ1-3Galβ-sp3 | 278 | 373 |
| Gala1-3(Gala1-4)Galβ1-4GlcNAcβ-sp3 | 279 | 374 |
| Galβ1-3GlcNAcβ1-3Galβ1-4Glcβ-sp4 | 280 | 376 |
| Galβ1-3GlcNAcβ1-3Galβ1-3GlcNAcβ-sp2 | 281 | 377 |
| Galβ1-3GlcNAca1-3Galβ1-4GlcNAcβ-sp3 | 282 | 378 |
| Galβ1-3GlcNAcβ1-3Galβ1-4GlcNAcβ-sp3 | 283 | 379 |
| Galβ1-3GlcNAca1-6Galβ1-4GlcNAcβ-sp2 | 284 | 380 |
| Galβ1-3GlcNAcβ1-6Galβ1-4GlcNAcβ-sp2 | 285 | 381 |
| Galβ1-4GlcNAcβ1-3Galβ1-4Glcβ-sp4 | 286 | 383 |
| Galβ1-4GlcNAcβ1-3Galβ1-4GlcNAcβ-sp2 | 287 | 384 |
| Galβ1-4GlcNAca1-6Galβ1-4GlcNAcβ-sp2 | 288 | 386 |
| Galβ1-4GlcNAcβ1-6Galβ1-4GlcNAcβ-sp2 | 289 | 387 |
| Galβ1-4GlcNAcβ1-6(Galβ1-3)GalNAca-sp3 | 290 | 388 |
| GalNAcβ1-3Gala1-4Galβ1-4Glcβ-sp3 | 291 | 389 |
| (Glcα1-4)4β-sp4 | 292 | 390 |
| GalNAca1-3(Fuca1-2)Galβ1-3GalNAca-sp3 | 293 | 392 |
| GlcNAcβ1-6(GlcNAcβ1-3)Galβ1-4GlcNAcβ-sp2 | 294 | 395 |
| (GlcNAcβ1)3-3,4,6-GalNAca-sp3 | 295 | 396 |
| Galβ1-3GlcNAcβ1-3Galβ1-3GlcNAcβ-sp3 | 296 | 401 |
| Galβ1-3GlcNAcβ1-3Galβ1-4GlcNAcβ-sp2 | 297 | 403 |
| GalNAca1-3Galβ1-4(Fuca1-3)GlcNAcβ-sp3 | 298 | 404 |
| GlcNAcβ1-4(GlcNAcβ1-3)Galβ1-4GlcNAcβ-sp3 | 299 | 408 |
| Galβ1-3GlcNAca1-3Galβ1-3GlcNAcβ-sp3 | 300 | 410 |

| | | |
|--|-----|-----|
| 3-O-SuGalβ1-4GlcNAcβ1-3Galβ1-4GlcNAcβ-sp3 | 301 | 419 |
| Galβ1-3GlcNAcβ1-3Galβ1-4Glcα-sp4 | 302 | 421 |
| Neu5Aca2-3Galβ1-4(Fuca1-3)GlcNAcβ-sp3 | 303 | 423 |
| Neu5Aca2-3Galβ1-4(Fucβ1-3)GlcNAcβ-sp3 | 304 | 425 |
| Neu5Aca2-3Galβ1-3(Fuca1-4)GlcNAcβ-sp3 | 305 | 426 |
| Neu5Aca2-3Galβ1-4(Fuca1-3)(6-O-Su-)GlcNAcβ-sp3 | 306 | 428 |
| Neu5Aca2-3(6-O-Su)Galβ1-4(Fuca1-3)GlcNAcβ-sp3 | 307 | 429 |
| Neu5Aca2-3Galβ1-4(2-O-Su-Fuca1-3)GlcNAcβ-sp3 | 308 | 431 |
| Neu5Aca2-3Galβ1-4(3-O-Su-Fuca1-3)GlcNAcβ-sp3 | 309 | 432 |
| Neu5Aca2-8Neu5Aca2-3Galβ1-4Glcβ-sp4 | 310 | 434 |
| Neu5Aca2-3Galβ1-4(2-O-Su-Fuca1-3)(6-O-Su-)GlcNAcβ-sp3 | 311 | 435 |
| 4-O-Su-Neu5Aca2-3(6-O-Su)Galβ1-4(Fuca1-3)GlcNAcβ-sp3 | 312 | 436 |
| GalNAca1-3(Fuca1-2)Galβ1-3GalNAcβ-sp3 | 313 | 437 |
| Fucβ1-2Galβ1-4(Fuca1-3)GlcNAcβ-sp3 | 314 | 438 |
| Neu5Aca2-6(Fuca1-2)Galβ1-4GlcNAcβ-sp3 | 315 | 441 |
| Neu5Aca2-3 (GalNAcβ1-4)Galβ1-4Glcβ-sp4 | 316 | 442 |
| Fuca1-2Galβ1-3GlcNAcβ1-3Galβ1-4Glcβ-sp4 | 317 | 479 |
| Gala1-3Galβ1-4GlcNAcβ1-3Galβ1-4Glcβ-sp4 | 318 | 481 |
| Gala1-3(Fuca1-2)Galβ1-3(Fuca1-4)GlcNAcβ-sp3 | 319 | 482 |
| Gala1-3(Fuca1-2)Galβ1-4(Fuca1-3)GlcNAcβ-sp3 | 320 | 483 |
| Galβ1-4GalNAca1-3(Fuca1-2)Galβ1-4GlcNAcβ-sp3 | 321 | 485 |
| Galβ1-4GlcNAcβ1-6(Galβ1-4GlcNAcβ1-3)GalNAca-sp3 | 322 | 488 |
| Galβ1-4GlcNAcβ1-3(GlcNAcβ1-6)Galβ1-4GlcNAcβ-sp2 | 323 | 489 |
| GalNAca1-3(Fuca1-2)Galβ1-4(Fuca1-3)GlcNAcβ-sp3 | 324 | 491 |
| (Glcα1-6)5β-sp4 | 325 | 492 |
| (GlcNAcβ1-4)5β-sp4 | 326 | 493 |
| Mana1-6(Mana1-3)Mana1-6(Mana1-3)Manβ-sp4 | 327 | 495 |
| Fuca1-2Galβ1-3(Fuca1-4)GlcNAcβ1-3Galβ1-4Glcβ-sp4 | 328 | 496 |
| Galβ1-4GlcNAcβ1-3Galβ1-4GlcNAcβ1-3Galβ1-4GlcNAcβ-sp3 | 329 | 498 |
| Galβ1-4GlcNAcβ1-6(Galβ1-4GlcNAcβ1-3)Galβ1-4GlcNAcβ-sp2 | 330 | 499 |
| Galβ1-3GalNAcβ1-3Gala1-4Galβ1-4Glcβ-sp4 | 331 | 501 |
| (Glcα1-6)6β-sp4 | 332 | 502 |
| (GlcNAcβ1-4)6-sp4 | 333 | 503 |
| (Aβ1-4GNβ1-2Ma1)2-3,6-Mβ1-4GNβ1-4GNβ-sp4 | 334 | 504 |
| (GNβ1-2Ma1)2-3,6-Mβ1-4GNβ1-4GNβ-sp4 | 335 | 505 |
| GalNAcβ1-3(Fuca1-2)Galβ1-4(Fuca1-3)GlcNAcβ-sp3 | 336 | 508 |
| GalNAca1-3GalNAcβ1-3Gala1-4Galβ1-4Glcβ-sp4 | 337 | 511 |
| Neu5Aca2-3Galβ1-4(Fuca1-3)GlcNAcβ1-3Galβ-sp3 | 338 | 528 |
| Neu5Aca2-6Galβ1-4GlcNAcβ1-3Galβ1-4GlcNAcβ-sp3 | 339 | 534 |
| Neu5Aca2-8Neu5Aca2-3(GalNAcβ1-4)Galβ1-4Glcβ-sp4 | 340 | 535 |
| Neu5Aca2-3Galβ1-3GlcNAcβ1-3Galβ1-4Glcβ-sp4 | 341 | 536 |
| Neu5Aca2-3Galβ1-4GlcNAcβ1-3Galβ1-4Glcβ-sp4 | 342 | 537 |
| (Siaa2-6Aβ1-4GNβ1-2Ma1)2-3,6-Mβ1-4GNβ1-4GNβ-sp4 | 343 | 627 |
| Trehalose-ethanolamine | 344 | 629 |
| (GlcAβ1-3GlcNAcβ1-4)20-NH(p-C6H4)CH2CH2NH2 | 345 | 630 |
| (GlcAβ1-3GlcNAcβ1-4)38-NH(p-C6H4)CH2CH2NH2 | 346 | 631 |
| (GlcAβ1-3GlcNAcβ1-4)13-NH(p-C6H4)CH2CH2NH2 | 347 | 632 |
| (Neu5Aca2-8)n-NH(p-C6H4)CH2CH2NH2 | 348 | 633 |
| GlcNAca1-4GlcNAcβ-sp3 | 349 | 800 |
| [Galβ1-4GlcNAcβ-OCH2CH2]2NH | 350 | 804 |
| GalNAcβ1-4(6-O-Bn)GlcNAcβ-sp3 | 351 | 805 |
| Gala1-6Glcα-sp3 | 352 | 806 |
| Gala1-6Glcβ-sp3 | 353 | 808 |
| GalNAcβ1-3GalNAca-sp3 | 354 | 809 |
| GalNGca1-3GalNAca-sp3 | 355 | 810 |
| 3,6-O-Me2-Glcβ1-4(2,3-O-Me2)Rhaβ-O(p-C6H4)-OCH2CH2NH2 | 356 | 811 |
| Galβ1-4Glcα-sp4 | 357 | 812 |
| Galβ1-3GalNGca-sp3 | 358 | 813 |
| Gala1-4GalNAca-sp3 | 359 | 815 |
| Galβ1-4GalNAca-sp3 | 360 | 816 |

| | | |
|---|-----|------|
| GalNAc β 1-4GalNAc α -sp3 | 361 | 817 |
| GalNAc α 1-4GalNAc α -sp3 | 362 | 818 |
| Glc β 1-4GalNAc α -sp3 | 363 | 819 |
| GlcNAc β 1-4GalNAc α -sp3 | 364 | 820 |
| Gal α 1-4Gal β -sp3 | 365 | 821 |
| GalNAc α 1-4Gal β -sp3 | 366 | 822 |
| GalNAc β 1-4Gal β -sp3 | 367 | 823 |
| Glc β 1-3GlcNAc β -sp3 | 368 | 825 |
| Glc β 1-3GalNAc α -sp3 | 369 | 826 |
| Glc β 1-3GalNAc β -sp3 | 370 | 827 |
| GlcNAc β 1-2Gal β -sp3 | 371 | 828 |
| GlcNAc β 1-4Gal β -sp3 | 372 | 829 |
| Gal β 1-3(6-O-Su)GalNAc α -sp3 | 373 | 850 |
| Gal α 1-3(6-O-Su)GalNAc α -sp3 | 374 | 851 |
| GlcNAc β 1-4-[HOOC(CH ₃)CH]-3-O-GlcNAc α -sp4 | 375 | 852 |
| 6-O-Su-Gal α 1-3GalNAc α -sp3 | 376 | 853 |
| Neu5Ac α 2-3(6-O-Su)Gal β -sp3 | 377 | 854 |
| Crypted formula, available on request | 378 | 855 |
| H-(Gly)6-NH ₂ Gly6-amide, linear | 379 | 900 |
| biot-CMG2-NH ₂ | 380 | 901 |
| Crypted formula, available on request | 381 | 927 |
| -4Qui3NA α 1-3Rha α 1-4Gal β 1-3(Glc β 1-4)GalNA α 1- | 382 | 1001 |
| -2Rib-ol5-P-6Gal α 1-3FucNAma α 1-3GlcN β 1- | 383 | 1002 |
| -4(Fuca α 1-3)GalNA α 1-6ManNA α 1-3Fuca α 1-3(Glc β 1-4)Gal β 1- | 384 | 1003 |
| -2Fuca α 1-2Gal β 1-3GalNAc α 1-3GlcNAc α 1- | 385 | 1004 |
| -4Qui3NAc α 1-3Rha α 1-4Gal β 1-3(Glc β 1-4)GalNAc α 1- | 386 | 1005 |
| -4(Fuca α 1-3)GalNAc α 1-6Man ₂ (20%)Ac ₃ (40%)Ac ₄ (20%)Ac α 1-3Fuca α 1-3(Glc β 1-4)Gal β 1- | 387 | 1006 |
| -2(Galf(80%)Ac α 1-4)Gal α 1-3ManNAc β 1-6Galf β 1-3GlcNAc β 1- | 388 | 1007 |
| -3Galf ₂ (30%)Ac β 1-3Gal α 1- | 389 | 1008 |
| -3(S-3HOBu α 1-2Ala α 1-4)Qui4N β 1-6GlcNAc α 1-3QuiNAc α 1-3GlcNAc α 1- | 390 | 1009 |
| -2Man β 1-4Glc α 1-3QuiNAc α 1-3GlcNAc α 1- | 391 | 1010 |
| -3(GalNAcA ₆ NH ₂ α 1-2)Rha α 1-2Rha α 1-3Rha α 1-2Rha α 1-3GlcNAc β 1- | 392 | 1011 |
| -2(Fuc3NFoa α 1-3)Man β 1-3Glc β 1-3GlcNAc β 1- | 393 | 1012 |
| -4Man α 1-2Man α 1-2Man β 1-3GalNAc α 1- | 394 | 1013 |
| -2Gal β 1-3GlcNAc α 1-4Rha α 1-3GlcNAc β 1- | 395 | 1014 |
| -3(ManNAc β 1-2)Rha α 1-2Rha α 1-2Gal α 1-3GlcNAc β 1- | 396 | 1015 |
| -2Ribf β 1-4Gal β 1-4GlcNAc α 1-4Gal β 1-3GlcNAc α 1- | 397 | 1016 |
| -3GlcNAc β 1-3(Man β 1-4)Gal α 1-4Rha α 1- | 398 | 1017 |
| -6Glc α 1-4(GlcNAc β 1-3)Gal β 1-3GalNAc α 1-3GlcNAc β 1- | 399 | 1018 |
| -2Glc α 1-6Glc α 1-4(GlcNAc β 1-3)Gal α 1-3GlcNAc β 1- | 400 | 1019 |
| -7Neu5Ac α 2-3FucNAma α 1-3GlcNAc ₆ Ac β 1- | 401 | 1020 |
| -3(GlcNAc β 1-2)Rha α 1-2Rha α 1-4Glc α 1-3GalNAc β 1- | 402 | 1021 |
| -3(Ser2Ac α 1-4)Qui4N β 1-3Ribf β 1-4GalNAc α 1-3GlcNAc α 1- | 403 | 1022 |
| -3(Gal β 1-4)Gal β 1-4(GlcNAc β 1-2)Glc β 1-3GalNAc β 1- | 404 | 1023 |
| -3(Rha ₂ (%)Ac ₃ (%)Ac ₄ (%)Ac α 1-4GalA α 1-2)Rha α 1-4Glc α 1-2Rha α 1-3GlcNAc β 1- | 405 | 1024 |
| -3FucNAc α 1-4(GlcNAc β 1-2)GalA α 1-3FucNAc α 1-3GlcNAc β 1- | 406 | 1025 |
| -2(Glc α 1-4)Glc β 1-2Fuc3NRHb β 1-6GlcNAc α 1-4GalNAc α 1-3(Glc α 1-6)GlcNAc β 1- | 407 | 1026 |
| -4Qui3NAc α 1-3Rha α 1-6GlcNAc α 1-4GlcA β 1-3(Glc β 1-4)GalNAc α 1- | 408 | 1027 |
| -4(Col α 1-3)(Col α 1-6)Glc α 1-4Gal α 1-3GlcNAc β 1- | 409 | 1201 |
| -2Gal β 1-3FucNAc α 1-3GlcNAc β 1- | 410 | 1202 |
| -2Man α 1-2(Glc α 1-4)Man β 1-3GlcNAc α 1-6Man α 1- | 411 | 1203 |
| -2(S-3HOBu α 1-4)Qui4NA α 1-4GalNAc β 1-4Rha α 1-3GlcNAc ₆ (30%)Ac β 1- | 412 | 1204 |
| -3(GlcNAc β 1-2)Rha α 1-2Rha α 1-4Glc α 1-3GalNAc β 1- | 413 | 1205 |
| -3Fucf ₂ (50%)Ac β 1-3-6dmanHep β 1- | 414 | 1206 |
| -2-DRha4NAc α 1-3Fuca α 1-4Glc β 1-3GalNAc α 1- | 415 | 1207 |
| -4(R-Lac2-3Rhap2Ac α 1-3)Man β 1-4Man α 1-3GalNAc β 1- | 416 | 1208 |
| -4Qui3NAc α 1-3Rha α 1-4Gal β 1-3GalNAc α 1- | 417 | 1209 |
| -6Man α 1-2(Glc α 1-4)Man α 1-2(Glc α 1-3)Man β 1-3GlcNAc α 1- | 418 | 1210 |
| -2(Galf α 1-4)Gal α 1-3ManNAc β 1-6Galf β 1-3GlcNAc β 1- | 419 | 1211 |
| -3)Fuca α 1-3Xluf β 1- | 420 | 1212 |

| | | |
|--|-----|------|
| -3(Glcα1-2)Rhaα1-2Rhaα1-2Rhaα1-3(Glcα1-2)Rhaα1- | 421 | 1213 |
| -4-8eLeg5Ac7Aca2-6Galβ1-3FucNAca1-3GlcNAca1- | 422 | 1214 |
| -4(GlcpNAcβ1-3)GalNAca1-2Glcα1-4L-IdoAa1-3GalNAcβ1- | 423 | 1215 |
| -3Rib-ol5-P-6Gala1-3FucNAma1-3GlcNAcβ1- | 424 | 1216 |
| -2(RhaNAc3NFoβ1-3)Manβ1-3Gala1-4Rhaα1-3GlcNAca1- | 425 | 1217 |
| -3(S-3HOBu1-2DAla1-4)Qui4Nb1-6GlcNAca1-3LQuiNAca1-3GlcNAc6(30%)Aca1- | 426 | 1218 |
| -2(Glcα1-3)Mana1-3Fuca1-3GalNAca1-4(Galb1-3)GalNAcβ1- | 427 | 1219 |
| -2Fuc3(65%)Ac4(35%)Aca1-2Galβ1-3GalNAca1-3GalNAca1- | 428 | 1220 |
| -4(GalNAcβ1-3)Gala1-6Glcβ1-3GalNAcβ1- | 429 | 1221 |
| -3Rhaα1-3Rhaα1-2Glcα1-3GlcNAca1- | 430 | 1222 |
| -3(S-Lac2-4)GlcNAcβ1-2Rhaα1-2Rhaα1-3(Glcβ1-2)Rhaα1-3GlcNAcβ1- | 431 | 1223 |
| -2Rib-ol5-P-6Gala1-3FucNAma1-3(GlcNAcβ1-4)GlcNAcβ1- | 432 | 1224 |
| -8(D-Ala1-7)Leg5Aca2-4GlcAβ1-3GlcNAcβ1- | 433 | 1225 |
| -4(Fuca1-3)GlcNAc6(30%)Aca1-4GlcAa1-3Fuca1-3GlcNAcβ1- | 434 | 1226 |
| -2Galβ1-4Manβ1-4Gala1-3GlcNAcβ1- | 435 | 1227 |
| -2)Gala1-3(Fuca1-2)Galβ1-3GalNAcβ1-3GalNAcβ1(- | 436 | 1228 |
| Escherichia coli O10a10b | 437 | 1230 |
| -2Glcβ1-6GlcNAca1-3FucNAca1-3GlcNAcβ1- | 438 | 1231 |
| Gala1-2Gala1-2(Galb1-4)Glcα1-3Glcα1-/inner core-lipid A/ | 439 | 1232 |
| -2Rhaα1-2Rhaα1-2Rhaα1-2Glcα1-3GlcNAc6Aca1- | 440 | 1233 |
| Escherichia coli O27 | 441 | 1234 |
| -4(Rhaα1-2Fuca1-3)Mana1-3Fuca1-3GlcNAcβ1- | 442 | 1235 |
| -4(D-Gro1-P-O-3)GalNAcβ1-3Gala1-4Galβ1-3GalNAcβ1- | 443 | 1236 |
| -3(R-3HOBu1-4)Qui4Nβ1-4(Gala1-3)Mana1-4Rhaα1-3GlcNAca- | 444 | 1237 |
| -3Gala1-3(GlcAb1-4)Fuca1-4GlcNAcβ1-3Fuca1-3GlcNAcβ1- | 445 | 1238 |
| Escherichia coli O54 | 446 | 1239 |
| Escherichia coli O62 | 447 | 1240 |
| Escherichia coli O81 | 448 | 1241 |
| -4GlcAβ1-4(GlcNAcβ1-2)GlcAβ1-3GlcNAca1- | 449 | 1242 |
| -4(Rhaα1-2Fuca1-3)Mana1-3Fuca1-3GlcNAcβ1- | 450 | 1243 |
| Escherichia coli O37 | 451 | 1244 |
| -2Galβ1-4Manβ1-4Gala1-3GlcNAcβ1- | 452 | 1245 |
| -4(D-aThr3(70%)Ac2-6)GlcAβ1-6Galβ1-6Glcβ1-3GalNAc6(15%)Acβ1- | 453 | 1246 |
| -6(Rhaα1-3)Mana1-2(Glcα1-3)Mana1-2Mana1-2Manb1-3GlcNAca1- | 454 | 1247 |
| GlcNAca1-2Glcα1-2Glcα1-3(Gala1-6)Glcα1-/inner core-lipid A/ | 455 | 1248 |
| Escherichia coli O102 | 456 | 1249 |
| -3(Rhaα1-4)GlcAa1-2Rhaα1-2Rhaα1-2Gala1-3GalNAcβ1- | 457 | 1250 |
| -2Rhaα1-2Rhaα1-3Rha2Aca1-3(Glcα1-6)GlcNAcβ1- | 458 | 1251 |
| -3(Galfα1-2Rhaα1-4)Galβ1-4Glcα1-4GlcAa1-3GalNAcβ1- | 459 | 1252 |
| -2Ribβ1-4Galβ1-4GlcNAca1-4Galβ1-3GlcNAca1- | 460 | 1253 |
| -2(ManNAca1-3)Rhaα1-3Rhaα1-3Rhaα1-3GalNAca1- | 461 | 1254 |
| -2Rha4NAca1-3Fuca1-4Glcβ1-3GalNAca1- | 462 | 1255 |
| -4(Rhaα1-3)(Glcα1-6)Glcα1-3GalNAca1-3GalNAcβ1- | 463 | 1256 |
| -2Manβ1-4GlcAβ1-3LQuiNAca1-3GlcNAca1- | 464 | 1257 |
| -4ManNAc3NAcAβ1-2Rhaα1-3Rhaβ1-4GlcNAca1- | 465 | 1258 |
| Escherichia coli O84-deAc | 466 | 1259 |
| -3(Qui3NFoa1-4)GalA6NH2α1-4GalNAca1-4Gala1-3GalNAcβ1- | 467 | 1301 |
| Providencia alcalifaciens O3_2 capsular polysaccharide | 468 | 1302 |
| -4GlcNAcβ1-3GlcAa1-4GlcNAca1-3Rha2Acβ1- | 469 | 1303 |
| -2Glcβ1-6Gala1-6GalNAca1-4(Glcβ1-3)GalNAca1-3GalNAca1- | 470 | 1304 |
| Providencia rustigianii O11 capsular polysaccharide | 471 | 1305 |
| -4(GlcNAcβ1-2Glcβ1-2)(GlcNAcβ1-3)Galβ1-3GalNAca1-4Galβ1-3GalNAcβ1- | 472 | 1306 |
| -4(D-GroA1NH2(2-P-3))GalNAcβ1-4Galβ1-3FucNAc4Nβ1- | 473 | 1307 |
| -3(Dhpa2-4Manβ1-4)Gala1-4GalNAcβ1-3GalNAcβ1- | 474 | 1308 |
| -4Qui3NFoβ1-3Gala1-3GlcAβ1-3GalNAcβ1- | 475 | 1309 |
| -3GlcAβ1-4(Glcα1-3)Fuca1-4Fuca1-2Glcβ1-3GlcNAca1- | 476 | 1310 |
| -3Mana1-2Fuca1-2GlcA4Acβ1-3GalNAca1- | 477 | 1311 |
| -4Glcβ1-3Gala1-4GalNAcβ1-4(L-Ser2-6)GlcAβ1-3GalNAcβ1- | 478 | 1312 |
| P. aeruginosa O1(F4) | 479 | 1401 |
| -3Rhaα1-4LGalNAca1-3QuiNAca1- | 480 | 1402 |

| | | |
|--|-----|------|
| -2LGlcβ1-3FucNAcα1-3DFucNAcβ1- | 481 | 1403 |
| -2Rhaα1-3Rhaα1-4GalNAcA3Aca1-3QuiNAcβ1- | 482 | 1404 |
| <i>P. aeruginosa</i> O13ac | 483 | 1405 |
| <i>P. aeruginosa</i> O14 | 484 | 1406 |
| -2Ribfβ1-3GalNAcα1- | 485 | 1407 |
| <i>Pseudomonas aeruginosa</i> O2abc | 486 | 1408 |
| -4ManNAc3NAmAβ1-4LGuINAc3NAcAα1-3DFucNAc4Nβ1- | 487 | 1409 |
| -4ManNAc3NAmAβ1-4LGuINAc3NAcAα1-3DFucNAcβ1- | 488 | 1410 |
| -4ManNAc3NAmAβ1-4ManNAc3NAcAβ1-3DFucNAcα1- | 489 | 1411 |
| -4LGuINAc3NAmAα1-4ManNAc3NAcAβ1-3DFucNAc4Aca1- | 490 | 1412 |
| -2LRha3Aca1-6GlcNAcα1-4LGalNAcA3Aca1-3(S-3HOBu1-4)QuiNAc4Nβ1- | 491 | 1413 |
| -2Rha3Aca1-6GlcNAcα1-4LGalNAcAα1-3QuiNAc4NSHbβ1- | 492 | 1414 |
| -2Rhaα1-3FucNAcα1-3FucNAcα1-3QuiNAcα1- | 493 | 1415 |
| -2Rhaα1-3FucNAcα1-3FucNAcα1-3DFucNAcα1- | 494 | 1416 |
| -2Rhaα1-4GalNAcA3Aca1-4GalNFoAα1-3QuiNAcα1- | 495 | 1417 |
| -3R-3HOBu1-7Pse4Ac5Acβ2-4DFucNAcα1-3QuiNAcβ1- | 496 | 1418 |
| <i>Pseudomonas aeruginosa</i> O10a10b | 497 | 1419 |
| <i>Proteus genomospecies</i> 5/6 O79 | 498 | 1501 |
| -3GalNAcβ1-4(L6dTalα1-3)Manα1-3L6dTalα1- | 499 | 1502 |
| -2Rhaα1-2Rhaα1-2Rhaα1-4GalAα1-3GlcNAcα1- | 500 | 1503 |
| -3Rhaβ1-4(Glcα1-3)Rhaα1-2Rhaα1-3Galα1-3DFucNAcα1- | 501 | 1504 |
| <i>Proteus mirabilis</i> 12B-r | 502 | 1601 |
| -3(Rib1(50%)Ac-ol5-P-6)Galβ1-4(GlcNAcβ1-2)Glcβ1-3GlcNAcβ1- | 503 | 1602 |
| -2Glcβ1-3L6dTal2(85%)Aca1-3GlcNAcβ1- | 504 | 1603 |
| -4(LAlpAα1-3)GalNAcα1-3GalAα1-3GlcNAcα1- | 505 | 1604 |
| -3(Glcα1-6)GlcNAcβ1-4(GlcNAcβ1-2)GlcAβ1-3(L-Thr2-6)GalAβ1- | 506 | 1605 |
| -3GlcNAcβ1-3(S,R-CetLys2-6GalAα1-4)Galα1- | 507 | 1606 |
| GalNAcβ1-4GalNAcα1-3GlcNAcα1-2Rib-ol | 508 | 1607 |
| -3GlcAβ1-4(Galα1-3)FucNAcα1-3GlcNAcα1- | 509 | 1608 |
| -4(Lys2-6)GalAα1-4Galα1-3(Ser-(2-6)GalA4Aca1-3GlcNAcβ1- | 510 | 1609 |
| -3LQuiNAcα1-3GlcNAcα1-6(S-Lac-1-3)GlcNAcα1- | 511 | 1610 |
| -2(Rib-ol5-P-3)Galβ1-3GlcNAcα1-3(EtN1-75%P-6)Glcβ1-3GlcNAcβ1- | 512 | 1611 |
| -2Fuc3N(R-3HOBu)4Acβ1-6Glc3Aca1-4GlcAβ1-3GlcNAcα1- | 513 | 1612 |
| -3(EtNAc1-P-6)GlcNAcα1-3D-Asp2Ac4-4)Qui4Nβ1-6Glcα1-4GalAα1- | 514 | 1613 |
| -6(GalA6(L-Lys)α1-4)GalNAcβ1-4(Glcα1-2)GlcAβ1-3GalNAcβ1- | 515 | 1614 |
| -4(GalA6(L-Thr)3Aca1-3)GalNAcβ1-3Rhaβ1-4GlcNAc6Acβ1- | 516 | 1615 |
| -4(GlcAα1-3)FucNAcα1-3GlcNAcβ1- | 517 | 1616 |
| -4(S,R-CetLys2-6)GlcAb1-6GalNAcα1-6GlcNAcβ1-3GlcNAcβ1- | 518 | 1617 |
| -6GlcNAcα1-3Galβ1-3GalNAcα1- | 519 | 1618 |
| -3GlcAβ1-4(Galα1-3)FucNAcα1-3GlcNAcα1- | 520 | 1701 |
| -3(Glcβ1-3GlcNAc4(S-Lac)b1-2)Rhaα1-2Rhaα1-2Gal6Aca1-3GlcNAcβ1- | 521 | 1702 |
| -4(Glcα1-2)GlcA3Acβ1-3GlcNAcα1-2(R-3HOBu1-3)Fuc3Nβ1-6Glc4Aca1- | 522 | 1703 |
| -6GlcNAc3(S-Lac)α1-3LQuiNAcα1-3GlcNAcα1- | 523 | 1704 |
| -3Galα1-4GalNAcα1-3FucNAcα1-3(EtN1-P-6)GlcAcβ1- | 524 | 1705 |
| -6(S-Lac2-3)GlcNAcβ1-3Galα1-3GlcNAc6Acβ1- | 525 | 1706 |
| -4(Glcα1-3)Glcβ1-3Galβ1-3GalNAcβ1-4Rib-ol5-P- | 526 | 1707 |
| -3(EtN1-P-6)GlcNAcα1-2(R-3HOBu1-3)Fuc3Nβ1-6Glcα1-4GlcAβ1- | 527 | 1801 |
| -4(L-Ala2-6)GlcAβ1-3GalNAcβ1-4Glcβ1-3Galα1-4GalNAcβ1- | 528 | 1802 |
| -4GalN6Aca1-3DFuc2Aca1-3(EtN1-P-6)GlcNAcβ1-3Galα1- | 529 | 1803 |
| -3GlcNAcβ1-3(Qui3NAc2(65%)Ac4Aca1-2)Rhaβ1-4Rhaα1-4GlcAβ1- | 530 | 1804 |
| -4GalNAcβ1-3GlcNAcβ1-2(R-Lac1-3Glcα1-3)Rhaα1-2Ribfβ1- | 531 | 1805 |
| -4GlcAβ1-3GlcNAcβ1-2(R-3HOBu1-2L-Ala1-4)Qui4Nβ1-3Galα1- | 532 | 1806 |
| -4Glc6(65%)Aca1-3GlcA4Acβ1-3GlcNAcα1-3GlcA4(87%)Acβ1- | 533 | 1807 |
| -4Glcβ1-3GalNAcβ1-4GalNAcβ1-4Galβ1- | 534 | 1808 |
| -4LQuiNAcα1-3GlcNAcα1-4(LQuiNAcα1-3)GalNAcα1-4Galα1-P | 535 | 1809 |
| -4Glcβ1-3GalNAcβ1-4GalNAcβ1-4Galβ1- | 536 | 1810 |
| <i>Acinetobacter baumannii</i> LUH5534 | 537 | 1901 |
| -3(Ribfβ1-4GlcAβ1-4)Galα1-6Manα1-2Manα1-3GalNAcβ1- | 538 | 2001 |
| -3GlcNAcβ1-4GlcA3Acβ1-2(Rha3Aca1-3)Manα1-4Galβ1- | 539 | 2002 |
| -6Galα1-4GlcAβ1-6Galβ1-4Galβ1-4GlcNAcβ1- | 540 | 2003 |

| | | |
|---|-----|------|
| -4(GlcNAcβ1-3)GalNAcα1-4Glcα1-4L-IdoAα1-3GalNAcβ1- | 541 | 2004 |
| -4GlcAβ1-2(Galα1-3)Man6(50%)Acβ1-4Manβ1-3GlcNAcβ1- | 542 | 2005 |
| -6(R-Lac2-4)Glcβ1-4GalNAcα1-3GalNAcβ1- | 543 | 2006 |
| -3Rhaβ1-4Rhaα1-2Rhaα1-2GalAα1-3GalNAcα1- | 544 | 2007 |
| -2Ribfβ1-4GalAα1-3GlcNAcα1-2(Galfb1-3)Rhaα1-2Rhaα1-2Ribfβ1-4GalAα1- | 545 | 2008 |
| -3(GlcAβ1-4)Galα1-6Mana1-2Mana1-3GalNAcβ1- | 546 | 2009 |
| -2Galfβ1-3GlcNAcα1-8(3HOBut1-7)Pse5Ac2-6Galα1-6Glcα1- | 547 | 2010 |
| -3GalNAcα1-4GlcAβ1-3GlcNAcβ1-2GalAβ1- | 548 | 2011 |
| -4Glcα1-4GlcAβ1-3GlcNAcα1-3Rhaα1- | 549 | 2012 |
| Shigella boydii type X | 550 | 2013 |
| -3Rhaα1-3Rhaα1-2Galα1-3GlcNAcα1- | 551 | 2101 |
| -1D-Gro3-P-6Glcβ1-4(Glcα1-6Gal2(25%)Aca1-3)FucNAcα1-3GlcNAcβ1- | 552 | 2102 |
| -3(R-Lac2-4Glcβ1-6Glcα1-4)Galβ1-6Galfβ1-3GalNAcβ1- | 553 | 2103 |
| -3GlcNAcα1-3(Fuc3Ac4Aca1-4)GlcNAcα1-4GlcAα1-3Fuca1- | 554 | 2104 |
| GalNAcA3Ac6NH2α1-4GalNAcAα1-3GlcNAc | 555 | 2105 |
| -4GlcAβ1-3GalNAcβ1-3(GlcNAcβ1-4Glcβ1-4)GalNAcβ1- | 556 | 2106 |
| -2Gal3,4(RPyr)b1-4Manβ1-4Galα1-3GlcNAcβ1- | 557 | 2107 |
| -3GlcNAcβ1-2Rhaα1-2Rhaα1-3(Glcβ1-4)Rhaα1- | 558 | 2201 |
| -3GlcNAcβ1-2(Glcα1-3)Rhaα1-2Rhaα1-3(Glcα1-4)Rhaα1- | 559 | 2202 |
| -3GlcNAcβ1-2(Glcα1-3)Rhaα1-2Rhaα1-3Rha2Aca1- | 560 | 2203 |
| -2Rhaα1-2Rhaα1-3Rha2Aca1-3GlcNAcβ1- | 561 | 2204 |
| -3(Glcα1-6)GlcNAcβ1-2Rhaα1-2Rhaα1-3Rhaα1- | 562 | 2205 |
| -3(Glcα1-6)GlcNAcβ1-2Rhaα1-2Rhaα1-3Rha2Aca1- | 563 | 2206 |
| -3GlcNAcβ1-2Rhaα1-2(Glcα1-3)Rhaα1-3Rhaα1- | 564 | 2207 |
| -3GlcNAcβ1-2(Glcα1-3)Rhaα1-2(Glcα1-3)Rhaα1-3Rhaα1- | 565 | 2208 |
| -2Rha3(%)Aca4(%)Aca1-2Rhaα1-4GalAb1-3GalNAcβ1- | 566 | 2209 |
| -2Rha3(60%)Aca4(30%)Aca1-2Rhaα1-4GalAb1-3GalNAcβ1- | 567 | 2210 |
| -3GlcNAcβ1-2(Glcα1-3)Rhaα1-2Rhaα1-3Rhaα1- | 568 | 2211 |
| -2Rhaα1-2Rhaα1-3Rhaα1-3GlcNAcβ1- | 569 | 2212 |
| -3Rhaα1-3(Glcα1-4)GlcNAcβ1-2Rhaα1-2Rhaα1- | 570 | 2213 |
| Shigella flexneri type 2c | 571 | 2214 |
| -2(EtN1-P-3)Rhaα1-2Rhaα1-3Rhaα1-3(Glcα1-6)GlcNAcβ1- | 572 | 2215 |
| Shigella flexneri type 5c | 573 | 2216 |
| -2(Glcα1-3)Rhaα1-2Rhaα1-3Rhaα1-3(Glcα1-4)GlcNAcβ1- | 574 | 2217 |
| -2Rhaα1-2Rhaα1-3Rhaα1-3GlcNAcβ1- | 575 | 2218 |
| -2Rha3(%)Aca1-2Rhaα1-3Rhaα1-3GlcNAc6(%)Acβ1- | 576 | 2219 |
| -2(EtN1-P-3)Rhaα1-2(20%EtN1-P-3)Rhaα1-3Rhaα1-3GlcNAc6(45%)Acβ1- | 577 | 2220 |
| -2(Glcα1-3)Rhaα1-2(EtN1-P-3)Rhaα1-3Rhaα1-3GlcNAcβ1- | 578 | 2221 |
| Streptococcus equi sp. hyaluronic acid sodium salt | 579 | 2501 |
| -4(2-O-Su)L-IdoAα1-4(6-O-Su)GlcNSua1- _4GlcAβ1-4GlcNAcα1- | 580 | 2502 |
| Acetobacter methanolicus LPS | 581 | 2601 |
| -3Glcβ1- | 582 | 3001 |
| -6Mana1- | 583 | 3002 |
| -3Glcβ1-6Glcβ1- | 584 | 3301 |
| -3Glcβ1- | 585 | 3302 |
| -4Glcβ1-4Glcβ1-3Glcβ1- | 586 | 3401 |
| Rha:Ara:Gal:GalA 9:3:79:9, MW 900-2000 kDa | 587 | 3501 |
| Rha:Ara:Gal:GalA 17:3:62:18, MW 100-400kDa | 588 | 3502 |
| -2)Galα1-3(Fuca1-2)Galβ1-3GalNAcβ1-3GalNAcβ(1-LPS | 589 | 8001 |
| -3Rhaα1-3Rhaα1-2Glcα1-3GlcNAcα1- LPS | 590 | 8002 |
| -4(Fuca1-3)GlcNAc6(30%)Aca1-4GlcAα1-3Fuca1-3GlcNAcβ1- LPS | 591 | 8003 |
| -4(GalNAcβ1-3)Galα1-6Glcβ1-3GalNAcβ1- LPS | 592 | 8004 |
| -2Rib-ol5-P-6Galα1-3FucNAma1-3(GlcNAcβ1-4)GlcNAcβ1- LPS | 593 | 8005 |
| -3(Glcα1-2)Rhaα1-2Rhaα1-2Rhaα1-3(Glcα1-2)Rhaα1- LPS | 594 | 8006 |
| -6Mana1-2(Glcα1-4)Mana1-2(Glcα1-3)Manβ1-3GlcNAcα1- LPS | 595 | 8007 |
| -3Rib-ol5-P-6Galα1-3FucNAma1-3GlcNAcβ1- LPS | 596 | 8008 |
| -4(R-Lac2-3Rhap2Aca1-3)Manβ1-4Mana1-3GalNAcβ1- LPS | 597 | 8009 |
| -4(GlcNAcβ1-3)GalNAcα1-2Glcα1-4L-IdoAα1-3GalNAcβ1- LPS | 598 | 8010 |
| -3(S-Lac2-4)GlcNAcβ1-2Rhaα1-2Rhaα1-3(Glcβ1-2)Rhaα1-3GlcNAcβ1- LPS | 599 | 8011 |
| Escherichia coli O40 LPS | 600 | 8012 |

| | | |
|---|-----|------|
| Escherichia coli O49 LPS | 601 | 8013 |
| Escherichia coli O81 LPS | 602 | 8014 |
| Escherichia coli O52 LPS | 603 | 8015 |
| -3Glc β 1-3Glc β 1-3(Glc β 1-6)Glc β 1- | 604 | 9001 |
| -3Glc β 1- | 605 | 9002 |
| -4GlcN(%)Ac β 1- | 606 | 9003 |
| Saccharomyces cerevisiae mannan SIGMA | 607 | 9004 |
| Bakers yeast glucan SIGMA | 608 | 9005 |
| Saccharomyces cerevisiae zymosan A SIGMA | 609 | 9006 |
| Hyaluronic acid E77-2 KBL6413 17kDa | 610 | 9007 |
| S488 (fluorescence control) | 611 | |
| S555 (fluorescence control) | 612 | |
| S647 (fluorescence control) | 613 | |
| Smix (fluorescence control) | 614 | |
| empty (background control) | 615 | |

Table S2. Row number assignment for Semiotic glycan ID.

trivial name, row number, SGID, mean fluorescence intensity, s.d.

| | | | | | | | | | | | | | | |
|----------|----|----|--------|--------|-------------|-----|-----|--------|--------|----------------------|-----|-----|--------|------|
| aF | 1 | 1 | 1600.7 | 30.0 | Bdi | 61 | 76 | 1544.5 | 4.8 | TF6'Su | 121 | 151 | 1545.2 | 7.7 |
| aA | 2 | 2 | 1557.7 | 10.7 | Tab | 62 | 77 | 1551.8 | 23.1 | Lac6'Su | 122 | 153 | 1542.0 | 0.0 |
| bA | 3 | 3 | 1579.0 | 90.1 | Taa | 63 | 78 | 1551.8 | 15.4 | LeC3'Su | 123 | 154 | 1546.0 | 10.8 |
| TnSer | 4 | 4 | 1541.7 | 0.5 | Aa3GN | 64 | 80 | 2226.7 | 1662.9 | LN3'Su-C2 | 124 | 156 | 1548.0 | 7.4 |
| Tn | 5 | 5 | 1540.8 | 2.9 | aLN | 65 | 81 | 1542.3 | 0.8 | LN4'Su-C2 | 125 | 158 | 1689.0 | 84.0 |
| bAN | 6 | 6 | 1556.5 | 16.7 | aLN-PEG | 66 | 82 | 1541.3 | 1.0 | LN4'Su | 126 | 159 | 1545.8 | 7.1 |
| aG | 7 | 7 | 1548.7 | 10.1 | Aa6G | 67 | 83 | 1545.5 | 8.5 | LeC6'Su-C2 | 127 | 160 | 1541.8 | 1.6 |
| bG | 8 | 9 | 1556.7 | 38.5 | Ab2A | 68 | 84 | 1552.2 | 17.6 | LeC6'Su | 128 | 161 | 1542.0 | 0.0 |
| GN | 9 | 10 | 1567.8 | 24.2 | LeC | 69 | 85 | 1544.0 | 3.6 | LN6'Su-C2 | 129 | 162 | 1546.3 | 11.1 |
| GN-C2 | 10 | 11 | 1572.3 | 33.6 | LeC-C2 | 70 | 86 | 2078.5 | 1274.1 | GUb3GN | 130 | 164 | 1541.2 | 1.3 |
| GN-PEG | 11 | 13 | 1541.8 | 0.4 | Ab3A | 71 | 87 | 1545.0 | 4.3 | GUb3A | 131 | 165 | 1545.7 | 9.0 |
| bGN(Gc) | 12 | 14 | 1549.2 | 17.6 | Tbb | 72 | 88 | 1548.3 | 9.0 | GUb6A | 132 | 166 | 1558.7 | 21.1 |
| glucitol | 13 | 15 | 1542.0 | 0.0 | TF | 73 | 89 | 1580.7 | 64.1 | GN-Mur | 133 | 167 | 1543.0 | 2.4 |
| aM | 14 | 16 | 1556.0 | 16.2 | Lac-C2 | 74 | 92 | 1547.7 | 7.4 | GMDPLys | 134 | 168 | 1550.5 | 10.3 |
| aM-Gly | 15 | 17 | 1550.5 | 14.2 | Lac-Gly | 75 | 93 | 1551.7 | 21.3 | GM4 | 135 | 169 | 1547.8 | 8.7 |
| bM | 16 | 18 | 1543.7 | 2.3 | Ab4A | 76 | 94 | 1542.3 | 0.8 | Sia6A | 136 | 170 | 1543.2 | 3.9 |
| bMN | 17 | 19 | 1541.3 | 0.8 | LN-C2 | 77 | 96 | 1549.3 | 17.0 | 3-SiaTn | 137 | 171 | 1547.2 | 15.7 |
| aR | 18 | 20 | 1547.7 | 6.3 | LN | 78 | 97 | 1546.8 | 11.8 | SiaTn | 138 | 172 | 1544.0 | 4.9 |
| bA-Gly | 19 | 21 | 1543.3 | 3.3 | LN-C8 | 79 | 98 | 1542.3 | 0.8 | bSiaTn | 139 | 173 | 1541.8 | 0.4 |
| GN-Gly | 20 | 22 | 1546.0 | 6.3 | LN-PEG | 80 | 99 | 1551.8 | 7.9 | Neu5GcTn | 140 | 174 | 1545.7 | 12.6 |
| bAN-Gly | 21 | 23 | 1551.3 | 8.9 | Ab6A | 81 | 100 | 1572.7 | 18.4 | LN3'6Su2 | 141 | 177 | 1547.7 | 8.4 |
| GNa | 22 | 24 | 1647.8 | 17.2 | Fs-2 | 82 | 101 | 1548.7 | 15.2 | Lac6,6'Su2 | 142 | 178 | 1542.8 | 2.0 |
| bAN-PEG2 | 23 | 25 | 1547.7 | 8.0 | Adi | 83 | 102 | 1552.8 | 14.3 | LeC6,6'Su2 | 143 | 179 | 1547.7 | 9.2 |
| bR | 24 | 26 | 1550.0 | 10.3 | core5 | 84 | 103 | 1543.2 | 1.8 | LN66'Su2 | 144 | 180 | 1546.3 | 6.7 |
| bXyl | 25 | 28 | 1542.5 | 1.2 | ANb3A | 85 | 104 | 1558.0 | 19.8 | LN3'4'Su2 | 145 | 181 | 1575.0 | 51.6 |
| bF | 26 | 29 | 1580.7 | 29.2 | para-Fs | 86 | 105 | 1551.7 | 12.7 | LN3'6'Su2 | 146 | 182 | 1545.8 | 9.9 |
| bG-Gly | 27 | 30 | 1545.8 | 5.5 | LacdiNAc | 87 | 106 | 1551.2 | 19.1 | LN4'6'Su2-C2 | 147 | 183 | 1543.7 | 2.7 |
| aAra | 28 | 31 | 1555.7 | 18.7 | LacdiNAc-C2 | 88 | 107 | 1545.2 | 8.3 | LN4'6'Su2 | 148 | 184 | 1545.0 | 7.3 |
| bANGc | 29 | 32 | 1545.5 | 12.3 | Malt2 | 89 | 110 | 1565.3 | 37.0 | (Sia)2Bn | 149 | 187 | 1544.2 | 4.8 |
| GNH2 | 30 | 33 | 2526.5 | 2408.6 | cello | 90 | 111 | 1555.8 | 8.6 | (Sia)2-bBn | 150 | 188 | 1701.5 | 89.7 |
| L-bG-Gly | 31 | 34 | 1542.0 | 0.0 | gent | 91 | 112 | 1568.3 | 50.0 | LN3'66'Su3 | 151 | 189 | 1551.2 | 12.3 |
| bA3Su | 32 | 37 | 1550.5 | 15.4 | core3 | 92 | 113 | 1559.2 | 12.4 | LN6P | 152 | 190 | 1541.5 | 1.2 |
| bAN3Su | 33 | 38 | 1541.3 | 3.9 | GN3M | 93 | 114 | 1546.7 | 11.4 | LN6'P | 153 | 191 | 1542.0 | 0.0 |
| aAN6Su | 34 | 41 | 1539.8 | 5.3 | Ch2 | 94 | 116 | 1545.0 | 6.5 | LacdiNAc6Su | 154 | 192 | 1542.2 | 0.4 |
| GN6Su | 35 | 43 | 1591.7 | 83.3 | Ch2-Gly | 95 | 117 | 1548.8 | 8.2 | LacdiNAc3'Su | 155 | 193 | 1543.8 | 3.5 |
| aGU | 36 | 44 | 1547.7 | 13.9 | core6 | 96 | 118 | 1548.2 | 10.4 | LacdiNAc6'Su | 156 | 194 | 1553.5 | 17.9 |
| bGU | 37 | 45 | 1559.0 | 25.9 | Ma4M | 97 | 121 | 1551.2 | 14.8 | 3Ac-LacdiNAc6'Su | 157 | 195 | 1559.5 | 11.4 |
| G6P | 38 | 46 | 1542.0 | 0.0 | Ma6M | 98 | 122 | 1558.5 | 32.8 | LacdiNAc3,3'Su2 | 158 | 196 | 1542.5 | 1.8 |
| M6P | 39 | 47 | 1548.5 | 16.4 | Mb4GN | 99 | 123 | 1584.7 | 89.6 | LacdiNAc3',6'Su2 | 159 | 197 | 1542.0 | 0.0 |
| Sia | 40 | 48 | 1546.3 | 6.0 | 6'Bn-LN | 100 | 125 | 1577.2 | 48.5 | LacdiNAc4',6'Su2 | 160 | 198 | 1549.3 | 10.6 |
| Sia-Bn | 41 | 49 | 1543.0 | 3.0 | Bn2-aLN | 101 | 126 | 1562.0 | 15.5 | 3Ac-LacdiNAc4',6'Su2 | 161 | 199 | 1552.5 | 15.9 |
| bSia | 42 | 50 | 1592.0 | 118.6 | Lac-Trp | 102 | 128 | 1546.7 | 5.9 | LacdiNAc4'Su | 162 | 200 | 1546.7 | 12.9 |
| bSia-Bn | 43 | 51 | 1542.3 | 1.4 | 6BnLeC | 103 | 129 | 1542.7 | 2.2 | LacdiNAc6,6'Su2 | 163 | 202 | 1541.8 | 1.6 |
| aNeu5Gc | 44 | 52 | 1548.7 | 10.2 | 6'BnLeC | 104 | 130 | 1572.7 | 31.6 | LN6Su | 164 | 203 | 1550.5 | 14.7 |
| bSia5Gc | 45 | 53 | 1593.7 | 81.6 | Bn2LeC | 105 | 131 | 1555.0 | 17.9 | LacdiNAc4'Su-C2 | 165 | 204 | 1547.8 | 14.8 |
| GN3Su | 46 | 55 | 1543.0 | 6.5 | TF-C8 | 106 | 132 | 1542.7 | 3.3 | 6SiaANb | 166 | 205 | 1540.2 | 3.3 |
| bRib | 47 | 57 | 1553.3 | 27.8 | Lac-Ala | 107 | 133 | 1546.0 | 5.2 | Neu5Gc3A | 167 | 206 | 1562.0 | 29.7 |
| bF | 48 | 58 | 1550.8 | 16.2 | Lac-Asn | 108 | 135 | 1541.0 | 1.7 | LeC-Gly | 168 | 208 | 1554.3 | 10.9 |
| A173 | 49 | 59 | 1549.7 | 14.2 | Lac-Ile | 109 | 136 | 1546.3 | 7.7 | A78 | 169 | 211 | 1541.7 | 2.0 |
| bA6Su | 50 | 60 | 1549.2 | 11.2 | Lac-Nle | 110 | 137 | 1543.5 | 6.7 | deltaGUb3A | 170 | 214 | 1549.5 | 18.6 |
| Tn3Su | 51 | 61 | 1541.5 | 0.8 | Lac-Val | 111 | 138 | 1553.3 | 25.4 | LeD | 171 | 215 | 1595.2 | 47.1 |
| bGN-C2 | 52 | 62 | 1557.3 | 20.6 | LNa | 112 | 139 | 1585.8 | 20.9 | Htype2 | 172 | 216 | 1542.2 | 2.0 |
| GN4Su | 53 | 63 | 1545.7 | 10.5 | Tab(f) | 113 | 140 | 1666.5 | 300.1 | Htype3 | 173 | 217 | 1546.2 | 8.4 |
| A4Su | 54 | 64 | 1541.7 | 2.9 | GNa3AN | 114 | 142 | 1553.7 | 17.8 | Htype6 | 174 | 219 | 1546.0 | 9.6 |
| Tn4Su | 55 | 65 | 1549.8 | 14.2 | Hdi3Su | 115 | 143 | 1545.0 | 6.4 | Gallii3 | 175 | 222 | 1544.0 | 4.9 |
| bAN4Su | 56 | 66 | 1544.0 | 4.9 | LeC6Su-C2 | 116 | 144 | 1679.0 | 73.3 | Pk-C2 | 176 | 223 | 1550.8 | 12.8 |
| Hdi | 57 | 71 | 1545.7 | 5.3 | LeC6Su | 117 | 145 | 1545.7 | 4.4 | P1 | 177 | 225 | 1589.2 | 37.6 |
| Fa3GN | 58 | 72 | 1544.5 | 4.7 | Lac6Su | 118 | 146 | 1550.5 | 15.7 | Btri | 178 | 226 | 1549.3 | 18.0 |
| Le | 59 | 73 | 1582.8 | 89.7 | Ch2-6Su | 119 | 149 | 1542.0 | 0.0 | Btri-C8 | 179 | 227 | 1543.3 | 4.5 |
| Aa2A | 60 | 75 | 1547.3 | 10.8 | TF3'Su | 120 | 150 | 1586.3 | 24.7 | Ab3'LN-Gly | 180 | 229 | 1541.5 | 1.2 |

| | | | | | | | | | |
|-------------|-----|-----|--------|--------|----------------|-----|-----|--------|-------|
| Fb2'LeC | 181 | 230 | 1546.3 | 10.1 | (3'SLN)2 | 241 | 310 | 1551.2 | 12.2 |
| LN3Tn | 182 | 231 | 1541.5 | 1.4 | 3'SLN6Su | 242 | 315 | 1548.3 | 12.4 |
| LN6Tn | 183 | 232 | 1549.0 | 13.3 | 6'SuHtype2 | 243 | 316 | 1543.2 | 2.4 |
| LeA | 184 | 233 | 1542.7 | 2.2 | 6'SLN6Su | 244 | 318 | 1545.7 | 8.5 |
| LeX | 185 | 234 | 1550.3 | 20.9 | 3'SLN6'Su | 245 | 319 | 1542.3 | 0.5 |
| Atri | 186 | 235 | 1560.7 | 34.4 | 3'SLN6',4''Su2 | 246 | 320 | 1578.0 | 40.5 |
| Atri-C8 | 187 | 236 | 1568.0 | 38.9 | (Sia)3 | 247 | 321 | 1546.2 | 10.2 |
| ABtri | 188 | 237 | 1545.5 | 9.6 | (Sia)3b | 248 | 322 | 1542.3 | 1.4 |
| Fa2(ANb3)A | 189 | 239 | 1543.3 | 2.1 | 6'SiaLeC | 249 | 323 | 1657.2 | 124.0 |
| (Ga4)3b | 190 | 240 | 1542.0 | 0.0 | 6'SiaLeC6Su | 250 | 324 | 1549.2 | 13.8 |
| (Ga6)3b | 191 | 241 | 1541.8 | 1.0 | 3'SL-Nle | 251 | 327 | 1546.0 | 10.3 |
| GNa3'LN-C2 | 192 | 242 | 2272.2 | 61.2 | 3'SL-Phe | 252 | 328 | 1542.0 | 0.0 |
| GNa3'LN | 193 | 243 | 2427.2 | 93.9 | 3'SL-Trp | 253 | 329 | 1545.3 | 6.7 |
| GNa6'LN | 194 | 245 | 1541.8 | 0.4 | 3'SiaLeC(Gc) | 254 | 331 | 1549.3 | 8.4 |
| GN2'TF | 195 | 246 | 1542.0 | 0.6 | 3'SLN(Gc)6Su | 255 | 334 | 1553.7 | 29.2 |
| GN3'TF | 196 | 247 | 1546.2 | 11.2 | 3'SiaLeC6Su | 256 | 335 | 1545.0 | 6.9 |
| GN3'LN-C2 | 197 | 249 | 1542.3 | 0.8 | ANa4'LN | 257 | 337 | 1543.7 | 5.1 |
| GN3'LN | 198 | 250 | 1541.5 | 1.8 | 6'SiaTF | 258 | 338 | 1542.2 | 1.6 |
| GN4'LN | 199 | 251 | 1546.7 | 7.5 | b6SiaTab | 259 | 340 | 1549.0 | 10.4 |
| Ch3 | 200 | 252 | 1547.8 | 9.8 | 6'Su3'SiaTF | 260 | 342 | 1557.0 | 13.4 |
| GN6'LN | 201 | 253 | 1546.3 | 13.1 | b3'SLN | 261 | 344 | 1544.0 | 3.7 |
| core2 | 202 | 254 | 1544.0 | 2.9 | 6Su3'SiaTF | 262 | 345 | 1546.2 | 6.9 |
| core4 | 203 | 255 | 1548.8 | 5.8 | 6,6'Su2-3'SLN | 263 | 346 | 1542.3 | 1.4 |
| GN2-4,6Tn | 204 | 256 | 1555.8 | 22.4 | 3'SL(Gc) | 264 | 350 | 1542.5 | 3.3 |
| (Ma)3b | 205 | 258 | 1540.7 | 2.8 | Btype1 | 265 | 359 | 1544.2 | 5.3 |
| (Ab)2-3,4GN | 206 | 259 | 1541.3 | 1.2 | Btype2 | 266 | 360 | 1541.8 | 0.4 |
| bLeA | 207 | 260 | 1552.7 | 12.2 | Btype2-C2 | 267 | 361 | 1597.7 | 60.8 |
| ANb-cluster | 208 | 263 | 1555.8 | 29.0 | Btype3 | 268 | 362 | 1547.8 | 10.3 |
| Ab4'LN | 209 | 264 | 1549.2 | 12.3 | Btype4 | 269 | 363 | 1542.0 | 0.0 |
| P1 | 210 | 266 | 1550.3 | 13.2 | aGalLeX | 270 | 364 | 1545.5 | 8.6 |
| GlcNAc3'Lec | 211 | 267 | 1548.3 | 12.4 | Aa4'(Fa2')LN | 271 | 365 | 1542.0 | 0.0 |
| Fa6Ch2 | 212 | 268 | 1544.8 | 8.0 | Atype1 | 272 | 366 | 1543.2 | 2.9 |
| 3'SL-Cit | 213 | 272 | 2050.7 | 1235.7 | Atype2 | 273 | 368 | 1547.0 | 7.7 |
| Fb2LN | 214 | 273 | 1547.5 | 8.4 | ANa4'(Fa2')LN | 274 | 369 | 1544.2 | 2.9 |
| ANa3'LN | 215 | 274 | 1547.3 | 11.8 | ANb3'(Fa2')LN | 275 | 370 | 1545.7 | 9.2 |
| ANb3'LN | 216 | 275 | 1550.5 | 10.3 | LeB | 276 | 371 | 1571.8 | 43.2 |
| GN4'LN-C3 | 217 | 276 | 1541.5 | 1.2 | LeY | 277 | 372 | 1550.5 | 17.0 |
| NGcAtri | 218 | 277 | 1560.0 | 22.9 | GalIII4 | 278 | 373 | 1543.8 | 4.5 |
| Fs-3 | 219 | 278 | 1541.8 | 0.4 | Aa2-3',4'LN | 279 | 374 | 1545.8 | 6.1 |
| LeCa3Tn | 220 | 279 | 1547.3 | 6.4 | LNT | 280 | 376 | 1584.0 | 44.7 |
| Htype4 | 221 | 281 | 1554.3 | 13.4 | LeCb3'LeC | 281 | 377 | 1572.7 | 74.6 |
| Ab3'LN | 222 | 282 | 1559.2 | 18.9 | LeCa3'LN | 282 | 378 | 1722.2 | 22.8 |
| 3'SuLeA | 223 | 287 | 1543.5 | 4.2 | LeC3'LN | 283 | 379 | 1541.8 | 0.4 |
| 3'SuLeX | 224 | 288 | 1574.2 | 57.2 | LeCa6'LN | 284 | 380 | 1929.2 | 930.3 |
| 6SiaTF | 225 | 289 | 1544.7 | 7.0 | LeC6'LN | 285 | 381 | 1546.0 | 9.8 |
| A3a(Sia)Tn | 226 | 290 | 1544.2 | 6.3 | LNnT | 286 | 383 | 1556.3 | 33.7 |
| b6SiaTF | 227 | 291 | 1553.7 | 16.8 | LN3'LN-C2 | 287 | 384 | 1545.0 | 4.1 |
| Sia3'TF | 228 | 292 | 1549.7 | 11.0 | LNa6'LN | 288 | 386 | 1548.5 | 17.5 |
| 3'SL | 229 | 293 | 1543.3 | 2.5 | LNb6'LN | 289 | 387 | 1604.2 | 70.4 |
| 3'SL-Gly | 230 | 294 | 1545.3 | 5.2 | LN6TF | 290 | 388 | 1543.0 | 2.4 |
| 6'SL-C2 | 231 | 295 | 1541.8 | 0.4 | Gb4 | 291 | 389 | 1556.5 | 17.5 |
| b6'SL | 232 | 297 | 1562.0 | 23.5 | (Ga4)4b | 292 | 390 | 1545.2 | 6.0 |
| 3'SLN | 233 | 298 | 1597.5 | 135.9 | A(type 3) | 293 | 392 | 1542.0 | 0.0 |
| 3'SiaLeC | 234 | 299 | 1831.0 | 701.1 | Tk | 294 | 395 | 1562.0 | 30.9 |
| 6'SLN | 235 | 300 | 1545.5 | 7.2 | GN3-3,4,6Tn | 295 | 396 | 1553.8 | 13.2 |
| b6'SLN | 236 | 302 | 1557.8 | 17.5 | LeC3'LeC | 296 | 401 | 1541.5 | 5.4 |
| 3'SLN(Gc) | 237 | 303 | 1545.3 | 7.2 | LeC3'LN | 297 | 403 | 1543.3 | 4.3 |
| 6'SLN(Gc) | 238 | 304 | 1549.5 | 18.0 | ANaLeX | 298 | 404 | 1545.3 | 5.6 |
| b6'SLN(Gc) | 239 | 305 | 1541.8 | 3.0 | GN2-3',4'LN-C3 | 299 | 408 | 1541.2 | 1.3 |
| Sia2-3,6Tn | 240 | 309 | 1542.0 | 0.6 | LeCa3'LeC | 300 | 410 | 1656.3 | 92.9 |

| | | | | | | | | | |
|------------------|-----|-----|--------|-------|-----------------------|-----|------|--------|--------|
| (3'SuLN)3'LN | 301 | 419 | 1570.3 | 44.4 | ANb4ANa | 361 | 817 | 1546.2 | 8.7 |
| LNTa | 302 | 421 | 1546.3 | 8.0 | ANa4ANa | 362 | 818 | 1564.7 | 55.5 |
| SiaLeX | 303 | 423 | 1543.5 | 3.7 | G4ANa | 363 | 819 | 1553.7 | 24.8 |
| bF-SiaLeX | 304 | 425 | 1544.2 | 6.0 | GN4ANa | 364 | 820 | 1542.5 | 1.2 |
| SiaLeA | 305 | 426 | 1563.7 | 27.0 | Aa4A | 365 | 821 | 1554.8 | 28.5 |
| SiaLeX6Su | 306 | 428 | 1560.2 | 45.6 | ANa4A | 366 | 822 | 1554.2 | 19.8 |
| SiaLeX6'Su | 307 | 429 | 1542.8 | 3.1 | ANb4A | 367 | 823 | 1557.3 | 15.0 |
| SiaLeX2''Su | 308 | 431 | 1543.5 | 4.7 | Gb3GN | 368 | 825 | 1549.0 | 8.6 |
| SiaLeX3''Su | 309 | 432 | 1552.8 | 12.4 | Gb3Tn | 369 | 826 | 1542.2 | 2.0 |
| GD3 | 310 | 434 | 1542.7 | 2.3 | Gb3ANb | 370 | 827 | 1548.5 | 7.4 |
| SiaLeX6,2''Su2 | 311 | 435 | 1545.2 | 4.3 | GNb2A | 371 | 828 | 1557.3 | 24.7 |
| SiaLeX6,4''Su2 | 312 | 436 | 1604.5 | 90.0 | GNb4A | 372 | 829 | 1542.2 | 2.0 |
| A(type 4) | 313 | 437 | 1541.7 | 0.8 | 6SuTF | 373 | 850 | 1541.8 | 0.4 |
| LeYbF | 314 | 438 | 1549.2 | 19.1 | 6SuTaa | 374 | 851 | 1570.7 | 53.0 |
| Sia6'Htype2 | 315 | 441 | 1543.3 | 3.3 | GN-aMur | 375 | 852 | 1563.7 | 34.6 |
| GM2 | 316 | 442 | 1555.3 | 13.8 | 6'SuTaa | 376 | 853 | 1544.2 | 8.4 |
| Htype1Lac | 317 | 479 | 1541.5 | 2.3 | Sia3A6Su | 377 | 854 | 1548.3 | 13.6 |
| Gallii5 | 318 | 481 | 1552.8 | 25.6 | Crypted formula | 378 | 855 | 1540.7 | 3.3 |
| BLeB | 319 | 482 | 1542.3 | 0.8 | Gly6 | 379 | 900 | 1547.2 | 11.1 |
| BLeY | 320 | 483 | 1544.3 | 4.5 | biot-CMG2 | 380 | 901 | 1546.3 | 7.6 |
| Ab4ANa3'(Fa2')LN | 321 | 485 | 1543.7 | 4.1 | Crypted formula | 381 | 927 | 1542.5 | 2.9 |
| LN2-3,6Tn | 322 | 488 | 1543.7 | 4.1 | S. enterica O28deAc | 382 | 1001 | 1603.8 | 9.4 |
| LN3'(GN6')LN | 323 | 489 | 1547.3 | 8.8 | S. enterica O47deAc | 383 | 1002 | 1548.3 | 15.5 |
| ALeY | 324 | 491 | 1550.8 | 9.2 | S. enterica O16deAc | 384 | 1003 | 1576.5 | 15.2 |
| (Ga6)5b | 325 | 492 | 1550.0 | 17.7 | S. enterica O13 | 385 | 1004 | 1578.7 | 34.0 |
| Ch5 | 326 | 493 | 1582.2 | 45.3 | S. enterica O28 | 386 | 1005 | 1663.3 | 47.8 |
| (Ma)5b | 327 | 495 | 5628.5 | 266.2 | S. enterica O16 | 387 | 1006 | 1717.3 | 196.8 |
| LeBLac | 328 | 496 | 1545.8 | 9.6 | S. enterica O17 | 388 | 1007 | 1568.2 | 8.5 |
| (LNb3')3 | 329 | 498 | 1551.2 | 17.3 | S. enterica O67 | 389 | 1008 | 1564.5 | 13.9 |
| LN2-3',6'LN | 330 | 499 | 1599.0 | 74.0 | S. enterica O58 | 390 | 1009 | 1570.0 | 8.2 |
| Gb5 | 331 | 501 | 1545.5 | 6.1 | S. enterica O41 | 391 | 1010 | 1545.0 | 7.3 |
| (Ga6)6b | 332 | 502 | 1559.2 | 14.9 | S. enterica O62 | 392 | 1011 | 1550.2 | 13.5 |
| Ch6 | 333 | 503 | 1560.3 | 44.9 | S. enterica O60 | 393 | 1012 | 1574.8 | 16.7 |
| 9-OS | 334 | 504 | 1560.5 | 16.7 | S. enterica O18 | 394 | 1013 | 1546.2 | 10.7 |
| 7-OS | 335 | 505 | 1619.7 | 6.3 | S. enterica O59 | 395 | 1014 | 1599.0 | 29.4 |
| ALeYb | 336 | 508 | 1558.0 | 14.0 | S. enterica O42 | 396 | 1015 | 1549.2 | 12.8 |
| Fs-5-Gly | 337 | 511 | 1542.0 | 0.0 | S. enterica O52 | 397 | 1016 | 1548.3 | 15.5 |
| SiaLeX3A | 338 | 528 | 1551.5 | 11.4 | S. enterica O11 | 398 | 1017 | 1547.8 | 14.3 |
| 6'SLN-LN | 339 | 534 | 1542.3 | 1.5 | S. enterica O51 | 399 | 1018 | 1599.2 | 15.7 |
| GD2-Gly | 340 | 535 | 1554.8 | 20.7 | S. enterica O44 | 400 | 1019 | 1589.7 | 14.7 |
| LSTa | 341 | 536 | 1544.8 | 4.7 | S. enterica O21 | 401 | 1020 | 1557.0 | 12.8 |
| LSTd | 342 | 537 | 1550.3 | 11.4 | S. enterica O57 | 402 | 1021 | 1584.8 | 31.3 |
| 11-OS | 343 | 627 | 1591.3 | 12.2 | S. enterica O56 | 403 | 1022 | 1551.0 | 11.9 |
| Treh | 344 | 629 | 1544.3 | 6.2 | S. enterica O38 | 404 | 1023 | 1546.5 | 8.8 |
| HyalU20-ol | 345 | 630 | 1547.0 | 11.3 | C. sakazakii G2356 O2 | 405 | 1024 | 1549.2 | 11.1 |
| HyalU38-ol | 346 | 631 | 1551.5 | 10.9 | C. sakazakii G2592 O7 | 406 | 1025 | 1543.8 | 6.1 |
| HyalU13-ol | 347 | 632 | 1549.5 | 9.7 | C. sakazakii G2594 O4 | 407 | 1026 | 3429.8 | 360.0 |
| (Neu5Aca2-8)n | 348 | 633 | 1546.7 | 6.6 | C. sakazakii G2726 O3 | 408 | 1027 | 1793.0 | 17.4 |
| GNa4GN | 349 | 800 | 1550.8 | 15.1 | E. coli O11 | 409 | 1201 | 2241.8 | 1694.7 |
| LN_dimer | 350 | 804 | 1563.7 | 21.2 | E. coli O15 | 410 | 1202 | 1544.3 | 2.7 |
| 6Bn-LacdiNAc | 351 | 805 | 1544.0 | 4.5 | E. coli O44 | 411 | 1203 | 1542.2 | 0.4 |
| Aa6Ga | 352 | 806 | 1546.0 | 9.8 | E. coli O49 | 412 | 1204 | 1557.5 | 29.7 |
| Aa6G-C3 | 353 | 808 | 1549.7 | 11.3 | E. coli O51 | 413 | 1205 | 1559.0 | 28.3 |
| ANb3ANa | 354 | 809 | 1545.3 | 6.3 | E. coli O52 | 414 | 1206 | 1546.5 | 11.5 |
| core5Gc | 355 | 810 | 1544.7 | 3.9 | E. coli O57 | 415 | 1207 | 1550.0 | 6.4 |
| KN05097 | 356 | 811 | 1540.8 | 2.3 | E. coli O58 | 416 | 1208 | 1556.3 | 15.8 |
| Laca | 357 | 812 | 1547.5 | 9.8 | E. coli O71 | 417 | 1209 | 1603.8 | 29.3 |
| TFGc | 358 | 813 | 1547.0 | 12.7 | E. coli O73 | 418 | 1210 | 2133.0 | 71.4 |
| Aa4ANa | 359 | 815 | 1543.0 | 2.0 | E. coli O85 | 419 | 1211 | 1875.2 | 41.9 |
| Ab4ANa | 360 | 816 | 1543.8 | 4.5 | E. coli O95 | 420 | 1212 | 1803.2 | 27.9 |

| | | | | | | | | | |
|--------------------------|-----|------|--------|-------|--------------------------|-----|------|--------|--------|
| E. coli O99 | 421 | 1213 | 1586.7 | 109.4 | P. aeruginosa O11ab | 481 | 1403 | 1551.0 | 11.9 |
| E. coli O108 | 422 | 1214 | 1643.3 | 14.0 | P. aeruginosa O13ab | 482 | 1404 | 1543.2 | 3.4 |
| E. coli O112ab | 423 | 1215 | 1591.7 | 95.4 | P. aeruginosa O13ac | 483 | 1405 | 1552.0 | 20.7 |
| E. coli O118 | 424 | 1216 | 1553.0 | 15.0 | P. aeruginosa O14 | 484 | 1406 | 1542.3 | 0.8 |
| E. coli O119 | 425 | 1217 | 1563.3 | 14.9 | P. aeruginosa O15 | 485 | 1407 | 1545.8 | 6.6 |
| E. coli O123 | 426 | 1218 | 1550.0 | 12.2 | P. aeruginosa O2abc | 486 | 1408 | 1625.7 | 190.9 |
| E. coli O125 | 427 | 1219 | 1604.8 | 150.5 | P. aeruginosa O2ac | 487 | 1409 | 1545.2 | 4.3 |
| E. coli O127 | 428 | 1220 | 1544.2 | 4.8 | P. aeruginosa O2ac(F3) | 488 | 1410 | 1619.3 | 181.6 |
| E. coli O130 | 429 | 1221 | 1586.3 | 72.5 | P. aeruginosa O2ad(F7) | 489 | 1411 | 1540.7 | 2.5 |
| E. coli O148 | 430 | 1222 | 1545.7 | 4.2 | P. aeruginosa O2adf | 490 | 1412 | 1544.8 | 6.5 |
| E. coli O150 | 431 | 1223 | 1543.3 | 2.0 | P. aeruginosa O3(Habs 3) | 491 | 1413 | 1554.2 | 20.8 |
| E. coli O151 | 432 | 1224 | 1597.3 | 16.9 | P. aeruginosa O3ab | 492 | 1414 | 1564.7 | 27.9 |
| E. coli O161 | 433 | 1225 | 4272.0 | 184.4 | P. aeruginosa O4ab | 493 | 1415 | 1574.2 | 33.5 |
| E. coli O168 | 434 | 1226 | 1546.7 | 14.0 | P. aeruginosa O4ac | 494 | 1416 | 1556.5 | 19.8 |
| E. coli O40 | 435 | 1227 | 1544.0 | 3.2 | P. aeruginosa O6(F1) | 495 | 1417 | 1615.7 | 166.0 |
| E. coli O86_B7 | 436 | 1228 | 1547.5 | 8.5 | P. aeruginosa O9ad | 496 | 1418 | 1945.7 | 975.1 |
| E. coli O10a10b | 437 | 1230 | 1544.0 | 4.9 | P. aeruginosa O10a10b | 497 | 1419 | 1544.8 | 4.5 |
| E. coli O12 | 438 | 1231 | 1541.5 | 2.3 | P. genomospecies 5/6 O79 | 498 | 1501 | 1542.0 | 0.0 |
| E. coli O14 | 439 | 1232 | 1544.5 | 6.6 | A. hydrophila O34deAc | 499 | 1502 | 4001.0 | 294.8 |
| E. coli O19ab | 440 | 1233 | 1543.8 | 3.3 | E. cloacae G2277 | 500 | 1503 | 2186.3 | 1367.7 |
| E. coli O27 | 441 | 1234 | 1548.7 | 8.7 | E. cloacae G3421 | 501 | 1504 | 1542.7 | 1.8 |
| E. coli O36 | 442 | 1235 | 1564.7 | 11.8 | P. mirabilis 12B-r | 502 | 1601 | 1545.3 | 8.3 |
| E. coli O37 | 443 | 1236 | 1570.8 | 11.4 | P. mirabilis 1B-m | 503 | 1602 | 1543.5 | 5.4 |
| E. coli O39 | 444 | 1237 | 1672.8 | 60.2 | P. mirabilis 3B-m | 504 | 1603 | 1552.0 | 14.9 |
| E. coli O41 | 445 | 1238 | 1545.2 | 6.1 | P. mirabilis HJ 4320 | 505 | 1604 | 1546.7 | 9.2 |
| E. coli O54 | 446 | 1239 | 1548.2 | 9.6 | P. mirabilis O11 | 506 | 1605 | 1578.7 | 75.5 |
| E. coli O62 | 447 | 1240 | 2495.5 | 143.1 | P. mirabilis O13 | 507 | 1606 | 1549.2 | 10.0 |
| E. coli O81 | 448 | 1241 | 1674.0 | 19.9 | P. mirabilis O16 | 508 | 1607 | 1596.8 | 133.8 |
| E. coli O30 | 449 | 1242 | 1575.2 | 18.2 | P. mirabilis O23 | 509 | 1608 | 1552.0 | 16.0 |
| E. coli O36 | 450 | 1243 | 1542.0 | 0.0 | P. mirabilis O28 | 510 | 1609 | 1554.8 | 20.1 |
| E. coli O37 | 451 | 1244 | 1553.2 | 27.8 | P. mirabilis O31 | 511 | 1610 | 1569.7 | 9.2 |
| E. coli O40 | 452 | 1245 | 1557.5 | 28.2 | P. mirabilis O33 | 512 | 1611 | 1579.3 | 17.2 |
| E. coli O46 | 453 | 1246 | 1559.5 | 32.7 | P. mirabilis O35 | 513 | 1612 | 1556.7 | 17.9 |
| E. coli O68 | 454 | 1247 | 1546.0 | 9.8 | P. mirabilis O38 | 514 | 1613 | 1551.3 | 24.4 |
| E. coli O100 | 455 | 1248 | 1602.5 | 31.6 | P. mirabilis O3ab | 515 | 1614 | 1550.7 | 19.9 |
| E. coli O102 | 456 | 1249 | 1575.7 | 37.0 | P. mirabilis O58 | 516 | 1615 | 1541.8 | 0.4 |
| E. coli O120 | 457 | 1250 | 1798.7 | 622.4 | P. mirabilis O6 | 517 | 1616 | 1605.8 | 10.9 |
| E. coli O135 | 458 | 1251 | 1860.3 | 72.6 | P. mirabilis O60 | 518 | 1617 | 1547.3 | 7.9 |
| E. coli O140 | 459 | 1252 | 1550.8 | 9.1 | P. mirabilis OE | 519 | 1618 | 1543.3 | 2.9 |
| E. coli O153 | 460 | 1253 | 1548.3 | 9.8 | P. penneri 107 | 520 | 1701 | 1541.7 | 3.2 |
| E. coli O154 | 461 | 1254 | 1557.8 | 39.8 | P. penneri 113 | 521 | 1702 | 1541.5 | 5.9 |
| E. coli O157 | 462 | 1255 | 1542.0 | 0.0 | P. penneri 17 | 522 | 1703 | 1549.5 | 13.6 |
| E. coli O158 | 463 | 1256 | 1553.0 | 20.6 | P. penneri 28 | 523 | 1704 | 1545.0 | 7.3 |
| E. coli O163 | 464 | 1257 | 1542.3 | 0.8 | P. penneri 31 | 524 | 1705 | 1598.0 | 98.0 |
| E. coli O180 | 465 | 1258 | 1630.7 | 15.3 | P. penneri 40 | 525 | 1706 | 1541.8 | 0.4 |
| E. coli O84deAc | 466 | 1259 | 1544.5 | 8.2 | P. penneri 75 | 526 | 1707 | 1541.8 | 6.3 |
| P. alcalifaciens O3 | 467 | 1301 | 1544.0 | 5.4 | P. vulgaris 32/57 O17 | 527 | 1801 | 1542.7 | 2.5 |
| P. alcalifaciens O3 CPS | 468 | 1302 | 1551.7 | 15.1 | P. vulgaris 70/57 O44 | 528 | 1802 | 1546.8 | 10.4 |
| P. alcalifaciens O7 | 469 | 1303 | 1544.8 | 2.9 | P. vulgaris O19ab | 529 | 1803 | 1541.7 | 0.5 |
| P. alcalifaciens O9 | 470 | 1304 | 1695.7 | 361.4 | P. vulgaris O22 | 530 | 1804 | 1546.8 | 10.3 |
| P. rustigianii O11 CPS | 471 | 1305 | 1542.7 | 1.6 | P. vulgaris O25 | 531 | 1805 | 1685.3 | 32.4 |
| P. alcalifaciens O12 | 472 | 1306 | 1544.8 | 8.0 | P. vulgaris O4 | 532 | 1806 | 1543.0 | 1.7 |
| P. alcalifaciens O22 | 473 | 1307 | 1545.3 | 4.7 | P. vulgaris O46 | 533 | 1807 | 1570.2 | 36.7 |
| P. alcalifaciens O31 | 474 | 1308 | 1542.0 | 0.6 | P. vulgaris O65 | 534 | 1808 | 1553.7 | 19.3 |
| P. alcalifaciens O40 | 475 | 1309 | 1545.8 | 3.9 | P. vulgaris OX19 | 535 | 1809 | 1553.7 | 18.0 |
| P. alcalifaciens O46deAc | 476 | 1310 | 1554.2 | 12.4 | P. vulgaris TG251 | 536 | 1810 | 1544.5 | 3.9 |
| P. alcalifaciens O48 | 477 | 1311 | 1546.7 | 9.8 | A.baumannii LUH5534 | 537 | 1901 | 1573.3 | 27.8 |
| P. alcalifaciens O60 | 478 | 1312 | 1768.7 | 29.5 | Sh. boydii type 10 | 538 | 2001 | 1570.3 | 13.0 |
| P. aeruginosa O1(F4) | 479 | 1401 | 1576.7 | 56.1 | Sh. boydii type 12 | 539 | 2002 | 1737.2 | 214.1 |
| P. aeruginosa O10ac(F5) | 480 | 1402 | 1548.0 | 14.7 | Sh. boydii type 14 | 540 | 2003 | 1551.2 | 13.6 |

| | | | | |
|-----------------------------|-----|------|--------|--------|
| Sh. boydii type 15 | 541 | 2004 | 1551.3 | 16.7 |
| Sh. boydii type 16 | 542 | 2005 | 1583.0 | 67.8 |
| Sh. boydii type 17 | 543 | 2006 | 1545.0 | 7.4 |
| Sh. boydii type 18 | 544 | 2007 | 1757.3 | 19.9 |
| Sh. boydii type 2 | 545 | 2008 | 1758.3 | 29.3 |
| Sh. boydii type 6 | 546 | 2009 | 1627.2 | 11.4 |
| Sh. boydii type 7 | 547 | 2010 | 1672.0 | 40.9 |
| Sh. boydii type 8 | 548 | 2011 | 1579.8 | 9.4 |
| Sh. boydii type 9 | 549 | 2012 | 1545.3 | 4.1 |
| Sh. boydii type X | 550 | 2013 | 1544.5 | 5.3 |
| Sh. dysenteriae type 1 | 551 | 2101 | 1552.2 | 8.3 |
| Sh. dysenteriae type 11 | 552 | 2102 | 1546.5 | 6.2 |
| Sh. dysenteriae type 3 | 553 | 2103 | 1542.7 | 1.2 |
| Sh. dysenteriae type 4 | 554 | 2104 | 1555.3 | 14.2 |
| Sh. dysenteriae type 7 | 555 | 2105 | 2111.0 | 59.7 |
| Sh. dysenteriae type 8 | 556 | 2106 | 1634.8 | 13.8 |
| Sh. dysenteriae type 9 | 557 | 2107 | 1548.5 | 7.9 |
| Sh. flexneri type 2a | 558 | 2201 | 1545.2 | 6.0 |
| Sh. flexneri type 2b | 559 | 2202 | 1607.7 | 24.7 |
| Sh. flexneri type 3a | 560 | 2203 | 1611.2 | 15.4 |
| Sh. flexneri type 3b | 561 | 2204 | 1587.2 | 18.6 |
| Sh. flexneri type 4a | 562 | 2205 | 1724.2 | 59.4 |
| Sh. flexneri type 4b | 563 | 2206 | 1582.3 | 12.2 |
| Sh. flexneri type 5a | 564 | 2207 | 1599.8 | 31.7 |
| Sh. flexneri type 5b | 565 | 2208 | 5738.3 | 377.4 |
| Sh. flexneri type 6 | 566 | 2209 | 1598.2 | 30.1 |
| Sh. flexneri type 6b | 567 | 2210 | 1611.3 | 21.4 |
| Sh. flexneri type X | 568 | 2211 | 1729.8 | 58.0 |
| Sh. flexneri type Y | 569 | 2212 | 1554.0 | 15.8 |
| Sh. flexneri type 1a | 570 | 2213 | 1562.7 | 11.7 |
| Sh. flexneri type 2c | 571 | 2214 | 1607.3 | 84.0 |
| Sh. flexneri 4av | 572 | 2215 | 1559.2 | 7.1 |
| Sh. flexneri type 5c | 573 | 2216 | 2794.7 | 223.1 |
| Sh. flexneri type 1d | 574 | 2217 | 2995.7 | 85.5 |
| Sh. flexneri type Y | 575 | 2218 | 1549.3 | 10.0 |
| Sh. flexneri type Y_2 | 576 | 2219 | 1540.8 | 2.0 |
| Sh. flexneri type Yv | 577 | 2220 | 1546.5 | 10.5 |
| Sh. flexneri type Xv | 578 | 2221 | 1577.2 | 36.5 |
| S. equi sp. hyaluronic acid | 579 | 2501 | 1541.5 | 0.8 |
| Heparin | 580 | 2502 | 1903.0 | 885.7 |
| A. methanolicus LPS | 581 | 2601 | 1561.8 | 23.7 |
| S. cerevisiae zymoza A | 582 | 3001 | 1564.7 | 14.4 |
| Mannan | 583 | 3002 | 6613.2 | 551.9 |
| Laminarin | 584 | 3301 | 1551.0 | 22.1 |
| Laminaran | 585 | 3302 | 1580.2 | 56.9 |
| bGlucan | 586 | 3401 | 1546.5 | 6.7 |
| Galactan-1 | 587 | 3501 | 1561.7 | 30.5 |
| Galactan-2 | 588 | 3502 | 1541.7 | 2.6 |
| E. coli O86_B7 LPS | 589 | 8001 | 1541.8 | 0.4 |
| E. coli O148 LPS | 590 | 8002 | 1542.0 | 0.0 |
| E. coli O168 LPS | 591 | 8003 | 1542.3 | 1.9 |
| E. coli O130 LPS | 592 | 8004 | 1557.3 | 26.5 |
| E. coli O151 LPS | 593 | 8005 | 1542.8 | 2.0 |
| E. coli O99 LPS | 594 | 8006 | 1561.0 | 27.6 |
| E. coli O73 LPS | 595 | 8007 | 1555.5 | 16.0 |
| E. coli O118 LPS | 596 | 8008 | 1541.7 | 0.5 |
| E. coli O58 LPS | 597 | 8009 | 1551.5 | 16.7 |
| E. coli O112ab LPS | 598 | 8010 | 1570.3 | 19.1 |
| E. coli O150 LPS | 599 | 8011 | 2692.3 | 2766.4 |
| E.coli O40 LPS | 600 | 8012 | 1549.8 | 11.2 |

| | | | | |
|----------------|-----|------|--------|-------|
| E.coli O49 LPS | 601 | 8013 | 1546.2 | 10.2 |
| E.coli O81 LPS | 602 | 8014 | 1590.8 | 20.4 |
| E.coli O52 LPS | 603 | 8015 | 1553.5 | 18.9 |
| Scleroglucan | 604 | 9001 | 1549.2 | 7.0 |
| Curdlan | 605 | 9002 | 1555.0 | 21.0 |
| Chitosan | 606 | 9003 | 1546.7 | 5.5 |
| Mannan | 607 | 9004 | 1547.3 | 9.9 |
| Glucan | 608 | 9005 | 1541.8 | 0.4 |
| Zymosan A | 609 | 9006 | 2797.2 | 108.4 |
| HyalU(E77-2) | 610 | 9007 | 1545.7 | 6.5 |
| S488 | 611 | 488 | 1843.5 | 39.6 |
| S555 | 612 | 555 | 5038.2 | 468.4 |
| S647 | 613 | 647 | 1554.0 | 15.7 |
| Smix | 614 | | 4614.2 | 127.6 |
| blank | 615 | | 1568.0 | 49.2 |

5.6. Isosteric Substitution of Acylhydrazones yields highly potent divalent LecA Inhibitors with excellent Solubility and metabolic Stability

Authors: Eva Zahorska¹⁻³, Sakonwan Kuhaudomlarp^{4,5,6}, Joscha Meiers¹⁻³, Dirk Hauck¹⁻², Emilie Gillon⁴, Katharina Rox^{2,7}, Anne Imberty⁴, Alexander Titz^{*1-3}

¹ Chemical Biology of Carbohydrates (CBCH), Helmholtz Institute for Pharmaceutical Research Saarland (HIPS), Helmholtz Centre for Infection Research, D-66123 Saarbrücken, Germany

² Deutsches Zentrum für Infektionsforschung (DZIF), Standort Hannover-Braunschweig ³ Department of Chemistry, Saarland University, D-66123 Saarbrücken, Germany

⁴ Université Grenoble Alpes, CNRS, CERMAV, 38000 Grenoble, France

⁵ Department of Biochemistry, Faculty of Science, Mahidol University, Bangkok 10400, Thailand;

⁶ Center for Excellence in Protein and Enzyme Technology, Faculty of Science, Mahidol University, Bangkok 10400, Thailand;

⁷ Department of Chemical Biology (CBIO), Helmholtz Centre for Infection Research, D-38124 Braunschweig, Germany

*corresponding author: alexander.titz@helmholtz-hzi.de

Manuscript in preparation.

The references of this chapter are listed at the end of this chapter.

E.Z. designed and synthesised LecA ligands. D.H. synthesised bis-aniline building blocks **C–F** and monovalent ligands **G2** and **K2**. E.Z. performed competitive LecA binding assay and ITC measurements. E.Z. and J.M. performed solubility determinations. K.R. obtained and analysed metabolic stability data. S.K. and E.G. performed and analysed SPR experiments with conceptual advice from A.I.. E.Z. and A.T. conceived the study. E.Z. and A.T. wrote the manuscript with input from all co-authors.

Intended Journal: Chemical Communications

RUNNING TITLE:

Divalent inhibitors with bisaminopyridine and sulfonated linkers as potent inhibitor of bacterial lectins with excellent solubility and metabolic stability

ABSTRACT

Bacterial adhesion and biofilm formation of the ESKAPE pathogen *Pseudomonas aeruginosa* are mediated by the tetravalent lectins LecA and LecB. Recently, we have reported rapidly accessible highly active divalent galactose-specific LecA inhibitors, albeit with relatively poor solubility. Here, we aim at increasing solubility and metabolic stability of the compounds by isosterically replacing the chemically labile and poorly soluble acylhydrazone linking motif and varied the linking unit between two galactosides. The resulting optimized divalent LecA ligands with improved metabolic stability were up to 5000-fold more soluble, enabling now the confirmation of their low-nanomolar activity by microcalorimetry.

Carbohydrate-protein interactions are essential recognition codes in many biological processes, including microbial and viral infections. Lectins of pathogenic origin involved in host-cell recognition, adhesion and/or biofilm formation are being recognized as new therapeutic targets.^{1,2} *Pseudomonas aeruginosa* is a Gram-negative opportunistic bacterium that belongs to the group of highly resistant ESKAPE pathogens.³ Resistance to an antimicrobial treatment can be further enhanced by its ability to grow biofilms – the causative mechanism of chronic infections.⁴ *P. aeruginosa* adhesion and biofilm formation are mediated by the tetravalent lectins LecA and LecB, encoded in its core genome and functionally conserved across clinical isolates.^{5–8} Thus, their inhibition is desired to counteract pathogenicity.⁹ Furthermore, it was shown that LecA acts as a lipid zipper upon binding to its cellular receptor Gb3 and triggers bacterial invasion.¹⁰ It was demonstrated that inhalation of D-galactose and L-fucose aerosols, the monosaccharide ligands of LecA and LecB, respectively, reduced bacterial burden in cystic fibrosis patients.¹¹

Numerous glycomimetics based on D-galactose ($K_d = 88 \mu\text{M}$)¹² and L-fucose/D-mannose ($K_d = 430 \text{ nM}$ for methyl α -L-fucoside, $K_d = 71 \mu\text{M}$ methyl α -D-mannoside)¹³ have been developed for LecA and LecB, respectively.^{2,9,14} Some of these compounds targeting LecB lack carbohydrate character and showed potent inhibition of LecB with beneficial pharmacokinetic properties.^{15–17} Numerous monovalent LecA glycomimetic inhibitors have also been reported^{18–20}, demonstrating the importance of an aromatic aglycon on the b-galactose moiety to reach micromolar affinity.^{8,19} We have recently introduced the first covalent lectin inhibitor targeting a surface exposed cysteine residue²¹ and the first non-carbohydrate lectin inhibitors for bacterial lectins, a catechol motif.²² However, all monovalent LecA inhibitors reached at best only moderate potencies in the 5 to 50 μM range.

In contrast to LecB, the quaternary structure of LecA²³ displays two adjacent binding sites that are optimally oriented in space for simultaneous binding to the two galactose moiety of a divalent ligand leading to an increased inhibitory potency. Notably, Pieters and coworkers developed low nanomolar LecA inhibitors (down to $K_d = 12 \text{ nM}$) by connecting two galactosides through a linker containing several copies of rigid glucose-triazole linkers.^{24,25} Despite the efficient CuAAC chemistry applied for the final assembly of the divalent ligands, 17 synthetic steps were required to prepare the individual azide and alkyne building blocks and assemble the final compound. Replacing one of the glucose-bistriazole spacers with cyclohexyl bistiourea moieties somewhat simplified the synthesis to 9 steps and one compound with 30 nM affinity was obtained.²⁶ Similarly, rather complex divalent LecA ligands with peptide-based

linkers obtained from a lengthy synthesis were reported by Novoa *et al.* ($K_d = 82$ nM) and Huang *et al.* ($K_d = 71$ nM).^{27,28}

We have recently reported a series of highly active divalent LecA inhibitors with acylhydrazone based linkers ($K_d = 11 - 81$ nM) synthesized in only four chemical steps.²⁹ While these molecules showed the highest potency among all published divalent LecA inhibitors, they suffer from an intrinsic hydrolytic lability of the acylhydrazone bond and very low aqueous solubility despite the presence of the two hydrophilic carbohydrate moieties. Furthermore, since acylhydrazones undergo hydrolysis at acidic pH, potentially toxic aldehydes and hydrazides may be formed *in vivo*.

Here, we report the optimization of these highly potent divalent LecA inhibitors by replacing the acylhydrazone motif with a more stable amide bond and varying linker identity and length to increase solubility and stability (Figure 1a). We chose two galactoside building blocks bearing coumaric acid (**1**, Figure 1b) or hydroxyphenyl propionic acid (**2**) as aglycons to investigate the effect of the more rigid olefin in **1**, comparable to the parent acylhydrazones, versus the flexible alkyl motif in **2**. These galactosylated carboxylic acids were intended for coupling to various bisanilines to yield the corresponding divalent LecA inhibitors. Since an optimal length and geometry is important for the divalent ligand to bind simultaneously to two neighbouring LecA sites, linker length was varied by stepwise introduction of methylene units. The aromatic moieties and linker lengths were varied: bisaniline linkers **B–F** and their monovalent control **A** (Figure 1c) were used to mimic previously used bis-benzaldehyde structures;²⁹ our rational solubility optimization included the introduction of hydrogen-bonding polar groups or ionizable moieties into bisaminopyridine linkers **H–J** and sulfonated linker **L** and their monovalent controls **G** and **K**, respectively.

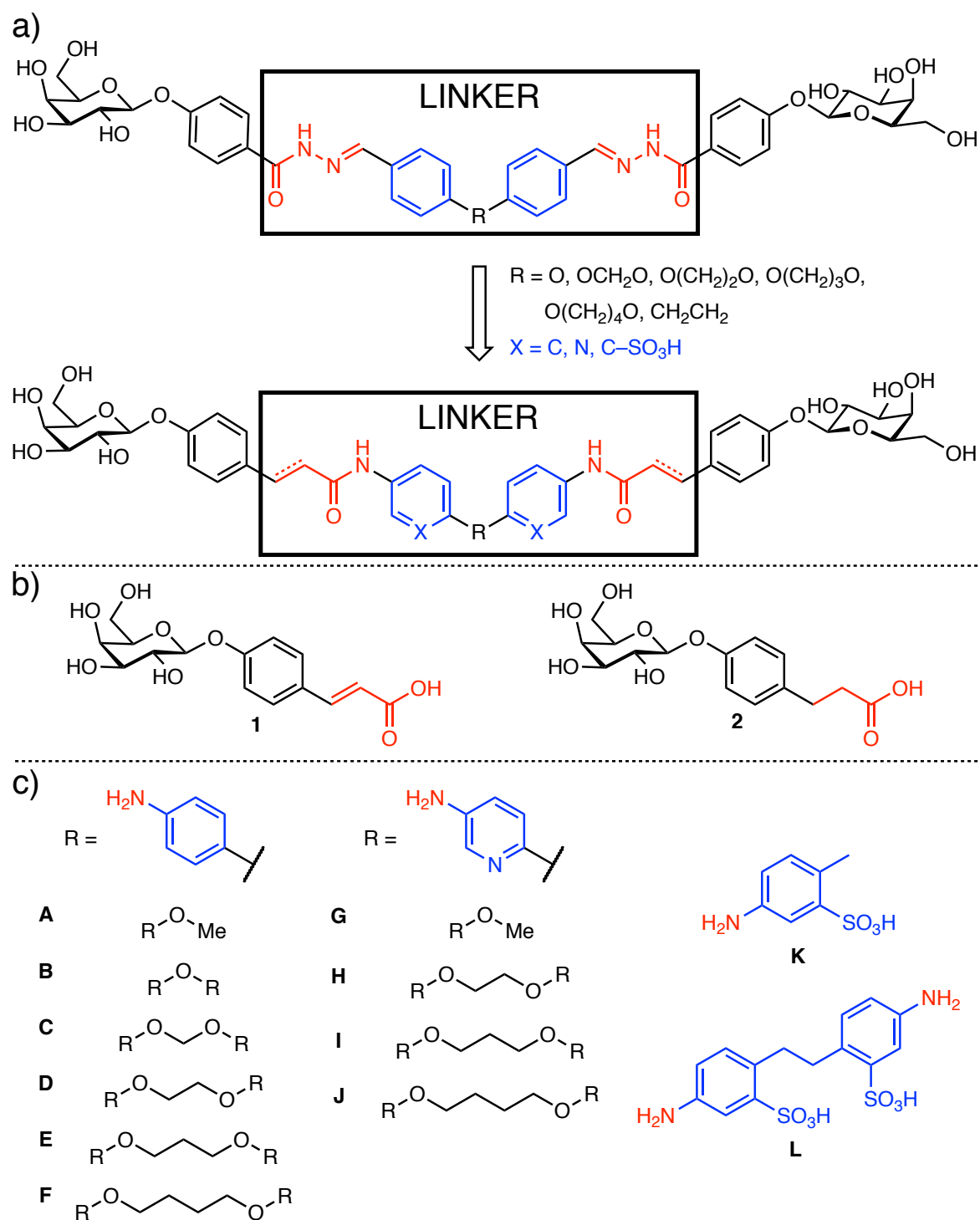
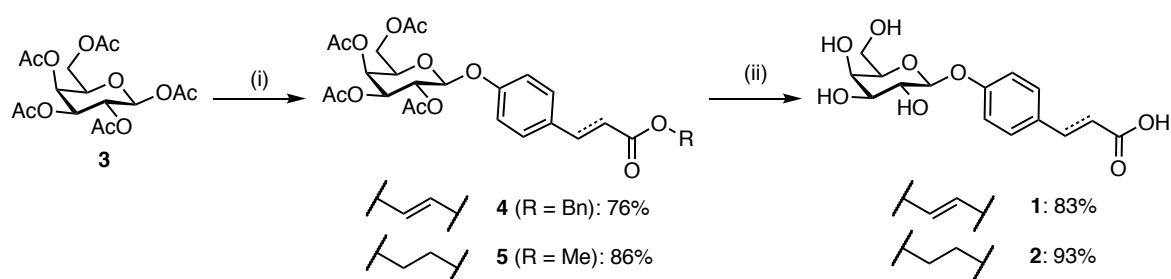


Figure 1: Divalent precision LecA ligands: (a) parent bisacylhydrazone LecA inhibitors (top) and new generation optimized bioisosters (bottom). Proposed chemical modifications are highlighted: amide linkage as acylhydrazone bioisoster in red and linker derivatizations in blue. (b) Galactoside building blocks with terminal α,β -unsaturated carboxylate **1** and its saturated analogue **2**. (c) Linker moieties: anilines **B–F**, aminopyridines **H–J** and sulfonated linker **L**, and their monovalent controls **A**, **G**, and **K**.

Synthesis of the two galactoside building blocks **1** and **2** started with β -selective glycosylation of benzyl coumarate or methyl 3-(4-hydroxyphenyl)propanoate with β -D-galactose pentaacetate (**3**) under Lewis acid catalysis (Scheme 1). β -Glycosides **4** and **5** were obtained in good yields (76-86%) and full saponification of the esters was achieved by treating with aqueous NaOH to give galactosides **1** and **2** in high yields. Synthesis of coumarate **1** was initially attempted using the methyl ester under identical glycosylation conditions as for compound **2**, but this transformation was unsuccessful most probably due to its poor solubility in dichloromethane and only poor yields were achieved when carried out in the more polar solvent chloroform instead. Changing the glycosyl acceptor from methyl to benzyl coumarate improved solubility in those solvents and the glycosylation yielded 76% of compound **4**.

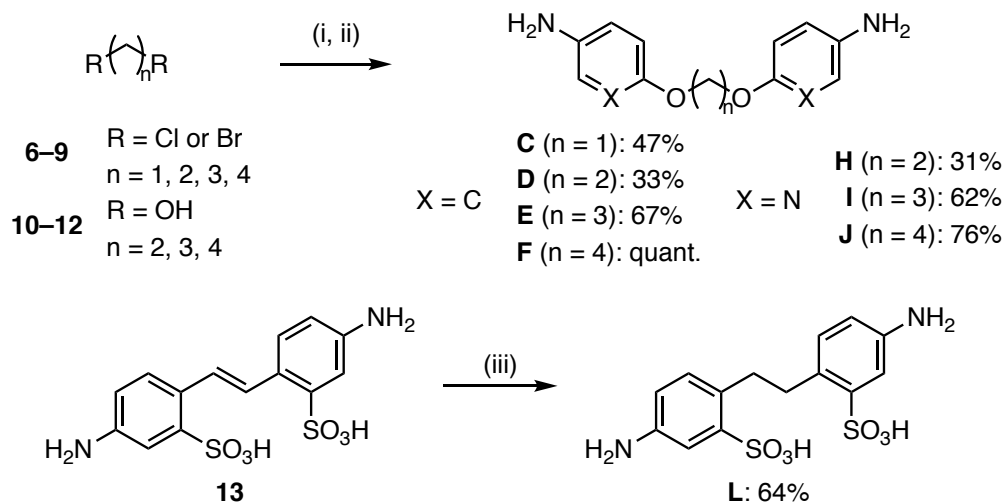


Scheme 1: Synthesis of galactoside building blocks **1** and **2**. Reagents and conditions: (i) benzyl *p*-coumarate/methyl 3-(4-hydroxyphenyl)propanoate, $\text{BF}_3 \cdot \text{Et}_2\text{O}$, CHCl_3 for **4** and CH_2Cl_2 for **5**, 0°C – r.t., overnight; (ii) NaOH, $\text{H}_2\text{O}/\text{MeOH}$ (1:1), 50°C for **1** and r.t. for **2**, 1 h – 2 h.

The linkers needed for assembly of those galactosides into divalent LecA inhibitors were synthesized or purchased. While, anilines **A** and **B**, amino pyridine **G** and sulfonated linker **K** were commercially available, linkers **C–F** and bis-aminopyridine linkers **H–J** were prepared in two steps: a double nucleophilic substitution of the α,ω -alkyldihalides (**6–9**) with 4-nitrophenol or a double nucleophilic aromatic substitution using α,ω -alkyldiols (**10–12**) with 2-chloro-5-nitro-pyridine followed in both cases by palladium-catalyzed hydrogenation to the desired bis-anilines or bis-aminopyridines, respectively (Scheme 2). Ethyl-spaced bissulfonated linker **L** was by obtained by reduction of 4,4'-diaminostilbene-2,2'-disulfonic acid (**13**) with hydrogen on Raney nickel.

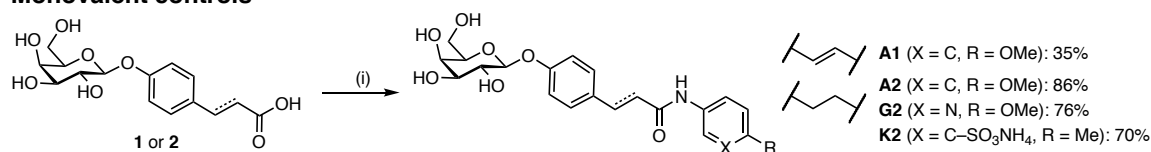
Final assembly of the divalent LecA inhibitors was achieved by coupling of the amino-substituted linkers **A–L** and carboxylate-containing galactosides **1** and **2** using HBTU or PyBOP as peptide coupling reagents (Scheme 3). High reaction turnovers were observed for all coupling reactions, but purification difficulties caused varying yields: lower solubility was responsible for isolated yields in the benzene series (**A1–F1** and **A2–F2**), whereas side product formation was observed in the pyridine series (**H1–I1** and **G2–J2**). After chromatographic

separation, the sulfonic acids induced acid catalysed hydrolysis of the glyosidic linkage upon solvent removal and concentration, thus the sulfonated ligands **K2** and **L2** had to be purified using buffered eluents as ammonium salts.

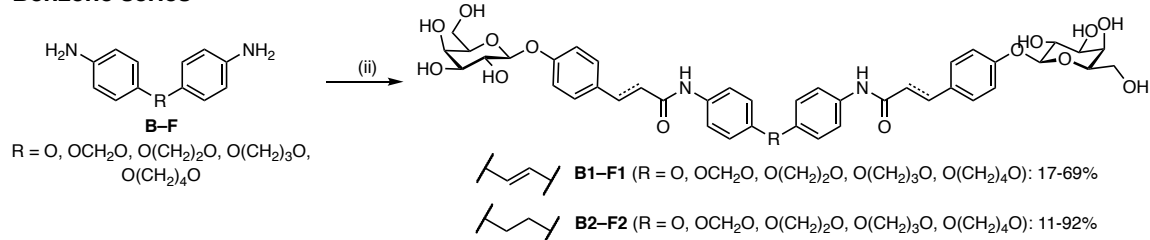


Scheme 2: Synthesis of benzene, pyridine and phenylsulfonate linkers. Reagents and conditions: (i) for **C-F**: 4-nitrophenol, K_2CO_3 , DMF, 70 °C, microwave, 11 h – 4 d (for **C** 10 days, no irradiation), for **H-J**: 2-chloro-5-nitropyridine, NaH, r.t., DMF, 1 h – 2 d (for **H** K_2CO_3 , 65 °C, DMF, 5 d); (ii) H_2 , Pd/C, $CH_2Cl_2/MeOH$ (2:1, 3:1 for **D-F**), r.t., 3h – o.n.; (iii) Raney Ni, H_2 , r.t., H_2O , 6 d.

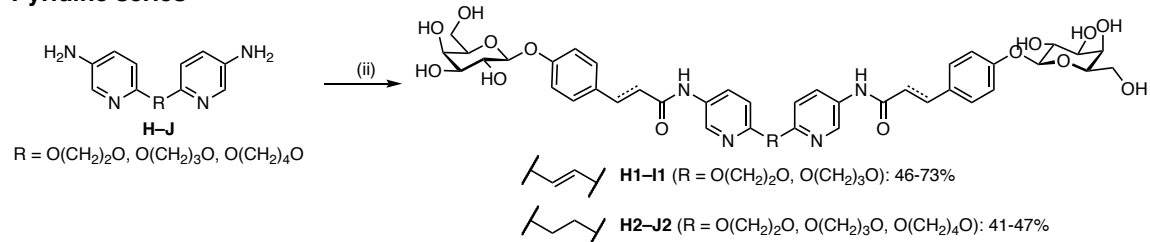
Monovalent controls



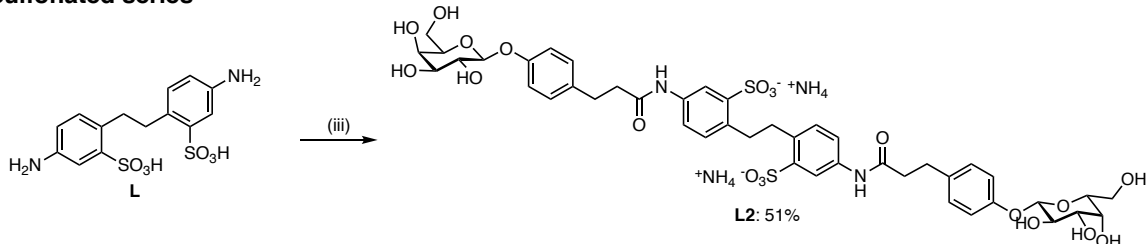
Benzene series



Pyridine series



Sulfonated series



Scheme 3: Synthesis of divalent LecA ligands and their monovalent analogues as controls. Reagents and conditions: (i) for **A** and **G**: HBTU, DIPEA, DMF, r.t., 1 h – overnight, for **K**: PyBOP, N-methylmorpholine, DMF, r.t., overnight; (ii) galactoside **1** or **2**, HBTU, DIPEA, DMF, r.t., 2 h – 2 d, (iii) galactoside **2**, PyBOP, N-methylmorpholine, DMF, r.t., overnight.

Previously, the parent acylhydrazone divalent LecA ligands²⁹ (Figure 1) suffered from poor aqueous solubility. Therefore, we tested selected representatives of each new class aiming at higher solubility and one of the parent bisacylhydrazones and quantified their solubility in aqueous media (Table 1). All tested new derivatives showed significantly improved solubility compared to the previous bisacylhydrazone **14**. The very low kinetic solubility of the bisacylhydrazone **14** ($S < 0.3 \mu\text{M}$) was increased at least fourfold in its α,β -unsaturated amide analogue **D1** ($S = 1.2 \pm 0.6 \mu\text{M}$) and at least over 20-fold in the saturated analogue **D2** ($S = 7.5 \pm 4.2 \mu\text{M}$). Substitution of the benzene ring with a pyridine moiety further increased solubility by 5- to 10-fold enhancement (**H1** $S = 5.5 \pm 1.4 \mu\text{M}$, **H2** $S = 71.4 \pm 14.9 \mu\text{M}$) compared to **D1/D2**. Generally, saturated propanamide divalent ligands **D1** and **H1** were more soluble than their unsaturated acrylamide-based analogues **D2** and **H2**. Excellent solubility was finally

achieved with sulfonated divalent ligand **L2**, which was fully dissolved from its solid form in an aqueous buffer ($S > 1.5$ mM).

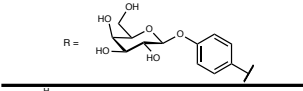
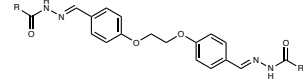
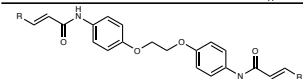
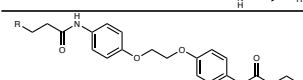
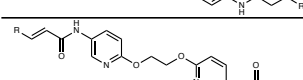
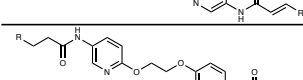
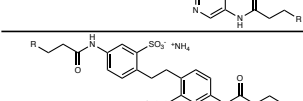
We then set out to determine early *in vitro* Absorption, Distribution, Metabolism, and Excretion (ADME) properties for a selected subset of the synthesized LecA inhibitors **D1**, **D2**, **H1**, **H2** and **L2** to evaluate their stability in blood plasma and against liver metabolism and compare it to one parent bisacylhydrazone compound **14** (Table 1). The data obtained from microsomal stability tests revealed a low intrinsic clearance (CL_{int}) by mouse microsomes ($CL_{int} = 6.8 - 23$ $\mu\text{L}/\text{min}/\text{mg}$ protein) for all tested compounds, except of the slightly elevated clearance by **D2** ($CL_{int} = 29.6$ $\mu\text{L}/\text{min}/\text{mg}$ protein) and by the sulfonated ligand **L2** ($CL_{int} = 29.5$ $\mu\text{L}/\text{min}/\text{mg}$ protein). On the other hand, significant differences in metabolic stability were observed in human liver microsomes. Introduction of the pyridine ring decreased the compound stability (**H1** $CL_{int} = 28.6$ $\mu\text{L}/\text{min}/\text{mg}$ protein, **H2** $CL_{int} = 32.5$ $\mu\text{L}/\text{min}/\text{mg}$ protein) compared to their benzene analogues (**D1** $CL_{int} = 21.9$ $\mu\text{L}/\text{min}/\text{mg}$ protein, **D2** $CL_{int} = 21.0$ $\mu\text{L}/\text{min}/\text{mg}$ protein) or even to the parent acylhydrazone ligand **14** ($CL_{int} = 19.6$ $\mu\text{L}/\text{min}/\text{mg}$ protein). The sulfonated ligand **L2** was the most stable compound in human microsomes ($CL_{int} = 9.2$ $\mu\text{L}/\text{min}/\text{mg}$ protein).

In plasma stability test, the parent acylhydrazone ligand **14** was rather quickly degraded ($t_{1/2} = 48.9$ min) in mouse plasma and a somewhat slower degradation was observed in human plasma ($t_{1/2} = 123.5$ min). In contrast, the new generation of ligands exhibited high stability in both mouse and human plasma ($t_{1/2} \geq 180$ min), with exception of coumarate-bearing pyridine **H2** in mouse plasma ($t_{1/2} = 81.1$ min) and coumarate-bearing benzene **D2** in human plasma ($t_{1/2} = 132.5$ min), both of which still showed superior stability to the bisacylhydrazone **14**. The observed higher plasma stability of all tested amide derivatives supports the isosteric replacement of the hydrolysis prone bisacylhydrazone linking motif. All tested compounds showed very high to full mouse and human plasma protein binding (PPB) with lowest PPB for saturated pyridyl amide **H2** at 97% except for the sulfonated ligand **L2** which showed remarkably low plasma protein binding in both species, mouse and human (14.48 % and 38.45 %, respectively).

All synthesized galactosides were then evaluated for LecA inhibition in the previously reported competitive binding assay based on fluorescence polarization (Figure S1).²⁰ Monovalent galactosides (**A1**, **A2**, **G2** and **K2**) showed similar IC_{50} values (between 14 – 19 μM). The monovalent ligand carrying the α,β -unsaturated acrylamide motif **A1** ($IC_{50} = 18.8 \pm 6.6$ μM) was equipotent to its saturated and more flexible propanamide analogue **A2** ($IC_{50} = 18.9 \pm 5.5$ μM). Replacement of the benzene ring with pyridine in **G2** ($IC_{50} = 14.3 \pm 7.2$ μM)

or addition of the sulfonate solubility tag in **K2** ($IC_{50} = 14.4 \pm 3.6 \mu M$) did not greatly alter the IC_{50} values. In contrast to the monovalent controls and similar to our previous observations for the bisacylhydrazones, the titrations of the fluorescent galactoside-LecA mixture with all divalent LecA ligands exhibited very steep Hill slopes with IC_{50} s in the single digit micromolar range indicating the high potency of divalent compounds reaching the lower assay limit.²⁹

Table 1: Aqueous solubility and early ADME data of selected LecA inhibitors. Kinetic solubility was determined in aqueous TBS/ Ca^{2+} buffer containing 1% DMSO by LC-MS. Averages and std. dev. from three independent experiments. *Thermodynamic solubility in TBS/ Ca^{2+} buffer (w/o DMSO), one replicate. Plasma stability, plasma protein binding and metabolic stability using S9-fractions were performed in triplicates. Data were analysed using LC-MS/MS measurements.

| R =  | Compound | Solubility S [μM] | CL_{int} [$\mu L/min/mg$ protein] | | Plasma stability $t_{1/2}$ [min] | | PPB [%] | |
|---|-----------|--------------------------|--------------------------------------|-------|----------------------------------|-------|-----------------|------------------|
| | | | Mouse | Human | Mouse | Human | Mouse | Human |
|  | 14 | < 0.3 | < 23 | 19.6 | 48.9 | 123.5 | 100 \pm 0 | 100 \pm 0 |
|  | D1 | 1.2 \pm 0.6 | 22.4 | 21.9 | 180.1 | 223.9 | 99.43 \pm 1.0 | 99.57 \pm 0.8 |
|  | D2 | 7.5 \pm 4.2 | 29.6 | 21.0 | 182.7 | 132.5 | 100 \pm 0 | 99.51 \pm 0.8 |
|  | H1 | 5.5 \pm 1.4 | 17.5 | 28.6 | > 180 | > 240 | 100 \pm 0 | 100 \pm 0 |
|  | H2 | 71.4 \pm 14.9 | 6.8 | 32.5 | 81.1 | 214.9 | 97.58 \pm 2.1 | 99.50 \pm 0.9 |
|  | L2 | > 1500* | 29.5 | 9.2 | > 240 | > 240 | 14.48 \pm 6.8 | 38.45 \pm 12.4 |

To circumvent the limit of the competitive binding assay for these highly potent inhibitors, direct binding to immobilised LecA was quantified using SPR (Figure 2, Figures S2–S4). In agreement with the competitive binding assay, no difference in binding affinity was observed for the monovalent ligands carrying the acrylamide motif **A1** ($K_d = 5.21 \pm 0.60 \mu M$) compared to the propanamide derivative **A2** ($K_d = 5.38 \pm 0.09 \mu M$). Interestingly, a striking difference in binding affinity was observed among the divalent inhibitors. Within the benzene series, the acrylamide-based ligands **B1–F1** showed K_d s in the nanomolar to micromolar range while their propanamide-based analogues **B2–F2** were two- to threefold more active when attached to the shorter linkers **B–D** and 100- to 200-fold more potent for the longest linkers **E** and **F**. With respect to the linker length, the acrylamide-based divalent ligands with linker **C** containing one methylene unit exhibited optimal binding affinity (**C1** $K_d = 37.7 \pm 11$ nM). Increasing the number of methylene to 4 units in **F1** led to a complete loss of divalent binding boost ($K_d = 2.25 \pm 0.3 \mu M$). Divalent ligands carrying the propanamide motif **B2–F2** showed

high binding affinity to LecA in 15–23 nM range. K_d values were oscillating based on the number of methylene units present in the linker, possibly as the results of “zig-zag” geometry of the hydrocarbon chain.

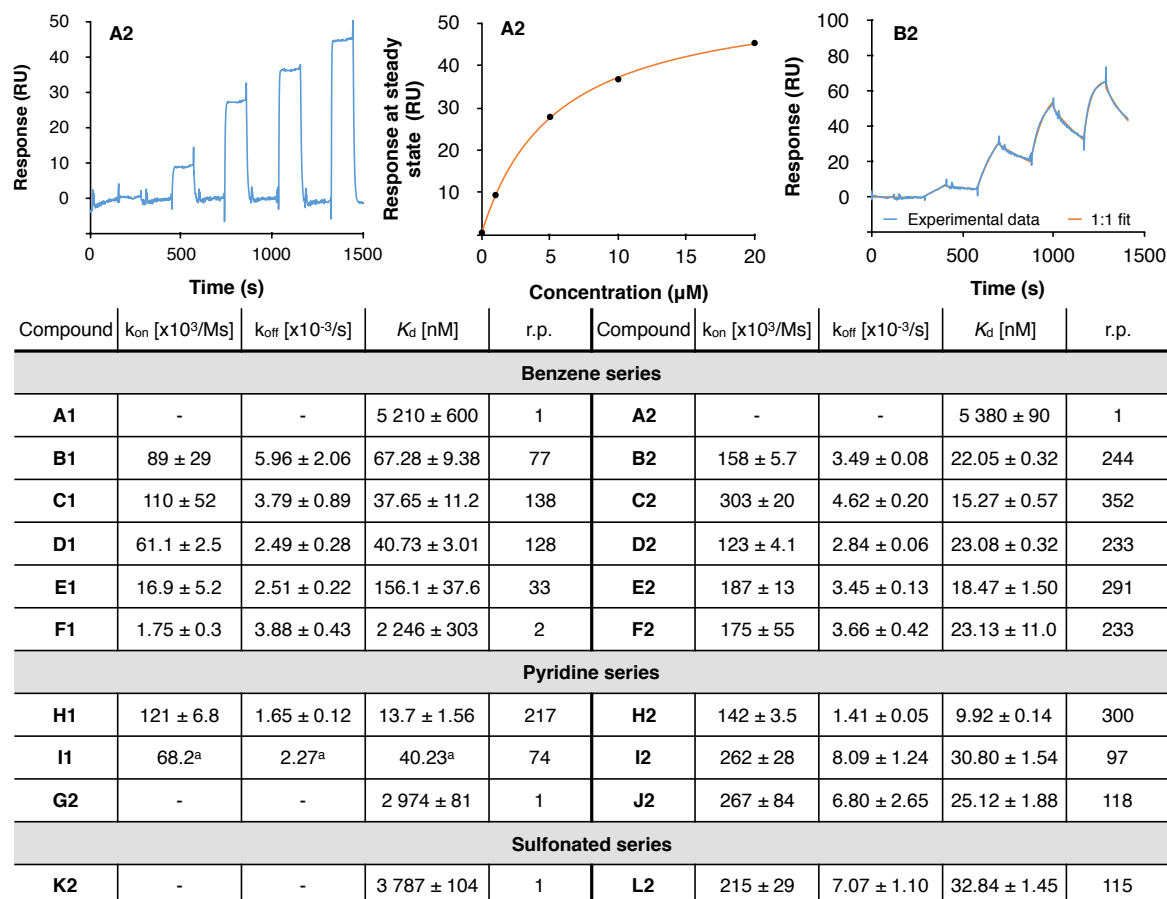


Figure 2: Direct binding of LecA ligands determined by SPR. Sensogram of monovalent ligand **A2** (left) with its affinity analysis (centre) and sensogram of divalent ligand **B2** (right) from single-cycle kinetics experiments (injections of 0, 10, 50, 100, 200 nM) are shown. Averages and std. dev. were calculated from three independent experiments (^aonly one experiment due to sample aggregation). Relative potencies (r.p.) were calculated compared to respective monovalent compound in each series and valency-normalized.

Compared to **A2**, monovalent ligands from the pyridine series **G2** and sulfonated series **K2** showed slightly enhanced binding affinity to LecA (**G2** $K_d = 2.97 \pm 0.08$ μ M, **K2** $K_d = 3.78 \pm 0.10$ μ M). In case of divalent ligands, substitution of the benzene ring with pyridine was also favoured. Three-fold and four-fold increase in binding affinity was observed for acrylamide-based ligand **H1** ($K_d = 13.7 \pm 1.56$ nM) and **I1** ($K_d = 40.23$ nM) when compared to their benzene analogues **D1** and **E1**, respectively. In the propanamide-based derivatives, the increase in binding affinity was less pronounced - **H2** ($K_d = 9.92 \pm 0.14$ nM) and **I2** ($K_d = 30.80 \pm 1.54$ nM) were roughly two times more active, while the longest ligand **J2** ($K_d = 25.12 \pm 1.88$ nM) was equipotent to **F2**. The observed potency boost might be a result of additional interactions

of the pyridine rings with the protein surface (e.g. H-bond) or a solvation contribution. Furthermore, the divalent sulfonated ligand **L2** ($K_d = 30.84 \pm 1.45$ nM) was also able to reach low nanomolar binding affinity to LecA, proving that ether functionality in the linkers was not essential and that the sulfonate solubility tag was tolerated.

Due to the superior solubility of the propanamide ligands in the pyridine series and an excellent solubility of the sulfonated ligand **L2**, we were able to determine their binding affinities and thermodynamic parameters using direct binding to LecA in solution by ITC (Figure 3, Figures S5–S9). K_d values measured for monovalent ligands **G2** and **K2** by ITC were in low micromolar range (**G2** $K_d = 5.27 \pm 0.03$ μ M, **L2** $K_d = 6.23 \pm 0.44$ μ M) but slightly higher than their SPR values. Binding affinities determined by ITC were in low nanomolar range for divalent pyridine-containing ligand **I2** ($K_d = 35.1 \pm 12.5$ nM) and divalent sulfonated ligand **L2** ($K_d = 39.9 \pm 3.6$ nM), the values which are comparable to SPR-measured values. In both cases, enthalpy contributions were roughly doubled (**I2** $\Delta H = -23.9 \pm 1.2$ kcal/mol, **L2** $\Delta H = -19.5 \pm 1.3$ kcal/mol) compared to their monovalent analogues (**G2** $\Delta H = -11.0 \pm 0.2$ kcal/mol, **K2** $\Delta H = -10.3 \pm 0.1$ kcal/mol), while the entropy costs were increased at least threefold (**G2** $\Delta S = -12.8 \pm 0.6$ cal/mol/deg vs. **I2** $\Delta S = -45.9 \pm 4.5$ cal/mol/deg, **K2** $\Delta S = -10.7 \pm 0.6$ cal/mol/deg vs. **L2** $\Delta S = -31.6 \pm 4.4$ cal/mol/deg). Divalent ligand with the longest linker **J2** was less potent, yet still in nanomolar range ($K_d = 79.5 \pm 32.8$ nM), with decreased enthalpy contribution ($\Delta H = -13.5 \pm 0.90$ kcal/mol) but also lower entropy costs ($\Delta S = -12.6 \pm 1.8$ cal/mol/deg), suggesting different binding mode for **J2**.

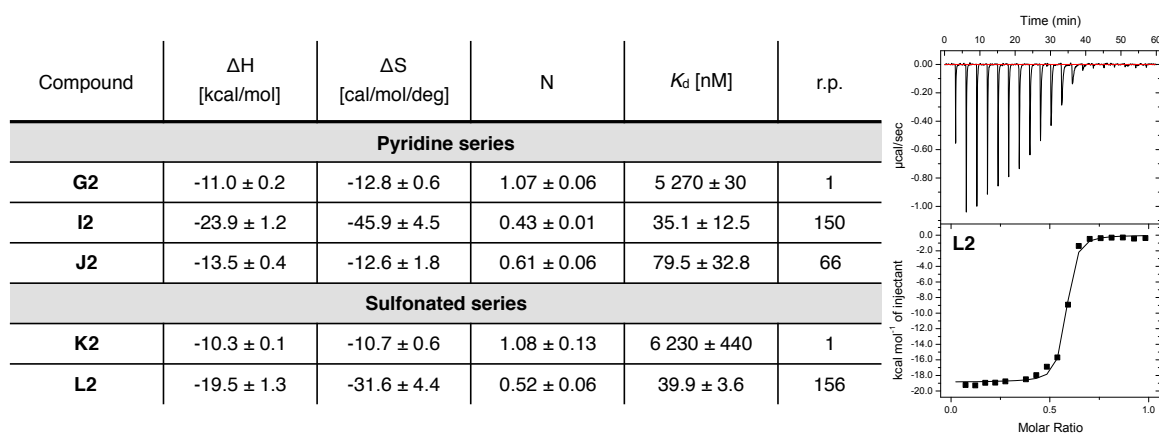


Figure 3: Direct binding of LecA ligands determined by ITC. Titration of LecA (50 μ M) with divalent sulfonated ligand **L2** (250 μ M) is shown. Averages and std. dev. were calculated from three independent experiments. Relative potencies (r.p.) were calculated compared to respective monovalent compound in each series and valency-normalized.

In conclusion, we synthesized a small library of divalent LecA ligands in only three to five chemical steps as bioisosters of the poorly soluble and chemical labile but highly potent

bisacylhydrazones reported previously. The aim of this work to increase solubility and stability while maintaining on target activity for LecA was achieved and all modifications (Figure1) lead to an increase in solubility. A remarkable solubility boost over 5000-fold was achieved with the sulfonated ligand **L2** ($S > 1.5$ mM). Furthermore, replacement of the chemically labile acylhydrazone linkage with its amide bioisoster enhanced compound stability in plasma. Divalent ligands from the benzene series (**D1**, **D2**) as well as the sulfonated ligand **L2** exhibited high stability in human liver microsomes while the pyridine **H1**, **H2** were slightly less stable. All ligands showed high plasma protein binding in mouse and human species, whereas the ligand **L2** exhibited remarkably low plasma protein binding properties. Low nanomolar binding affinities associated with a strong divalent potency boost could be retained for all synthesized compounds with a single exception of the longest acrylamide-based ligand **F1** (**I1** not yet measured). Good solubility of propanamide ligands in the pyridine series **H2–J2** and the divalent sulfonated ligand **L2** allowed evaluation of the thermodynamics binding parameters with ITC in addition to kinetic parameters determined by SPR. These highly optimized compounds will be studied in experiments with *P. aeruginosa*. The inhibition of LecA virulence may provide an alternative treatment option for *P. aeruginosa* infections.

Acknowledgments

The authors are grateful to Jelena Konstantinovic (HIPS, Saarbrücken) for assisting with HRMS. K.R. thanks Jennifer Wolf and Kimberley Vivien Sander for excellent technical assistance. K.R. receives support from the German Center for Infection Research (DZIF, TTU 09.710 and 09.719). A.T. acknowledges the European Research Council (ERC Starting Grant, Sweetbullets). S.K. thanks the French National Research Agency [ANR-17-CE11-0048] project ‘Glycomime’. For support and AI acknowledges Glyco@Alps (ANR-15-IDEX-02) and Labex Arcane/CBH-EUR-GS (ANR-17-EURE-0003).

REFERENCES

- 1 B. Ernst and J. L. Magnani, *Nat. Rev. Drug Discov.*, 2009, **8**, 661–677.
- 2 J. Meiers, E. Siebs, E. Zahorska and A. Titz, *Curr. Opin. Chem. Biol.*, 2019, **53**, 51–67.
- 3 L. B. Rice, *J. Infect. Dis.*, 2008, **197**, 1079–1081.
- 4 D. Davies, *Nat. Rev. Drug Discov.*, 2003, **2**, 114–122.
- 5 D. Tielker, S. Hacker, R. Loris, M. Strathmann, J. Wingender, S. Wilhelm, F. Rosenau and K. E. Jaeger, *Microbiology*, 2005, **151**, 1313–1323.
- 6 S. P. Diggle, R. E. Stacey, C. Dodd, M. Cámara, P. Williams and K. Winzer, *Environ. Microbiol.*, 2006, **8**, 1095–1104.
- 7 R. Sommer, J. C. Paulson, A. Titz, A. Varrot, S. Wagner, A. Khaledi, S. Häussler, C. M. Nycholat and A. Imberty, *Chem. Sci.*, 2016, **7**, 4990–5001.
- 8 A. M. Boukerb, A. Decor, S. Ribun, R. Tabaroni, A. Rousset, L. Commin, S. Buff, A. Doléans-Jordheim, S. Vidal, A. Varrot, A. Imberty and B. Cournoyer, *Front. Microbiol.*, 2016, **7**, 1–16.
- 9 S. Wagner, R. Sommer, S. Hinsberger, C. Lu, R. W. Hartmann, M. Empting and A. Titz, *J. Med. Chem.*, 2016, **59**, 5929–5969.
- 10 T. Eierhoff, B. Bastian, R. Thuenauer, J. Madl, A. Audfray, S. Aigal, S. Juillot, G. E. Rydell, S. Muller, S. de Bentzmann, A. Imberty, C. Fleck and W. Romer, *Proc. Natl. Acad. Sci.*, 2014, **111**, 12895–12900.
- 11 H. P. Hauber, M. Schulz, A. Pforte, D. Mack, P. Zabel and U. Schumacher, *Int. J. Med. Sci.*, 2008, **5**, 371–376.
- 12 R. U. Kadam, M. Bergmann, M. Hurley, D. Garg, M. Cacciarini, M. A. Swiderska, C. Nativi, M. Sattler, A. R. Smyth, P. Williams, M. Cámara, A. Stocker, T. Darbre and J. L. Reymond, *Angew. Chemie - Int. Ed.*, 2011, **50**, 10631–10635.
- 13 C. Sabin, E. P. Mitchell, M. Pokorná, C. Gautier, J. P. Utile, M. Wimmerová and A. Imberty, *FEBS Lett.*, 2006, **580**, 982–987.
- 14 S. Cecioni, A. Imberty and S. Vidal, *Chem. Rev.*, 2015, **115**, 525–561.
- 15 D. Hauck, I. Joachim, B. Frommeyer, A. Varrot, B. Philipp, H. M. Möller, A. Imberty, T. E. Exner and A. Titz, *ACS Chem. Biol.*, 2013, **8**, 1775–1784.
- 16 R. Sommer, S. Wagner, K. Rox, A. Varrot, D. Hauck, E. C. Wamhoff, J. Schreiber, T. Ryckmans, T. Brunner, C. Rademacher, R. W. Hartmann, M. Brönstrup, A. Imberty and A. Titz, *J. Am. Chem. Soc.*, 2018, **140**, 2537–2545.
- 17 R. Sommer, K. Rox, S. Wagner, D. Hauck, S. S. Henrikus, S. Newsad, T. Arnold, T. Ryckmans, M. Brönstrup, A. Imberty, A. Varrot, R. W. Hartmann and A. Titz, *J. Med. Chem.*, 2019, **62**, 9201–9216.

- 18 J. Rodrigue, G. Ganne, B. Blanchard, C. Saucier, D. Giguère, T. C. Shiao, A. Varrot, A. Imberty and R. Roy, *Org. Biomol. Chem.*, 2013, **11**, 6906–6918.
- 19 R. U. Kadam, D. Garg, J. Schwartz, R. Visini, M. Sattler, A. Stocker, T. Darbre and J. L. Reymond, *ACS Chem. Biol.*, 2013, **8**, 1925–1930.
- 20 I. Joachim, S. Rikker, D. Hauck, D. Ponader, S. Boden, R. Sommer, L. Hartmann and A. Titz, *Org. Biomol. Chem.*, 2016, **14**, 7933–7948.
- 21 S. Wagner, D. Hauck, M. Hoffmann, R. Sommer, I. Joachim, R. Müller, A. Imberty, A. Varrot and A. Titz, *Angew. Chemie - Int. Ed.*, 2017, **56**, 16559–16564.
- 22 S. Kuhaudomlarp, E. Siebs, E. Shanina, J. Topin, I. Joachim, S. Figueiredo, C. Gomes, A. Varrot, D. Rognan, A. Imberty and A. Titz, *Angew. Chem. Int. Ed.*, 2021, **60**, 2–13.
- 23 G. Cioci, E. P. Mitchell, C. Gautier, M. Wimmerová, D. Sudakevitz, S. Pérez, N. Gilboa-Garber and A. Imberty, *FEBS Lett.*, 2003, **555**, 297–301.
- 24 F. Pertici and R. J. Pieters, *Chem. Commun.*, 2012, **48**, 4008–4010.
- 25 G. Yu, A. C. Vicini and R. J. Pieters, *J. Org. Chem.*, 2019, **84**, 2470–2488.
- 26 A. V. Pukin, A. J. Brouwer, L. Koomen, H. C. Quarles Van Ufford, J. Kemmink, N. J. De Mol and R. J. Pieters, *Org. Biomol. Chem.*, 2015, **13**, 10923–10928.
- 27 A. Novoa, T. Eierhoff, J. Topin, A. Varrot, S. Barluenga, A. Imberty, W. Römer and N. Winssinger, *Angew. Chemie - Int. Ed.*, 2014, **53**, 8885–8889.
- 28 S. F. Huang, C. H. Lin, Y. T. Lai, C. L. Tsai, T. J. R. Cheng and S. K. Wang, *Chem. - An Asian J.*, 2018, **13**, 686–700.
- 29 E. Zahorska, S. Kuhaudomlarp, S. Minervini, S. Yousaf, M. Lepsik, T. Kinsinger, A. K. H. Hirsch, A. Imberty and A. Titz, *Chem. Commun.*, 2020, **56**, 8822–8825.

References

Note: References of chapter 1.2 , chapter 3.1 and chapter 5.6 are listed at the end of the individual chapters.

1. Sender, R.; Fuchs, S.; Milo, R. Revised Estimates for the Number of Human and Bacteria Cells in the Body. *PLOS Biology* **2016**, e1002533.
2. Meynard, J.-L.; Barbut, F.; Guiguet, M.; Batissel, D.; Lalande, V.; Lesage, D.; Guiard-Schmid, J.-B.; Petit, J.-C.; Frottier, J.; Meyohas, M.-C. *Pseudomonas aeruginosa* infection in human immunodeficiency virus infected patients. *Journal of Infection* **1999**, 38, 176-181.
3. Bodey, G. P. *Pseudomonas aeruginosa* infections in cancer patients: have they gone away? *Current Opinion in Infectious Diseases* **2001**, 14, 403-407.
4. Busi Rizzi, E.; Schininà, V.; Bordi, E.; Buontempo, G.; Narciso, P.; Bibbolino, C. HIV-related bronchopulmonary infection by *Pseudomonas aeruginosa* in the HAART era: radiological findings. *Acta Radiologica* **2006**, 47, 793-797.
5. European Centre for Disease Prevention and Control, Healthcare-associated infections acquired in intensive care units, Annual Epidemiological Report for 2017. In <https://www.ecdc.europa.eu/> (09.11.2021).
6. Deutsche Gesellschaft für Pneumologie und Beatmungsmedizin e.V., Lungenerkrankung bei Mukoviszidose: *Pseudomonas aeruginosa*. <https://www.awmf.org/leitlinien/detail/anmeldung/1/II/026-022.html> (09.11.2021).
7. Severe Infections Caused by *Pseudomonas Aeruginosa*. Springer US: 2003.
8. Nau, R.; Sorgel, F.; Eiffert, H. Penetration of Drugs through the Blood-Cerebrospinal Fluid/Blood-Brain Barrier for Treatment of Central Nervous System Infections. *Clinical Microbiology Reviews* **2010**, 23, 858-883.
9. Klockgether, J.; Cramer, N.; Wiehlmann, L.; Davenport, C. F.; Tummeler, B. *Pseudomonas aeruginosa* Genomic Structure and Diversity. *Frontiers in Microbiology* **2011**, 2, 150.
10. Lee, D. G.; Urbach, J. M.; Wu, G.; Liberati, N. T.; Feinbaum, R. L.; Miyata, S.; Diggins, L. T.; He, J. X.; Saucier, M.; Deziel, E.; Friedman, L.; Li, L.; Grills, G.; Montgomery, K.; Kucherlapati, R.; Rahme, L. G.; Ausubel, F. M. Genomic analysis reveals that *Pseudomonas aeruginosa* virulence is combinatorial. *Genome Biology* **2006**, 7.
11. Poole, K. *Pseudomonas aeruginosa*: Resistance to the Max. *Frontiers in Microbiology* **2011**, 2.
12. Cross, A. S. What is a virulence factor? *Critical Care* **2008**, 12, 196.
13. Azam, M. W.; Khan, A. U. Updates on the pathogenicity status of *Pseudomonas aeruginosa*. *Drug Discovery Today* **2019**, 24, 350-359.
14. Lee, J.; Zhang, L. The hierarchy quorum sensing network in *Pseudomonas aeruginosa*. *Protein & Cell* **2015**, 6, 26-41.
15. Fong, J. N. C.; Yildiz, F. H. Biofilm Matrix Proteins. *Microbiology Spectrum* **2015**, 3.
16. Davies, D. Understanding biofilm resistance to antibacterial agents. *Nature Reviews Drug Discovery* **2003**, 2, 114-122.

17. Ma, L.; Lu, H.; Sprinkle, A.; Parsek, M. R.; Wozniak, D. J. *Pseudomonas aeruginosa* Psl Is a Galactose- and Mannose-Rich Exopolysaccharide. *Journal of Bacteriology* **2007**, 189, 8353-8356.
18. Jennings, L. K.; Storek, K. M.; Ledvina, H. E.; Coulon, C.; Marmont, L. S.; Sadvovskaya, I.; Secor, P. R.; Tseng, B. S.; Scian, M.; Filloux, A.; Wozniak, D. J.; Howell, P. L.; Parsek, M. R. Pel is a cationic exopolysaccharide that cross-links extracellular DNA in the *Pseudomonas aeruginosa* biofilm matrix. *Proceedings of the National Academy of Sciences of the United States of America* **2015**, 112, 11353-11358.
19. Debeer, D.; Stoodley, P.; Roe, F.; Lewandowski, Z. Effects of Biofilm Structures on Oxygen Distribution and Mass-Transport. *Biotechnology and Bioengineering* **1994**, 43, 1131-1138.
20. Flemming, H.-C.; Wingender, J. The biofilm matrix. *Nature Reviews Microbiology* **2010**, 8, 623-633.
21. Gilboa-Garber, N. Purification and properties of hemagglutinin from *Pseudomonas aeruginosa* and its reaction with human blood cells. *Biochimica et Biophysica Acta - General Subjects* **1972**, 273, 165-173.
22. Gilboa-Garber, N.; Mizrahi, L.; Garber, N. Mannose-binding hemagglutinins in extracts of *Pseudomonas aeruginosa*. *Canadian Journal of Biochemistry* **1977**, 55, 975-981.
23. Gilboa-Garber, N. *Pseudomonas aeruginosa* lectins. In *Methods in Enzymology*, Academic Press: **1982**, Vol. 83, 378-385.
24. Tielker, D.; Hacker, S.; Loris, R.; Strathmann, M.; Wingender, J.; Wilhelm, S.; Rosenau, F.; Jaeger, K.-E. *Pseudomonas aeruginosa* lectin LecB is located in the outer membrane and is involved in biofilm formation. *Microbiology* **2005**, 151, 1313-1323.
25. Diggle, S. P.; Stacey, R. E.; Dodd, C.; Cámara, M.; Williams, P.; Winzer, K. The galactophilic lectin, LecA, contributes to biofilm development in *Pseudomonas aeruginosa*. *Environmental microbiology* **2006**, 8, 1095-1104.
26. Stover, C. K.; Pham, X. Q.; Erwin, A. L.; Mizoguchi, S. D.; Warrenner, P.; Hickey, M. J.; Brinkman, F. S.; Hufnagle, W. O.; Kowalik, D. J.; Lagrou, M.; Garber, R. L.; Goltry, L.; Tolentino, E.; Westbrook-Wadman, S.; Yuan, Y.; Brody, L. L.; Coulter, S. N.; Folger, K. R.; Kas, A.; Larbig, K.; Lim, R.; Smith, K.; Spencer, D.; Wong, G. K.; Wu, Z.; Paulsen, I. T.; Reizer, J.; Saier, M. H.; Hancock, R. E.; Lory, S.; Olson, M. V. Complete genome sequence of *Pseudomonas aeruginosa* PAO1, an opportunistic pathogen. *Nature* **2000**, 406, 959-964.
27. Winzer, K.; Falconer, C.; Garber, N. C.; Diggle, S. P.; Camara, M.; Williams, P. The *Pseudomonas aeruginosa* Lectins PA-IL and PA-IIL Are Controlled by Quorum Sensing and by RpoS. *Journal of Bacteriology* **2000**, 182, 6401-6411.
28. Sommer, R.; Wagner, S.; Varrot, A.; Nycholat, C. M.; Khaledi, A.; Häussler, S.; Paulson, J. C.; Imbert, A.; Titz, A. The virulence factor LecB varies in clinical isolates: consequences for ligand binding and drug discovery. *Chemical Science* **2016**, 7, 4990-5001.
29. Joachim, I.; Rikker, S.; Hauck, D.; Ponader, D.; Boden, S.; Sommer, R.; Hartmann, L.; Titz, A. Development and optimization of a competitive binding assay for the

galactophilic low affinity lectin LecA from *Pseudomonas aeruginosa*. *Organic & Biomolecular Chemistry* **2016**, 14, 7933-7948.

30. Zahorska, E.; Kuhaudomlarp, S.; Minervini, S.; Yousaf, S.; Lepsik, M.; Kinsinger, T.; Hirsch, A. K. H.; Imberty, A.; Titz, A. A rapid synthesis of low-nanomolar divalent LecA inhibitors in four linear steps from d-galactose pentaacetate. *Chemical Communications* **2020**, 56, 8822-8825.

31. Sommer, R.; Rox, K.; Wagner, S.; Hauck, D.; Henrikus, S. S.; Newsad, S.; Arnold, T.; Ryckmans, T.; Brönstrup, M.; Imberty, A.; Varrot, A.; Hartmann, R. W.; Titz, A. Anti-biofilm Agents against *Pseudomonas aeruginosa*: A Structure–Activity Relationship Study of C-Glycosidic LecB Inhibitors. *Journal of Medicinal Chemistry* **2019**, 62, 9201-9216.

32. Passos da Silva, D.; Matwichuk, M. L.; Townsend, D. O.; Reichhardt, C.; Lamba, D.; Wozniak, D. J.; Parsek, M. R. The *Pseudomonas aeruginosa* lectin LecB binds to the exopolysaccharide Psl and stabilizes the biofilm matrix. *Nature Communications* **2019**, 10, 2183.

33. Jiang, Z. W.; Nero, T.; Mukherjee, S.; Olson, R.; Yan, J. Searching for the Secret of Stickiness: How Biofilms Adhere to Surfaces. *Frontiers in Microbiology* **2021**, 12:686793.

34. Mitchell, E.; Houles, C.; Sudakevitz, D.; Wimmerova, M.; Gautier, C.; Pérez, S.; Wu, A. M.; Gilboa-Garber, N.; Imberty, A. Structural basis for oligosaccharide-mediated adhesion of *Pseudomonas aeruginosa* in the lungs of cystic fibrosis patients. *Nature Structural Biology* **2002**, 9, 918-921.

35. Mewe, M.; Tielker, D.; Schonberg, R.; Schachner, M.; Jaeger, K. E.; Schumacher, U. *Pseudomonas aeruginosa* lectins I and II and their interaction with human airway cilia. *Journal of Laryngology and Otology* **2005**, 119, 595-599.

36. Chemani, C.; Imberty, A.; de Bentzmann, S.; Pierre, M.; Wimmerová, M.; Guery, B. P.; Faure, K. Role of LecA and LecB Lectins in *Pseudomonas aeruginosa*-Induced Lung Injury and Effect of Carbohydrate Ligands. *Infection and Immunity* **2009**, 77, 2065-2075.

37. Eierhoff, T.; Bastian, B.; Thuenauer, R.; Madl, J.; Audfray, A.; Aigal, S.; Juillot, S.; Rydell, G. E.; Muller, S.; de Bentzmann, S.; Imberty, A.; Fleck, C.; Römer, W. A lipid zipper triggers bacterial invasion. *Proceedings of the National Academy of Sciences of the United States of America* **2014**, 111, 12895-900.

38. Zheng, S.; Eierhoff, T.; Aigal, S.; Brandel, A.; Thuenauer, R.; de Bentzmann, S.; Imberty, A.; Römer, W. The *Pseudomonas aeruginosa* lectin LecA triggers host cell signalling by glycosphingolipid-dependent phosphorylation of the adaptor protein CrkII. *Biochimica et Biophysica Acta - Molecular Cell Research* **2017**, 1864, 1236-1245.

39. Thuenauer, R.; Landi, A.; Trefzer, A.; Altmann, S.; Wehrum, S.; Eierhoff, T.; Diedrich, B.; Dengjel, J.; Nyström, A.; Imberty, A.; Römer, W. The *Pseudomonas aeruginosa* Lectin LecB Causes Integrin Internalization and Inhibits Epithelial Wound Healing. *mBio* **2020**, 11, e03260-19.

40. Adam, E. C.; Mitchell, B. S.; Schumacher, D. U.; Grant, G.; Schumacher, U. *Pseudomonas aeruginosa* II lectin stops human ciliary beating: therapeutic implications of fucose. *American Journal of Respiratory and Critical Care Medicine* **1997**, 155, 2102-2104.

41. Moodley, Y.; Linz, B.; Bond, R. P.; Nieuwoudt, M.; Soodyall, H.; Schlebusch, C. M.; Bernhoft, S.; Hale, J.; Suerbaum, S.; Mugisha, L.; van der Merwe, S. W.; Achtman, M. Age

of the Association between *Helicobacter pylori* and Man. *PLOS Pathogens* **2012**, 8, e1002693.

42. Maixner, F.; Krause-Kyora, B.; Turaev, D.; Herbig, A.; Hoopmann, M. R.; Hallows, J. L.; Kusebauch, U.; Vigl, E. E.; Malfertheiner, P.; Megraud, F.; O'Sullivan, N.; Cipollini, G.; Coia, V.; Samadelli, M.; Engstrand, L.; Linz, B.; Moritz, R. L.; Grimm, R.; Krause, J.; Nebel, A.; Moodley, Y.; Rattai, T.; Zink, A. The 5300-year-old *Helicobacter pylori* genome of the Iceman. *Science* **2016**, 351, 162-165.

43. Capasso, L. 5300 years ago, the Ice Man used natural laxatives and antibiotics. *Lancet* **1998**, 352, 1864-1864.

44. Walsh, C. Where will new antibiotics come from? *Nature Reviews Microbiology* **2003**, 1, 65-70.

45. Clatworthy, A. E.; Pierson, E.; Hung, D. T. Targeting virulence: a new paradigm for antimicrobial therapy. *Nature Chemical Biology* **2007**, 3, 541-548.

46. Tooke, C. L.; Hinchliffe, P.; Bragginton, E. C.; Colenso, C. K.; Hirvonen, V. H. A.; Takebayashi, Y.; Spencer, J. beta-Lactamases and beta-Lactamase Inhibitors in the 21st Century. *Journal of Molecular Biology* **2019**, 431, 3472-3500.

47. Yoshida, H.; Bogaki, M.; Nakamura, M.; Yamanaka, L. M.; Nakamura, S. Quinolone resistance-determining region in the DNA gyrase gyrB gene of *Escherichia coli*. *Antimicrobial Agents and Chemotherapy* **1991**, 35, 1647-1650.

48. Flensburg, J.; Sköld, O. Massive overproduction of dihydrofolate reductase in bacteria as a response to the use of trimethoprim. *European Journal of Biochemistry* **1987**, 162, 473-476.

49. United-Nations. New report calls for urgent action to avert antimicrobial resistance crisis. <https://www.who.int/news/item/29-04-2019-new-report-calls-for-urgent-action-to-avert-antimicrobial-resistance-crisis> (accessed 13.08.21).

50. Nikaido, H. Outer-Membrane Barrier as a Mechanism of Antimicrobial Resistance. *Antimicrobial Agents and Chemotherapy* **1989**, 33, 1831-1836.

51. Li, X. Z.; Nikaido, H.; Poole, K. Role of mexA-mexB-oprM in antibiotic efflux in *Pseudomonas aeruginosa*. *Antimicrobial Agents and Chemotherapy* **1995**, 39, 1948-1953.

52. Li, X.-Z.; Nikaido, H. Efflux-Mediated Drug Resistance in Bacteria: an Update. *Drugs* **2009**, 69, 1555-1623.

53. Moore, N. M.; Flaws, M. L. Treatment Strategies and Recommendations for *Pseudomonas aeruginosa* Infections. *American Society for Clinical Laboratory Science* **2011**, 24, 52-56.

54. Wagner, S.; Sommer, R.; Hinsberger, S.; Lu, C.; Hartmann, R. W.; Empting, M.; Titz, A. Novel Strategies for the Treatment of *Pseudomonas aeruginosa* Infections. *Journal of Medicinal Chemistry* **2016**, 59, 5929-5969.

55. Nyfeler, B.; Hoepfner, D.; Palestrant, D.; Kirby, C. A.; Whitehead, L.; Yu, R.; Deng, G.; Caughlan, R. E.; Woods, A. L.; Jones, A. K.; Barnes, S. W.; Walker, J. R.; Gaulis, S.; Hauy, E.; Brachmann, S. M.; Krastel, P.; Studer, C.; Riedl, R.; Estoppey, D.; Aust, T.; Movva, N. R.; Wang, Z.; Salcius, M.; Michaud, G. A.; McAllister, G.; Murphy, L. O.; Tallarico, J. A.; Wilson, C. J.; Dean, C. R. Identification of Elongation Factor G as the Conserved Cellular Target of Argyrin B. *PLOS ONE* **2012**, 7, e42657.

56. Baumann, S.; Herrmann, J.; Raju, R.; Steinmetz, H.; Mohr, K. I.; Hüttel, S.; Harmrolfs, K.; Stadler, M.; Müller, R. Cystobactamide: Topoisomerase-Inhibitoren aus Myxobakterien mit hoher antibakterieller Aktivität. *Angewandte Chemie* **2014**, 126, 14835-14839.
57. Werneburg, M.; Zerbe, K.; Juhas, M.; Bigler, L.; Stalder, U.; Kaech, A.; Ziegler, U.; Obrecht, D.; Eberl, L.; Robinson, J. A. Inhibition of lipopolysaccharide transport to the outer membrane in *Pseudomonas aeruginosa* by peptidomimetic antibiotics. *ChemBioChem* **2012**, 13, 1767-1775.
58. Martin-Loeches, I.; Dale, G. E.; Torres, A. Murepavadin: a new antibiotic class in the pipeline. *Expert Review of Anti-Infective Therapy* **2018**, 16, 259-268.
59. ClinicalTrials.gov, Pivotal Study in VAP Suspected or Confirmed to be Due to *Pseudomonas Aeruginosa* (PRISM-MDR). <https://clinicaltrials.gov/ct2/show/NCT03409679?term=murepavadin&draw=2&rank=2> (accessed 31.08.21).
60. Clatworthy, A. E.; Pierson, E.; Hung, D. T. Targeting virulence: a new paradigm for antimicrobial therapy. *Nature Chemical Biology* **2007**, 3, 541-548.
61. Calvert, M. B.; Jumde, V. R.; Titz, A. Pathoblockers or antivirulence drugs as a new option for the treatment of bacterial infections. *Beilstein Journal of Organic Chemistry* **2018**, 14, 2607-2617.
62. Schütz, C.; Empting, M. Targeting the *Pseudomonas* quinolone signal quorum sensing system for the discovery of novel anti-infective pathoblockers. *Beilstein Journal of Organic Chemistry* **2018**, 14, 2627-2645.
63. Cathcart, G. R. A.; Quinn, D.; Greer, B.; Harriott, P.; Lynas, J. F.; Gilmore, B. F.; Walker, B. Novel Inhibitors of the *Pseudomonas aeruginosa* Virulence Factor LasB: a Potential Therapeutic Approach for the Attenuation of Virulence Mechanisms in Pseudomonas Infection. *Antimicrobial Agents and Chemotherapy* **2011**, 55, 2670-2678.
64. Sommer, R.; Joachim, I.; Wagner, S.; Titz, A. New Approaches to Control Infections: Anti-biofilm Strategies against Gram-negative Bacteria. *CHIMIA International Journal for Chemistry* **2013**, 67, 286-290.
65. Sommer, R.; Wagner, S.; Rox, K.; Varrot, A.; Hauck, D.; Wamhoff, E.-C.; Schreiber, J.; Ryckmans, T.; Brunner, T.; Rademacher, C.; Hartmann, R. W.; Brönstrup, M.; Imberty, A.; Titz, A. Glycomimetic, Orally Bioavailable LecB Inhibitors Block Biofilm Formation of *Pseudomonas aeruginosa*. *Journal of the American Chemical Society* **2018**, 140, 2537-2545.
66. Rezzoagli, C.; Archetti, M.; Mignot, I.; Baumgartner, M.; Kummerli, R. Combining antibiotics with antivirulence compounds can have synergistic effects and reverse selection for antibiotic resistance in *Pseudomonas aeruginosa*. *PLOS Biology* **2020**, 18, e3000805.
67. Schütz, C.; Ho, D. K.; Hamed, M. M.; Abdelsamie, A. S.; Rohrig, T.; Herr, C.; Kany, A. M.; Rox, K.; Schmelz, S.; Siebenburger, L.; Wirth, M.; Borger, C.; Yahiaoui, S.; Bals, R.; Scrima, A.; Blankenfeldt, W.; Horstmann, J. C.; Christmann, R.; Murgia, X.; Koch, M.; Berwanger, A.; Loretz, B.; Hirsch, A. K. H.; Hartmann, R. W.; Lehr, C. M.; Empting, M. A New PqsR Inverse Agonist Potentiates Tobramycin Efficacy to Eradicate *Pseudomonas aeruginosa* Biofilms. *Advanced Science* **2021**, 8, e2004369.
68. Theuretzbacher, U.; Outterson, K.; Engel, A.; Karlen, A. The global preclinical antibacterial pipeline. *Nature Reviews Microbiology* **2020**, 18, 275-285.

69. Mohammadi, M.; Khayat, H.; Sayehmiri, K.; Soroush, S.; Sayehmiri, F.; Delfani, S.; Bogdanovic, L.; Taherikalani, M. Synergistic Effect of Colistin and Rifampin Against Multidrug Resistant *Acinetobacter baumannii*: A Systematic Review and Meta-Analysis. *Open Microbiological Journal* **2017**, 11, 63-71.
70. Pokrovskaya, V.; Baasov, T. Dual-acting hybrid antibiotics: a promising strategy to combat bacterial resistance. *Expert Opinion in Drug Discovery* **2010**, 5, 883-902.
71. Parkes, A. L.; Yule, I. A. Hybrid antibiotics - clinical progress and novel designs. *Expert Opinion in Drug Discovery* **2016**, 11, 665-680.
72. Khongorzul, P.; Ling, C. J.; Khan, F. U.; Ihsan, A. U.; Zhang, J. Antibody-Drug Conjugates: A Comprehensive Review. *Molecular Cancer Research* **2020**, 18, 3-19.
73. Devarajan, P. V.; Dawre, S. M.; Dutta, R. Infectious Diseases: Need for Targeted Drug Delivery. In *Targeted Drug Delivery : Concepts and Design*, Eds. Springer International Publishing, **2015**, 113-148.
74. Lehar, S. M.; Pillow, T.; Xu, M.; Staben, L.; Kajihara, K. K.; Vandlen, R.; DePalatis, L.; Raab, H.; Hazenbos, W. L.; Hiroshi Morisaki, J.; Kim, J.; Park, S.; Darwish, M.; Lee, B.-C.; Hernandez, H.; Loyet, K. M.; Lupardus, P.; Fong, R.; Yan, D.; Chalouni, C.; Luis, E.; Khalfin, Y.; Plise, E.; Cheong, J.; Lyssikatos, J. P.; Strandh, M.; Koefoed, K.; Andersen, P. S.; Flygare, J. A.; Wah Tan, M.; Brown, E. J.; Mariathasan, S. Novel antibody-antibiotic conjugate eliminates intracellular *S. aureus*. *Nature* **2015**, 527, 323-328.
75. Peck, M.; Rothenberg, M. E.; Deng, R.; Lewin-Koh, N.; She, G.; Kamath, A. V.; Carrasco-Triguero, M.; Saad, O.; Castro, A.; Teufel, L.; Dickerson, D. S.; Leonardelli, M.; Tavel, J. A. A Phase 1, Randomized, Single-Ascending-Dose Study To Investigate the Safety, Tolerability, and Pharmacokinetics of DSTA4637S, an Anti-*Staphylococcus aureus* Thiomab Antibody-Antibiotic Conjugate, in Healthy Volunteers. *Antimicrobial Agents and Chemotherapy* **2019**, 63, e02588-18.
76. ClinicalTrials.gov. Study to Investigate the Safety, Tolerability, and Pharmacokinetics of DSTA4637S in Participants With Staphylococcus Aureus Bacteremia Receiving Standard-of-Care (SOC) Antibiotics. <https://www.clinicaltrials.gov/ct2/show/NCT03162250?term=DSTA4637S&rank=2> (accessed 01.09.21).
77. van Dongen, G. A.; Visser, G. W.; Lub-de Hooge, M. N.; de Vries, E. G.; Perk, L. R. Immuno-PET: a navigator in monoclonal antibody development and applications. *Oncologist* **2007**, 12, 1379-1389.
78. Cazzamalli, S.; Dal Corso, A.; Widmayer, F.; Neri, D. Chemically Defined Antibody- and Small Molecule-Drug Conjugates for in Vivo Tumor Targeting Applications: A Comparative Analysis. *Journal of the American Chemical Society* **2018**, 140, 1617-1621.
79. Tegge, W.; Guerra, G.; Holtke, A.; Schiller, L.; Beutling, U.; Harmrolfs, K.; Grobe, L.; Wullenkord, H.; Xu, C.; Weich, H.; Bronstrup, M. Selective Bacterial Targeting and Infection-Triggered Release of Antibiotic Colistin Conjugates. *Angewandte Chemie International Edition* **2021**, 60, 17989-17997.
80. Klahn, P.; Brönstrup, M. Bifunctional antimicrobial conjugates and hybrid antimicrobials. *Natural Product Reports* **2017**, 34, 832-885.
81. O'Shea, R.; Moser, H. E. Physicochemical Properties of Antibacterial Compounds: Implications for Drug Discovery. *Journal of Medicinal Chemistry* **2008**, 51, 2871-2878.

82. Busse, H.-J.; Wöstmann, C.; Barker, E. P. The bactericidal action of streptomycin: membrane permeabilization caused by the insertion of mistranslated proteins into the cytoplasmic membrane of *Escherichia coli* and subsequent caging of the antibiotic inside the cells due to degradation of these proteins. *Microbiology* **1992**, 138, 551-561.
83. Hancock, R. E.; Farmer, S. W.; Li, Z. S.; Poole, K. Interaction of aminoglycosides with the outer membranes and purified lipopolysaccharide and OmpF porin of *Escherichia coli*. *Antimicrobial Agents and Chemotherapy* **1991**, 35, 1309-1314.
84. Yadav, R.; Bulitta, J. B.; Schneider, E. K.; Shin, B. S.; Velkov, T.; Nation, R. L.; Landersdorfer, C. B. Aminoglycoside Concentrations Required for Synergy with Carbapenems against *Pseudomonas aeruginosa* Determined via Mechanistic Studies and Modeling. *Antimicrobial Agents and Chemotherapy* **2017**, 61, e00722-17.
85. Müsken, M.; Pawar, V.; Schwebs, T.; Bähre, H.; Felgner, S.; Weiss, S.; Häussler, S. Breaking the Vicious Cycle of Antibiotic Killing and Regrowth of Biofilm-Residing *Pseudomonas aeruginosa*. *Antimicrobial Agents and Chemotherapy* **2018**, 62, e01635-18.
86. Nichols, W. W.; Dorrington, S. M.; Slack, M. P.; Walmsley, H. L. Inhibition of tobramycin diffusion by binding to alginate. *Antimicrobial Agents and Chemotherapy* **1988**, 32, 518-523.
87. Hatch, R. A.; Schiller, N. L. Alginate lyase promotes diffusion of aminoglycosides through the extracellular polysaccharide of mucoid *Pseudomonas aeruginosa*. *Antimicrobial Agents and Chemotherapy* **1998**, 42, 974-7.
88. Chiang, W. C.; Nilsson, M.; Jensen, P. O.; Hoiby, N.; Nielsen, T. E.; Givskov, M.; Tolker-Nielsen, T. Extracellular DNA shields against aminoglycosides in *Pseudomonas aeruginosa* biofilms. *Antimicrobial Agents and Chemotherapy* **2013**, 57, 2352-2361.
89. Tseng, B. S.; Zhang, W.; Harrison, J. J.; Quach, T. P.; Song, J. L.; Penterman, J.; Singh, P. K.; Chopp, D. L.; Packman, A. I.; Parsek, M. R. The extracellular matrix protects *Pseudomonas aeruginosa* biofilms by limiting the penetration of tobramycin. *Environmental Microbiology* **2013**, 15, 2865-2878.
90. Vicens, Q.; Westhof, E. Crystal structure of a complex between the aminoglycoside tobramycin and an oligonucleotide containing the ribosomal decoding site. *Chemistry & biology* **2002**, 9, 747-755.
91. Garneau-Tsodikova, S.; Labby, K. J. Mechanisms of Resistance to Aminoglycoside Antibiotics: Overview and Perspectives. *MedChemComm* **2016**, 7, 11-27.
92. Zaunbrecher, M. A.; Sikes, R. D., Jr.; Metchock, B.; Shinnick, T. M.; Posey, J. E. Overexpression of the chromosomally encoded aminoglycoside acetyltransferase eis confers kanamycin resistance in *Mycobacterium tuberculosis*. *Proceedings of the National Academy of Sciences of the United States of America* **2009**, 106, 20004-20009.
93. Guchhait, G.; Altieri, A.; Gorityala, B.; Yang, X.; Findlay, B.; Zhanel, G. G.; Mookherjee, N.; Schweizer, F. Amphiphilic Tobramycins with Immunomodulatory Properties. *Angewandte Chemie International Edition* **2015**, 54, 6278-6282.
94. Joachim, I.; Rikker, S.; Hauck, D.; Ponader, D.; Boden, S.; Sommer, R.; Hartmann, L.; Titz, A. Development and optimization of a competitive binding assay for the galactophilic low affinity lectin LecA from *Pseudomonas aeruginosa*. *Organic & Biomolecular Chemistry* **2016**, 14, 7933-7948.

95. Wiegand, I.; Hilpert, K.; Hancock, R. E. W. Agar and broth dilution methods to determine the minimal inhibitory concentration (MIC) of antimicrobial substances. *Nature Protocols* **2008**, 3, 163-175.
96. Rice, L. B. Federal Funding for the Study of Antimicrobial Resistance in Nosocomial Pathogens: No ESKAPE. *The Journal of Infectious Diseases* **2008**, 197, 1079-1081.
97. Boucher, H. W.; Talbot, G. H.; Bradley, J. S.; Edwards, J. E.; Gilbert, D.; Rice, L. B.; Scheld, M.; Spellberg, B.; Bartlett, J. Bad bugs, no drugs: no ESKAPE! An update from the Infectious Diseases Society of America. *Clinical Infectious Diseases: An Official Publication of the Infectious Diseases Society of America* **2009**, 48, 1-12.
98. Rice, L. B. Progress and Challenges in Implementing the Research on ESKAPE Pathogens. *Infection Control & Hospital Epidemiology* **2010**, 31, S7-S10.
99. Church, D.; Elsayed, S.; Reid, O.; Winston, B.; Lindsay, R. Burn Wound Infections. *Clinical Microbiology Reviews* **2006**, 19, 403-434.
100. Narten, M.; Rosin, N.; Schobert, M.; Tielen, P. Susceptibility of *Pseudomonas aeruginosa* Urinary Tract Isolates and Influence of Urinary Tract Conditions on Antibiotic Tolerance. *Current Microbiology* **2012**, 64, 7-16.
101. Pachori, P.; Gothalwal, R.; Gandhi, P. Emergence of antibiotic resistance *Pseudomonas aeruginosa* in intensive care unit; a critical review. *Genes & Diseases* **2019**, 6, 109-119.
102. World Health Organization, WHO publishes list of bacteria for which new antibiotics are urgently needed. <https://www.who.int/news/item/27-02-2017-who-publishes-list-of-bacteria-for-which-new-antibiotics-are-urgently-needed> (accessed 15.12.21)
103. European Centre for Disease Prevention and Control, Antimicrobial resistance in the EU/EEA (EARS-Net), Annual Epidemiological Report for 2019. In <https://www.ecdc.europa.eu>, (accessed 03.10.21)
104. Suci, P. A.; Mittelman, M. W.; Yu, F. P.; Geesey, G. G. Investigation of ciprofloxacin penetration into *Pseudomonas aeruginosa* biofilms. *Antimicrobial Agents and Chemotherapy* **1994**, 38, 2125-2133.
105. Bundesinstitut für Arzneimittel und Medizinprodukte, Rote-Hand-Brief zu Fluorchinolon-Antibiotika: Schwerwiegende und anhaltende, die Lebensqualität beeinträchtigende und möglicherweise irreversible Nebenwirkungen.
106. Bundesinstitut für Arzneimittel und Medizinprodukte, Rote-Hand-Brief zu systemisch und inhalativ angewendeten Fluorchinolonen: Risiko einer Herzklappenregurgitation/-insuffizienz.
107. Tanne, J. H. FDA adds “black box” warning label to fluoroquinolone antibiotics. *British Medical Journal* **2008**, 337, 135.
108. Hargas, A.; Aasumets, K. Ciprofloxacin impairs mitochondrial DNA replication initiation through inhibition of Topoisomerase 2. *Nucleic Acids Research* **2018**, 12, 9625-9636.
109. Bisaccia, D. R.; Aicale, R.; Tarantino, D.; Peretti, G. M.; Maffulli, N. Biological and chemical changes in fluoroquinolone-associated tendinopathies: a systematic review. *British Medical Bulletin* **2019**, 130, 39-49.

110. Pouzaud, F.; Dutot, M.; Martin, C.; Debray, M.; Warnet, J. M.; Rat, P. Age-dependent effects on redox status, oxidative stress, mitochondrial activity and toxicity induced by fluoroquinolones on primary cultures of rabbit tendon cells. *Comparative Biochemistry and Physiology Part C: Toxicology & Pharmacology* **2006**, 143, 232-241.
111. Dalhoff, A.; Eickenberg, H. U. Tissue distribution of ciprofloxacin following oral and intravenous administration. *Infection* **1985**, 13, 78-81.
112. Rautio, J.; Meanwell, N. A.; Di, L.; Hageman, M. J. The expanding role of prodrugs in contemporary drug design and development. *Nature Reviews Drug Discovery* **2018**, 17, 559-587.
113. Klahn, P.; Bronstrup, M. Bifunctional antimicrobial conjugates and hybrid antimicrobials. *Natural Product Reports* **2017**, 34, 832-885.
114. Tielker, D.; Hacker, S.; Loris, R.; Strathmann, M.; Wingender, J.; Wilhelm, S.; Rosenau, F.; Jaeger, K. E. *Pseudomonas aeruginosa* lectin LecB is located in the outer membrane and is involved in biofilm formation. *Microbiology* **2005**, 151, 1313-1323.
115. Cott, C.; Thuenauer, R.; Landi, A.; Kühn, K.; Juillot, S.; Imberty, A.; Madl, J.; Eierhoff, T.; Römer, W. *Pseudomonas aeruginosa* lectin LecB inhibits tissue repair processes by triggering β -catenin degradation. *Biochimica et Biophysica Acta - Molecular Cell Research* **2016**, 1863, 1106-1118.
116. Landi, A.; Mari, M.; Wolf, T.; Kleiser, S.; Gretzmeier, C.; Wilhelm, I.; Kiritsi, D.; Thünauer, R.; Geiger, R.; Nyström, A.; Reggiori, F.; Claudinon, J.; Römer, W. *Pseudomonas aeruginosa* lectin LecB impairs keratinocyte fitness by abrogating growth factor signalling. *Cell Biology* **2019**, 2, e201900422.
117. Wilhelm, I.; Levit-Zerdoun, E.; Jakob, J.; Villringer, S.; Frensch, M.; Übelhart, R.; Landi, A.; Müller, P.; Imberty, A.; Thuenauer, R.; Claudinon, J.; Jumaa, H.; Reth, M.; Eibel, H.; Hobeika, E.; Römer, W. Carbohydrate-dependent B cell activation by fucose-binding bacterial lectins. *Science Signaling* **2019**, 12.
118. Cecioni, S.; Imberty, A.; Vidal, S. Glycomimetics versus multivalent glycoconjugates for the design of high affinity lectin ligands. *Chemical Reviews* **2015**, 115, 525-561.
119. Bernardi, A.; Jimenez-Barbero, J.; Casnati, A.; De Castro, C.; Darbre, T.; Fieschi, F.; Finne, J.; Funken, H.; Jaeger, K. E.; Lahmann, M.; Lindhorst, T. K.; Marradi, M.; Messner, P.; Molinaro, A.; Murphy, P. V.; Nativi, C.; Oscarson, S.; Penades, S.; Peri, F.; Pieters, R. J.; Renaudet, O.; Reymond, J. L.; Richichi, B.; Rojo, J.; Sansone, F.; Schaffer, C.; Turnbull, W. B.; Velasco-Torrijos, T.; Vidal, S.; Vincent, S.; Wennekes, T.; Zuilhof, H.; Imberty, A. Multivalent glycoconjugates as anti-pathogenic agents. *Chemical Society Reviews* **2013**, 42, 4709-27.
120. Meiers, J.; Siebs, E.; Zahorska, E.; Titz, A. Lectin antagonists in infection, immunity, and inflammation. *Current Opinion in Chemical Biology* **2019**, 53, 51-67.
121. Zahorska, E.; Kuhadomlarp, S.; Minervini, S.; Yousaf, S.; Lepsik, M.; Kinsinger, T.; Hirsch, A. K. H.; Imberty, A.; Titz, A. A rapid synthesis of low-nanomolar divalent LecA inhibitors in four linear steps from D-galactose pentaacetate. *Chemical Communications* **2020**, 56, 8822-8825.
122. Kuhadomlarp, S.; Siebs, E.; Shanina, E.; Topin, J.; Joachim, I.; da Silva Figueiredo Celestino Gomes, P.; Varrot, A.; Rognan, D.; Rademacher, C.; Imberty, A.; Titz, A. Non-

Carbohydrate Glycomimetics as Inhibitors of Calcium(II)-Binding Lectins. *Angewandte Chemie International Edition* **2021**, 60, 8104-8114.

123. Wagner, S.; Hauck, D.; Hoffmann, M.; Sommer, R.; Joachim, I.; Müller, R.; Imberty, A.; Varrot, A.; Titz, A. Covalent lectin inhibition and application in bacterial biofilm imaging. *Angewandte Chemie International Edition* **2017**, 56, 16559-16545.

124. Meiers, J.; Zahorska, E.; Rohrig, T.; Hauck, D.; Wagner, S.; Titz, A. Directing Drugs to Bugs: Antibiotic-Carbohydrate Conjugates Targeting Biofilm-Associated Lectins of *Pseudomonas aeruginosa*. *J Med Chem* **2020**, 63, 11707-11724.

125. Zhu, J.; Cai, X.; Harris, Tyler L.; Gooyit, M.; Wood, M.; Lardy, M.; Janda, Kim D. Disarming *Pseudomonas aeruginosa* Virulence Factor LasB by Leveraging a *Caenorhabditis elegans* Infection Model. *Chemistry & Biology* **2015**, 22, 483-491.

126. Kany, A. M.; Sikandar, A.; Haupenthal, J.; Yahiaoui, S.; Maurer, C. K.; Proschak, E.; Köhnke, J.; Hartmann, R. W. Binding Mode Characterization and Early in Vivo Evaluation of Fragment-Like Thiols as Inhibitors of the Virulence Factor LasB from *Pseudomonas aeruginosa*. *ACS Infectious Diseases* **2018**, 4, 988-997.

127. Kany, A. M.; Sikandar, A.; Yahiaoui, S.; Haupenthal, J.; Walter, I.; Empting, M.; Köhnke, J.; Hartmann, R. W. Tackling *Pseudomonas aeruginosa* Virulence by a Hydroxamic Acid-Based LasB Inhibitor. *ACS Chemical Biology* **2018**, 13, 2449-2455.

128. Wretling, B.; Pavlovskis, O. R. *Pseudomonas aeruginosa* Elastase and Its Role in *Pseudomonas* Infections. *Reviews of Infectious Diseases* **1983**, 5, S998-S1004.

129. Schmidtchen, A.; Frick, I.-M.; Andersson, E.; Tapper, H.; Björck, L. Proteinases of common pathogenic bacteria degrade and inactivate the antibacterial peptide LL-37. *Molecular Microbiology* **2002**, 46, 157-168.

130. Kamath, S.; Kapatral, V.; Chakrabarty, A. M. Cellular function of elastase in *Pseudomonas aeruginosa*: role in the cleavage of nucleoside diphosphate kinase and in alginate synthesis. *Molecular Microbiology* **1998**, 30, 933-941.

131. Yu, H.; He, X.; Xie, W.; Xiong, J.; Sheng, H.; Guo, S.; Huang, C.; Zhang, D.; Zhang, K. Elastase LasB of *Pseudomonas aeruginosa* promotes biofilm formation partly through rhamnolipid-mediated regulation. *Canadian Journal of Microbiology* **2014**, 60, 227-235.

132. Ropponen, H.-K.; Richter, R.; Hirsch, A. K. H.; Lehr, C.-M. Mastering the Gram-negative bacterial barrier – Chemical approaches to increase bacterial bioavailability of antibiotics. *Advanced Drug Delivery Reviews* **2021**, 172, 339-360.

133. Nishino, N.; Powers, J. C. *Pseudomonas aeruginosa* elastase. Development of a new substrate, inhibitors, and an affinity ligand. *Journal of Biological Chemistry* **1980**, 255, 3482-3486.

134. Mesaros, N.; Nordmann, P.; Plésiat, P.; Roussel-Delvallez, M.; Eldere, J. V.; Glupczynski, Y.; Laethem, Y. V.; Jacobs, F.; Lebecque, P.; Malfroot, A.; Tulkens, P. M.; Bambeke, F. V. *Pseudomonas aeruginosa*: resistance and therapeutic options at the turn of the new millennium. *Clinical Microbiology and Infection* **2007**, 13, 560-578.

135. Bassetti, M.; Vena, A.; Russo, A.; Croxatto, A.; Calandra, T.; Guery, B. Rational approach in the management of *Pseudomonas aeruginosa* infections. *Current Opinion in Infectious Diseases* **2018**, 31, 578-586.

136. Chu, D. T.; Fernandes, P. B. Structure-activity relationships of the fluoroquinolones. *Antimicrobial Agents and Chemotherapy* **1989**, 33, 131-135.
137. Gootz, T. D.; Brighty, K. E. Fluoroquinolone antibacterials: SAR, mechanism of action, resistance, and clinical aspects. *Medicinal Research Reviews* **1996**, 16, 433-486.
138. Werner, H. M.; Cabalteja, C. C.; Horne, W. S. Peptide Backbone Composition and Protease Susceptibility: Impact of Modification Type, Position, and Tandem Substitution. *ChemBioChem* **2016**, 17, 712-718.
139. Sanchez, J. P.; Domagala, J. M.; Hagen, S. E.; Heifetz, C. L.; Hutt, M. P.; Nichols, J. B.; Trehan, A. K. Quinolone antibacterial agents. Synthesis and structure-activity relationships of 8-substituted quinoline-3-carboxylic acids and 1,8-naphthyridine-3-carboxylic acids. *Journal of Medicinal Chemistry* **1988**, 31, 983-991.
140. Ledoussal, B.; Bouzard, D.; Coroneos, E. Potent non-6-fluoro-substituted quinolone antibacterials: synthesis and biological activity. *Journal of Medicinal Chemistry* **1992**, 35, 198-200.
141. Sanchez, J. P.; Gogliotti, R. D.; Domagala, J. M.; Gracheck, S. J.; Huband, M. D.; Sesnie, J. A.; Cohen, M. A.; Shapiro, M. A. The Synthesis, Structure-Activity, and Structure-Side Effect Relationships of a Series of 8-Alkoxy- and 5-Amino-8-alkoxyquinolone Antibacterial Agents. *Journal of Medicinal Chemistry* **1995**, 38, 4478-4487.
142. Novoa, A.; Eierhoff, T.; Topin, J.; Varrot, A.; Barluenga, S.; Imberty, A.; Römer, W.; Winssinger, N. A LecA Ligand Identified from a Galactoside-Conjugate Array Inhibits Host Cell Invasion by *Pseudomonas aeruginosa*. *Angewandte Chemie* **2014**, 126, 9031-9035.
143. Sommer, R.; Exner, T. E.; Titz, A. A Biophysical Study with Carbohydrate Derivatives Explains the Molecular Basis of Monosaccharide Selectivity of the *Pseudomonas aeruginosa* Lectin LecB. *PLOS ONE* **2014**, 9, e112822.
144. Lal, B.; Pramanik, B. N.; Manhas, M. S.; Bose, A. K. Diphenylphosphoryl azide a novel reagent for the stereospecific synthesis of azides from alcohols. *Tetrahedron Letters* **1977**, 18, 1977-1980.
145. Ilgin, S.; Can, O. D.; Atli, O.; Ucel, U. I.; Sener, E.; Guven, I. Ciprofloxacin-induced neurotoxicity: evaluation of possible underlying mechanisms. *Toxicology Mechanisms and Methods* **2015**, 25, 374-381.
146. Lawrence, J. W.; Darkin-Rattray, S.; Xie, F.; Neims, A. H.; Rowe, T. C. 4-Quinolones cause a selective loss of mitochondrial DNA from mouse L1210 leukemia cells. *Journal of Cellular Biochemistry* **1993**, 51, 165-174.
147. Abd-Allah, A. R. A.; Gannam, B. B.; Hamada, F. M. A. The impact of ofloxacin on rat testicular DNA: application of image analysis. *Pharmacological Research* **2000**, 42, 145-150.
148. Daschner, F. D.; Westenfelder, M.; Dalhoff, A. Penetration of ciprofloxacin into kidney, fat, muscle and skin tissue. *European Journal of Clinical Microbiology* **1986**, 5, 212-213.
149. Meiers, J.; Zahorska, E.; Röhrig, T.; Hauck, D.; Wagner, S.; Titz, A. Directing Drugs to Bugs: Antibiotic-Carbohydrate Conjugates Targeting Biofilm-Associated Lectins of *Pseudomonas aeruginosa*. *Journal of Medicinal Chemistry* **2020**, 63, 11707-11724.

150. Sommer, R. First glycomimetic, orally bioavailable LecB inhibitors block biofilm formation of *Pseudomonas aeruginosa*. *Journal of the American Chemical Society* **2018**, 140, 2537-2545.
151. Boukerb, A. M.; Rousset, A.; Galanos, N.; Méar, J.-B.; Thépaut, M.; Grandjean, T.; Gillon, E.; Cecioni, S.; Abderrahmen, C.; Faure, K.; Redelberger, D.; Kipnis, E.; Dessein, R.; Havet, S.; Darblade, B.; Matthews, S. E.; de Bentzmann, S.; Guéry, B.; Cournoyer, B.; Imberty, A.; Vidal, S. Antiadhesive Properties of Glycoclusters against *Pseudomonas aeruginosa* Lung Infection. *Journal of Medicinal Chemistry* **2014**, 57, 10275-10289.
152. Cecioni, S.; Imberty, A.; Vidal, S. Glycomimetics versus Multivalent Glycoconjugates for the Design of High Affinity Lectin Ligands. *Chemical Reviews* **2015**, 115, 525-561.
153. Palmioli, A.; Sperandio, P.; Polissi, A.; Airoidi, C. Targeting Bacterial Biofilm: A New LecA Multivalent Ligand with Inhibitory Activity. *Chembiochem* **2019**, 20, 2911-2915.
154. Pertici, F.; Pieters, R. J. Potent divalent inhibitors with rigid glucose click spacers for *Pseudomonas aeruginosa* lectin LecA. *Chemical Communications* **2012**, 48, 4008-4010.
155. Visini, R.; Jin, X.; Bergmann, M.; Michaud, G.; Pertici, F.; Fu, O.; Pukin, A.; Branson, T. R.; Thies-Weesie, D. M. E.; Kemmink, J.; Gillon, E.; Imberty, A.; Stocker, A.; Darbre, T.; Pieters, R. J.; Reymond, J. L. Structural Insight into Multivalent Galactoside Binding to *Pseudomonas aeruginosa* Lectin LecA. *ACS Chemical Biology* **2015**, 10, 2455-2462.
156. Huang, S.-F.; Lin, C.-H.; Lai, Y.-T.; Tsai, C.-L.; Cheng, T.-J. R.; Wang, S.-K. Development of *Pseudomonas aeruginosa* Lectin LecA Inhibitor by using Bivalent Galactosides Supported on Polyproline Peptide Scaffolds. *Chemistry – An Asian Journal* **2018**, 13, 686-700.
157. Yu, G. Y.; Vicini, A. C.; Pieters, R. J. Assembly of Divalent Ligands and Their Effect on Divalent Binding to *Pseudomonas aeruginosa* Lectin LecA. *The Journal of Organic Chemistry* **2019**, 84, 2470-2488.
158. Sanchez, J. P.; Domagala, J. M.; Heifetz, C. L.; Priebe, S. R.; Sesnie, J. A.; Trehan, A. K. Quinolone antibacterial agents. Synthesis and structure-activity relationships of a series of amino acid prodrugs of racemic and chiral 7-(3-amino-1-pyrrolidiny)quinolones. Highly soluble quinolone prodrugs with in vivo pseudomonas activity. *Journal of Medicinal Chemistry* **1992**, 35, 1764-1773.
159. Sanderson, T. J.; Black, C. M.; Southwell, J. W.; Wilde, E. J.; Pandey, A.; Herman, R.; Thomas, G. H.; Boros, E.; Duhme-Klair, A.-K.; Routledge, A. A Salmochelin S4-Inspired Ciprofloxacin Trojan Horse Conjugate. *ACS Infectious Diseases* **2020**, 6, 2532-2541.
160. Pinkert, L.; Lai, Y. H.; Peukert, C.; Hotop, S. K.; Karge, B.; Schulze, L. M.; Grunenberg, J.; Bronstrup, M. Antibiotic Conjugates with an Artificial MECAM-Based Siderophore Are Potent Agents against Gram-Positive and Gram-Negative Bacterial Pathogens. *Journal of Medicinal Chemistry* **2021**, 64, 15440-15460.
161. Wu, J. Y.; Srinivas, P.; Pogue, J. M. Cefiderocol: A Novel Agent for the Management of Multidrug-Resistant Gram-Negative Organisms. *Infectious Diseases and Therapy* **2020**, 9, 17-40.

162. Rathnavelu, V.; Alitheen, N. B.; Sohila, S.; Kanagesan, S.; Ramesh, R. Potential role of bromelain in clinical and therapeutic applications. *Biomedical Reports* **2016**, *5*, 283-288.
163. de Lencastre Novaes, L. C.; Jozala, A. F.; Lopes, A. M.; de Carvalho Santos-Ebinuma, V.; Mazzola, P. G.; Pessoa Junior, A. Stability, purification, and applications of bromelain: A review. *Biotechnology Progress* **2016**, *32*, 5-13.
164. Arshad, Z. I.; Amid, A.; Yusof, F.; Jaswir, I.; Ahmad, K.; Loke, S. P. Bromelain: an overview of industrial application and purification strategies. *Applied Microbiology and Biotechnology* **2014**, *98*, 7283-7297.
165. Gross, P.; Seelert, H.; Meiser, P.; Müller, R. Characterization of bromelain indicates a molar excess of inhibitor vs. enzyme molecules, a Jacalin-like lectin and Maillard reaction products. *Journal of Pharmaceutical and Biomedical Analysis* **2020**, *181*, 113075.
166. Azarkan, M.; Feller, G.; Vandenameele, J.; Herman, R.; El Mahyaoui, R.; Sauvage, E.; Vanden Broeck, A.; Matagne, A.; Charlier, P.; Kerff, F. Biochemical and structural characterization of a mannose binding jacalin-related lectin with two-sugar binding sites from pineapple (*Ananas comosus*) stem. *Scientific Reports* **2018**, *8*, 11508.
167. Damme, E. J. M. V.; Peumans, W. J.; Barre, A.; Rougé, P. Plant Lectins: A Composite of Several Distinct Families of Structurally and Evolutionary Related Proteins with Diverse Biological Roles. *Critical Reviews in Plant Sciences* **1998**, *17*, 575-692.
168. Peumans, W. J.; Van Damme, E. J. Lectins as plant defense proteins. *Plant Physiology* **1995**, *109*, 347-352.
169. Swanson, M. D.; Winter, H. C.; Goldstein, I. J.; Markovitz, D. M. A lectin isolated from bananas is a potent inhibitor of HIV replication. *Journal of Biological Chemistry* **2010**, *285*, 8646-8655.
170. Swanson, M. D.; Boudreaux, D. M.; Salmon, L.; Chugh, J.; Winter, H. C.; Meagher, J. L.; Andre, S.; Murphy, P. V.; Oscarson, S.; Roy, R.; King, S.; Kaplan, M. H.; Goldstein, I. J.; Tarbet, E. B.; Hurst, B. L.; Smee, D. F.; de la Fuente, C.; Hoffmann, H. H.; Xue, Y.; Rice, C. M.; Schols, D.; Garcia, J. V.; Stuckey, J. A.; Gabius, H. J.; Al-Hashimi, H. M.; Markovitz, D. M. Engineering a therapeutic lectin by uncoupling mitogenicity from antiviral activity. *Cell* **2015**, *163*, 746-58.
171. Fornstedt, N.; Porath, J. Characterization studies on a new Lectin found in Seeds of *Vicia ervilia*. *FEBS Letters* **1975**, *57*, 187-191.
172. Klonis, N.; Sawyer, W. H. Spectral properties of the prototropic forms of fluorescein in aqueous solution. *Journal of Fluorescence* **1996**, *6*, 147-157.
173. Oyelaran, O.; Gildersleeve, J. C. Glycan arrays: recent advances and future challenges. *Current Opinions in Chemical Biology* **2009**, *13*, 406-413.
174. Hauck, D.; Joachim, I.; Frommeyer, B.; Varrot, A.; Philipp, B.; Möller, H. M.; Imberty, A.; Exner, T. E.; Titz, A. Discovery of Two Classes of Potent Glycomimetic Inhibitors of *Pseudomonas aeruginosa* LecB with Distinct Binding Modes. *ACS Chemical Biology* **2013**, *8*, 1775-1784.
175. Beshr, G.; Sikandar, A.; Jemiller, E.-M.; Klymiuk, N.; Hauck, D.; Wagner, S.; Wolf, E.; Koehnke, J.; Titz, A. Photorhabdus luminescens lectin A (PIIA): A new probe for detecting α -galactoside-terminating glycoconjugates. *The Journal of Biological Chemistry* **2017**, *292*, 19935-19951.

176. Watanabe, Y.; Allen, J. D.; Wrapp, D.; McLellan, J. S.; Crispin, M. Site-specific glycan analysis of the SARS-CoV-2 spike. *Science* **2020**, 369, 330-333.
177. Richter, M. F.; Drown, B. S.; Riley, A. P.; Garcia, A.; Shirai, T.; Svec, R. L.; Hergenrother, P. J. Predictive compound accumulation rules yield a broad-spectrum antibiotic. *Nature* **2017**, 545, 299-304.
178. Vergalli, J.; Bodrenko, I. V.; Masi, M.; Moynié, L.; Acosta-Gutiérrez, S.; Naismith, J. H.; Davin-Regli, A.; Ceccarelli, M.; van den Berg, B.; Winterhalter, M.; Pagès, J.-M. Porins and small-molecule translocation across the outer membrane of Gram-negative bacteria. *Nature Reviews Microbiology* **2020**, 18, 164-176.
179. O'Leary, M. K.; Chen, S. S.; Westblade, L. F.; Alabi, C. A. Design of a PEGylated Antimicrobial Prodrug with Species-Specific Activation. *Biomacromolecules* **2021**, 22, 984-992.
180. Boyce, J. H.; Dang, B. B.; Ary, B.; Edmondson, Q.; Craik, C. S.; DeGrado, W. F.; Seiple, I. B. Platform to Discover Protease-Activated Antibiotics and Application to Siderophore-Antibiotic Conjugates. *Journal of the American Chemical Society* **2020**, 142, 21310-21321.
181. Boulware, K. T.; Daugherty, P. S. Protease specificity determination by using cellular libraries of peptide substrates (CLiPS). *Proceedings of the National Academy of Sciences of the United States of America* **2006**, 103, 7583-7588.
182. Yogo, T.; Umezawa, K.; Kamiya, M.; Hino, R.; Urano, Y. Development of an Activatable Fluorescent Probe for Prostate Cancer Imaging. *Bioconjugate Chemistry* **2017**, 28, 2069-2076.
183. Zieba, A.; Maslankiewicz, A.; Sitkowski, J. ¹H, ¹³C and ¹⁵N NMR spectra of ciprofloxacin. *Magnetic Resonance in Chemistry* **2004**, 42, 903-904.
184. Huang, X. Fluorescence Polarization Competition Assay: The Range of Resolvable Inhibitor Potency Is Limited by the Affinity of the Fluorescent Ligand. *Journal of Biomolecular Screening* **2003**, 8, 34-38.
185. Blixt, O.; Head, S.; Mondala, T.; Scanlan, C.; Huflejt, M. E.; Alvarez, R.; Bryan, M. C.; Fazio, F.; Calarese, D.; Stevens, J.; Razi, N.; Stevens, D. J.; Skehel, J. J.; van Die, I.; Burton, D. R.; Wilson, I. A.; Cummings, R.; Bovin, N.; Wong, C. H.; Paulson, J. C. Printed covalent glycan array for ligand profiling of diverse glycan binding proteins. *Proceedings of the National Academy of Sciences of the United States of America* **2004**, 101, 17033-17038.
186. Olivera-Ardid, S.; Khasbiullina, N.; Nokel, A.; Formanovsky, A.; Popova, I.; Tyrtys, T.; Kunetskiy, R.; Shilova, N.; Bovin, N.; Bello-Gil, D.; Mañez, R. Printed Glycan Array: A Sensitive Technique for the Analysis of the Repertoire of Circulating Anti-carbohydrate Antibodies in Small Animals. *Journal of Visualized Experiments* **2019**, 144, e57662.

